Durham University

Durham E-Theses

Modelling the differentiation and development of human tissues using mammalian stem cells and advanced cell technologies

LUCY ANNE SMITH

How to cite:

SMITH, LUCY ANNE (2020) Modelling the differentiation and development of human tissues using mammalian stem cells and advanced cell technologies. Doctoral thesis, Durham University.

Use policy

The full-text may be used and/or reproduced, and given to third parties in any format or medium, without prior permission or charge, for personal research or study, educational, or not-for-profit purposes provided that:

- a full bibliographic reference is made to the original source
- a https://etheses.durham.ac.uk/id/eprint/13432/ is made to the metadata record in Durham E-Theses
- the full-text is not changed in any way

The full-text must not be sold in any format or medium without the formal permission of the copyright holders.

Please consult the full Durham E-Theses policy for further details.

Academic Support Office, The Palatine Centre, Durham University, Stockton Road, Durham, DH1 3LE
e-mail: e-theses.admin@durham.ac.uk Tel: +44 0191 334 6107
https://etheses.durham.ac.uk



Department of Biosciences

Modelling the differentiation and development of human tissues using mammalian stem cells and advanced cell technologies

Lucy Anne Smith

September 2019

A thesis submitted for the degree of Doctor of Philosophy

Abstract

Human tissue development is a complex process which remains poorly understood. A variety of different techniques are currently used to study the events involved, yet each has associated limitations. Human embryo work is subject to ethical and logistical issues, animal studies are not necessarily representative of human processes, traditional cell culture lacks complexity and embryoid body formation suffers from viability and size related issues. The study of this process is crucial to the better understanding of this topic, as well as allowing for the development of reproducible differentiation protocols for regenerative medicine applications and the study and characterisation of pluripotent stem cells.

The overall aim of this project was to develop a novel *in vitro* model to be used to study the differentiation of human tissues. Based on work from the literature and previous work carried out within the group, it was hypothesised that the culture of pluripotent stem cell derived embryoid bodies (EBs) on the surface of a porous scaffold to enhance cell maturation over time and for the formation of complex tissue structures not previously possible. EBs show self-organisation, recapitulating some events of early embryogenesis, but have limited viability on increasing EB size and agglomeration, preventing long term studies. It was theorised that the reduction of cellular diffusion distances by changing the structure of the EB into a flattened tissue disc structure on the scaffold allows for improved nutritional and oxygen support, as well as the influence of attachment mediated signalling, which in turn would allow sufficient time for complex structure formation.

Proof of concept was confirmed using embryonal carcinoma cells, as was the ability to study specific signalling pathways through directing the differentiation of EBs using known morphogens. The incorporation of additional microenvironmental cues to the model was also undertaken, with co-culture and perfusion successfully introduced into the tissue disc model, impacting on the structure and phenotype of the cells. Long term culture with murine ES cell derived EBs resulted in the formation of a variety of complex structures which have not previously been seen *in vitro*. Tissue discs were successfully directed towards specific germ layers using various combinations of morphogens, and the introduction of physiological conditions impacted significantly on tissue disc morphology, with perfusion in particular showing an enhancement of differentiation. Validation against teratomas formed from the same cell populations confirmed the complexity of the *in vitro* structures and their similarity to the *in vivo* samples, and pilot studies confirmed the ability to culture human pluripotent stem cell derived tissue discs within the system also.

The model developed in this project has shown the ability to form varied and complex tissue structures *in vitro* in response to a variety of microenvironmental cues. As well as being used to study the events of human tissue development, this model also offers a controllable and reproducible *in vitro* alternative to the teratoma assay.

Acknowledgments

There are many people and organisations to thank for their support and contributions to this work. I would like to acknowledge the Anatomical Society, without whose support this project could not have taken place and the members of which I found enthusiastic, helpful and encouraging. I would also like to thank the EPSRC for additional support received to complete work during this project. Thank you to my supervisor, Professor Stefan Przyborski, for giving me the opportunity to complete this project and be a member of the Przyborski lab. Thank you also for your advice, guidance, support and enthusiasm during this time. I also would like to thank members of the Faculty of Science at Durham University for their subject specific help: Dr Lian Gan of the Department of Engineering, Prof Gareth William, Dr Lars Olof Pålsson and Aaron Brown of the Department of Chemistry. Thanks also to go to Professor Majlinda Lako of Newcastle University for facilitating the completion of the teratoma assay.

To the members of the Przyborski laboratory, past and present, thank you so much. There really aren't words to describe how much I appreciate everyone's help and friendship. I would like to thank Dr Mathilde Roger, Dr Frederique Tholozan and Dr Nicola Fullard for all of their technical help and advice over the past 4 years. Kirsty, thank you for sharing the sometimes long journey to work and my love of reading. Rebecca, thank you for being my stem cell partner and for listening to me when I was overly anxious. Nicole, thank you for your continual kindness, support and encouragement. Henry, thank you for your help with the perfusion system, the associated physics and for showing me that crazy ideas can work. Lydia, thank you for being so optimistic and bringing positivity to the lab every day. Matt, thank you for your straight talking and being my slightly messy lab bench neighbour. Ben, thank you for punctuating my days with film review discussions and always being willing to help out. Thank you to Amy and Steve for your friendship and support, and Claire, for being truly thoughtful and kind. Thank you also to Alex, Kelly, Melissa, Eve, Felicity, Antonio, Dom and Pam.

To all of my family and friends, thank you for being so supportive and understanding during my studies. To Sophie and Jess, thank you for letting me tell you every trivial detail about my work day, reminding me of the importance of time away from the lab and making it enjoyable.

Finally, none of this would have been possible without the love and support of my mum. Mum, thank you for always encouraging me to do what I love. Thank you for caring so deeply and listening to me when things didn't work and putting up with my need for perfection. I will always be grateful to you.

This thesis is dedicated to Ernie and Alan, who both knew the value and importance of hard work.

Declaration

The work described within this text was carried out in the Department of Biosciences, Durham University between October 2015 and August 2019. All of the work is my own, except where specifically stated otherwise. No part has previously been submitted for a degree at this or any other university.

Statement of Copyright

The copyright of this thesis rests with the author. No quotations from it should be published without prior written consent and information derived from it should be acknowledged.

Publications arising from this work:

Applications of novel bioreactor technology to enhance the viability and function of cultured cells and tissues. (2019) Interface Focus; H. W. Hoyle, L. A. Smith, R. J. Williams and S. A. Przyborski – submitted and under review

Pluripotent phenotype vs pluripotent function: the teratoma assay in a modern day context. L. A. Smith, R. H. Quelch, F. V. P. S Liu, and S. A. Przyborski - In preparation

Modelling the development of human tissue *in vitro* using mammalian stem cells in a novel scaffold based model L.A. Smith, D. D. G. Owens, E. G. Knight and S. A. Przyborski - In preparation

Poster Presentations:

Modelling the Development of Human Tissues *In Vitro* Using Mammalian Stem Cells and Advanced Cell Technologies (2019) IFAA, London, UK

Modelling the Development of Human Tissues *In Vitro* Using Advanced Cell Technologies and Mammalian Stem Cells (2019) BSCB BSDB Joint Meeting, Coventry, UK

Modelling the Development of Human Tissues *In Vitro* Using Advanced Cell Technologies and Mammalian Stem Cells (2018) Anatomical Society Winter Meeting, York, UK

Modelling the Development of Human Tissues *In Vitro* Using a Combination of Advanced Cell Technologies and Mammalian Stem Cells (2018) EMBO EMBL Symposium: Organoids, Heidelberg, Germany

Modelling the Development of Human Tissues *In Vitro* Using a Combination of Advanced Cell Technologies and Mammalian Stem Cells (2017) Anatomical Society Winter Meeting, Dundee, UK

Modelling the development of human tissues *in vitro* using a combination of three dimensional cell culture technologies (2016) Anatomical Society Winter Meeting, London, UK

Modelling the development of human tissues *in vitro* using a combination of three dimensional cell culture technologies (2016) White Rose Consortium Work In Progress Meeting, Durham, UK

Investigating Modelling Human Tissue Development *In Vitro* Using Three Dimensional Cell Culture Technologies (2016) Anatomical Society Summer Meeting, Brighton, UK

Investigating Modelling Human Tissue Development *In Vitro* Using Three Dimensional Cell Culture Technologies (2016) BSCB BSDB Joint Meeting, Coventry, UK

Oral Presentations:

Modelling the Development of Human Tissues *In Vitro* Using a Combination of Advanced Cell Technologies and Mammalian Stem Cells (2018) Anatomical Society Summer Meeting, Oxford, UK

Modelling the Development of Human Tissues *In Vitro* Using a Combination of Advanced Cell Technologies and Mammalian Stem Cells (2018) Durham University Department of Biosciences Postgraduate Conference, Durham, UK

Modelling the Development of Human Tissues *In Vitro* Using a Combination of Advanced Cell Technologies and Mammalian Stem Cells (2017) North East Postgraduate Conference, Newcastle, UK

Contents

List of Figures **17**

List of Tables **27**

Abbreviations **29**

1.1 Introduction **31**

1.2 Project Background **33**

1.2.1 Mammalian embryonic development 33

1.2.1.1 Preimplantation events of early embryogenesis 33

1.2.1.2 Blastocyst formation 34

1.2.1.3 Implantation 34

1.2.1.4 Gastrulation 35

1.2.1.5 Organogenesis 38

1.2.2 Pluripotent stem cells: a useful tool from the study of embryos 40

1.2.2.1 Embryonal carcinoma cells 40

1.2.2.2 Embryonic stem cells 40

1.2.2.3 Induced pluripotent stem cell populations 41

1.2.2.4 Assessment of pluripotency 42

1.2.3 Advanced cell culture technologies for the improvement of the cellular microenvironment 46

1.2.3.1 Traditional ‘two dimensional’ cell culture techniques 47

1.2.3.2 Aggregation based techniques 48

1.2.3.3 Scaffold based technologies 51

1.2.3.4 Physiological culture conditions 54

1.2.4 Techniques used to model human tissue development 55

1.2.4.1 Human embryo work 55

1.2.4.2 Use of model organisms 56

1.2.4.3 Teratoma formation 56

1.2.4.4 Pluripotent stem cell studies 57

1.2.5 Conclusion 58

1.3 Project Aims and Objectives 59

1.3.1 Aims 59
1.3.2 Objectives 60
2. Materials and Methods 61
2.1 Introduction 61
2.2 Routine cell culture and three dimensional cell culture techniques 61
2.2.1 Routine culture, maintenance and cryopreservation of TERA2.cl.SP12 embryonal carcinoma cells 61
2.2.2 Formation, maintenance and morphogen treatment of TERA2.cl.SP12 cell aggregates 63
2.2.3 Preparation of Alvetex® Polaris inserts 64
2.2.4 Seeding and maintenance of TERA2.cl.SP12 aggregates as tissue discs on Alvetex® inserts 65
2.2.5 Routine culture, pluripotency maintenance and cryopreservation of CGR8 embryonic stem cells 65
2.2.6 Formation, maintenance and morphogen treatment of CGR8 embryoid bodies 66
2.2.7 Seeding and maintenance of CGR8 embryoid bodies as tissue discs on Alvetex® Polaris 68
2.2.8 Routine culture, maintenance and cryopreservation of I18002 induced pluripotent stem cell line 69
2.2.9 Routine culture, maintenance and cryopreservation of H9 human embryonic stem cells 71
2.2.10 Formation and maintenance of I18002 and H9 embryoid bodies 72
2.2.11 Routine culture, maintenance and cryopreservation of human neonatal dermal fibroblasts 72
2.2.12 Isolation of severe combined immunodeficient (SCID) mouse fibroblast cell line and creation of cell line 73
2.2.13 Routine culture, maintenance and cryopreservation of SCID mouse fibroblast cell line 74
2.2.14 Seeding and culture of cells on glass coverslips 75
2.2.15 Formation of dermal equivalents using Alvetex® Scaffold 76
2.2.16 Seeding of aggregates/EBs on dermal equivalents for co-culture 76
2.3 Processing, sectioning and histological staining for assessment of tissue structure 78
2.3.1 Sample processing for wax embedding – aggregates and embryoid bodies 78
2.3.2 Sample processing for wax embedding – Alvetex® samples 78

2.3.3 Sample sectioning 79
2.3.4 Haematoxylin and Eosin staining 79
2.3.5 Masson's Trichrome staining 80
2.3.6 Weighert's staining 80
2.3.7 Periodic Acid Schiff with Alcian Blue Staining 81
2.4 Techniques to assess cell and tissue identity 82
2.4.1 Immunofluorescent staining of paraffin sections 82
2.4.2 Immunofluorescent staining of glass coverslips 82
2.4.3 Microscopy 84
2.4.4 Flow cytometry 84
2.4.5 Western blotting: Lysate preparation and protein concentration determination 87
2.4.6 Western blotting: Gel casting, loading, running and transfer 87
2.4.7 Western blotting: Membrane blocking, antibody incubations and exposure 87
2.4.8 PCR analysis: RNA lysate preparation 89
2.4.9 PCR analysis: cDNA synthesis 89
2.4.10 PCR analysis: Primer preparation and SYBR PCR reaction 90
2.5 Techniques to assess structure, size and viability 92
2.5.1 Aggregate measuring 92
2.5.2 Cell layer and infiltration measuring 92
2.5.3 TUNEL assay 93
2.5.4 MTT assay 94
3. Assessment of the methods used to confirm the pluripotency and developmental potential of human pluripotent stem cells 95
3.1 Introduction 95
3.1.1 Pluripotency as a cell state 95
3.1.2 Developmental potency: pluripotency as a cell function 97
3.1.3 The teratoma assay to assess the developmental potential of PSCs 99
3.1.4 Routes to standardisation for pluripotency assessment 102
3.1.5 Conclusion 103
3.2 Aims and Hypotheses 105
3.3 Objectives 105

3.4 Results....106
3.4.1 Investigation into phenotypic and functional analyses used to assess human pluripotent stem cells....106
3.4.1.1 The majority of human pluripotent stem cell lines have characterisation data available for assessment....107
3.4.1.2 Analyses which assessed the pluripotent state showed varying frequency of usage....108
3.4.1.3 The teratoma assay is one of the most infrequently used techniques in the assessment pluripotency as a function....110
3.4.1.4 In depth analysis of teratoma assay protocols reveals a lack of congruency and trends within these assays....111
3.5 Discussion....117
3.5.1 The availability of characterisation data for registered human PSCs....117
3.5.2 Use of analyses which assess the pluripotent state....118
3.5.3 Current use of the teratoma assay to assess developmental potency....119
3.5.4 In depth analysis of teratoma assay protocols....120
3.6 Conclusion....122
4. The application of technologies to enhance the microenvironment of PSCs using EC cells as a working model....123
4.1 Introduction....123
4.1.1 Embryoid bodies as a model of human tissue development....123
4.1.2 Cell death and diffusion in embryoid bodies....125
4.1.3 Combining embryoid bodies with advanced cell culture technologies....127
4.1.4 Use of Alvetex® scaffolds for three dimensional cell culture....129
4.1.5 TERA2.cl.SP12: Embryonal carcinoma cells as models of human development....130
4.1.6 Conclusion....132
4.2 Aims and Hypotheses....133
4.3 Objectives....133
4.4. Materials and Methods....134
4.4.1 Propidium iodide staining and flow cytometry of EBs....134
4.4.2 Caspase 3/7 live staining of EBs....134
4.4.3 Fluorescence Lifetime Imaging Microscopy....134
4.5 Results....136

4.4.1 Investigations into the effects of cell density on the formation, viability and differentiation of TERA2.cl.SP12 derived EBs 136
4.4.2 Investigation into the interaction between cellular EBs and Alvetex® membranes 152
4.4.3 Characterisation of the model and investigations into known signalling pathways 163
4.5 Discussion 169
4.5.1 The impact of cell seeding density on EB properties 169
4.5.2 Optimisation of TERA2.cl.SP12 EB formation 171
4.5.3 Optimisation of porous scaffold to maintain EBs long term as tissue discs 171
4.5.4 Analysis of cell death and oxygen tension in TERA2.cl.SP12 EBs and tissue discs 173
4.5.5 The study of developmental pathways using tissue discs cultured on Alvetex® Polaris 176
4.6 Conclusion 178
5. Increasing the complexity of the *in vitro* cellular microenvironment to further enhance the differentiation of PSC derived structures 180
5.1 Introduction 180
5.1.1 The complexity of the *in vivo* environment 180
5.1.2 Co-culture studies *in vitro*: Methods, techniques and rationale 183
5.1.2.1 The development of *in vitro* tissue models co-culture models 184
5.1.3 Introduction of perfusion into the *in vitro* setting and its use with PSCs 185
5.1.4 The incorporation of physiological factors to the current TERA2.cl.SP12 model 192
5.1.5 Conclusion 194
5.2 Aims and Hypotheses 195
5.3 Objectives 195
5.4 Materials and Methods 196
5.4.1 Technical specifications of equipment used for perfusion experiments 196
5.4.2 Analysis of fluid flow dynamics 199
5.4.3 Analysis of fluid flow dynamics – Image J analysis 199
5.4.4 Particle Image Velocimetry studies 200
5.4.5 Seeding of cells/EBs for static sandwich culture 200
5.4.6 Seeding cells in Matrigel on Alvetex® inserts 201
5.4.7 Seeding cells/EBs on Alvetex® inserts for static culture 201
5.4.8 Seeding cells/EBs for perfused culture 202

5.5 Results....203
5.5.1 Characterisation of neonatal human dermal fibroblast model and optimisation for culture of pluripotent stem cell EBs with fibroblasts....203
5.5.2 Creation and use of more relevant dermal fibroblast model using SCID mouse dermal fibroblasts....216
5.5.3 The introduction of perfusion to tissue disc culture and technical optimisation....229
5.5.4 Optimisation of novel perfusion system using TERA2.cl.SP12....244
5.6 Discussion....263
5.6.1 The use of an established dermal fibroblast model to undertake proof of concept co-culture studies....263
5.6.2 Development of a relevant, novel co-culture model to enhance the differentiation of PSC derived EBs....265
5.6.3 The impact of fibroblasts on PSC derived tissue discs....265
5.6.4 The optimisation of the novel perfusion system....268
5.6.5 The impact of fluid flow and perfusion on the pluripotency and differentiation of PSCs....270
5.7 Conclusions....271
6. The application of novel technologies to enable the formation of rudimentary tissue structures from mammalian PSCs....272
6.1 Introduction....272
6.1.1 EC cells: a truly pluripotent population?....272
6.1.2 Alternative pluripotent populations: mouse pluripotent stem cells....273
6.1.3 Comparing mouse and human developmental processes: the use of murine PSCs in developmental studies....275
6.1.4 Organogenesis and the identification of mature complex tissues....278
6.1.5 The creation of complex tissues *in vitro*....288
6.1.6 Conclusion....288
6.2 Aims and Hypotheses....291
6.3 Objectives....291
6.4 Materials and Methods....292
6.4.1 Morphogen treatment of CGR8 embryoid bodies....292
6.4.2 Paracrine and Topography experiments: Preparation of conditioned media and fixed

scaffolds 293
6.4.3 Paracrine and Topography experiments: EB seeding and maintenance 293
6.4.4 Long term perfusion using CGR8 cells 294
6.5 Results 295
6.5.1 Long term culture of CGR8 embryoid bodies as tissue discs on Alvetex® Polaris 295
6.5.2 Modulation of tissue disc differentiation using exogenous morphogen stimulation 310
6.5.3 Investigation into lineage specification events: Ectodermal fate decisions 335
6.5.4 Co-culture of CGR8 tissue discs with SCID fibroblast dermal equivalent 356
6.5.5 Utilisation of CGR8 murine stem cells in perfusion culture system 367
6.6 Discussion 376
6.6.1 The long term differentiation of murine embryoid bodies as tissue discs on Alvetex® Polaris 376
6.6.2 Directing the differentiation of murine EBs and tissue discs towards specific germ layers 377
6.6.3 Investigating lineage commitment in the ectoderm germ layer 381
6.6.4 The effects of fibroblasts on murine tissue disc formation and differentiation 382
6.6.5 Enhancing the PSC microenvironment using perfusion culture 384
6.7 Conclusion 386
7. Further validation and application of the *in vitro* model using the teratoma assay and human pluripotent stem cell populations 388
7.1 Introduction 388
7.1.1 Standardising the culture of human pluripotent stem cells and the assessment of cellular pluripotency 388
7.1.2 Standardising the assessment of developmental potency 389
7.1.3 Confirming developmental potency using the teratoma assay 390
7.1.4 Human pluripotent stem cells and models of human tissue development 393
7.1.5 Conclusions 395
7.2 Aims and Hypotheses 396
7.3 Objectives 396
7.4 Materials and Methods 397
7.4.1 Alkaline Phosphatase Staining 397

7.4.2 Teratoma assay protocols: Cell maintenance and syringe loading 397
7.4.3 Teratoma assay protocols: Injection and animal maintenance 397
7.4.4 Teratoma assay protocols: Tumour processing and sectioning 398
7.5 Results 399
7.5.1 Histological and immunofluorescent analysis of TERA2.cl.SP12 teratomas and tissue disc samples 399
7.5.2 Histological and immunofluorescent analysis and comparison of CGR8 teratomas and tissue disc samples 406
7.5.3 Use of human pluripotent stem cell lines to form tissue discs 422
7.6 Discussion 427
7.6.1 Comparison of the differentiation within tissue disc samples and teratoma samples 427
7.6.2 The tissue disc model as an *in vitro* alternative to the teratoma assay 429
7.6.3 Use of multiple human pluripotent stem cell populations in the EB based *in vitro* model 430
7.7 Conclusion 432
8. General Discussion, Future Directions and Conclusion 433
8.1 Summary of key findings 433
8.2 Discussion 433
8.2.1 The current use of the teratoma assay to assess developmental potency 434
8.2.2 Differentiation of EC cell derived structures using advanced cell technology 435
8.2.3 Creating a more physiological culture environment 435
8.2.4 Application of the model to a more relevant murine PSC population 436
8.2.5 Validation against teratoma samples and with human pluripotent stem cell lines 437
8.3 Future Directions 439
8.3.1 Differentiation of specific cell populations using more complex morphogen based protocols 439
8.3.2 Integration of multiple cues to create a more complex and physiological microenvironment 439
8.3.3 Further work using human pluripotent stem cell lines 439
8.3.4 Investigation into the effects of other environmental cues on tissue disc differentiation 440
8.3.5 Embryonic toxicity testing for therapeutic compounds 440

8.4 Conclusion 441

9. Bibliography 433

10. Appendices 458

10.1 Appendix 1 – Abstracts and Posters 458

10.1.1 Investigating Modelling Human Tissue Development *In Vitro* Using Three Dimensional Cell Culture Technologies (2016) BSCB BSDB Joint Meeting, Coventry, UK 458

10.1.2 Investigating Modelling Human Tissue Development *In Vitro* Using Three Dimensional Cell Culture Technologies (2016) Anatomical Society Summer Meeting, Brighton, UK 460

10.1.3 Modelling the development of human tissues *in vitro* using a combination of three dimensional cell culture technologies (2016) White Rose Consortium Work In Progress Meeting, Durham, UK 462

10.1.4 Modelling the development of human tissues *in vitro* using a combination of three dimensional cell culture technologies (2016) Anatomical Society Winter Meeting, London, UK 465

10.1.5 Modelling the Development of Human Tissues *In Vitro* Using a Combination of Advanced Cell Technologies and Mammalian Stem Cells (2017) Anatomical Society Winter Meeting, Dundee, UK 466

10.1.6 Modelling the Development of Human Tissues *In Vitro* Using a Combination of Advanced Cell Technologies and Mammalian Stem Cells (2018) EMBO EMBL Symposium: Organoids, Heidelberg, Germany 468

10.1.7 Modelling the Development of Human Tissues *In Vitro* Using Advanced Cell Technologies and Mammalian Stem Cells (2018) Anatomical Society Winter Meeting, York, UK 470

10.1.8 Modelling the Development of Human Tissues *In Vitro* Using Advanced Cell Technologies and Mammalian Stem Cells (2019) BSCB BSDB Joint Meeting, Coventry, UK 472

10.1.9 Modelling the Development of Human Tissues In Vitro Using Mammalian Stem Cells and Advanced Cell Technologies (2019) IFAA, London, UK 474

10.2 Appendix 2 – Oral presentations 476

10.2.1 Modelling the Development of Human Tissues *In Vitro* Using a Combination of Advanced Cell Technologies and Mammalian Stem Cells (2017) North East Postgraduate Conference, Newcastle, UK 476

10.2.2 Modelling the Development of Human Tissues *In Vitro* Using a Combination of Advanced Cell Technologies and Mammalian Stem Cells (2018) Durham University Department of Biosciences Postgraduate Conference, Durham, UK 476

10.2.3 Modelling the Development of Human Tissues *In Vitro* Using a Combination of Advanced Cell Technologies and Mammalian Stem Cells (2018) Anatomical Society Summer Meeting, Oxford, UK 477
10.3 Appendix 3 – Histological stain recipes 478
10.3.1 Haematoxylin and Eosin staining 478
10.3.2 Masson's Trichrome staining 478
10.3.3 Weighert's staining 479
10.4 Appendix 4 – Western Blotting recipes 481
10.4.1 Gel Casting recipe 481
10.4.2 Buffer recipes 481
10.4.2.1 10x Tank buffer recipe 481
10.4.2.2 1x Tank buffer recipe 481
10.4.2.3 10x Transfer buffer recipe 481
10.4.2.4 1x Transfer buffer recipe 482
10.5 Appendix 5 – PCR primer optimisation data 483
10.5.1 Cytokeratin 10 483
10.5.2 Cytokeratin 14 483
10.5.3 Class III β-tubulin 484
10.5.4 E-cadherin 484
10.5.5 Brachyury 485
10.5.6 Alpha fetoprotein 485
10.5.7 FOXA2 486
10.5.8 GATA6 486
10.5.9 SOX17 487
10.5.10 GAPDH 487
10.6 Appendix 6 – Teratoma assay supplemental data 488

List of Figures

1. Introduction

Figure 1.1: Compaction of the early mammalian embryo

Figure 1.2: Structure of the mammalian blastocyst

Figure 1.3: Proccesses of Zona hatching and implantation

Figure 1.4: Schematic of the mammalian gastrulation process

Figure 1.5: The retinoic acid signalling pathway

Figure 1.6: Various sources of pluripotent stem cells

Figure 1.7: *In vitro* methods of assessing developmental potency

Figure 1.8: Schematic of a general teratoma assay

Figure 1.9: Microenvironmental cues which impact on cell structure and function

Figure 1.10: Adaptation of cells to the external microenviroment

Figure 1.11: Phenotype and morphology of cells cultured in the traditional two dimensional environment

Figure 1.12: Phenotype and morphology of cells cultured using three dimensional culture techniques

Figure 1.13: Techniques used to create cellular aggregates

Figure 1.14: Methods used to synthesise scaffolds for cell culture applications

2. Materials and Methods

Figure 2.1: TERA2.cl.SP12 cells in vitro at subconfluent and fully confluent densities

Figure 2.2: TERA2.cl.SP12 cells in suspension culture in vitro at various timepoints during the aggregate formation process

Figure 2.3: Assembling an Alvetex® insert

Figure 2.4: Schematic of creation of TERA2.cl.SP12 tissue discs

Figure 2.5: CGR8 pluripotent stem cells *in vitro*

Figure 2.6: Formation of embryoid bodies using murine embryonic stem cell line CGR8

Figure 2.7: Two phase embryoid body formation process using Aggrewell plates and suspension culture

Figure 2.8: I18002 pluripotent stem cells in culture *in vitro*

Figure 2.9: Washing of I18002 colonies from 6 well plate

Figure 2.10: H9 pluripotent stem cells *in vitro*

Figure 2.11: Neonatal human dermal fibroblasts *in vitro*

Figure 2.12: Outgrowth of immunodeficient mouse fibroblasts from dermal explant *in vitro*

Figure 2.13: Murine dermal fibroblasts in culture *in vitro*

Figure 2.14: Schematic for the creation of dermal equivalent using fibroblasts in Alvetex® Scaffold

Figure 2.15: Schematic for the creation of co-culture model using dermal equivalents and stem cell aggregates

Figure 2.16: Stem cell aggregates stained with 0.01% crystal on the Polaris membrane and in a wax block

Figure 2.17: Secondary antibody controls for Rabbit and Mouse secondary antibodies

Figure 2.18: Representative control settings and antibody histograms from flow cytometry analysis

Figure 2.19: Phase contrast image of TERA2.cl.SP12 aggregate in suspension culture opened in Image J for measurement

Figure 2.20: H&E stained image of TERA2.cl.SP12 aggregates cultured in the sandwich culture set up prepared for measuring cell layer infiltration

Figure 2.21: Antibody control slides generated for TUNEL staining

3. Assessment of the methods used to confirm the pluripotency and developmental potential of human pluripotent stem cells

Figure 3.1: Methods used to assess the pluripotency as a state during the characterisation of putative human PSC lines

Figure 3.2: Methods used to assess developmental potency during the characterisation of putative human PSC lines

Figure 3.3: Comparison of the *in vivo* functional tests of developmental potency

Figure 3.4: Representative structures from a human pluripotent stem cell derived teratoma

Figure 3.5: Outline of the process used to collect data for in depth analysis of the characterisation of human pluripotent stem cell lines

Figure 3.6: Analysis of characterisation data availability for entire dataset and for separate ESC and iPSC populations

Figure 3.7: Breakdown of the phenotypic analyses used to characterise human pluripotent stem cell lines

Figure 3.8: Breakdown of the functional analyses used to characterise human pluripotent stem cell lines

Figure 3.9: Evaluation of frequency of teratoma assay analysis on registered human pluripotent stem cell

Figure 3.10: Analysis of initial cell number used on implantation in teratoma assay protocols of registered human pluripotent cells

Figure 3.11: Assessment of anatomical site used for implantation in teratoma assay protocols of registered human pluripotent cells

Figure 3.12: Analysis of mouse strains used in teratoma assays performed on registered human pluripotent stem cells

Figure 3.13: Identification of endpoint definition of teratoma assays performed on registered human pluripotent stem cells

Figure 3.14: Assessment of the reporting of teratoma assay success rate in registered human pluripotent stem cell lines

4. The impact of microenvironmental factors on the differentiation of embryonal carcinoma cell derived tissue discs

Figure 4.1: PSC derived EB in culture

Figure 4.2: Schematic of the internal structure of PSC derived EBs

Figure 4.3: The heterogeneity of the embryoid body microenvironment

Figure 4.4: Characterisation of TERA2.cl.SP12 cells in traditional 2D culture

Figure 4.5: Phase contrast images of TERA2.cl.SP12 EBs seeded at different cell densities during the first 3 days of suspension culture and analysis of the morphology of the structures

Figure 4.6: TERA2.cl.SP12 EBs cultured at varied cell densities for up to 21 days

Figure 4.7: Analysis of TERA2.cl.SP12 EBs cultured at varied cell densities for up to 21 days

Figure 4.8: Assessment of apoptotic cell death in TERA2.cl.SP12 EBs at various cell densities using live caspase 3/7 stain

Figure 4.9: Quantitative analysis of necrotic cell death in TERA2.cl.SP12 EBs at various cell densities via flow cytometry

Figure 4.10: Assessment of necrotic cell death in TERA2.cl.SP12 EBs at various cell densities using propidium iodide

Figure 4.11: Assessment of the pluripotency and epithelial ectodermal differentiation of TERA2.cl.SP12 EBs seeded at various densities

Figure 4.12: Assessment of the neural differentiation of TERA2.cl.SP12 EBs seeded at various densities

Figure 4.13: Behaviour of TERA2.cl.SP12 EBs cultured on the surface of Alvetex® Scaffold for 7 days

Figure 4.14: Behaviour of TERA2.cl.SP12 EBs cultured on the surface of Alvetex® Strata for 7 days

Figure 4.15: Behaviour of TERA2.cl.SP12 EBs cultured on the surface of Alvetex® Polaris for 7 days

Figure 4.16: Comparison of cell death in TERA2.cl.SP12 EBs and the Alvetex® tissue disc model

Figure 4.17: Figure 4.16: Assessment of Pt[dpyb]Cl decay time and therefore oxygen tension in TERA2.cl.SP12 EBs and tissue discs

Figure 4.18: Treatment of TERA2.cl.SP12 aggregates with organic retinoid all-trans retinoic acid (ATRA) to promote neural differentiation, and subsequent culture on Alvetex® Polaris

Figure 4.19: Treatment of TERA2.cl.SP12 EBs with synthetic retinoid analogue EC23 to promote neural differentiation, and subsequent culture on Alvetex® Polaris

Figure 4.20: Treatment of TERA2.cl.SP12 EBs with morphogen bone morphogenetic 2 (BMP-2) to promote non-neural ectodermal differentiation, and subsequent culture on Alvetex® Polaris

Figure 4.21: Histological and marker expression analysis of teratocarcinoma formed from human EC cells

Figure 4.22: Changes to the EB microenvironment on culture on Alvetex® Polaris

Figure 4.23: Schematic of the PSC derived EB internal structure and the corresponding interaction of the fluorescent platinum compound

Figure 4.24: Schematic of the PSC derived tissue disc structure and the corresponding interaction of the fluorescent platinum compound

5. The incorporation of more microenvironmental cues to enhance the physiological relevance of the in vitro tissue disc model

Figure 5.1: Microenvironmental cues which impact on cell structure and function

Figure 5.2: The microenvironment of the developing embryo

Figure 5.3: The teratoma microenvironment

Figure 5.4: Additional microenvironmental cues which can be fulfilled through co-culture

Figure 5.5: The structure of a hollow fibre bioreactor and example structures created from PSCs

Figure 5.6: Examples of microfluidic technology device designs

Figure 5.7: Examples of dynamic bench top cell culture systems

Figure 5.8: Overview of novel perfusion system equipment

Figure 5.9: Perfusion system glassware and specifications

Figure 5.10: Stirrer system used for perfused experiments and specifications

Figure 5.11: Potential device holder stand designs

Figure 5.12: Overview of novel perfusion system equipment

Figure 5.13: Assessment of fluid flow dynamics of the system using crystal violet dye

Figure 5.14: Schematic for the creation of static sandwich culture models

Figure 5.15: Schematic for the creation perfused culture models

Figure 5.16: Characterisation of current HDFn dermal equivalent model cultured for up to 28 days in M106 with TGF-β and ascorbic acid supplementation

Figure 5.17: Full thickness human skin equivalent model formed on HDFn dermal equivalent

Figure 5.18: Characterisation of HDFn cells cultured in M106 and DMEM

Figure 5.19: HDFn growth in M106 and DMEM

Figure 5.20: Characterisation of HDFn dermal equivalents cultured for up to 28 days in DMEM with TGF-β and ascorbic acid supplementation

Figure 5.21: Characterisation of TERA2.cl.SP12 EBs cultured on HDFn dermal equivalents for 7 days

Figure 5.22: Characterisation of TERA2.cl.SP12 EBs treated with EC23 and cultured on HDFn dermal equivalents for 7 days

Figure 5.23: Characterisation of TERA2.cl.SP12 EBs treated with BMP-2 and cultured on HDFn dermal equivalents for 7 days

Figure 5.24: Isolation and characterisation of SCID Mouse dermal fibroblast cell line

Figure 5.25: Characterisation of SCID Mouse Fibroblast dermal equivalents cultured for up to 28 days in DMEM

Figure 5.26: Characterisation of SCID Mouse Fibroblast dermal equivalents cultured for up to 28 days in DMEM with ascorbic acid and TGF-β supplementation

Figure 5.27: Characterisation of T2SP12 EBs cultured on SCID dermal equivalents for 7 days

Figure 5.28: Characterisation of T2SP12 EBs treated with EC23 and cultured on SCID dermal equivalents for 7 days

Figure 5.29: Characterisation of T2SP12 EBs treated with BMP-2 and cultured on SCID dermal equivalents for 7 days

Figure 5.30: Fluid flow analysis data for anticlockwise fluid flow cone design

Figure 5.31: Fluid flow analysis data for anticlockwise fluid flow cone design with Alvetex® holder in place

Figure 5.32: Fluid flow analysis data for clockwise fluid flow cone design

Figure 5.33: Fluid flow analysis data for clockwise fluid flow cone design with Alvetex® holder in place

Figure 5.34: Fluid flow analysis data for platform with angled slots design

Figure 5.35: Fluid flow analysis data for platform with angled slots design with Alvetex® holder in place

Figure 5.36: Fluid flow analysis data for clockwise fluid flow cone final design

Figure 5.37: Fluid flow analysis data for clockwise fluid flow cone final design with Alvetex® holder in place

Figure 5.38: Morphology and viability of cells cultured in PTFE conditioned media

Figure 5.39: The sandwich culture technique used for perfusion experiments

Figure 5.40: Morphology and behaviour of TERA2.cl.SP12 EBs seeded into various combinations of Alvetex® sandwich culture in the static setting

Figure 5.41: Quantification of invasion of TERA2cl.SP12 EBs into base and top membrane of sandwich culture

Figure 5.42: Characterisation of TERA2.cl.SP12 EBs cultured in Polaris Polaris sandwich culture combinations

Figure 5.43: TERA2.cl.SP12 EBs cultured in Polaris based sandwich culture combinations in the novel perfusion system

Figure 5.44: TERA2.cl.SP12 cells cultured static culture in the novel sandwich culture setting at varying cell densities

Figure 5.45: TERA2.cl.SP12 cells cultured static culture in the novel sandwich culture setting at varying cell densities

Figure 5.46: Variability of TERA2.cl.SP12 in perfused sandwich culture is dependent on cell seeding density

Figure 5.47: Characterisation of TERA2.cl.SP12 cells in perfusion system

Figure 5.48: Characterisation of TERA2.cl.SP12 cells cultured using a reoptimised culture methodology

Figure 5.49: Characterisation of TERA2.cl.SP12 cells cultured using a reoptimised culture methodology

Figure 5.50: The benefits of sandwich culture techniques

6. The application of the in vitro tissue model to more relevant mammalian pluripotent stem cell populations

Figure 6.1: Phenotype and culture conditions of human and mouse PSCs

Figure 6.2: The hourglass model of development

Figure 6.3: Comparison of key signalling pathways involved in pluripotency and differentiation in humans and mice

Figure 6.4: Current overview of work completed using TERA2.cl.SP12 EBs as tissue discs in the model

Figure 6.5: Characterisation of 2D CGR8 murine embryonic stem cells in the pluripotent state

Figure 6.6: CGR8 murine embryonic stem cells successfully form embryoid bodies which show evidence of spontaneous differentiation

Figure 6.7: Culture and characterisation of murine embryoid bodies on Alvetex® Polaris for 7 days

Figure 6.8: Culture and characterisation of murine embryoid bodies on Alvetex® Polaris for 7 days

Figure 6.9: Culture and characterisation of murine embryoid bodies on Alvetex® Polaris for 14 days

Figure 6.10: Culture and characterisation of murine embryoid bodies on Alvetex® Polaris for 14 days

Figure 6.11: Culture and characterisation of murine embryoid bodies on Alvetex® Polaris for 21 days

Figure 6.12: Culture and characterisation of murine embryoid bodies on Alvetex® Polaris for 21 days

Figure 6.13: Culture and characterisation of murine embryoid bodies on Alvetex® Polaris for 28 days

Figure 6.14: Culture and characterisation of murine embryoid bodies on Alvetex® Polaris for 28 days

Figure 6.15: Culture and characterisation of murine embryoid bodies on Alvetex® Polaris for 35 days

Figure 6.16: Culture and characterisation of murine embryoid bodies on Alvetex® Polaris for 35 days

Figure 6.17: Directed differentiation of CGR8 embryoid bodies with synthetic retinoid EC23 and their maintenance on Alvetex® inserts

Figure 6.18: Directed differentiation of CGR8 embryoid bodies with Activin A and their maintenance on Alvetex® inserts

Figure 6.19: Maintenance of embryoid bodies differentiated towards ectodermal lineages as tissue discs on Alvetex® Polaris for 14 days

Figure 6.20: Assessment of 14 day ectodermal tissue disc differentiation and structure identity via immunostaining for germ layer markers

Figure 6.21: Maintenance of embryoid bodies differentiated towards mesodermal lineages as tissue discs on Alvetex® Polaris for 14 days

Figure 6.22: Assessment of 14 day mesodermal tissue disc differentiation and structure identity via immunostaining for germ layer markers

Figure 6.23: Maintenance of embryoid bodies differentiated towards endodermal lineages as tissue discs on Alvetex® Polaris for 14 days

Figure 6.24: Assessment of 14 day endodermal tissue disc differentiation and structure identity via immunostaining for germ layer markers

Figure 6.25: Assessment of gene expression in 14 day germ layer differentiated tissues discs

Figure 6.26: Assessment of gene expression in 14 day germ layer differentiated tissues discs

Figure 6.27: Assessment of protein expression in 14 day germ layer differentiated tissues discs

Figure 6.28: Maintenance of embryoid bodies differentiated towards ectodermal lineages as tissue discs on Alvetex® Polaris for 28 days

Figure 6.29: Assessment of 28 day ectodermal tissue disc differentiation and structure identity via immunostaining for germ layer markers

Figure 6.30: Maintenance of embryoid bodies differentiated towards mesodermal lineages as tissue discs on Alvetex® Polaris for 28 days

Figure 6.31: Assessment of 28 day mesodermal tissue disc differentiation and structure identity via immunostaining for germ layer markers

Figure 6.32: Maintenance of embryoid bodies differentiated towards endodermal lineages as tissue discs on Alvetex® Polaris for 28 days

Figure 6.33: Assessment of 28 day endodermal tissue disc differentiation and structure identity via immunostaining for germ layer markers

Figure 6.34: Assessment of gene expression in 28 day germ layer differentiated tissues discs

Figure 6.35: Assessment of protein expression in 28 day germ layer differentiated tissues discs

Figure 6.36: SB431542 treated embryoid bodies cultured as tissue discs on Alvetex® Polaris for 14 days

Figure 6.37: BMP-4 treated embryoid bodies cultured as tissue discs on Alvetex® Polaris for 14 days

Figure 6.38: SB431542 and BMP-4 treated embryoid bodies cultured as tissue discs on Alvetex® Polaris for 14 days

Figure 6.39: Assessment of gene expression in 14 day ectoderm differentiated tissues discs

Figure 6.40: Assessment of gene expression in 14 day ectoderm differentiated tissues discs

Figure 6.41: Assessment of protein expression in 14 day ectoderm differentiated tissues discs

Figure 6.42: SB431542 treated embryoid bodies cultured as tissue discs on Alvetex® Polaris for 28 days

Figure 6.43: BMP-4 treated embryoid bodies cultured as tissue discs on Alvetex® Polaris for 28 days

Figure 6.44: SB431542 and BMP-4 treated embryoid bodies cultured as tissue discs on Alvetex® Polaris for 28 days

Figure 6.45: Assessment of gene expression in 28 day ectoderm differentiated tissues discs

Figure 6.46: Assessment of gene expression in 28 day ectoderm differentiated tissues discs

Figure 6.47: Assessment of protein expression in 28 day ectoderm differentiated tissues discs

Figure 6.48: SCID Mouse Fibroblast growth curve in DMEM and GMEM

Figure 6.49: Structure and viability of SCID dermal equivalents cultured in stem cell media

Figure 6.50: CGR8 tissue discs cultured on SCID dermal equivalents for 14 days

Figure 6.51: CGR8 tissue discs cultured on SCID dermal equivalents for 21 days

Figure 6.52: CGR8 tissue discs cultured on SCID dermal equivalents for 28 days

Figure 6.53: CGR8 tissue discs cultured on HDFn dermal equivalents for 28 days

Figure 6.54: CGR8 tissue discs cultured with SCID fibroblast conditioned media or on fixed fibroblast populated scaffolds for up to 28 days

Figure 6.55: Complex structure formation following 56 days of perfusion culture of CGR8 cells

Figure 6.56: Complex structure formation throughout the tissue disc structure of 56 day CGR8 derived tissue disc

Figure 6.57: Multiple CGR8 derived tissue discs show the formation of complex, mature structures following 56 day perfusion

Figure 6.58: Identification of germ layer structures following 56 days of perfusion culture of CGR8 cells

Figure 6.59: Identification of germ layer structures following 56 days of static control culture of CGR8 cells

Figure 6.60: Identification of germ layer structures following 56 days of static control culture of CGR8 cells

Figure 6.61: Variability in tissue disc structure formation following differentiation towards specific germ layers

7. Further validation and application of the in vitro tissue disc model using the teratoma assay and human pluripotent stem cell populations

Figure 7.1: Histological and immunofluorescent characterisation of H9 teratomas using various tissue stains

Figure 7.2: OECD guidelines for the Testing of Chemicals

Figure 7.3: Characterisation of TERA2.cl.SP12 teratomas

Figure 7.4: TERA2.cl.SP12 tissue discs formed from the same cell suspension show successful tissue disc formation after 14 days on the scaffold

Figure 7.5: TERA2.cl.SP12 tissue discs formed from the same cell suspension show successful tissue disc formation with complex structures after 28 days on the scaffold

Figure 7.6: Analysis of TERA2.cl.SP12 tissue discs cultured for 42 days on the scaffold

Figure 7.7: Histological characterisation of CGR8 teratomas using H&E

Figure 7.8: Histological characterisation of CGR8 teratma using Masson's trichrome

Figure 7.9: Histological characterisation of CGR8 teratoma using Weighert's stain

Figure 7.10: Immunofluorescent staining of CGR8 teratoma samples from markers from the three germ layers

Figure 7.11: Histological analysis of CGR8 tissue disc samples cultured for 14 days using H&E staining

Figure 7.12: Immunofluorescent staining of 14 day CGR8 tissue discs for markers from the three germ layers

Figure 7.13: Histological analysis of CGR8 tissue disc samples cultured for 28 days using H&E staining

Figure 7.14: Immunofluorescent staining of 28 day CGR8 tissue discs for markers from the three germ layers

Figure 7.15: Histological analysis of CGR8 tissue disc samples cultured for 42 days using H&E staining

Figure 7.16: Immunofluorescent staining of 42 day CGR8 tissue discs for markers from the three germ layers

Figure 7.17: Histological analysis of CGR8 tissue disc samples cultured for 56 days using H&E staining

Figure 7.18: Immunofluorescent staining of 56 day CGR8 tissue discs for markers from the three germ layers

Figure 7.19: Characterisation of human induced pluripotent stem cell line H9

Figure 7.20: Histological analysis of H9 stem cell derived tissue discs cultured for up to 28 days

Figure 7.21: Characterisation of human induced pluripotent stem cell line I18002

Figure 7.22: Histological analysis of I18002 stem cell derived tissue discs cultured for up to 28 days

8. General Discussion

Figure 8.1: Overview of the studies conducted in this project

Figure 8.2: Comparing the use of the teratoma assay and the *in vitro* model to assess developmental potency

Appendices

Figure 10.1: Primer optimisation for cytokeratin 10

Figure 10.2: Primer optimisation for cytokeratin 14

Figure 10.3: Primer optimisation for Class III β-tubulin

Figure 10.4: Primer optimisation for E-cadherin

Figure 10.5: Primer optimisation for Brachyury

Figure 10.6: Primer optimisation for Alphafetoprotein

Figure 10.7: Primer optimisation for FOXA2

Figure 10.8: Primer optimisation for GATA6

Figure 10.9: Primer optimisation for SOX17

Figure 10.10: Primer optimisation for GAPDH

List of Tables

Table 1.1: Primary germ layers and the organs and tissues derived from each

Table 1.2: Aggregation based techniques used to achieve three dimensional cell interactions

Table 1.3: Examples of common methods used to create solid scaffolds for cell culture

Table 2.1: Morphogens used to direct the differentiation of TERA2.cl.SP12 aggregates

Table 2.2: Morphogens used to direct the differentiation of CGR8 embryoid bodies during culture

Table 2.3: Colouration of structures as stained by Masson's Trichrome protocol

Table 2.4: Colouration of structures as stained by Weighert's staining protocol

Table 2.5: Colouration of structures as stained by Periodic Acid Schiff with Alcian Blue stain

Table 2.6: Primary antibodies used for immunofluorescent staining

Table 2.7: Secondary antibodies used for immunofluorescent staining

Table 2.8: Primary antibodies used for flow cytometry analysis

Table 2.9: Secondary antibodies used for flow cytometry analysis

Table 2.10: Primary antibodies used for Western Blotting analysis

Table 2.11: Secondary antibodies conjugated to horseradish peroxidase used for Western Blotting

Table 2.12: Primer sequences used for PCR analysis of gene expression

Table 2.13: Reagents used to create stock solution of primers

Table 2.14: SYBR reaction mix reagent volumes

Table 4.1: Void and pore sizes of the three formats of Alvetex®

Table 4.2: Summary of results from EB cell densities studies and impact on optimisation decisions

Table 4.3: Three formats of Alvetex® and its structural features

Table 4.4. Decay times of the Pt[dpyb]Cl compound in various areas within TERA2.cl.SP12 EBs and tissue discs

Table 5.1: Summary of results from co-culture studies

Table 6.1. Examples of histology and expression profile of tissues derived from the ectoderm

Table 6.2. Examples of histology and expression profile of tissues derived from the mesoderm

Table 6.3. Examples of histology and expression profile of tissues derived from the mesoderm

Table 6.4. Examples of histology and expression profile of tissues derived from the mesoderm

Table 6.5. Examples of histology and expression profile of tissues derived from the endoderm

Table 6.6. Examples of histology and expression profile of tissues derived from the endoderm

Table 6.7: Morphogens used for simple directed differentiation and final concentrations

Table 6.8: Morphogen combinations used to differentiate the embryoid bodies towards each germ layer and final concentrations

Table 6.9: Morphogen concentrations used to differentiate the embryoid bodies towards specific ectodermal lineages

Table 7.1. Current examples of human PSC based embryonic toxicity testing methods

Table 10.1. Recipes for making polyacrylymide gels

Table 10.2. Mouse identification data and assay end dates

Abbreviations

2D	Two dimensional
3D	Three dimensional
ATRA	All-Trans Retinoic Acid
bFGF	Basic Fibroblast growth factor
BMP-2	Bone Morphogenetic Protein 2
BMP-4	Bone Morphogenetic Protein 4
CK8	Cytokeratin 8
CK10	Cytokeratin 10
CK14	Cytokeratin 14
DMEM	Dulbecco's Modified Eagle's Medium
DMSO	Dimethyl sulfoxide
DNA	Deoxyribose nucleic acid
dH_2O	Demineralised water
EB	Embryoid body
EC23	Synthetic analogue to ATRA
EC cell	Embryonal Carcinoma cell
ECM	Extracellular Matrix
ES cell	Embryonic Stem cell
FBS	Foetal Bovine Serum
GMEM	Glasgow Minimum Essential Medium
HDFn	Neonatal Human Dermal Fibroblasts
HIPE	High Internal Phase Emulsion
ICM	Inner Cell Mass
ISCBI	International Stem Cell Banking Initiative
ISCI	International Stem Cell Initiative
iPS cell	Induced Pluripotent Stem cell
LIF	Leukaemia Inhibitory Factor
MSC	Mesenchymal Stem Cell
OECD	Organisation for Economic Co-operation and Development
PAGE	Polyacrylamide Gel Electrophoresis
PBS	Phosphate Buffered Saline
PFA	Paraformaldehyde
PSCs	Pluripotent Stem Cells
PTFE	Polytetrafluoroethylene
qFBS	Pluripotent Stem Cell Qualified Foetal Bovine Serum
qPCR	Quantitative Polymerase Chain Reaction
RA	Retinoic Acid
RNA	Ribose Nucleic Acid
SCID	Severe Combined Immunodeficient
SSEA-1	Stage specific embryonic antigen 1

SSEA-3	Stage specific embryonic antigen 3
SSEA-4	Stage specific embryonic antigen 4
TE	Trophoectoderm
TUNEL assay	Terminal deoxynucleotidyl transferase dUTP nick end labelling assay

1.1 Introduction

Human developmental processes have long fascinated society. For centuries, scientists, artists and philosophers including Aristotle, Da Vinci and Darwin have explored the meaning, and more importantly, sought to understand the biological events involved in this unique human process.

For many years the most reliable and only method which allowed for the study human development remained direct observation and experimentation of embryonic processes, both human and proxy studies using various model organisms. While these are informative and relevant, they are fraught with ethical issues, and in the case of animal studies, underlying assumptions regarding the similarity of developmental processes between human and other species.

The derivations of human embryonic stem cells and later induced pluripotent stem cells were heralded as a key moments in scientific history. These sources of pluripotent stem cells would provide ample opportunity for the study of events involved in human tissue development in a more controlled, reproducible and large scale manner. A wide range of molecular events and signalling pathways have been elucidated using a wide range of techniques, yet many aspects of the developmental process remain poorly characterised. In particular, events involved in mature tissue formation are understudied, which remains due to the limitations of the various methods used to study human development.

Recent advances and improvements in cell culture practices, including a shift towards the use of more relevant and physiological culture systems, provide a range of novel options to now attempt to solve these issues. The refinement of three dimensional cell culture technologies, such as hydrogels, spheroid type cultures and solid scaffolds means that these technologies can now be applied to the maintenance and differentiation of pluripotent stem cell populations. Combining these techniques can result in even more complex differentiation in *in vitro* systems, a phenomenon which has the potential to be applied to the study of human tissue development, as well as the related field of cellular pluripotency.

In this thesis, the stepwise development of a novel three dimensional model using a solid scaffold based technology and pluripotent stem cells will be described. A thorough review of the literature is first conducted covering a number of areas relevant to the project. The series of events involved in early embryogenesis, including the impact of morphogens and the differentiation of complex tissues from the three germ layers is described, as are the properties of the different human pluripotent stem cell populations currently available to researchers. Advanced cell culture methods are briefly covered, as are the current models used to study the process of human tissue development and the rationale for a new model of human tissue development is discussed.

Each Results Chapter is preceded by a detailed review of the literature pertaining to the specific topics and culture methods explored within the Chapter. Chapter 3 covers a review of registered human pluripotent stem cell lines, and their characterisation data, focussing in detail on the use and

parameters of the teratoma assays conducted. This is with the aim of identifying trends in these assays for potential standardisation and in order to direct and inform the following *in vitro* work. In Chapter 4, the human embryonal carcinoma cell line TERA2.cl.SP12 is used to optimise an *in vitro* tissue disc model, by investigating the effects of altering aspects of the microenvironment, including cell seeding density, scaffold topography and the addition of morphogens. The introduction of more physiological properties to the model, co-culture and perfusion, is explored in Chapter 5. These properties are optimised in this chapter, with the aim of enhancing the differentiation of the tissue discs formed, again using the human embryonal carcinoma cell line, TERA2.cl.SP12. Chapter 6 uses a murine embryonic stem cell line, CGR8, in the model in order to better explore the differentiation which can be achieved and begin to model the events of mammalian tissue differentiation. The differentiation of the tissue discs is directed using a variety of morphogens to achieve germ layer specific structure formation. The optimised physiological properties are also applied to the system and the effects of these on the differentiation phenotype assessed. Chapter 7 aims to validate the model optimised in the previous Chapters against a teratoma assay, as well undertaking pilot studies using human pluripotent stem cell lines, both human embryonic stem cell lines and induced pluripotent stem cell lines, within the model. The impact of the results obtained and their applications are considered within the General Discussion, as well as the variety of Future Directions that could be taken following this project.

1.2 Project Background

1.2.1 Mammalian embryonic development

Embryonic development is a highly complex process, during which the single cell formed at the initiation of the process undergoes an intricate, tightly controlled series of proliferations, migrations and progressive specialisations that eventually result in the complete organism, producing all somatic lineages and germline cells. It is a fundamental process to living organisms, and one which warrants close study.

1.2.1.1 Preimplantation events of early embryogenesis

Embryogenesis begins with the fertilisation event, at which the male and female gametes meet. Cellular and nuclear fusion follow, as the separate oocyte and sperm form a single totipotent zygote, a cell of around 100 µm diameter (Gilbert, 2000). This cell represents a genetically unique entity, and has the greatest differentiation potential, with the ability to form all of the extraembryonic tissues, as well as those within the embryo proper. The lifespan of the zygote as a single cell is short lived, as the cell proceeds to the cleavage stage, undergoing a number of cell divisions every 12-24 hours to increase cell number, over the first 3 days. At the 12 cell stage, the entity is termed a morula. The cells remain genetically, phenotypically and transcriptionally similar up until this point, with each retaining the ability to form both the embryonic and extraembryonic lineages (Niakan et al., 2012). Following this, on around day 4, cells undergo compaction (see Figure 1.1), during which the cells increase their intercellular contacts through changes in gap junctions and tight junctions, redistribute surface microvilli and show cytoplasmic polarisation (Iwata et al., 2014; Rossant and Tam, 2009).

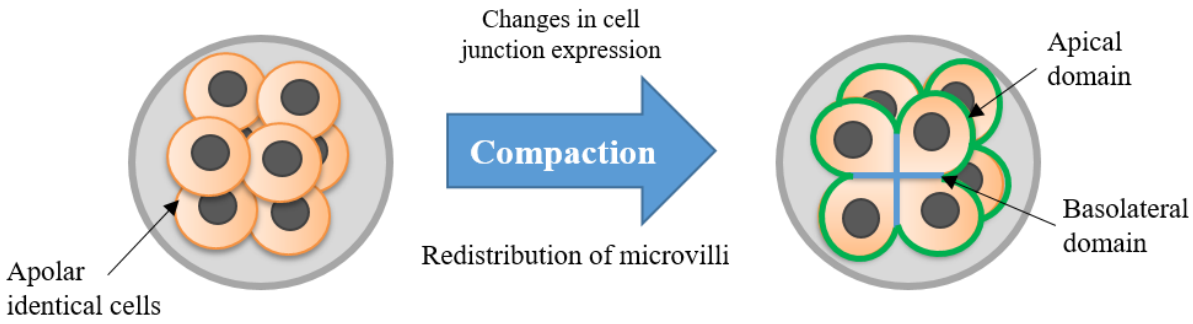


Figure 1.1: Compaction of the early mammalian embryo: A series of subtle changes in the distribution of tight junctions and gap junctions, as well as the redistribution of microvilli to the apical surface, results in the polarisation of the cells within the early embryo. Adapted from Rossant and Tam 2009.

Cells then proceed to segregate into two distinct groups while still undergoing division, each of which will form a distinct population of cells: the trophoblast cells are located on the outer edge of the

structure, and will form the trophoectoderm (TE), whereas the remaining cells inside the will form the inner cell mass (ICM) (Niakan et al., 2012). This is the first lineage decision which occurs in the developing embryo, and is required for attachment and implantation to occur successfully.

1.2.1.2 Blastocyst formation

As a result of cellular segregation, the trophoblast cells subsequently begin to secrete fluid into the centre of the solid cell mass, resulting in the process of cavitation. As the cells of the ICM migrate and position at one end of the morula, this forms an asymmetrical structure composed of trophoblast cells surrounding a newly formed blastocoel at one end, a fluid filled cavity, and the cells of the ICM at the opposite end (see Figure 1.2) (Gilbert, 2000; Tam and Behringer, 1997). This structure is the blastocyst. The blastocyst continues to increase in size due to active ion importation into the blastocoel by the trophoblast cells and subsequent osmosis (Sathananthan et al., 2003). The events described up to this point take place within the oviduct as the developing embryo travels towards the uterus in order to undergo the next crucial event in the developmental cascade: implantation.

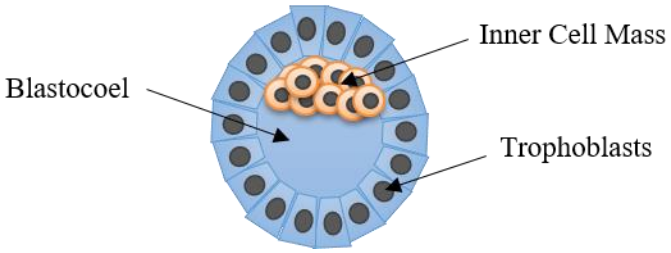


Figure 1.2: Structure of the mammalian blastocyst: The blastocyst is an asymmetrical structure composed of two cell populations: an Inner Cell Mass and the fluid filled blastocoel cavity surrounded by a layer of trophoblast cells.

1.2.1.3 Implantation

Prior to the fertilisation event, the ovum is surrounded by the zona pellucida, a thick glycoprotein extracellular matrix, which initially protects the ovum (Nichols and Smith, 2012) and prevents multiple fertilisation events occurring (Gilbert, 2000). After fertilisation has occurred, this proteinaceous substance prevents ectopic implantation into non uterine sites, such as the fallopian tube. On reaching the uterus, zona hatching occurs in order for implantation to take place successfully. This usually takes place around 6 days after fertilisation; successful implantation is crucial in order for the embryo to develop further (Niakan et al., 2012), and is dependent on a 'competent embryo and receptive endometrium' and their ability to communicate in order to orchestrate the event (Weimar et al., 2013). The combination of mechanical pressure from the increasing blastocyst size and the secretion of proteolytic enzymes causes hatching, after which the blastocyst is able to come into direct contact with the endometrium, the uterine epithelium, and attach

to the complex extracellular matrix of the uterus, which in humans usually occurs at around day 7 (Niakan et al., 2012). Trophoblast cells secure attachment in conjunction with the endometrium and continue to communicate with the diverse cell populations of the endometrium as seen in Figure 1.3, allowing for the eventual full implantation of the blastocyst into the uterine wall.

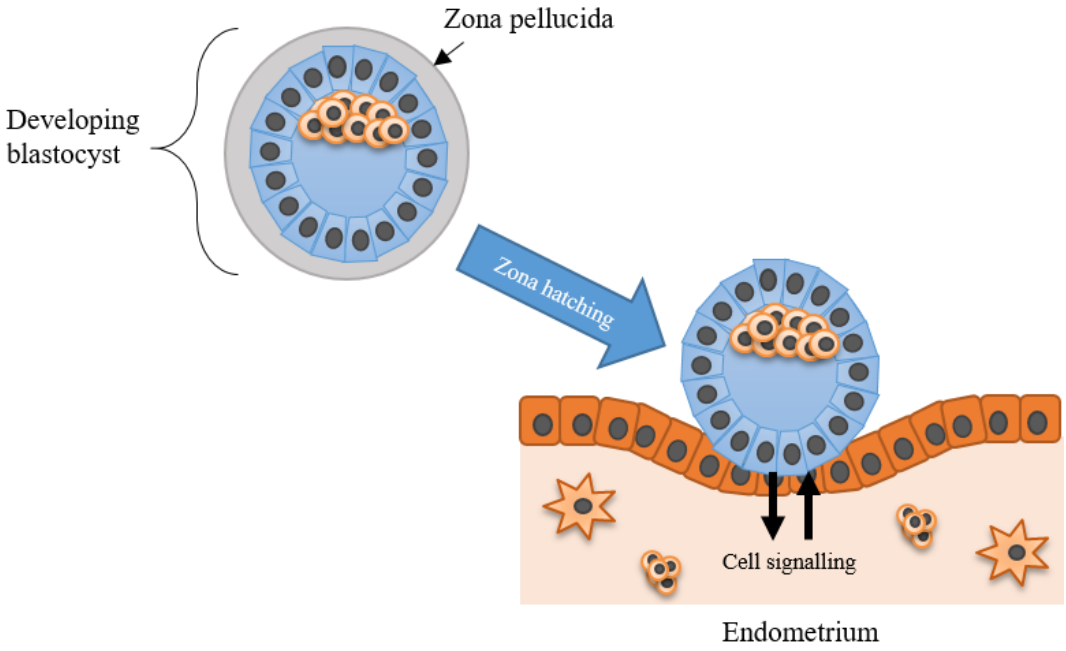


Figure 1.3: Processes of Zona hatching and implantation: The developing blastocyst must hatch from the thick extracellular matrix surrounding it in order to be able to come into contact with the endometrium and securely implant in the uterus. Both of these steps are crucial to the progression of the blastocyst into the next stages of the developmental cascade.

1.2.1.4 Gastrulation

Further lineage decision events are now required for embryonic development to continue. Cells segregate to form the hypoblast, also known as the primitive endoderm, within the ICM and migrate to line the blastocoel cavity. These hypoblast cells will later form the extraembryonic yolk sac, which is part of the extraembryonic endoderm, supporting the embryo through nutrient transfer and eventually forming part of the placenta (Freyer and Renfree, 2009). The cells left within the ICM are now the epiblast, which will further segregate into cells which form the embryo proper. The epiblast cells then proceed to a series of migrations which lead to the formation of the primitive streak and the eventual formation of the gastrula, which is normally around 14 days after fertilisation. This process of gastrulation is the point at which embryo formation begins and germ layer specification occurs, each of which, ectoderm, mesoderm and endoderm, is responsible for the formation of specific organs and body structures (Tam and Behringer, 1997) (see Figure 1.4 for brief schematic). Initially, the epiblast forms a bilaterally symmetrical disc known as the primitive streak, which will guide the gastrulation process. Mesenchymal cells arrange along the potential midline of the structure, which elongates and undergoes a symmetry breaking event, creating the anterior and

posterior axis of the developing organism. Mesodermal and endodermal progenitors then migrate towards the newly formed primitive groove in the centre of the primitive streak, before migrating into this structure, as seen in Figure 1.4. This results in the formation of a trilayer disc of the three germ layers, which is organised according to the eventual body plan: endoderm is the innermost layer, followed by mesoderm, and the ectoderm is the outermost layer. Now that the progenitor populations are spatially arranged, organogenesis can take place.

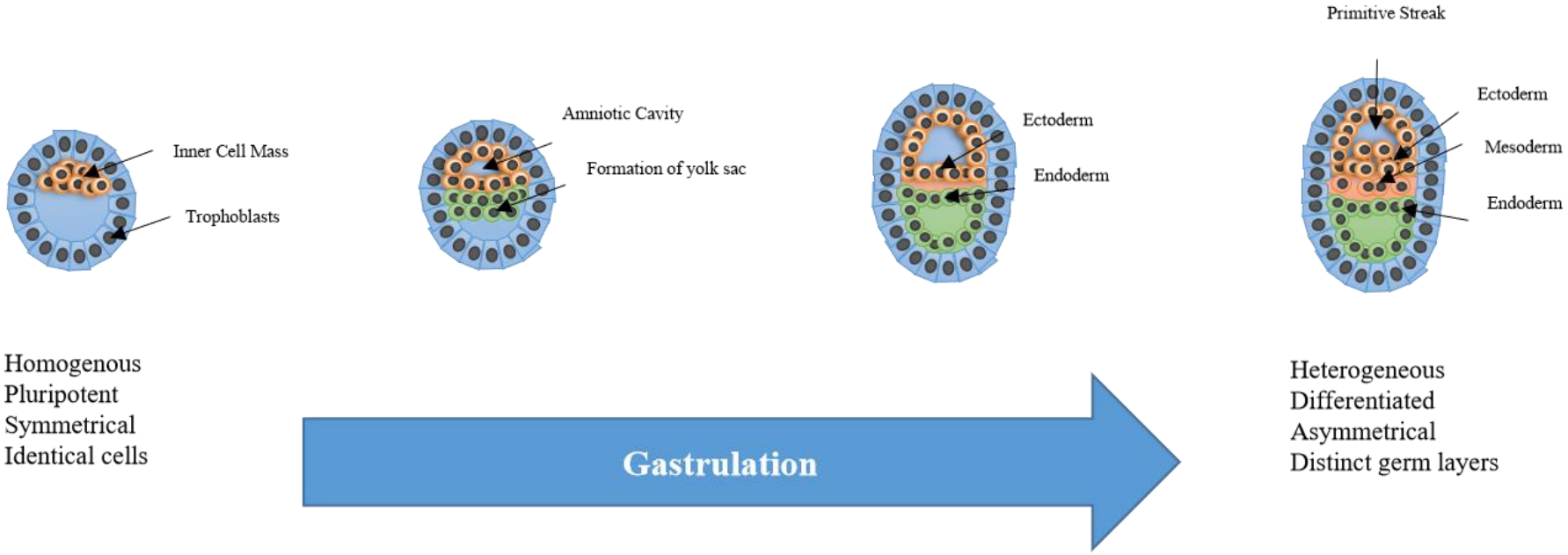


Figure 1.4: Schematic of the mammalian gastrulation process: Gastrulation takes place around 14 days after the fertilisation event, and is a key event in the developmental cascade. The blastocyst, which is formed of an outer layer of trophoblast cells and a homogenous pluripotent Inner Cell Mass, undergoes a series of complex cellular migrations resulting in the formation of a trilayer disc, which serves as an indicator of the organism's body plan. Key support structures such as the yolk sac begin to form, and the pluripotent stem cells of the Inner Cell Mass undergo lineage segregation.

1.2.1.5 Organogenesis

Organogenesis is the process by which progenitor cells within each germ layer form the mature organs through a series of differentiation and specialisation events. This is in response to a variety of extracellular signals, which are both chemical and physical in nature. Spatiotemporal control is a key aspect of this process, whereby signals are delivered to specific locations at a specific time in a continuous and cohesive process. While each germ layer is separately responsible for the formation of specific organ structures (see Table 1.1), signalling from each germ layer is crucial to the differentiation processes occurring in other germ layers and to ensure correct spatial organisation and orientation (Grapin-Botton and Melton, 2000; Tam and Behringer, 1997). This is achieved through the formation of morphogen gradients across the organism, resulting in differential differentiation of cells within tissue structures and organs.

Table 1.1. Primary germ layers and the organs and tissues derived from each

Germ Layer	**Organs, structures and cell populations derived from this germ layer**
Ectoderm	Skin, specifically the epidermis All neural tissues – central and peripheral nervous systems, and associated sensory cells
Mesoderm	Connective tissues All skeletal bone and cartilage Smooth and skeletal muscle tissues Haematopoetic tissues Kidneys
Endoderm	Gastrointestinal tract Respiratory system Urinary tract Endocrine glands including the pancreas

A classic example of these complex interactions is the retinoid pathway. The retinoid pathway is a key developmental signalling pathway which has been well characterised and studied, having a wide range of roles during the developmental process. Retinoic acid (RA) performs its main functions in the nucleus, binding to specific receptor proteins and influencing gene expression through the recruitment of transcriptional activators, as seen in Figure 1.5 (Rhinn and Dollé, 2012).

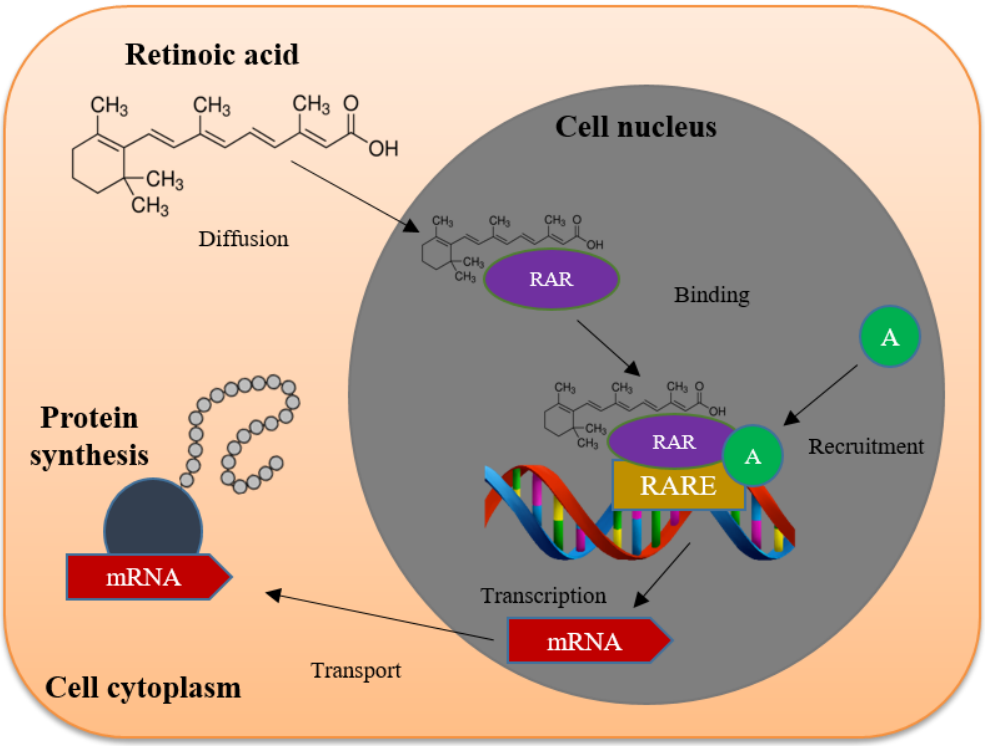


Figure 1.5: The retinoic acid signalling pathway: Retinoic acid is a Vitamin A derived compound which has a number of essential and well established roles within the developing embryo and the adult human. It controls the fate of a number of cell populations, and acts on cells in a concentration dependent manner. Retinoic acid binds to specific nuclear receptor proteins (RARs/RXRs), which bind DNA motifs (RAREs) and recruit transcriptional activators (A) to alter gene expression.

In the developing organism, retinoic acid is responsible for the formation and patterning of a number of organs. The organisation and patterning of the hindbrain into separate neuroepithelial compartments is influenced by retinoic acid signalling from the adjacent somitic mesoderm; the formation of a gradient of retinoic acid results in differential gene expression, with Hox gene in particular involved in the process (Kiecker and Lumsden, 2005). RA signalling is also involved in the formation of branchial arches from the endoderm, structures which lead to the formation of a variety of tissues including the thyroid and thymus; again, the RA synthesis is localised to this area. It is known to have functions in the formation and elongation of the neural tube and associated somites in combination with a Wnt/FGF gradient (Aulehla and Pourquié, 2010). The involvement of RA in limb bud patterning has also been extensively studied, although the effects of RA are indirect, as the molecule regulates a number of downstream cascades, such as sonic hedgehog and FGF signalling (Cunningham and Duester, 2015). Additional roles include involvement in eye formation, liver and heart development and spermatogenesis. The retinoic acid pathway is only one example of a signalling pathway from the developmental process, but it is representative due to the complex nature of its effects in combination with other morphogens on the developing organism.

1.2.2 Pluripotent stem cells: a useful tool from the study of embryos

Pluripotent stem cells (PSCs) have revolutionised the field of stem cell biology and regenerative medicine, and are defined by their ability to self renew and form differentiated progeny. They provide an opportunity to study embryonic development closely and better understand the differentiation processes for clinical applications and regenerative medicine therapies.

1.2.2.1 Embryonal carcinoma cells

The first PSC line derived and successfully cultured *in vitro*, embryonal carcinoma (EC) cells are known to represent the undifferentiated malignant aspect of germ cell tumours and teratocarcinomas, as well as being the malignant counterpart to embryonic stem cells (Evans, 1981; Martin, 1980). Initially discovered in strain 129 mice showing an increased incidence of testicular tumours (Stevens and Little, 1954), following their isolation years later the self renewal properties of murine EC cells were elucidated through their retransplantation into various body sites and the successful formation of teratocarcinomas, with both differentiated and undifferentiated tumour compartments. Systematic analysis of their marker expression profile revealed concurrent expression of markers found on murine blastocysts (Artzt et al., 1973), confirming the relationship between EC cells and the pluripotent cell populations found in the blastocyst (Evans, 1981; Martin, 1980). The subsequent isolation of human EC cells in the 1970s confirmed their similarities to the human embryo, as well as highlighting the subtle differences in pluripotent stem cell phenotype and function and developmental processes between species (Henderson et al., 2002). This cell population is a useful tool for the study for a variety of developmental processes and the nature of pluripotency itself, with novel lines proving useful in specific applications including the process of neurogenesis (Przyborski, 2001) and cardiomyocyte formation (van der Heyden and Defize, 2003). Nevertheless, due to their malignant origin EC cells do have some limitations. EC cells are often limited in their differentiation capacity (Andrews et al., 2005), due to the accumulation of karyotypic abnormalities and the acquisition of survival promoting mutations as tumour stem cells (Mueller et al., 2006), an inherent part of their cancerous nature. These mutations may also interfere further with the stem cell phenotype, bringing into question whether the cells accurately represent a true PSC population.

1.2.2.2 Embryonic stem cells

In the same way as seen with EC cells, murine embryonic stem (ES) cells were isolated from the mouse blastocyst before cells were isolated from the human blastocyst. The term ‘embryonic stem cells’ was purportedly coined by Gail Martin when the murine cells were isolated (Martin, 1981): human ES cells were isolated almost 20 years after this, famously by Thomson et al (Thomson et al., 1998). Since the initial isolation of these populations, more efficient derivation processes have been

developed, leading to more widespread methods which do not result in embryonic destruction or wastage either by more efficient use of the cells within the blastocyst, or simply through improved technique (González et al., 2010; Hovatta et al., 2014; Zdravkovic et al., 2015). Naturally, these cells also share an expression profile with the early blastocyst, and as EC cells do, ES cells have been shown to fulfil the properties of pluripotency, both the ability to self renew and produce differentiated progeny derived from the three germ layers (Thomson et al., 1998). ES cells are defined specifically as cells derived from the ICM of the preimplantation blastocyst (Nichols and Smith, 2012), although embryonic stem cell populations have also been derived from the morula (Strelchenko et al., 2004) and the epiblast (Brons et al., 2007), with both representing subtly different states of pluripotency.

1.2.2.3 Induced pluripotent stem cell populations

Induced pluripotent stem (iPS) cell populations are the third, and most recently derived pluripotent stem cell population. The key difference in this cell population is their source of origin: EC and ES cells are derived from tumorigenic and embryonic populations respectively, whereas iPS cells may theoretically be derived from any somatic cell. A key set of genes associated with the pluripotent state, named Yamanaka factors (Oct 3/4, Sox 2, Klf4 and c-Myc) (Liu et al., 2008), are transfected into the selected population often via viral delivery, which results in cellular reprogramming and a return to the undifferentiated state, imbuing the cells with the ability to self renew and produce differentiated progeny again (Takahashi et al., 2007; Takahashi and Yamanaka, 2006). Of particular interest to the personalised medicine sector, the number of iPS cells derived has increased exponentially, with 693 new hPSC lines added to the registration site hPSC.reg alone in 2018.

Since the initial creation of iPS cell lines from adult fibroblasts using a lentiviral system (Takahashi et al 2007), a range of different delivery systems, including viral, non-viral, integrative and non integrative have been optimised and trialled, indicating variation in reprogramming success (Telpalo-Carpio et al., 2013). Additionally, iPS cells have now been successfully created from a range of somatic cell types, including fibroblasts (Takahashi et al., 2007), peripheral blood mononuclear cells (Kim et al., 2016) and umbilical card blood cells (Fernandes et al., 2017). iPS cell lines are also of interest for disease modelling, with the ability to create cell lines from patients with a range of disease statuses and aberrant genotypes. Conditions which already have iPS cell lines available include genetic mosaicism (Luo et al., 2018), type 1 diabetes (Maehr et al., 2009) and Parkinson's (Li et al., 2018). Research into a number of conditions has already yielded some small scale transplantation studies, with the first iPSC therapies being used to treat patients suffering from macular degeneration (Cyranoski, 2017) and clinical trials for the treatments of Parkinson's disease also ongoing (Cyranoski, 2018). However, therapies of this type are often delayed by low differentiation yields, the risks of dedifferentiation of transplanted cells and potential neoplasias.

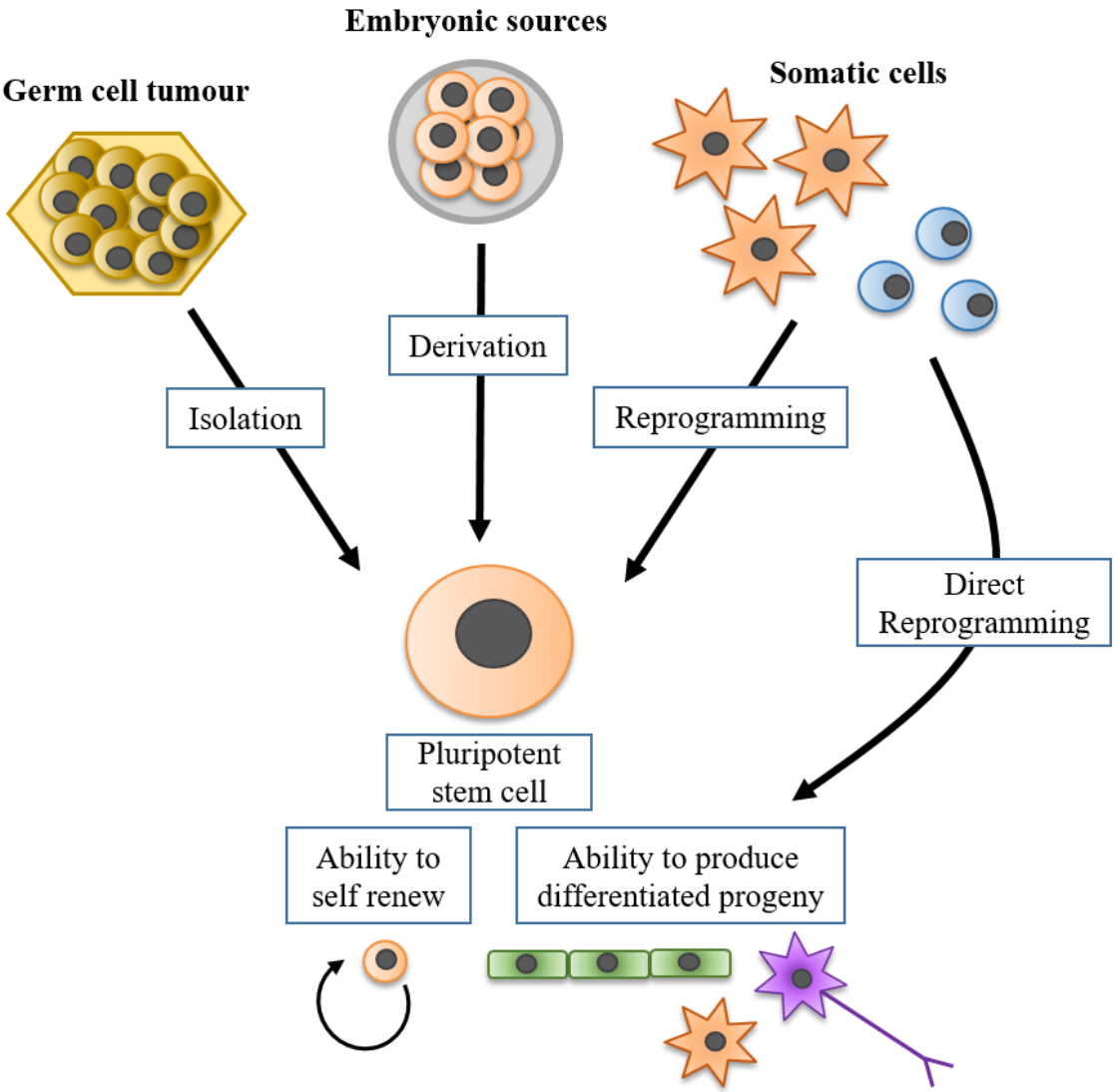


Figure 1.6: Various sources of pluripotent stem cells: While the three categories of pluripotent stem cell are derived from very different sources, each population displays the hallmarks of pluripotency: the ability to self renew and the ability to produce differentiated progeny from the three germ layers. Cells can also be directly reprogrammed towards a specific cell phenotype, bypassing the need to create a pluripotent population.

1.2.2.4 Assessment of pluripotency

The derivation of iPS cells and their potential use in regenerative medicine applications has further emphasised the need to fully characterise novel PS cell lines, in order to rigorously confirm their pluripotency. Currently, a range of methods and techniques can be used to assess the markers and functions associated with pluripotent stem cell populations. These include detection of specific transcription factors known to be involved in maintaining the pluripotent state, Oct 3/4, Sox 2 and Nanog; extracellular markers such as SSEA-4, TRA-1-60 and TRA-1-81 and enzymatic activity such as alkaline phosphatase (Asprer and Lakshmipathy, 2015), among others. These analyses only confirm the pluripotent state, which is not necessarily an indicator of differentiation capacity, also termed developmental potency. The expression of these pluripotency associated factors singly does

not necessarily correlate with the expression of other pluripotency associated markers (Cahan and Daley, 2013), nor does it indicate a capacity to differentiate (Palmqvist et al., 2005). As such, differentiation based assays are also required to ascertain the developmental potential of novel pluripotent stem cell lines i.e. their ability to successfully form derivatives from the three germ layers. The variation between different human pluripotent stem cell populations, particularly in terms of their developmental potency, is acknowledged as an issue within the field. Heterogeneity of marker expression between pluripotent cell lines is also an acknowledged occurrence, but variation in differentiation capacity impacts on responses to differentiation protocols and the subsequent differentiated cell yield, a factor critical to regenerative medicine therapies. The sources of this variation are myriad, and may be as a result of genetic anomalies, environmental conditions or reprogramming methods used (Asprer and Lakshmipathy, 2015; Cahan and Daley, 2013; International Stem Cell Initiative et al., 2007; Ortmann and Vallier, 2017), and complex differentiation based assays are best suited to assessing this. While directed differentiation of PSCs using morphogens or the formation of embryoid bodies can provide some data as to the differentiation capabilities and developmental potency of a PSC population (see Figure 1.7), previously the teratoma assay has been considered to be the gold standard method to assess this property in human pluripotent stem cell populations (Buta et al., 2013; Müller et al., 2010a). More stringent germline experiments are an option available for the assessment of novel non-human pluripotent stem cell lines, such as germline transmission (Peng et al., 2014) or the tetraploid complementation assay (Nagy et al., 1993). The restrictions and ethical implications of forming animal-human chimeras (DeWitt, 2002; Hyun et al., 2007; Lensch et al., 2007) and the 14 day embryo rule prevent these type of studies being used for the assessment of the developmental potency of human PSCs.

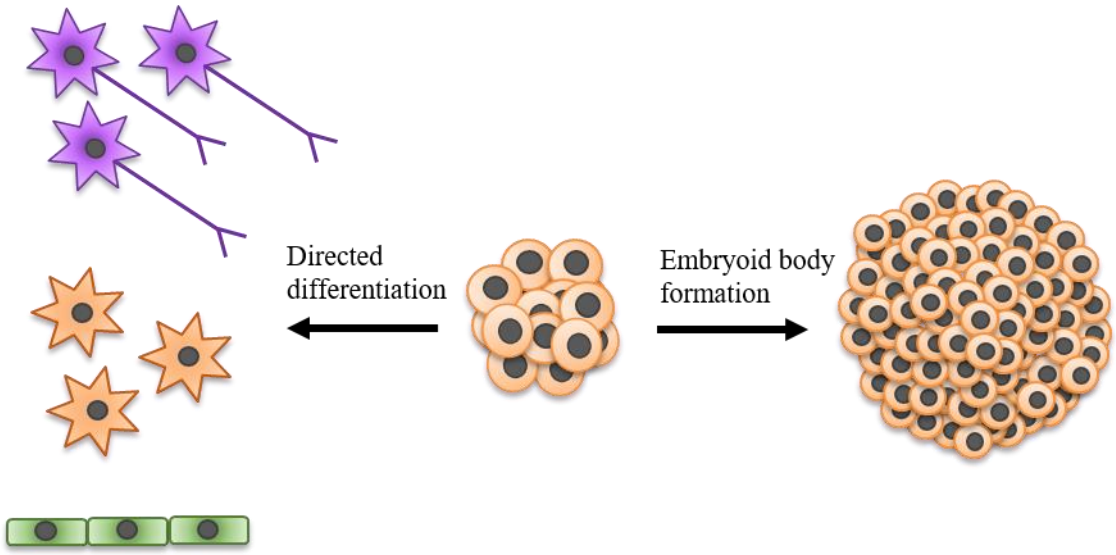


Figure 1.7: *In vitro* methods of assessing developmental potency: PSCs can be treated with exogenous morphogens to direct their differentiation towards specific cell lineages as a way to confirm the developmental potency of a cell line. The formation of embryoid bodies can also be used to assess this property, as these structures recapitulate some aspects of early development.

A general teratoma assay protocol involves the implantation of the putative pluripotent stem cell population into an immunodeficient mouse host, and the subsequent formation of a differentiated tumour, see Figure 1.8. The presence of structures from the three germ layers is considered as confirmatory of pluripotency, although it is well recognised in the stem cell biology field that the assay has limitations, and requires standardisation or replacement (Bouma et al., 2017; Buta et al., 2013; Gropp et al., 2012; Masuda et al., 2012; Müller et al., 2010a). Of particular concern is the variation in protocols, many of the parameters of which have been shown to affect the differentiation trajectories of the PSC population being analysed, including the histocompatibility and immune status of the mouse host (Dressel, 2011), initial cell seeding number (Lee et al., 2009), anatomical site of implantation and inclusion of other reagents such as Matrigel (Prokhorova et al., 2009).

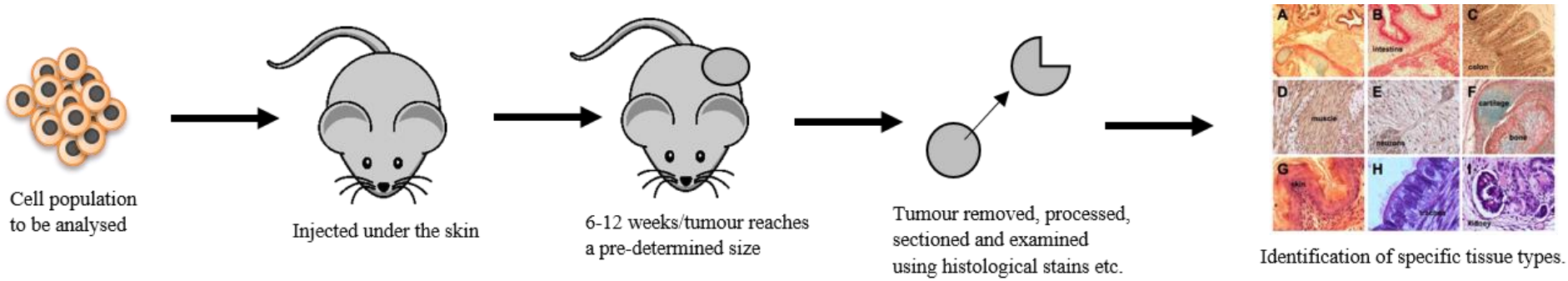


Figure 1.8: Schematic of a general teratoma assay: Putative pluripotent stem cells are injected under the skin of an immunodeficient mouse host, and left to form a teratoma. Once a defined tumour size has been reached or time period has passed, the tumour is excised from the mouse and examined histologically for the presence of complex structures from the three germ layers as confirmation of developmental potency.

1.2.3 Advanced cell culture technologies for the improvement of the cellular microenvironment

Cell culture techniques have changed markedly since the establishment of routine cell culture practices in the 1950s, with the introduction of more defined culture systems and culture environments which introduce additional elements that make them more closely aligned with sources of cellular origin or intended anatomical locations following differentiation. Even since the derivation of human pluripotent stem cells in the 1990s, culture options have become more wide ranging as the need for a complex tailored microenvironment which takes into account the myriad chemical and physical cues cells are exposed to (see Figure 1.9) is required to enhance cellular structure, and therefore function, is acknowledged (Baker and Chen, 2012; Cukierman et al., 2002). These concepts are particularly important for downstream applications, such as regenerative medicine therapies, where physiological cellular function is essential for a successful treatment outcome.

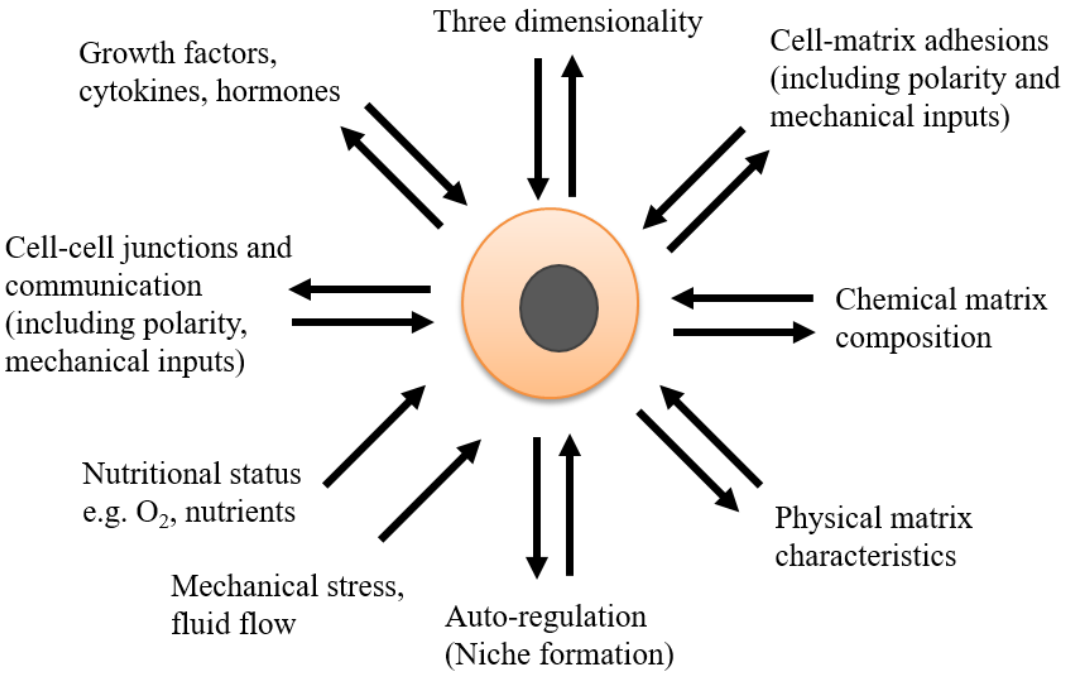


Figure 1.9: Microenvironmental cues which impact on cell structure and function: A wide variety of physical and chemical cues influence the cell affecting its structure and therefore function; in the case of pluripotent stem cells, this impacts on pluripotency and differentiation trajectory. Adapted from Yamada and Cukierman, 2007.

1.2.3.1 Traditional 'two dimensional' cell culture techniques

Traditional cell culture techniques have routinely relied on the culture of cell populations on flat surfaces, previously glassware but more recently plasticware. While culture methods such as these are homogenous, inexpensive and simple to undertake, they expose cells to a number of abnormal microenviromental stimuli (Baker and Chen, 2012), which results in the adoption of a non physiological structure and therefore impacts on cell function, as shown in Figure 1.10.

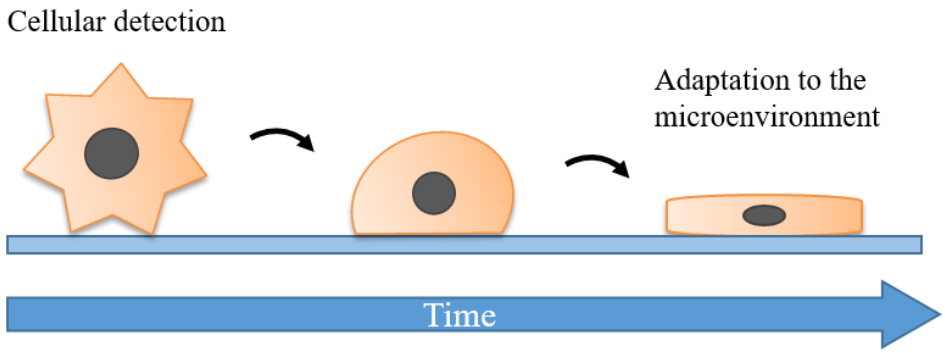


Figure 1.10: Adaptation of cells to the external microenviroment: Cells which are transferred to the *in vitro* environment from *in vivo* adapt to their new microenvironment, which results in changes to cell and nuclear shape. This new morphology is very different from that adopted *in vivo*, and impacts significantly on cell function.

These cues and stimuli include exposure to a non physiological material which has properties far removed from the original source of the cells and is spatially very different, as well as lacking in complexity, dynamics and heterogeneity, as is highlighted in Figure 1.11. Exposure to these cues leads to an abnormal cellular orientation with an enforced polarisation in relation to the growth surface and reduced contact with adjacent cells. The combination of these abnormal stimuli and responses leads to the adoption of a flat, two dimensional cell structure, preventing cells from adopting a three dimensional morphology or forming complex tissue structures as would be found *in* vivo, ultimately impacting on cell function. Data gathered from *in vitro* experiments conducted in this way are not necessarily representative of cellular responses *in vivo*.

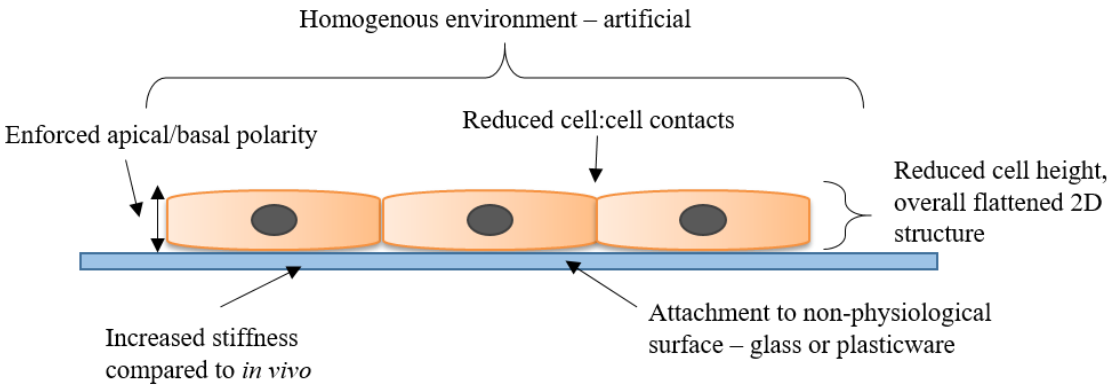


Figure 1.11: Phenotype and morphology of cells cultured in the traditional two dimensional environment: Cells cultured using traditional methods are exposed to a number of non physiological cues, which influence cell structure and ultimately, cell function. Adapted from Baker and Chen 2012

A number of studies have illustrated the impact of creating a cellular microenvironment which is phenotypically and structurally more representative of *in vivo* architecture, providing appropriate and complex cues which allow cells to adopt a more physiological structure and therefore improving cell function (Petersen et al., 1992), as seen in Figure 1.12. There has been a particular focus on the introduction of culture methods which allow cells to adopt a three dimensional structure; there are a number of different methods employed to do this, the uses of which are dependent on the requirements of the application and the cell population in use. Three dimensional culture systems are naturally highly employed in the regenerative medicine field for tissue engineering purposes, allowing for the creation of more physiologically relevant and functional tissue replacement therapies. These methods are also now heavily used to better understand the normal physiological function of human and animal organ systems, as well as creating more accurate predictive models for the drug validation process.

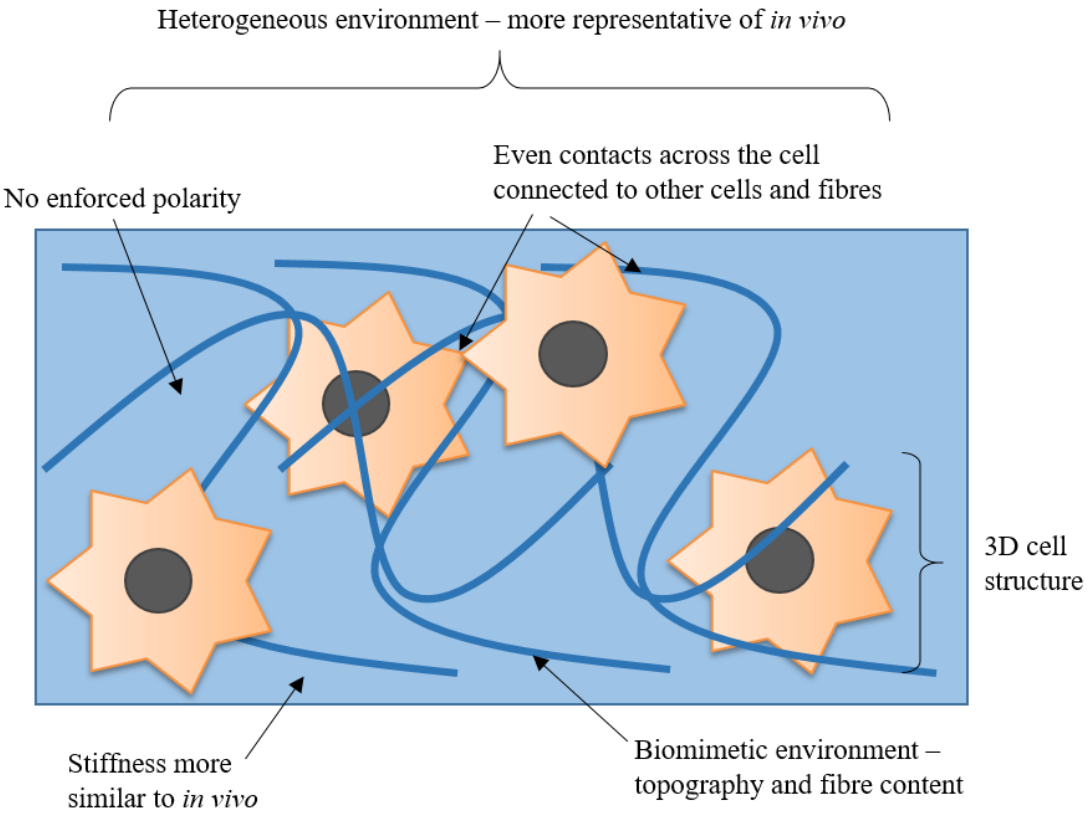


Figure 1.12: Phenotype and morphology of cells cultured using three dimensional culture techniques: Cells cultured in the three dimensional environment are exposed to very different cues, which are more physiologically relevant. Adapted from Baker and Chen 2012

1.2.3.2 Aggregation based techniques

Methods which focus on bringing cells into close contact in clumps or aggregates have long been used to assess the differentiation capacity of PSCs in the *in vitro* context (Martin et al., 1977). Aggregates, spheroids, embryoid bodies and organoid culture all rely on the same principle of

bringing cell populations into highly close contact to form a spherical structure which is self organising and synthesises its own extracellular matrix, resulting in a self dependent collection of cells which are arranged in a three dimensional space and functioning in an organised manner, in response to physical and chemical cues from the neighbouring cells (Meng et al., 2014).

The terminology used for the structure depends on the cell population and intended uses. Pluripotent stem cell derived structures are embryoid bodies (EBs) due to their morphological similarity to the early embryo and ability to recapitulate some of the events involved in the early embryogenesis process (Itskovitz-Eldor et al., 2000; Martin, 1980; Martin et al., 1977). Tumorigenic cells, often cancer cell lines, are generally aggregates or spheroids, and are increasingly popular in tumour biology studies due to their ability to mimic the tumour structure and local microenvironment, in particular the interactions with host cell populations, in a more physiological manner (Carlsson and Nederman, 1989). Organoid cultures also rely on the fundamental principles of this method – self organisation, ECM synthesis and close cellular interactions – but for the purpose of creating miniature functional organs *in vitro* using either organ specific stem cell populations or PSCs subject to complex morphogen directed differentiation protocols (Lancaster and Knoblich, 2014a). Initial successful work in this area was carried out using intestinal stem cells (Sato et al., 2009), and more recent studies using cerebral organoids in particular have shown that the structures share features with the developing brain, including maintenance of the neural plate progenitor population, correct direction of neural tract formation and a variety of neural and glial cell populations within the structure (Lancaster et al., 2013). Techniques used to create these different spherical structures are as diverse as the cell populations involved, and again, depend on the cell population and intended use, with each having its own merits and limitations (Kurosawa, 2007) (See Table 1.2 and Figure 1.13).

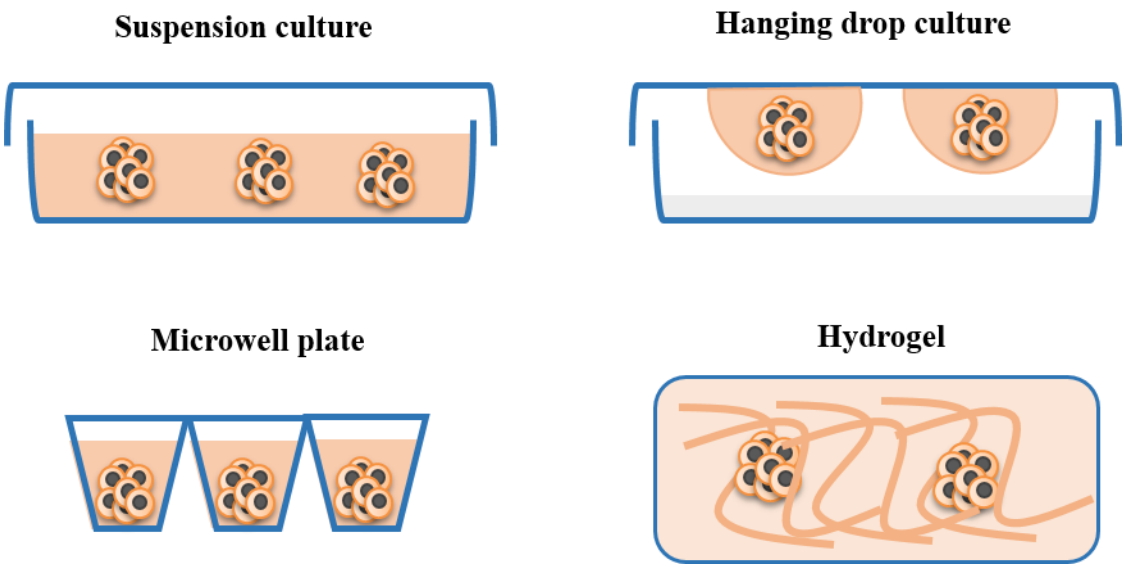


Figure 1.13: Techniques used to create cellular aggregates: Various methods can be used to create cellular aggregates, each relying on the same principle of bringing cells into very close contact to form self organising structures. The technique used depends on the cell type and intended downstream applications.

Table 1.2: Aggregation based techniques used to achieve three dimensional cell interactions

Technique	Outline	Merits	Limitations	References
Suspension culture	Cells seeded into a large volume of media in a low adherence vessel, such as a Petri dish, and allowed to aggregate naturally.	Cheap, simple, low maintenance, creates large numbers of aggregates for study	Aggregates do not have a defined cell number or size. Aggregates also clump together resulting in large unusable structures	(Doetschman et al., 1985; Gothard et al., 2009; Rohani et al., 2008)
Hanging drop culture	Cells seeded into a small drop of media and cultured hanging from the top of a Petri dish lid. Cells aggregate due to gravity.	Aggregates of a defined cell number. Allows for analysis of individual aggregates. Cheap and simple.	Can be laborious to maintain. Only small numbers of aggregates can be created.	(Joshi and Lee, 2015; Kurosawa, 2007)
Low adherence microwell plates	Cells seeded into a well plate and spun down into microwells in the base or cells seeded into a 96 well plate. To encourage aggregation.	Aggregates of a defined cell number. Large numbers of aggregates can be created easily with minimum space requirements. Rapid aggregation process.	Transfer to other culture vessels required due to small media volumes in well. Media changes may be technically challenging.	(Pettinato et al., 2015; Ungrin et al., 2008)
Hydrogels	Cells seeded into a hydrogel and allowed to proliferate and form aggregates encapsulated in the gel.	Creation of clonal aggregates possible from a single cell. Hydrogel environment may be more representative of the *in vivo* environment.	Aggregates need to be removed from the hydrogel for use in further analyses of applications which could affect structural integrity. Hydrogel may also be providing cues which cells are responding to.	(Kurosawa, 2007)

1.2.3.3 Scaffold based technologies

A large proportion of the work involved in creating three dimensional culture spaces relies on the use of scaffold based technologies, which provide an exogenous scaffold that cells can be seeded onto or into to facilitate the formation of a more physiologically relevant cell or tissue structure. These can be broadly split into two categories dependent on their inherent properties: hydrogels and solid scaffolds. The methods discussed are summarised in Figure 1.14.

Hydrogels are composed of a three dimensional linked network of polymers – often proteins – which have the ability to absorb and retain multiple times their own weight in water molecules, resulting in a thick gel like consistency (Caliari and Burdick, 2016). This composition provides hydrogels with properties very similar to the endogenous extracellular matrix which cells normally reside within and provides a suitable support system for them to adopt a three dimensional structure through interacting with the protein network (El-Sherbiny and Yacoub, 2013). Natural hydrogels are those which are created using naturally occurring proteins such as collagen and fibrin, often the secreted ECM components of cells in culture (Tsou et al., 2016), the most well known of these being the common cell culture reagent Matrigel. A product secreted by Engelbreth-Holm-Swarm mouse sarcoma cells, Matrigel contains a variety of complex molecules, growth factors and proteins including common ECM proteins laminin and type IV collagen (Caliari and Burdick, 2016). While natural hydrogels are obviously highly compatible with cells, issues with variability in protein and growth factor content naturally impact on reproducibility, having led to the creation of synthetic hydrogels using various polymers. Synthetic hydrogels are inherently customisable, with a wide range of options available for tailoring to specific cell or tissue needs, and customisable aspects include, but are not limited to, polymer identity, hydrogel stiffness, and gel responsiveness to properties such as heat, light, pH and mechanical forces (Drury and Mooney, 2003; Tibbitt and Anseth, 2009).

Solid scaffold based technologies are, as the name suggests, rigid supports used for cell culture. The materials used for these vary widely, from natural ECM proteins such as collagen and fibrin to synthetic materials such as ceramic and various plastics. The arrangement and topography of the scaffolds are customisable depending on the manufacturing technique used to create the scaffold, of which there are naturally a very wide array, some of which are described below. In the same way as hydrogels, solid scaffolds are also fully customisable according to application. Examples include coating of scaffolds with bioactive molecules, degradation and remodelling by resident cell populations and sensitivity to external stimuli such as heat.

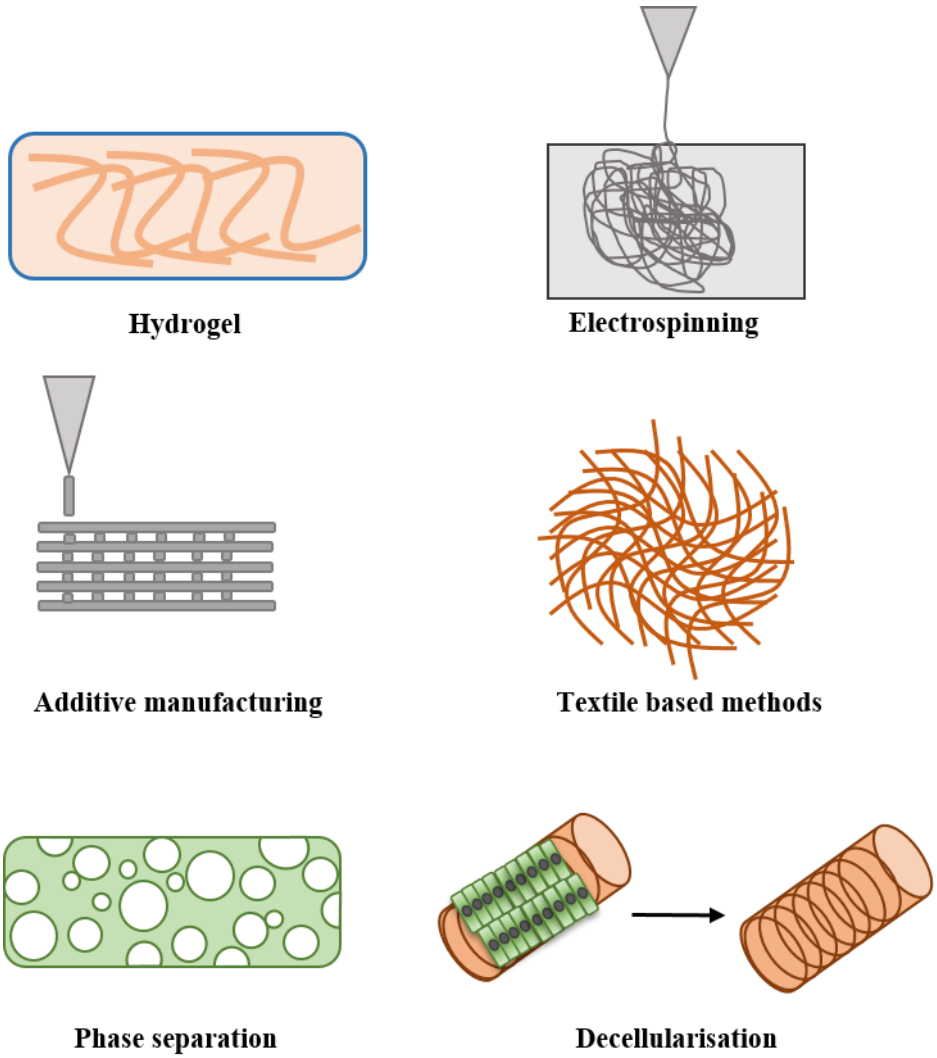


Figure 1.14: Methods used to synthesise scaffolds for cell culture applications: There are myriad methods and techniques used to fabricate scaffolds for cell culture. The choice of technique is dependent on the desired properties in the finished scaffold, including material composition, topography and biodegradability to name a few, with each method producing a combination of physically and chemically unique cues.

Table 1.3: Examples of common methods used to create solid scaffolds for cell culture

Technique	Outline	References
Electrospinning	Uses electrostatic forces and a charged polymer jet to deposit the selected material (natural or synthetic) onto a metallic collection surface, creating fibres arranged in customised microscale and nanoscale topographies.	(Bhattarai et al., 2018; Jun et al., 2018)
Additive manufacturing	Also known as 3D printing. Encompasses a variety of different printing techniques which essentially involve the creation of a product through the laying down of consecutive thin layers of polymer following a three dimensional digital design.	(Gleadall et al., 2018; Jammalamadaka and Tappa, 2018)
Textile based methods	The desired polymers are woven or braided together to create an interlinked network for cell seeding.	(Aibibu et al., 2016)
Phase separation	A solution with multiple different solvents is created; the removal of one solvent either chemically or thermally results in the creation of a scaffold with pores. Examples of these include polyHIPEs (High Internal Phase Emulsions).	(Ghalia and Dahman, 2016)
Decellularisation	Involves the stripping of cells from an intact organ or tissue, leaving behind the complex protein rich extracellular matrix with signalling cues intact.	(Gupta et al., 2017)

1.2.3.4 Physiological culture conditions

While the use of three dimensional culture techniques to create a more physiological cell structure has been shown to impact significantly on the function of cells, spatial arrangement alone is insufficient to fully recapitulate the complexity of the physiological environment. A host of factors are known to contribute to the local cellular microenvironment and provide signalling cues to cells (Yamada and Cukierman, 2007), as seen previously in Figure 1.9.

Various studies are also working to incorporate these factors into cell culture systems to make them more representative of the physiological environment, with the aim of eliciting even more appropriate functions and responses from cells. In the context of PSCs, the aim is to create a microenvironment that stimulates differentiation through recapitulating the physical and chemical cues that are present *in vivo*. This includes the microenvironmental properties previously mentioned, such as three dimensional spatial arrangement and the physical and chemical cues provided by the local microenvironment, but encompasses a range of other local factors. In the study of PSCs and the induction of their differentiation, the importance of a physiological oxygen tension on pluripotency and differentiation (Csete, 2005; Murugesan and Premkumar, 2018; Simon and Keith, 2008) has been studied as well as the impact of the introduction of media perfusion and fluid flow on differentiation trajectory (Wolfe et al., 2012; Yoshimitsu et al., 2014). The introduction of other cell populations to better represent diverse *in vivo* environments including stem cell niches and the complex developmental microenvironment has also been investigated in a number of systems (Park et al., 2009a). Work continues to incorporate a multitude of these factors in combination to enhance the cellular microenvironment to the point at which the physiological functions of cells and tissues *in vitro* can fully recapitulate the functions which take place *in vivo* (Gerlach et al., 2010a; Schmelzer et al., 2010; Wertheim et al., 2018; Xie et al., 2006).

1.2.4 Techniques used to model human tissue development

As outlined in section 1.2.1, human embryonic development is a complex process involving a variety of morphogens and complicated cell movements. Yet it is an area whose study can benefit a number of scientific fields, particularly regenerative medicine applications, as well as better informing our understanding of the actual process. Embryonic organisation and axial formation in particular are increasingly popular areas of study, as is the study of the effects of toxic compounds on normal embryonic development. Currently, a range of methods are used to assess and study these phenomena.

1.2.4.1 Human embryo work

Working with human blastocysts offers a unique opportunity to closely study the events of early embryogenesis and work of this nature provides genuine physiological results which are highly valuable and directly translatable to other studies. However, the finite nature of human embryo work due to the guidelines as implemented and regulated by the Human Fertilisation and Embryology Authority means that this type of study is ultimately limited by time. As detailed in the Human Fertilisation and Embryology Act 2008, Section 3:

A licence cannot authorise—

(a) keeping or using an embryo after the appearance of the primitive streak,

(b) placing an embryo in any animal, or

(c) keeping or using an embryo in any circumstances in which regulations prohibit its keeping or use.

(4) For the purposes of subsection (3)(a) above, the primitive streak is to be taken to have appeared in an embryo not later than the end of the period of 14 days beginning with the day on which the process of creating the embryo began, not counting any time during which the embryo is stored.

Taken from The National Archives, The Human Fertilisation and Embryology Act 2008.

These guidelines are crucial to prevent the further development of embryos which have been exposed to experimental conditions, and allow for study up until the moment at which a unique organism is deemed to have formed i.e. 14 days, which is around the time of primitive streak formation. As a result, only the study of the very earliest events in the process of human embryogenesis can be successfully undertaken using this method, preventing the ability to study the later events including germ layer specification, organogenesis and tissue differentiation. Associated ethical issues with the general use of human embryos for research purposes also makes work of this nature problematic, an issue which society continues to struggle with (Cavaliere, 2017).

1.2.4.2 Use of model organisms

Model organisms have been used for decades in many fields such as fundamental cell biology and ageing to study basic cellular processes. Accessibility, short lifespans, large populations, the ability to undertake experimental manipulation in a number of ways and differences in regulatory practices make the use of other species highly attractive for the study of developmental processes (Holloway et al., 2019). Many fundamental studies into development were completed on *Xenopus laevis* (Cannatella and de Sa, 1993) and chick embryos, based on the assumptions that the biology of these organisms is representative of other species. Other common model organisms include the fruit fly *Drosophila Melanogaster* (Jennings, 2011), the roundworm *Caenorhabditis Elegans* (Leung et al., 2008) and the zebrafish *Danio Rerio* (Meyers, 2018). The conservation of key developmental and cellular processes between species, particularly those within the same taxonomic Class (i.e. Mammalia) means that the study of mouse development in particular has yielded results highly indicative of the human developmental process (Toxicology, 2000). Yet, there still remains the fact that the study of alternative species as model organisms can never be truly conclusive or completely elucidate the events of human development and renders this type of study indicative more than conclusive.

1.2.4.3 Teratoma formation

Although the teratoma assay has primarily been used for the characterisation of novel pluripotent stem cell lines, it also has a number of applications in the study of human development. Martin recognised the value of teratocarcinomas in the 1970s, as a model for the study of embryogenesis and neoplasias. Since then, a small number of studies have been undertaken using teratomas to study various aspects of development, including the lymphatic system (Al-Jomard and Amarin, 2017) and the tumours have also been described as providing an embryonic niche for the study of neoplasias specific to children, such as neuroblastoma (Jamil et al., 2013). As pluripotency is closely linked to development, the assay can also be used to study the nature of cellular differentiation, particularly in response to the treatment or manipulation of the pluripotent stem cell population used to form the tumour. However, the complex differentiation that can be achieved within the assay is offset by the highly variable protocol, briefly mentioned in section 1.2.2.2. While this doesn't necessarily limit the use of the assay in isolation, it does reduce the utility of the data obtained and prevent comparison between cell lines. The use of animals introduces another highly variable biological element, as well as being a source of ethical concern and a potential waste of animal resources, as the animals are utilised only as hosts for the tumour.

1.2.4.4 Pluripotent stem cell studies

Pluripotent stem cell lines provide a continuous source of cells and can be used as a surrogate model of human tissue development. Known to be phenotypically and functionally similar to cells in the early human embryo, human pluripotent stem cells have been used in a number of ways to study tissue differentiation. Two dimensional studies using traditional culture methods have been able to elucidate cellular signalling pathways and mechanisms. Three dimensional cell culture methods have been extensively used, with EB formation allowing for the analysis of lineage specification and differentiation mechanisms – this technique is a key initial step in many complex differentiation protocols. More recently, complex culture techniques have been used to better understand the events involved in early embryogenesis without using embryos, mainly in combination with EB formation. Co-culture with trophoblast cells has been used both to study blastocyst signalling (Rivron et al., 2018) and this culture system combined with hydrogels has be utilised to study lineage specification and implantation events (Shahbazi et al., 2017, 2016). These studies have again allowed for the study of early embryogenesis events, and EB formation has been used in a diverse range of applications to study differentiation. As with many other models however, there are limitations. The constraints of traditional cell culture techniques were discussed in section 1.2.3.1, but the formation and use of EBs is a technique which is also flawed. As the structures increase in size, the diffusion distances to the centre of the EB increase, resulting in a gradient of oxygen, nutrients and cytokines (Van Winkle et al., 2012). This results in a hypoxic core at the centre of the EB, which in turn effects the ability of the EB to differentiate and form complex structures preventing their use in long term studies. However, the importance of timing during the developmental process is well recognised, and is noted by some to be more important than the actual number of cells in the developing embryo (Niakan et al., 2012), a concept which also translates to the *in vitro* situation. Sufficient time is also required for complex tissue structures form if studies on the events later in the developmental cascade are to be successfully undertaken, which is not possible if EB viability cannot be maintained.

1.2.5 Conclusion

This literature review has explored the nature of the human developmental process and highlighted a number of concepts relevant to the following project. Human embryogenesis and the resulting tissue formation process are complex events subject to the influence of a number of cues, including signals from other cell populations and interactions with a range of morphogens. Studies of this process have resulted in the isolation of pluripotent stem cell lines, which provide a source of cells useful for a range of developmental biology studies and regenerative medicine applications. The introduction of more relevant culture techniques, which better represent the *in vivo* environment, allows for the achievement of more complex differentiation. This is particularly useful in the study of pluripotent stem cell developmental potency and differentiation, as well as the study of human tissue development. A number of models are available for the study of these events and states, but these are limited in their value due to tight regulation, fundamental biological differences or unrepresentative environments. The use of three dimensional technologies has been employed, with embryoid body formation particular being able to recapitulate the events of human development. EB formation is limited however, due to increasing size and the formation of hypoxic cores, meaning that highly complex differentiation cannot be achieved within these structures. EB formation also has the potential to allow for the assessment of developmental potency as well in a more controlled and reproducible manner if complex structure formation can be achieved, yet the only method which can currently be used to achieve tissue complexity with human pluripotent stem cells is the teratoma assay.

This review has underlined the need for an *in vitro* method which can allow for complex tissue differentiation to occur. Ideally, this differentiation would be as complex as that seen in the teratoma assay, so that the model could be used to assess both developmental potency and study the events of human development. The use of three dimensional cell culture techniques and the incorporation of more physiological culture conditions can be used to enhance the differentiation of pluripotent stem cells in order to better achieve this.

1.3 Project Aims and Objectives

1.3.1 Aims

The aim of this project is to create a novel *in vitro* model using pluripotent stem cells, which can be used for the purposes of studying the development of human tissues and assessing the pluripotency of human pluripotent stem cell lines. The model will use the commonly used technique of embryoid body formation in combination with a solid scaffold, with the overall aim of greatly enhancing the differentiation that can be achieved by forming a tissue disc structure. A variety of additional three dimensional and physiological culture techniques which have already been used to improve the differentiation of pluripotent stem cells will also be incorporated and explored within the model. It is hypothesised that the differentiation which can be achieved within these tissue disc structures will be more complex and diverse than that seen in EBs.

1.3.1.1 Optimise the model using a well characterised human embryonal carcinoma cell line

Optimisation stages will involve the use of an embryonal carcinoma cell line, TERA2.cl.SP12, as these cells are known to share properties with embryonic stem cells, but are simple and inexpensive to culture, as well as being a well characterised system in terms of differentiation. Initial work will focus on the study of EC cell aggregates, with a view to optimising the culture time and cell density of aggregates prior to seeding in the scaffold. Following this, appropriate scaffold selection and the maintenance of differentiated tissue discs on the scaffold will be completed. It is hypothesised that the aggregates most appropriate for the model will be of a low seeding density and an early time point. The most appropriate scaffold is expected to be one which allows for the maintenance of an entire tissue disc structure.

1.3.1.2 Create a more physiological microenvironment *in vitro* to enhance differentiation

Additional properties and cues will be introduced into the model to increase physiological relevance, again, with the overall aim of improving the cellular microenvironment and the differentiation within the tissue discs. Co-culture with a relevant murine dermal fibroblast cell line will be undertaken, as well as the introduction of media perfusion to the system. It is expected that the introduction of these properties to the tissue disc model will result in an enhanced differentiated phenotype, with increased complexity in the tissue structures.

1.3.1.3 Use a more relevant pluripotent stem cell population in the model

The results of the previous work will then be translated to a murine embryonic stem cell line, in order to further explore the differentiation that can be achieved within the model, and as an intermediary

step to using a human pluripotent stem cell lines. The ability to direct the differentiation of the tissue discs in a more specific manner will also be examined, to prove that the model can be directed to form derivatives from each germ layer. It is hypothesised that highly complex differentiation from the three germ layers will be achieved within this version of the model, which will also be highly receptive to the physiological properties previously investigated and optimised.

1.3.1.4 Validate the model using a teratoma assay and human pluripotent stem cells

Finally, model validation will be conducted in parallel with a teratoma assay, in order to directly compare the differentiation between the gold standard *in vivo* model and the novel *in vitro* model. It is speculated that structures of equal complexity will be able to be achieved in the *in vivo* and *in vitro* systems. Some pilot studies using human pluripotent stem cell lines will be carried out to prove that these populations can be successfully cultured in the model. This is hypothesised to be the case, with both ES cells and iPS cells expected to be able to form tissue discs on the scaffold.

1.3.2 Objectives

The objectives for this project are as follows:

- Develop a novel *in vitro* model using human embryonal carcinoma cell aggregates and three dimensional solid scaffold technologies to enhance the differentiation which can be achieved.
- Incorporate more physiological properties, co-culture and perfusion, in order to enhance the differentiation within the model and make the model more physiologically relevant.
- Use the previously optimised conditions with a murine embryonic stem cell line, assessing the differentiation of the cells into structures derived from all three germ layers.
- Undertake validation of the model using *in vivo* teratoma assay studies and through forming tissue discs using other human pluripotent stem cell populations.

2. Materials and Methods

2.1 Introduction

A wide range of methods and techniques have been used throughout this project in order to undertake relevant experiments and analyse the data obtained. This has involved a number of different cell lines and populations and multiple advanced cell culture techniques, including three dimensional cell culture methods and physiologically relevant culture systems such as co-culture and perfusion. Analytical methods have included various qualitative staining techniques, both histological and immunofluorescent, and a range of quantitative methods including flow cytometry, Western blotting and PCR.

Within this chapter, the following is detailed:

- Routine cell culture and maintenance for each cell line used

- Common three dimensional techniques used throughout

- General analytical techniques used throughout

Methods and techniques which are specific to the work completed in a single chapter are more closely detailed at the beginning of each Chapter.

2.2 Routine cell culture and three dimensional cell culture techniques

Unless stated otherwise, all cell culture practices were performed under sterile conditions in a Class 2 Biological Safety Cabinet.

2.2.1 Routine culture, maintenance and cryopreservation of TERA2.cl.SP12 embryonal carcinoma cells

The human embryonal carcinoma cell line TERA2.cl.SP12 was maintained using Dulbecco's Modified Eagles Medium (DMEM, Gibco, Invitrogen, Paisley, Scotland) supplemented with 10 % heat treated Foetal Bovine Serum (FBS, Gibco), 2 mM L-glutamine (Lonza, Basel, Switzerland) and 100U/mL of Penicillin/Streptomycin (Gibco) in appropriate T25 and T75 flasks (BD Biosciences, Oxford, UK), with media changes every 1 to 2 days as necessary. Cells were passaged on reaching 100 % confluency by rolling acid washed glass beads across the surface to dislodge cells in a small amount of maintenance media, before transferring the cell suspension to new flasks, splitting at a ratio of 1:3. Cells were incubated and maintained at 37°C and 5 % CO_2.

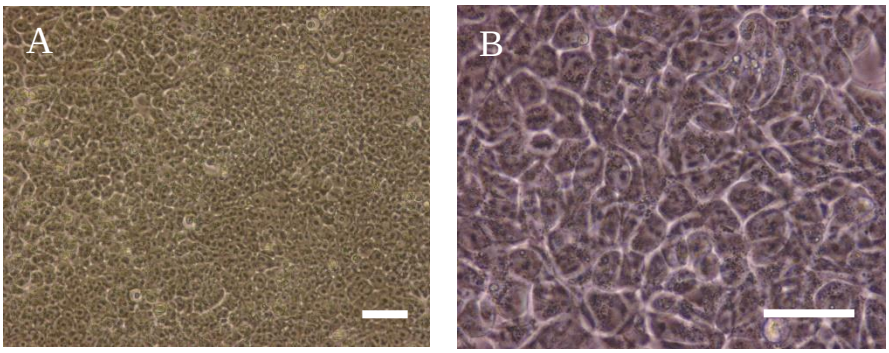


Figure 2.1: TERA2.cl.SP12 cells *in vitro* at subconfluent and fully confluent densities: Phase contrast images of the human embryonal carcinoma cell line TERA2.cl.SP12 at (A) full confluency prior to use or passage and (B) at a higher magnification to highlight the stem cell phenotype. TERA2.cl.SP12 show a typical stem cell morphology: cells are small with a high nuclear to cytoplasmic ratio and prominent nucleoli. Scale bars: 50 μm and 25 μm

For the creation of cell banks and working stocks, TERA2.cl.SP12 cells in culture were washed using sterile phosphate buffered saline (PBS) before detachment using acid washed glass beads as described. Cells were centrifuged at 1000 rpm for 3 minutes, supernatant media removed and resuspended in freezing media consisting of 90 % heat treated FBS and 10 % dimethyl sulfoxide (DMSO, Sigma Aldrich, Dorset, UK). Cells were resuspended at a ratio of 1 T25 flask per mL, and 1 mL was placed in each cryovial (Fisher Scientific UK, Winsford, UK). Cryovials were stored in Mr Frosty™ (Fisher Scientific UK) containers for at least 24 hours at -80°C before being transferred to -150°C for long term storage.

To revive for culture, one cryovial of frozen TERA2.cl.SP12 was thawed rapidly in a 37°C waterbath, before being resuspended in 9 mL of pre-warmed media in a Falcon tube (Greiner Bio-One, Stonehouse, UK). Cells were centrifuged at 1000 rpm for 3 minutes, supernatant media was aspirated, and the cells resuspended in 10 mL of pre-warmed media, placed in a T25 flask and maintained as described above.

2.2.2 Formation, maintenance and morphogen treatment of TERA2.cl.SP12 cell aggregates

TERA2.cl.SP12 cells in tissue culture flasks were washed using sterile PBS and incubated in 0.25 % trypsin/2 mM EDTA (Gibco) for 3 minutes at 37°C and 5 % CO_2 to obtain a single cell suspension. Maintenance media was added to neutralise the reaction, and cells were centrifuged at 1000 rpm, supernatant removed and resuspended in 1 mL maintenance media. Viable cells were counted using a Neubauer Improved Haemocytometer, with the Trypan Blue Exclusion Assay used to identify dead cells and obtain accurate cell numbers. To count, a sample of the resuspended pellet was combined with Trypan Blue (Sigma Aldrich) in a ratio of 1:10 cell suspension to dye. The volume required for the desired number of cells was calculated, and added to 20 mL maintenance media in a sterile, untreated 90 mm Petri dish (Fisher Scientific UK). Petri dishes were incubated at 37°C, 5 % CO_2 with media changes every 3-4 days. To change media, the aggregate suspension medium was transferred to a 50 mL Falcon (Greiner Bio-One) and aggregates were allowed to settle at the bottom of the tube. Used media was then aspirated from the tube and 20 mL fresh media added, before the lid was replaced and the tube was inverted to resuspend the aggregates. The suspension was then poured into a new Petri dish for further culture. Aggregates were both allowed to spontaneously differentiate and were treated with morphogens to direct their differentiation. Aggregates were maintained for up to 21 days, dependent on morphogen treatment applications.

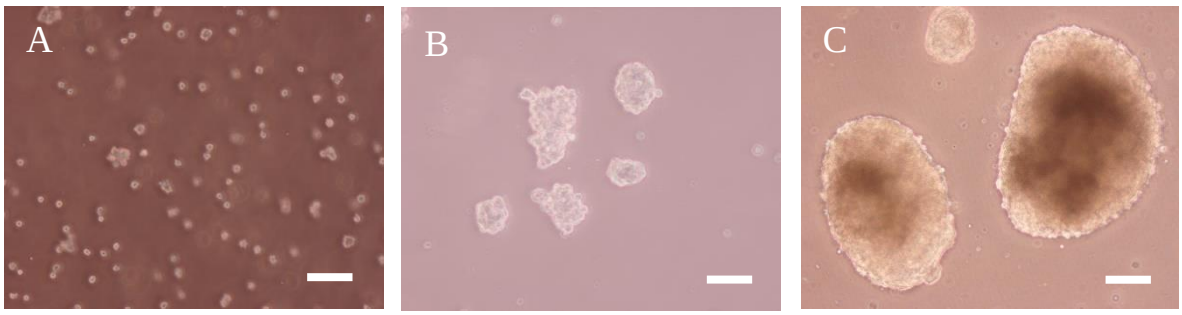


Figure 2.2: TERA2.cl.SP12 cells in suspension culture *in vitro* at various timepoints during the aggregate formation process: TERA2.cl.SP12 cells (A) on the day of seeding, (B) 1 day post seeding and (C) 14 days post seeding. Cells quickly clump together to form aggregates, as seen in Image B after only 24 hours. By 14 days, aggregates are quite large, having accumulated a significant number of cells. Scale bars: 100 μm

To direct the differentiation of the cell aggregates, morphogens were added to the culture medium 1 day after seeding in the concentrations described below, dissolved in the appropriate vehicle.

Table 2.1: Morphogens used to direct the differentiation of TERA2.cl.SP12 aggregates

Morphogen	Vehicle	Supplier	Final concentration
All-*trans* Retinoic Acid (ATRA)	DMSO	Sigma Aldrich	0.01 µM
EC23	DMSO	Reprocell UK, Sedgefield, UK	0.01 µM
Bone Morphogenetic Protein 2 (BMP-2)	20 mM Acetic Acid	Gibco	50 ng/mL

2.2.3 Preparation of Alvetex® Polaris inserts

Alvetex® inserts (Reprocell Europe Ltd, Sedgefield, UK) were prepared for use according to previously established protocols. Alvetex® inserts must be treated in order to render the hydrophobic surfaces hydrophilic, and so allow cellular adhesion. Alvetex® Scaffold and Strata inserts were received already assembled, and so were placed into 70 % ethanol for treatment for at least 5 minutes on the day of use. Alvetex® Polaris inserts required assembly and were prepared at least a day before they were required for use; the Alvetex® Polaris discs were placed in 70 % ethanol to become hydrophilic, before placing into the base piece and clipping the body piece on (see Figure 2.3). The newly assembled Polaris insert was then placed in 70 % ethanol until required for cell culture. On the day of use, all assembled inserts were then washed twice in sterile PBS for 5 minutes in the cell culture hood. Inserts were placed into 6 well plates and a small amount of appropriate media added to the insert and aspirated before seeding of cellular material.

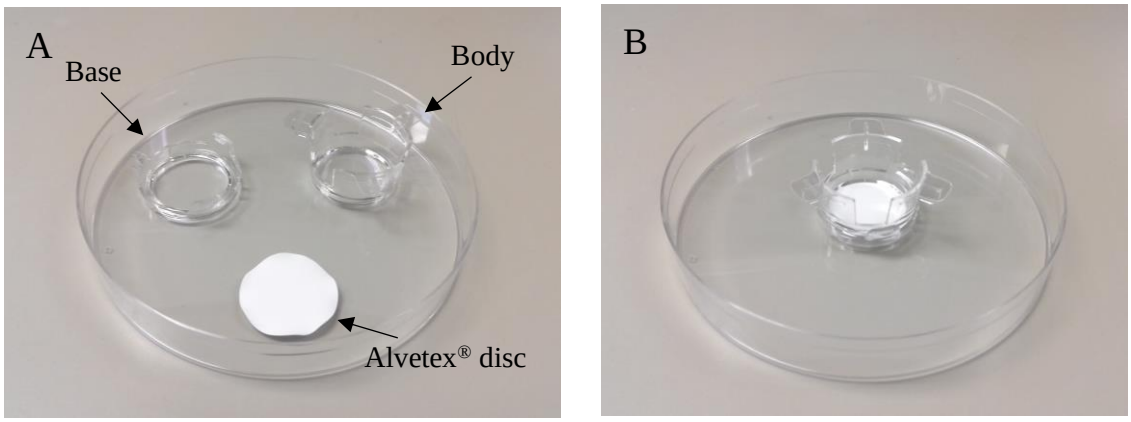


Figure 2.3: Assembling an Alvetex® insert: The Alvetex® inserts consist of (A) a base piece, a body piece and a porous, polystryrene insert (Alvetex® disc). Polaris inserts were assembled 24 hours prior to use as shown in image (B), Strata and Scaffold inserts were received preassembled, ready for use.

2.2.4 Seeding and maintenance of TERA2.cl.SP12 aggregates as tissue discs on Alvetex® inserts

Alvetex® inserts which had been prepared as previously described were placed in a 6 well plate (Greiner Bio-One) and 10 mL of TERA2.cl.SP12 media added to each well. TERA2.cl.SP12 aggregates which had reached the appropriate timepoint were then transferred from the Petri dish using a cut off 200 µL pipette tip (Sarstedt, Leicester, UK) in a volume of around 50 µL and placed on the insert in submerged culture. 6 to 10 aggregates were placed on each insert for the culture period and were incubated at 37°C, 5 % CO_2. Half and full media changes were performed as required, around every 3-4 days, until the desired timepoint, and prepared for analysis as appropriate.

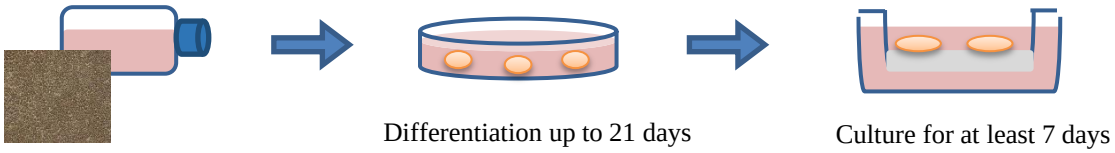


Figure 2.4: Schematic of creation of TERA2.cl.SP12 tissue discs: TERA2.cl.SP12 cells are seeded as aggregates and cultured in suspension until the mature timepoint is reached. Aggregates are then transferred to the Alvetex® Polaris membrane and cultured for a further 7 days, before analysis via a range of techniques.

2.2.5 Routine culture, pluripotency maintenance and cryopreservation of CGR8 embryonic stem cells

The murine embryonic stem cell line CGR8 (ECACC, Porton Down, UK) was maintained in a basal medium consisting of Glasgow Minimum Essential Medium (GMEM, Sigma Aldrich) supplemented with 10 % Pluripotent Stem Cell Qualified FBS (qFBS, Gibco), 2 mM L-glutamine, 100U/mL Penicillin/Streptomycin and 55 µM β-mercaptoethanol (Sigma Aldrich).

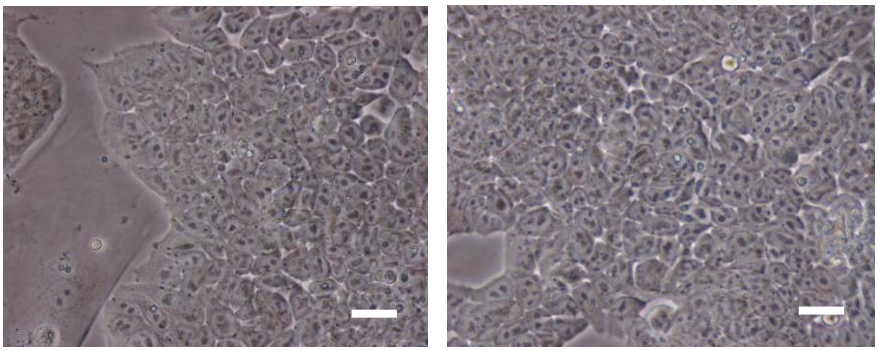


Figure 2.5: CGR8 pluripotent stem cells *in vitro*: CGR8 murine embryonic stem cells maintained under pluripotent conditions at 70 % confluency, prior to use or passage. CGR8 embryonic stem cells show a typical stem cell morphology: cells are small with prominent nucleoli and a high nuclear to cytoplasmic ratio, growing in a colony formation. Scale bars: 50 µm

To maintain the pluripotent phenotype, CGR8 cells were cultured in Nunc™ T25 flasks (Fisher Scientific UK) coated with 0.2 % gelatin (Sigma Aldrich) solution in sterile PBS, incubated at 37°C, 5 % CO_2 for at least 20 minutes prior to use. Cells were grown in a pluripotency medium consisting of the basal medium with the addition of mouse recombinant Leukaemia Inhibitory Factor (LIF, Amsbio, Abingdon) at a concentration of 1000 U/mL. Media was changed every day, and cells were passaged once 70-80 % confluency was reached, around every 2-3 days. To passage, cells were washed in sterile PBS and incubated in 0.25 % trypsin/2 mM EDTA for 3 minutes, before the reaction was neutralised with pluripotency medium. The cell suspension was transferred to a Falcon tube, centrifuged at 1000 rpm for 3 minutes and the supernatant removed. Cells were resuspended in an appropriate volume of pluripotency medium, and split at a ratio of 1:9 into fresh gelatin coated flasks.

Frozen stocks were created in a way similar to that previously described. Briefly, cells were washed with sterile PBS and detached using the trypsin method. The freezing medium used consisted of 90 % qFBS and 10 % DMSO, and cells were frozen down at the confluent density into cryovials, at a ratio of one T25 per cryovial. Cells were revived in the same way as previously described by rapid thawing and centrifugation, resuspended in pluripotency medium and placed into a T25 coated with 0.2 % gelatin.

2.2.6 Formation, maintenance and morphogen treatment of CGR8 embryoid bodies

To form embryoid bodies, CGR8 cells maintained in the pluripotent state were treated with 0.25 % trypsin/2 mM EDTA to form a single cell suspension and counted using the Trypan Blue Exclusion Assay to obtain accurate cell numbers. Culture medium was swapped to a differentiation medium, which consisted of the basal medium with no additional supplements. Aggrewell 800™ plates (Stem Cell Technologies, Cambridge, UK) were used to form the embryoid bodies, and were prepared as follows (see Figure 2.6). Wells to be used for culture were rinsed with 2 mL of differentiation medium, which was then aspirated. 500 µL of the differentiation medium was then added to each well, and plates were centrifuged at 2000 g for 5 minutes to displace air bubbles in the microwells. This was confirmed under the microscope, before the appropriate cell volume was added to the well to form embryoid bodies of the required size. Differentiation media was added so that the final volume in the well was 2 mL, and pipetted up and down gently several times to distribute the cells evenly. The plates were then centrifuged at 100 g for 3 minutes to capture the cells at the bottom of the microwells. Aggrewell™ plates were incubated for 3 days at 37°C, 5 % CO_2, with half media changes on days 1 and 2 post seeding.

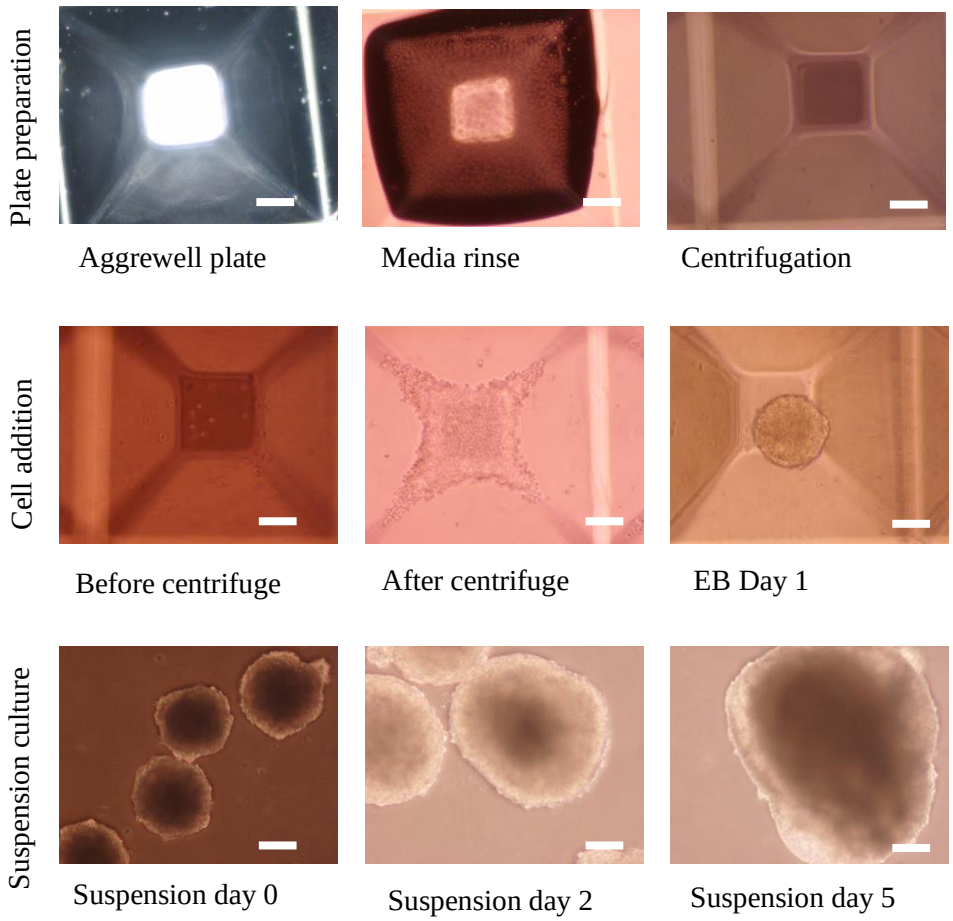


Figure 2.6: Formation of embryoid bodies using murine embryonic stem cell line CGR8: Phase contrast images of embryoid body creation. Aggrewell 800™ plates were prepared as advised in the manufacturer's instructions. Cells were added and the plates centrifuged to pellet the cells at the base of the microwells, encouraging aggregation. After 3 days culture in the plates, embryoid bodies were transferred to Petri dishes for suspension culture, to allow EBs to mature and increase in size. Scale bar: 100 μm

On day 3, embryoid bodies which had formed were removed from the microwells by pipetting the medium up and down firmly, and transferring the suspension to a sterile, untreated 90 mm Petri dish. Wells were repeatedly washed using differentiation media to remove embryoid bodies if required. The medium in the Petri dish was topped up to 20 mL using the differentiation medium, and embryoid bodies were cultured in the Petri dish for 5 days before fixing or transfer to Alvetex® inserts. CGR8 embryoid bodies were both allowed to spontaneously differentiate and treated with morphogens during culture to direct the differentiation, as detailed in Table 2.2.

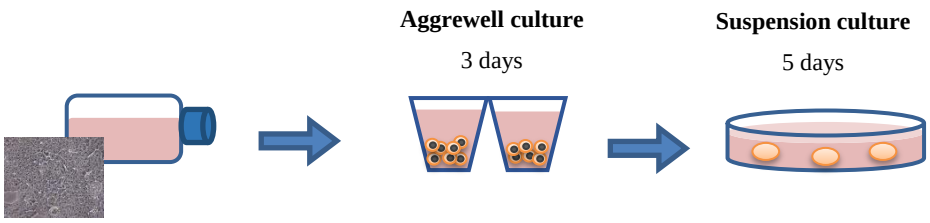


Figure 2.7: Two phase embryoid body formation process using Aggrewell plates and suspension culture: Schematic showing the overall process used to create embryoid bodies with low adherence microwell plates, Aggrewell 800™. The process is two step: embryoid bodies are initially allowed to form over 3 days in the microwell plates before being transferred to suspension culture, allowing for formation and maturation of the structures.

Table 2.2: Morphogens used to direct the differentiation of CGR8 embryoid bodies during culture

Morphogen	Vehicle	Supplier	Final Concentrations
Activin A	0.1% Bovine Serum Albumin in sterile PBS	Gibco	100 ng/mL, 50 mg/mL, 20 ng/mL
Basic Fibroblast Growth Factor (bFGF)	10 mM Tris	Gibco	100 ng/mL
BMP-4	4 mM Hydrochloric acid / 0.1% bovine serum albumin	Gibco	50 ng/mL, 20 ng/mL, 1 ng/mL
Dorsomorphin	DMSO	Sigma Aldrich	10 µM
EC23	DMSO	Reprocell Reinnervate	0.01 µM
SB431542	DMSO	Sigma Aldrich	10 µM

Further details of the combinations of morphogens used to direct the embryoid bodies can be found in the Material and Methods in Chapter 4.

2.2.7 Seeding and maintenance of CGR8 embryoid bodies as tissue discs on Alvetex® Polaris

Following suspension culture in Petri dishes, CGR8 embryoid bodies were seeded onto Alvetex® Polaris inserts as previously described, using a cut off pipette tip to transfer 6-8 embryoid bodies onto the insert. Inserts were maintained in the differentiation medium at 37°C, 5 % CO_2, with half and full media changes as required.

2.2.8 Routine culture, maintenance and cryopreservation of I18002 induced pluripotent stem cell line

I18002 induced pluripotent stem cell line was obtained from Reprocell Europe Ltd at p11. To maintain the pluripotent phenotype, I18002 colonies were cultured and maintained in feeder free conditions using NutriStem hPSC XF media (Reprocell Europe Ltd) in 6 well plates coated with iMatrix 511 (recombinant laminin 511 fragments) (Reprocell Europe Ltd), according to the manufacturer's protocol. Briefly, the iMatrix solution was diluted in sterile PBS, with 9.6 µL added per 2 mL sterile PBS to make the working coating solution. 2 mL of the working solution was added to each well, and incubated for 60 minutes at 37°C, 5 % CO_2. Following this, plates were either sealed with Parafilm for storage at 4°C for up to 1 week prior to use, or coating solution was aspirated for immediate use. Plates which had been stored at 4°C were allowed to reach room temperature before cell seeding. Media was also allowed to reach room temperature before use, and changed daily, with a total volume of 2 mL used per well.

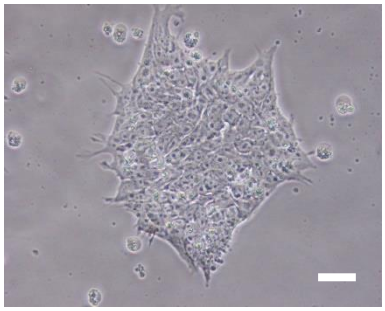


Figure 2.8: I18002 pluripotent stem cells in culture *in vitro*: I18002 human induced pluripotent stem cell line, with a typical colony shown. Cells display the morphological hallmarks of pluripotency, including a small cell size, prominent nucleoli and high nuclear to cytoplasmic ratio. Scale bar: 100 µm

To passage, cells were allowed to reach 70-80 % confluency. Cells were washed gently in 1 mL 0.48 mM Versene (EDTA solution) (Fisher Scientific UK), before 1 mL Versene was added to the plates and incubated at 37°C for 5 minutes. Cells were checked under a phase contrast microscope to ensure colonies were beginning to detach, with gaps appearing between the cells. If this was not the case, cells were further incubated in the Versene solution, for up to a total time of 10 minutes, with regular checking every 1-2 minutes. Versene was then aspirated from the wells and colonies quickly washed from the surface of the plate using a 1 mL micropipette and 1 mL of NutriStem media. Cells were washed from the plate surface in one pipetting motion as shown in the Figure below, with the plate held at a 45° angle and the tip held very close to the well surface also at an angle of around 45°. It was important to wash the cells in one motion to prevent the cells breaking into a single cell suspension from repeated pipetting.

The cell suspension was then split at an appropriate ratio, usually 1:3 into coated wells already containing 1 mL of NutriStem, with further media added to bring the final total volume to 2 mL. The plate was gently rocked in each direction to evenly distribute the cells within the wells.

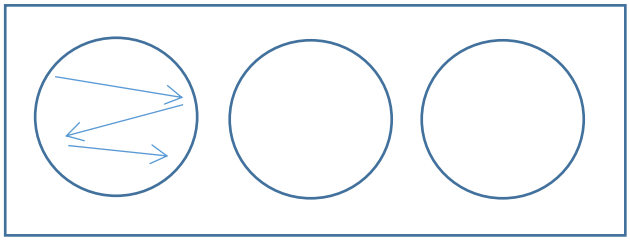


Figure 2.9: Washing of I18002 colonies from 6 well plate: Pipette tip was brought close to the surface of the well, and the cells washed off in one motion using the force created by the tip. In order to maximise the number of cells washed from the plate, the pipette tip was moved in a zig-zig motion across the well to cover a large surface area.

Frozen cell stocks were created by detaching cells from the wells using the Versene method as described. Colonies were washed from the plate, placed in a 15 mL Falcon and centrifuged at 200 g for 3 minutes. Media was aspirated and cells gently resuspended in CryoStem freezing medium (Reprocell Europe Ltd), at a ratio of 1 well per 500 µL of CryoStem, which was placed into 1 cryovial. Cryovials were stored at -150°C as previously stated.

To revive, 1 cryovial was thawed as quickly as possible using a 37°C waterbath, until a small ice crystal remained in the cryovial. Using a serological pipette, the thawed cell suspension was transferred to a 15 mL Falcon tube. The cryovial was gently washed with 1 mL NutriStem media, which was transferred to the Falcon tube. 8.5 mL of NutriStem media was very slowly added to the Falcon tube in 2-3 mL volumes, with mixing in between each addition to reduce osmotic stress on the cells, to reach a final total volume of 10 mL. The cell suspension was then centrifuged at 200 g for 3 minutes. The supernatant was aspirated from the tube, and the tube was gently flicked to dislodge the cell pellet. The cells were then gently resuspended in 1 mL of NutriStem media, and split into 2 coated wells containing the correct volume of media at a ratio of 80 % and 20 % of the vial, giving a final media volume of 2 mL per well.

2.2.9 Routine culture, maintenance and cryopreservation of H9 human embryonic stem cells

H9 human embryonic stem cells were kindly donated by Professor Majlinda Lako, Institute of Genetic Medicine, Newcastle University. Cells were cultured in feeder free conditions in 6 well plates coated with Corning Matrigel Human Embryonic Stem Cell (hESC) qualified Matrix (Fisher Scientific UK) using mTESR 1 medium (Stem Cell Technologies). Briefly, hESC qualified Matrigel was diluted in mTESR according to the dilution factor provided with the coating matrix to create a coating solution. Coating solution was added to the wells in a 6 well plate, with 1 mL per well, and plates incubated at 37°C, 5 % CO_2 for 60 minutes. After incubation, plates were either: sealed with Parafilm and stored at 4°C or the coating solution aspirated and plates used immediately. mTESR was made up according to the manufacturer's instructions, and stored in aliquots at -20°C. Medium and plates that had been stored in temperature controlled conditions were allowed to reach room temperature before use, and media was stored at 4°C after defrosting for up to 1 week.

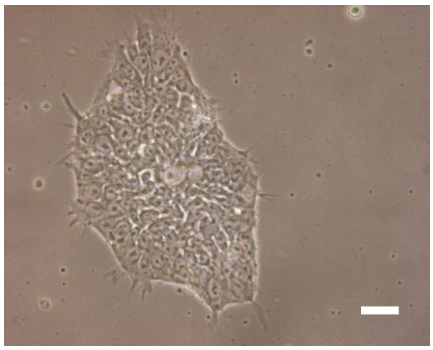


Figure 2.10: H9 pluripotent stem cells *in vitro*: H9 human embryonic stem cell line in culture, with a typical colony shown. Cells also display morphological hallmarks of pluripotency, with a high nuclear to cytoplasmic ratio, prominent nucleoli and a small cell size. Scale bar: 100 μm

To passage, colonies were allowed to reach around 70 % confluency before detaching using ReLeSR (Stem Cell Technologies) according to the manufacturer's protocol. Briefly, cells were washed in DPBS, before 1 mL of ReLeSR was added to each well. ReLeSR was aspirated after 30-60 seconds, to leave a thin film of ReLeSR liquid covering the cells. Wells were then incubated at 37°C, 5 % CO_2 for 6 minutes, before 1 mL of mTESR was added to each well. Plates were then firmly tapped for 30-45 seconds to detach colonies, and the cell suspension transferred to a 15 mL Falcon tube using a serological pipette. The cell suspension was pipetted up and down gently to break up any large colonies, and seeded at the appropriate ratio into Matrigel coated plates containing mTESR.

For the creation of cell stocks, H9 cells were cryopreserved in mFreSR (Stem Cell Technologies). Cells were passaged as described using ReLeSR and transferred to a 15 mL Falcon tube, before centrifuging at 300 g for 5 minutes at room temperature. The supernatant was aspirated, and cells gently resuspended in mFreSR using a serological pipette. 1 well was resuspended in 1 mL of

mFreSR, which was placed into 1 cryovial using a serological pipette. Cryovials were then placed into a Mr Frosty as previously described, before transfer to long term storage at -150°C.

All plates and reagents were prepared prior to revival to allow for thawing to be completed quickly. To revive, one cryovial of frozen H9 cells was quickly thawed in a 37°C waterbath until only a small ice crystal remained. Cell suspension was removed from the cryovial using a serological pipette and transferred to a 15 ml Falcon tube. 7 mL of mTESR was slowly added to the cell suspension, intermittently mixing the media. Cells were centrifuged at 300 g for 5 minutes at room temperature, supernatant aspirated and cells resuspended in 1 mL mTESR, which was split between 2 Matrigel coated wells. Media was then changed daily.

2.2.10 Formation and maintenance of I18002 and H9 embryoid bodies

Cells were maintained according to the above protocols in 6 well plates prior to embryoid body formation. On the day EBs were to be made, cells were incubated in Rho kinase (ROCK) inhibitor Y27632 (Tocris Biosciences, Abingdon, UK) at a final concentration of 10 µM for 60 minutes prior to use by addition of the chemical to the media already in the culture plates. Wells were gently swirled to ensure distribution of the Y27632 and placed back in the cell culture incubator at 37°C, 5 % CO_2. Following incubation, cells were detached using the appropriate detachment method as described, with 10 µM Y27632 added to the media used to wash the cells from the plate. Cells were washed from the plate firmly to create a single cell suspension, centrifuged at 200 g for 3 minutes, and resuspended in a differentiation medium, consisting of KnockOut DMEM/F12 (Fisher Scientific), 10 % Multispecies KnockOut Serum Replacement (Fisher Scientific), 2 mM L-glutamine, 100 U/mL Penicillin/Streptomycin and 55 µM β-mercaptoethanol. Y27632 was also added at this point at a final concentration of 10 µM. Following this, cells were counted using the Trypan Blue method, before seeding and culture in Aggrewell 800™ plates as previously described using the aforementioned differentiation medium. ROCK inhibitor was added to the medium initially on seeding for 24 hours. Subsequent half media changes were performed using differentiation medium without ROCK inhibitor, and embryoid bodies were allowed to form over 2-3 days.

2.2.11 Routine culture, maintenance and cryopreservation of human neonatal dermal fibroblasts

Human neonatal dermal fibroblasts (HDFn, cell line number 1366356 from Life Technologies, (Invitrogen, Fisher Scientific UK)) were initially acquired and previously cultured in M106 (Gibco) supplemented with a low serum growth supplement (Gibco) in Nunc™ flasks, seeding at a ratio of 2.5 x 10^3 cells per cm^2. Medium was changed every 2-3 days. Cells were passaged on reaching 70 %

confluency, using the 0.25 % trypsin/ 2mM EDTA method, and reseeded into new flasks at the stated ratio.

On passage and thereafter, cell medium was swapped to a medium consisting of DMEM, 10 % FBS, 2 mM L-glutamine and 100U/mL Penicillin/Streptomycin. Cell stocks were created in the manner previously described, with freezing media consisting of 90 % FBS and 10 % DMSO. Cells were frozen down at a density of 1 x10^6 cells per 1 mL per cryovial. Cells were revived as previously described, and seeded according to the density stated above.

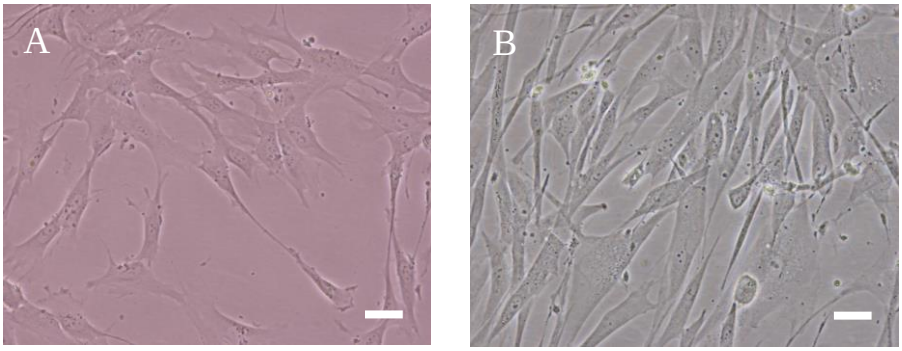


Figure 2.11: Human dermal fibroblasts *in vitro*: Neonatal human dermal fibroblasts at (A) low density and (B) high density prior to use or passage. HDFns show a typical fibroblast morphology, with an elongated shape. Scale bars: 50 μm

2.2.12 Isolation of severe combined immunodeficient (SCID) mouse fibroblast cell line and creation of cell line

The isolation procedure was carried out in a laminar flow hood. A dermal explant was removed from the flank of a SCID mouse which had been shaved to remove fur. Adipose tissue was cut away from the sample, which was washed several times in sterile PBS containing 200 U/mL Penicillin/Streptomycin. The tissue was then cut into pieces around 1 mm^3. Dermal explant pieces were placed with the dermis in contact with the plate surface of a 6 well plate which had been scored with a scalpel in a cross hatch manner to facilitate attachment, with 1-2 pieces per well.

Explants were left to adhere to the surface of the plate for around 2 hours at 37°C, 5 % CO_2, before 10 mL maintenance media was slowly added to the plate, careful to prevent detachment. Explants were maintained in culture at 37°C, 5 % CO_2 in a medium consisting of DMEM, 20 % FBS, 2 mM L-glutamine, 200 U/mL Penicillin/Streptomycin and Amphotericin B. The media was changed every 3 days, and explants were left for around 10-12 days to allow for cell migration.

After sufficient migration was achieved, wells were incubated in 0.25 % trypsin/ 2 mM EDTA for a sufficient time to detach cells and explants. The reaction was neutralised using maintenance media,

and explants removed from the well and placed in a fresh, scored 6 well plate to encourage further fibroblast migration. The cell suspension was pooled, centrifuged at 1000 rpm for 3 minutes, supernatant removed and resuspended in maintenance medium. The cells were then transferred to a Nunc T25 and labelled P0, and explants were placed into a fresh scored 6 well plate to encourage more cellular migration, maximising cell retrieval. Media was changed every 2-3 days, and cells were maintained in the original isolation medium until passaging, whereas explants were maintained as described above. At the first passage, cells were passaged at a ratio 1:2, and swapped to a medium consisting of DMEM, 10 % FBS, 2 mM L-glutamine and 100 U/mL Penicillin/Streptomycin.

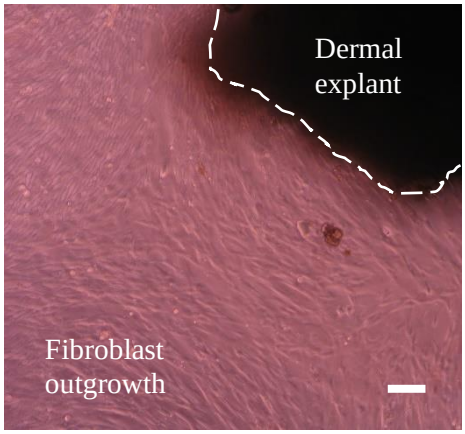


Figure 2.12: Outgrowth of immunodeficient mouse fibroblasts from dermal explant *in vitro*: The dermal explants were placed onto scored tissue culture plastic in 6 well plates to aid attachment and outgrowth. Fibroblasts grew out of the explant as a lawn across the plate and are clearly visible in the image. Scale bar: 50 µm

For initial creation of a cell bank, cells were cryopreserved as previously described by detachment using 0.25 % trypsin/ 2 mM EDTA, with the freezing medium consisting of 90 % FBS and 10 % DMSO. Cells were frozen down with ½ T25 per 1 mL, which was placed into one cryovial and stored as previously indicated. Cells were revived as previously described and placed into a Nunc™ T25 flask.

2.2.13 Routine culture, maintenance and cryopreservation of SCID mouse fibroblast cell line

For routine culture, SCID mouse fibroblasts were maintained in the medium used after the first passage, as detailed above, in Nunc™ flasks, with media changes every 2-3 days at 37°C, 5 % CO_2. On reaching 70 % confluency, cells were passaged using the 0.25 % trypsin/ 2 mM EDTA method, and split at a ratio of 1:6 into new flasks.

Frozen working stocks were created as described, using the same freezing media. Cells were frozen down at a ratio of 1:4 to 1:6, depending on flask size and confluency.

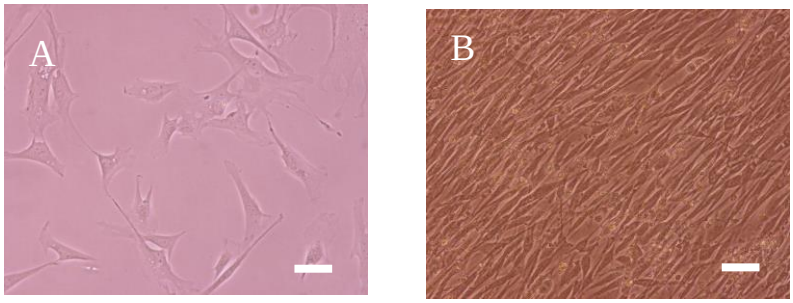


Figure 2.13: Murine dermal fibroblasts in culture *in vitro*: SCID mouse fibroblast cells in culture at (A) low density and (B) high density. SCID fibroblasts also show the typical elongated fibroblast morphology. Scale bars: 50 μm

2.2.14 Seeding and culture of cells on glass coverslips

In order to assess the phenotype and identity of 2D cells prior to use in 3D systems, cells were cultured on glass coverslips to allow for staining. Coverslips were washed in 70 % ethanol, before being placed in a 12 well plate (Greiner Bio-One). Coverslips were washed in sterile PBS twice in the plate, before being incubated in 500 μL of 10 μg/mL Poly-d-lysine (PDL, Sigma Aldrich) solution at room temperature overnight. Before use, PDL solution was aspirated and coverslips washed in sterile PBS. 2 mL of the appropriate media was added to the wells, and cells were seeded onto the coverslip according to the correct seeding density. Cells were cultured until the appropriate confluency was reached. At this point, media was aspirated from the wells and coverslips were gently washed in PBS. Coverslips were fixed in either 4 % Paraformaldehyde (PFA, Fisher Scientific UK) for 20 minutes at room temperature, or in ice cold 1:1 methanol:acetone solution at -20°C for 20 minutes. After fixing, coverslips were washed twice in PBS and stored at 4°C until staining.

2.2.15 Formation of dermal equivalents using Alvetex® Scaffold

Alvetex® Scaffold (6 well inserts) was prepared for culture as previously described, and placed into 6 well plates without the addition of the full volume of culture medium. The same seeding and maintenance protocol was used to create dermal equivalents (DEs) from both SCID fibroblasts and HDFns.

A single cell suspension was obtained of the cell line being used using the 0.25 % trypsin/ 2 mM EDTA method as previously described. Cells were counted using the Trypan Blue Exclusion method, to obtain accurate cell numbers. The volume of the cell suspension was adjusted to a density of 1 x10^6 cells per 100 µL, and 100 µL of the cell suspension was seeded onto the surface of the scaffold. Cells were left to adhere to the scaffold for at least 2 hours, before 10 mL medium was carefully added to the well. DEs were maintained in the normal cell maintenance media supplemented with Transforming Growth Factor β (Gibco) at a final media concentration of 5 ng/mL, and ascorbic acid at a final media concentration of 100 µg/mL. Scaffolds incubated at 37°C, 5 % CO_2, and were media changed every 3-4 days until required for further culture applications. At the first media change, the culture plate was replaced to account for cells falling through the scaffold and growing on the base of the plate.

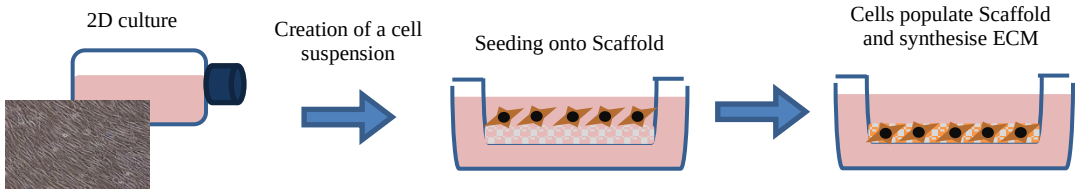


Figure 2.14: Schematic for the creation of dermal equivalent using fibroblasts in Alvetex® Scaffold: 1 million dermal fibroblasts were seeded onto the surface of a 6 well membrane in a 6 well plate and allowed to attach for at least 2 hours before the addition of 10 ml media. The fibroblasts are allowed to infiltrate and synthesise an endogenous extracellular matrix.

2.2.16 Seeding of aggregates/EBs on dermal equivalents for co-culture

To set up the co-culture model, dermal equivalents were set up in parallel with aggregates/EBs so that dermal equivalents and aggregates/EBs reached the appropriate mature time point on the same day.

On the day of seeding, maintenance media was aspirated from DEs, inserts were placed in a new 6 well plate and wells were topped up with the media of the aggregates/EBs to be seeded on the DE. Using a cut off pipette tip, 6-8 aggregates/EBs were transferred to the surface of the DE. Half and full media changes were performed every 3-4 days as required.

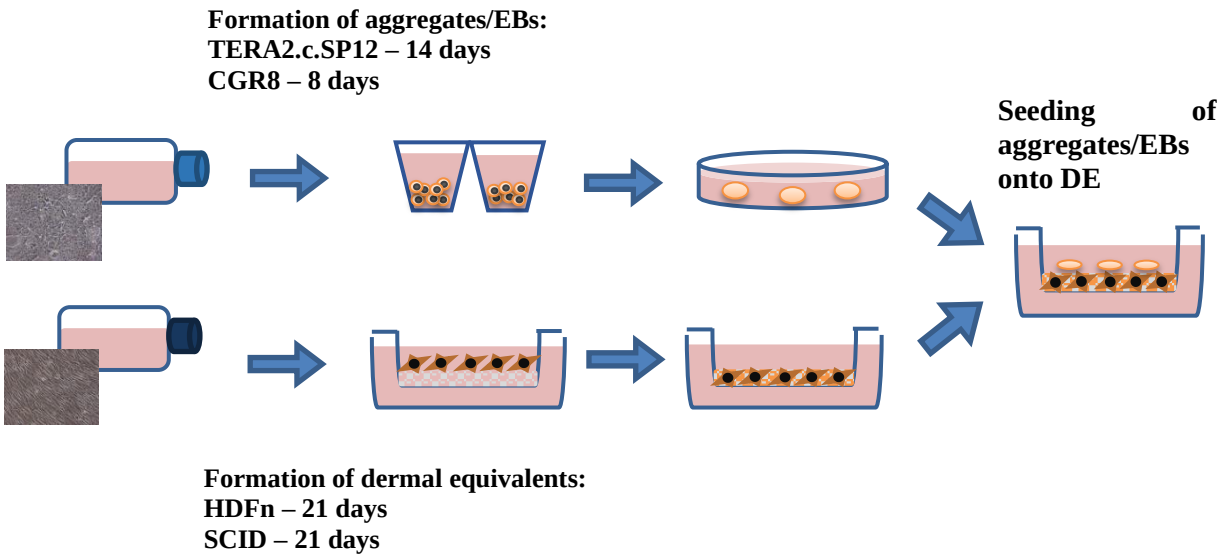


Figure 2.15: Schematic for the creation of co-culture model using dermal equivalents and stem cell aggregates: Dermal equivalents were set up initially due to the length of time required for the dermal equivalents to sufficiently form. Stem cell aggregates were subsequently set up following this to ensure that both cell cultures reach the mature timepoint in the same day.

2.3 Processing, sectioning and histological staining for assessment of tissue structure

2.3.1 Sample processing for wax embedding – aggregates and embryoid bodies

Aggregates/EBs were removed from Petri dishes and placed into a Falcon tube to settle to the bottom. Media was aspirated and aggregates/EBs resuspended in sterile PBS to wash. PBS was aspirated and fresh sterile PBS added again to wash. PBS was aspirated again, and 4% PFA added to the tube for fixation. Aggregates/EBs were fixed for 30 minutes at room temperature, before washing twice in PBS. Aggregates/EBs were then dehydrated by washing through a series of ethanols in the Falcon tube for a minimum of 15 minutes at room temperature as follows: 30 %, 50 %, 70 % with 0.1 % crystal violet for visualisation, 80 %, 90 %, 95 % and 100 %. Aggregates/EBs were then placed in Histoclear II (National Diagnostics, Lichfield, UK) for at least 30 minutes at room temperature. Liquid paraffin wax (Fisher Scientific UK) was added to the aggregates/EBs in a 1:1 ratio with the Histoclear II, and aggregates/EBs incubated at 60°C for at least 30 minutes. The Histoclear II:wax mixture was removed and 100 % paraffin wax added to the aggregates/EBs, which were incubated at 60°C for at least 60 minutes. To embed, Dispomoulds (CellPath, Powys, UK) were used, and a small amount of paraffin wax added to the base of the mould and allowed to partially set. Pre-warmed Pasteur pipettes were used to transfer the aggregates/EBs in liquid wax to the Dispomould. Once the wax had partially set, a tissue embedding cassette (Fisher Scientific UK) was placed on top, and more wax added to fill the mould. Wax blocks were left to completely set at room temperature overnight.

2.3.2 Sample processing for wax embedding – Alvetex® samples

Alvetex® inserts in culture were removed from the culture plates and unclipped to remove the Alvetex® disc. This was placed in fresh 6 well plate and washed in sterile PBS twice. PBS was aspirated and 4 % PFA was added to the well to fix, with the samples stored at 4°C overnight for fixation. Samples were then subsequently washed twice in PBS and dehydrated through the series of ethanols as described above for at least 15 minutes at room temperature. Samples were then placed in embedding cassettes, and transferred to a glass beaker for incubation in Histoclear II for at least 30 minutes at room temperature. Liquid paraffin wax was added to the glass beaker at the ratio of 1:1 with the Histoclear II and incubated at 60°C for at least 30 minutes. The Histoclear II:wax mixture was removed and replaced with 100 % liquid paraffin wax, and incubated at 60°C for at least 60 minutes. Dispomoulds had a small amount of wax added, which was allowed to partially set. The discs were removed from the embedding cassettes, cut in half, flattened on a surface and allowed to partially set before standing upright in the mould with the cut surface facing down. When the wax in the mould had further cooled, more wax was added to fill the mould, and the embedding cassette placed on top. Wax blocks were left to completely set at room temperature overnight.

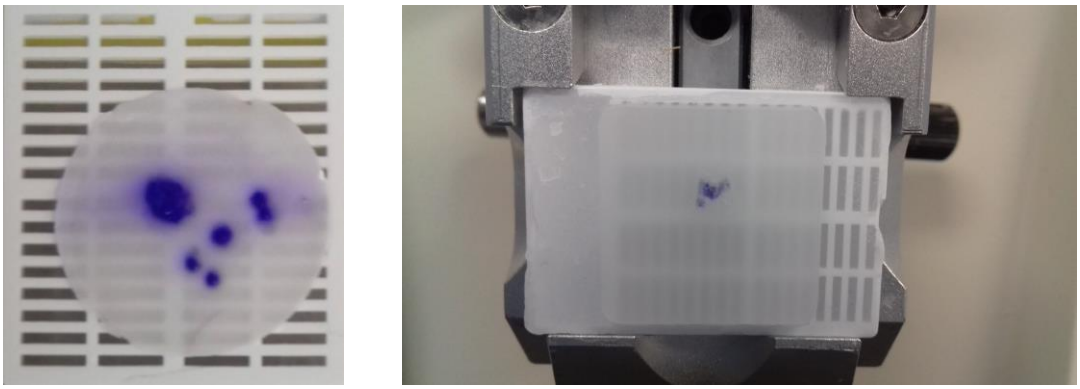


Figure 2.16: Stem cell aggregates stained with 0.01% crystal on the Polaris membrane and in a wax block: Aggregates/EBs and tissue discs are much easier to visualise when stained with crystal violet during the dehydration process, as can be seen in the wax block in the right image.

2.3.3 Sample sectioning

Wax blocks were mounted into a Leica EG1120 Microtome and sample sections of 5-7 µm cut. These were transferred to a waterbath set at 40°C, before mounting into SuperFrost™ Plus Microscope slides (Fisher Scientific UK). Slides were left to dry on a heated slide rack for at least 2 hours, or overnight, before staining.

2.3.4 Haematoxylin and Eosin staining

To analyse overall tissue structure, Haematoxylin and Eosin (H&E) staining was carried out according to the following protocol. Slides were deparaffinsed in Histoclear II for 15 minutes, before rehydration through 100 % ethanol for 2 minutes, 95 % ethanol for 1 minute, 70 % ethanol for 1 minute, and demineralised water (dH_2O) for 1 minute. Slides were stained in Mayer's Haematoxylin (Sigma Aldrich) for 5 minutes, before washing in dH_2O for 30 seconds, and incubating in alkaline alcohol for 30 seconds to blue the nuclei. Slides were dehydrated in 70 % ethanol and 95 % ethanol for 30 seconds each. Slides were stained in Eosin for 1 minute before 2 washes in 95 % ethanol for 10 seconds. Slides were then dehydrated in 100 % ethanol for 15 seconds, and then again in 100 % ethanol for 30 seconds. Slides were cleared twice in Histoclear II for at least 5 minutes in each. To mount, excess Histoclear II was carefully removed from the slides, and a small amount of DPX (Fisher Scientific UK) or Omni-mount (National Diagnostics) placed on the slide, before a coverslip was added to the top. Slides were left to dry and set for at least 30 minutes before imaging using a Leica Microscope.

2.3.5 Masson's Trichrome staining

Masson's Trichrome staining was used to ascertain the identity of tissue structures formed. Samples were stained as follows. Slides were deparaffinsed and rehydrated as described for H&E staining, finishing in dH_2O. Samples were then stained for 15 minutes in Weighert's Iron Haematoxylin, or until nuclei were stained, before washing in running tap water for around 10 minutes. Slides were rinsed in dH_2O, before staining in Biebrich Scarlet/Acid Fuschin for 8-10 minutes, and rinsing in dH_2O again. Slides were incubated in Phosphotungstic/Phosphomolybdic acid for 12 minutes, until collagen lost the red colouration as confirmed by microscopy. Slides were washed in dH_2O before staining in Aniline blue for 7 minutes. Slides were washed in dH_2O, before differentiation in 1 % acetic acid to remove excess stain. Slides were washed a final time in dH_2O, before dehydration in 70 %, 95 % and 100 % ethanol for 20 seconds each. Slides were cleared twice in Histoclear II for at least 5 minutes in each before mounting on coverslips in Omni-mount as described above.

Table 2.3: Colouration of structures as stained by Masson's Trichrome protocol

Structure	Staining colour
Nuclei	Black
Collagen, Cartilage, Bone	Blue
Muscle, Cytoplasm, Keratin	Red

2.3.6 Weighert's staining

Weighert's staining was also used alongside the other histological stains to identify the structures which formed. Slides were deparaffinsed and rehydrated as described for H&E staining, finishing in dH_2O. Slides were stained in Alcian Blue for 5 minues, before washing in dH_2O. Slides were then stained in Weighert's Iron Haematoxylin for 20 minutes, before rinsing in running tap water for around 10 minutes. Slides were washed in dH_2O, before washing 50 % ethanol and then 1 % acid alcohol. Slides were dehydrated in 70 % ethanol, washed in dH_2O and then stained in Ponceau S solution for 10 seconds. Slides were dehydrated in 95 % ethanol for 10 seconds, and 100 % ethanol for 1 minute, before clearing twice in Histoclear II for 5 minutes in each. Slides were mounted on coverslips as described using Omni-mount.

Table 2.4: Colouration of structures as stained by Weighert's staining protocol

Structure	Staining colour
Nuclei	Brown/Black
Cartilage	Pale blue
Bone	Red
Cytoplasm	Pink

2.3.7 Periodic Acid Schiff with Alcian Blue Staining

A Periodic Acid Schiff with Alcian Blue staining kit (Atom Scintific, Cheshire, UK) was used to confirm the identity and cellular distribution within epithelial surfaces. The staining was conducted in accordance with the manufacturers protocol Slides were deparraffinised and rehydrated as described for H&E staining, before staining using Alcian Blue solution for 10 minutes. Slides were washed well in dH_2O and treated with 1 % periodic acid for 5 minutes. Slides were then washed in dH_2O again before incubating in Schiff reagent for 20 minutes. Slides were washed in hot running tap water for 20 minutes, and stained in Haemalum Mayer for 30 seconds. Samples were then rinsed in running tap water, differentiated in 0.5 % acid alcohol and blued in tap water. Slides were then dehydrated through 70 % ethanol, 95 % ethanol and 100 % ethanol for 30 seconds each, and incubated in Histoclear II for 5 minutes, twice. Slides were then mounted as described using Omni-mount.

Table 2.5: Colouration of structures as stained by Periodic Acid Schiff with Alcian Blue stain

Structure	Staining colour
Acid mucins (sulfomucins and sialmucins)	Blue
Mixtures of both	Purple
Neutral mucins, Glycogen, various glycoproteins	Red
Proteoglycans and hyaluronic acid	Blue
Nuclei	Pale Blue

2.4 Techniques to assess cell and tissue identity

2.4.1 Immunofluorescent staining of paraffin sections

Immunofluorescent staining was used to identify the presence of specific transcription factors and proteins within tissue samples. Slides were first deparaffinised in Histoclear II for at least 15 minutes, before rehydration for 5 minutes each in 100 % ethanol, 95 % ethanol, 70 % ethanol and dH_2O. Antigen retrieval was performed by incubation in citrate buffer at 95°C for 20 minutes, and slides were cooled by the addition of dH_2O. Blocking buffer was made up with either 20 % normal goat serum (NGS, Sigma Aldrich) or, for CGR8 teratoma slides, 20 % newborn calf serum (NCS, Fisher Scientific UK) in 0.4 % Triton-X-100 in PBS, and slides were blocked for at least 1 hour at room temperature. Primary antibodies diluted in blocking buffer were added at the appropriate concentrations, and incubated at 4°C overnight. The next day, slides were washed 3 times in PBS before addition of appropriate fluorescently conjugated secondary antibodies and the nuclear stain Hoescht diluted in blocking buffer. Slides were incubated at room temperature for one hour before washing 3 times in PBS. Slides were mounted in Vectashield™ (Vector Labs, Peterborough, UK) and a cover slip placed on top, which was sealed around the edges using nail varnish. Slides were stored at 4°C until imaging.

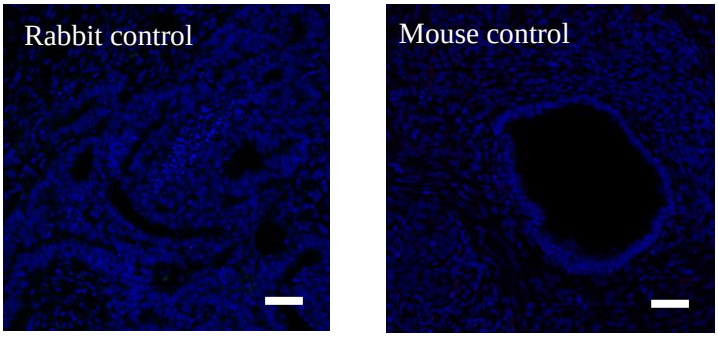


Figure 2.17: Secondary antibody controls for Rabbit and Mouse secondary antibodies: To detect levels of secondary antibody background staining, slides with the same sample or cell type (aggregate, tissue disc or teratoma) were incubated with the secondary antibody only. These samples were used to adjust the laser power and gain on the confocal microscope in order to reliably detect positive staining. Scale bars: 100 µm

2.4.2 Immunofluorescent staining of glass coverslips

Coverslips in a 12 well plate were placed on ice, and permeabilised in 0.1 % Triton-X-100 in PBS for 15 minutes. Permeabilisation solution was removed from the well using a Pasteur pipette, and coverslips were then blocked in a buffer consisting of 10 % NGS in 0.1 % Tween20 in PBS solution for 60 minutes. 50 µL of the desired antibody at the appropriate concentration was pipetted onto Parafilm (Fisher Scientific UK) in a plastic tray, coverslips were removed from the plate and placed on the Parafilm with the cells in contact with the antibody solution. Primary antibodies were

incubated for 60 minutes, and coverslips were washed in blocking buffer by moving onto 50 µL droplets of blocking buffer on the Parafilm for 10 minutes. This was repeated 3 times. Coverslips were then placed onto 50 µL droplets of the appropriate secondary antibody and Hoescht nuclear stain at the correct concentration for 60 minutes, before washing again as described. To mount, a small amount of Vectashield™ was placed on a SuperFrost™ Plus slide, excess PBS carefully blotted from the coverslip, and the coverslip placed onto the Vectashield™ on the slide. The coverslips were sealed with nail varnish, allowed to dry and stored at 4°C until imaging.

Table 2.6: Primary antibodies used for immunofluorescent staining

Marker	Description	Supplier	Product code	Concentration	Species
Oct 4	Pluripotency associated transcription factor	Abcam	ab19857	1:100	Rabbit
Sox 2	Pluripotency associated transcription factor	Abcam	ab97959	1:100	Rabbit
SSEA4	Pluripotency associated extracellular protein	Abcam	ab16287	1:100	Mouse
SSEA-1	Pluripotency associated extracellular protein	Abcam	ab16285	1:100	Mouse
TRA-1-60	Pluripotency associated extracellular protein	Abcam	ab16288	1:100	Mouse
Nestin (Human)	Early neural differentiation marker	Merck Millipore	MAB 5326	1:200	Mouse
Nestin (Mouse)	Early neural differentiation marker	Abcam	ab11306	1:200	Mouse
Class III β-tubulin	Mature neuronal marker	Biolegend	802001	1:600	Rabbit
Cytokeratin 8	Epithelial ectoderm marker	Sigma	C5301	1:200	Mouse
E-cadherin	Cell junctional marker	BD Biosciences	610181	1:200	Mouse
Collagen 4	Basement membrane protein	Abcam	ab6586	1:100	Rabbit
α smooth muscle actin	Myofibroblast cytoskeletal protein	Abcam	ab7817	1:100	Mouse
GATA4	Mesoendoermal transcription factor	Abcam	ab84593	1:50	Rabbit
Cytokeratin 10	Stratum corneum differentiation protein	Abcam	ab76318	1:100	Rabbit

Collagen 3	Extracellular matrix protein	Abcam	ab7778	1:100	Rabbit
Fibronectin	Extracellular matrix protein	Abcam	ab23750	1:100	Rabbit
Vimentin	Fibroblast cytoskeletal markers	Abcam	ab92547	1:200	Rabbit
Collagen 1	Extracellular matrix protein	Abcam	ab34710	1:100	Rabbit
Loricrin	Terminal differentiation marker	Abcam	ab85679	1:100	Rabbit
Filaggrin	Terminal differentiation marker	Abcam	ab17808	1:100	Mouse
Cytokeratin 14	Epidermal basal cell marker	Abcam	ab7800	1:100	Mouse

Table 2.7: Secondary antibodies used for immunofluorescent staining

Secondary antibody	Concentration	Supplier	Product code
Goat anti Mouse Alexa Fluor 594	1:1000	Invitrogen	A11005
Goat anti Rabbit Alexa Fluor 488	1:600	Invitrogen	A11034
Donkey anti Mouse Alexa Fluor 594	1:1000	Invitrogen	A21203
Donkey anti Rabbit Alexa Fluor 488	1:600	Invitrogen	A21206
Hoescht 33342	1:1000	Life Technologies, Fisher Scientific UK	H3570

2.4.3 Microscopy

Histological staining was imaged using the Leica DM500 (Leica Microsystems, Wetzlar DE).

Immunostained samples were imaged using the Zeiss LSM 880 confocal microscope with Airyscan or Zeiss Axioscope.

2.4.4 Flow cytometry

To more quantitatively assess the identity of both 2D and 3D cells, flow cytometry was used. 2D cells were washed in sterile PBS and detached from the culture flask using the appropriate detachment method to obtain a single cell suspension. 3D aggregates and tissue discs on Alvetex®

Polaris were also washed and treated with 0.25 % trypsin/2 mM EDTA in a Falcon and plate respectively, in order to detach and dissociate the structures to form a single cell suspension. The cell suspension was then counted, and washed 2 times in PBS by centrifugation. For extracellular markers, cells were resuspended in blocking buffer, consisting of 0.1 % bovine serum albumin (Sigma Aldrich) in PBS until staining was performed. For intracellular markers, cells were fixed on ice in 4 % PFA for 20 minutes, washed twice in PBS, and permeabilised in a buffer consisting of 0.2 % Triton-X-100 in PBS for 15 minutes before resuspending in blocking buffer ready for staining.

Prepared cells were seeded into a round bottom 96 well plate at a density of 2 x 10^5 cells per well, with three wells used per antibody. The plate was centrifuged to pellet cells and excess buffer removed. Cells were resuspended in 50 µL of primary antibody and left to incubate on ice for 60 minutes. Cells were washed 3 times by centrifugation and resuspension in 150 µL blocking buffer, before cells were resuspended in 50 µL of fluorescently conjugated secondary antibody. Cells were incubated in the dark on ice before washing twice by centrifugation and resuspending in 200 µL to be read using the Guava EasyCyte Flow cytometer. Appropriate negative, species and secondary antibody controls were run with each plate in order to gate the data obtained.

Table 2.8: Primary antibodies used for flow cytometry analysis

Marker	Description	Supplier	Product code	Concentration	Species
SSEA-1	Pluripotency associated extracellular protein	Abcam	ab16285	1:100	Mouse
SSEA-4	Pluripotency associated extracellular protein	Abcam	ab16287	1:100	Mouse
TRA-1-60	Pluripotency associated extracellular protein	Abcam	ab16288	1:200	Mouse
A2B5	Neural associated extracellular protein	R&D systems	MAB1416	1:100	Mouse
Oct 4	Pluripotency associated transcription factor	Abcam	ab19857	1:100	Rabbit
Sox 2	Pluripotency associated transcription factor	Abcam	ab97959	1:100	Rabbit
Nanog	Pluripotency associated transcription factor	Abcam	ab21624	1:100	Rabbit
Nestin	Early neural differentiation marker	Merck Millipore	MAB 5326	1:200	Mouse
Class III β-tubulin	Late neural differentiation marker	Biolegend	802001	1:600	Rabbit
Cytokeratin 8	Epithelial ectoderm marker	Sigma Aldrich	C5301	1:200	Mouse

Table 2.9: Secondary antibodies used for flow cytometry analysis

Secondary antibody	Concentration	Supplier	Product code
Goat anti Mouse IgG Alexa Fluor 488	1:100	Invitrogen	A11001
Goat anti Rabbit IgG Alexa Fluor 488	1:600	Invitrogen	A11034
Goat anti Mouse IgM FITC	1:100	Sigma Aldrich	M8644

In order to determine the single cell population to be analysed, cellular fragments, debris and clumps of cells were excluded by assessing the forward and side scatter of an unstained well and placing the gate around the selected population. Species specific sera were used to assess non-specific primary antibody binding, and thereby set a gate for true antibody binding and the corresponding areas of the histograms to be analysed. Secondary antibody controls were also carried out, although these did not generally produce any more notable non specific binding than the serum controls.

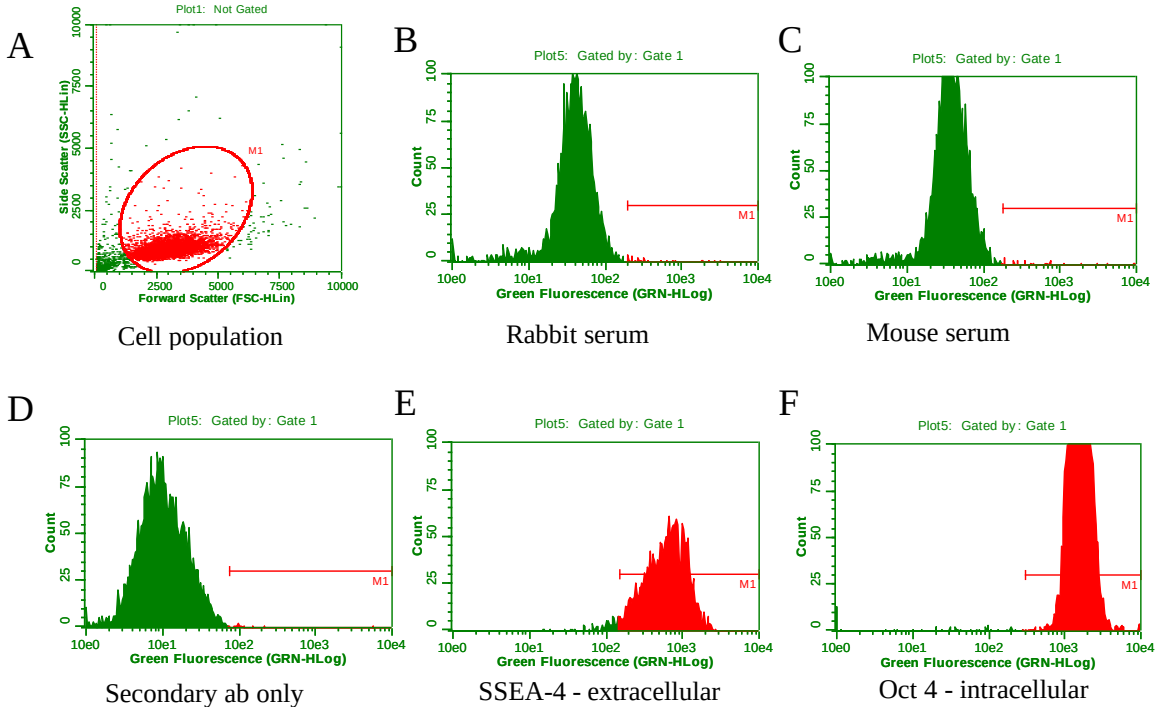


Figure 2.18: Representative control settings and antibody histograms from flow cytometry analysis: The relevant cell population was gated out using the scatter plot as shown in (A), with the relevant cell population contained in the circle in red. Images (B) and (C) show representative histograms of non specific binding for rabbit and mouse serum respectively. An appropriate gate was placed at the point at which the peak ended, in order to allow for the selection of positively stained populations. As shown by image (D), secondary antibody non specific binding did not interfere with the detection of positive staining. Images (E) and (F) are examples of extracellular marker SSEA4, and intracellular markers Oct 4, respectively.

2.4.5 Western blotting: Lysate preparation and protein concentration determination

To assess protein expression, samples were analysed by Western Blotting. Protein lysates were created by lysing PBS washed samples in Mammalian Protein Extracting Reagent™ (MPER, Fisher Scientific UK) with 1 % Protease and Phosphatase Inhibitor Cocktail (Fisher Scientific UK) on ice. Lysates were vortexed every 5 minutes for 30 minutes, and sonicated for 30 minutes to ensure that samples were thoroughly homogenised. Samples were centrifuged at 12,000 rpm for 20 minutes, supernatant removed and stored at -80°C until use.

Protein concentration was ascertained using a Bradford Assay. 5 µL of sample was combined with 250 µL of Bradford Reagent (Bio-Rad, Oxford, UK) in a flat bottom 96 well plate, and left to incubate for at least 10 minutes before reading at 595 nm on a Microplate Spectrophotometer. A series of protein standards were also run at the same time in order to create a standard curve to determine protein concentration using the equation of the line.

2.4.6 Western blotting: Gel casting, loading, running and transfer

Polyacrylamide gels were cast using the Mini Protean Gel Casting System (Bio-Rad) at 8 % or 10 %, depending on the size of proteins to be assessed. Prior to loading, samples were combined 4:1 with Laemmli sample buffer (Bio-Rad) and boiled at 95°C to ensure samples were denatured. 10 µg of sample was loaded into each well, with the PageRuler Protein Ladder (Fisher Scientific UK) for comparison and samples were run at 100 V for 90 to 120 minutes, or until the samples were fully separated within the gel. Gels were transferred onto Nitrocellulose membranes (GE Healthcare Life Sciences, Buckinghamshire, UK) overnight at 4°C, before staining with Ponceau S to check protein transfer and separation and washed in dH_2O to remove excess stain.

2.4.7 Western blotting: Membrane blocking, antibody incubations and exposure

Membranes were blocked in 5 % milk solution for at least 2 hours. Primary antibodies were diluted in 5 mL milk, and placed in Falcon tubes with membranes on a roller to incubate overnight at 4°C. The next day, membranes were washed in Blot Rinse Buffer (BRB) 3 times for 10 minutes each. Membranes were placed in a Falcon with the appropriate secondary antibody conjugated to horse radish peroxidase, and incubated on a roller for 60 minutes at room temperature. Membranes were then washed in BRB 3 times for 10 minutes each, and placed on clingfilm. Clarity™ ECL (Bio-Rad) was made up by combining the two solutions (peroxide reagent and enhancer solution) in a 1:1 ratio, with 1 mL total solution made up per membrane. The solution was applied and the membrane enclosed in the clingfilm, and left to incubate for around 5 minutes. Membranes were then taken to the dark room and exposed to CL-Xposure X-ray film (Fisher Scientific UK) for an appropriate time,

and developed to visualise protein expression. Developed films were scanned at high resolution, converted to JPEG format and analysed using Image J software.

Table 2.10: Primary antibodies used for Western Blotting analysis

Marker	Description	Supplier	Product code	Concentration	Species
β-actin	Housekeeping protein	Abcam	ab8224	1:5000	Mouse
Class III β-tubulin	Late neural differentiation marker	Biolegend	802001	1:1000	Rabbit
E-cadherin	Epithelial junctional protein	BD Biosciences	610181	1:500	Mouse
α smooth muscle actin	Myofibroblast cytoskeletal protein	Abcam	ab7817	1:500	Mouse
GATA4	Mesoendodermal transcription factor	Abcam	ab84593	1:500	Rabbit
Cytokeratin 10	Stratum corneum differentiation protein	Abcam	ab76318	1:100	Rabbit

Table 2.11: Secondary antibodies conjugated to horseradish peroxidase used for Western Blotting

Secondary antibody	Concentration	Supplier	Product code
Goat anti Mouse HRP	1:5000	Sigma	A4416
Donkey anti Goat HRP	1:10000	Merck Millipore	AP18P
Donkey anti Rabbit HRP	1:10000	Merck Millipore	AP182P

2.4.8 PCR analysis: RNA lysate preparation

RNA isolation was performed using the Reliprep RNA Cell Miniprep Kit (Promega UK, Southampton UK), all reagents were prepared and protocols followed according to the maunfacturer's instructions. Briefly, samples were removed from their culture conditions: embryoid bodies were placed into a sterile Eppendorf and allowed to collect in the base of the tube and Alvetex inserts were unclipped and placed in the bottom of a 12 well plate. Samples were washed in ice cold PBS which was then aspirated, before BL+TG buffer was applied to the samples to lyse. The buffer was pipetted over the samples several times to aid lysis of the samples, before storage at -80°C until RNA isolation was performed. Samples were allowed to thaw on ice, before isopropanol was added to the samples, which were mixed by vortexing. Samples were then transferred to Minicolumns in collection tubes, and centrifuged at 13,000 rpm for 30 seconds. The column eluate was discarded, and 500 µL of RNA column wash was added to the column, which was then centrifuged again at 13,000 rpm for 30 seconds, and the eluate discarded. A DNase incubation mix was created by combining the following reagents for each sample:

Reagent	**Volume/µL**
Yellow Core Buffer	24
0.09M $MnCl_2$	3
DNase 1	3

Reagents were mixed by gentle pipetting, and 30 µL added to each sample column, covering the membrane. Samples were incubated for 15 minutes at room temperature, after which 200 µL of Column Wash Buffer was added to Minicolumns. Minicolumns were centrifuged at 13,000 rpm for 15 seconds, and 500 µL of RNA Wash buffer was added to the Minicolumns, which were centrifuged again at 13,000 rpm for 30 seconds. Collection tubes and eluate were discarded, and the Minicolumns placed in new collection tubes, with 300 µL of RNA Wash buffer added. Minicolumns were centrifuged again at 13,000 rpm for 2 minutes, and the collection tubes and eluate discarded. The Minicolumns were placed into 1.5 mL Elution tubes, and 20 µL of Nuclease Free water added to the columns for RNA collection. Minicolumns were centrifuged at 13,000 rpm for 1 minute to collect the RNA. RNA yield and quality was assessed using the Nanodrop Spectrophotometer (Fisher Scientific UK). Samples were stored at -80°C until cDNA synthesis.

2.4.9 PCR analysis: cDNA synthesis

cDNA synthesis was performed using the High Capacity cDNA Reverse Transcription Kit (Applied Biosystems, Fisher Scientific UK). Protocols were followed according to the manufacturer's

instructions. The appropriate volume of RNA required to make 1 µg, 0.5 µg or 0.25 µg of cDNA was calculated for each sample, and a 2X Master Mix was made, with the following reagent volumes.

Reagent/component	**Volume per sample reaction/µL**
10x RT buffer	2 µL
25x dNTP mix (100 mM)	0.8 µL
10x RT Random primers	2 µL
MultiScribe™ Reverse Transcriptase	1 µL
Nuclease Free water	4.2 µL
RNA sample	10 µL
Total reaction volume	*20 µL*

The components were placed in a 0.2 mL PCR tube, centrifuged briefly to ensure all components were at the base of the tube and placed in a thermocycler on the appropriate programme as specified in the manufacturer's instructions. The thermocycler programme was set as follows:

Settings	**Step 1**	**Step 2**	**Step 3**	**Step 4**
Temperature	25°C	37°C	85°C	4°C
Time	10 minutes	120 minutes	5 minutes	∞

2.4.10 PCR analysis: Primer preparation and SYBR PCR reaction

Primers sequences used were obtained from PrimerBank (Massachusetts General Hospital, The Center for Computational and Integrative Biology and Harvard Medical School) and from the Li et al 2015 paper where appropriate. Primer sequences were as follows:

Table 2.12 Primer sequences used for PCR analysis of gene expression

Gene	**Forward primer**	**Reverse primer**
Cytokeratin 10	GCCTCCTACATGGACAAAGTC	GCTTCTCGTACCACTCCTTGA
Cytokeratin 14	AAGGTCATGGATGTGCACGAT	CAGCATGTAGCAGCTTTAGTTCTTG
Class III β-tubulin	CCCAGCGGCAACTATGTAGG	CCAGACCGAACACTGTCCA
E-cadherin	CAGGTCTCCTCATGGCTTTGC	CTTCCGAAAAGAAGGCTGTCC
Brachyury	GCTTCAAGGAGCTAACTAACGAG	CCAGCAAGAAAGAGTACATGGC
Alpha fetoprotein	CTTCCCTCATCCTCCTGCTAC	ACAAACTGGGTAAAGGTGATGG
FOXA2	CCCTACGCCAACATGAACTCG	GTTCTGCCGGTAGAAAGGGA
GATA6	TTGCTCCGGTAACAGCAGTG	GTGGTCGCTTGTGTAGAAGGA
SOX17	CGAGCCAAAGCGGAGTCTC	TGCCAAGGTCAACGCCTTC
GAPDH	AGGTCGGTGTGAACGGATTTG	TGTAGACCATGTAGTTGAGGTCA

Custom made oligonucleotides based on the primer sequences were ordered from Sigma Aldrich in the salt format and reconstituted at a concentration of 1 mg/mL. A stock solution for each gene was created by combining the following:

Table 2.13 Reagents used to create stock solution of primers

Component	**Volume**
Forward Primer	10 µL
Reverse Primer	10 µL
RNase free dH_2O	80 µL
Total volume	*100 µL*

Primers were further diluted 1 in 4 with RNase free dH_2O prior to use in the PCR reaction.

The SsoAdvanced™ Universal SYBR® Green Supermix dye (Biorad) was used to detect PCR products. Primers, samples and reagents were thawed on ice prior to use and pipetted into a low profile Hard-Shell Skirted 96 well PCR plate (Biorad). Dependent upon the reaction volume used, samples and reagents were calculated and pipetted as follows:

Table 2.14: SYBR reaction mix reagent volumes

Reagent/component	**20 µL reaction**	**10 µL reaction**
2X SYBR dye	10 µL	5 µL
Forward/Reverse Primer	1 µL	1 µL
Sample	Variable	Variable
RNase Free dH_2O	Variable	Variable
Total volume	*20 µL*	*10 µL*

Plates were sealed with an adhesive Plate Seal (Biorad). The plate was centrifuged for 3 minutes at 1000 rpm to ensure the reagents and components were mixed at the bottom of each well. Plates were then stored at 4°C for up to 3 hours prior to running in the thermocycler.

The thermocycler programme was set as follows:

Polymerase activation and DNA denaturation	**Denaturation at 95°C**	**Annealing/Extension and Plate Read at 60°C**	**Cycles**	**Melt Curve Analysis**
30 seconds at 95°C	15 seconds	15 seconds	40	95°C

All primers were validated prior to use, using a range of cDNA amounts – 60 ng, 30 ng, 15 ng and 7.5 ng (see Appendix for primer optimisation data).

2.5 Techniques to assess structure, size and viability

2.5.1 Aggregate measuring

In order to measure the size of cellular aggregates, phase contrast or H&E stained images were opened in Image J software. An appropriate haemocytometer image was opened to set the scale correctly, and aggregates were traced around continuously using the Freehand line tool. Only aggregates which were fully visible in the field of view were measured. When it was unclear whether a structure was composed of one of two aggregates, the structure was not measured. Measurement values were generated automatically by Image J software (https://imagej.nih.gov/ij/).

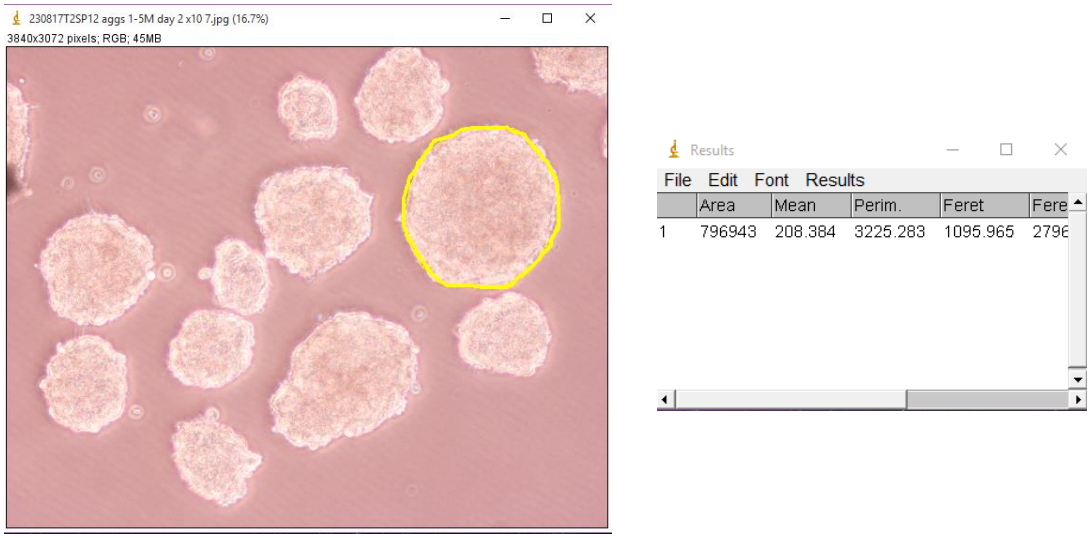


Figure 2.19: Phase contrast image of TERA2.cl.SP12 aggregate in suspension culture opened in Image J for measurement: Aggregates were traced around using the Freehand tool and measurements taken using the automatic measuring function in Image J.

2.5.2 Cell layer and infiltration measuring

In order to assess the height of the cell layer or the level of infiltration into the Alvetex® insert, H&E stained images were taken across the length of the insert at random at x10 or x20 magnification. Images were opened in Image J software, and a square grid overlaid onto the image using the Grid function. A random number generator was used to select 10 squares across the insert to measure the infiltration. Cell layer height was measured by measuring from the edge of the Alvetex® insert to the highest point of the intact cellular layer in that square. Infiltration was measured by measuring the invasion of the cells from the edge of the Alvetex® insert to the furthest point into the insert in that square. This was repeated over 5 images per insert, and the mean cell layer height or infiltration

calculated. This was repeated for the top and base insert in any sandwich culture where infiltration was assessed.

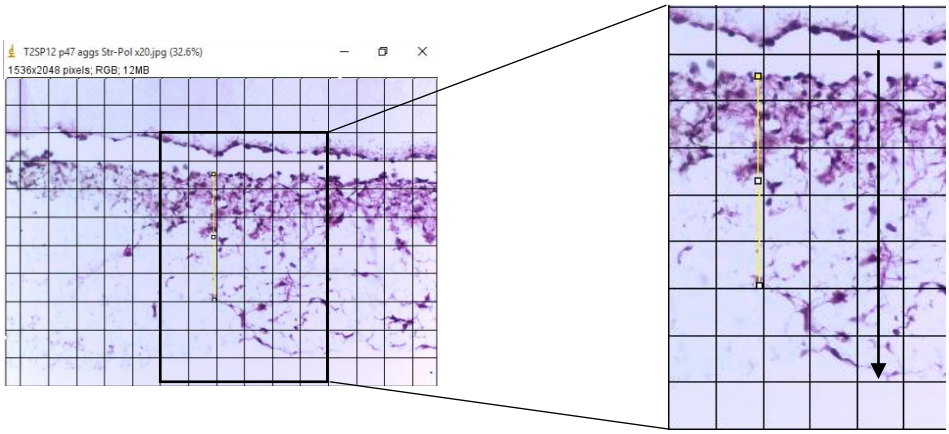


Figure 2.20: H&E stained image of TERA2.cl.SP12 aggregates cultured in the sandwich culture set up prepared for measuring cell layer infiltration: A grid was overlaid onto the image to be measured and a random number generator used to determine which column to measure the infiltration or cell layer height. The furthest cellular migration from the surface of the Alvetex® was measured.

2.5.3 TUNEL assay

The DeadEnd™ Fluorometric TUNEL assay system (Promega) was used to assess apoptotic cell death in PFA fixed, paraffin wax embedded sample sections. The manufacturer's protocol was followed as described.

Slides were deparaffinised in Histoclear II twice for at least 5 minutes per wash, before washing in 100 % ethanol for 5 minutes. Slides were then rehydrated through series of ethanols for 3 minutes in each: 100 %, 95 %, 80 %, 70 % and 50 %. Slides were washed in 0.85 % NaCl solution for 5 minutes, before washing in PBS for 5 minutes. Samples were fixed in 4 % PFA at room temperature for 15 minutes, before 2 further washes in PBS for 5 minutes. Excess liquid was blotted from the slide, and a 20 µg/mL Proteinase K solution added and incubated at room temperature for 8-10 minutes. Slides were washed in PBs for 5 minutes. Samples were fixed in 4 % PFA again for 5 minutes at room temperature, and again washed in PBS for 5 minutes. At this point, a positive control slide was created by the addition of 100 U/mL DNase solution to a slide for 5 minutes. Following this, excess liquid was removed from the slides, and Equilibration buffer added for 5-10 minutes. During sample equilibration, Nucleotide Mix and rTdT enzyme were thawed on ice, and calculations for reaction mix completed. A master reaction mix was created, with 45 µL of Equilibration buffer, 5 µL of Nucleotide Mix and 1 µL of rTdT enzyme per slide. Equilibration buffer was removed from the slides, 50 µL of the reaction mix was added to each slide directly onto the sample, with parafilm used to keep the solution in place. Slides were incubated in a humidified chamber at incubated at 37°C for 60 minutes. To terminate the reaction, slides were washed in the dark in 2X SSC buffer for 15 minutes

at room temperature. Slides were washed twice in PBS for 5 minutes to wash away unincorporated nucleotides, nuclei stained using Hoescht and coverslips mounted in Vectasheild™ with nail varnish. Slides were stored at 4°C until imaging.

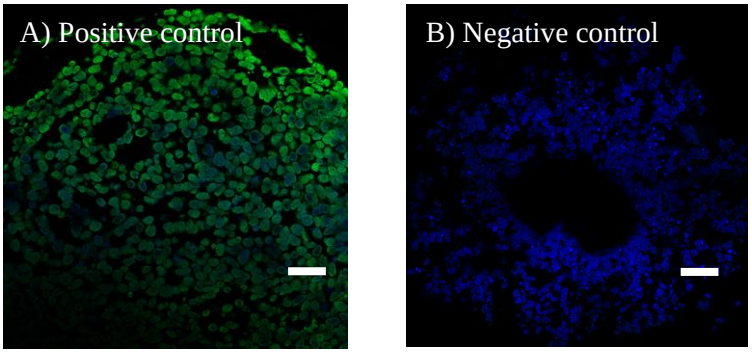


Figure 2.21: Antibody control slides generated for TUNEL staining: Images show representative confocal images of (A) positive control generated by treating samples with a DNase prior to incubation with the reaction mix, and (B) negative control samples generated by adding dH_2O to the reaction mix in place of rTdT enzyme. Scale bars: 100 µm

2.5.4 MTT assay

In order to assess the viability of cells after culture using various methods, cells were subject to an MTT assay. 2D cells in culture plates were washed in sterile PBS, or Alvetex® inserts were transferred to 12 well plates before washing in sterile PBS. PBS was then aspirated, Thiazolyl Blue Tetrazolium Bromide powder (MTT, Sigma Aldrich) was dissolved in phenol free DMEM (Fisher Scientific UK) at a concentration of 1 mg/mL, and 1 mL added to each well. Cells were incubated at 37°C, 5 % CO_2 for 60 minutes, before MTT solution was aspirated. 1 mL of acidified isopropanol was added to each well to lyse cells, which were placed in the dark on a shaker set at 80 rpm for 10 minutes. Sample solution was then diluted appropriately in isopropanol to a total volume of 200 µL and placed in a flat bottomed 96 well plate. Samples were then read at 570 nm on a microplate spectrophotometer.

3. Assessment of the methods used to confirm the pluripotency and developmental potential of human pluripotent stem cells

3.1 Introduction

The study of human developmental processes is inherently linked to the study of cellular pluripotency, and with that, the techniques and methods which are used to confirm this property in stem cell populations. Characterisation of the more subtle yet critical property of developmental potency is also a fundamental aspect of this, as biological variability in the differentiation capacity of pluripotent stem cells is a key issue in the creation of robust differentiation protocols for studying developmental processes and future regenerative therapies.

3.1.1 Pluripotency as a cell state

Pluripotent stem cells are defined by their ability to both self-renew and produce differentiated progeny comprising of cells from the three germ layers – Ectoderm, Mesoderm and Endoderm. Confirmation of pluripotency is an essential aspect of the characterisation of novel stem cell populations, as it is this property that makes these cells so desirable and useful. The pluripotent state has a characteristic profile: this can be exploited to confirm the property in putative stem cell populations at both the cellular and molecular levels. PSCs have a characteristic morphology *in vitro*, with a small cell size, large nuclear to cytoplasmic ratio and prominent nucleoli (Takahashi et al., 2007; Thomson et al., 1998), allowing for a very basic identification following initial derivation. The detection of alkaline phosphatase activity is also a rapid method for ascertaining pluripotent populations (O'Connor et al., 2008). The detection of factors which are known to be involved in the regulation of pluripotency, such as the core set of transcription factors Oct 4, Sox 2 and Nanog (De Los Angeles et al., 2015) and extracellular epitopes which are expressed in known pluripotent populations, such as glycosphingolipids SSEA-3 and SSEA-4 and carbohydrates TRA-1-60 and TRA-1-81 (Brimble et al., 2007; Natunen et al., 2011) provides a very simple method to ascertain the pluripotent state and allows for the collection of quantitative data. Techniques involving the detection of these transcription factors and extracellular proteins are wide ranging, and include flow cytometry, immunocytochemistry and analysis of gene expression (Asprer and Lakshmipathy, 2015), and it is common practice to undertake multiple methods of analysis during the characterisation process, with representative results for each shown in Figure 3.1.

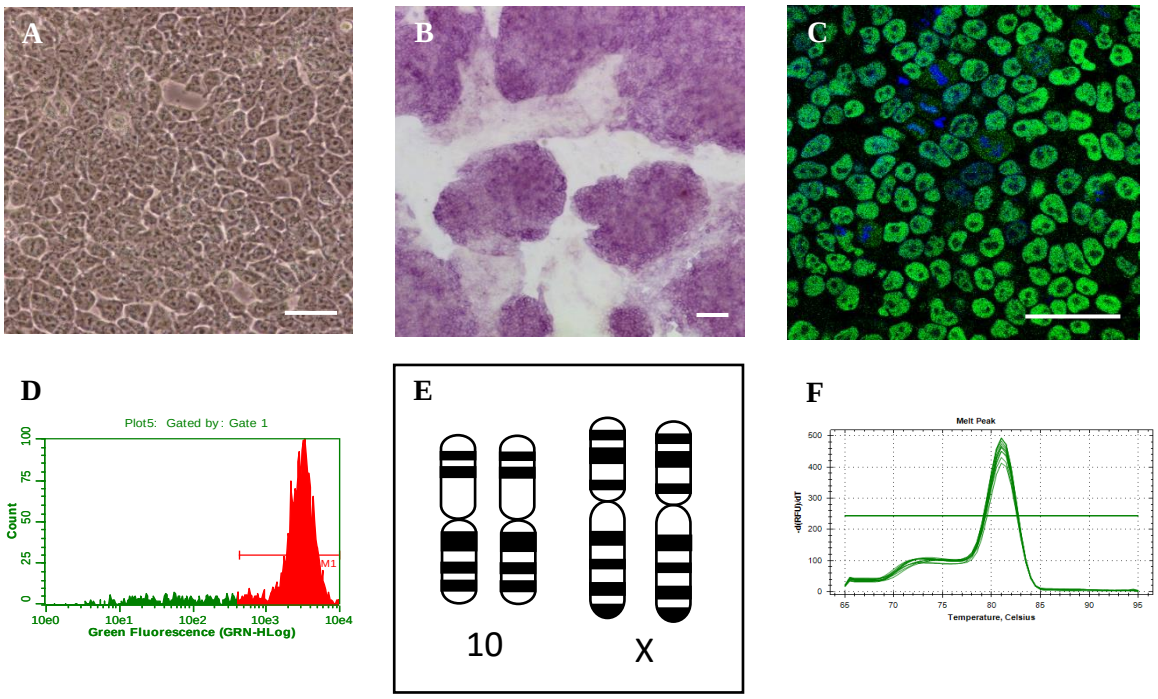


Figure 3.1: Methods used to assess the pluripotency as a state during the characterisation of putative human PSC lines: Representative results from analyses used to phenotypically detect cellular pluripotency. Single analyses alone are insufficient for confirmation; multiple methods need to be used in order to conclusively establish this property. A) Phase contrast image of human PSCs *in vitro* shows typical stem cell morphology with prominent nucleoli and high nuclear to cytoplasmic ratio. B) ES cell colonies stained positively for alkaline phosphatase activity show a typical positive result. C) Immunocytochemistry for the pluripotency associated transcription factor Oct 4 with strong expression and expected nuclear localisation in the majority of cells. D) Representative histogram showing strong expression of the extracellular marker Oct 4 following flow cytometric analysis of a PSC population. E) Schematic of a typical chromosomal banding pattern from cellular karyotyping. F) Melt curve indicating a pure PCR product during qPCR analysis of gene expression. Scale bars: (A, B) 100 µm, (C) 50 µm

The possession of a set of definitive markers known to be detected only in pluripotent stem cell populations would be of great use to the stem cell community (Singh et al., 2016), and while variability in expression profiles dependent on the cell population is noted (International Stem Cell Initiative et al., 2007), many of the factors mentioned above are strongly associated with the stem cell phenotype. However, the identification of markers solely specific to pluripotent stem cell populations has proven difficult to achieve, introducing difficulty and doubt into the process of PSC characterisation. Other non-pluripotent stem cell populations have been shown to express the same transcription factors and extracellular markers, including mesenchymal stem cells (Matic et al., 2016) and peripheral blood mononuclear cells (Zangrossi et al., 2007). This is a particularly important issue for the characterisation of induced pluripotent stem cell populations. Due to their derivation from somatic cell lineages, it may be more difficult to detect cells which have not fully responded to the reprogramming process if the original cell source expressed any of these markers used to determine

pluripotency. In addition, the expression of a given pluripotency marker does not necessarily correlate with the expression of any other pluripotency marker, and, perhaps more pertinently, the phenotypic expression profile of a PSC population does not always correlate with the functional capacity of a stem cell population to differentiate (Palmqvist et al., 2005) as the mechanisms which execute lineage determination and differentiation are somewhat independent from those that regulate and maintain access to the ability to enter these pathways (Cahan and Daley, 2013). De Los Angeles sums this up succinctly and clearly, commenting that 'molecular signatures can suggest pluripotency,' but that 'only functional tests can establish the true developmental potential of a cell' (De Los Angeles et al., 2015). Thus, functional tests for the characterisation of PSCs are critical to this process, providing more comprehensive information on what is possibly considered the most desirable property of PSC populations: their ability to differentiate.

3.1.2 Developmental potency: pluripotency as a cell function

As discussed in section 3.1.1, techniques which assess pluripotency as a state or phenotype are insufficient for the full characterisation of PSC populations due to their lack of specificity and inability to determine the differentiation capacity of PSC populations. These phenotypic analyses also fail to indicate the ability of PSCs to differentiate into specific cell lineages (Ortmann and Vallier, 2017), a key factor for future studies in development and regenerative medicine. Functional assays are even more important when the natural biological heterogeneity among PSCs is considered, a factor which impacts both on expression profile and differentiation capacity. The heterogeneity in differentiation capacity, termed developmental potency, is impacted on by differences in mechanisms including gene expression, cell signalling, DNA methylation and epigenetics, the latter two of which is especially important in iPSC populations (Ortmann and Vallier, 2017).

The functional tests available for the assessment of developmental potency are wide ranging in their nature, but all rely on promoting differentiation within these putative stem cell populations. Using traditional cell culture, this can be achieved simply by removing pluripotency maintaining conditions from PSCs in order to encourage spontaneous differentiation. In feeder based systems, this is the removal of mitotically inhibited fibroblast feeder layers (Thomson et al., 1998), whereas in feeder free systems, differentiation can be promoted by the removal of cytokines which maintain the pluripotent state, which in the case of human PSCs, is usually basic Fibroblast Growth Factor (Eiselleova et al., 2009). The addition of exogenous morphogens to cultures can provide more definitive results on the ability of PSCs to differentiate towards specific cell lineages (Schuldiner et al., 2000). The formation of differentiated cells using this method is fairly quick, and when combined with immunofluorescent and quantitative analytical techniques such as PCR, a good overview of the differentiation which has occurred can be established. However, these methods are naturally restricted by the two dimensional cellular microenvironment, many of the flaws of which were discussed in section 1.2.3.1. This means that while simple cellular differentiation can be achieved,

the formation of complex or mature structures is unlikely due to the artificial microenvironmental cues that cells are exposed to. In a similar way to the assessment of the pluripotent state, this method is perhaps more indicative than comprehensive, and is not considered to be a stringent assessment of developmental potency.

Embryoid body formation is also well used as a method to establish the developmental potency of pluripotent stem cell lines, with many techniques used to form these structures, some of which were highlighted in section 1.2.3.2. Another relatively rapid technique, the spontaneous self-organisation of PSCs and their differentiation towards the three primary germ layers is more conclusive than spontaneous two dimensional differentiation (Sheridan et al., 2012), particularly when combined with other analyses or the addition of exogenous morphogens to create lineage specific structures. It should be noted however, that undertaking short term EB formation assays can only ever be indicative of the ability of PSCs to self-organise and form progenitor cell populations, which is not necessarily indicative of their ability to form mature tissue structures. The formation of complex, mature structures provides a better overview of developmental potency and, more critically, it is these mature structures that will be required for future regenerative medicine therapies. However, the formation of these tissue structures can be difficult in this cellular system. The ability to maintain EBs for the lengths of time that would be required for these structures to form is hampered by the fact that increasing EB size over time leads to the formation of a hypoxic core, which severely impacts on cellular and structure viability (Gothard et al., 2009; Van Winkle et al., 2012; Wu et al., 2014).

While these *in vitro* options are controllable and reproducible, and can be combined with a range of additional analyses to assess differentiation, they are ultimately limited in their ability to produce mature tissue structures and as such are currently considered to be one of the least stringent methods of assessing developmental potency (Buta et al., 2013). Although *in vivo* options are considerably less desirable to use because of a number of animal related issues, currently it is the teratoma assay that can produce the most complex tissue differentiation achieved by human pluripotent stem cells, and as a result, continues to be considered the ‘gold standard’ method to investigate developmental potency.

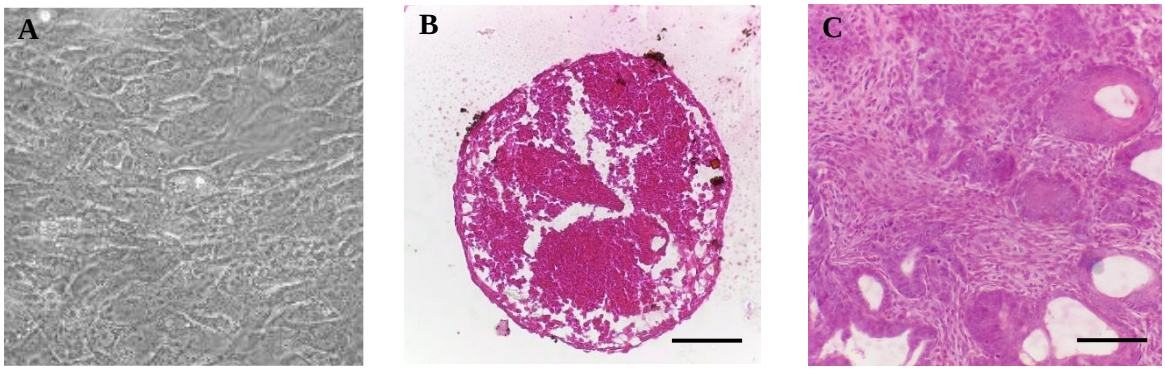


Figure 3.2: Methods used to assess developmental potency during the characterisation of putative human PSC lines: Representative data from techniques used to assess the developmental potency of human PSCs. It is crucial that functional tests are also conducted in order to establish the differentiation capacity of the cells. A) ES cells exposed to exogenous morphogen Activin A to direct their differentiation towards a mesodermal lineage, showing highly altered morphology *in vitro*. B) 8 day old embryoid body formed from ES cells by suspension culture, showing a heterogeneous structure. C) Complex tissue structures as seen in a teratoma formed from human PSCs, with evidence of complex differentiation from all three germ layers. Scale bars: 100 µm

3.1.3 The teratoma assay to assess the developmental potential of PSCs

The origins of the teratoma assay lie in the very first experiments investigating cellular pluripotency, when in 1954 Stevens and Little noted the formation of complex tumours with a variety of 'embryonic and adult tissues not normally found in the testis' (Stevens and Little, 1954). Subsequent experiments elucidated the role of PSCs in tumour formation (Stevens, 1970; Stevens and Varnum, 1974), confirming the link between pluripotency and teratocarcinoma tumours, malignant tumours with both undifferentiated and disorganised differentiated tissue structures. The teratoma is actually the differentiated aspect of these malignant growths, and is itself benign due to the lack of persistence of undifferentiated cells in this part of the tumour.

In the stem cell field today, the teratoma assay is a method used to assess the developmental potency of human pluripotent stem cell populations, and has been considered the 'gold standard' method to do so for a number of years (Brivanlou et al., 2003; Müller et al., 2010b). When compared to other *in vivo* techniques used to assess the developmental potency and differentiation capacity of stem cell populations, it is considered one of the least stringent (Aoi, 2016) (see Figure 3.3). However, these alternative techniques involve the incorporation of the putative stem cell population into blastocysts and as the formation of human-animal chimeras is currently not legally permitted and still under debate (DeWitt, 2002; Hyun et al., 2007; Lensch et al., 2007), these methods are used exclusively with non human PSC populations. As a result, the teratoma assay is the more stringent method available for use with human PSCs, and is regarded as an essential part of the PSC characterisation process, being previously endorsed by the International Stem Cell Initiative (International Stem Cell Initiative et al., 2007).

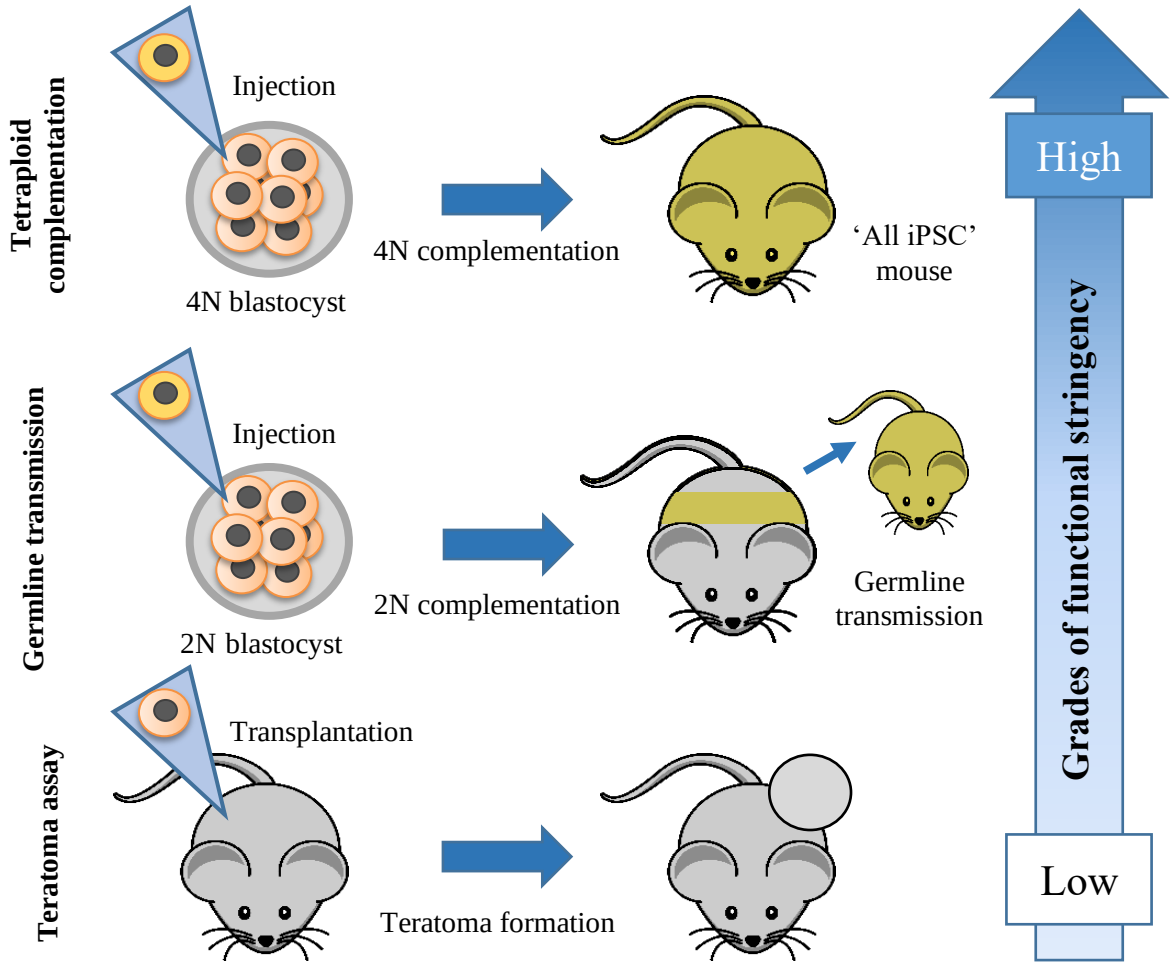


Figure 3.3: Comparison of the *in vivo* functional tests of developmental potency: Schematic representations of the *in vivo* methods used to assess the developmental potency of novel pluripotent stem cell populations. Only the final technique, teratoma formation, can be used to assess human pluripotent stem cells. Tetraploid complementation is the most stringent as this tests the ability of the stem cells to direct the differentiation of the entire organism. Germline transmission can confirm the ability of the cells to integrate into the developing organism, and the production of function gametes is an indicator of chromosomal integrity and functional pluripotency. The teratoma assay assesses the ability of the cells to undergo spontaneous differentiation into cells from the three germ layers. Adapted from Aoi 2016.

A general teratoma assay protocol involves the implantation of the putative pluripotent stem cell population into a specific site in an immunodeficient mouse host. The cells are then allowed to develop into a tumour over several weeks, which is excised, and normally analysed via various histological and immunofluorescent staining methods. The presence of structures from all three germ layers is 'reliable and comprehensive' proof of pluripotency (Zhang, 2014), and the maturity and range of structures which form are a strong indicator of the developmental potency of the PSCs in question, with example histology shown in Figure 3.4. The assay has also been said to offer a 'tremendous amount of information….. beyond their use as proof of pluripotency' (Müller et al., 2010b), having been used as a method to study developmental biology (Hultman et al., 2014;

Przyborski, 2005) and cancer (Jamil et al., 2013). Importantly, the assay can also provide information on the tumourigenicity of PSC populations (International Stem Cell Initiative, 2018). The persistence of undetected undifferentiated cells in regenerative therapies could pose a risk to patients and the formation of a teratocarcinoma, with undifferentiated stem cell elements from putative PSCs during characterisation serves as an indicator of their ability to undergo malignant transformation (Buta et al., 2013).

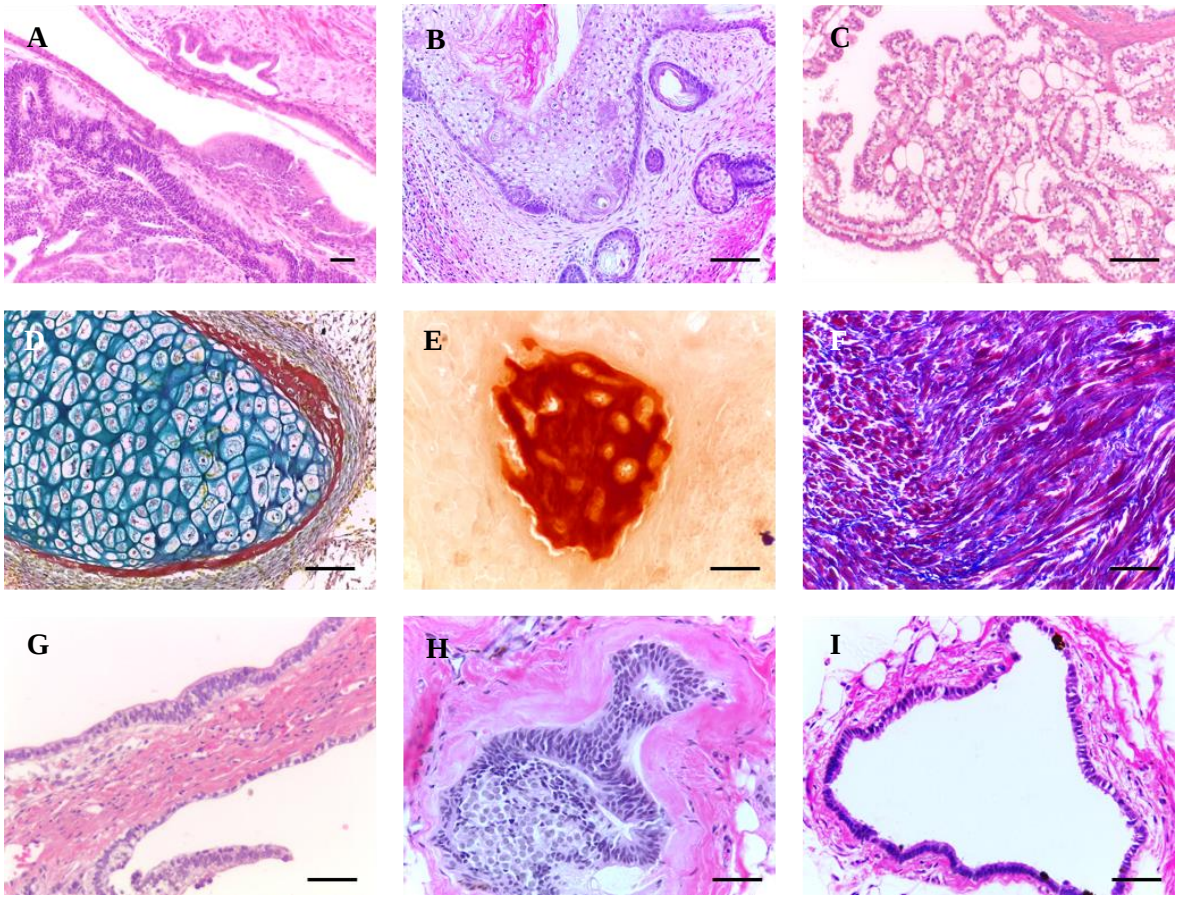


Figure 3.4: Representative structures from a human pluripotent stem cell derived teratoma: Over several weeks, PSCs are able to form highly complex structures within a teratoma and the presence of tissues from all three germ layers is indicative of cellular pluripotency. Images are H&E stain unless otherwise stated. A) Typical section through a teratoma showing multiple germ layer structures. B) Skin tissue. C) Primitive respiratory tissue. D) Cartilage with surrounding bone stained using Weighert's stain. E) Bone tissue stained using Alizarin Red. F) Muscle tissue stained using Masson's Trichrome. G) Respiratory epithelia. H) Neural tissue. I) Epithelia lined lumen. Scale bars (A-F) 100 µm and (G-I) 50 µm

There are, however, a number of limitations to this assay relating to several aspects of the protocol. Initial assessment of a general protocol highlights the use of animals as hosts, a practice which the scientific community is actively trying to reduce through initiatives involving the refinement and replacement of animal based studies ("The 3Rs | NC3Rs," 2019). This is further compounded by the fact that teratoma formation is not always successful, leading to the waste of animal resources. Biological variation between individual mice is another matter which complicates the assay, as this

naturally leads to differences in tumour success and structure formation which cannot be controlled for. Assay length is also a major issue, which can prevent continuing work with novel PSC lines due to the need to wait the 2-3 months it takes for tumours to form. Significant variation also exists at the technical level, an issue which is well recognised by many in the stem cell biology field (Buta et al., 2013; Gropp et al., 2012) and was investigated more closely by Müller et al in a systematic review in 2010. The review found that protocols vary widely between laboratories in every technical aspect, including cell preparation, implantation and assay length. What is most concerning is that many of these parameters have been shown to impact on the differentiation trajectory of the cells in the developing teratoma. Additional studies have shown that variation in cell number (Lee et al., 2009), injection site (Cooke et al., 2006; Prokhorova et al., 2009), mouse strain (Dressel, 2011), implantation with other cell populations (Hentze et al., 2009) and use of reagents such as Matrigel (Prokhorova et al., 2009) influences the identity of the tissue structures and the success rate of tumour formation. This lack of similarity in protocols also prevents comparison between cell lines and tumours, and therefore prevents a reliable comparison of the developmental potency of different PSC populations. This is a loss of valuable data and prevents the maximisation of animal resources to gain as much useful data as possible. Furthermore, differences in reporting standards of both protocols and results from teratoma assays is another obstacle to comparing developmental potency. This ranges from complete reporting of both protocol information and resultant tumour data to no evidence of the assay having been performed at all. Müller found that many hESC lines within his study did not have teratoma assay data available in the manuscripts which reported their initial characterisation, which is concerning. Whilst this could be due to the data not being published, this remains a problem, as it prevents comparison between different PSC populations and within the same PSC population when repeat teratoma assays are conducted, and is another loss of valuable data.

3.1.4 Routes to standardisation for pluripotency assessment

The notion of standardising or replacing the teratoma assay has also been discussed within the field for almost a decade (Buta et al., 2013; Gropp et al., 2012; Müller et al., 2010b), with many advocating for a change in practices to make this assay more efficient, transparent and valuable, or to focus on research into novel alternatives of the *in vitro* and the *in silico* type.

Standardisation of the assay has been suggested, and is a desirable option due to its ability to conclusively assess developmental potency and provide an indication of malignant potential in novel PSCs, as well as allowing for comparison between cell populations, both from different lineages and the same lineage. Attempts have been made to do so in both *in vivo* and *in vitro* settings. Gropp et al analysed a number of the parameters including cell number, inclusion of mitotically inhibited fibroblasts in the injection suspension and the use of Matrigel (Gropp et al., 2012). While covering a range of the parameters which are known to affect the differentiation trajectory of PSCs, these decisions ultimately seem arbitrary. There is an inherent difficulty in the standardisation of an assay

with so many parameters, which is performed by many different laboratories within the field. How does one begin to undertake such a process? Masuda et al offered a different approach, using an *in vitro* technique. Using embryonic rat metanephroi which were cultured *ex vivo*, putative PSCs were injected into the structure and left to form a tumour (Masuda et al., 2012). Differentiated structures formed after 2 weeks in culture, but these do not appear to achieve the maturity and complexity of actual teratomas, although this complexity was achieved following relay transplantation into a mouse host. While this attempt provides better standardisation potential due to the use of *in vitro* methods, the use of biological material such as rat metanephroi maintains an uncontrollable level of variability, and is perhaps more wasteful of animal resources due to the use of embryonic kidneys only. While the standardisation of the protocol may prove difficult, the introduction of minimum reporting standards for the assay protocol and results is certainly an idea which would greatly benefit the field and remedy some issues, as was seen on the introduction of similar standards for microarray analysis (Brazma et al., 2001; Müller et al., 2010b).

Masuda et al's study touched on the idea of standardising the teratoma assay in a way which did not involve the use of the animal host, and since then, others have started to develop alternative methods which can be used to determine developmental potency. These have included the use of traditional culture methods as well as the incorporation of more advanced cell culture techniques including bioreactors (Gerlach et al., 2010a; Stachelscheid et al., 2013) to form teratoma like constructs *in vitro*. *In silico* methods assessing the gene expression of PSC derived differentiated structures include ScoreCard (Tsankov et al., 2015) and TeratoScore (Avior et al., 2015), but perhaps the most well known and successful of these is the bioinformatic application PluriTest which analyses the gene expression data of putative PSC populations. Through the comparison of microarray data, PluriTest can distinguish between pluripotent and somatic cell populations, providing a Pluripotency Score and a Novelty Score for each cell line, which indicate pluripotent abilities of the cell line, any technical and biological variation respectively (Müller et al., 2011, 2008). A recent study by the International Stem Cell Initiative concluded that methods such as PluriTest could be used to screen PSCs that meet other pluripotency criteria, whereas embryoid body formation could be used when more quantitative analyses are required. Interestingly, the study concluded that the technique required depended on the intended application of the PSC population (International Stem Cell Initiative 2018), but conceded that the teratoma assay is still currently required for the assessment of malignant potential in PSC populations, stating that 'it is prudent to carry out the teratoma assay on cells destined for clinical use'. As clinical therapies is likely the intended use of most PSC populations, this suggestion does not significantly improve the characterisation process.

3.1.5 Conclusion

The assessment of pluripotency and developmental potency in putative stem cell populations is a complex process. While pluripotency can be easily identified as a state, the confirmation of

developmental potency is much more useful when future applications of PSCs in studies into human development and regenerative medicine are considered. The teratoma assay is currently the 'gold standard' method to do this, although this technique is fraught with issues and limitations. Attempts have been made to standardise the assay or develop alternatives but the only previous review assessing the use of the teratoma assay was conducted in 2010, which was prior to these attempts. Returning to review the characterisation data of human pluripotent stem cell lines can offer valuable information on a number of aspects of the assay, including whether steps have been taken towards its standardisation and if these novel methods have been adopted. If this is not the case, these data can provide information on trends in assay protocols, therefore suggesting potential standardisation parameters. Finally, as the teratoma assay is the test of functional pluripotency which can achieve the formation of the most mature tissue structures, these data can also inform further work *in vitro* in this project.

3.2 Aims and Hypotheses

The aim of this chapter is to critically assess the use of methods used to confirm the pluripotency and developmental potency of novel human stem cell populations, focussing in particular on the use of the teratoma assay and its associated parameters. Investigation will be restricted to those cell lines registered as being available for public use at well known UK and US repositories, as this data should be freely and easily accessible online. Following the collation of this characterisation data, the frequencies of the methodologies and parameters of the teratoma assay will be assessed, in order to attempt to identify standardisation options and trends for the formation of complex tissues prior to commencing the development of an *in vitro* model. It is hypothesised that data will be available for the majority of the cell lines listed in the repositories, and that the methodologies previously established within the literature review will be used at a high frequency. It is expected that most cell lines will be analysed used multiple methods. As for the teratoma assay, while variation between protocols is highly likely, it is hypothesised that there will be some trend in the data which will be of use in informing the proposed *in vitro* work.

3.3 Objectives

- Collate data regarding human pluripotent stem cell characterisation from the human pluripotent stem cell lines held at the following cell banks and repositories:
  European Collection of Authenticated Cell Cultures (ECACC, UK)
  Medical Research Council (MRC, UK)
  National Institutes of Health (NIH, USA)
  American Type Culture Collection (ATCC, USA)
- Assess the techniques and methodologies used to characterise the human pluripotent stem cell lines, including whether these methods assess phenotypic or functional pluripotency.
- Assess the use of the teratoma assay, its parameters and protocols.
- Identify any potential trends or commonalities in the teratoma assay protocols which would be useful for the optimisation of an *in vitro* model.

3.4 Results

3.4.1 Investigation into phenotypic and functional analyses used to assess human pluripotent stem cells

In preparation for analysis, complete lists of registered human pluripotent stem cell lines, both ESC and iPSC, were obtained from the cell banks and repositories stated previously: ECACC, MRC, NIH and ATCC. As shown in the schematic in Figure 3.5, these were sorted for the removal of duplicate lines, and initial characterisation data sourced in order to perform the analysis. Where characterisation data could not be obtained, the original depositors were contacted in an attempt to source the information. Due to these cell lines being registered for public use, this data is expected to be freely and easily available.

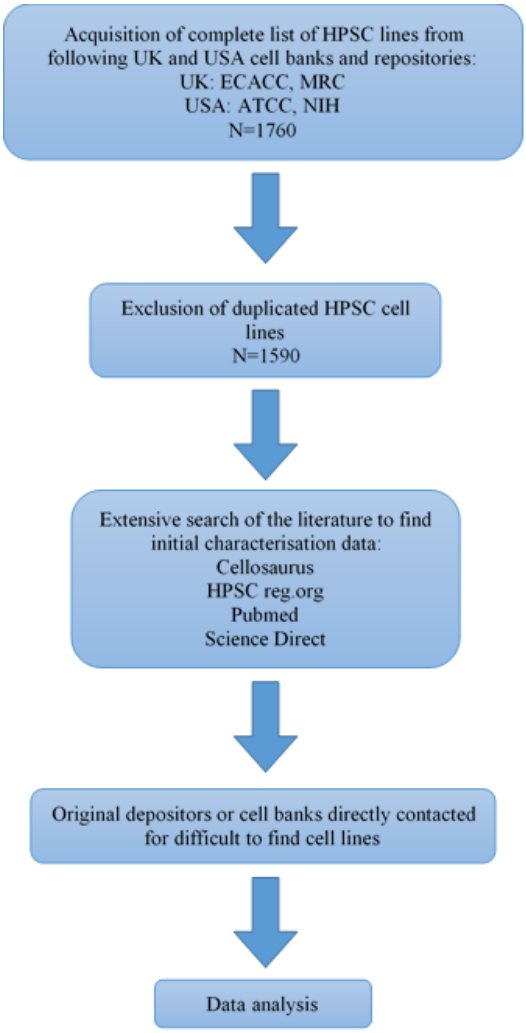


Figure 3.5: Outline of the process used to collect data for in depth analysis of the characterisation of human pluripotent stem cell lines: Major UK and US cell banks were identified and complete lists of human PSC lines obtained from online catalogues. Lists were cross referenced to prevent duplicate analysis: a total of 1590 cell lines were deemed eligible. For each cell line, an extensive literature search was conducted to find the initial characterisation data. For those cell lines which did not have data available online, original depositors were contacted to attempt to obtain the relevant information. In cases where manuscripts were not available, data from the cell bank or repository was used. If data was not sourced, the cells were marked as 'No data available'.

3.4.1.1 The majority of human pluripotent stem cell lines have characterisation data available for assessment

Initial assessment of data availability showed that only 11 % of the cell lines in this study did not have data available for analysis, as shown in Figure 3.6, giving a final number of cell lines with data of 1418. The cell lines which did not have any characterisation data available were exclusively embryonic stem cell lines. Splitting the cell lines into subgroups shows that while almost half of the ES cell lines did not have any data available, all of the iPS cell lines analysed in this study had characterisation data available. This is likely due to many iPSC lines having been derived for commercial purposes, and in large numbers, and so routine characterisation data is required for commercial catalogues.

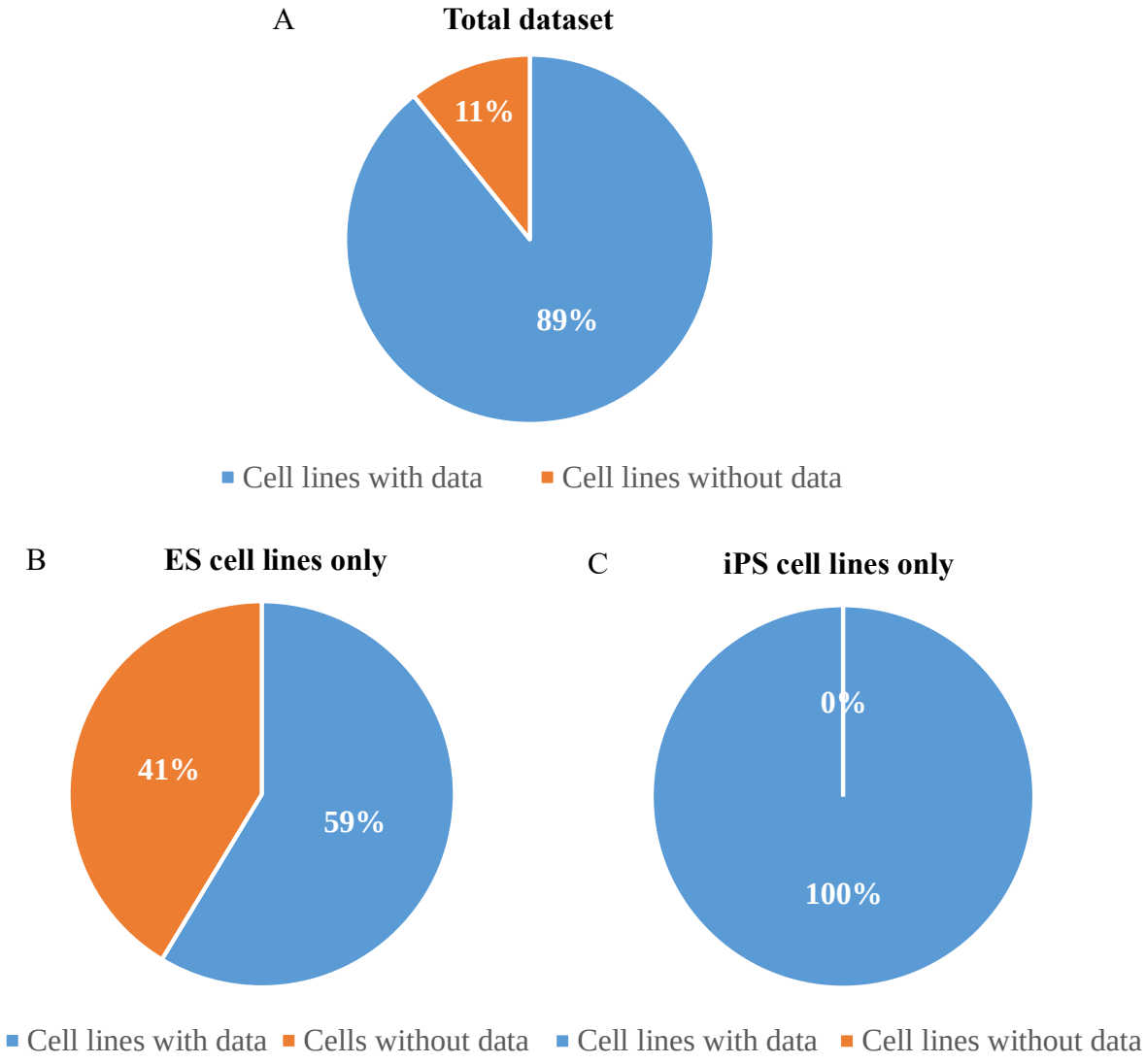


Figure 3.6: Analysis of characterisation data availability for entire dataset and for separate ESC and iPSC populations: (A) Initial data was obtained regarding the availability of characterisation data for the human pluripotent stem cell lines. Of the total dataset, around 11 % of cell lines did not have characterisation data available. When the availability of the data was considered dependent on the cell line identity, the results were significantly more revealing. Of ES cell lines (B), only 59 % of cell lines had characterisation data available. In contrast, all iPSC lines analysed (C) had characterisation data freely available to access.

3.4.1.2 Analyses which assessed the pluripotent state showed varying frequency of usage

The frequency of analyses performed on each cell line was then assessed. Analyses were divided into two groups; those which assess the pluripotent state and those which assess developmental potency. Pluripotent state is defined here as any analysis which detects the following: transcription factors, cell surface markers, proteins and gene expression signatures associated with pluripotency, and encompasses immunocytochemistry, flow cytometry, PCR, alkaline phosphatase assays, karyotyping (a standard analysis on PSCs to detect for aneuploidies) and bioinformatics applications such as PluriTest. Analyses which assess developmental potency are defined here as those which assess the ability of pluripotent stem cells to differentiate into other cell types, generally from the three germ layers, and includes embryoid body formation, spontaneous differentiation, directed differentiation and the teratoma assay. When both types of analysis are considered, nearly all cell lines assessed, 98 %, had at least one phenotypic and one functional assessment performed, indicating a more thorough approach to the assessment of pluripotency and developmental potency. In depth assessment of the analyses reveals a number of trends surrounding those performed. No single analysis was performed on all of the cell lines assessed in this study. As shown in Figure 3.7, of the phenotypic analyses, immunocytochemistry was the modal technique, with around 60 % of all cell lines having had the analysis performed. Generally, this involved the detection of specific proteins associated with cellular pluripotency: extracellular markers such as SSEA-4, TRA-1-60 and TRA-1-81 and transcription factors such as Oct 4, Sox 2 and Nanog. The next most common techniques used were PCR and Bioinformatics based assessments, also simple, high throughput methods which can be easily performed in any laboratory. Around 42 % of cell lines had flow cytometry performed, which also relied on the detection of the same specific proteins associated with pluripotency and is again high throughput and rapid. Very few cell lines, around 11 %, had the alkaline phosphatase assay performed, which is interesting given the simplicity of the colorimetric enzyme assay. Karyotyping of these cell lines was also not performed as frequently as expected, with only 17 % of lines having had the analysis performed.

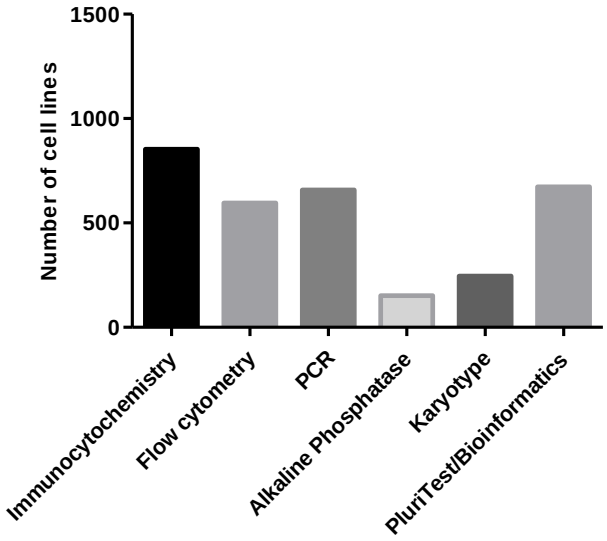


Figure 3.7: Breakdown of the phenotypic analyses used to characterise human pluripotent stem cell lines: Methodologies were categorised as described, dependent on whether the technique assessed the pluripotent phenotype or pluripotency as a function, i.e. developmental potential and differentiation capacity. Of those which assess the pluripotent state, no single analysis is completed on all of the cell lines assessed. Those methods which are rapid and simple to perform and are relatively inexpensive appear to be slightly more frequently used, with immunocytochemistry being the most frequent by a small margin, closely followed by PCR and bioinformatics based techniques.

3.4.1.3 The teratoma assay is one of the most infrequently used techniques in the assessment pluripotency as a function

Of the techniques which assess pluripotency as a function, i.e. assess developmental potency, directed differentiation was by far the most common methodology used, with Figure 3.8 showing that 84 % of the cell lines have had some form of directed differentiation experiment performed. Again, due to the fact that many novel iPSC lines are derived with a view to use in modelling a specific tissue or condition, or are derived in a high throughput manner, this seems relatively unsurprising. The protocols used and tissues achieved were varied and included differentiation into cardiomyocytes, neurones and trophoblast lineages, as well as more general germ layer differentiation. Embryoid body formation was the next most popular methodology at 44 % of cell lines, which is again, another simple, high throughput methodology that can provide data regarding developmental potency in a matter of days. The teratoma assay, considered to be the current 'gold standard' method, was performed on only around 12 % of the cell lines assessed in the study. This is unexpected; there is currently no alternative methodology which is considered to give such conclusive evidence of developmental potency and malignant potential. Spontaneous differentiation of cells, perhaps the simplest of all of the functional analyses, was performed on only around 40 cell lines, around 3 %, which was unsurprising in some respect; this could be a reflection on attitudes towards the lack of information regarding actual developmental potency from this technique.

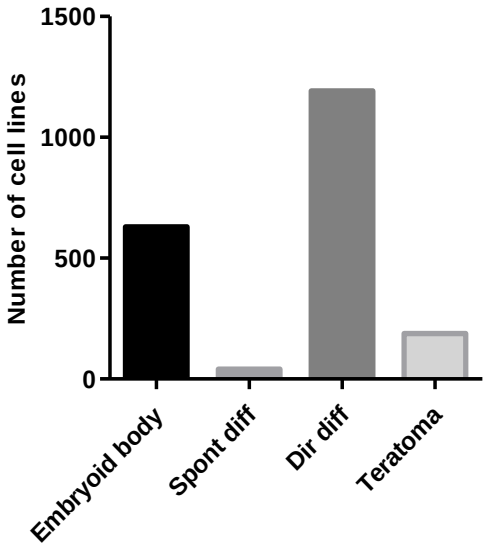


Figure 3.8: Breakdown of the functional analyses used to characterise human pluripotent stem cell lines: Methodologies were categorised as described, dependent on whether the technique assessed the pluripotent phenotype or pluripotency as a function, i.e. developmental potential and differentiation capacity. Of those analyses which assess the pluripotent function, directed differentiation is clearly the most frequently used method of establishing developmental potency, while spontaneous differentiation is rarely used.

3.4.1.4 In depth analysis of teratoma assay protocols reveals a lack of congruency and trends within these assays

General analysis of the methods used to assess both pluripotency and developmental potency indicated that the teratoma assay was performed on only 12 % of the cell lines in this study. Further investigation revealed that of those cell lines which had the assay performed, most were ES cell lines, 94 %, whereas a mere 6 % were iPS cell lines, as can be seen in Figure 3.9.

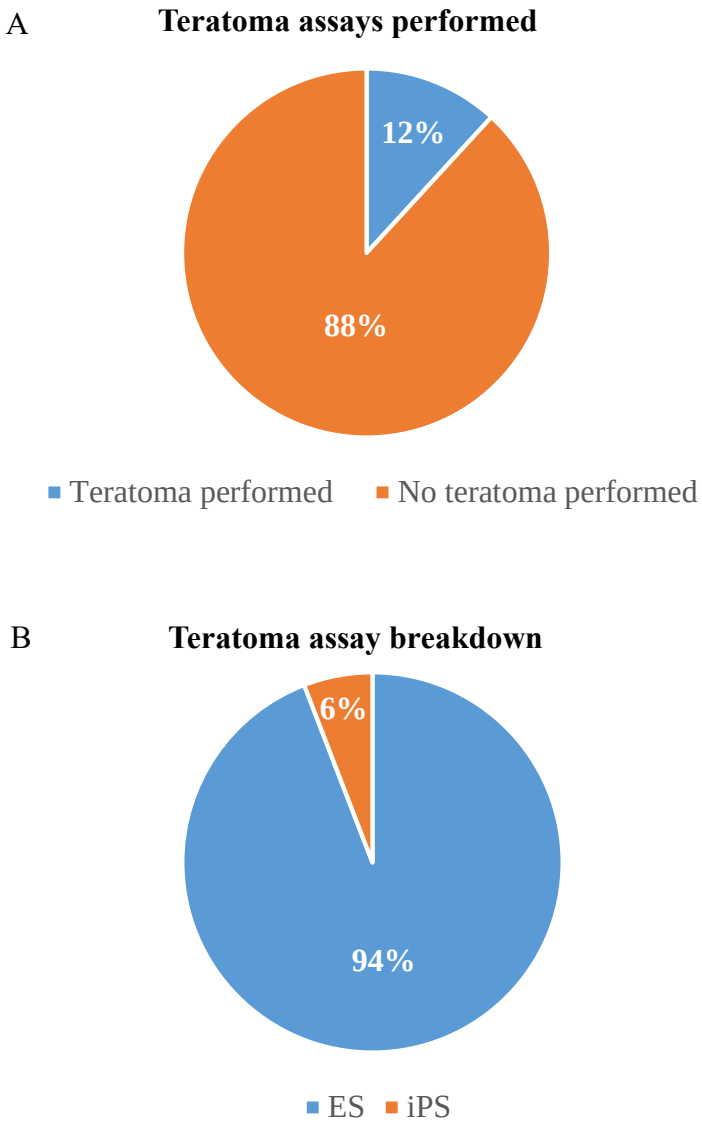


Figure 3.9: Evaluation of frequency of teratoma assay analysis on registered human pluripotent stem cell: The teratoma assay was selected for further analysis due to its use in various applications such as developmental studies, and the 'gold standard' status of the method. The percentage of cell lines which had a teratoma assay performed as a fraction of the study data set was found to be only 12 %, as seen in chart A. Following further analysis of those cell lines which had the teratoma assay performed (B), the majority, 94 %, were ES cells, whereas a mere 6 % were iPSCs.

A deeper analysis into the protocols was performed in order to identify any trends which would provide suggestions for assay standardisation as well as informing the *in vitro* work. A number of key assay parameters were selected for analysis, particularly those which have been shown to affect differentiation trajectory. The number of cells initially seeded per injection in the assay was assessed; values were grouped to simplify analysis due to the wide range of values used in the assay, with the resultant data represented in Figure 3.10. Categories assessing specific cell numbers included less than 1 million cells, 1-2 million cells and more than 2 million cells. A number of protocols used cells in a manner which did not involve seeding a specific cell number, such as stem cell clumps/colonies or entire wells of a culture plate; these were grouped into the clumps/colonies/wells category. The final two categories were for assays which used multiple initial cell numbers, or did not provide a value or description of the amount of cells seeded. Very few teratoma assays used less than 1 million cells, only 3 % of all assays performed. The next cell number grouping of 1-2 million cells, encompassed 16 % of the teratoma assays performed, and around 11 % of assays used more than 2 million cells. The remaining assays did not use a consistent cell number: 10 % of assays used a range of different values and 15 % of assays used the arbitrary measure of cell clumps, colonies or wells of a culture plate. However the modal response, a very significant 45 % of the assays, did not provide any information on the number of cells used in the assay.

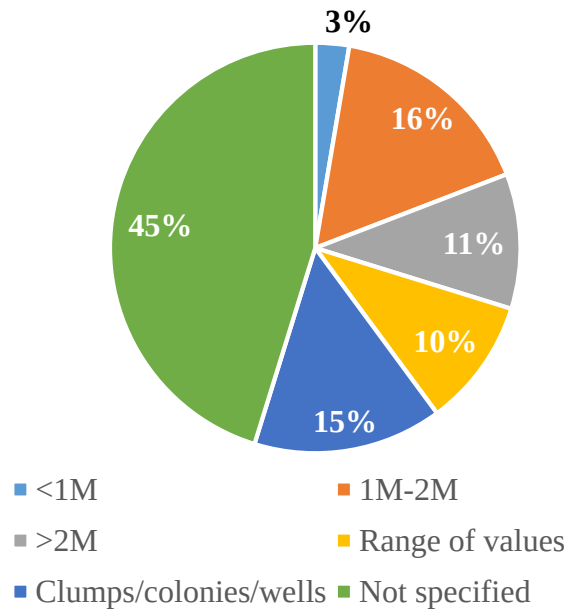


Figure 3.10: Analysis of initial cell number used on implantation in teratoma assay protocols of registered human pluripotent cells: Deeper analysis of the protocols used was undertaken in order to identify trends and common practices. Parameters were grouped to simplify the analysis. Initial cell seeding number is a key parameter in the teratoma assay; analysis revealed that there was no single starting cell number which was used more frequently than the rest, and that almost half of the protocols analysed did not provide information regarding the number of cells used at implantation in the assay.

Anatomical site used for the implantation of the cell population is another key parameter of the assay, one in particular which has been shown to impact extensively on the differentiation trajectory of the pluripotent stem cells. Due to the fact that a wide number of anatomical sites are used in the assay, again, these were roughly grouped according to mouse body area to simplify analysis, with resulting data shown in Figure 3.11. For clarification, unspecified intramuscular and subcutaneous sites refer to instances when cells were said to have been injected either intramuscularly or subcutaneously, but no specific body site was mentioned. Specific body site locations were grouped into the same categories, whether they were subcutaneous or intramuscular, as this was deemed to be the most logical and efficient method of grouping. Flank/back sites and unspecified intramuscular sites were rarely used, with each comprising only 3 % and 2 % respectively of the assays assessed. Unspecified subcutaneous sites and testicular sites were the next most used, at 11 % and 13 % respectively. Thigh/leg sites comprised 18 % of the assays, whereas surprisingly, the most popular anatomical location was actually the kidney, with 23 % of assays using this as the site of implantation. Once again, many of the assays did not specify the anatomical site used, with 30% of assays not disclosing this information.

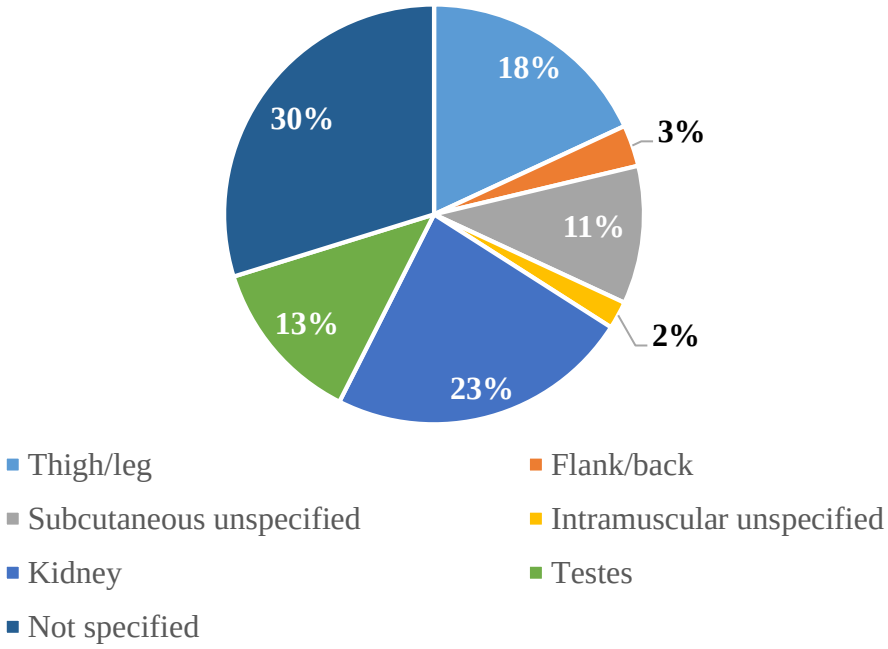


Figure 3.11: Assessment of anatomical site used for implantation in teratoma assay protocols of registered human pluripotent cells: Deeper analysis of the protocols used to perform the teratoma assay was undertaken in order to identify trends and common practices. Parameters were grouped to simplify the analysis, with anatomically close regions grouped together. The injection site used in the assay was also assessed: no single site predominated as the most frequently used, and sites used were highly varied. Again, a number of protocols did not specify the anatomical location used.

The strain of immunocompromised mouse used to conduct the teratoma assay was another parameter which was investigated. No grouping was used in this analysis; mouse strains were categorised as

they were recorded in the assay protocols, with those using the exact same strain placed together. If the immunodeficiency of the mouse was not specifically given, this was classed as immunocompromised unspecified. As can be seen in Figure 3.12, there were a number of mouse strains that are not routinely used for this assay which were found in this analysis: CB17 SCID and Rag 2 -/- each comprised only 1 % of the assays surveyed. Immunocompromised nude and NOD/SCID mice were 2 % and 5 % of assays, and so were also not frequently used. 8 % of assays used multiple strains of immunocompromised mice, whereas another 8 % used mice with an unspecified immunodeficiency. Nude mice were used in around 11 % of assays, however, the most commonly used strains of mouse were SCID strains. SCID mice were used in 18 % of assays, with the most popular strain being SCID/Beige, at 23 % of the assays surveyed. Again though, the modal response for the analysis of the immunocompromised mouse strain used was that the information was not given; this occurred in 26 % of the assays assessed.

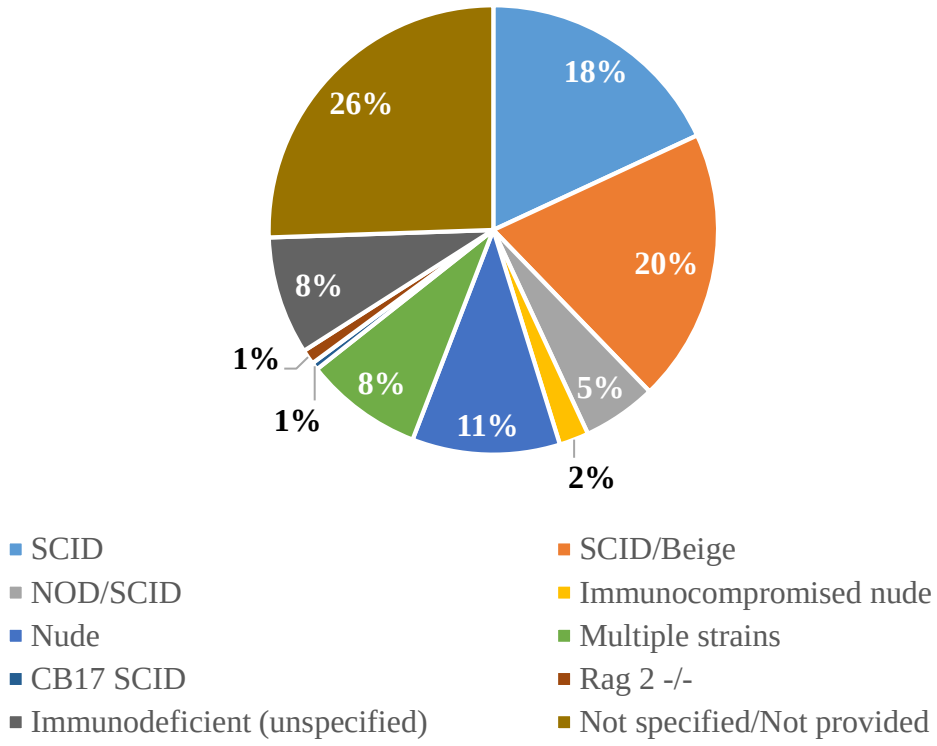


Figure 3.12: Analysis of mouse strains used in teratoma assays performed on registered human pluripotent stem cells: The mouse strain used during the assay is another key parameter which was also analysed. In a similar way to other parameters, the mouse strains used in the protocols were highly varied, and there was no predominantly used strain. The most frequent finding was that the mouse strain was not specified or provided in the protocol, with 26 % of the protocols assessed showing this.

Assay endpoint is another parameter which can indirectly affect the differentiation which occurs during the assay, as not defining the endpoint clearly or using properties such as tumour size to determine when to the excise the tumour could provide more variable results within the same teratoma assay study. Of course, this does not include the unexpected rapid growth of tumours which

have the potential to impact on mouse health and must be excised, but rather, how the endpoint was defined prior to the completion of the assay. Again, grouping of results was used to simplify the analytical process. Tumour endpoints were categorised as to whether they were based on time or tumour dimensions (size). A defined and undefined category was also created for each, depending on whether the assay had a specific time scale or tumour size that was to be reached, or not. Protocols which stated a range of endpoint times without justifiable endpoint decisions were recorded as undefined time. Assay endpoints which were determined as undefined size were those that simply used tumour visibility as a reason to stop the assay and excise the tumour sample. The data in Figure 3.13 shows that very few assays used an undefined size to determine assay endpoint, with only 3 % choosing this. The three other categories of endpoint were almost evenly split: defined time, undefined time and defined size comprised of 19 %, 21 % and 21 % of the assays surveyed respectively. Once again however, the modal response for this parameter was that the manner in which the endpoint was defined was not provided, with 36 % of assays falling into this category.

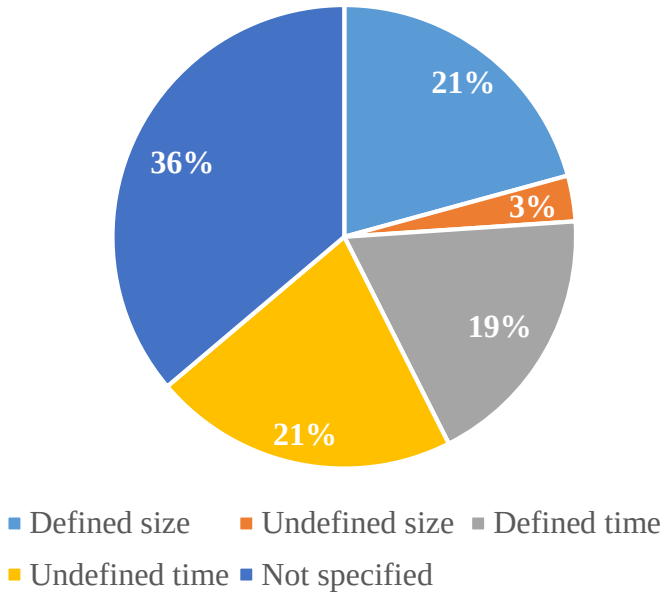


Figure 3.13: Identification of endpoint definition of teratoma assays performed on registered human pluripotent stem cells: The definition of the assay endpoint was also assessed. The manner in which the endpoint of the assay was determined in the protocols were grouped dependent on whether this was done by assay time or tumour size. As has been seen with other assay parameters, the most frequent finding was that the way in which the endpoint of the assay was determined was not provided or specified in the protocol, with most of the other groupings being around 20 % of the teratoma assays performed

The final parameter considered in the analysis of teratoma assay protocols was assay success rate. This is indicative of a number of properties, including protocol reliability and the ability of the pluripotent stem cells to be successfully implanted and form differentiated tissues. Of all assays surveyed, Figure 3.14 shows that only 2 % provided data on the success rate of the assay, which

included how many tumours formed compared to the number of mice implanted with the cell population.

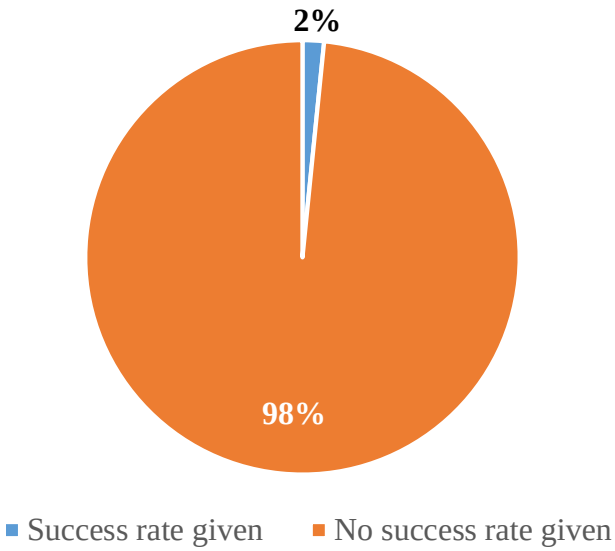


Figure 3.14: Assessment of the reporting of teratoma assay success rate in registered human pluripotent stem cell lines: The frequency of the reporting of assay success rate was also analysed. The tumour formation success rate of the assay is a determinant of protocol success and cell line compatibility with transplantation and therefore a useful piece of assay information. However, only 2 % of the protocols assessed provided data regarding the success rate of tumour formation during the assay.

3.5 Discussion

The aim of this Chapter was to systematically assess the characterisation data of human pluripotent stem cell lines registered as publicly available for use at the major UK and US cell banks and repositories. Whilst both phenotypic and functional methods were investigated, particular attention was focussed on the use and protocol parameters of the teratoma assay. This was in light of the fact that the only previous formal study analysing this data was conducted in 2010, and that since then a number of attempts have been made to standardise, replace or provide guidance on the use of the teratoma assay for the characterisation of human pluripotent stem cell populations. The stages of the data collection process are detailed in Figure 3.5, with in depth analysis taking place after this. The relevance of the data collected on the current status of human PSC characterisation is present here, along with the significance of this in terms of assay standardisation and future *in vitro* work.

3.5.1 The availability of characterisation data for registered human PSCs

As mentioned in the Aims at the beginning of this Chapter, this study concentrated on analysing human pluripotent stem cells registered at major UK and US cell banks and repositories. These were chosen due to the fact that this provided a reasonably restricted set of human PSCs to analyse in detail. More importantly, as these cells lines are registered with cell banks and repositories as publicly available for use, detailed characterisation data for these cell lines should also be available either through the repository or from the original characterisation manuscript.

A final total of 1590 cell lines were found to be eligible for analysis after the acquisition of lists of cell lines from ECACC, MRC, ATCC and NIH websites. During the following data acquisition process, a brief analysis was conducted to ascertain whether the assumption that data would be available for all of the cell lines at the repositories was true. Following an extensive online search across cell line databases, journals and public data repositories, contact details were also sourced for PSC lines which proved difficult to find, and the original depositors contacted in an attempt to complete the dataset. After these attempts, 11 % of the cell lines in the dataset were found not to have characterisation data available. Initially, this does not seem an inordinate number of cell lines, when the converse is considered, that 89 % of cell lines did have characterisation data available. Numerically, this equates to around 170 cell lines with no data, but deeper analysis of how this correlates with the stem cell type reveals a clear bias. Characterisation data was available for all of the induced pluripotent stem cell lines in the dataset, but for only half of the embryonic stem cell lines surveyed. Many of the iPSC lines were derived in large scale studies, most likely for commercial reasons, so the availability of complete characterisation data is beneficial as a service for future users. The lack of data for embryonic stem cell lines is concerning, given that these are a public resource available for use in other studies and the fact that human ESCs have been available as a resource for around 20 years (Thomson et al., 1998), suggesting that extensive characterisation should have been

performed. Whether this is due to the data simply not having been published, or more worryingly not having been conducted, this raises other issues regarding the responsibilities and requirements of publishing basic cell line data. These will not be covered in detail in this discussion, but is perhaps another issue that needs to be addressed by not only the stem cell field, but by all fields involved in cell culture practices.

3.5.2 Use of analyses which assess the pluripotent state

As discussed in section 3.1, pluripotency can be assessed as a state, or as a function, termed developmental potency, using a number of different methods; these were grouped into these two categories and the characterisation for each cell line was analysed. Initial analysis of the technique used highlighted that almost all cell lines in this study, 98 %, were subjected to at least one phenotypic and one functional assay during their characterisation process, and suggests a recognition of the need to assess both aspects of this property due to the lack of correlation between these two properties.

Of the analyses which assess the pluripotent state, there appears to be a trend towards the analyses which are rapid and simple, which can provide information on various defined markers of pluripotency, particularly immunocytochemistry and flow cytometry. The methods which assess gene expression are also popular, with the relatively new PluriTest showing a similar frequency to the use of the more traditional technique of PCR. Analyses which provide less information overall, the alkaline phosphatase assay and karyotyping, are used less frequently, which is understandable, although both assays still have some value in the characterisation process. Alkaline phosphatase assays are another rapid method which can be used to screen cell populations which show evidence of other pluripotency hallmarks. While the karyotyping of human PSCs is not indicative of pluripotency, it is recommended in order to detect genetic abnormalities in PSC populations, and so should be expected to have been performed on a newly derived cell line. Karyotypic abnormalities are also another source of PSC heterogeneity, which can impact on pluripotency and developmental potency.

Of the assays used to assess developmental potency, the use of directed differentiation assays far surpasses the other assays in this category. Directed differentiation encompasses all forms of this technique, both two dimensional and three dimensional, and almost all of the cell lines had this assay performed. The large scale iPSC derivation projects which were listed on the ECACC website were responsible for this bias, due to the fact that these large numbers of cell lines all had this assay performed. Additionally many iPSC lines, in particular disease lines, are derived for the study of the disease phenotype in specific mature cell populations, and so differentiation into these cell populations is often also performed as a part of the characterisation process. The ease of this technique also explains its use on this large scale, as there is no need for specific equipment and the use of morphogens from each germ layer can provide a comprehensive overview of developmental potency. Only around one third of cell lines were characterised used the embryoid body formation

assay, which may be representative of the fact that it can only indicate the ability to self-organise and form progenitor populations. Spontaneous differentiation is used the least, a fact reflective of its inconsistent nature as an assay to test developmental potency and the ability to only form immature cell types. The teratoma assay however, was used on only 12% of cell lines in this study, data at odds with the high regard in which this technique is held by the field.

3.5.3 Current use of the teratoma assay to assess developmental potency

Although considered a 'gold standard' method, the teratoma assay was used for only 12 % of the cell lines surveyed in this study. Considering that the assay holds such a high status, is endorsed by the ISCI and considered the only stringent method to assess this property and malignant potential. More in depth analysis highlights the fact that the majority of these assays, a very significant 94 %, were performed on ES cell lines, whereas a mere 4 % of the assays were performed on iPS cell lines, which numerically is only 11 iPS cell lines and 177 ES cell lines. This result was not expected. As a percentage of the actual ES cell lines (for which characterisation data was sourced), this is around 72 % of ES cell lines in this study which had a teratoma assay conducted. For iPS cell lines, this is only 0.9 % of the cell lines in this study.

When compared to the data that Müller obtained in 2010 after assessing manuscripts published between 1998 and 2009, this in an improvement for ES cells. Within Müller's data set, only 44 % of ES cell lines had associated teratoma assay data, and while this study analyses a slightly different selection of human PSC lines, this increase of almost 30 % may to represent a collective effort by the field to confirm functional pluripotency by the most stringent means possible. This dataset concerns PSCs registered at repositories whereas Müller's dataset consisted of PSCs in published manuscripts, and although subtly different, both of these datasets should have full characterisation data available for access. However, it is possible that as the cell lines in this study are from cell banks and repositories, there could be an increased likelihood that more characterisation has been undertaken for commercial purposes compared to those derived for purely academic reasons.

The striking difference in the teratoma data for human iPSC lines – Müller found that only 36 % of iPSCs in his study had teratoma data, compared to a mere 0.9 % in this study, could be due to a number of reasons. Müller's study dataset covers only two years after the derivation of murine iPSCs from fibroblasts (manuscript published in 2006), and a year after the same was achieved using human fibroblasts (manuscript published 2007). It is most likely that iPSCs were still being derived in small scale studies while techniques were still be optimised at this point in time and the rate of reprogramming success still relatively low. Even with this in mind, 36 % of cell lines is still a surprisingly low number of teratoma assays at a time when the methods of derivation were still novel. The nature of iPSC line derivation is now high throughput, due to efficient optimisation of the source cell population and reprogramming techniques (Aoi, 2016; Omole and Fakoya, 2018), allowing for large scale generation of iPSC lines. This means that performing the teratoma assay on all of these

novel iPSC lines is not practical, and as there are two large scale derivation projects encompassed by this dataset – EBISC and HiPSC – this is reflected in the very low number of teratoma assays performed on iPSCs. This considered, the recommendations as made by Aoi and more recently the ISCI, are that the teratoma assay is the only method currently capable for determining the malignant potential of PSC lines, which is crucial information for clinical therapies. iPSCs are particularly appealing for transition to the clinic, and although few iPSC derived therapies have been subject to clinical trial yet, determination of this property is essential.

3.5.4 In depth analysis of teratoma assay protocols

Müller's review did not seek to assess teratoma assay protocols in depth, but did comment on methodology that was 'poorly reported' and proceeded to describe several representative anecdotes to illustrate the variation in reporting and protocols. In this study, key parameters of the teratoma assay protocol and its reporting were selected in order to better understand any variation, trends or standardisation present. Many different parameters of the assay could have been chosen for this analysis, but those that were chosen represent the absolute minimum amount of data that would be required to replicate a teratoma assay from a specific protocol, as well as those parameters that are considered those most likely to impact on differentiation trajectory.

Cell number is a parameter which has been shown to affect the differentiation of PSCs both as embryoid bodies (Park et al., 2007) and in the teratoma assay (Lee et al., 2009). For ease, the number of cells used was split into categories. Data analysis showed that assays performed with low specific cell numbers, less than 1 million, were rare, but that those with 1-2 million or 2 million or more cells were relatively similar, at 11 % and 16 % respectively. Categories were also required for those protocols which did not use specific cell numbers, a practice which is problematic in terms of reproducibility. Those assays which used a range of values or used arbitrary measures such as clumps/colonies were also similar in terms of their proportions, 10 % and 15 %, showing no real overall trend for any initial cell seeding number. Again, the most common response analysed was that the cell number was not given in the protocol, an issue in terms of reporting clarity and reproducibility.

Injection site for the assay is another parameter known to affect the differentiation trajectory (Cooke et al., 2006; Prokhorova et al., 2009). This analysis does show a modal response of the kidney as the most commonly used anatomical site, which is surprising when it is considered that more difficulties are likely to be encountered on undertaking internal implantation and excision compared to subcutaneous or intramuscular implantation and excision. However, more protocols did not provide information on the site of implantation than used the kidney site, 30 % compared to 23 % which used kidney as the site for teratoma formation, which is another reproducibility issue.

Mouse strain is another parameter which varies surprisingly. While there is a popularity in the use of severe combined immunodeficient (SCID) mice, with SCID and SCID/Beige mice being used in 18 % and 20 % of protocols respectively, 8 different specific mouse strains were identified overall, as well as mice which were described as having an unspecified immunodeficiency. This was more than expected, and while some strains were only used by 1 % of protocols, it represents another large source of biological variation, with the effects of differences in histocompatibility complex and mouse strain known to impact on tumour formation and differentiation (Dressel, 2011). Other sources of variation will be present in anatomical sites and cytokine levels between mouse species, further affecting teratoma formation. However, once again, the most common protocol response was that the mouse strain was not given at all in the protocol details.

The definition of teratoma endpoint is another parameter which indirectly impacts on the differentiation within the tumour, as tumours left to grow for longer are perhaps more likely to contain complex and mature cellular structures. The ways in which endpoint was determined fell into 2 categories: tumour dimensions (size) or time since the original implantation. The endpoint was taken to be the parameter which was mentioned at tumour excision. Undefined endpoints, those not dependent on specific measurements or a specific timescale, are a concern due to the uncontrolled for differential tumour growth rates and the lack of comparability and poor clarity in reporting methods. Very few studies opted for an undefined size as the tumour endpoint, which was described in the protocol as simply the visibility of a tumour at the implantation site. The other three categories of assay endpoint, undefined time, defined size and defined time, showed very similar frequencies in the dataset, of 21 %, 21 % and 19 %, showing no clear trend for this parameter. Again, perhaps unsurprisingly, the modal response taken from teratoma protocols was that the endpoint of the assay was not stated in the protocol.

The final aspect of the teratoma assay which was studied in depth was the reporting of teratoma formation success rate. The reporting of tumour success rates can provide valuable information on a number of areas of the assay, including PSC viability, protocol success and assay utility, as well as providing comparison for the assessment of different populations of PSCs, including those which have been manipulated and subject to a teratoma assay (Bouma et al., 2017; Gutierrez-Aranda et al., 2010; Lee et al., 2009; Tao et al., 2018). Out of all of the teratoma assays analysed in this study, only 3 cell lines had success rate data detailed in the manuscript, which equates to around 2 %. This again was surprising, and represents a loss of valuable data and a lack of transparency in experimental data reporting. The variability in experimental success, particularly when animals are involved, is an unavoidable part of the scientific process, but the severe lack of success rate reporting is still unexpected, and could be due to the desire of researchers not to be judged on their technical skills due to teratoma failure rates.

3.6 Conclusion

Throughout this Chapter, the characterisation data of human PSCs registered at major UK and US cell banks and repositories has been analysed in order to investigate the availability of characterisation data for registered human PSC lines, as well as the methods used to confirm pluripotency as a state and as a function in putative human PSCs. In particular, this Chapter has focussed on the protocols used to undertake the teratoma assay in order to identify and possible trend to inform *in vitro* work.

Analysis of the characterisation data found that while characterisation data could be found for all of the iPSC lines in the dataset, only half of ES cell lines had characterisation data available, which is concerning given that these cells lines are available for use from public cell banks and repositories. Methods which are rapid and simple showed a high frequency, such as immunocytochemistry in phenotypic analyses, and directed differentiation for functional analyses. Almost all of the cell lines used both phenotypic and functional analyses to assess pluripotency and developmental potency, showing an understanding in the field of the need to undertake both due to the lack of correlation between pluripotency and developmental potency. However, the 'gold standard' technique of the teratoma assay was performed on only 12 % of all cell lines in the dataset, which was not expected, as the value and stringency of the assay is well recognised across the field, for assessing the developmental potency and malignant potential of PSCs. In depth analysis of the protocols used to conduct teratoma assays also produced unexpected results. These included:

- Significant variation in all assay parameters assessed
- A lack of trends for any single protocol, and therefore a persistence in the lack of standardisation
- A lack of clarity and transparency in protocol reporting, with very minimal information in some cases and many not reporting the parameters and conditions used.

The need for the standardisation of this assay has been well recognised for years, yet the data from this review suggests this has not occurred. Additionally, there was very little information on tumour success rates. The variability of these parameters and the frequency with which information regarding the protocol was not provided matches with Müller's description of 'poor reporting' in the study conducted in 2010, demonstrating that the reporting of protocols and results has not moved forward since the previous study. The lack of trends and standardisation of teratoma assay protocols as assessed by this study suggests that this process is one which is more difficult than previously realised by the field and that there are no clear trends which could suggest parameters for assay standardisation. Given these findings, the need for standardised alternatives to the teratoma assay is clear. Due to the difficulties of doing this with the *in vivo* assay, new strategies to develop *in vitro* work is an option which can offer both standardisation and reproducibility, as well as increasing complexity with the incorporation of advanced cell culture techniques.

4. The application of technologies to enhance the microenvironment of PSCs using EC cells as a working model

4.1 Introduction

As established in the Introduction and Results Chapter 1, there is a need for a novel *in vitro* model to assess the developmental potential of pluripotent stem cells and study complex tissue differentiation, which could also be used as an animal free alternative to the teratoma assay. Of the three dimensional cell culture techniques discussed in Section 1.2.3, aggregation based techniques in particular have been used in conjunction with pluripotent stem cells to study cellular differentiation, and the resultant structures, termed embryoid bodies, are known to recapitulate some of the events of early human development. The use of embryoid bodies is a therefore a logical starting place in the development of a novel *in vitro* model.

4.1.1 Embryoid bodies as a model of human tissue development

Cells have an intrinsic ability to self-assemble on contact with other cells (Simunovic and Brivanlou, 2017) and aggregation and self-organisation into structures has been shown to be possible in a number of different pluripotent, somatic and tumorigenic cell populations, in order to allow for understanding and study of concepts such as human development, organ function and tumour biology in the *in vitro* context. Embryoid bodies (EBs) derived from PSCs have also long been used to rapidly assess the pluripotency of novel human PSC lines, as the spontaneous self-organisation and differentiation which takes place within these structures is indicative of the ability to undergo early lineage specification (Sheridan et al., 2012). Due to these intrinsic properties and the events which occur during EB formation, EBs are also now an important primary stage in many differentiation protocols attempting to create specific cell lineages, as the EB provides an environment for PSCs to transition from a pluripotent state to lineage commitment (Desbaillets et al., 2000a; Dvash et al., 2006) as well as providing a physical environment for the initiation of structure formation (Eiraku et al., 2011; Suga et al., 2011; Takasato et al., 2014). Importantly, the differentiation trajectory of EBs can be externally manipulated and tightly controlled by altering factors such as EB size and cell number (Dang et al., 2002; Lach et al., 2018; Van Winkle et al., 2012), thereby allowing for specific germ layer populations to be selected for, and improving the yields of progenitor populations in differentiation protocols (Yanai et al., 2013).

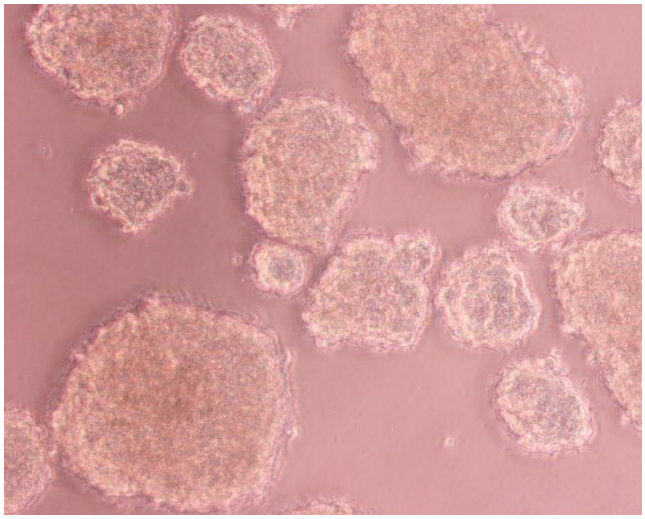


Figure 4.1: PSC derived EB in culture: Pluripotent stem cells naturally self-organise into spherical structures termed embryoid bodies (EBs). These recapitulate events of early embryogenesis and differentiate towards the three germ layers spontaneously.

The ability of EBs to self-organise is mediated through increased cell contacts and interactions (Meng et al., 2014) as cells are spatially arranged in a three dimensional environment, as well as through the creation of internal cytokine, nutrient and oxygen gradients across the structures, which further recapitulates the morphogen gradients which are established in the developing embryo. EBs have been shown to display organised regional expression of markers pertaining to the three germ layers (Itskovitz-Eldor et al., 2000), which suggests that a gastrulation event takes place in the developing structure (Fuchs et al., 2012), further confirming the similarity of these structures to the early embryo. Additional treatment and manipulation of PSC derived EBs using exogenous morphogens and other physical and chemical stimuli allows for a wide variety of complex structures to be achieved. Examples include many focussed on the study of early developmental processes. Spontaneously forming and differentiating EBs naturally allow for the study of very early embryonic processes, with the term 'embryoid' being considered to apply to very specific organised structures which show polarisation and correct spatial organisation of cells directly correlated with known stages of embryogenesis (Simunovic and Brivanlou, 2017). More recent studies focussing on the formation of an EB *in vitro* from single cells have allowed for insights into the first cell divisions and organisation events that take place as the human embryo develops, allowing for a better understanding of the lineage decision events and polarisation taking place within the structure (Shahbazi et al., 2016). The study of gastrulation, a later yet critical process in the developmental cascade, can be achieved through simple cell number restriction and treatment with exogenous morphogens, allowing for the polarisation of EBs and symmetry breaking to occur within the structures, now termed 'gastruloids' (Baillie-Johnson et al., 2015). Organ specific developmental processes have also been well studied using this technique, often using EB formation as an initial lineage commitment step. Strictly

speaking, the resultant structures are organoids, not embryoid bodies, although the ability to form such complex, recognisable and functional models of a wide variety of organ systems indicates the power and potential of EBs and EB based techniques in the study of the formation complex tissue structures, given appropriate cues.

4.1.2 Cell death and diffusion in embryoid bodies

While the utility of EBs is well recognised for differentiation based protocols, there still exist limitations to the method. The creation of cytokine, nutrient and oxygen gradients across the developing EB is a major driver of differentiation within the structure, and yet the creation of these gradients also poses a significant problem with increasing EB size and culture time (Van Winkle et al., 2012). The phenomenon of significant gradient formation within EBs has been noted and studied in depth by a number of groups, particularly concerning oxygen and cell death.

The presence of differential oxygen gradients within EBs has previously been established as a phenomenon (Gassmann et al., 1996), but a more recent in depth study by Van Winkle focussed on modelling the mass transfer of a number of factors within EBs, including oxygen, nutrients and cytokines, provides more detailed data and rationale as to the cause (Van Winkle et al., 2012). Importantly, study simulation data indicated that the oxygen concentration under atmospheric conditions at the centre of large human PSC derived EBs, those with a 400 μm radius, is around 50 % lower than that at the centre of smaller human derived EBs of 200 μm radius. This highlights the heterogeneity within the larger developing EB, illustrated in Figure 4.2, as the differential oxygen tensions can impact on both cellular differentiation and, more crucially, cellular viability (Wu et al., 2014). Critically, Van Winkle's study assumed that the oxygen concentration was at a steady state in liquid media in the simulation; the actual dynamics of oxygen concentration in *in vitro* cultures is unlikely to be so homogenous (covered in more detail in Chapter 5), and therefore will impact more severely on EB structure. Van Winkle and others link this to cell density within the outer layers of EBs impeding diffusion (Gothard et al., 2009; Van Winkle et al., 2012) with others noting that this effect on mass transfer could be even more pronounced with longer term cultures (Son et al., 2011). The effects of metabolic consumption on the establishment and maintenance of this diffusion gradient also cannot be ignored, with highly metabolic cells driving a more severe gradient than cells with a lower metabolic activity (Rouwkema et al., 2010). Wu and colleagues found similar results when investigating oxygen transfer to EBs in stirred suspension bioreactors, with the differences in oxygen concentration in smaller EBs of 100 μm being negligible but being more detectable and pronounced in EBs of 300 μm radius, with almost 25 % of cells having a partial pressure of oxygen less than 30 mm Hg (Wu et al., 2014). The correlation of these radial values is unsurprising, given that the tissue diffusion limit (the distance which cells/tissue can effectively receive nutrients including glucose and oxygen by passive diffusion, without specialised circulatory support) is

understood to be approximately 100 - 200 µm, although actual values *in vitro* may vary dependent on application (Asthana and Kisaalita, 2012; Rouwkema et al., 2010).

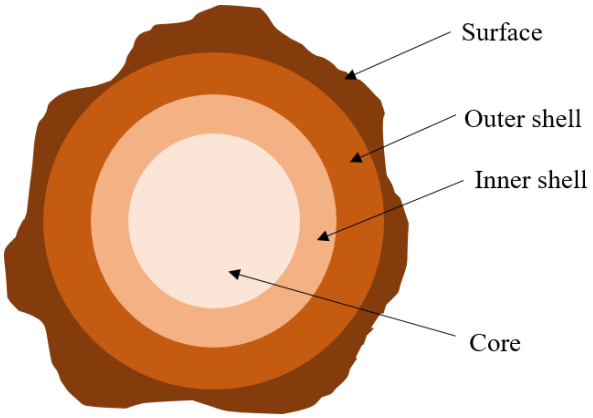


Figure 4.2: Schematic of the internal structure of PSC derived EBs: As PSC derived EBs increase in size, the internal structure of the EB become heterogeneous, with a number of cell layers, each with a subtly different microenvironment. This results in a gradient of nutrients and oxygen, and differences in cell function and viability. Adapted from Gothard et al 2009.

Assessment of papers which utilise aggregation based techniques reveals the ubiquitous prevalence of reduced EB viability and death within the centre of structures. Central necrosis is a well established phenomenon in tumour spheroids (Groebe and Mueller-Klieser, 1996), but the development of areas of necrosis and hypoxia in large tumour spheroids is considered to be analogous to areas which form in tumours *in vivo*, therefore providing an improved and more representative study model rather than limiting their use (Mehta et al., 2012). The same cannot be said for PSC derived EBs and organoids, where this impacts significantly on differentiation, function and usage. Gothard *et al* noted that all human EB samples in a study focussing on comparing size engineered EBs to less controlled methods became necrotic by day 9, even though necrosis had been decreased in the size controlled EBs. In fact, after around 5 days many EBs showed the formation of a layered structure which contained a core of cell death and a densely populated outer surface (Gothard et al., 2009). Son *et al* found that, as hypothesised, prolonged culture of human EBs without passaging resulted in a significant increase in apoptotic markers after 4 weeks in culture, which only continued to increase at week 5 (Son et al., 2011). The prolonged culture of cerebral organoids enhances the differentiation and structure of the resultant tissues, but was also found to contribute to significant apoptosis within the structures after around 30 days in culture, which again only increased with increasing culture time (Giandomenico et al., 2019; Mansour et al., 2018). While it can be posited that apoptosis is a mechanism used in development in various remodelling events such as cavity formation , the detection of both necrotic (Smith et al., 1987) and apoptotic events within developing EBs and EB derived structures and their increasing prevalence over time suggests a strong connection with the increasing diffusion distance and reduced nutritional support.

Even if individual EBs do not form a severe gradient across their structure (there is some evidence that EBs may limit their size to prevent the above scenario (Dang et al., 2002; Gassmann et al., 1996)), EB aggregation is a well documented yet unavoidable aspect of techniques such as suspension culture, which is used to generate large numbers of EBs for improved statistical significance in a non laborious manner (Flamier et al., 2017). EB aggregation and the formation of large multi EB structures results in highly heterogeneous cultures, with the resultant structures being unsustainable due to the creation of large diffusion distances and a suboptimal internal microenvironment and therefore rendering them unusable (Gothard et al., 2009).

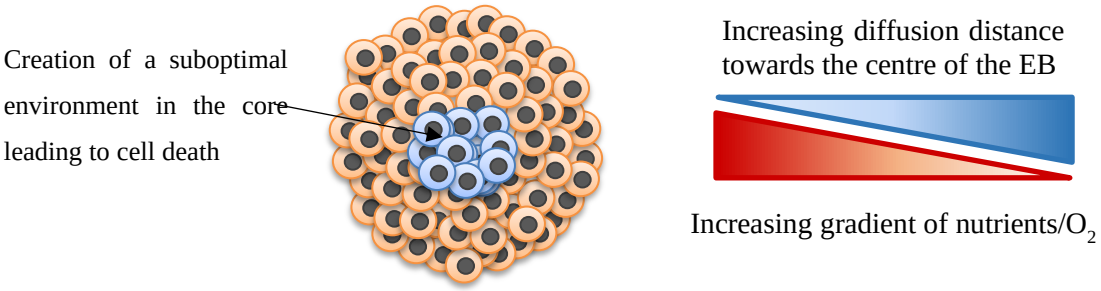


Figure 4.3: The heterogeneity of the embryoid body microenvironment: As EB size increases, this results in the creation of large diffusion distances to the centre of the structure, which also results in the creation of a severe gradient of oxygen and nutrients. This leads to a suboptimal microenvironment in the centre of the EB, which induces cell death and interferes with EB viability and structure formation.

4.1.3 Combining embryoid bodies with advanced cell culture technologies

The advantages of EB culture for the differentiation of pluripotent stem cells both as an initiator of lineage commitment and to provide appropriate space and cellular connections for the formation of complex structures cannot be understated. Yet, the issue of severe gradient formation, particularly oxygen, across the developing EB severely restricts their use in the long term studies required to form complex tissue structures. Time is an integral part of the developmental process, and sufficient time is required to allow for the formation and maturation of complex human tissues, whether *in vitro* or *in vivo*. Multiple attempts have been undertaken in order to improve the viability of EBs, allowing for prolonged culture and the encouragement of complex tissue like structure formation. As discussed in Section 1.2.3 of the Introduction, there are a number of advanced cell culture techniques now available to do this.

Scaffold based technologies have been used to direct the differentiation of a variety of cell populations via seeding the cell suspension directly onto or into the scaffold, as discussed previously. These techniques have also been used to support the prolonged culture of EBs and their differentiated derivatives in order to overcome the issues associated with increasing EB size. Extensive work has

been conducted in the neuroscience field, culturing PSC derived neurospheres and organoids on solid scaffolds to improve both viability and functionality, essentially through the process of reducing diffusion distances within these cellular constructs. To overcome the issues encountered with cerebral organoids, Lancaster *et al* followed a similar methodology to organotypic slice culture, taking 300 μm thick sections of mature cerebral organoids and culturing them on porous cell culture inserts at the air liquid interface (Giandomenico et al., 2019). As well as prolonged viability, improvements in nerve tract diversity compared to the organoids and a demonstration of functionality through the induction of muscle contractions were also observed. Nestor saw a comparable output using a similar technique with PSC derived neurospheres and porous cell culture inserts. Neurospheres were seeded onto the insert with the aim of reducing their thickness for imaging, with the methodology producing structures that were comparable to the neural tissues of the EB but also showed increased viability and maturity, with the presence of synapses (Nestor et al., 2013). Interestingly, Nestor also noted that the overall structure was 'inside out' compared to the EB culture, although attributed this phenomenon simply to the presence of the scaffold for adherence. Abbasi and colleagues also studied the induction of neural differentiation using nanofiber scaffolds produced by electrospinning, a departure from the simple porous scaffolds discussed in the previous examples. In this case, the EBs both treated with morphogens and allowed to spontaneously differentiate prior to seeding on the plasma-treated nanofibrous polycaprolactone scaffolds (Abbasi et al., 2016). EBs were cultured on two different topographical surfaces, attaching and successfully differentiating towards the neural phenotype under both spontaneous and differentiating conditions. While the effects of the study on EB viability were not assessed, Abbasi also found that culture of EBs on nanofibers resulted in more effective differentiation towards mature neural phenotypes.

Studies in 2D using gelatin coated surfaces have actually noted the importance of attachment in EB size, growth and differentiation, observing highly different results when compared to EBs in suspension culture conditions, including a significantly increased size and the absence/presence of specific cell populations (Dang et al., 2002; Ho et al., 2010). Dang postulates that the finite EB size observed in culture could be due to the absence of developmental cues, and suggests that attachment mediated growth signals are responsible for the differences in EB size and growth observed in the attached EBs. Given that the attachment of the blastocyst is a crucial step in the developmental process to permit further development of the embryo, as outlined in section 1.2.1.3, and the similarity of the EB structure and morphology to the blastocyst, it seems highly likely and plausible that attachment to surfaces, including 2D coated surfaces and solid scaffolds, allows for the differentiation of highly complex structures. The adherence of EBs to coated plastic surfaces is a technique used commonly in the study of human development and PSC derived EBs, and although this may activate attachment mediated signals, this does not solve some of the other issues of EB culture as well as perpetuating issues associated with traditional cell culture methods. These are namely the formation of gradients of oxygen within the structure due to an asymmetrical nutritional

support and enforced polarisation of cells attached to the surface, potentially leading to the formation of a heterogeneous EB environment again.

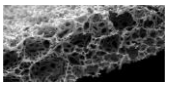
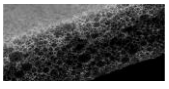
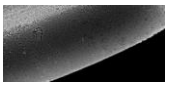
While centred mainly to the study of neural differentiation, good evidence exists that the combination of EB culture with technologies such as solid scaffolds can allow for improvements in differentiation and viability, which crucially, will allow for longer term studies and support the formation of even more complex mature tissue structures.

4.1.4 Use of Alvetex® scaffolds for three dimensional cell culture

Solid physical scaffolds for cell culture purposes can be created using a wide range of techniques, as briefly outlined in Section 1.2.3.3. The polymerisation of high internal phase emulsions is a phase separation technique used to create porous scaffolds with interconnected pores and voids, with the resultant cell scaffolds termed polyHIPEs.

Following the combination and mixing of the oil phase which will form the scaffold structure and an aqueous phase to create the pores and voids within the scaffold, polyHIPEs are created through the curing of the oil phase to form a solid scaffold structure and the subsequent removal of the aqueous phase (Knight, 2014). Pore and void size can be altered dependent on the reaction conditions, allowing for customisation dependent on cell culture and model requirements. One commercially available polyHIPE scaffold which is available in a range of pore and void sizes, and has been used for a variety of *in vitro* applications is Alvetex®. The three formats available are outlined in Table 4.1; Alvetex® Scaffold has the largest pore and void sizes, followed by Alvetex® Strata. Alvetex® Polaris is not yet commercially available, and has the smallest pore and void sizes of the scaffolds, although all three are fully porous and composed of polystyrene, the same material most common tissue culture plastic is composed of.

Table 4.1: Void and pore sizes of the three formats of Alvetex®

Alvetex® format	Commercially available	Void sizes (µm)	Pore sizes (µm)	Ultrastructure
Alvetex® Scaffold	Yes	38	13	
Alvetex® Strata	Yes	13	5	
Alvetex® Polaris	No	3	0.5	

SEM images kindly provided by R Quelch.

Alvetex® cell culture scaffolds have been used in a wide range of applications, including the routine culture of cell populations for drug testing on Alvetex® Scaffold (Schutte et al., 2011) and the formation of *in vitro* organotypic models, including skin models using Alvetex® Scaffold as the basis

of a co-culture system to study epidermal and dermal biology (Costello et al., 2019; Hill et al., 2015; Roger et al., 2019) and respiratory epithelia models (Marrazzo et al., 2016). In the field of stem cell biology, Alvetex® has been used for the propagation of PSCs (Knight, 2014) and the priming of PSCs prior to use in other differentiation based assays (Quelch, 2018). Both studies showed that the culture of PSCs on Alvetex® resulted in an improved differentiation capacity, as illustrated using *in vitro* and *in vivo* techniques usually used to assess the developmental potency of PSC populations. The scaffold has been used in a number of other studies investigating differentiation, including the differentiation of neural stem cells into functional neurones (Stevanato et al., 2015). Focussing on the use of Alvetex® in the context cellular viability and differentiation, a variety of work has also been conducted using both cell lines and tissue slices. Similarly to that described in section 4.1.4, the enhancement of neural differentiation and neurite outgrowth from PSC derived neurospheres has been demonstrated using the Alvetex® Scaffold format of the technology (Clarke et al., 2017; Goncalves, 2017). Alvetex® has also been used to maintain tumour tissue slices (Davies et al., 2015) and create tissue like samples for further study (MacDonald et al., 2014). Studies have been undertaken using EBs also, seeding the structures onto all three forms of the scaffold in order to assess the ability to maintain EBs in this way and observe the effects on differentiation. While the culturing of PSC derived EBs on the Scaffold resulted in the loss of EB structure and full infiltration into the polystyrene insert, EB structures could be maintained on the surface of Strata, showing evidence of complex differentiation from the three germ layers (Knight, 2014). Knight showed that this was possible for short term studies where EBs were allowed to spontaneously differentiate for 7 days, and confirmed the potential for using Alvetex® for this application. Further work by Owens expanded on that completed by Knight, demonstrating the ability to culture human and murine PSC derived EBs on Alvetex® Polaris, which resulted in the complete maintenance of EB structure, and highlighted the ability to culture the structures for longer term and the potential for the formation of complex tissue structures (Owens, 2015). These studies by Owens were focussed on proof of concept and simple differentiation, but again, highlighted the ability to use scaffolds for this application, indicating the utility of the Polaris format.

4.1.5 TERA2.cl.SP12: Embryonal carcinoma cells as models of human development

Much of the work described above has focussed on the use of human PSC populations, mainly embryonic with some iPSC work also described. While these cell populations are able to offer the most appropriate physiological response and the greatest opportunity for the study of a range of differentiation events, their culture requirements can be fairly restrictive, as human ESC and iPSC populations require complex and finely tuned culture conditions in order to maintain the pluripotent state. This entails either the maintenance and management of feeder layers concurrently with the PSC populations, or the purchase of expensive coating matrices and defined media with the necessary morphogens to prevent spontaneous differentiation (Chen et al., 2014). These options are laborious

or expensive, and can prevent large scale studies, which are often required for optimisation of novel models and for in depth investigation into cellular processes such as the events of human development. The wide range of differentiation which can occur may also complicate matters when attempting to compare established techniques with novel culture practices, due to the wide range of differentiated phenotypes to be assessed and compared.

Human EC cells are a tumorigenic pluripotent population, which are highly similar to human ES cells in a number of ways (Andrews et al., 2005). Displaying the typical pluripotent phenotype and morphology and with an expression profile similar to that of the human blastocyst (Artzt et al., 1973; Evans, 1981; Henderson et al., 2002; Martin, 1975), human EC cells offer a simpler, cheaper and more robust option for the development of a novel model investigating PSC differentiation, with minimal culture requirements for the maintenance of the pluripotent state. The N-Tera2 line is a popular EC cell line which has been used to study the process of neurogenesis in particular, responding well to retinoic acid exposure, which results in the direction of their differentiation towards the neural phenotype. The N-Tera2 line was originally derived from the Tera2 population, an EC cell line derived from a lung metastasis of a primary testicular embryonal carcinoma (Andrews et al., 1984), and further subclones have been derived from the N-Tera2 population, including TERA2.cl.SP12. The TERA2.cl.SP12 clone was isolated using magnetic sorting (Przyborski, 2001), selected for a high expression of extracellular pluripotency markers and transcription factors, including SSEA-3, TRA-1-60 and Oct 4, and naturally low expression of neural differentiation markers such as A2B5. TERA2.cl.SP12 has been used in a number of studies focussing on embryonic development and pluripotency, including early ectodermal fate decisions and signalling pathways (Horrocks, 2007) and the impact of various microenvironmental stimuli on pluripotency and developmental potency including hypoxia (Morales, 2018) and the three dimensional microenvironment (Quelch, 2018), all of which have used EB formation as a crucial aspect of the study process. The TERA2.cl.SP12 cell line has also been used in the aforementioned neurite outgrowth studies (Goncalves, 2017), with the cell line showing a strong response to retinoic acid induced differentiation towards the neural lineage, and having been well characterised in the differentiated phenotype, showing an increased expression of key markers of neural differentiation Nestin and Class III β-tubulin. Additionally, retinoic acid is a key developmental morphogen involved in various differentiation events including the development of the spinal cord and the spatial organisation of neural and mesodermal tissues, rendering it a highly suitable morphogen in the optimisation of the model. TERA2.cl.SP12 cells also show the ability to differentiate towards epithelial ectoderm on exposure to bone morphogenetic proteins, providing two distinct differentiated phenotypes for study during the optimisation process. The application of BMP-2 to the cells has previously been shown to successfully induce epithelial differentiation in this cell line: BMP family morphogens are also critical in spatial patterning and differentiation during the developmental process.

4.1.6 Conclusion

Embryoid bodies are a useful tool for the study of human development, due to their ability to self-organise and commit PSCs to a differentiation cascade. The ability to control their differentiation trajectory by changing cell seeding density and EB size is highly useful, and a number of studies have been conducted using these structures to investigate the various stages of human development. However, EBs as structures are limited in a number of ways. Long term culture protocols are required to create complex structures from PSC derived EBs, but this is not possible due to the creation of large diffusion gradients across the EB structure as a consequence of increasing EB size over time. The severity of these diffusion gradients impacts on oxygen distribution within the EB, which creates a suboptimal environment in the EB interior, resulting in cell death and an impact on EB differentiation. This currently limits the use of EBs as a model, due to the inability to undertake long term studies which would allow for the formation of mature tissues. Combining EBs with solid scaffold technologies can prolong their viability through the reduction of these diffusion distances, with subsequent effects including an increased complexity and maturity of the EB derived tissue structures which form on the scaffold, which may also be due to the activation of attachment mediated signals. Alvetex® is a porous polystyrene scaffold which has been used in a number of three dimensional culture studies, in particular having been shown to enhance the differentiation capacity of PSCs, support the maintenance of tissue slices and the differentiation of PSC derived EBs. EC cells offer a simple and robust system for the optimisation of the novel model, with less demanding culture requirements and a well characterised differentiated phenotype, having already been used in studies into early embryogenesis and neural differentiation. These cells can be used as a working model to optimise growth conditions and develop methods before moving onto cells with more complex growth requirements, such as ES and iPS cells. Thus, combining TERA2.cl.SP12 EC cell derived EBs with Alvetex® scaffolds provides an option for the creation of a novel model of human tissue development.

4.2 Aims and Hypotheses

The aim of this chapter is to investigate the two key aspects of EB formation, cell death and differentiation, by creating EBs using a model cell line, TERA2.cl.SP12. Once the optimum culture time to maintain EB viability with sufficient differentiation is determined, EBs will be seeded onto the aforementioned polyHIPE scaffolds to determine the most appropriate scaffold to extend EB viability and maintain complex differentiation. Following this, the novel model will be subject to simple differentiation in order to ensure that the manipulation of differentiation by exogenous means can still be achieved, and that the model retains the differentiated phenotype as seen in the TERA2.cl.SP12 EB population. It is expected that increasing seeding density will result in an increase in cell death in TERA2.cl.SP12 EBs; therefore a lower seeding density is expected to be more appropriate for seeding EBs in the model. It is hypothesised that the appropriate scaffold will be one which prevents the infiltration of the EB into the insert will be most suitable to form a tissue model. Finally, seeding treated EC EBs into the model is expected to result in the maintenance or enhancement of the differentiated EB phenotype.

4.3 Objectives

- Create EBs using the TERA2.cl.SP12 cell line and assess both cell death and differentiation within the structures
- Choose the optimum polystyrene polyHIPE scaffold for the formation and maintenance of a tissue disc with an extended viability and differentiated phenotype
- Differentiate EBs prior to use in the model using known morphogens such as retinoids and BMPs, and ensure that the phenotype is maintained in the tissue disc model

4.4. Materials and Methods

Routine maintenance of TERA2.cl.SP12 EBs and their seeding onto Alvetex® inserts is described in the general Materials and Methods in Chapter 2. Below are techniques specific to the work in this Chapter.

4.4.1 Propidium iodide staining and flow cytometry of EBs

To assess necrotic cell death in live EBs, EBs were incubated with propidium iodide. EBs were maintained as previously described until the staining time point. A sample of the EBs were transferred to a 15 mL Falcon, and incubated in propidium iodide diluted 1:1000 in PBS for 20 minutes at room temperature, before washing in PBS and staining in Hoescht solution. EBs were washed in PBS again before transferring to ibidi µ Cell Culture Imaging dishes (ibidi, Martinsried, Germany) in a small amount of PBS for imaging immediately using the confocal microscope.

For flow cytometry, EBs washed in sterile PBS and carefully dissociated using 0.25% trypsin/EDTA. The reaction was neutralised using maintenance media and cells washed three times in sterile PBS. Cells were incubated in propidium iodide diluted in PBS at a final concentration of 10 µg/mL for 10 minutes, before washing 3 times in PBS and reading using the Guava easyCyte Flow Cytometer.

4.4.2 Caspase 3/7 live staining of EBs

To assess apoptotic cell death in live EBs, a caspase 3/7 stain was used. EBs were maintained as previously described until the staining time point. A sample of the EBs were transferred to a sterile 96 well round bottom plate. Nexcelom ViaStain™ Live Caspase 3/7 stain (Nexcelom Bioscience Ltd, Manchester, UK) was prepared according to the manufacturer's protocol, diluting the 1 mM stock solution in EB maintenance media to a final concentration of 2 µM. The media was removed from the EBs and 200 µl of the staining media was added to each well of EBs in the 96 well plate. EBs were incubated overnight in the stain, before washing in PBS the following day and staining for 5-10 minutes in Hoescht solution in PBS. EBs were then washed in PBS again and transferred to ibidi µ dishes in a small amount of PBS to image immediately on the confocal microscope.

4.4.3 Fluorescence Lifetime Imaging Microscopy

Fluorescence Lifetime Imaging Microscopy (FLIM) was conducted to assess the oxygen tension within EBs and tissue discs on Alvetex® Polaris, and was conducted with kind assistance from Dr Lars-Olof Pålsson, of the Department of Chemistry, Durham University.

To prepare samples, Platinum dipyrobenzene chloride (Pt[dpyb]Cl), which was kindly provided by Professor JA Gareth Williams, Department of Chemistry, Durham University, was dissolved in 0.5% DMSO in sterile PBS at a stock concentration 100 mM. EBs were placed into sterile 96 well plates,

and Polaris inserts were unclipped from their holders and placed into the bottom of 12 well plates. Samples were incubated in a final concentration of Pt[dpyb]Cl of 100 µM, diluted in appropriate cell culture media at 37°C, 5 % CO_2 overnight for at least 16 hours.

The following day, samples were partially prepared for imaging: EBs were transferred from the 96 well plate to a 15 mL Falcon tube, and the Falcon and plate containing the Polaris inserts were covered in foil for transport directly to the Imaging Facility in the Department of Chemistry. Samples were washed in PBS to remove excess stain and placed into Cavity Microscope Slides (Agar Scientific, Essex, UK): EBs were left in a small amount of PBS to prevent drying and EBs floating during imaging. Polaris membranes were cut to size, so that the tissue disc was surrounded by a small amount of membrane, and placed upside down in the cavity. Imaging was conducted as per the probe requirements, the excitation and emission filters used were $\lambda_{ex} = 405$ nm, $\lambda_{em} = 500–550$ nm, respectively (Raza et al., 2017; Williams et al., 2003).

4.5 Results

4.4.1 Investigations into the effects of cell density on the formation, viability and differentiation of TERA2.cl.SP12 derived EBs

The TERA2.cl.SP12 cell line has been used for a number of other applications involved in the study of pluripotency, differentiation and human tissue development. Previous studies have involved the culture and maintenance of pluripotent stem cell derived EBs on the surface of the polyHIPE scaffold, however, the growth of these EBs, including TERA2.cl.SP12 EBs, prior to use in the model had not been well studied. This is particularly important in terms of optimising the length of time required to culture EBs prior to use in the model, as well as comparing the effects of prolonged culture of the EBs both in suspension and on the scaffold. The presence of cell death and oxygen gradients can be established, as well as the differentiation profile of the EBs over a specified time period, which will then allow for the establishment of whether the model improves these properties. In order for the model to be successful, EBs must be seeded onto the polystyrene scaffold with the minimum cell death, as the activation of cell death pathways can result in a cascade effect on the resulting cells, with more widespread cell death ensuing. Additionally, the presence of significant cell death in the model would compromise the differentiated phenotype and likely prevent any more complex structure formation. This is critical when the formation of these complex structures is investigated even more closely following the introduction of more physiological microenvironmental cues to stimulate differentiation, such as perfusion and co-culture as in Chapter 3. Initial experiments involved the assessment of growth, differentiation and cell death in TERA2.cl.SP12 EBs seeded at a range of densities over a prolonged time period, in order to allow for a sufficient time range to select from. Two different types of cell death were assessed, as were the two differentiated phenotypes of TERA2.cl.SP12 investigated.

4.4.1.1 TERA2.cl.SP12 embryonal carcinoma cells display typical hallmarks of pluripotency

Initial cell line characterisation highlights the pluripotent phenotype of the TERA2.cl.SP12 cell line, and confirms its suitability in these differentiation studies, with a characteristic stem cell morphology; cells have a high nuclear to cytoplasmic ratio and prominent nucleoli as seen in the phase contrast images in Figure 4.4, part A. The cells also show a high expression of common pluripotency markers TRA-1-60, Oct 4, Sox 2 and low expression of differentiated markers such as Nestin, Class III β-tubulin and cytokeratin 8 when cultured at confluency, as would be expected: these culture conditions promote the pluripotent phenotype. Flow cytometry analysis provides more quantitative data, indicating that cells have a high expression of pluripotency markers SSEA-4, TRA-1-60, Oct 4 and Sox 2 and low expression of neural marker A2B5.

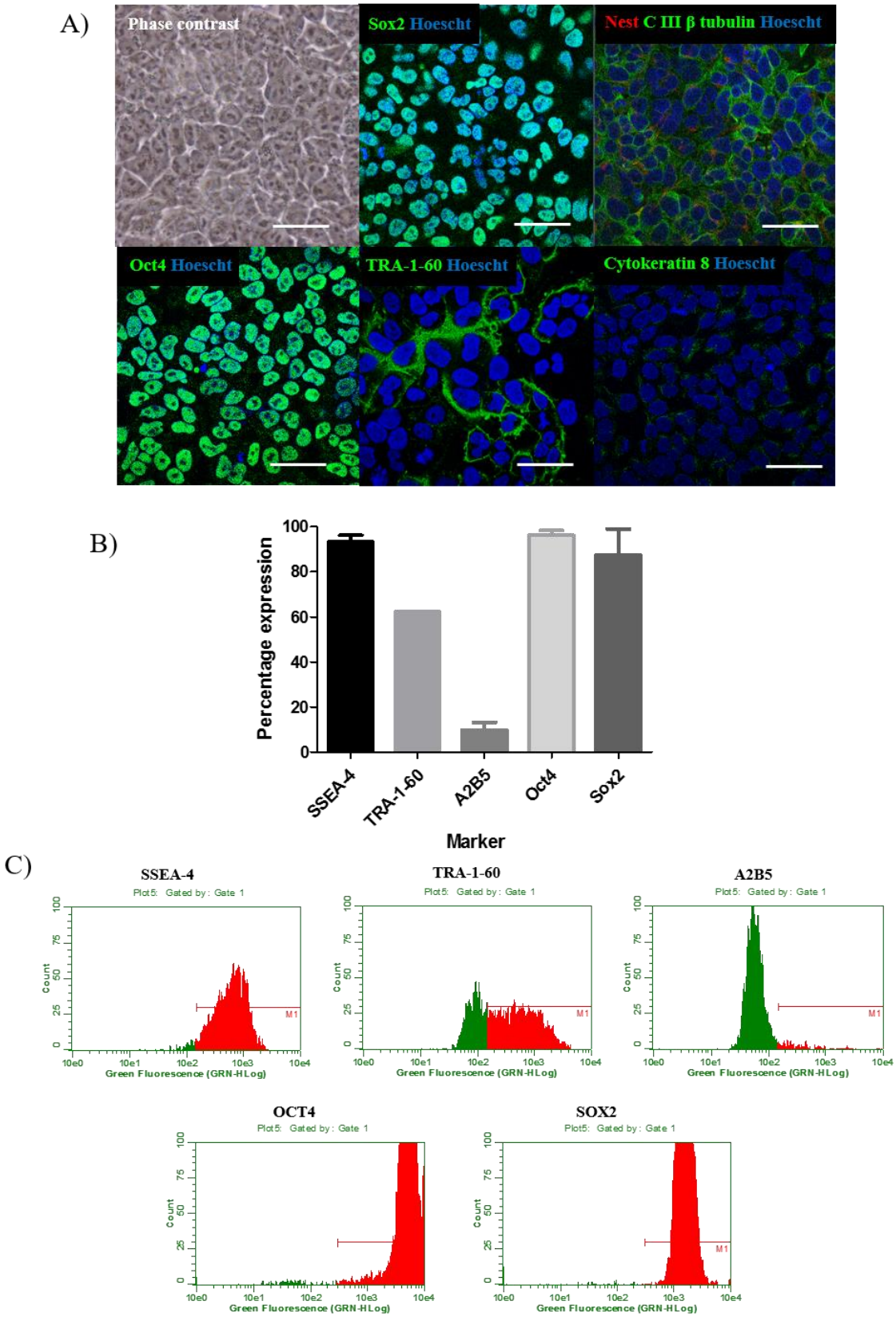


Figure 4.4: Characterisation of TERA2.cl.SP12 cells in traditional 2D culture: Figure legend on next page.

(Previous page) Figure 4.4: Characterisation of TERA2.cl.SP12 cells in traditional 2D culture: Pluripotency analysis of TERA2.cl.SP12 cells via immunostaining and flow cytometry detection of a variety of markers. For both analyses, cells were cultured until fully confluent. Cells on coverslips were fixed and stained for pluripotency markers Oct 4, Sox 2 and TRA-1-60 and differentiation markers Nestin, Class III β-tubulin and cytokeratin 8. For flow cytometry, cells were dissociated into a single cell suspension and stained using appropriate antibodies. Cells show pluripotent phenotype and appropriately high expression of pluripotency associated markers, with low expression of differentiation associated markers when maintained in 2D culture conditions, indicating their pluripotent nature. Representative histograms are shown. Data represents mean ± SEM from 3 independent experiments. (n=3) Scale bar: 50 μm

4.4.1.1 Differences in cell seeding density only impact on EB size during the early phase of formation

A range of cell densities were selected to seed EBs which incorporated values previously used in other studies with this cell line, in order to select the appropriate density for EBs to be used during the optimisation of the model using the TERA2.cl.SP12 cells. Previous studies have used 1 million cells (Knight, 2014; Quelch, 2018) and 1.5 million cells (Goncalves, 2017) in suspension culture to create EBs for various analyses. As the cell line is inexpensive to culture, suspension culture was used again to promote EB formation, as this allowed for the creation of large numbers of EBs for thorough analysis and eventual seeding onto the scaffold. The range of values to be seeded per Petri dish were selected as 0.5, 1, 1.5, 2 and 3 million (M) cells per Petri dish. The growth of these EBs was monitored closely over the first three days of suspension culture, as during this time EBs generally form compact aggregated structures (Zhou et al., 2010), with phase contrast images taken in order for the EBs to be measured. The measurements chosen to be conducted were EB circumference and area, as well as Feret's diameter. Feret's diameter is defined as the perpendicular distance between two tangents to the particle to be measured, and in Image J, is measured as the longest distance between two points on the selection boundary (Walton, 1948). This was chosen due to the often non circular/elliptical shape of the EBs, which complicated the measurement of diameter due to differences across the EB structure. Measurements were taken by tracing the circumference of the EB and using the automatic measuring functions in Image J. Phase contrast images and corresponding measurement data show trends as would be expected: EBs increase in size over the first three days of culture, and increasing seeding density leads to increasingly larger EBs at comparable time points, as can be seen in Figure 4.5. This effect is most pronounced on day three, when the differences in the circumference, area and Feret's diameter of the EBs are significantly more pronounced for the cells initially seeded at 2M and 3M cells per Petri dish, something which is again, notable in the phase contrast images.

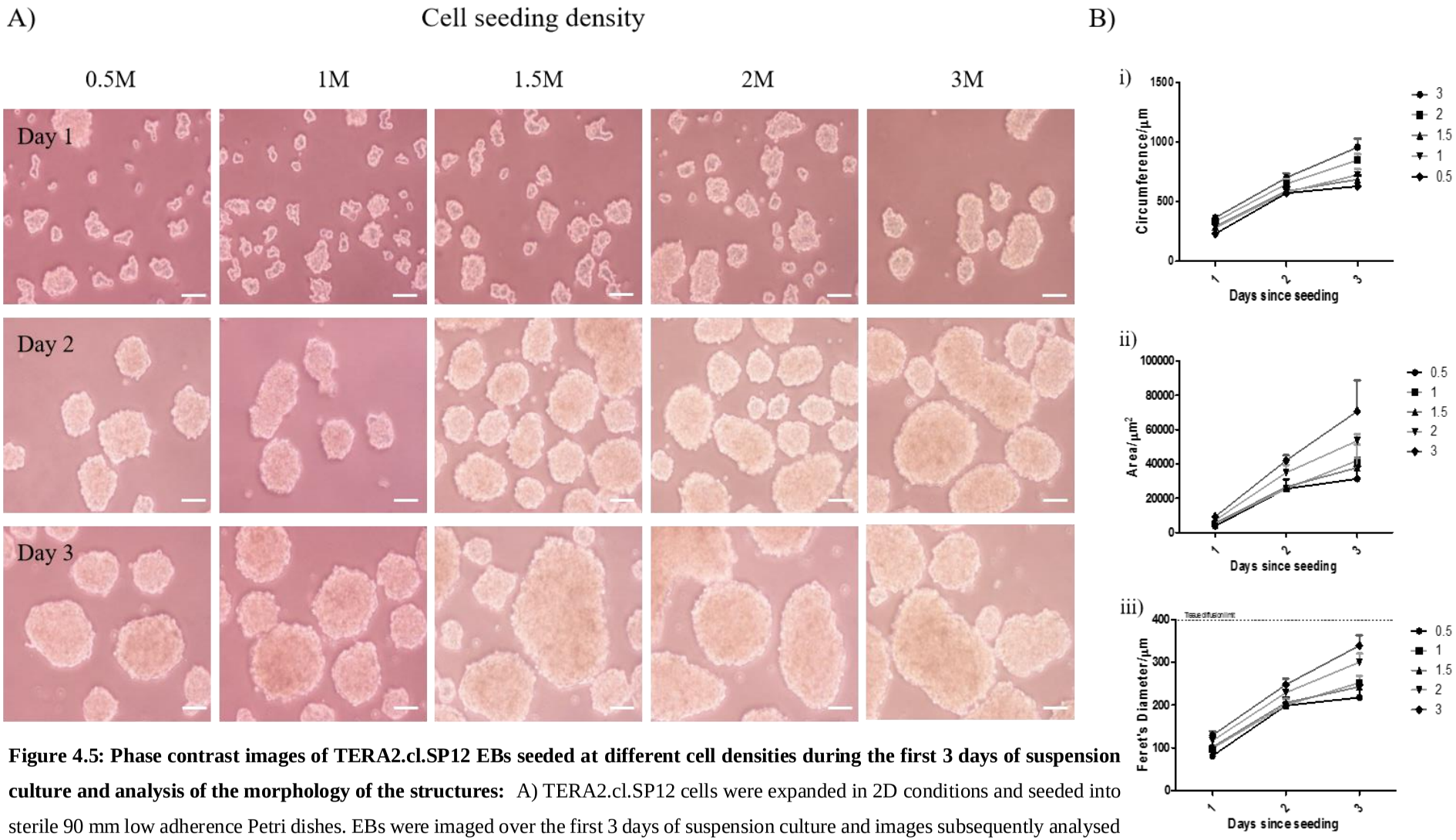


Figure 4.5: Phase contrast images of TERA2.cl.SP12 EBs seeded at different cell densities during the first 3 days of suspension culture and analysis of the morphology of the structures: A) TERA2.cl.SP12 cells were expanded in 2D conditions and seeded into sterile 90 mm low adherence Petri dishes. EBs were imaged over the first 3 days of suspension culture and images subsequently analysed using the measuring functions in Image J, with subsequent data in part B). As seen in section A), by day 3, there are clear differences between EB sizes corresponding to the initial seeding density, which is reflected in the quantitative analysis. Representative histograms are shown. Data represents mean ± SEM from 3 independent experiments. (n=3) Scale bar: 100 µm

Following further culture, differences in EB size were less perceptible. Figure 4.6 shows representative H&E images of the EBs at 7, 14 and 21 days suspension culture. At 7 days, there are slight differences in the size of EBs dependent on the initial seeding density, with EBs seeded at 1M and 1.5M appearing larger at this time point than EBs seeded at other densities. By 14 days, differences in EB size are much less visible, and at 21 days, there is no real difference in the size of the EBs regardless of the initial seeding density. This is confirmed by quantitative measurements of EBs that can be seen in Figure 4.7, with the same set of measurements taken as in Figure 4.5, with no significant differences in seeding density and subsequent EB dimensions as analysed via a one way ANOVA. The data confirms that at and after 14 days in culture in particular, there are no clear differences in EB size, suggesting that there is an inherent upper limit to TERA2.cl.SP12 EB size. Within the EBs, evidence of differentiation can be detected through the formation of neural rosettes within the EB body. These are not detectable in any of the EBs at 7 days, although at and after 14 days, some more heterogeneous structures including neural rosettes can be identified in some of the EBs, particularly 0.5M and 1.5M seeding densities. These can also be identified at the 21 day time point in a number of the EBs, showing the more differentiated phenotype in the EBs. Also of note are the subtle differences in the morphology of the centre of the EB in Figure 4.6, which is more noticeable in the 21 day EBs, particularly the 1M and 1.5M seeding densities. The centre of these EBs appears to have adopted a different structure compared to the rest of the EBs, with the cells appearing to be slightly looser in their overall arrangement. This is potentially the formation of a layered structure as alluded to by Gothard (Gothard et al., 2009). (The fragmentation of some EBs is an artefact of processing, most likely due to the fragility of some EB structures, and is not taken to be of significance in this study.)

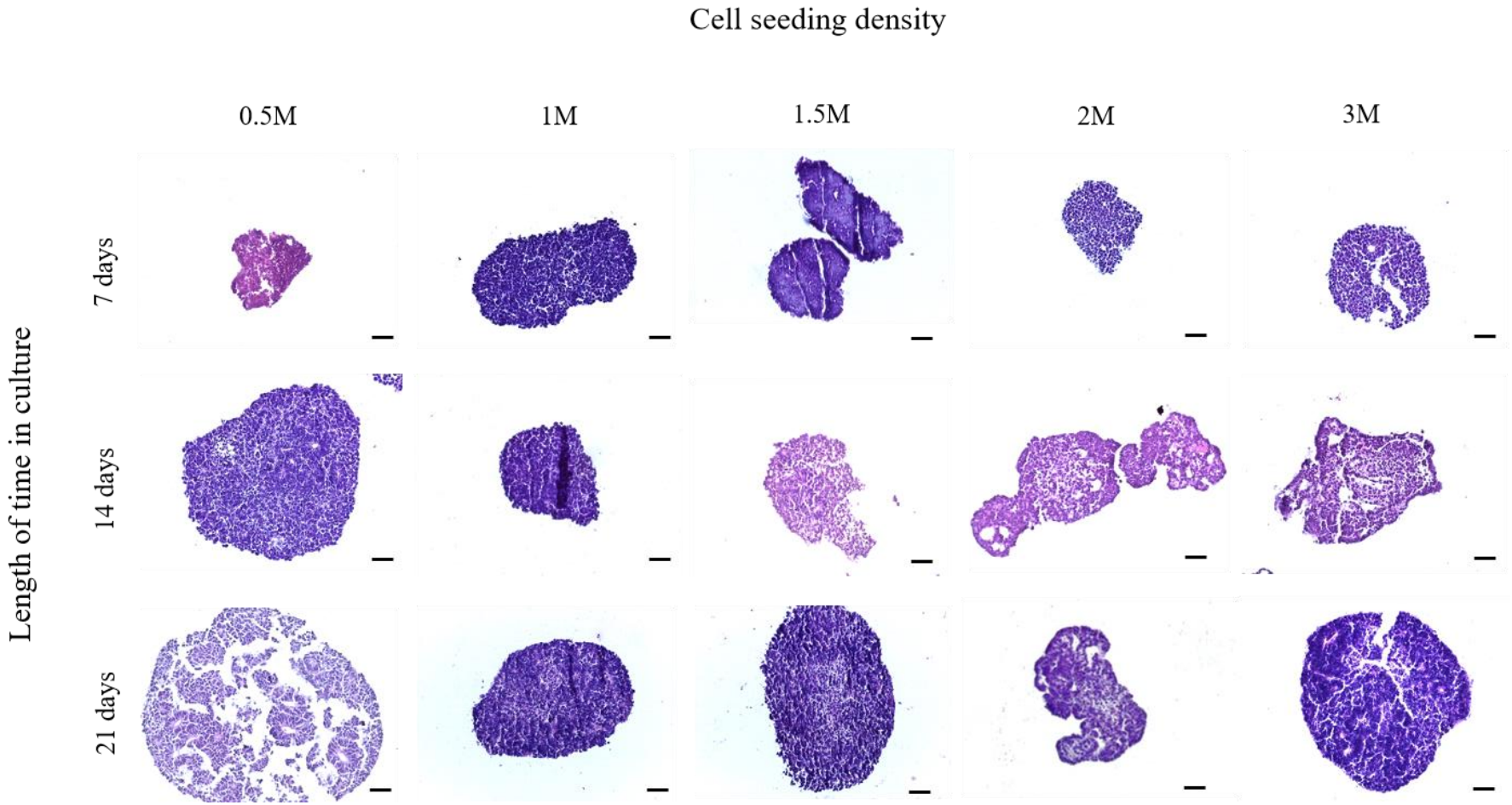


Figure 4.6: TERA2.cl.SP12 EBs cultured at varied cell densities for up to 21 days: H&E images of TERA2.cl.SP12 EBs seeded at different cell densities at 7, 14 and 21 days of culture post seeding with analysis of morphology: TERA2.cl.SP12 cell EBs were fixed in 4% PFA before subsequent dehydration and embedding in paraffin wax. Sections were stained using H&E. Differences in initial aggregate seeding density translate into differences in aggregate size at early time points as observed in the previous Figure, but less so at the later time points as shown here. Representative images shown from three independent experiments. (n=3) Scale bar: 100 µm

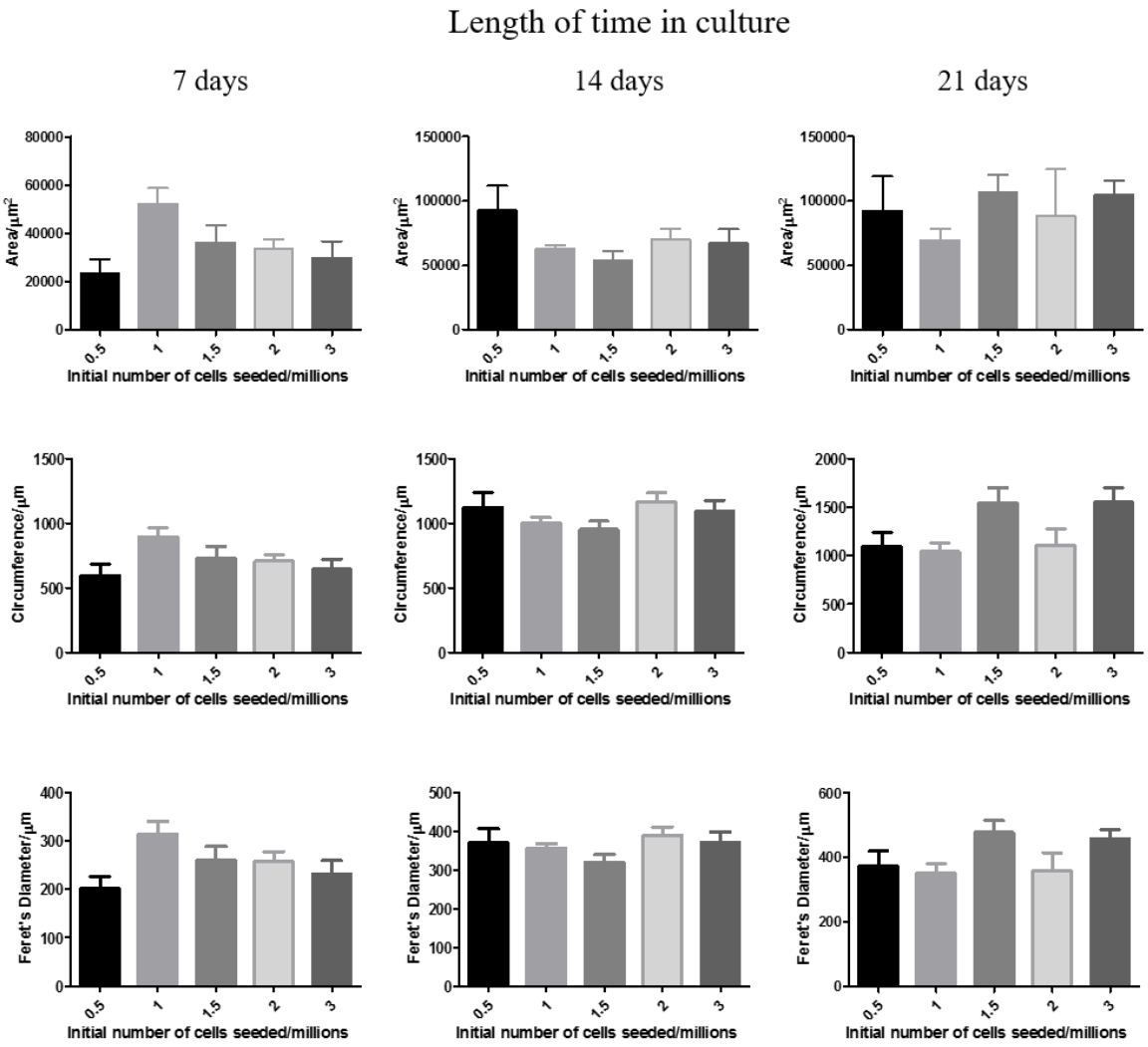


Figure 4.7: Analysis of TERA2.cl.SP12 EBs cultured at varied cell densities for up to 21 days: H&E images of TERA2.cl.SP12 EBs seeded at different cell densities at 7, 14 and 21 days were analysed using the measuring functions in Image J. As with Figure 4.5, there some small differences between the EBs seeded at different cell densities, particularly at the earlier time point of 7 days. While there is natural variability using suspension culture as a method of EB formation, overall there are no significant differences in the size of EBs after 14 days culture. No significant differences were found as analysed using one way ANOVA. Data represents mean ± SEM from 3 independent experiments (n=3).

4.4.1.2 Cell death reaches a level of consistency in TERA2.cl.SP12 EBs after 14 days culture

Determining the localisation and level of cell death in the EBs is key prior to seeding them onto the scaffold, yet EBs also require sufficient time in culture to differentiate and mature prior to use in a model intended to create complex structures. Additionally, cell death occurs via a number of different mechanisms within EBs, dependent upon various factors, including EB size and local microenvironmental conditions. Both apoptotic and necrotic events have previously been identified in developing EBs, prompting the need to assess both in the structures developing here.

Apoptosis is a controlled form of cell death, which may be in response to irreparable cell or DNA damage or a part of a controlled developmental process, and the pathways controlling this process are heavily regulated by caspase family proteins. Caspases 3 and 7 are key executioner proteins or effector caspases (Walsh et al., 2008), involved in the cleavage of many other proteins in the apoptotic cascade as well as other crucial apoptotic events such as chromatin condensation (Porter and Jänicke, 1999). Thus, the activation of these proteases is an indicator of entry into apoptosis, a fact which can be exploited to detect apoptotic cell death *in vitro*. A live active Caspase 3/7 stain was used to assess apoptotic cell death within the EBs over 3 time points; 7, 14 and 21 days, in order to determine a suitable length of time to culture EBs prior to seeding in the model. Live staining highlighted that almost all EBs at all seeding densities have some low level of cell death within the internal structures. After 7 days in suspension, EBs continue to show a trend as would be expected when the seeding density is considered in regards to levels of apoptotic cell death, with the lowest seeded densities showing very little apoptotic cell death, if any. The EBs seeded at the higher cell densities 2M and 3M, show some small amount of apoptotic cell death but at this stage, the staining is not well localised to any specific point within the EBs. By the 14 day time point, positive apoptotic staining appears to be more apparent and consistent between the EBs, as well as more localised to central areas within the EBs or areas with high cell density, in particular where individual EBs have clumped together. The only exception to this is the 3M cell seeding density, which shows a large amount of positive staining within the EB. This consistent staining phenotype is replicated at the 21 day time point, where cell death is generally more centrally localised in the EBs or to areas of a high cell density.

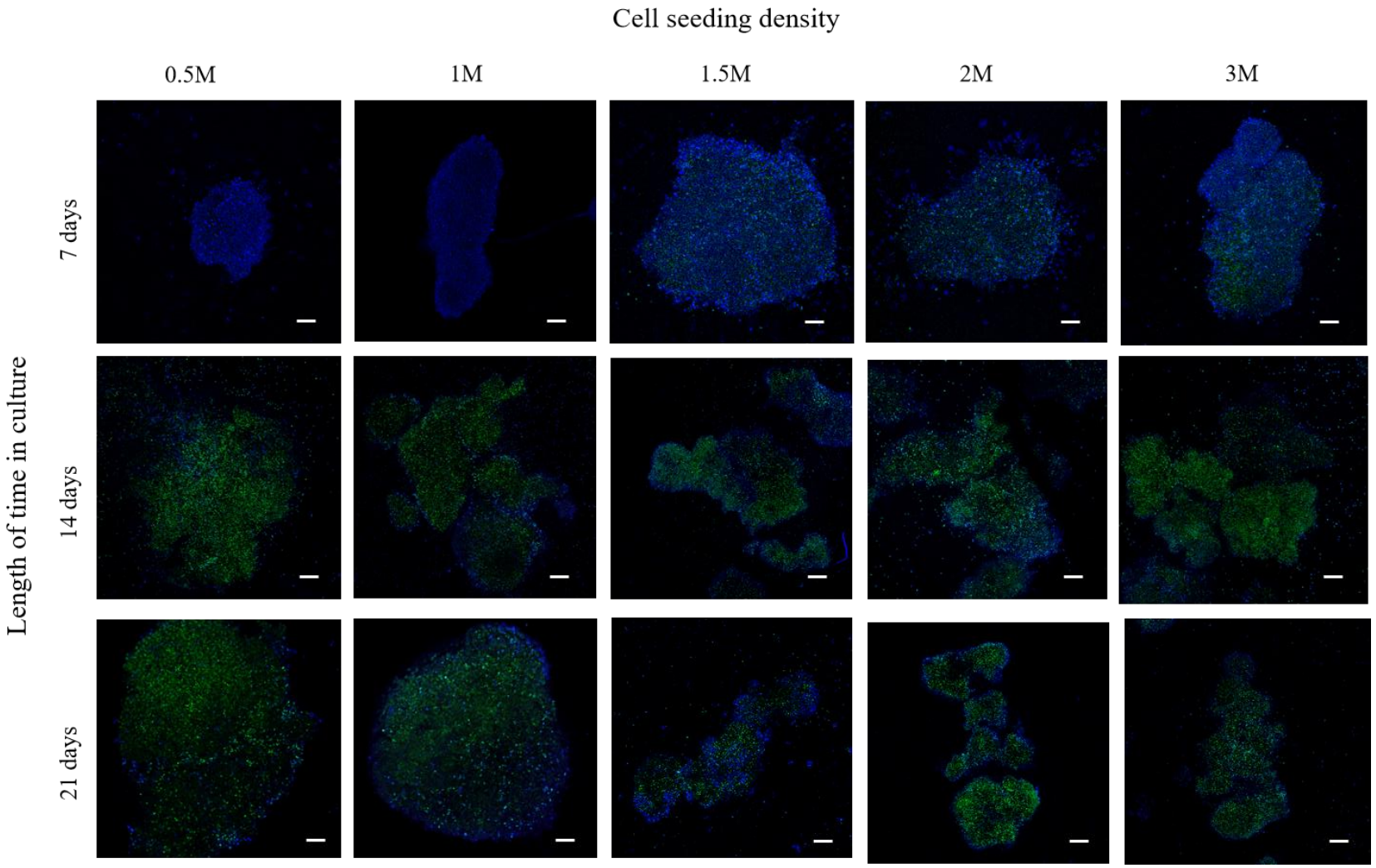


Figure 4.8: Assessment of apoptotic cell death in TERA2.cl.SP12 EBs at various cell densities using live caspase 3/7 stain: EBs were transferred to a round bottomed 96 well plate, before incubation in 2µM of the live Caspase 3/7 stain overnight at 37°C. Aggregates were then washed and stained with Hoechst before transferring to 35 mm Petri dishes for imaging. Images were taken on a Zeiss 880 Confocal Microscope. Small differences in the cell death at the various cell densities are more apparent at the earlier time points. There is a significant amount of cell death present at the later time points, although this appears to be consistent between seeding densities. Representative images shown. Scale bar: 100 µm

Necrotic cell death was also assessed. Necrotic cell death is a chaotic process in response to cellular trauma, such as injury, exposure to extreme temperature or hypoxic conditions, and results in the uncontrolled breakdown of the cell. Features include nuclear swelling and the loss of membrane integrity (Fink and Cookson, 2005), a factor which can be used to detect necrosis through the use of dyes such as propdium iodide (PI), which only enter cells with impaired membranes. PI staining reveals a similar pattern of positive staining within the TERA2.cl.SP12 EBs. Positive staining is not easily detected in the confocal images in Figure 4.10 for the 7 day time point, correlating with the lack of apoptotic cell death also observed after 7 days. As was seen in the previous Figure with the Caspase staining, propidium iodide staining can be seen in EBs from the two later time points. Again, a similar trend as was observed with the 14 and 21 day EBs is visible, with cell death localised to central and cell dense areas, yet consistent in terms of frequency between EBs of differing cell densities. Flow cytometry performed on dissociated TERA2.cl.SP12 EBs confirms this phenotype for the later time point EBs, with differences in staining found not to be significant in these EB populations. This analysis also reveals a similar staining profile as observed with Caspase 3/7 staining in the EBs cultured for only 7 days in suspension, with an increase in positive staining in concordance with the increase in seeding density.

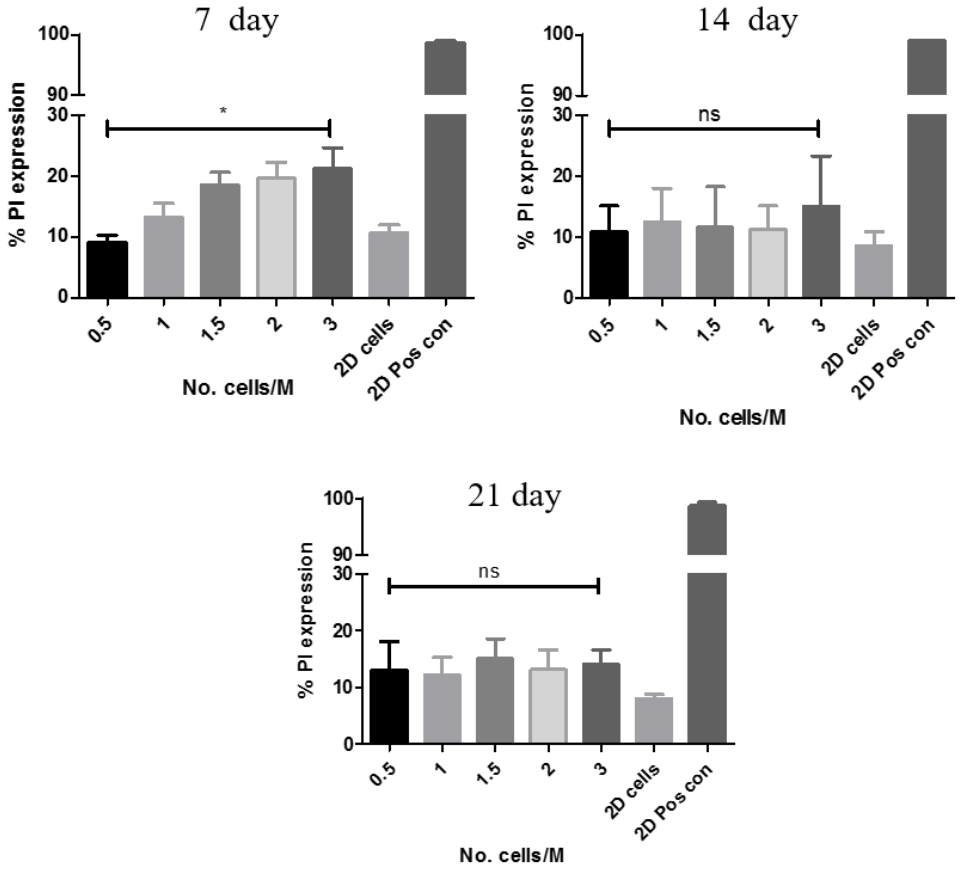


Figure 4.9: Quantitative analysis of necrotic cell death in TERA2.cl.SP12 EBs at various cell densities via flow cytometry: EBs were dissociated to create a single cell suspension; cells were washed in PBS and incubated in 10µg/ml propidium iodide solution, before detection using Guava easyCyte Flow Cytometer. At the 7 day time point, there is a significant trend in the amount of cell death present, highlighting the impact of cell seeding density. After this, cell death as identified by propidium iodide staining is consistent in all cell densities. Data represents mean ± SEM from 3 independent experiments. (n=3)

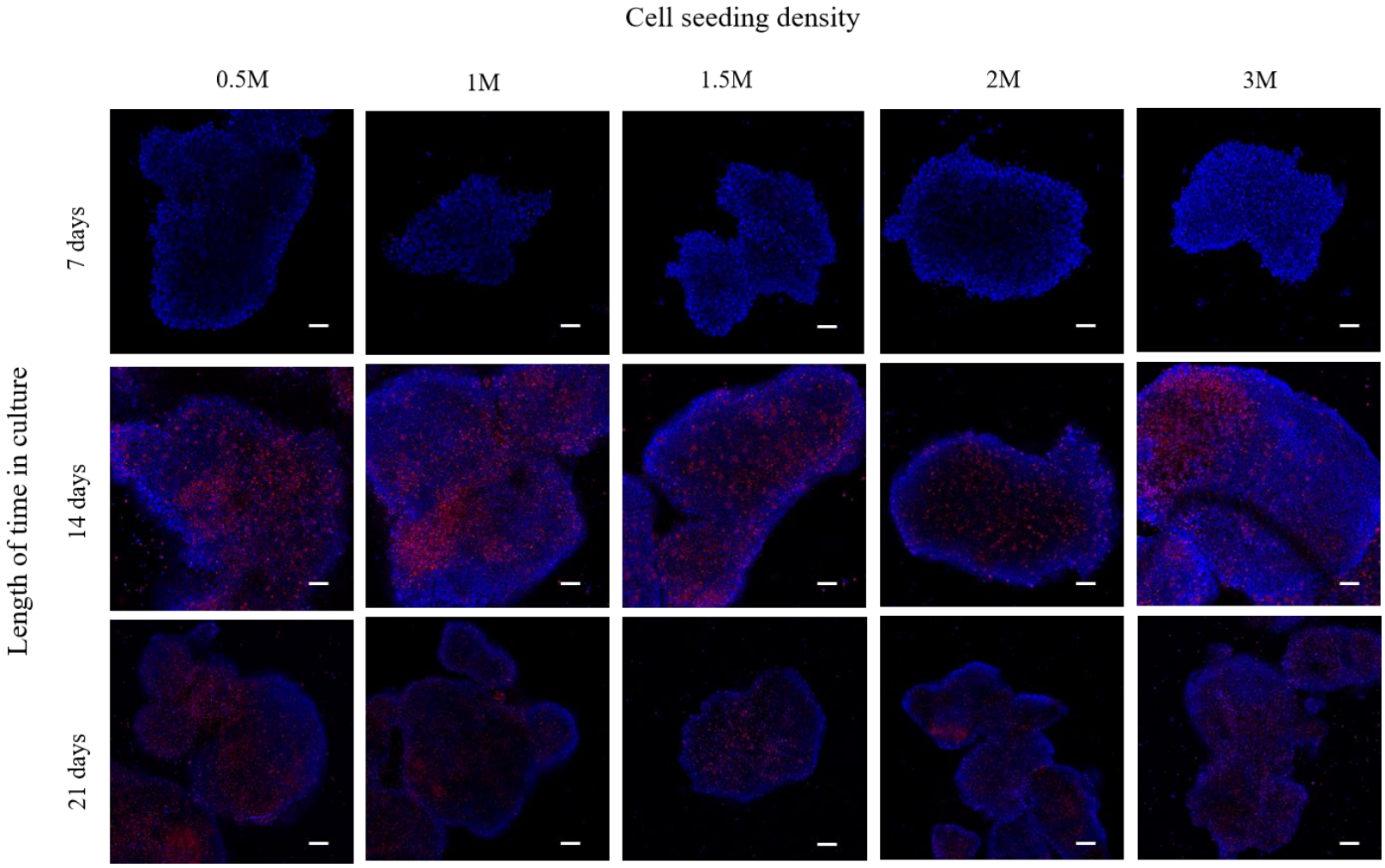


Figure 4.10: Assessment of necrotic cell death in TERA2.cl.SP12 EBs at various cell densities using propidium iodide: Confocal microscope images of TERA2.cl.SP12 EBs of different cell densities at 7, 14 and 21 days of suspension culture, stained with propidium iodide. EBs were washed before incubation in 10µg/ml propidium iodide solution for 20 minutes at room temperature. Aggregates were then washed twice again before fixing with 4% PFA. After washing, aggregates were stained with Hoechst for 20 minutes before mounting on slides in Vectashield mounting medium. Images were taken on a Zeiss 880 Confocal Microscope. Propidium iodide cell death appears to be more pronounced at 14 days and after, at all cell densities. Representative images shown. Scale bar: 100 µm

4.4.1.3 In TERA2.cl.SP12 EBs, seeding density has some modest effects on pluripotency and differentiation

Limiting the amount of cell death which occurs in TERA2.cl.SP12 EBs during their formation in the suspension phase needs to be balanced with sufficient maturation of EBs prior to seeding into a model to allow for differentiation to occur and continue. Additionally, the effects of seeding density on the property of pluripotency and subsequent differentiation has not been well explored in EC cell derived EBs in order to inform decisions regarding seeding density and culture time. EBs which were seeded at the densities stated above were subject to analysis of ectodermal differentiation, both neural and non-neural epithelial, and pluripotency analysis over the same 21 day time period, via the expression of the following 4 markers. Oct 4 is a transcription factor which contributes to the maintenance of the pluripotent state through mutualistic antagonism with two other key transcription factors, Sox 2 and Nanog, and is known to be strongly associated with the pluripotent phenotype. Nestin is a marker of neural stem cells, an intermediate filament marker which is detected in particular in neural progenitor populations during the developmental process. The microtubule protein Class III β-tubulin is a marker of mature neural differentiation, as the protein is detected in the outgrowing neural processes. The epithelial marker cytokeratin 8 is expressed in simple epithelial populations derived from the ectoderm. As TERA2.cl.SP12 EBs preferentially differentiate towards these two ectodermal phenotypes, which are distinct in their expression profile, this will allow for the detection of complex differentiation within the structures.

While the expression of pluripotency marker Oct 4 is not significantly different between differentially seeded EBs at the early 7 day time point, a trend is clearly visible. Flow cytometry analysis of dissociated EBs shows that EBs seeded at the higher densities of 2M and 3M cells per Petri dish demonstrate a reduced expression of Oct 4 in comparison to the lower seeded densities at the same time point. After this time, there is little correlation between the continued expression of pluripotency markers and cell density. These differences in Oct 4 expression are visible in the immunostaining as seen in Figure 4.11. EBs cultured for 7 days show some differences in the expression of the pluripotency marker, as is seen with the flow cytometry data. At and after 14 days in culture, Oct 4 expression cannot be detected in the immunostaining images, with the flow cytometry data representing this residual low level expression in particular at 21 days. The expression of cytokeratin 8, an early epithelial ectoderm marker, was found to be highly significant when the highest and lowest seeding densities were compared after 7 days of culture, possibly correlating with differences in pluripotent nature of the cells seeded at the lower density as seen with the trend in Oct 4 staining. After this time point, the expression of cytokeratin 8 is relatively consistent between the various seeding densities, as reflected by the lack of significance in the flow cytometry data obtained for both the 14 day and 21 day time points and the lack of staining in the Figure. Given that the default differentiation pathway of TERA2.cl.SP12 is neural, this is not unexpected.

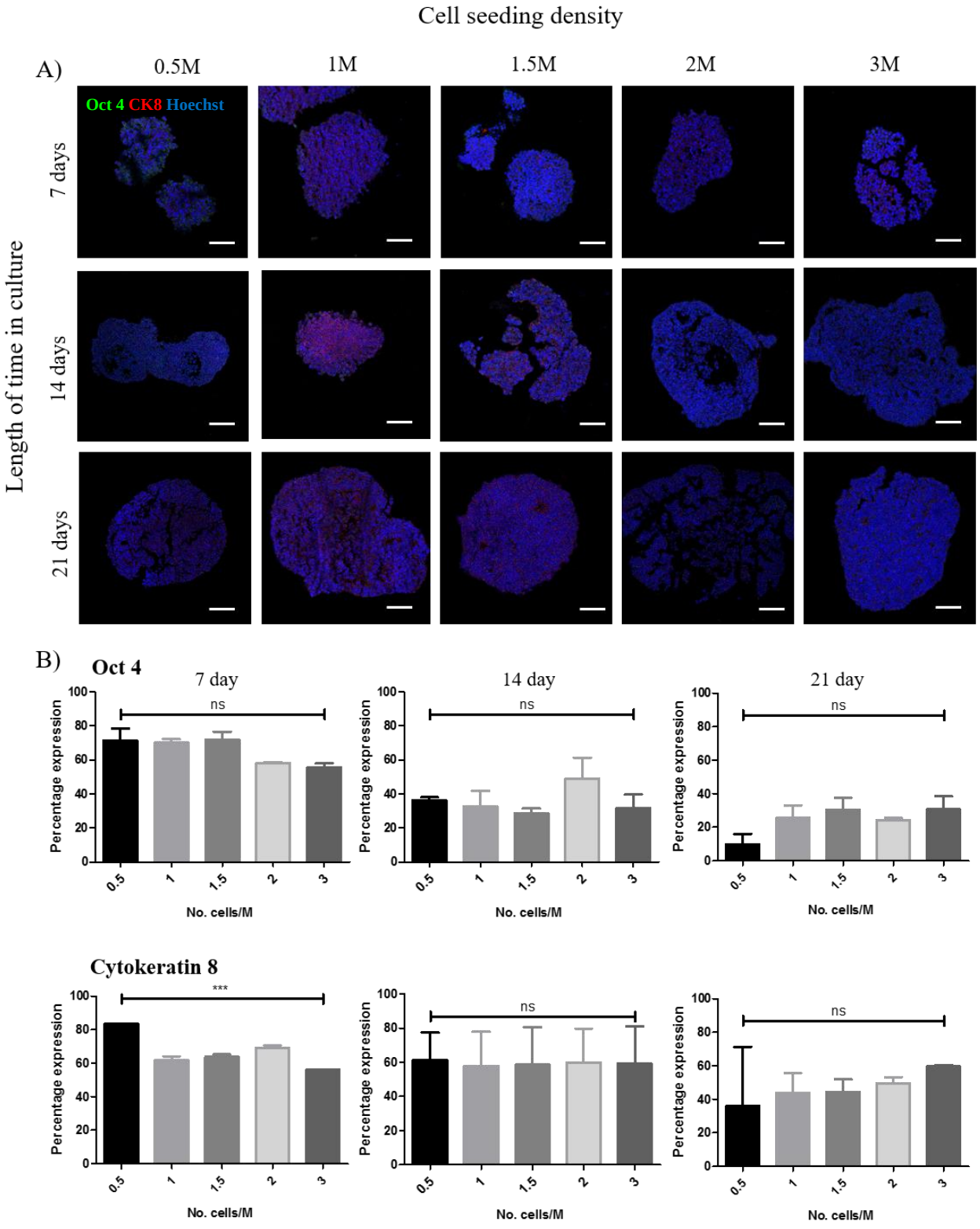


Figure 4.11: Assessment of the pluripotency and epithelial ectodermal differentiation of TERA2.cl.SP12 EBs seeded at various densities: A) 6 µm wax sections of EBs were stained to detect the expression of pluripotency marker Oct 4 (green) and the epithelial marker cytokeratin 8 (red) and imaged using a Zeiss 880 confocal microscope. B) Flow cytometry on EBs was carried out as described previously although the effects are not significant, there is a general trend in the effects of seeding density on both pluripotency and epithelial differentiation. Representative images shown. Flow cytometry data analysed using a one way ANOVA. Data represents mean ± SEM from 3 independent experiments. (n=3) Scale bar: 50 µm

The analysis of neural differentiation was also conducted, due to the propensity of TERA2.cl.SP12 to form neural derived tissues. As was seen with pluripotency marker Oct 4, neural progenitor marker Nestin also shows a trend in expression in correlation with EB seeding density. EBs seeded at the lower cell densities show a higher expression of the marker compared to those seeded at the higher cell density. In this case, the trend is much more gradual, and persists beyond the 7 day time point until the end of the culture period at 21 days, although the differences are again, not significant. Some small amounts of Nestin staining can be detected in the TERA2.cl.SP12 EBs, although this is often alongside stronger Class III β-tubulin staining. The expression of the pan-neuronal marker Class III β-tubulin is an indicator of more mature neuronal differentiation, and its expression in the developing EBs was also assessed using flow cytometry and immunostaining. The expression of this marker was found not to be significant between the various seeding densities at all time points, but selected seeding densities show an increased expression, notably 0.5 and 1.5 million cells. The immunostaining reveals that although Class III β-tubulin is expressed at the earlier time point of 7 days, it is not until 14 days that expression is more global in the EB structure and there is evidence of differentiated structures such as neural rosettes. These structures are even more visible at the 21 day time points, with clear evidence in the EBs seeded at 1 and 1.5 million cells, highlighting the need for sufficient time for EBs to undergo lineage specification and form complex differentiated structures.

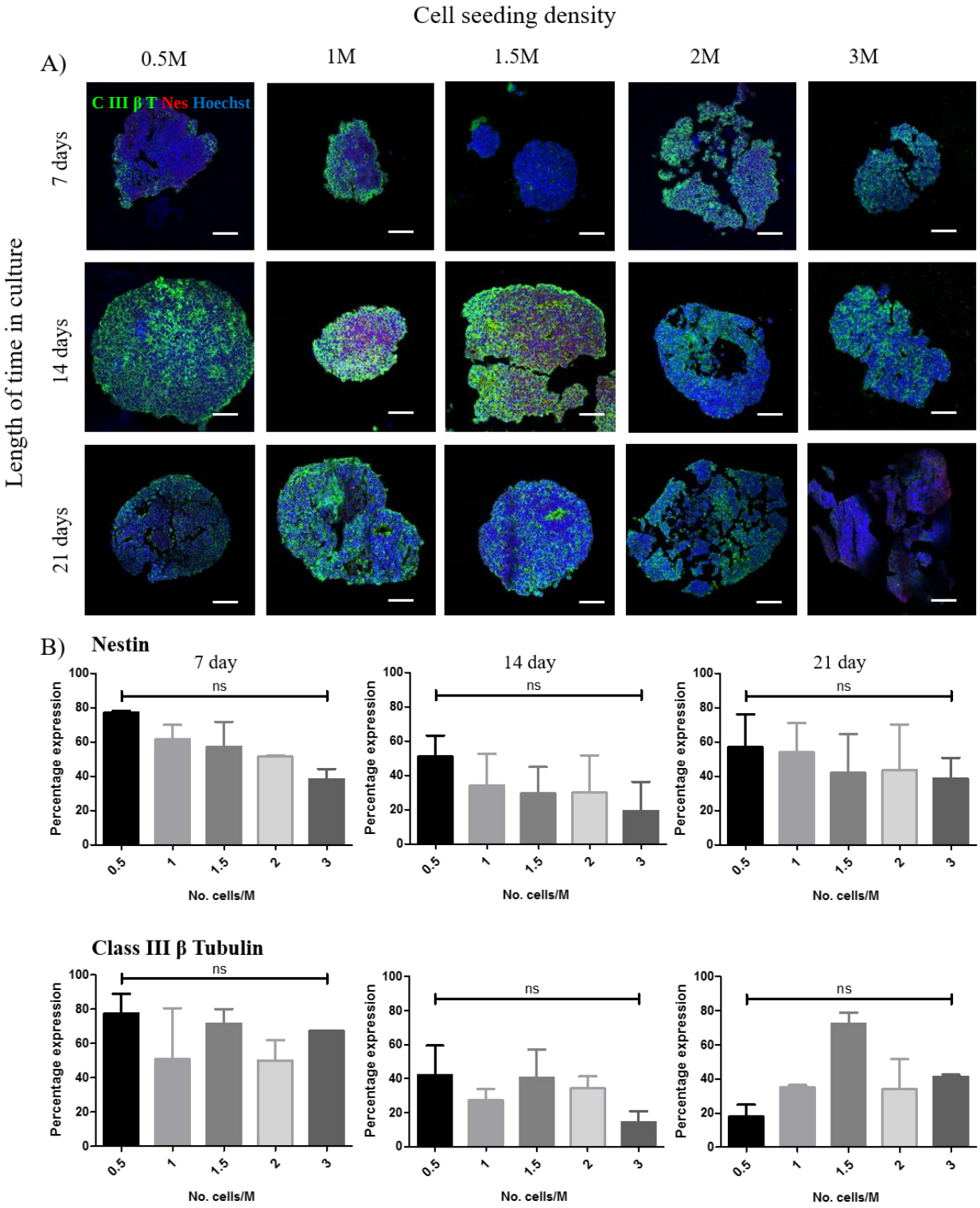


Figure 4.12: Assessment of the neural differentiation of TERA2.cl.SP12 EBs seeded at various densities: A) 6 µm wax sections of EBs were stained to detect the expression of early neural marker Nestin (red) and late neural differentiation marker Class III β-tubulin (green) and imaged using a Zeiss 880 confocal microscope. B) Flow cytometry was carried out on EBs as previously described. Again, although the effects observed are not significant, there are trends and differences in the expression of the neural markers dependent on the seeding density. Representative images shown. Flow cytometry data analysed using one way ANOVA. Data represents mean ± SEM from 3 independent experiments. (n=3) Scale bar: 50 µm

4.4.1.4 EB seeding density and culture time optimised to 1.5M cells and 14 days respectively

The various studies carried out investigating the dimensions, cell death and differentiation within TERA2.cl.SP12 EBs at 5 different seeding densities yielded a number of interesting results that allow for the selection of the optimal seeding density and culture period for EBs prior to seeding on the scaffold.

Table 4.2: Summary of results from EB cell densities studies and impact on optimisation decisions

Property	Results	Optimal conditions
EB dimensions	**Early time points up to 3 days** – high cell densities approach the tissue diffusion limit, risk of forming a hypoxic core and increased cell death **7, 14 and 21 days** – Small differences at 7 days, but no significant differences in EB size after 14 days in culture. No complex structures at 7 days, some evidence of more complex structures at day 14.	0.5M and 1.5M show heterogeneity in structure at 14 days indicating differentiation
Cell death	**Apoptotic cell death** – some evidence of a trend correlating with seeding density at 7 days, with a more consistent amount of cell death after 14 days in culture at all time points **Necrotic cell death** – Significant difference between high and low densities at 7 days. Consistency in cell death at and after 14 days in culture.	All densities show consistency at 14 days
Pluripotency and differentiation	**Pluripotency -** Oct 4 expression trend visible but not significant, higher densities show lower expression. **Epithelial differentiation** – CK8 expression significantly different at 7 days between low and high seeding densities. Consistently low cytokeratin 8 expression in general after 14 days in culture. **Neural differentiation** – Early marker Nestin shows a trend with seeding density, persisting until 21 days. Class III β-tubulin expression high in selected densities but not significantly so. Evidence of complex structures not until 14 days in immunostaining.	0.5M and 1.5M show an enrichment for Class III β-tubulin expression, 1.5M particularly at 21 days.

Based on the fact that cell death is consistent after 14 days in culture in all cell densities, but complex differentiated structures are not visible until this point in histological and immunostained images, 14

days is the minimum length of time TERA2.cl.SP12 EBs can be cultured to ensure EBs show a differentiated phenotype. Given that the higher cell densities reach a diameter approaching the tissue diffusion limit early in the culture period, there is a reluctance to select these EBs due to the risk of forming a hypoxic core early during the differentiation process. At the 14 day time point, differentiation was not significantly different in any of the seeding densities although selected densities showed persistent enrichment for the neural marker Class III β-tubulin, the preferred differentiation route of this cell line. Due to this trend of increased mature neural marker expression, the presence of complex differentiated structures and a consistency in cell death, 1.5M cells for 14 days was selected as the optimal EB seeding density and suspension culture time prior to seeding on the scaffolds.

4.4.2 Investigation into the interaction between cellular EBs and Alvetex® membranes

A key aim of this novel model is increasing the viability of pluripotent stem cell EBs for prolonged culture, in order to allow for the development of complex structures which can be analysed to assess cellular pluripotency, as well as study aspects of human tissue development and cellular differentiation. In the Introduction to this chapter, the use of Alvetex®, a polyHIPE scaffold, was discussed in the context of numerous cell types, as was its ability to maintain stem cells, embryoid bodies and tissue slices. Initial experiments sought to explore the interaction of TERA2.cl.SP12 EBs with the multiple forms of Alvetex®, in order to select the form most suitable for maintaining pluripotent stem cell EBs as a 'tissue disc' and allow for more complex differentiation.

4.4.2.1 Alvetex® Polaris is the only form of the scaffold that allows for the full preservation of the EB as a tissue discs

Alvetex® comes in three forms, each with different void and pore sizes, as detailed in Table 4.3. All three formats, Scaffold, Strata and Polaris, have previously been used in small scale studies successfully to maintain pluripotent stem cell derived EBs as tissue discs. However, in order to directly compare the use of these formats, as well as now using the optimised EB culture period, it was considered appropriate to test all three forms of Alvetex® in order to ascertain the most suitable form for this novel model.

TERA2.cl.SP12 EBs which had been seeded at a density of 1.5M cells and cultured in suspension for 14 days were seeded onto Alvetex® inserts and maintained for a further 7 days on each form of the scaffold before analysis. As Figure 4.13 shows, TERA2.cl.SP12 EBs adhere and flatten out onto the surface of Alvetex® Scaffold, and the tissue disc shows a dense, compact structure on the surface of the scaffold. However, a significant proportion of the EB has infiltrated the scaffold itself; there are many cells below the dashed line, which indicates the surface of the scaffold. In fact, cells from the EB infiltrate the full 200 μm width of the scaffold, with cells clearly visible on the underside of the scaffold in the H&E image. There are no characteristic differentiated structures which are indicative of ectodermal differentiation in this cell line, namely neural rosettes and epithelial surface structures. The lack of Oct 4 expression in the associated immunostaining highlights that pluripotency is not maintained or stimulated by the scaffold. Positive staining for both cytokeratin 8 and Class III β-tubulin supports the fact that the scaffold is able to maintain the EBs with a level of disorganised differentiation in the tissue disc format. Class III β-tubulin expression is high, indicating mature differentiation, but a large proportion of the positive cells are within the scaffold itself.

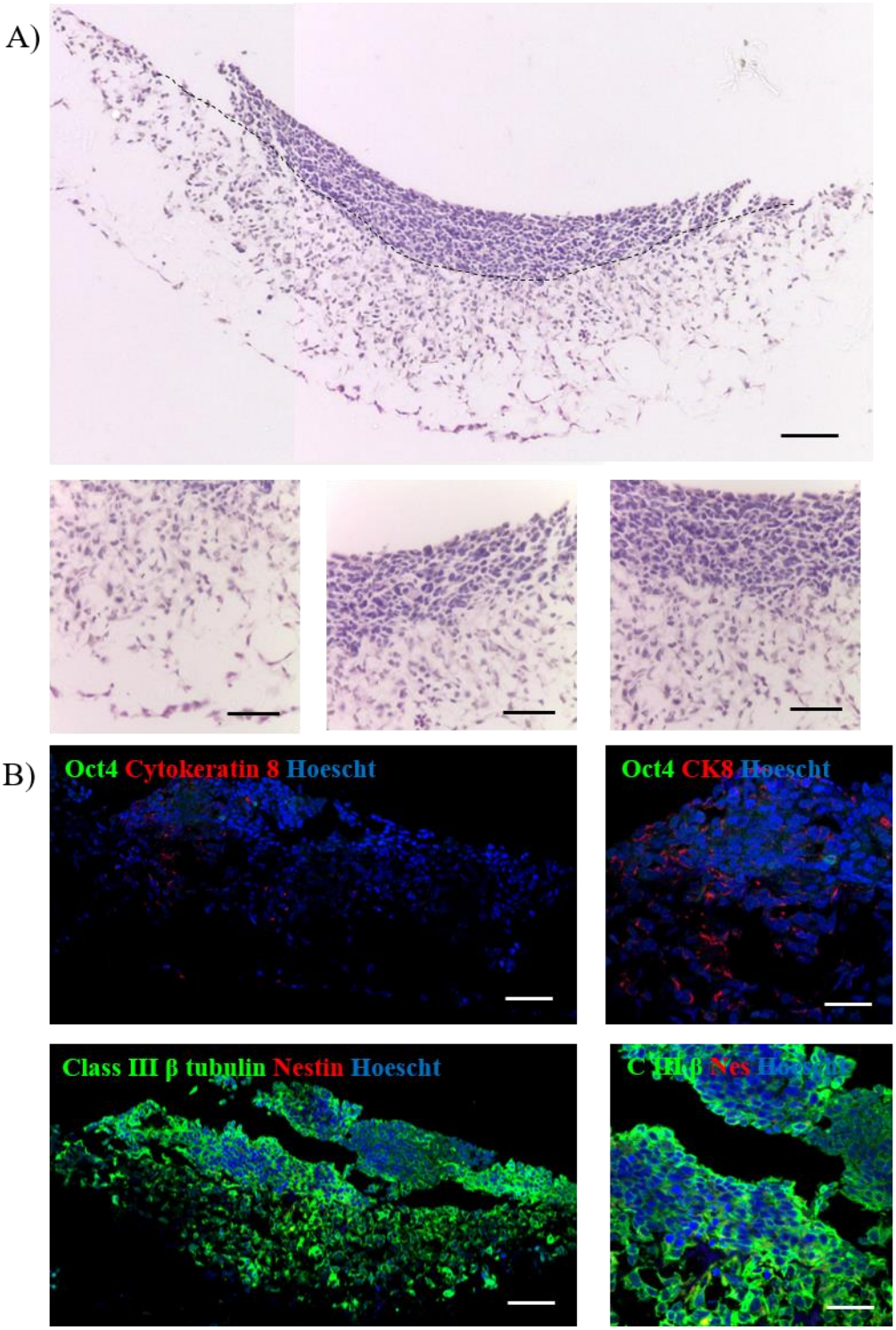


Figure 4.13: Behaviour of TERA2.cl.SP12 EBs cultured on the surface of Alvetex® Scaffold for 7 days: TERA2.cl.SP12 cells were seeded at a density of 1.5M cells into a sterile, low adherence Petri dish and cultured for 14 days before transferring to Alvetex® Scaffold for 7 days. Inserts were then fixed in 4 % PFA for histological analysis. Dashed line indicates the upper boundary of the Alvetex® insert. Note that while some of the structure of the EB remains on the surface of the insert, much has migrated below into the supporting scaffold, invading the full thickness of the insert. While there is positive staining for differentiation, there is no evidence of complex structure formation due to EB disintegration. Additionally, there are no pluripotent regions. Representative images shown. Scale bars: 100 µm and 50 µm

When cultured on Alvetex® Strata, TERA2.cl.SP12 EBs again show evidence of flattening and adherence to the scaffold, due to the elongated shape of the tissue disc. The level of infiltration into the scaffold is significantly less compared to Alvetex® Scaffold, with cells only having infiltrated partially into the insert; no cells have reached the base of the insert in this case. There is evidence of complex differentiation in the form of neural rosettes within the tissue disc structure. Immunostaining again shows no evidence of Oct 4 positive pluripotent areas, indicating that EBs cultured on this scaffold strongly follow a differentiation pathway. Class III β-tubulin staining is positive within the EBs and the infiltrated cells, indicating the maintenance of differentiated areas, although there is no evidence of neural structure formation with regard to neural rosettes. The lack of cytokeratin 8 positive structures indicates an absence of non-neural epithelial ectoderm differentiation within the tissue disc structure.

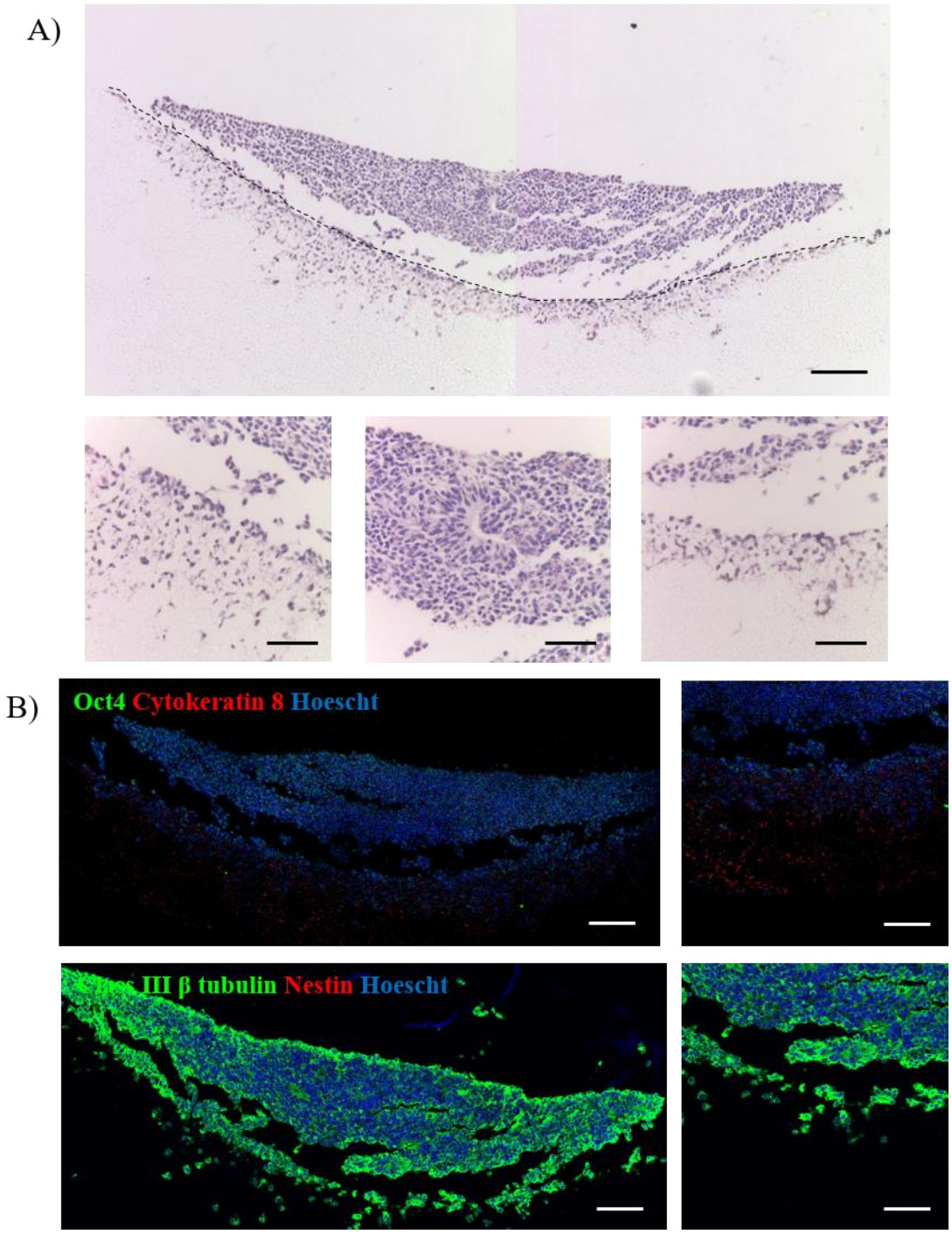


Figure 4.14: Behaviour of TERA2.cl.SP12 EBs cultured on the surface of Alvetex® Strata for 7 days: TERA2.cl.SP12 cells were seeded at a density of 1.5M cells into a sterile, low adherence Petri dish and cultured for 14 days before transferring to Alvetex® Strata for 7 days. Inserts were then fixed in 4 % PFA for histological analysis. Dashed line indicates the upper boundary of the Alvetex® insert. While there is evidence of cellular migration into the supporting scaffold as seen with Alvetex® Scaffold, there is significantly less invasion into the depth of the insert. This has resulted in more of the EB structure remaining on the surface of the scaffold, with neuroepithelial differentiation clearly visible in the centre of the EB. Neural differentiation is detected through positive staining for Class III β-tubulin. Representative images shown. Scale bars: 100 µm and 50 µm

The culture of TERA2.cl.SP12 EBs on Alvetex® Polaris results in a final structure which differs significantly to the culture of these EBs on the previous two forms of the scaffold in one major way. Due to the small pore and void size, 0.5 μm and 3 μm respectively, cells are unable to enter into the scaffold itself. This results in a final structure which comprises of the entire EB which was initially seeded onto the scaffold, which again adheres and elongates into a tissue disc structure as previously observed. Neural rosette structures are also visible in the tissue disc, confirming the differentiated phenotype with the presence of progenitor populations and its maintenance when EBs are seeded onto the scaffold. Immunostaining for the detection of Oct 4 positive pluripotent zones results in weak positive staining in some small areas within the tissue disc structure. Distinct zones of positively stained Class III β-tubulin are also visible, confirming the more mature neural differentiation observed within the EB. There are no cytokeratin 8 positive areas within the tissue disc, indicating a lack of epithelial ectodermal differentiation, as was seen on Alvetex® Strata.

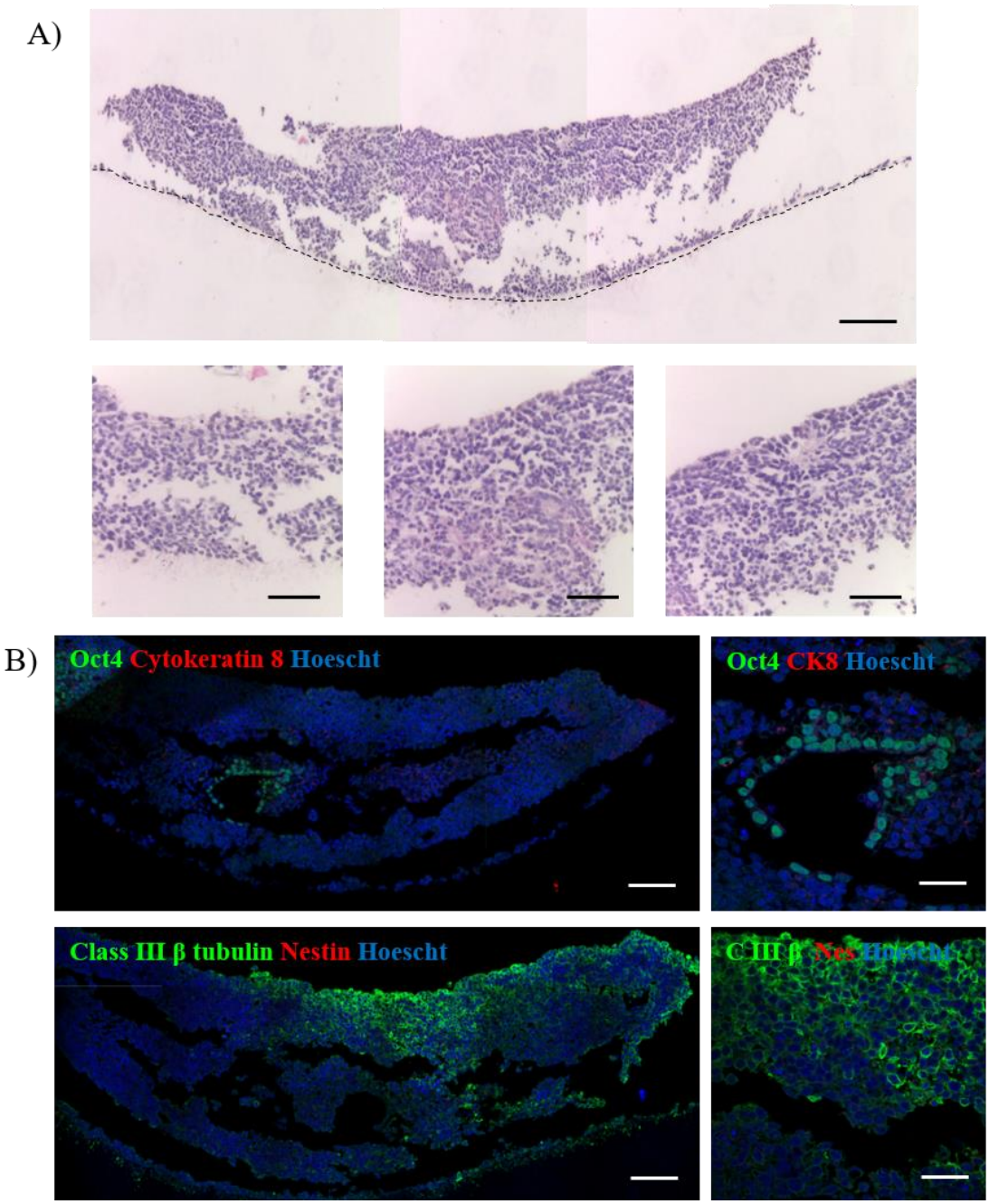


Figure 4.15: Behaviour of TERA2.cl.SP12 EBs cultured on the surface of Alvetex® Polaris for 7 days: TERA2.cl.SP12 cells were seeded at a density of 1.5M cells into a sterile, low adherence Petri dish and cultured for 14 days before transferring to Alvetex® Polaris for 7 days. Inserts were then fixed in 4 % PFA for histological analysis. Dashed line indicates the upper boundary of the Alvetex® insert. Due to the small pore size, cells have not been able to invade into the polystyrene scaffold, and as such, the entire EB structure remains on the surface of the scaffold. Small cellular projections are visible where the EB is anchored to the insert. Evidence of neural differentiation is clear through the positive staining for Class III β-tubulin as are areas of pluripotency through the expression of Oct 4. Representative images shown. Scale bar: 100 µm and 50 µm

4.4.2.2 TERA2.cl.SP12 tissue discs show improved viability compared to time matched TERA2.cl.SP12 EBs in suspension

While the appropriate scaffold for the maintenance of an entire tissue disc structure has been selected, attention must now be given to the viability of such tissue structures. In particular, this must be compared to EBs of the same age cultured solely in suspension, in order to prove that the tissue disc model is a more suitable *in vitro* alternative.

As with previous studies, TERA2.cl.SP12 EBs which had been cultured in suspension for 14 days were seeded onto Alvetex® Polaris scaffold and cultured for a further 7 days, with EBs also maintained in suspension during this time. These samples were then assessed in parallel in order to determine whether tissue disc viability was improved upon when compared to EBs cultured in suspension.

TERA2.cl.SP12 EBs and tissue discs were stained with propidium iodide as previously described, in order to assess general and necrotic cell death within the structures. Propidium iodide staining was detected within the EBs maintained in suspension, throughout the structure. By contrast, propidium iodide staining was not detected within the tissue disc cultured on the surface of Alvetex® Polaris, indicating the improvement of viability. Use of the Caspase 3/7 live stain previously employed to assess the amount of non-necrotic, mainly apoptotic, cell death within the EBs was again used to compare the cell death present in tissue discs. Direct comparison highlights that extensive areas of cell death are present within the EB at 21 days, with localisation at specific points. In contrast, no positive staining can be detected in the tissue disc cultured on the surface of the Polaris scaffold. This is visible in multiple EBs and tissue discs stained in the same way, with representative images shown in Figure 4.16. Analysis of processed and cut samples reveals the same phenotypes, through use of terminal deoxynucleotide transferase dUTP nick end labelling (TUNEL), which stains DNA fragmentation during the late phase of apoptosis, specifically the blunt ends of double stranded DNA breakages (Kyrylkova et al., 2012). As with the previous staining methods, positive TUNEL staining for cell death is present within the EB maintained in suspension, whereas no positive staining can be detected in the tissue disc cultured on the surface of Alvetex® Polaris, indicating that there is little cell death ongoing in the tissue disc.

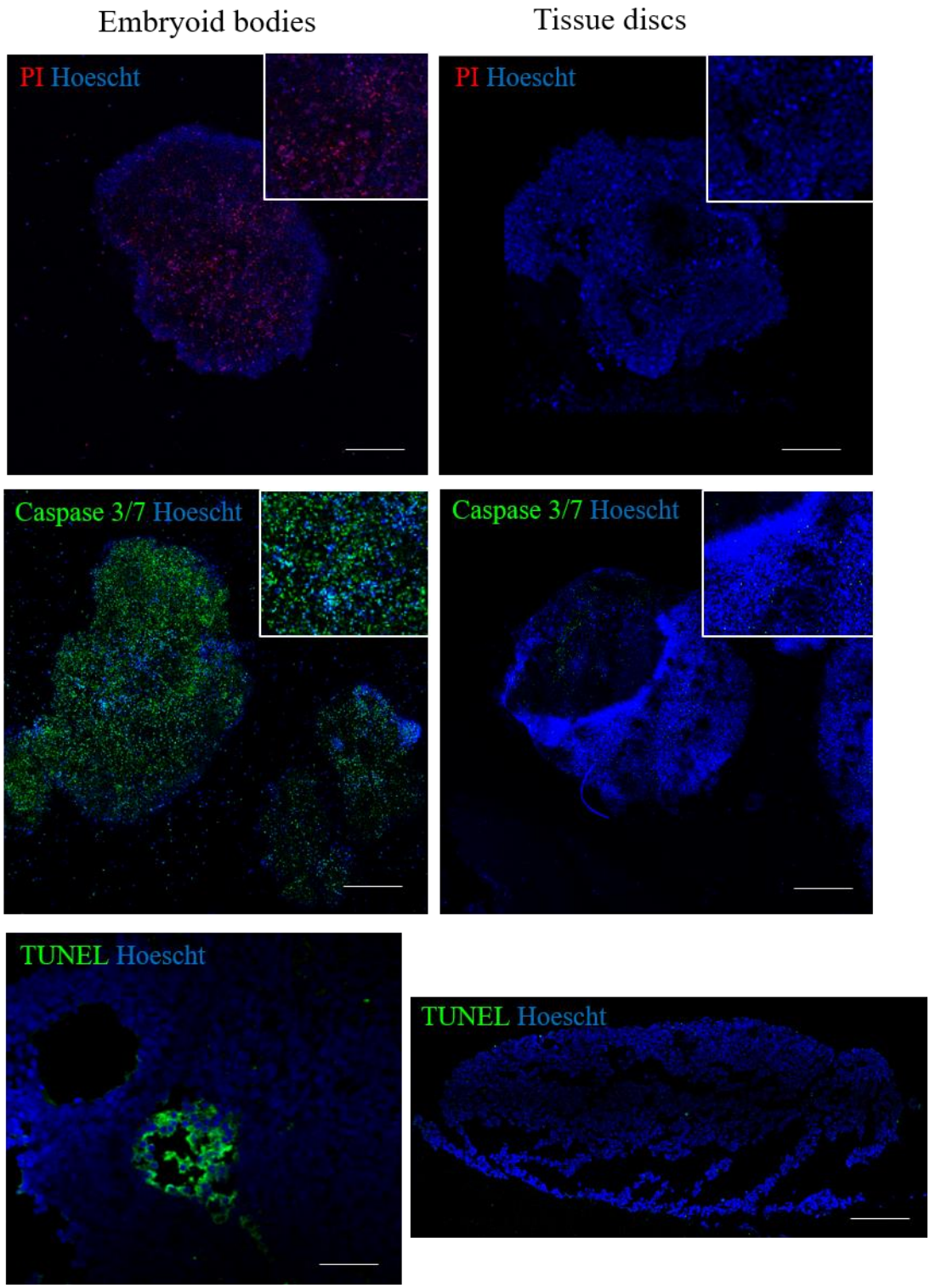


Figure 4.16: Comparison of cell death in TERA2.cl.SP12 EBs and the Alvetex® tissue disc model: Cell death was assessed in the EBs and tissue discs using methods previously used on live EBs. TUNEL staining was also used to assess the amount of cell death in the two culture methodologies. All three staining methods showed evidence of cell death in the EB model, but no cell death within tissue disc structure cultured in the Alvetex® based model. Representative images shown. Scale bar: 100 µm

4.4.2.3 Comparison of internal oxygen in EBs and tissue discs reveals differences in oxygen content

The analyses used in the previous section show that the viability of TERA2.cl.SP12 EBs is improved through their culture on Alvetex® Polaris scaffolds, through a reduction in cell death. As EB viability is thought to be compromised by the creation of an oxygen gradient within EBs, this was investigated and compared to the oxygen content of tissue discs cultured on the scaffold. Platinum dipyrobenzene chloride is a metal based probe which fluoresces differentially in response to different oxygen tensions in the local microenvironment. This is due to the fact that under excitation, metal complexes emit from a triplet excited state, which molecular oxygen is known to quench in a concentration dependent manner (Raza et al., 2017). In biological systems, this means that in a high oxygen environment the fluorescence of the metal compound is quenched, resulting in a low fluorescence with a short half-life. Conversely, in a low oxygen environment, fluorescence is not quenched, leading to a longer fluorescent half-life in the microsecond range. This can be detected using fluorescence lifetime imaging microscopy (FLIM), allowing for the establishment of differential oxygen tensions in biological systems, with this technique having previously been used to assess the oxygen content of 2D cells and tumour spheroids (Raza et al., 2017; Williams et al., 2003). Using the above mentioned compound, FLIM was employed here to infer the oxygen tension in EBs and tissue discs, in order to establish whether a gradient was present in the EBs, and whether oxygen content was consistent in tissue discs on the scaffold. In this case, the method was used indicatively as a proxy method rather than as a quantitative method to obtain a measurable oxygen tension.

Due to a number of technical difficulties with the imaging equipment, pilot studies only were conducted using this method, and so preliminary conclusions only can be drawn from these analyses. Assessment of the decay time of the compound in TERA2.cl.SP12 EBs revealed the presence of differential areas of fluorescence within the EB. In the centre, the decay time was found to be longer than that at the edge of the EB, as seen in Table 4.4. This was assessed in EBs cultured for 21 days, comparable to the tissue discs, and 28 days, an increased length of time used as a positive control for the analytical method. The decay time was found to be variable in the centre of EBs, but this was generally higher that the decay time at the edge of the EBs, indicating a differential oxygen concentration and the presence of a gradient. In the tissue discs, the decay time was found to be more consistent between locations, which in turn was similar to the decay time at the edge of EBs.

Table 4.4. Decay times of the Pt[dpyb]Cl compound in various areas within TERA2.cl.SP12 EBs and tissue discs

Sample	Location	Decay time	Oxygen content
T2SP12 28d EB	Centre	2.14-3.48 µs	Low
	Edge	0.90 µs	High
T2SP12 21d EB	Centre	1.11 – 4.81 µs	Low
	Edge	0.84 µs	High
T2SP12 14d + 7d Pol	Location 1	~ 0.9 µs	High
	Location 2	~ 0.9 µs	High

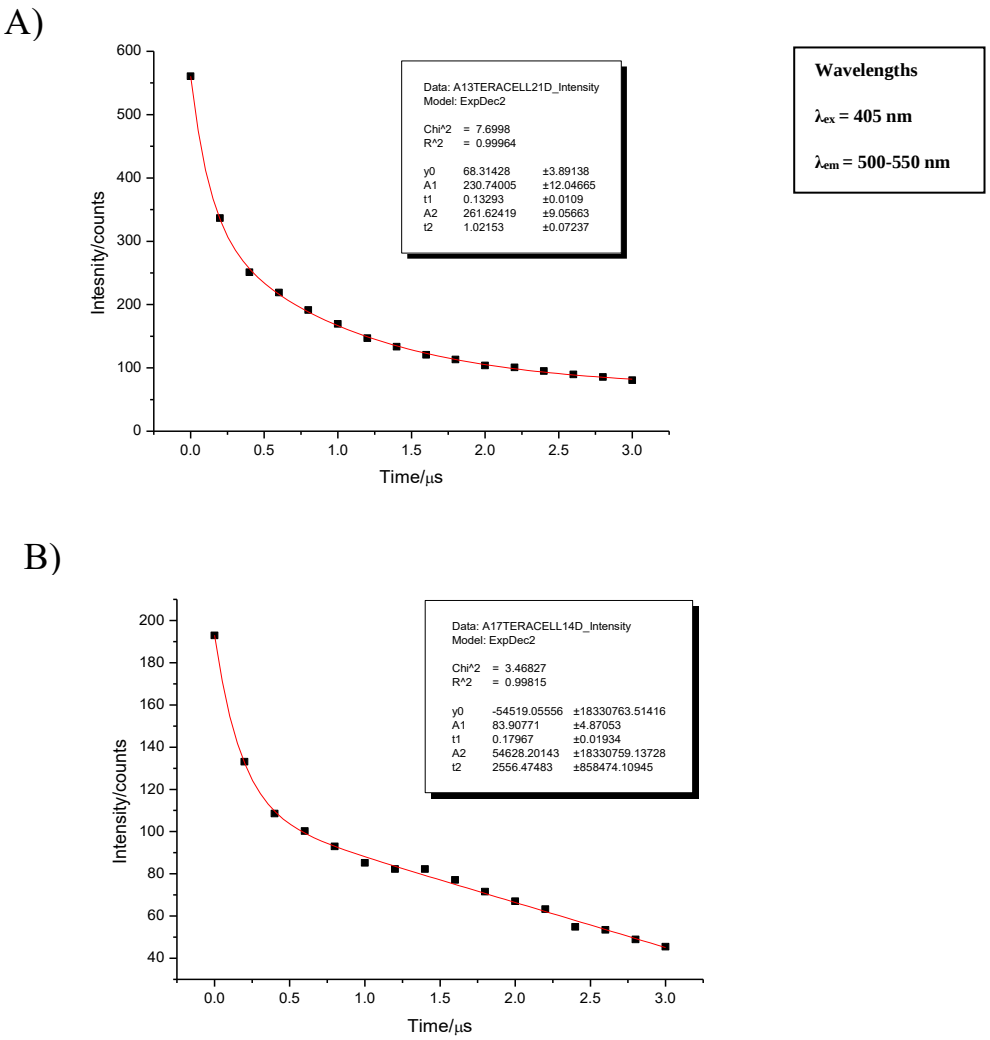


Figure 4.17: Assessment of Pt[dpyb]Cl decay time and therefore oxygen tension in TERA2.cl.SP12 EBs and tissue discs: The decay time in A) TERA2.cl.SP12 EBs and B) TERA2.cl.SP12 tissue discs. The decay time was calculated as function of the measurements taken. The decay time was found to be increased in the centre of EBs, and decreased at the edge of EBs and in tissue discs, suggesting a higher oxygen tension. Representative data shown. Data from 1 independent experiment.

4.4.3 Characterisation of the model and investigations into known signalling pathways

Given that the ability to manipulate the differentiation of EBs and embryoid bodies allows for more in depth study of the developmental process, it is critical that these same structures which have been differentiated can be maintained on the surface of the scaffold, while retaining their differentiated phenotype.

4.4.3.1 ATRA treated TERA2.cl.SP12 EBs retain their neural phenotype when cultured as tissue discs

Organic retinoids such as All-*Trans* Retinoic Acid (ATRA) have been used extensively to direct the differentiation of TERA2.cl.SP12, a process which has been well studied previously in a number of different applications, both to induce neural differentiation specifically, and to study the effects of the microenvironment on developmental potential. TERA2.cl.SP12 cells respond well to ATRA, forming neurospheres over a 21 day differentiation period, which show a clear neural phenotype through the expression of the mature pan-neuronal marker Class III β-tubulin, as shown in Figure 4.18. Due to the unstable nature of these morphogens in response to heat and light, the differentiation induced by ATRA is intermittent across the neurosphere, as evidenced by the uneven expression of the neural markers across the EB structure. In the same way, TERA2.cl.SP12 EBs which were differentiated using ATRA over 21 days and subsequently seeded onto Alvetex® Polaris adhere well to the scaffold and show the same differentiated phenotype as seen in the EBs, with a similarly intermittent expression pattern of the neural marker across the tissue disc structure. Flow cytometry assessment of the differentiation of these two culture systems shows no significant difference in the overall expression of the markers assessed. Both display prominent expression of Class III β-tubulin, low expression of pluripotency marker Oct 4 and neural progenitor marker Nestin, and epithelial marker cytokeratin 8.

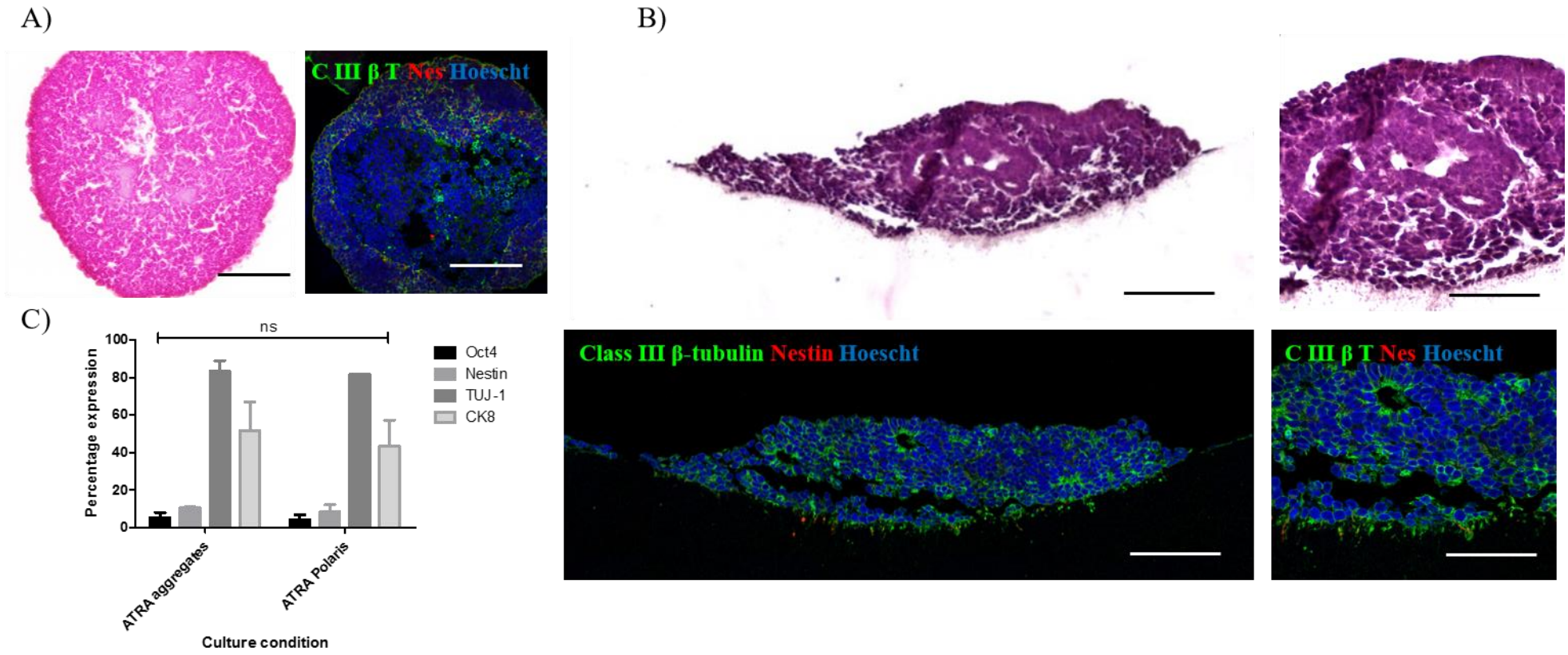


Figure 4.18: Treatment of TERA2.cl.SP12 aggregates with organic retinoid all-trans retinoic acid (ATRA) to promote neural differentiation, and subsequent culture on Alvetex® Polaris: TERA2.cl.SP12 EBs were cultured in suspension, and treated with ATRA at a final concentration of 0.01µM to promote the differentiation of the EBs into neurospheres. These were subsequently cultured on Alvetex® Polaris for 7 days. Immunostaining for neural markers Class III β-Tubulin and Nestin reveals intermittent differentiation within the EB, which is replicated within the tissue disc. Flow cytometry analysis of the neurospheres and tissue discs confirmed that the phenotype is consistent between the two culture conditions, with an enrichment for the neural cell type. Representative images shown. Data represents mean ± SEM from 3 independent experiments. Scale bars: 100 µm and 50 µm

4.4.3.2 EC23 treated TERA2.cl.SP12 EBs retain their neural phenotype when cultured as tissue discs

Due to the instability of compounds such as ATRA, which is a key developmental morphogen and therefore highly used in differentiation protocols, the creation of synthetic morphogens in order to increase the reliability of differentiation protocols is significantly more commonplace. Due to this, it is necessary to test the ability to maintain these more strongly differentiated tissues on the scaffold, which may interact differentially with the Alvetex® Polaris. EC23 is a synthetic retinoid which has been used extensively to direct the differentiation of TERA2.cl.SP12 cells and EBs towards the neural phenotype. As shown in Figure 4.19, EBs stained using this compound show a highly homogenous differentiated phenotype, with strong, even expression of Class III β-tubulin, as well as some expression of neural progenitor marker Nestin. This phenotype is confirmed through flow cytometry analysis of the EBs. TERA2.cl.SP12 EBs which were differentiated using EC23 and seeded onto Alvetex® Polaris adhere well to the scaffold as tissue discs, and also show a homogenously differentiated phenotype, with strong expression of Class III β-tubulin and Nestin. The lack of neural rosettes in the tissue disc reflects the EB phenotype and confirms the potency of the EC23 in inducing mature neural differentiation. Flow cytometry analysis of the EC23 treated tissue discs confirms their similarity to the EC23 treated EBs analysed in the same way, with a similar expression profile of the pluripotent and differentiated markers.

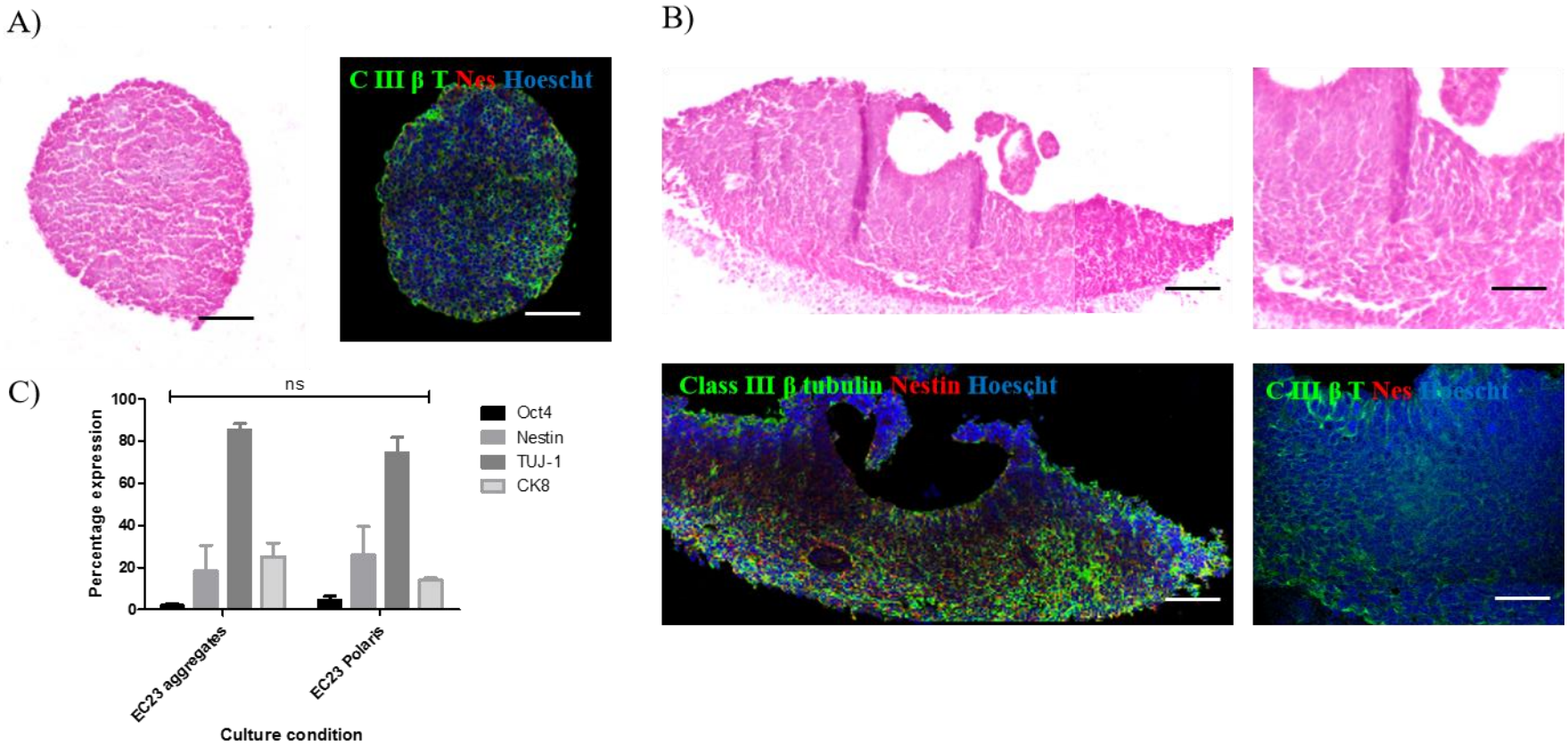


Figure 4.19: Treatment of TERA2.cl.SP12 EBs with synthetic retinoid analogue EC23 to promote neural differentiation, and subsequent culture on Alvetex® **Polaris:** TERA2.cl.SP12 EBs were cultured in suspension, and treated with synthetic compound EC23 at a final concentration of 0.01µM to promote the differentiation of the EBs into neurospheres. These were subsequently cultured on Alvetex Polaris for 7 days. Immunostaining for neural markers Class III β-tubulin and Nestin reveals strong homogeneous differentiation within the EB, which is also replicated within the tissue disc cultured on the insert. Flow cytometry analysis of the neurospheres and tissue discs confirmed that the phenotype is consistent between the two culture conditions, with an enrichment for the neural cell type. Representative images shown. Data represents mean ± SEM from 3 independent experiments. Scale bar: 100 µm 50 µm

4.4.3.3 BMP-2 treated TERA2.cl.SP12 EBs retain their non-neural phenotype when cultured as tissue discs

As an embryonal carcinoma cell line, TERA2.cl.SP12 cells preferentially differentiate into ectodermal derivatives, and have been proven to do so previously on a number of occasions, in both 2D and 3D culture conditions. The use of BMPs induces a non-neural differentiated phenotype, with evidence of a wider variety of differentiated structures within the EBs. TERA2.cl.SP12 EBs differentiated using BMP-2 show a heterogeneous phenotype, with both neural differentiation and lumen structures, as well as a loose mesenchymal element. EBs treated with BMP-2 and seeded onto Alvetex® Polaris show maintenance of their heterogeneous structure, with dense neural differentiation and neural rosettes as well lumen structures visible within the tissue disc. There is a significant mesenchyme element within the tissue disc also, where cells are loosely packed and there are large areas of extracellular matrix visible. Immunostaining of these tissue discs highlights very distinct areas of differentiation, with areas strongly positive for Class III β-tubulin indicating mature neural differentiation and significant areas of organised cytokeratin 8 differentiation on the edges of the tissue disc and mixed within the mesenchymal element. There are no areas of Oct 4 positive staining, with no pluripotent populations maintained within the tissue disc as is seen in the EB.

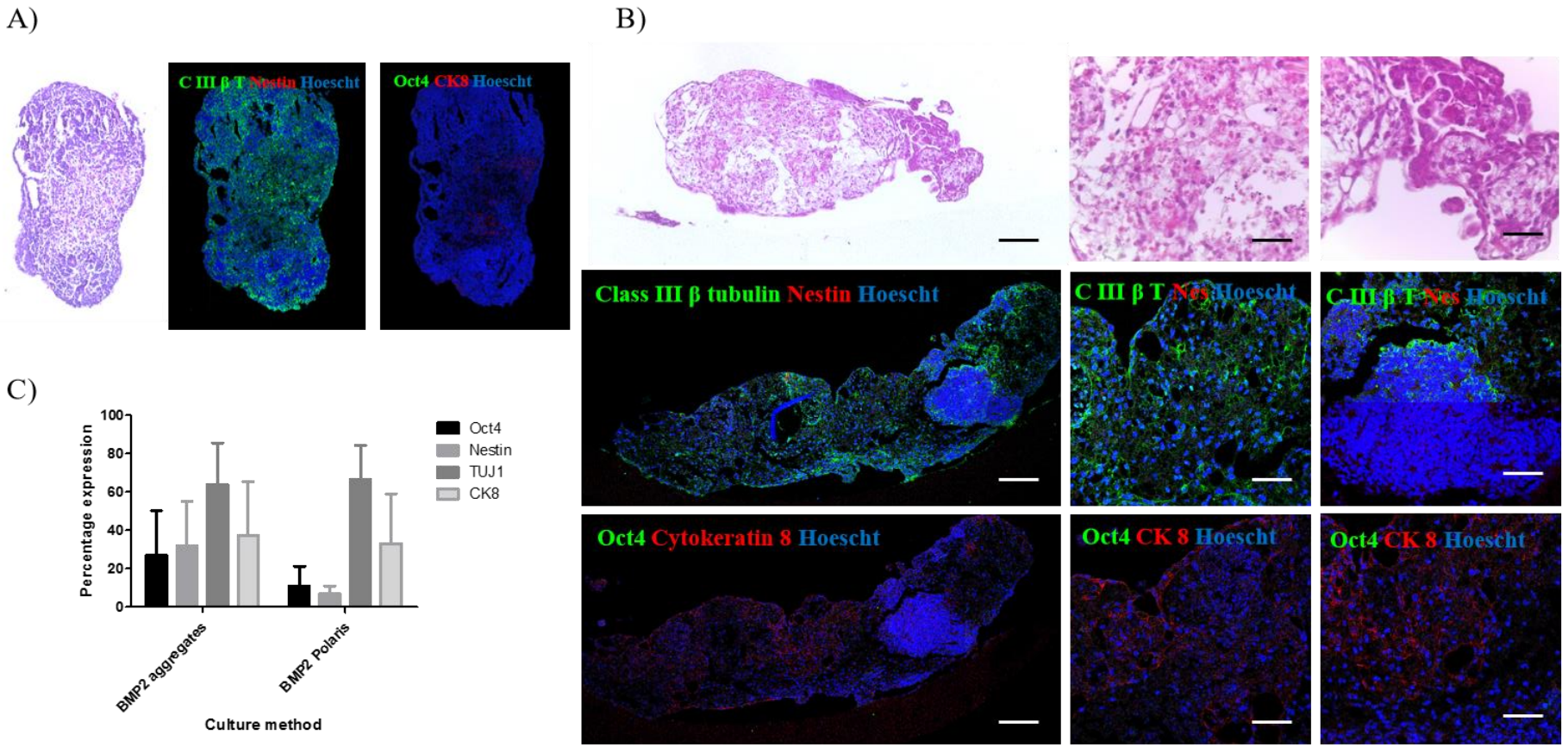


Figure 4.20: Treatment of TERA2.cl.SP12 EBs with morphogen bone morphogenetic 2 (BMP-2) to promote non-neural ectodermal differentiation, and subsequent culture on Alvetex® Polaris: TERA2.cl.SP12 EBs were cultured in suspension, and treated with BMP-2 at a final concentration of 50 ng/ml to promote the differentiation of the EBs into non-neural ectoderm. These were subsequently cultured on Alvetex® Polaris for 7 days. Immunostaining for various ectodermal markers, including neural Class 3 β-Tubulin and Nestin, as well as epithelial marker cytokeratin 8 reveal the phenotype and structures present in the EB. Flow cytometry analysis of the EBs and tissue discs confirmed that the phenotype is consistent between the two culture conditions. Representative images shown. Data represents mean ± SEM from 3 independent experiments. Scale bar: 100 µm - 25 µm

4.5 Discussion

The aim of this Chapter was to optimise a novel model which can be used to study human development using pluripotent stem cells and three dimensional cell culture techniques. The embryonal carcinoma cell line TERA2.cl.SP12 was used due to its extensive use in other developmental biology studies, its inexpensive, simple culture requirements and limited yet well characterised differentiation towards ectodermal derivatives (Przyborski et al., 2004). Initial studies investigated the formation of EBs from these cells in order to optimise the time and seeding density for EB formation to allow for sufficient differentiation but to reduce cell death within the structures. EBs were then seeded onto the three formats of Alvetex®, to assess the interactions of the EBs and determine the appropriate scaffold for use in the model. Cell death and oxygen content was then assessed (oxygen indirectly) and compared in the EB and the model to confirm an improvement in viability and microenvironment. Finally, the ability to maintain differentiated EBs in the model was assessed through the use of three different morphogens.

4.5.1 The impact of cell seeding density on EB properties

The model under development in this chapter combines two separate three dimensional cell culture techniques: use of cell aggregation and use of a solid porous scaffold. Prior to use in the model, TERA2.cl.SP12 cells show the typical hallmarks of pluripotency: the characteristic morphology, high expression of pluripotency associated factors such as SSEA-4, TRA-1-60, Oct 4 and Sox 2, and low expression of differentiation markers including A2B5, Nestin, cytokeratin 8 and Class III β-tubulin, rendering them useful for this study and confirming their similarity to cells from the blastocyst. TERA2.cl.SP12 EBs have been used in projects by Horrocks, Knight and Owens to study the differentiation and development of human tissues and confirmed to recapitulate aspects of this process. Some also combined these techniques as in this Chapter, although systematic optimisation of the EB formation process prior to seeding on the scaffold was not undertaken.

Initially, the optimisation of EB culture prior to seeding in the scaffold involved investigating the impact of seeding density and culture time on three key EB properties: EB dimensions, cell death and pluripotency. This is an important point to consider, as seeding density is known to impact on the differentiation and size of PSC derived EBs (Dang et al., 2002; Lach et al., 2018; Van Winkle et al., 2012), the latter of which will also impact on the creation of gradients across the developing EB and ultimately, the level of cell death (Giandomenico et al., 2019; Gothard et al., 2009; Mansour et al., 2018; Martin, 1975). TERA2.cl.SP12 EBs were seeded at a range of densities in order to ascertain whether the impact of seeding density on various EB properties recorded in other PSC populations also applies to TERA2.cl.SP12 EC cells, and whether there is indeed a limit to EB size as postulated (Dang et al., 2002; Gassmann et al., 1996). The aim was also to identify the optimum time point with the least cell death which showed sufficient levels of differentiation within the developing EB. As

expected, initial seeding density of TERA2.cl.SP12 impacted significantly on the size of the EBs over the first three days of culture. Of particular interest is the fact that the highest seeded EBs reach diameters of almost 350 µm after only 3 days in culture, which is approaching the tissue diffusion limit, marked as 400 µm on graph C (a radius of 200 µm would represent the tissue diffusion limit, which would be a diameter of 400 µm), suggesting that prolonged culture after this would be detrimental at these seeding densities and could result in large amounts of cell death, an observation which would align with data obtained by Gothard, where necrosis was identified in EBs after only 5 days (Gothard et al., 2009). At day 7, some of these differences were still visible, but there were no significant differences in EB dimensions after this point, suggesting that PSC derived EBs do have size limit, or at least, the EC cell line TERA2.cl.SP12 does. However, what is noticeable in EBs at the 21 day time point in particular is differences in the internal structure of the EBs, with the formation of the layered internal EB structure as described by Gothard (Gothard et al., 2009), and providing visual evidence of the formation of a hypoxic core. While it can be conceded suspension culture is a more heterogeneous method of EB formation, differences in the size of EBs were clearly visible in the early formation stages, combined with the observation that only those seeded at the higher density reached sizes near to the tissue diffusion limit, indicating their potential unsuitability in the model. The confirmation of a limit to EB size in these initial analyses highlights some interesting ideas. An upper limit to EB size regardless of initial seeding density, as seen in this study and by others would suggest that cell death will be consistent between the EBs, a phenomenon which is also confirmed within these analyses. Both propidium iodide staining and live Caspase 3/7 staining are present within the EBs, fitting with the mixed reports of the identity of the cell death occurring within EB structures (Giandomenico et al., 2019; Gothard et al., 2009; Son et al., 2011).

Assessment of cell death using the two different staining techniques shows that after 7 days in culture, a trend is still visible in the amount of cell death present which correlates with the initial seeding density as would be expected: higher seeding densities appear to show more cell death in EBs compared to lower seeding densities. A consistency in cell death is reached across all seeding densities, a result particularly prominent in the flow cytometry data, with very similar results at 14 days and 21 days, suggesting that EBs have not increased in size and therefore have not increased their diffusion gradients. However, the fact that EB size is limited still lends support as to why EBs are unable to form the complex structures that are seen in teratomas. This would involve further proliferation and structural organisation which would likely surpass the EB size limit. When the blastocyst formation process is considered, the EB size limit is most likely inherently controlled, linked to the requirement of implantation into the uterine lining for further development of the blastocyst (Dang et al., 2002), further strengthening the case for combining EBs with other advanced cell technologies to encourage more complex differentiation and maturation to occur.

The effects of seeding density on the differentiation and pluripotency of the EBs was also fairly modest. Mixed ectodermal differentiation was observed within the EBs, as Horrocks observed when studying TERA2.cl.SP12 EBs which were untreated; few significant differences were detected in the

flow cytometry analysis of pluripotency and differentiation markers. Differences in the immunostaining did highlight that strong global EB differentiation, particularly in terms of neural markers, was not observed until at least 14 days in culture also in line the differentiation trajectories noted by Horrocks both with and without morphogens (and further highlighting the importance of time in differentiation based studies). This was also the time point at which more complex differentiated structures could be detected in the formation of some neural rosettes. A modest trend in Oct 4 suggests that there is a maintenance of pluripotency in the EBs seeded at a lower density, and although this, as with the similar trend in Nestin expression, is only observed at the 7 day time point, it does indicate that seeding density has some small impact on the differentiation of TERA2.cl.SP12 EBs as with other PSC populations EBs (Dang et al., 2002; Lach et al., 2018; Van Winkle et al., 2012).

4.5.2 Optimisation of TERA2.cl.SP12 EB formation

The collation of the analyses conducted on TERA2.cl.SP12 EBs allowed for the identification of the optimal parameters for EB formation prior to seeding in the proposed model. The lack of appearance of complex differentiated structures prior to around 14 days, indicated the need for sufficient time for EB maturation, a concept established by various studies. Additionally, the consistency EB size and cell death within EBs highlights that seeding density does not impact greatly on the viability of the structures when using this cell line, although does show some impact on pluripotency and differentiation. The 14 day time point was selected to allow for sufficient maturation of EBs, and the 1.5 million cell seeding density due to the small increases in neural marker Class III β-tubulin. Inadvertently, these parameters also allow for some level of comparison with other studies previously conducted using this cell line.

4.5.3 Optimisation of porous scaffold to maintain EBs long term as tissue discs

Based on the success of a variety of previous studies in enhancing the differentiation of PSCs and allowing for the culture of EBs on the surface, the polyHIPE Alvetex® was selected for the creation of the *in vitro* model. Knight and Owens in particular had attempted to culture various PSC derived EBs on the scaffold, with a view of developing a model with enhanced EB differentiation.

As would be expected due to the pore sizes of the scaffold, seeding of TERA2.cl.SP12 derived EBs onto Alvetex® Scaffold resulted in much of the EB structure being lost, with cells migrating into the scaffold. This was a phenomenon observed by both Knight and Owens on use of this format of Alvetex®. The analysis of differentiation however, did show evidence of an enhanced phenotype, with staining for cytokeratin 8 detected as well as the strong staining for Class III β-tubulin which was seen in the EBs. Knight also saw that structure was lost, although in a more complete manner, and the culture of the RC-10 EB derived structures, tissue discs, in that study actually had a reduced

differentiated phenotype compared to the EBs cultured on gelatin coated plates, with only 2 germ layers detected. However, Knight also observed very similar results in terms of pluripotency, with a lack of Oct 4 staining in PSC derived tissue discs in both these data and the results obtained by Knight.

The culture of the tissue discs (flattened EB derived structures) on Strata scaffolds showed similar results to both Knight and Owens with a reduced loss of structure into the scaffold and improvements in structure formation. This is replicated in the culture of TERA2.cl.SP12 EBs on Strata in this study, with neural rosettes in particular visible in the tissue disc structure. The level of infiltration into the scaffold is actually reduced compared to that which was observed by Knight, with a large proportion of the EB still on the surface of the scaffold. While the enhanced differentiation that was observed by Knight is not present due to the lack of cytokeratin 8 staining in this sample, this is likely representative of the heterogeneity of structure formation when TERA2.cl.SP12 EBs are allowed to spontaneously differentiate. However, the loss of some tissue disc structure, as was also observed with Alvetex® Scaffold, renders Strata unsuitable for studies where complex structure formation is the aim. (Fragmentation of the tissue discs can be noted particularly in Figures 4.14 and 4.15. This is likely due to the fact that the tissue discs were allowed to spontaneously differentiate in this instance, resulting in overall weaker differentiation and therefore decreased deposition of ECM due to the retention of some pluripotent characteristics, leading to fragmentation. This phenomenon was also observed by Owens when using TERA2.cl.SP12 EB to form tissue discs.)

The culture of TERA2.cl.SP12 EBs on Alvetex® Polaris has only previously been conducted by Owens due to the fact that Alvetex® Polaris is not yet commercially available, although the structure of Polaris, with its small void and pore size, shares similarities with other porous structures used for the maintenance of complex PSC derived structures such as organoid slices and neurospheres as described in the Introduction. Full EB structure is maintained on the surface of the scaffold as a tissue disc, with complex structures visible and intact, as observed also by Owens. This maintenance of EB structure is accompanied by intermittent neural differentiation within the newly developed tissue disc and weak Oct 4 positive staining, suggesting an overall enhancement of the microenvironment to be more similar to the *in vivo* teratocarcinoma (see Figure 4.21) rather than a simple enhancement of differentiation. This is consistent with the results Knight observed on Strata.

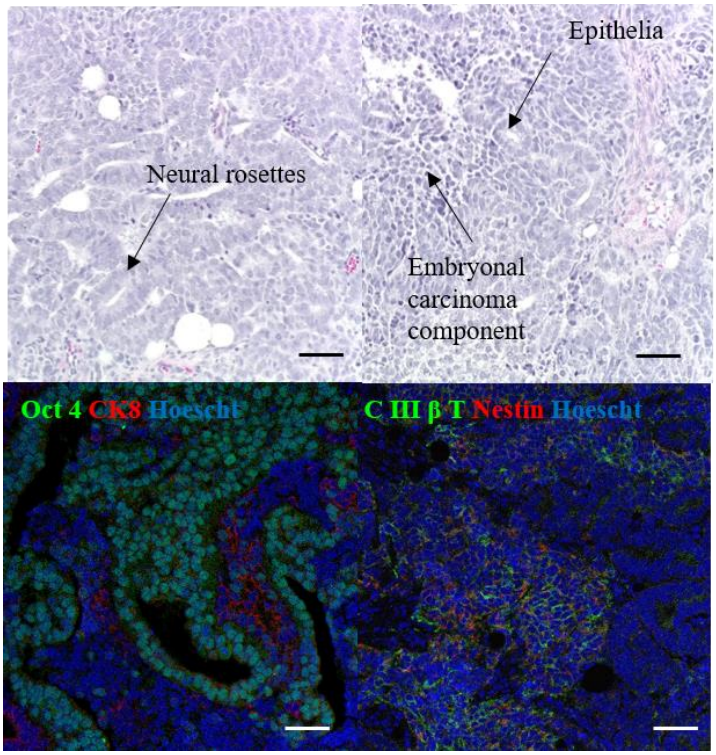


Figure 4.21: Histological and marker expression analysis of teratocarcinoma formed from human EC cells: TERA2.cl.SP12 cells were subject to a teratoma assay, with the resultant tumour containing both types of ectodermal differentiation, neural and epithelial. There are also areas displaying the embryonal carcinoma phenotype, which are Oct 4 positive. Tissue discs cultured on Alvetex® Polaris show evidence of EC cell populations in addition to the differentiated structures. Scale bars: 50 µm

4.5.4 Analysis of cell death and oxygen tension in TERA2.cl.SP12 EBs and tissue discs

The reduction of cell death in PSC derived EBs through their maintenance as tissue discs on the surface of Alvetex® is an important factor in the further use of Alvetex® Polaris for the *in vitro* model. Cell death was analysed using the previously used live methods of propidium iodide staining and a live Caspase 3/7 stain, as well as using TUNEL staining on fixed samples. The use of multiple methods to assess cell death within cellular structures is recommended due to the possibility of the lack of specificity with methods such as TUNEL (double stranded DNA breaks are not exclusive to apoptotic events, but can also occur during necrosis (Kyrylkova et al., 2012)). This also provides a more comprehensive overview of the cell death within the EBs and tissue discs. All three methods of staining showed a reduction in cell death in tissue discs maintained on the scaffold compared to those maintained in suspension culture for the same length of time. This confirms that the culture of PSC derived EBs as tissue discs on Alvetex® Polaris does result in an improvement in viability, correlating with data obtained by Lancaster in the culture of brain organoid slices on porous permeable membranes; in this study a reduction in TUNEL staining was also observed when scaffold culture was undertaken (Giandomenico et al., 2019; Lancaster and Knoblich, 2014b).

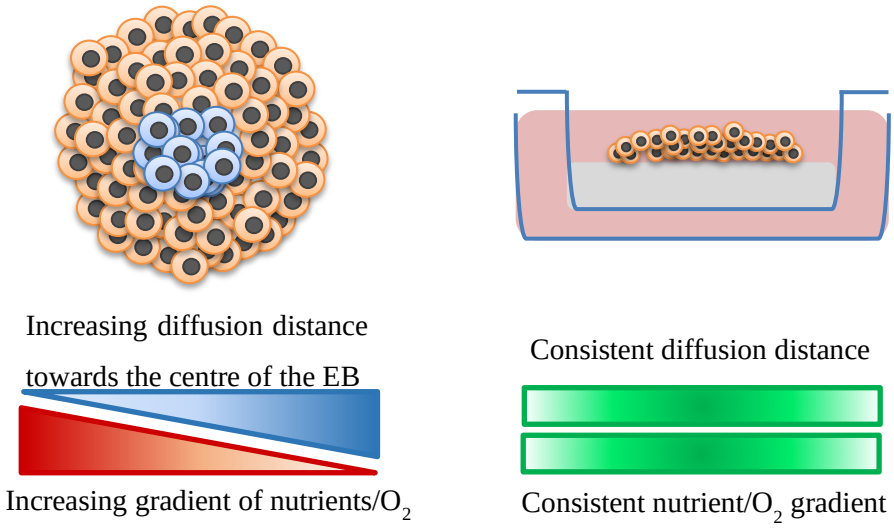


Figure 4.22: Changes to the EB microenvironment on culture on Alvetex® Polaris: When the TERA2.cl.SP12 EBs are cultured in suspension, a heterogeneous microenvironment is created due to the diffusion distance to the centre of the structure, leading to poor nutritional support. This is resolved when EBs are seeded onto a porous scaffold, as the EB forms a flattened tissue disc which has a consistent diffusion distance and therefore more consistent nutritional support and oxygenation.

Following the confirmation of differences in cell death and viability between PSC derived EBs and PSC derived tissue discs, the potential cause of this was investigated: multiple sources as discussed in the Introduction confirmed the presence of an oxygen gradient in EBs, and it was hypothesised that seeding the EBs onto the scaffold resulted in the removal of this gradient. The technique of FLIM was employed in conjunction with a platinum based compound which fluoresces differentially in response to the local oxygen tension of the cellular microenvironment and has previously been used to infer the oxygen content of melanoma tumour spheroids (Raza et al., 2017), structures which are highly similar to PSC derived EBs.

Analysis of 21 day TERA2.cl.SP12 EBs showed that there were differential areas of fluorescence within the EB, as would be expected from the literature regarding differences in internal EB structure, and correlating with the data obtained by Raza et al using melanoma spheroids. A longer decay time was recorded in the centre of EBs, inferring the presence of a low oxygen environment, and a shorter decay time was recorded at the edge of the EBs, inferring a higher local oxygen tension, see Figure 4.23. This also aligns with work by Van Winkle and Gassman, and provides real data regarding the oxygen dynamics in actual EB culture, as well and agreeing with the cell death data indicating the presence of cell death in the centre of the EBs, which is likely due to this low oxygen environment.

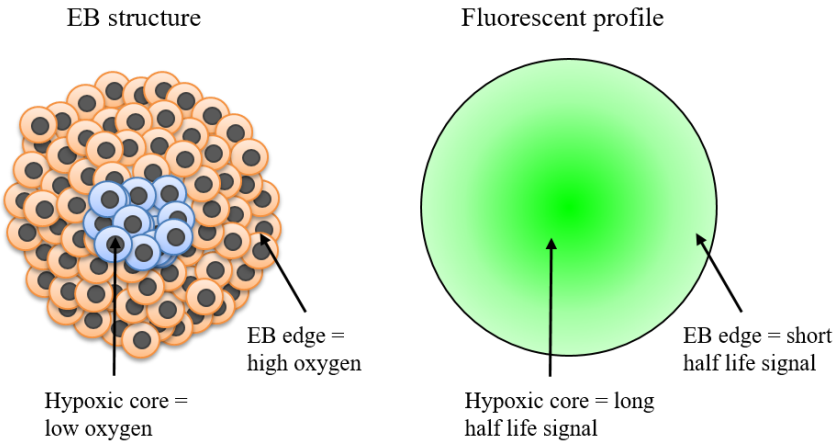


Figure 4.23: Schematic of the PSC derived EB internal structure and the corresponding interaction of the fluorescent platinum compound: The platinum based compound is quenched by oxygen in a concentration dependent manner, which can be detected by using FLIM. In high oxygen environments, the signal is quenched, resulting in short lived fluorescence. In low oxygen environment, the fluorescence takes longer to decay, resulting in a fluorescent signal with a long lifetime. In the EB, the low oxygen microenvironment is in the centre of the EB, whereas the high oxygen environment is at the edge of the structure.

Assessment of TERA2.cl.SP12 tissue discs cultured in suspension for 14 days and on the Polaris membrane for 7 days produced preliminary results that also correlated with the cell death analyses. The measurements of the decay time were found to be more consistent in the different locations in the tissue disc, as well as correlating with the measurements of the decay time at the edge of the EBs. This infers that the oxygen tension within the tissue discs is comparable with the oxygen tension at the edge of the EBs, and that this is generally consistent across the tissue disc (see Figure 4.24), providing further evidence in support of the original hypothesis that the reduction diffusion distance through seeding EBs on solid scaffold results in better nutritional support and oxygenation. These studies are only preliminary due to major technical difficulties with imaging equipment, but these initial data provide good support for the model and the use of this technique. Additional studies need to be completed in order to obtain more statistically robust data and in order to better understand the variability in oxygen tension between EBs and tissue discs of this nature. The use of samples exposed to specific oxygen tensions could aid in the accurate measurement of oxygen tension in the cell structures.

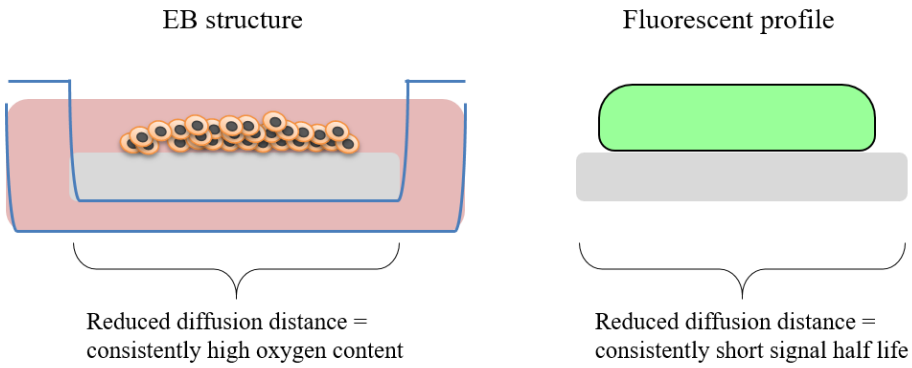


Figure 4.24: Schematic of the PSC derived tissue disc structure and the corresponding interaction of the fluorescent platinum compound: The platinum based compound used is quenched by oxygen in a concentration dependent manner, which can be detected by using FLIM. In the tissue disc, the reduced diffusion distance results in a consistently high oxygen concentration throughout the structure. In the analysis using FLIM, this translates to a short half-life of the platinum compound throughout the tissue disc structure, confirming the high oxygen content.

4.5.5 The study of developmental pathways using tissue discs cultured on Alvetex® Polaris

An essential property of any model studying human tissue development is the ability to study the differentiation of specific tissues, which in most cases is through the modulation of differentiation by the application of exogenous morphogens. As an embryonal carcinoma cell line, TERA2.cl.SP12 has a preferential differentiation route of ectodermal derivatives, which has been demonstrated and well characterised in 2D culture and EBs. This can be achieved both by spontaneous differentiation through the removal of pluripotency maintaining conditions and the application of morphogens. TERA2.cl.SP12 cells respond well to all *trans* retinoic acid (ATRA) to direct their differentiation towards the neural phenotype, and bone morphogenetic protein 2 (BMP-2) for differentiation towards the non-neural epithelial phenotype.

TERA2.cl.SP12 EBs treated with ATRA show an intermittent neural phenotype across the EB structure, which is replicated in the treated tissue disc cultured on the surface of Alvetex® Polaris. The presence of neural rosette structures in the tissue disc confirms the presence of organised neural progenitors, showing an increased tissue complexity as previously hypothesised, with the same structures not visible in the comparable EB. While the characterisation of the differentiated tissues in this system is simple, it does align with some previous data obtained by Nestor and Lancaster, in which the complexity, diversity and function of neurally differentiated tissues was improved through the culture on permeable membranes. As was observed by Nestor in the study of neural networks, some small neurite outgrowth into the scaffold is observed, as highlighted by the Class III β-tubulin staining, indicating increased tissue disc maturity.

The use of synthetic retinoids is a more practical option for *in vitro* studies due to the instability of organic retinoid compounds when exposed to light and heat sources. EC23 is a synthetic retinoid analogue which has been used highly successfully in studies of neural differentiation using TERA2.cl.SP12, and is a potent inducer of the neural phenotype. Application of EC23 to TERA2.cl.SP12 EBs results in strong homogenous differentiation as previously observed by Clarke *et al*, a phenotype which is replicated in the differentiated tissue disc cultured on Alvetex® Polaris. The lack of neuroepithelial structures in the EC23 treated EB and tissue disc reflects the potency of EC23 as an exogenous morphogen, and the fact that EC23 strongly drives the differentiation of the cells to a more mature neural phenotype. The instability of ATRA naturally results in a heterogeneous action on the EBs, resulting in areas with early neural differentiation with neuroepithelia and areas of more mature differentiation in the final tissue disc.

Treatment of TERA2.cl.SP12 cells with BMP-2 has previously been shown to supress the neural phenotype in 2D culture and embryoid body culture, and increase the propensity for epithelial differentiation (Horrocks, 2007; Owens, 2015). This was again observed on the use of BMP-2 to differentiate EBs in this study. The BMP-2 treated EBs show a much more heterogeneous phenotype, with various epithelial and mesenchymal structures, a phenotype which is again replicated in the resultant tissue disc on Alvetex® Polaris. Small areas of neural differentiation are still visible, possibly due to heterogeneity of action of BMP-2 on the EB during the suspension culture phase. The large areas of cytokeratin 8 staining however, confirm the shift towards the non neural phenotype, indicating the ability to successfully maintain highly different phenotypes on the scaffold. This correlates with the study conducted by Owens, which also maintained differentiated TERA2.cl.SP12 tissue discs on Alvetex® Polaris.

4.6 Conclusion

In this Chapter, the aim was to optimise an *in vitro* model to be used for the study of human development. Due to the fact that one of the current models used to study human embryogenesis, EB formation, can only be used to study early events of this process, a novel model is required for long term studies with sufficient time for complex structure formation to occur. EB use is limited due to the heterogeneity of the EB internal microenvironment as the EB size increases, creating differences in oxygen tension across the EB structure. A number of studies have combined the common technique of EB formation with the use of solid scaffolds to enhance the complexity and viability of EBs, allowing for more in depth studies of the developmental process. In response to these studies and previous studies conducted in the laboratory, it was hypothesised that this could be further developed as a model of human development, following some optimisation of the EB formation process.

TERA2.cl.SP12 cells were used in the optimisation process due to their similarity to ES cells, less demanding culture requirements and well characterised differentiation phenotypes. Optimisation of the EB formation process revealed that TERA2.cl.SP12 embryoid bodies have an upper size limit, regardless of the initial seeding density. Although some EBs seeded at the higher density approach the tissue diffusion limit after as little as 3 days in culture and analysis of cell death at 7 days shows a trend which correlates with the initial seeding density, ultimately cell death within EBs is consistent regardless of initial seeding density after 14 days in culture. Quantitative analysis via flow cytometry showed seeding density had modest effects on pluripotency and differentiation of EBs, although immunostaining highlighted that the presence of global differentiation and complex structures was not identified until around 14 days in culture. Thus, the EB formation process was optimised to 14 days, with 1.5 million cells chosen as the initial seeding density.

The optimised EBs were seeded onto the three formats of Alvetex® available, with the only scaffold format maintaining the entire EB structure as a flattened tissue disc being Alvetex® Polaris. The improvement of viability in the novel model was confirmed through the comparison of cell death in tissue discs on the scaffold and EBs maintained in suspension culture for the same length of time. The rationale as to this was also elucidated in part by the analysis of the oxygen tension within EBs and tissue discs, revealing a consistent oxygen tension across the entire tissue disc structure and the presence of gradients as predicted in EBs. Finally, the ability to maintain differentiated tissue discs and the retention or enhancement of the differentiated phenotype was tested, with differentiation towards the neural and non neural epithelial phenotypes successfully completed. Both phenotypes showed at least a retention of the phenotype observed in the EB, with ATRA and BMP-2 treated tissue discs showing an improvement in the complexity of the structures present. The effects of the improvement of the EB microenvironment through the reduction of diffusion distance and oxygen gradients are clear when the data is considered, as are the effects of attachment mediated signalling mechanisms resulting in the presence of more complex structure, particularly in the BMP-2 treated

EBs. However, this model has investigated only ectodermal differentiation in a pluripotent population with a restricted differentiation capacity; the formation of tissue structures from all three germ layers is required for a comprehensive and informative model of human tissue development.

In summary, the optimisation of the two stages of the novel *in vitro* model undertaken in this Chapter was successful. The resultant model shows an improved viability compared to traditional EB formation and the ability to maintain tissue discs which have been manipulated using exogenous morphogen application. This now provides a basis model, which can be adapted for use with other cell lines, to further study PSC differentiation.

5. Increasing the complexity of the *in vitro* cellular microenvironment to further enhance the differentiation of PSC derived structures

5.1 Introduction

The local microenvironment which cells are exposed to is highly complex: many different physical and chemical signalling cues inform the structure and function of cell populations. Thus the introduction of three dimensionality into the *in vitro* environment, whilst impacting significantly on the structure and therefore function of cells, is insufficient to fully recapitulate *in vivo* cellular morphology and activities. A range of advanced cell culture techniques have been developed which encompass these other complex cues, in order to better represent the complex microenvironment.

5.1.1 The complexity of the *in vivo* environment

No cell resides in the *in vivo* environment singularly: the synthesis and homeostasis of all biological tissues is dependent on the interactions between separate cell populations (Bogdanowicz and Lu, 2013). All cells are subject to a wide range of physical and chemical cues, controlled by neighbouring cell populations, the extracellular matrix and *in vivo* mass transport systems. These factors contribute to create the unique local cellular microenvironment, providing a series of signals which cells respond to in a manner of ways (see Figure 5.1). Many of these factors are interdependent, with multiple different microenvironmental factors affecting the same cellular functions; for example, adhesion to the extracellular matrix is impacted on by the chemical composition of the matrix, its physical and topological properties and the three dimensional confirmation of the cell. This interdependence creates a number of complex feedback loops and interactions between neighbouring cells, the extracellular matrix and *in vivo* homeostatic control systems.

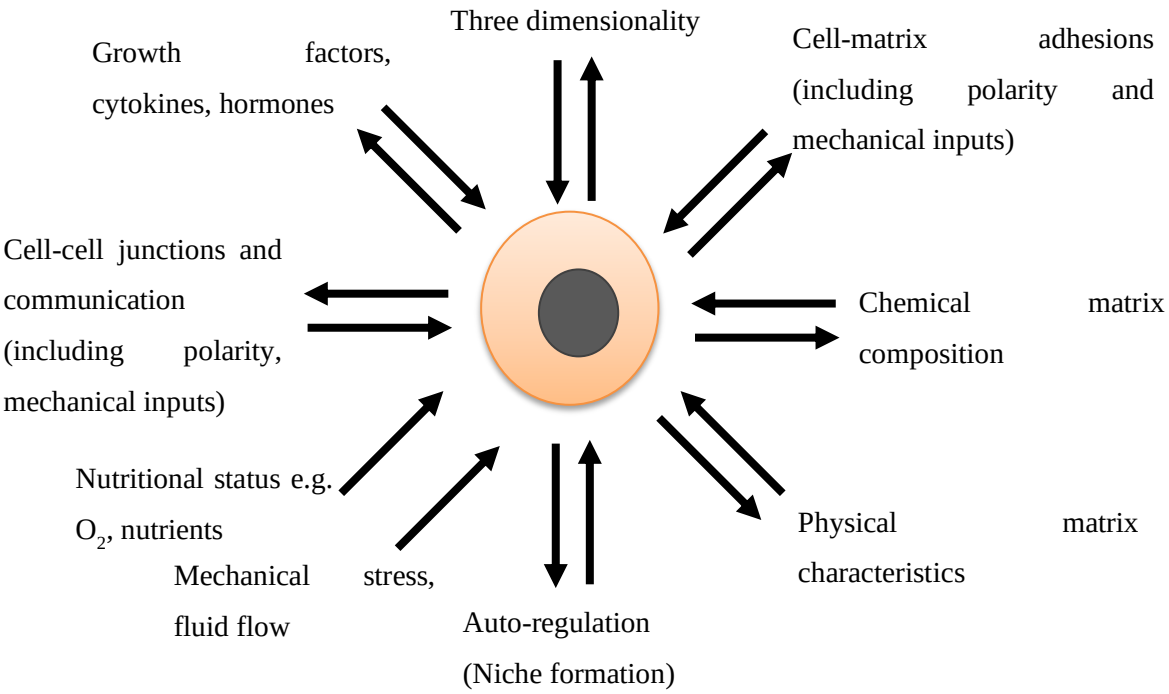


Figure 5.1: Microenvironmental cues which impact on cell structure and function: A wide variety of physical and chemical cues influence the cell, affecting its structure and therefore function; in the case of pluripotent stem cells, this impacts on pluripotency and differentiation trajectory. Adapted from Yamada and Cukierman, 2007.

Naturally, the phenotype and expression profile of any given microenvironment differs depending on a host of factors – anatomical location, identity of resident cell populations, vascularisation and ECM protein composition. Two different microenvironments are of interest to the work in this study: the environment which the developing embryo is exposed to and the local teratoma microenvironment.

The microenvironment that the developing embryo is exposed to is constantly changing in response to the transit of and cues from the embryo itself, the uterine cell populations and chemical/hormonal cues from the mother. At each stage of the developmental process, environmental cues are crucial to the successful transition of the developing organism to the next developmental stage. Within the developing embryo, the segregation of cells into multiple lineages creates different populations, signalling between which induces differentiation, migration and further lineage segregation. Communication with and attachment to the uterine endometrium results in the initiation of blastocyst implantation, and further signalling from uterine stromal cell populations (Atwood and Meethal, 2016) supports further development of the blastocyst. Vascularisation of the developing embryo allows for efficient nutrition and oxygenation once the structure has surpassed the tissue diffusion limit, altering the responses and differentiation trajectories of the cells in the structure and supporting the formation of a full sized foetus. Signalling from adjacent germ layers and cell populations is essential for the correct polarisation, migration and spatial organisation of developing organs within

the embryo (Grapin-Botton and Melton, 2000; Tam and Behringer, 1997), underlining in particular the importance of the microenvironment in cellular function.

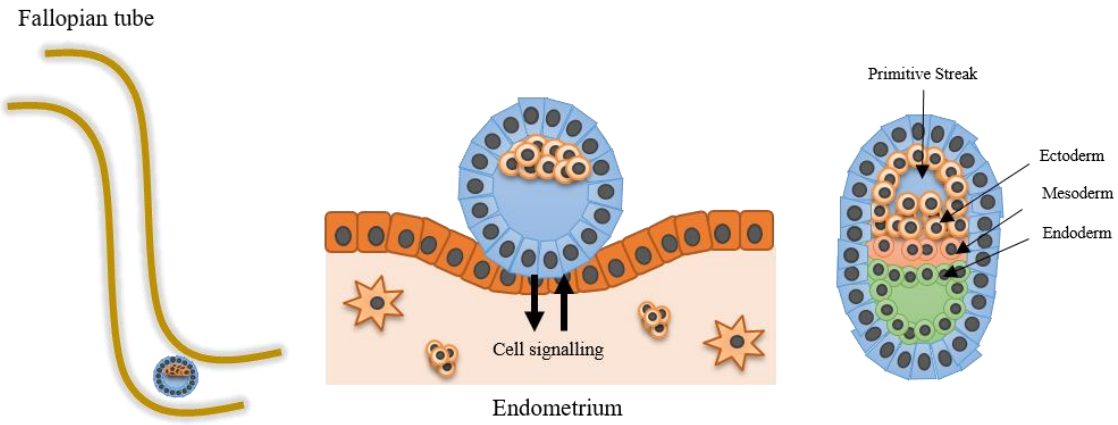


Figure 5.2: The microenvironment of the developing embryo: The microenvironment that the developing embryo is exposed to is highly dynamic, due to the transit of the developing structure along the fallopian tube and its subsequent interactions with the uterus. This is in addition to the changes ongoing in the embryo itself, with the creation of separate lineages and changes in cellular identity.

By contrast, the teratoma microenvironment could be considered more consistent, or homeostatic. As a mature tissue location, the cells and ECM are not subject to the same changes as the developing embryo. Although many of the environmental factors dependent on the actual anatomical location which is chosen as the site of implantation, there are a number of general factors which are consistent between the locations. PSCs come into contact with the extracellular matrix generated by the fibroblasts within the implantation site, which provides physical attachment, a three dimensional space and chemical signals to direct the proliferation and differentiation of the implanted PSCs. Host vascularisation of the developing tumour is crucial to its successful formation, again allowing for the structure to surpass the size limitations of the oxygen tissue diffusion limit and create complex structures from each germ layer. Signalling between differentiating populations within the developing teratoma will also impact on the development of neighbouring structures, in a similar manner to that seen in the developing embryo.

The diversity in the physical and chemical cues that PSCs are exposed to in both of these environments is clear, as is the impact that these cues will ultimately have on the successful differentiation of these populations.

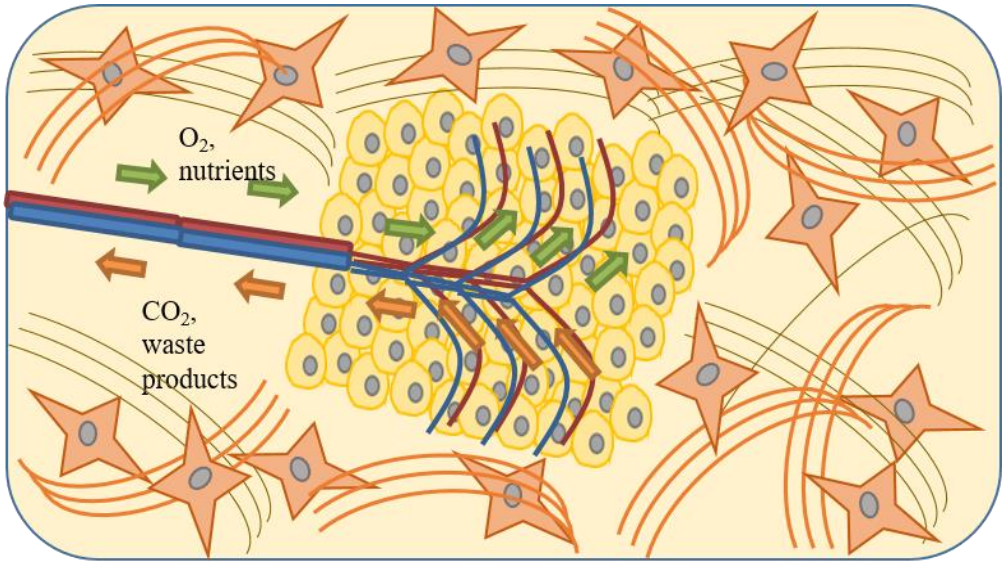


Figure 5.3: The teratoma microenvironment: Following the subcutaneous xenografting of PSCs into a mouse host, the microenvironment that the developing tumour is exposed to is dependent upon the anatomical location of implantation, although there is a level of consistency in the diverse cues that the PSCs are exposed to: paracrine signals from additional cell populations, attachment and interaction with a complex extracellular matrix and vascularisation by the host circulatory system.

5.1.2 Co-culture studies *in vitro*: Methods, techniques and rationale

The unique complexity of the cellular microenvironment *in vivo* underlines the importance of incorporating more elements into *in vitro* culture systems in order to better recapitulate physiological functions and responses of cells. A simple way to fulfil many of the cues described in Figure 5.1 is to incorporate the co-culture of other cell populations, such as supportive fibroblasts, into current three dimensional *in vitro* models. This can allow for the formation of a supportive (stem) cell niche, the effects of the paracrine secretion of growth factors/cytokines and the deposition of an extracellular matrix with specific physical and chemical cues which allows for appropriate cell junction expression and adhesion.

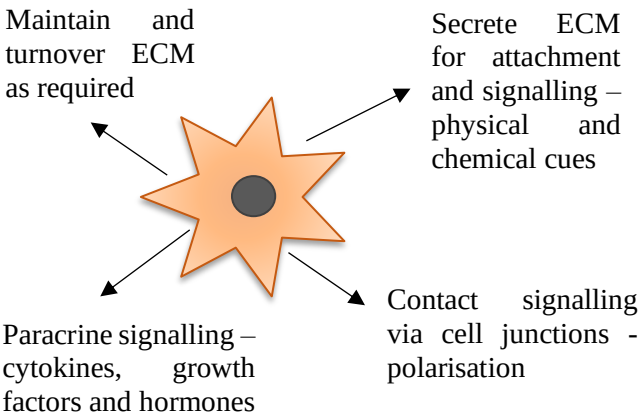


Figure 5.4: Additional microenvironmental cues which can be fulfilled through co-culture: Cell populations such as fibroblasts normally have a supportive role *in vivo*, making these cells a potential choice for co-culture studies due to their ability to fulfil many complex microenvironmetnal cues, including the secretion of cytokines and extracellular matrix proteins.

5.1.2.1 The development of *in vitro* tissue models co-culture models

Co-culture systems are used for a range of *in vitro* biological studies, where interactions between separate cell populations are of interest or essential for success, including studies into pathogen-host interactions, maintenance culture of specific cell populations e.g. mouse embryonic fibroblasts and PSCs and the creation of *in vitro* models of *in vivo* tissue environments (Goers et al., 2014). In the tissue modelling field, the creation of normal *in vitro* tissue models relies heavily on the technique of co-culture in order to recreate complex mature organ function. Examples are myriad, although the general concept involves the combined culture of an epithelial cell population on the surface supportive stromal cell population which provides appropriate chemical and physical cues, often also involving other advanced cell culture techniques such as scaffold culture to enforce correct spatial organisation. Successful reports include the creation of *in vitro* models of skin (Nayak et al., 2013; Roger et al., 2019), intestinal epithelia (Viney et al., 2009), respiratory epithelia (Blom et al., 2016; Ishikawa et al., 2017), and neural interactions (Daud et al., 2012), which are being used to understand normal biological functions, host pathogen interactions and responses to therapeutic drugs. Co-culture techniques are also being adopted in a number of differentiation based studies. PSCs have been incorporated into various co-culture situations, again often using scaffold technologies, in order to direct their differentiation towards specific cell populations, including chondrocytes (Bigdeli et al., 2009), primordial germ cells (Park et al., 2009b), cardiomyocytes (Mummery et al., 2003) and endometrium-like cells (YU et al., 2015). While there are challenges in the use of co-culture systems, such as differences in nutritional requirements, competition between different cell populations and difficulties in data normalisation when undertaking analysis, the recapitulation of the heterogeneity of the *in vivo* microenvironment through co-culture provides an excellent opportunity for creating more relevant *in vitro* cultures. Few studies though have used co-culture to study developmental processes, with the only examples focussing on the use of trophoblast cell lines with PSCs to better

understand the dynamic interactions between these cells in the developing blastocyst (Rivron et al., 2018). The use of multiple cell populations in the creation of organoids could also be considered a study of human development, specifically organogenesis, although these studies are generally limited to single organ processes, often use organ specific progenitors and focus as much on morphogenesis, the creation of structure, as they do on the process of differentiation.

5.1.2.2 The use of co-culture in tumour biology models

In the field of tumour biology, the importance of the co-culture of cancerous cell populations with the various cell populations involved in tumour support, progression or response, such as fibroblast, endothelial cells and immune cell populations, has been noted to impact significantly on the functions of tumour cells. This technique has been ubiquitously adopted into a variety of different culture techniques, with some models using up to three different cell populations within co-culture situations to better understand tumour biology (Lazzari et al., 2018). *In vivo*, fibroblasts create a niche which facilitates tumour growth (Majety et al., 2015), with endothelial cells providing the vasculature network to further support tumour progression, and the interactions between these populations in *in vitro* models have been shown to affect tumour growth, metastasis and response to therapeutic drugs (Amann et al., 2014; Courau et al., 2019; Lazzari et al., 2018; Timmins et al., 2004). Methods used have included co-culture within tumour spheroids and again, the use of hydrogels and solid scaffolds to create a stromal compartment as would be found *in vivo*. The data from these models is significantly more representative of tumour responses *in vivo*, allowing for better predictive drug testing and improved understanding of tumour biology due to the recapitulation of the physiological microenvironment and its complex intercellular interactions.

Thus, the incorporation of co-culture into any *in vitro* system offers the opportunity to more accurately recreate the local cellular microenvironment, increasing physiological relevance and improving cell functions and responses.

5.1.3 Introduction of perfusion into the *in vitro* setting and its use with PSCs

Another key component of the *in vivo* environment which contributes significantly to the local cellular microenvironment is vasculature. Vascularisation of the developing embryo and teratoma allows each structure to reach dimensions which far surpass the limits of the tissue diffusion distance, providing nutrition and removing metabolites but more importantly, allowing for efficient oxygenation of tissues. As well as providing nutritional and oxygen support, vascularisation, and by extension the introduction of perfusion to *in vitro* culture systems, can also provide mechanical/shear stress cues to guide the differentiation and function of cells.

A critical limitation of many current *in vitro* culture systems is the formation of unstirred layers, a phenomenon which occurs when using both traditional and three dimensional culture techniques. Unstirred layers form at the boundary between cells and culture media and in the spaces between cells, where depleted media and metabolites accumulate, affecting the ability of cells to take up molecules using both passive and active transport routes (Ng et al., 1993; Spivak et al., 2006). This in turn affects efficient gaseous exchange and nutrient support, as well as the uptake of any other compounds added to culture medium, such as therapeutic drugs. While the static nature of current culture systems already lacks in the support it provides (due to its relatively simplicity when compared to the *in vivo* microenvironment), the formation of unstirred layers further exacerbates the detrimental effects of static cell culture, necessitating the introduction of media circulation to improve cellular viability and function. Perfusion, fluid flow and shear stress have all been introduced to a wide range of cell types and *in vitro* models, with the techniques used to do so also being wide ranging in nature. Many somatic cell types have been shown to benefit and respond to these cues, including hepatocytes, osteocytes and chondrocytes (Lijuan et al., 2014; Pazzano et al., 2000; Schmelzer et al., 2010). It should be noted that these properties are subtly different in their nature and are mutually exclusive in some respects: perfusion and fluid flow, essentially fluid movement, can be introduced to a system with varying degrees or even the absence of shear stress, which is defined as the frictional movement of fluid on a surface (Adamo and García-Cardeña, 2011). Both of these factors have been shown to influence the function of cells *in vitro*.

5.1.3.1 Large scale cell culture bioreactors

While the synthesis of a supportive vasculature network to maintain cells and tissue constructs *in vitro* is a complex undertaking, a number of techniques have been used to introduce fluid flow into cell culture systems. On the macro scale, bioreactors are a popular choice for the maintenance of large cell masses, particularly for the synthesis of recombinant proteins and other products. As well as providing a three dimensional culture environment, the ability to closely monitor and tightly control nutrition, oxygenation and the removal of metabolites makes this technology highly useful, and allows for relatively successful large scale production of desired proteins. More recently, bioreactors have been employed in the culture of PSCs, both for expansion of the cell population and with the aim of developing an *in vitro* alternative to the teratoma assay. Gerlach and Knospel both used a form of novel hollow fibre capillary bioreactor to expand mouse embryonic stem cells, interestingly, in a co-culture with inactivated MEFs. Results showed a successful increase in cell number, good culture support, and most importantly, a maintenance of the 'stemness' of these populations confirmed by various analyses, including a teratoma assay (Gerlach et al., 2010b; Knöspel et al., 2016). Gerlach also used this novel hollow fibre technology to investigate the spontaneous differentiation of mouse embryonic stem cells, comparing the resultant differentiation to mouse foetal tissues and static culture controls. Culture of the mouse ESCs in the three dimensional

perfused environment for ten days resulted in differentiation of primitive structures which more closely resembled similar samples from the mouse foetus than comparable samples cultured using traditional two dimensional culture techniques, as confirmed by multiple marker expression (Gerlach et al., 2010a). Using a very similar hollow fibre bioreactor, Stachelscheid undertook a similar long term study focussing on the development of an *in vitro* replacement for the teratoma assay, using humans ESCs both with and without fibroblasts in the bioreactor cultures (Stachelscheid et al., 2013). As well as histological and immunostaining analysis, Stachelsheid also measured the output of various different proteins to monitor the differentiation process. It was found that after 50 days in bioreactor culture, human ESCs had formed highly complex tissue structures, which were significantly more successful than PSC derived EBs cultured for the same length of time.

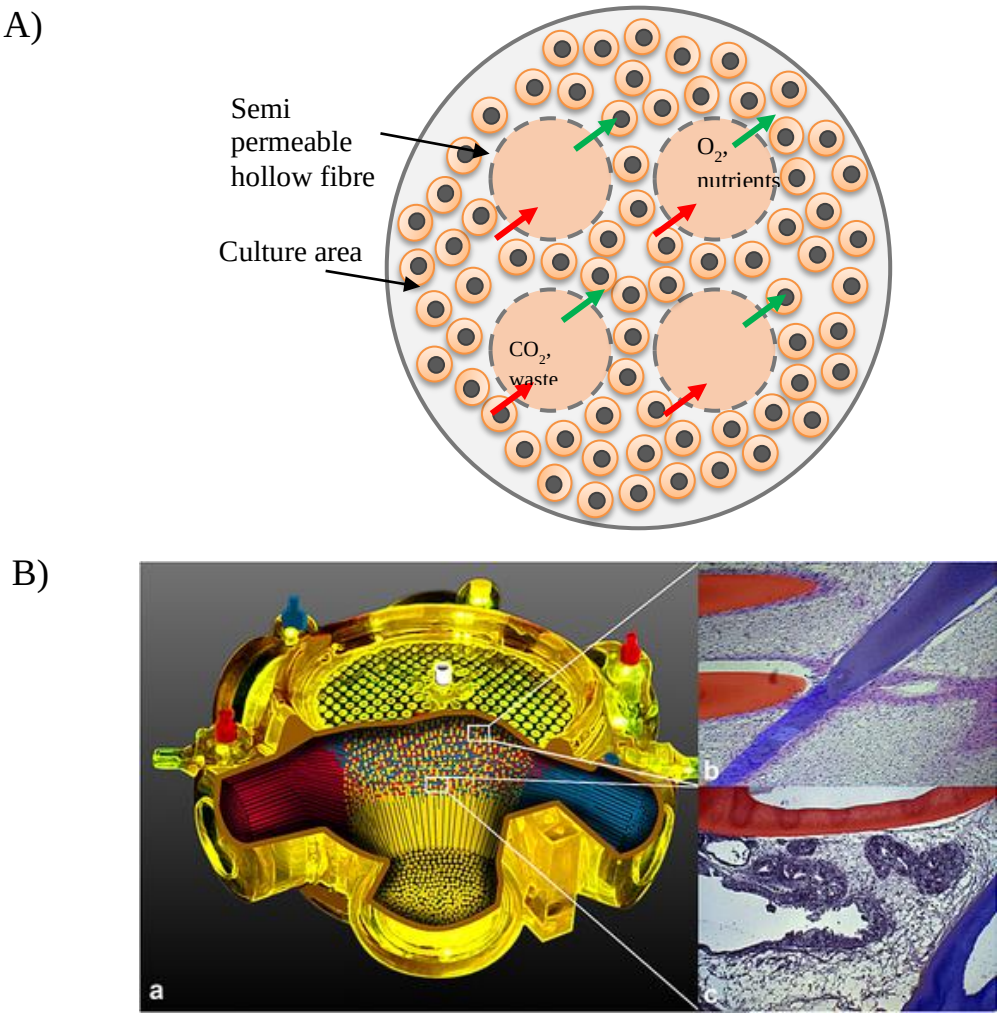


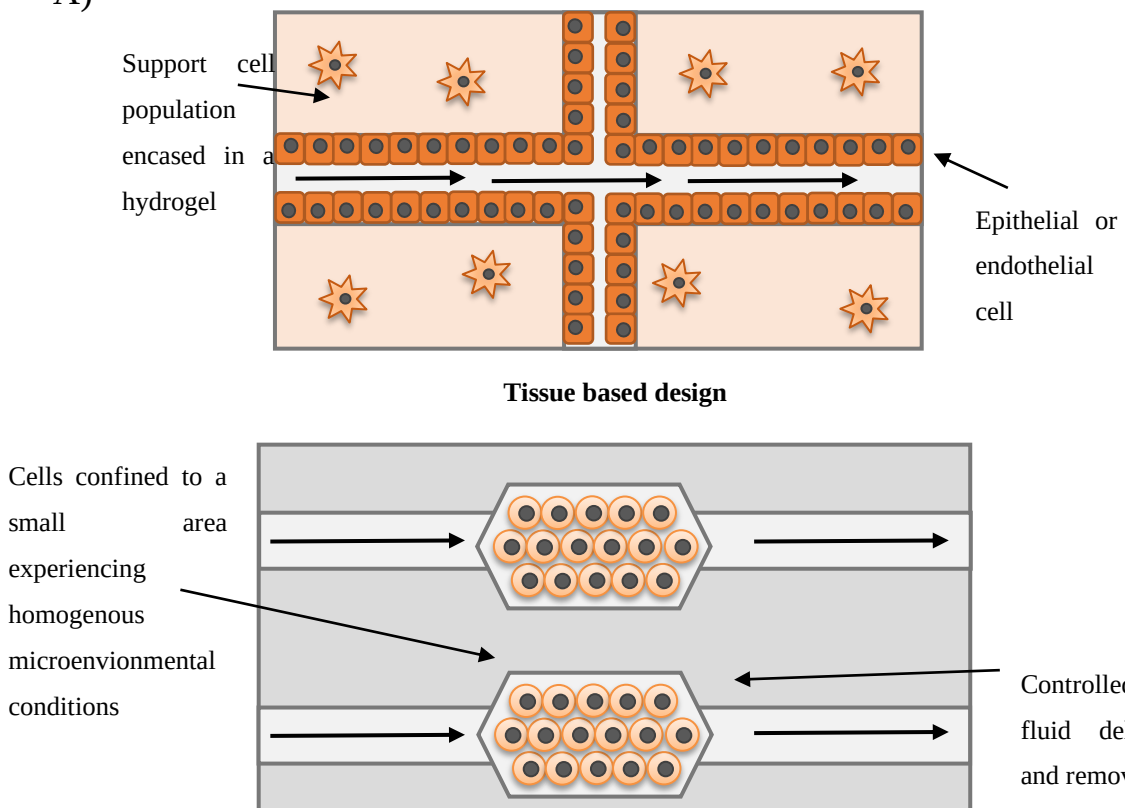
Figure 5.5: The structure of a hollow fibre bioreactor and example structures created from PSCs: Hollow fibre bioreactors have been used successfully to introduce fluid flow to PSCs, allowing for their maintenance and differentiation. A) Multiple semi permeable hollow capillary fibres are arranged within a bioreactor receptacle, at intervals to ensure that cells are homogenously provided with sufficient oxygen and nutrient support. Cells are seeded into the bioreactor culture area, and pack densely around the fibre locations. B) Three dimensional computer render of a hollow fibre bioreactor and example histology data from the differentiation of PSCs in the system show a variety of structures and cell morphologies. Image B adapted from Stachelschied 2012.

5.1.3.2 Microfluidic technology

While large bioreactors have demonstrated excellent results in terms of PSC differentiation, the associated expenses with the need for specific equipment and constant monitoring inhibits the adoption of these systems. Much more work on the introduction of perfusion and fluid flow has been completed on a smaller scale, using bench top bioreactors, stirred suspension cultures and microfluidics/chip technology, which can be used in a more high throughput manner and generate more samples, are less costly and of a more appropriate physical and physiological scale.

Microfluidic technology can be used to study the effects of highly controlled non turbulent fluid flow in various cell systems, and their advantages include controlled fluid mixing and laminar fluid flow, homogeneity and more often than not, a very small scale (Chiu et al., 2017). This in itself is advantageous due to the low cell number requirements and the ability to conduct large high through put studies. Generally, microfluidic systems are synthesised through the creation of microchannels in a material such as glass, or plastic, or through the patterning of materials such as hydrogels to create a series of interconnected channels, all of which media can be passed through (see examples in Figure 5.6). In the field of stem cell biology, microfluidics have also been applied to the maintenance and differentiation of pluripotent stem cells. Multiple studies have illustrated the impact of tight control of the local cellular microenvironment by fluid flow regulation, and its resulting impact on maintaining pluripotency (Titmarsh et al., 2011) or inducing lineage commitment in response to various morphogens (Cimetta et al., 2013; Giobbe et al., 2015). Studies have shown that the microfluidic environment can improve the reprogramming efficiency of iPSCs (Gagliano et al., 2019; Luni et al., 2016) and has been used to derive cells from all three germ layers, including cardiomyocytes, hepatocytes, neurones (Cosson and Lutolf, 2014; Luni et al., 2016). While microfluidics can be used to elucidate the effects of morphogens and cell functions even at the single cell level, as well as having applications in the modelling of tissue vascularisation, the interactions studied in the system are potentially not representative of the *in vivo* situation as a result of this small scale. A small scale system would suffer a greater impact from any media evaporation compared to large culture systems. In addition these systems do not necessarily take into account system wide effects from distal locations (Liu and Lu, 2016), the physics of larger mass transport systems and the fact that some microfluidic systems are ‘confined to two dimensions’ (Chiu et al., 2017).

A)



B)

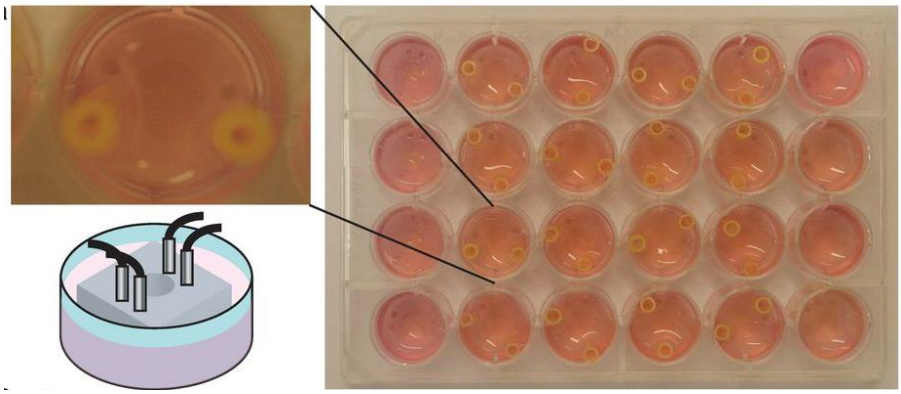


Figure 5.6: Examples of microfluidic technology device designs: Microfluidic chips can be designed using a variety of techniques, including 3D printing and thermal curing of hydrogels. A) The structure of the channels could reflect a miniature bioreactor or recapitulate the more complex structure of a specific organ, a shown here. B) In the example shown, a microfluidic system used to deliver morphogens to PSCs for differentiation in a 24 well plate. Adapted from Cusson and Lutlof 2014.

5.1.3.3 Bench top bioreactor systems

Bench top bioreactors and stirred suspension bioreactors are the third broad category of fluid flow system which are used to introduce perfusion, fluid flow and shear stress into cellular systems. These systems are, importantly, of a more physiological scale and allow the user to more easily manipulate and control the parameters as well as being cheaper than large scale bioreactors. Additionally, the improved flexibility and customisability of these systems over large scale bioreactors means that users are not constrained by the equipment/design, as demonstrated by the range of applications and techniques found in the literature. Dependent on equipment design, the inclusion of three dimensional techniques such as cell aggregation and solid scaffolds are often employed in these systems to provide the appropriate space for cells to attach to and grow (see example of a stirred suspension bioreactor in Figure 5.7). Work in this area using pluripotent stem cells has again focussed on the two key areas of stem cell culture; maintenance of pluripotency and differentiation. In the same way as observed in other systems, the introduction of fluid flow in bench top bioreactors promotes the maintenance of pluripotency through the control of the local microenvironment, with examples including Yeo through encapsulating PSCs in alginate in perfusion bioreactor (Yeo et al., 2013) and Kropp in a stirred suspension bioreactor (Kropp et al., 2016). Significant amounts of work have been devoted to the use of bioreactors for the development of reproducible differentiation protocols which result in mature, functional tissues. A common technique for differentiation protocols is to seed tissue specific progenitor populations into the system with the aim of achieving mature functional tissue constructs, as is usually the case with bone tissue engineering studies (Sailon et al., 2009; Schmelzer et al., 2010), but PSC populations have also been used in a number of differentiation based studies. Bench top systems have been used in particular to differentiate PSCs towards mesoendodermal lineages, such as cardiomyocytes (Bauwens et al., 2005; Shafa et al., 2011), with some noting the ability of dynamic culture to enhance lineage commitment to this germ layer (Lei et al., 2014). Stirred suspension culture has also been used in the creation of cerebral organoids; the technique used in the final stages of the differentiation protocol to enhance tissue expansion and maturation (Lancaster and Knoblich, 2014b). Additional work has elucidated the effects of the mechanical cues in perfused culture such as shear stress on germ layer specification (Wolfe et al., 2012; Wolfe and Ahsan, 2013).

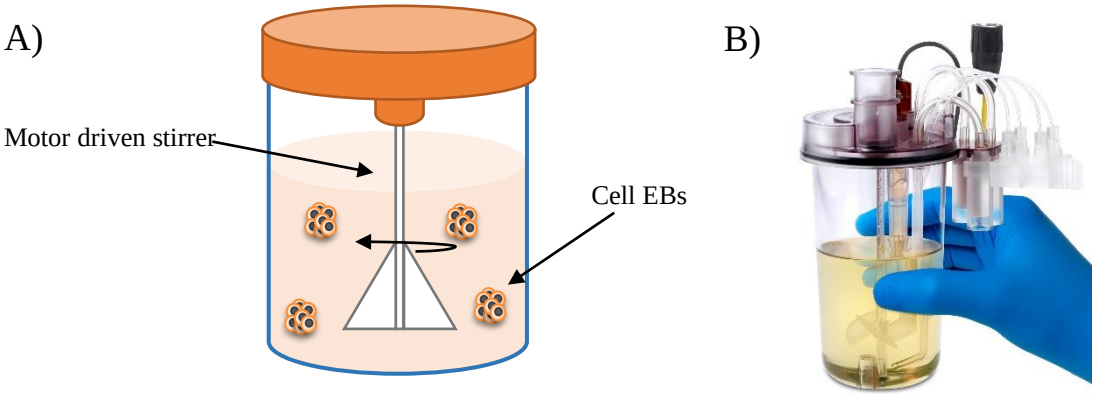


Figure 5.7: Examples of dynamic bench top cell culture systems: Stirred suspension bioreactors represent a simple yet popular type of bench top perfusion system, whereby three dimensional aggregates are cultured in a vessel which contains a mechanical stirrer to prevent the formation of unstirred layers and introduce shear stress if desired. A) Schematic of a stirred suspension bioreactor, used in various PSC expansion and differentiation applications. B) Image of a miniature stirred bioreactor for cell culture. From www.laboratoryequipment.com.

The impact of using dynamic culture systems *in vitro* to enhance the cellular microenvironment through improved nutrition, oxygenation and the introduction of mechanical signalling cues is apparent in the literature discussed here. Incorporating this property into the model developed in Chapter 4 could offer the opportunity to further enhance the differentiation within the system.

5.1.4 The incorporation of physiological factors to the current TERA2.cl.SP12 model

As detailed above, the use of both co-culture and perfusion in the differentiation of human PSCs has revealed the importance of introducing more microenvironmental cues to three dimensional culture models, in order to increase physiological relevance and therefore cell function. In the case of pluripotent stem cells, the hypothesis is that the introduction of more physiological cues would result in improved differentiation and tissue structure formation.

The current model created using TERA2.cl.SP12 EBs and Alvetex® Polaris in the previous Chapter incorporates three dimensionality and improved support of PSC derived structures, but does not provide any of the additional cues as described in Figure 5.1. Due to the versatility of Alvetex® and its availability in three different formats with various pore sizes, there are a number of options which can be explored to incorporate more microenvironmental cues.

Alvetex® has already been shown to be able to support the culture of a number of different cell populations. In particular, it is currently used to create a number of organ specific *in vitro* tissue models where multiple cell populations are cultured in close contact. All are based on a similar culture method, with the initial creation of a supportive fibroblast compartment using the Alvetex®

Scaffold format, with the corresponding epithelial population seeded onto the top. Using this technique, a representative model of human skin has been created as mentioned previously (Roger et al., 2019), and similar models are in development recreating the human intestine, buccal tissue and the respiratory tract. This can be translated to the tissue disc model through the exchange of Alvetex® Polaris for an Alvetex® Scaffold insert with cells cultured within to create a supportive stromal compartment. Due to the ubiquity of fibroblasts in tissues, their importance in the deposition of ECM, their role in signalling in cell niches and the ease with which these cells can be obtained and cultured, this cell population can be used in a model of tissue development and teratoma formation. These current models as detailed above all use fibroblast populations, and provide the opportunity to test the feasibility of PSC tissue disc co-culture before the incorporation of a more relevant fibroblast population. These optimisation experiments will be completed with TERA.cl.SP12 again, due to the distinct restricted differentiation phenotypes, which can be easily identified. The teratoma assay is the technique which allows for the formation of the most complex differentiated structures derived from PSCs, and so a fibroblast population which correlates with this assay would be most appropriate. The analysis conducted in Chapter 3 highlighted the lack of congruency in implantation site for the teratoma assay, but it can be surmised from the data that all cells come into contact with ECM and signals synthesised by fibroblast populations. This analysis also highlighted that SCID mouse strains were among the most popular choice of mouse host for conducting the teratoma assay. As dermal fibroblasts are easy to derive and are likely to come into contact with PSCs at many of the implantation site, SCID mouse dermal fibroblasts are a logical population to use in a co-culture model.

The effectiveness of using hollow fibre bioreactors in the differentiation of PSCs was well established in section 5.1.3, but their use is not practical in this setting. Microfluidic culture is also not appropriate due to its small scale, which prevents complex structure formation and is not necessarily representative of the teratoma size and microenvironment. The porous nature of the Alvetex® means that it should be able to be incorporated into a fluid flow system as it will permit the passage of fluid through the scaffold, with a bench top system being the obvious choice due to the dimensions of the Alvetex® insert. In order to achieve the desired effects and allow for complete customisation, a novel bench top bioreactor system will be developed for the culture of TERA2.cl.SP12 derived EBs on Alvetex® in a perfused system. The system must adhere to the following requirements:

- Can be incorporated into normal cell culture facility/equipment
- Easy to set up
- Minimal maintenance during culture
- Reusable and relatively inexpensive
- Be able to incorporate Alvetex® inserts
- Elements of customisation

These properties will allow for the maximisation of the resources and equipment, as well as use by any cell culture facility and adaptation dependent on the application or experimental set up.

While the introduction of multiple physiological factors would allow for the significant enhancement of the microenvironmental cue within the mode, these two culture conditions will be applied in isolation to the model in the hopes of better understanding their effects on differentiation and pluripotency.

5.1.5 Conclusion

The *in vivo* microenvironment which cells are subject to is highly complex; cells are exposed to a wide range of integrated physical and chemical microenvironmental cues which guide their structure and function. While both very different in some aspects, the *in vivo* microenvironments that the developing embryo and the developing teratoma are exposed to share a number of similarities. Of particular importance are the signalling cues and ECM support provided by neighbouring cell populations and the vascularisation of the developing structures as they increase in size. *In vitro* cell culture environments need to recapitulate these complex integrated signals in order to elicit a more representative, physiological functions from cells in culture. A significant amount of work has been undertaken to incorporate cues such as these into various culture practices, including into three dimensional culture systems. Co-culture has been used extensively in the creation of *in vitro* model organ systems and tumour biology studies, with some work also completed undertaking differentiation based experiments using PSCs. A wide variety of perfused culture systems have also been developed for the introduction of fluid flow and shear stress to *in vitro* culture, ranging from large scale bioreactor culture to user friendly bench top systems to high throughput microfluidics. The ability to both maintain pluripotency and induce the differentiation of PSCs within these systems has been demonstrated as possible, depending on the parameters of the system in use. These microenvironmental factors have been shown to impact on PSC function, and so their incorporation into the tissue disc model would be highly beneficial in terms of enhancing the differentiation, structure and function of PSC derived tissues. Fibroblasts are a ubiquitous cell population which is heavily involved in ECM production and cell signalling, making them a suitable choice for use in a co-culture version of this model. For the introduction of perfusion and fluid flow, a novel bench top bioreactor system will be developed to allow for flexibility and desired customisation.

5.2 Aims and Hypotheses

The aim of this chapter is to enable improved cell differentiation in the current model through incorporating properties which will make the model more representative of the physiological environment. Two different methodologies will be investigated.

Continuing to use the TERA2.cl.SP12 cell line to form stem cell derived embryoid bodies, fibroblasts will be incorporated into the model to create a co-culture environment to mimic the subcutaneous implantation of PSCs in a teratoma assay, with the overall aim of enhancing the differentiation of the tissue discs cultured in the model. In line with tumour biology studies which commonly utilise co-culture, it is hypothesised that the introduction of fibroblast contact, endogenous extracellular matrix and signalling cues into the model will enhance the function of the pluripotent stem cells, resulting in enhanced differentiation, with the formation of more complex structures as seen *in vivo*

The property of perfusion will also be investigated using the TERA2.cl.SP12 cell line, by utilising a simple, novel perfusion system to enable media recirculation during the culture period, with a view to recapitulating aspects of vasculature by reducing areas of static media. In a similar way to co-culture, the introduction of perfusion is also expected to improve the differentiation within the tissue discs, showing a wider range of structure formation and bringing the phenotype closer to that observed in the teratocarcinoma.

5.3 Objectives

- Utilise an established neonatal human dermal fibroblast model to determine whether co-culture with stem cell derived embryoid bodies is possible.
- Develop a novel dermal equivalent model using a more relevant fibroblast population: dermal fibroblasts from a severe combined immunodeficient (SCID) mouse.
- Co-culture TERA2.cl.SP12 EBs in the SCID mouse fibroblast co-culture model and assess the differentiation which occurs.
- Optimise the technical aspects of the novel perfusion system to select the appropriate equipment for successful media recirculation.
- Optimise the culture method for seeding cells into the perfusion system.
- Utilise the optimised culture method in the novel perfusion system and investigate the subsequent differentiation.

5.4 Materials and Methods

The routine maintenance of TERA2.cl.SP12, both fibroblast populations and the seeding of dermal equivalents is detailed in the Materials and Methods in Chapter 2, as is the seeding of EBs onto dermal equivalents for co-culture. The culture techniques and analytical techniques specific to this Chapter, mainly those related to the perfusion experiments, are detailed below.

5.4.1 Technical specifications of equipment used for perfusion experiments

The perfusion system used in this Chapter was custom designed, with many parts being made by various departments within Durham University.

5.4.1.1 Holder for Alvetex® inserts

The device used in the perfusion system was designed by Professor Stefan Przyborski for use with Alvetex® membranes of a 6 well format. It is made from polystyrene and composed of two identical pieces which clip together with the Alvetex® inserts positioned in the centre, as seen in Figure 5.8.

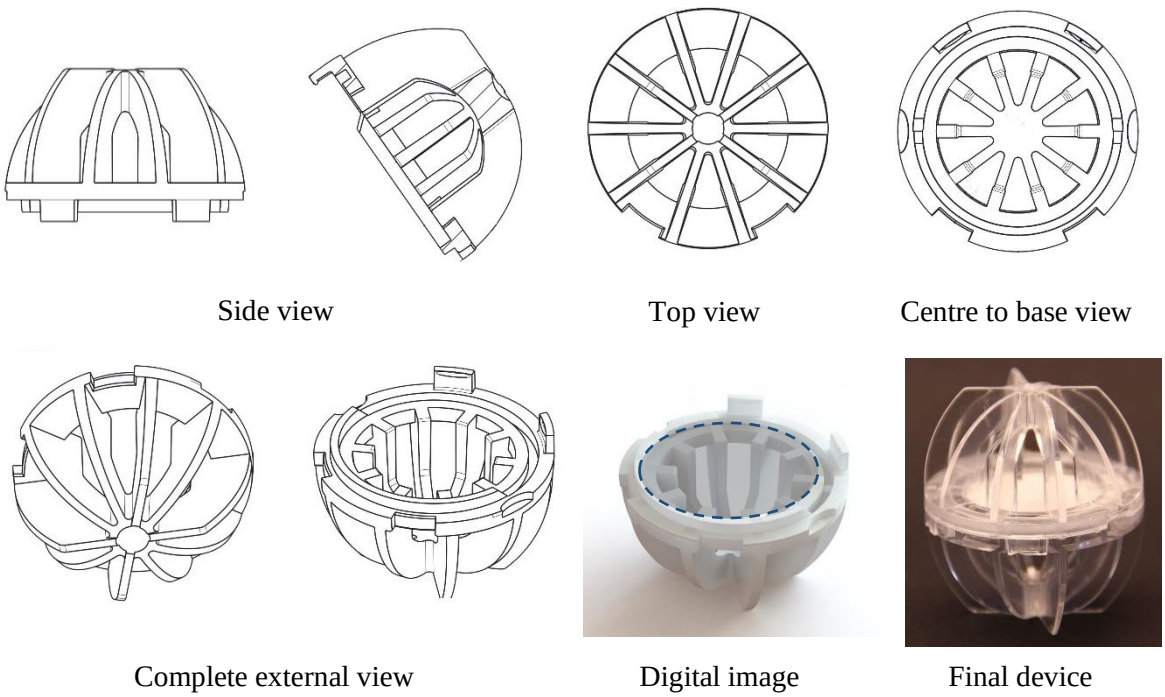
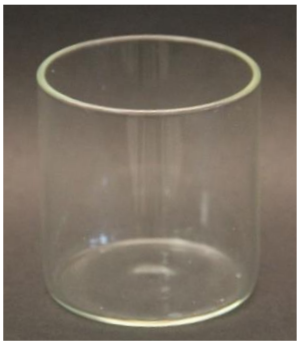


Figure 5.8: Overview of novel perfusion system equipment: Schematics showing computer aided design renders of the plans for the Alvetex® holder in multiple orientations, as well as a digital image and photograph of the final complete device. The device is composed of two identical parts which clip together to form an ovoid shaped holder, in which 6 well format Alvetex® inserts can be cultured.

5.4.1.1 Media reservoir

The glass beakers used to contain the system were kindly made by Aaron Brown, a member of the Durham University Glass Blowing Workshop, in the Department of Chemistry and designed in collaboration with Henry Hoyle. Specifications and a photograph of the equipment are shown in Figure 5.9. A Petri dish style lid was used to enclose the system.

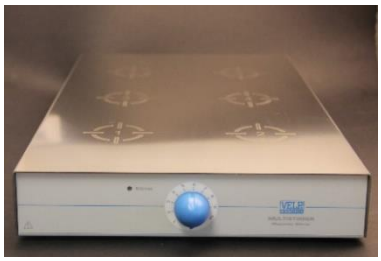


Parameter	Measurements
Internal diameter	65 mm
Height	69 mm
Wall thickness	2 mm
Total volume	228960 mm^3

Figure 5.9: Perfusion system glassware and specifications: Custom designed beakers were made by the Glassblowing Workshop in the Department of Chemistry. These were made from standard glass tubing of internal diameter 65 mm.

5.4.1.2 Magnetic stirrer driving perfusion

For fluid movement, glass beakers with a magnetic stir bar in the bottom and cellular material/media set up as described below were placed onto a Velp 6 point Magnetic Stirrer (Velp Scientifica, Usmate, Italy) in a standard cell culture incubator. To prevent rusting and other detrimental effects on the electrical equipment, the humidifying pan was removed from the incubator.



Parameter	Measurements
Total number of positions	6
Highest rotational speed	850 rpm
Lowest rotational speed	50 rpm

Data as per manufacturer's instruction manual.

Figure 5.10: Stirrer system used for perfused experiments and specifications: 6 point stirrers were used with magnetic stir bars to create fluid movement within the system, and therefore introduce perfusion. Three Velp stirrers were used in total in the incubator, allowing for up to 18 bioreactor experiments to be run at the same time.

5.4.1.3 Device holders for directing media flow

A series of different stand designs were created in collaboration with fellow PhD student Henry Hoyle in order to ascertain which was most appropriate for creating optimum fluid flow in the system. Prototype stands were made from Polytetrafluoroethylene (PTFE) by the Durham University Physics Workshop for testing, as detailed below.

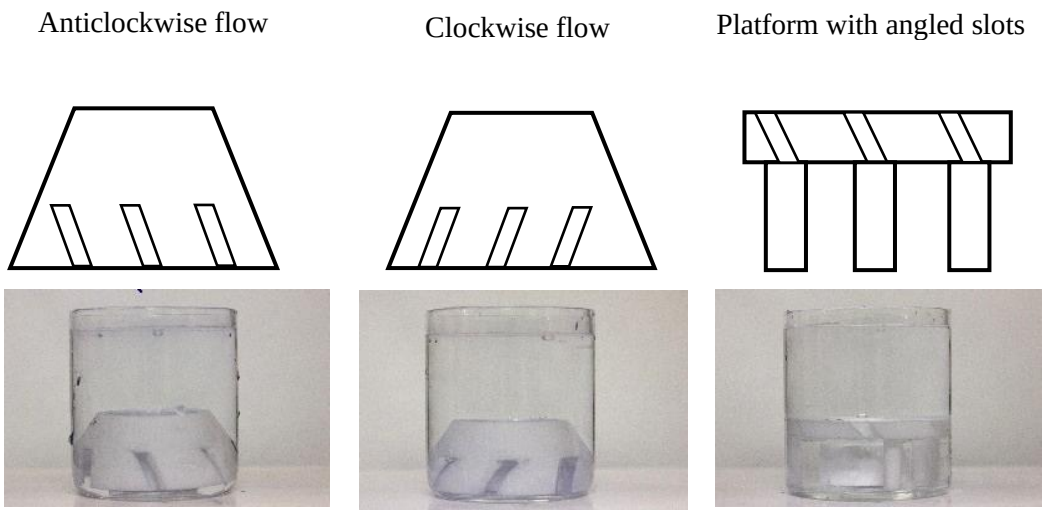


Figure 5.11: Potential device holder stand designs: Three different design prototypes were obtained for testing to assess the fluid flow within the system for optimisation. These were subject to a variety of physical tests, including fluid flow analysis using a dye and particle image velocimetry. Prototype stands were kindly made by the Physics Workshop, Durham University.

Once the final design had been confirmed, the final stands were kindly made by the Durham University Materials Workshop in the Department of Chemistry.

5.4.1.4 Complete bench top bioreactor system

The final equipment set up used combined the above elements into the perfusion culture system as seen in Figure 5.12 below.

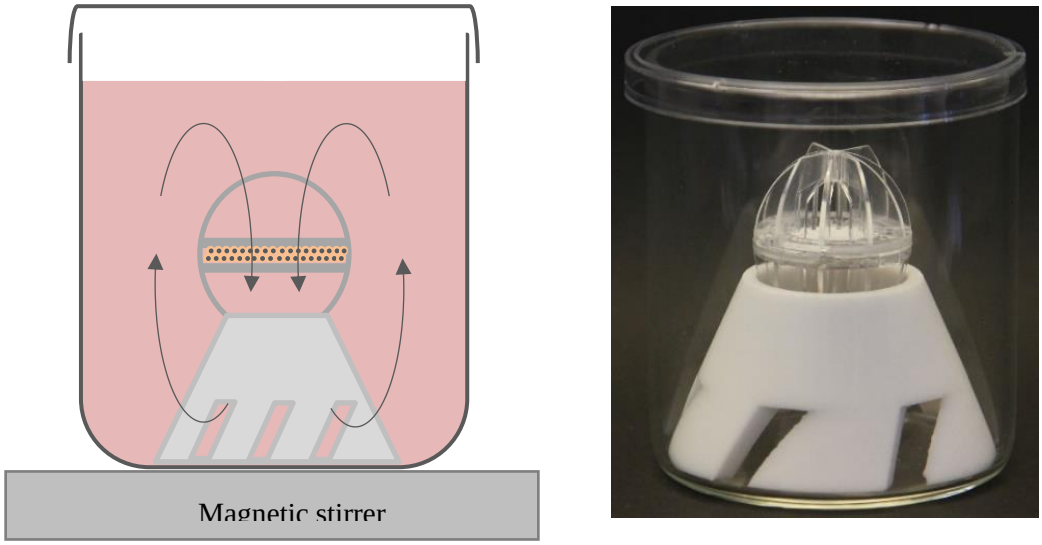


Figure 5.12: Overview of novel perfusion system equipment: The schematic and photograph show the equipment set up of the perfusion system. The Alvetex® holder is placed on a stand in a glass beaker with a Petri dish style lid, below which a magnetic stirrer is positioned, to continually move the culture medium through the device, resulting in the constant perfusion of the cellular material seeded onto the Alvetex®.

5.4.2 Analysis of fluid flow dynamics

The fluid flow dynamics of the fluid body in the glass beaker was assessed during the optimisation of the novel perfusion system. 150 mL of water was placed into the perfusion system with the stand to be analysed and a magnetic stirrer. The system was placed centrally on a magnetic stir plate in front of a plain white background and set to stir at 125 rpm. 200 µl of 0.1 % crystal violet in 70 % ethanol was added to the surface of the water at 0 seconds, and imaged automatically every 2 seconds for a total time of 60 seconds using a Canon camera.

5.4.3 Analysis of fluid flow dynamics – Image J analysis

To analyse the fluid flow within the images taken, images were first cropped so that only the vessel was visible in the image, and subsequently opened in Image J. A custom made Macro was used to create a consistent multi-point grid to overlay on the vessel, to measure the intensity of the dye across the entire vessel. The grid was created to cover the main body of fluid within the vessel, avoiding areas of heterogeneity and turbulence, such as the fluid surface and the base of the device holder, see Figure 5.13. This was then split into 3 sections, the top, middle and bottom of the vessel, and the mean dye intensity in each section calculated for each image. These values were then plotted as White intensity against time since the dye was added using GraphPad Prism.

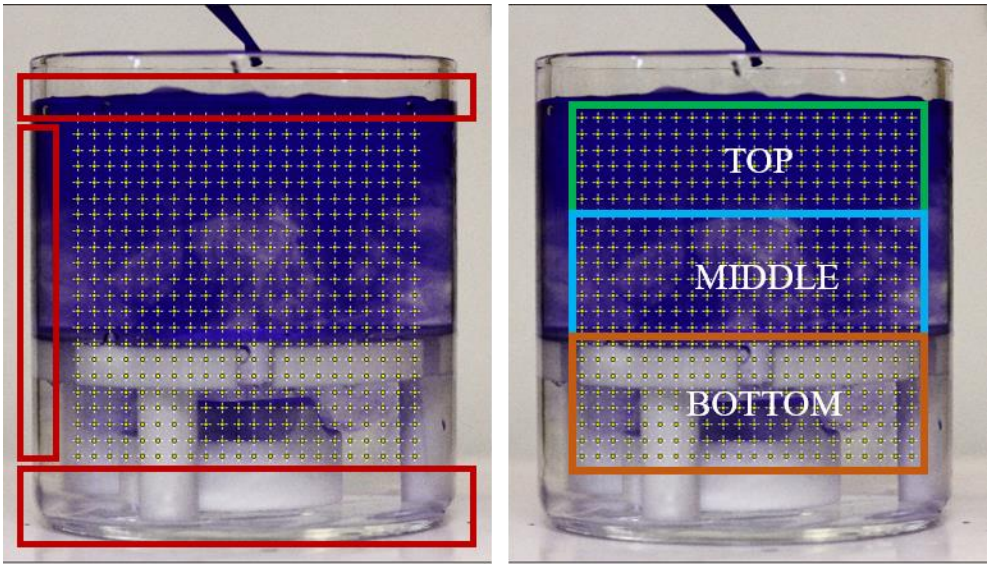


Figure 5.13: Assessment of fluid flow dynamics of the system using crystal violet dye: A multipoint grid was overlaid onto the image of the vessel using ImageJ, avoiding the areas of interference and turbulence at the top, base and sides of the vessel, as shown in the left hand image. The grid was then split into three equal sections, in order to measure the changes in dye intensity as is was circulated through the system. The average intensity was recorded for each section in each image and plotted against time.

5.4.4 Particle Image Velocimetry studies

Particle Image Velocimetry (PIV) was used to assess the effects of mixing and turbulence within the novel perfusion system, and conducted with kind assistance from Dr Lian Gan, Department of Engineering at Durham University. The flow field was measured in a horizontal plane across the centre of the custom made glass beaker by assessing the position over time of tracer particles added to the fluid in the beaker at a speed of 125 rpm (Raffel et al., 2018). The simple two-dimensional PIV measurement in a horizontal plane resolved the two-component in-plane velocity distribution, viz. (u,v) on (x,y) capturing most of the energy content there, (the out-of-plane velocity component is considered to be relatively unimportant). The PIV sample rate is 4Hz and the spatial resolution is 0.05 mm. The mean velocity magnitude and the rms contours are calculated from a time-mean of 400 fields. The turbulence level and hence the mixing efficiency can be inferred by the rms contours, with the data shown in the Figure later in this Chapter.

5.4.5 Seeding of cells/EBs for static sandwich culture

To prepare for sandwich culture, Alvetex® inserts were prepared as previously described and placed in a 6 well plate. Cells or EBs were first seeded onto the insert as previously described in the Materials and Methods. Media was topped up to 10 mL, and cells/EBs were left to adhere in culture for 1-2 days. After this time, inserts were carefully unclipped, the body piece retained in a sterile Petri dish and the disc left in the base piece and placed in a separate sterile Petri dish. Additional Alvetex®

inserts were prepared as previously described were unclipped from the inserts if necessary to release the discs. A top disc was then carefully placed on the insert with the cellular material adhered, and the body piece clipped back on the base piece to secure the 2 discs in a sandwich culture. The assembled sandwich culture was then placed in a fresh 6 well plate and topped up with 10 mL of appropriate media.

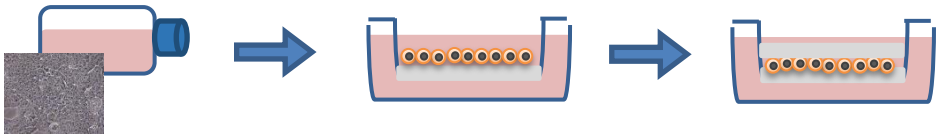


Figure 5.14: Schematic for the creation of static sandwich culture models: Pluripotent stem cells or EBs were seeded onto the Alvetex® inserts. Cells were allowed to attach for 1-2 days before the addition of the second insert to create a sandwich culture. Sandwich cultures were then returned to submerged culture in a 6 well plate.

5.4.6 Seeding cells in Matrigel on Alvetex® inserts

In some perfusion experiments, cells were combined with Matrigel for seeding to provide support in the sandwich culture.

Cells were detached using the 0.25 % trypsin/2 mM EDTA method and counted using the Trypan Blue exclusion assay as described to obtain accurate cell numbers. The appropriate cell volume for the number of inserts was then transferred to a 1.5 mL Eppendorf tube. In order to combine cells with Growth Factor Reduced (GFR) Matrigel matrix (Corning®, Fisher Scientific UK), the appropriate volume was calculated dependent on the batch concentration to obtain a final concentration of 3 mg/mL. The appropriate amount of cell culture medium to give a final volume of 200 µl per insert was also calculated following this. The additional media was added to the cell suspension, and the inserts were placed in 6 well plates ready for seeding. The GFR Matrigel matrix was kept on ice, and the appropriate volume was added to the cell suspension using cooled pipette tips to delay gelling. The cell suspension/Matrigel mixture was then immediately transferred to the insert, again using cooled tips, and incubated at 37°C, 5 % CO_2 for at least 30 minutes to allow the Matrigel to set. Where cell suspension/Matrigel combinations were left on the insert for two days, after setting, 6 mL of media was added to the outside of the insert in the well to prevent disturbing the cell layer. Inserts were then used as desired for sandwich culture or perfusion.

5.4.7 Seeding cells/EBs on Alvetex® inserts for static culture

Following some optimisation, cells and EBs were cultured without an additional insert. Cells and EBs were seeded in the same manner as previously described for seeding in the static model system.

Cells were added to the insert and allowed to attach for at least 1 hour before the addition of media, whereas EBs were added to the insert already submerged in media.

5.4.8 Seeding cells/EBs for perfused culture

To conduct perfused culture, cells/EBs were initially seeded as desired using the techniques described above and following the methods previously described for general cell seeding and static sandwich culture.

Perfusion devices were soaked in 70 % ethanol for at least 24 hours prior to use. To set up, perfusion devices were washed in sterile PBS, and placed in a sterile Petri dish with the flat centre facing upwards. The inserts with the cellular material adhered were very carefully unclipped to release the discs, which were then placed in the perfusion device. If required, a second prepared Alvetex® disc was then placed on top as previously described. Then, the second half of the perfusion device was clipped on to secure the disc/discs. 120 mL of media was added to the perfusion beaker, and the perfusion device slowly lowered into the media to rest on the stand while allowing the media to permeate the scaffold. Once the device was settled in the beaker, the lid was added and the beaker carefully placed on a Velp 6 point Magnetic Stirrer in the cell culture incubator and cultured at 37°C, 5 % CO_2.

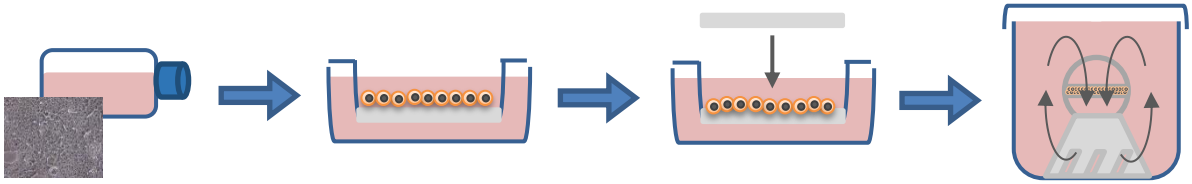


Figure 5.15: Schematic for the creation perfused culture models: Pluripotent stem cells or EBs were seeded onto the Alvetex® inserts as previously described and allowed to adhere to the scaffold for 1-2 days. Scaffolds were then carefully unclipped and placed into the perfusion device, and the second insert placed in top if required. The second piece of the perfusion device was clipped onto the piece containing the scaffold, and placed into the perfusion beaker.

5.5 Results

5.5.1 Characterisation of neonatal human dermal fibroblast model and optimisation for culture of pluripotent stem cell EBs with fibroblasts

The neonatal human dermal fibroblast model (HDFn) is well established within the group as a platform for both investigation into the properties and responses of the human dermis and the support and maintenance of a novel *in vitro* full thickness human skin model. As fibroblasts are to be incorporated into the model to increase physiological relevance, this reproducible model provides an ideal starting point to establish whether co-culture of pluripotent stem cell EBs with fibroblasts is possible.

5.5.1.1 Neonatal human dermal fibroblast cells can be used to create a dermal equivalent using synthetic media within a 3D scaffold, which can be replicated using stem cell media.

Currently, HDFn cells and the dermal equivalent are cultured in Medium 106 (M106), a synthetic medium created for the culture of human dermal fibroblasts, with a low serum growth supplement added. This media is used both in 2D culture and when forming the 3D dermal equivalent using Alvetex®, further supplemented with 5 ng/mL TGF-β and 100 µg/mL ascorbic acid. When cultured in M106, the dermal equivalent which forms shows a progressive increase in the number of fibroblasts within the scaffold with increasing culture time, as well as increasing deposition of appropriate ECM proteins, as shown by the histology and immunostaining in Figure 5.16. Vimentin is a cytoskeletal protein associated with the fibroblast phenotype, and collagen I is the most abundant ECM protein in the human body. These markers allow for the identification of fibroblasts within the scaffold and an appreciation of the deposition of ECM. In particular, using this technique results in the layering of the fibroblasts at the top and bottom of the scaffold, and after as little as 14 days in culture, a continuous layer of fibroblasts can be identified. The dermal equivalent tissue is currently capable of maintaining a fully differentiated epidermis when primary human keratinocytes are seeded onto the surface as can be seen in Figure 5.17; these cells are able to stratify into the distinct layers of the epidermis, achieving terminal differentiation and the formation of a keratinised top layer. This indicates that co-culture and continued support of other cell types on this dermal equivalent is possible, as is their differentiation and formation of mature complex tissue structures.

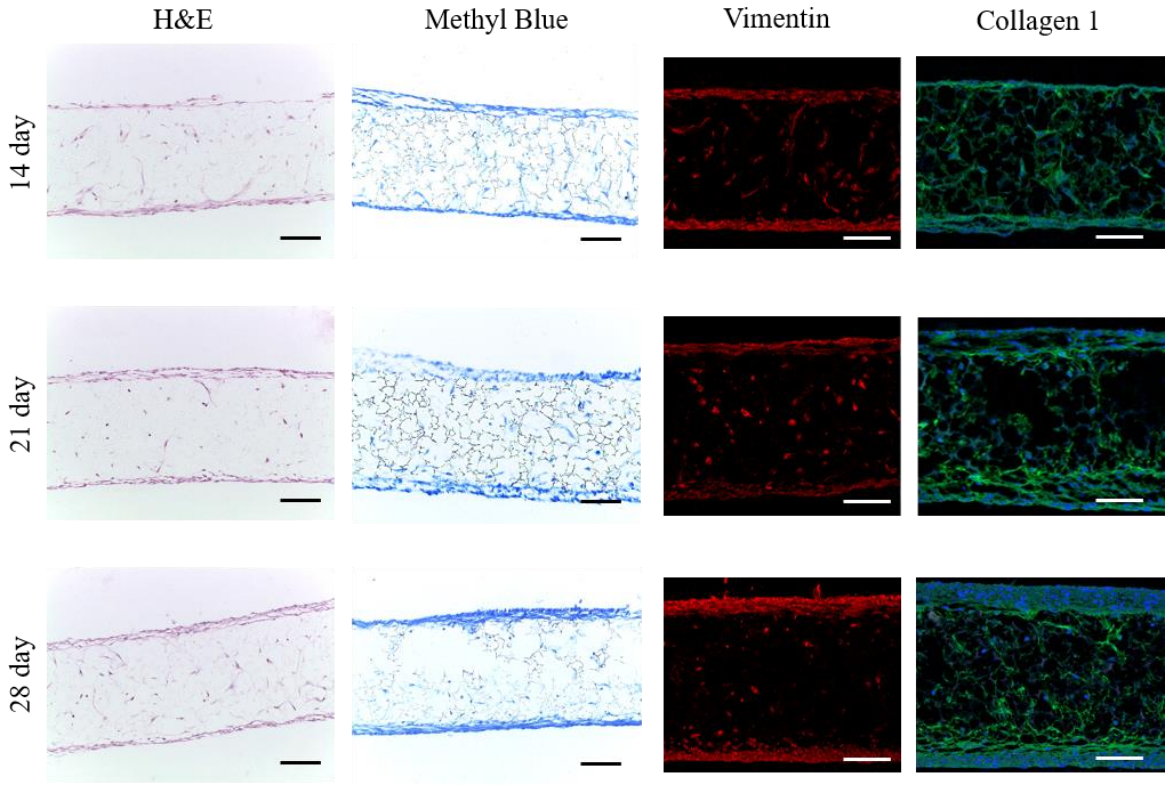


Figure 5.16: Characterisation of current HDFn dermal equivalent model cultured for up to 28 days in M106 with TGF-β and ascorbic acid supplementation: 0.5M HDFn cells were seeded onto the 12 well format of Alvetex® Scaffold to form a dermal equivalent tissue over 28 days before fixing in PFA. This current protocol results in the formation of a substantial dermal equivalent compartment within the inert scaffold, as shown by H&E staining, which is well populated with cells and endogenous extracellular matrix. Immunostaining for appropriate extracellular matrix proteins shows a homogenous distribution of proteins across the model, with multiple layers of fibroblasts at the upper and lower surfaces. Representative images shown. Samples courtesy of Nicole Darling. Scale bars: 100 µm

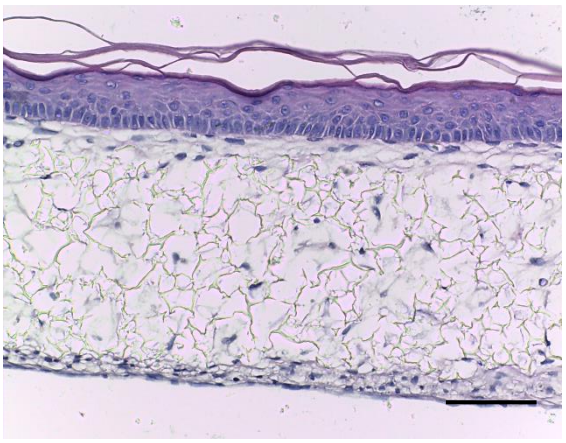


Figure 5.17: Full thickness human skin equivalent model formed on HDFn dermal equivalent: Dermal equivalent was cultured for 28 days as described before human epidermal keratinocytes were seeded onto the model. These were maintained in submerged culture before raising to the air liquid interface to allow for stratification of the epidermis, resulting in the formation of a fully differentiated skin equivalent model which recapitulates the structure of human skin. Image courtesy of Lydia Costello. Scale bar: 100 µm

As TERA2.cl.SP12 EBs will again be used to optimise a co-culture model, it is important to determine whether human dermal fibroblasts are viable and express the appropriate markers and ECM proteins when cultured in the TERA2.cl.SP12 media – DMEM supplemented with 10 % heat treated FBS. This media also offers a more cost effective option when undertaking large scale co-culture studies. As shown in Figure 5.18, HDFns were cultured in the two media types in 2D on coverslips to broadly assess morphology and protein expression. Fibroblasts have a highly similar typical morphology when grown in both media types, and show strong expression of the fibroblast cytoskeletal marker vimentin, as well as some low level expression of α-smooth muscle actin. In addition, the cells express the variety of ECM proteins as would be expected – Collagen I, III, IV and fibronectin – in both media types. In particular, immunostaining for collagen I and IV appears to show an increased expression in the production of these ECM proteins.

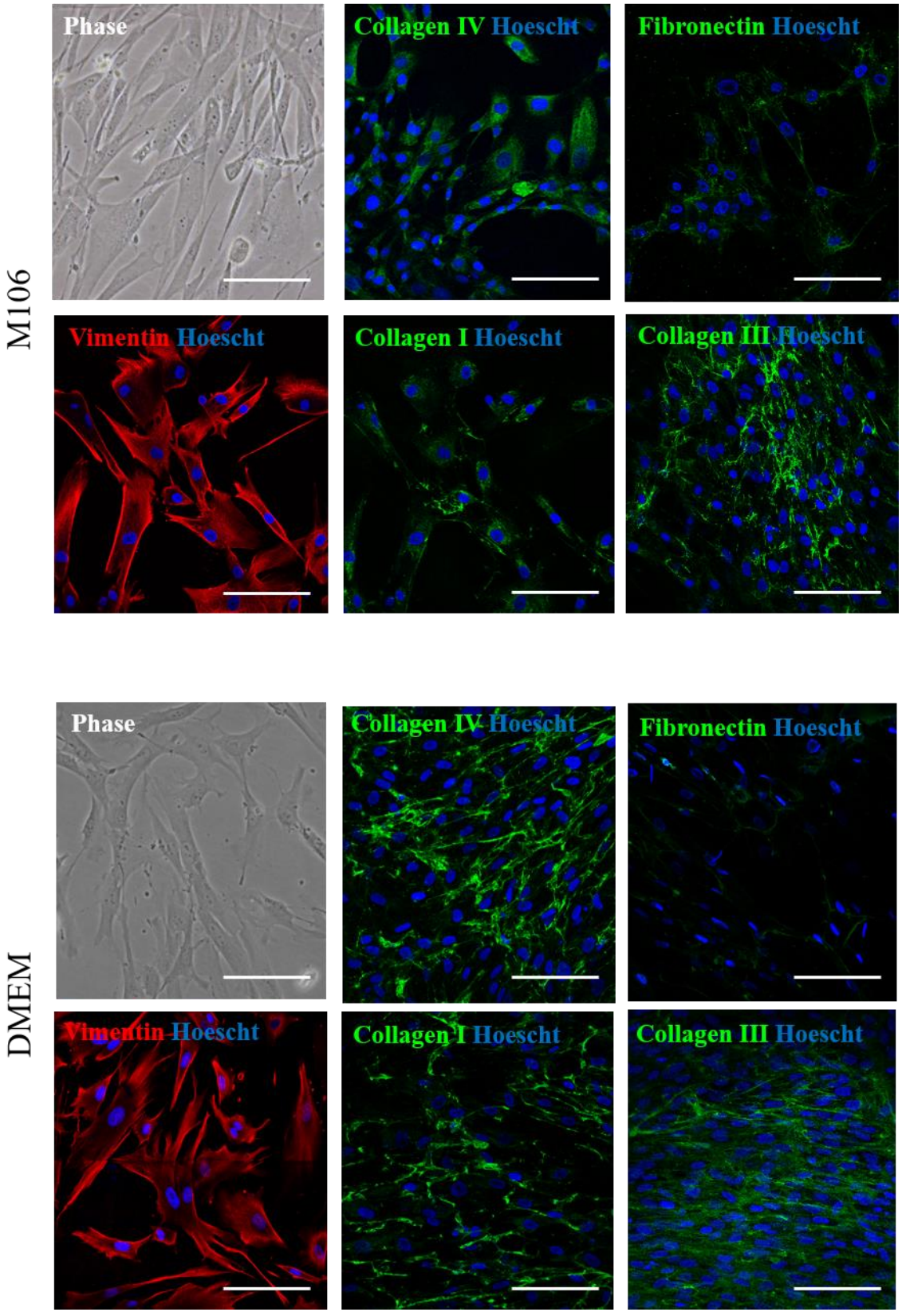
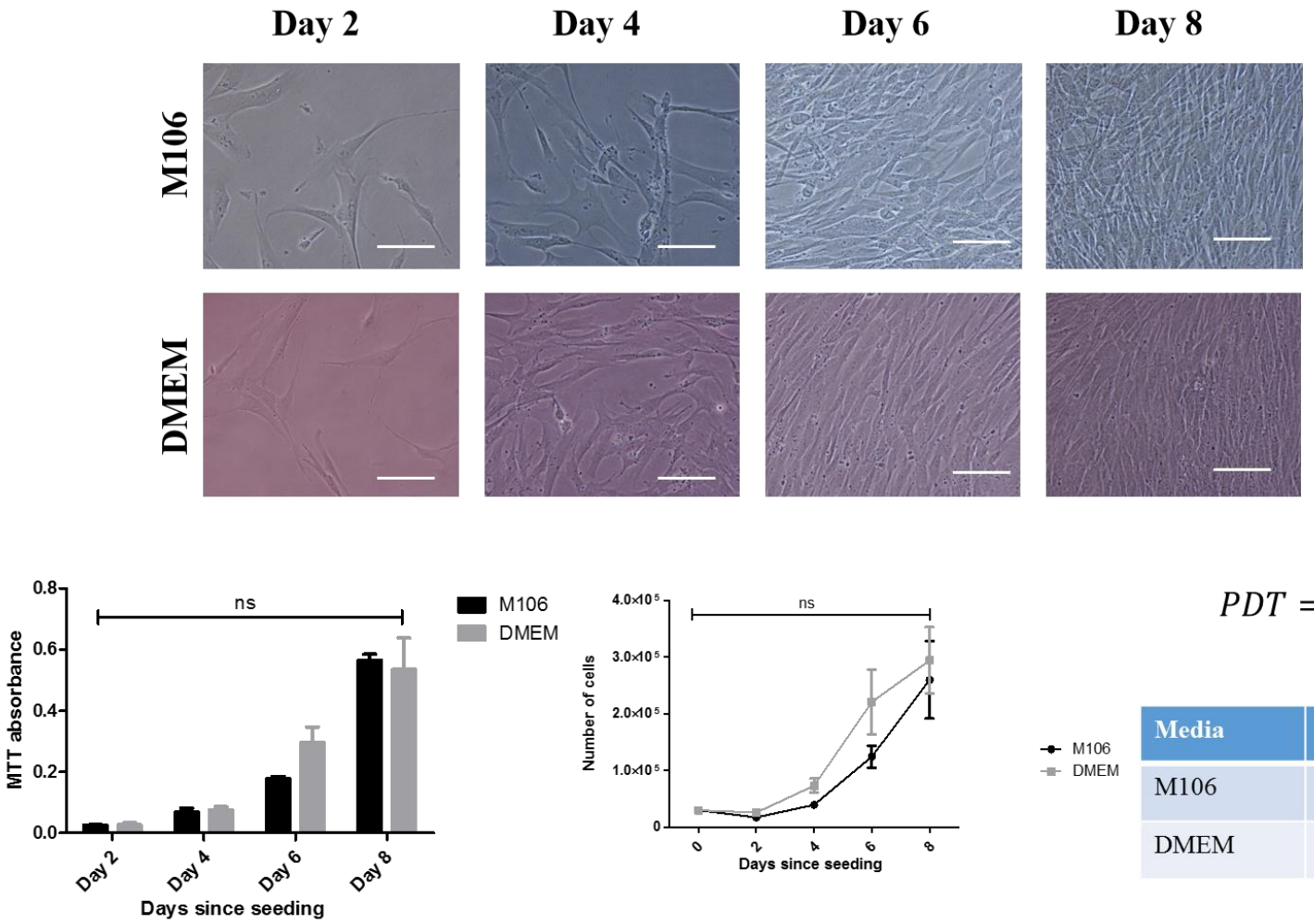


Figure 5.18: Characterisation of HDFn cells cultured in M106 and DMEM: HDFn cells were seeded onto PDL coated glass coverslips and cultured until around 70% confluent, before fixing in PFA at room temperature or methanol/acetone solution (50:50) at -20°C. Coverslips were stored in PBS at 4°C until immunocytochemistry was performed. HDFns show a typical fibroblast morphology, as well as synthesis of ECM proteins and expression of the appropriate fibroblast markers when cultured in both M106 and DMEM. Representative images shown. Scale bars: 100 µm and 50 µm

The growth rate and viability of HDFns was also assessed in both M106 and DMEM due to the nutritional differences in the two media types. Cells were seeded at a density of 30,000 per well in a 6 well plate and monitored over 8 days, with cell counts and MTT assay performed every 48 hours. Cell counts show a small increase in the number of fibroblasts when cultured in the DMEM, compared to those cultured in M106, with a reduction in the population doubling time (PDT) of around a day: the PDT for fibroblasts cultured in DMEM is around two days, whereas the PDT for those cultured in M106 is around three days. Cells seem to reach the same level of confluency after 8 days, regardless of the media used. There appear to be no differences in cell viability when the cells are cultured in the two media types, with MTT assays reflecting the differences in cell number which are also seen in the cell counts. Statistical analysis using a two way ANOVA showed no significant differences.



$$PDT = \frac{T \ \ln 2}{\ln \frac{Ne}{Nb}}$$

Media	PDT/days
M106	2.92
DMEM	2.06

Figure 5.19: HDFn growth in M106 and DMEM: HDFn cells were seeded into 6 well plates at a density of 30,000 cells per well on day 0, with either M106 media or DMEM. Cells were trypsinised, resuspended and counted on days 2, 4, 6 and 8, and the remaining wells were media changed. Phase contrast images show that there are few morphological differences evident in the cells in the two media types. Average cell number per well was calculated and plotted for each day cells were counted. The Population Doubling Time (PDT) was calculated using the equation shown. T = Incubation time (days), Xb = Cell number at the beginning of the incubation time, Xe = Cell number at the end of the incubation time. The PDT was calculated using the exponential growth phase of the graph. Results were found not to be statistically significant via two way ANOVA. Data represents mean ± SEM from 3 independent experiments (n=3). Representative images shown. Scale bar: 100 µm

As the HDFns grew successfully and show the same morphology and phenotype when cultured in DMEM compared to M106 yet with a shorter PDT, the use of DMEM to form dermal equivalents was employed. HDFns continue to be able to form a dermal equivalent when cultured in DMEM, supplemented in the same way as M106 with TGF-β and ascorbic acid. Cells were seeded onto the 6 well format of Alvetex® Scaffold in order to allow for seeding of EBs in the same size area as the previous version of the model, and to also allow for potential transfer of the model to other applications within the project, namely the perfusion system discussed later in this chapter. Due to the differences in media volume compared to the original dermal equivalent cultured in M106 in the 12 well format of Alvetex® Scaffold, the amount of fibroblast layering on the top of the insert is slightly reduced. However, the fibroblasts still form a continuous barrier across the scaffold, and express the appropriate ECM proteins, as seen in Figure 5.20. The decision was made to use HDFn DEs after 21 days in culture, due to the presence of a continuous fibroblast layer across the top of the insert and significant ECM deposition in the scaffold to support EB seeding.

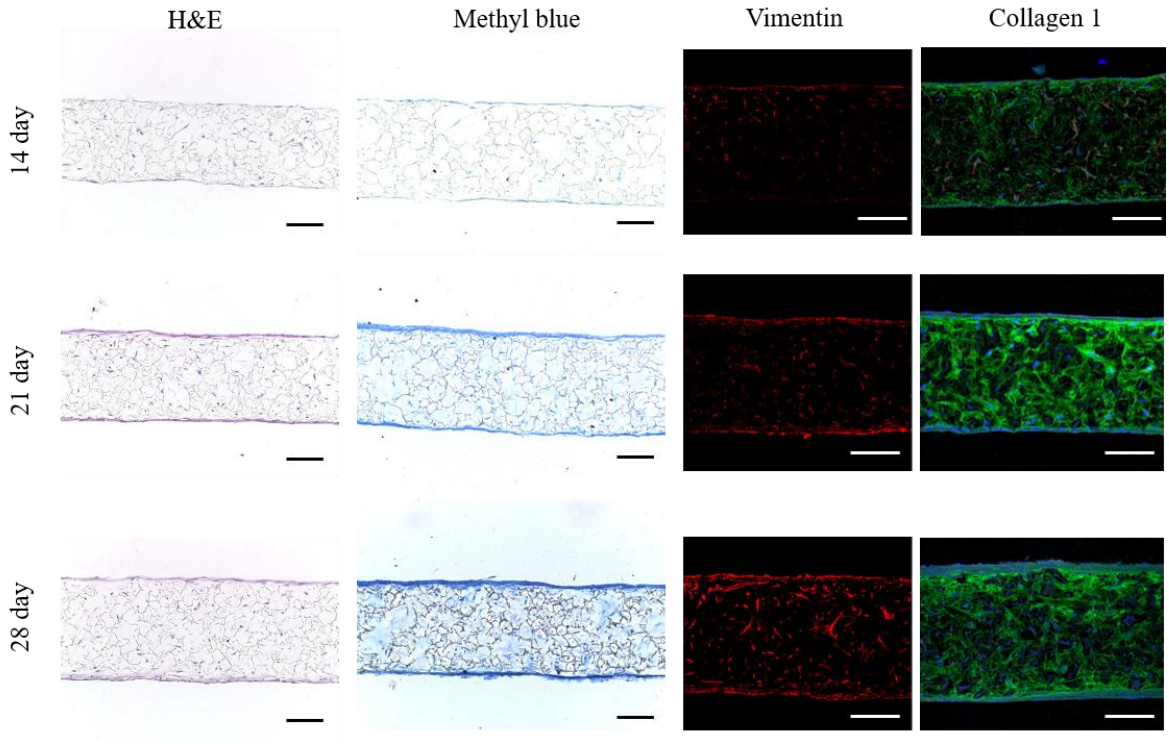


Figure 5.20: Characterisation of HDFn dermal equivalents cultured for up to 28 days in DMEM with TGF-β and ascorbic acid supplementation: The seeding density of the original DE model was scaled up appropriately for larger inserts, so that 1M HDFn cells were seeded onto the 6 well format of Alvetex® Scaffold at day 0 and allowed to form a dermal equivalent tissue over 28 days. By the 21 day time point, the cells have populated the scaffold and a substantial dermal compartment has formed, with a clear barrier. Again, the scaffold show a homogeneous distribution of HDFns throughout the insert, as well as homogenous production of ECM proteins, as highlighted by immunostaining for a variety of proteins. Representative images shown. Scale bars: 100 µm

5.5.1.2 Untreated and treated TERA2.cl.SP12 EBs can be successfully cultured on the human fibroblast dermal equivalent

TERA2.cl.SP12 EBs were cultured as previously described in suspension culture for 14 days without any morphogen treatments before seeding onto the surface of the 21 day HDFn dermal equivalent, with the histology and immunostaining data shown in Figure 5.21. EBs were maintained for a further 7 days on the dermal equivalents as tissue discs before analysis. The lack of EB infiltration into the scaffold reflects the integrity of the HDFn layer at the top of the dermal equivalent, and illustrates the successful formation of an entire tissue disc in the co-culture setting. This dissipates a potential issue in the form of loss of the tissue disc structure due to infiltration into the Alvetex® Scaffold, which was previously seen when the scaffolds were initially tested for suitability in the model in Chapter 2, and confirms the ability to undertake co-culture of stem cell EBs with the dermal equivalent. Differences in the tissue disc are noticeable; the formation is slightly looser, resembling a more mesenchymal structure, and there appears to be some organised epithelial like structures within the disc. A large area of the tissue disc expresses Class III β-tubulin, indicating the support of spontaneous neural differentiation with extensive Oct 4 expression also detected throughout the tissue disc, more so than was previously detected in the tissue discs cultured on the surface of Alvetex® Polaris.

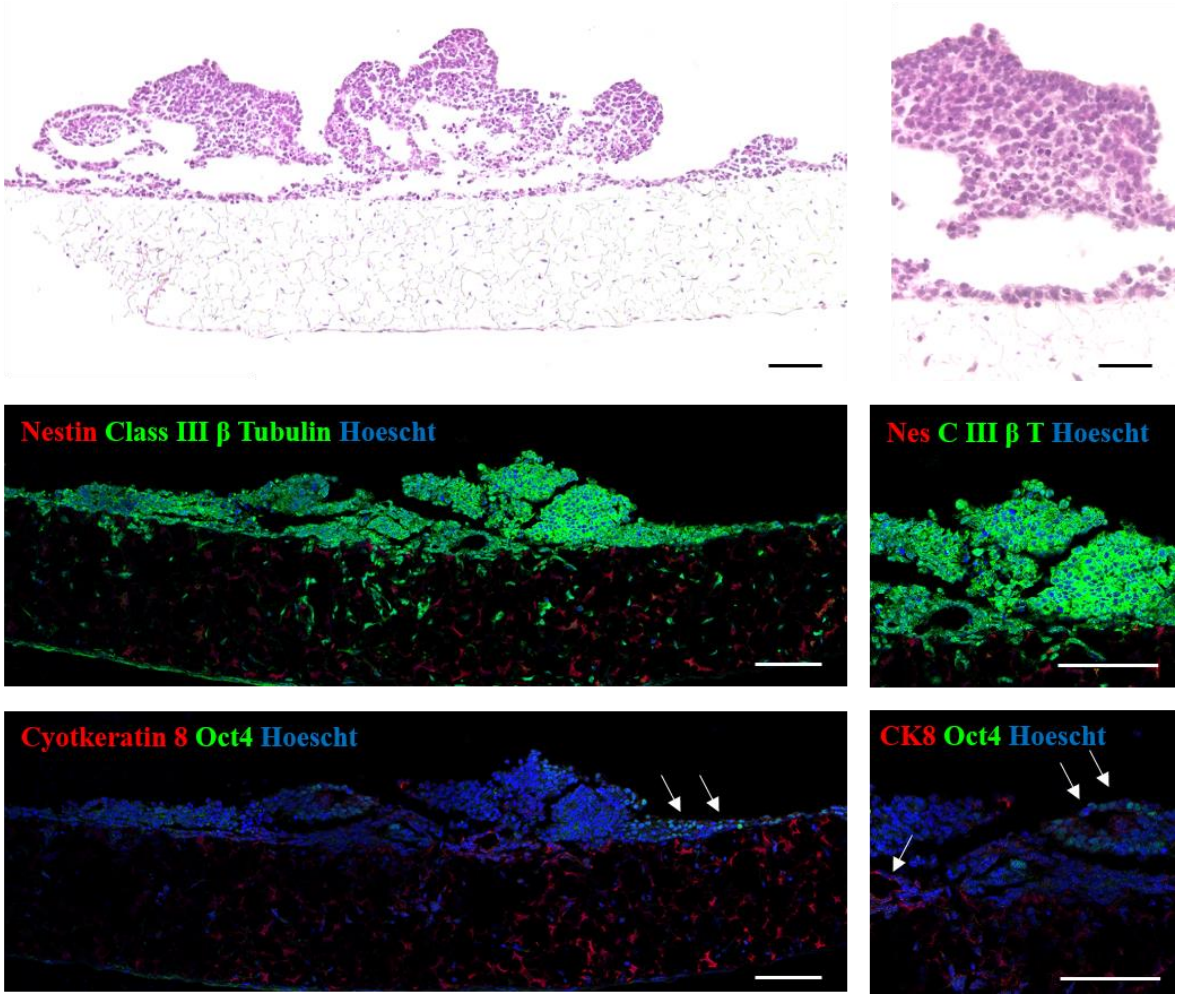


Figure 5.21: Characterisation of TERA2.cl.SP12 EBs cultured on HDFn dermal equivalents for 7 days: HDFn dermal equivalents were cultured for 21 days using the established protocol before TERA2.cl.SP12 EBs were seeded onto the surface of the dermal equivalent and cultured for a further 7 days. As can be seen in the H&E, the stem cell EBs do not infiltrate the scaffold when the fibroblasts are present, and are successfully maintained on the surface of the model. In addition to Class III β-tubulin positive areas, immunostaining shows the presence of small areas of Cytokeratin 8 and Oct 4 positive cells, as shown by the single and double arrows respectively. Oct 4 is particularly located where the EB has formed a monolayer along the surface of the dermal equivalent. Representative images shown. Scale bars: 100 µm and 25 µm

Interestingly Figure 5.22 shows that TERA2.cl.SP12 EBs treated with EC23, a highly potent morphogen and inducer of the neural phenotype, and subsequently cultured on the HDFn dermal equivalent also display a similar phenotype, in addition to confirming that differentiated EBs can successfully be cultured in the model. As would be expected, there are large areas of the tissue disc which stain positively for the neural maker Class III β-tubulin, and very little staining for the early neural marker Nestin. The areas which do not stain positively for Class III β-tubulin appear to express the pluripotency marker Oct 4, staining for which is fairly consistent throughout the tissue disc, and the intensity quite strong. This is also a phenotype which was not seen in the EC23 treated tissue disc cultured on the surface of Polaris, and would not be expected in an EB treated with EC23 due to the potency of the compound. The lack of cytokeratin 8 staining is consistent with the mature neural phenotype which is normally induced by the use of EC23.

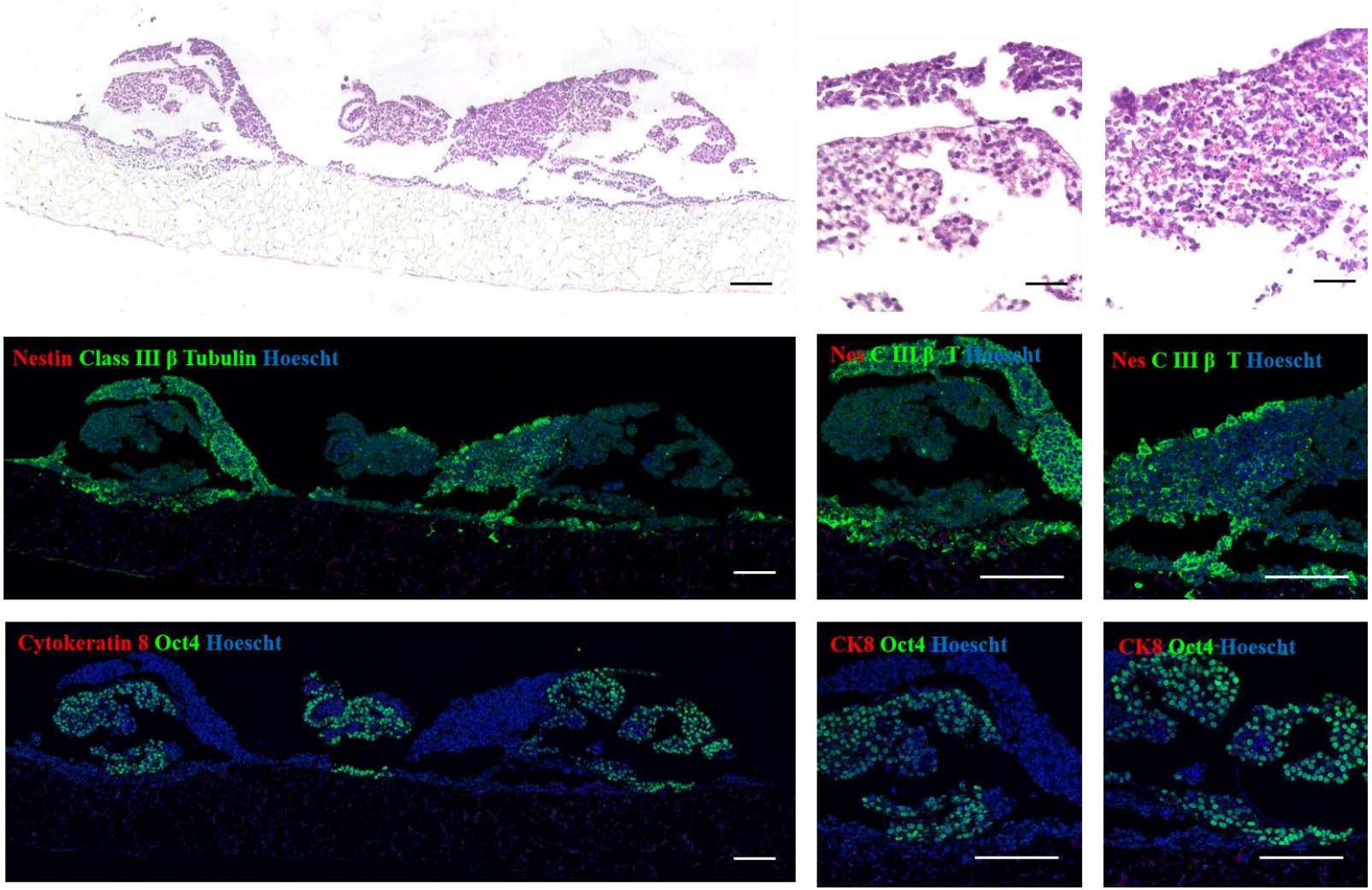


Figure 5.22: Characterisation of TERA2.cl.SP12 EBs treated with EC23 and cultured on HDFn dermal equivalents for 7 days: HDFn dermal equivalents were cultured for 21 days as previously described, with EC23 treated TERA.cl.2SP12 EBs seeded onto and cultured on the DE for a further 7 days. As previously seen, TERA2.cl.SP12 EBs do not infiltrate the scaffold when the fibroblasts are present, and are successfully maintained on the surface of the model, with the tissue disc showing a more heterogeneous morphology again. Immunostaining shows the maintenance of the mature neural phenotype through the Class III β-tubulin positive staining, as well as the presence of large areas of Oct 4 positive pluripotent cells, a feature not previously seen in EC23 treated tissue discs. No neural progenitors or epithelial differentiation is present, as there is no positive Nestin or cytokeratin 8 staining in the tissue disc respectively. Representative images shown. Scale bars: 100 µm and 25 µm

Figure 5.23 shows that TERA2.cl.SP12 EBs treated with the morphogen BMP-2 also show a similar phenotype to the TERA2.cl.SP12 EBs which were allowed to spontaneously differentiate when cultured on the surface of the HDFn dermal equivalent. Again, there are large areas which as Class III β-tubulin positive, as well as areas which stain positively for pluripotency marker Oct 4, as see in the EBs allowed to spontaneously differentiate. In fact, there is considerably more Oct 4 positive staining in the BMP-2 treated tissue discs than in the spontaneously differentiated tissue disc, although this is not as extensive as seen in the EC23 treated tissue disc. In addition, the EBs appear to have spread across the dermal equivalent surface more, forming a more flattened tissue disc structure. The Oct 4 positive areas of the tissue disc seem to correlate with the areas of the tissue disc which are in contact with the HDFn dermal equivalent. When compared to the BMP-2 treated EBs cultured on Alvetex® Polaris, there is a difference in the structure and morphology of the tissue disc, with an absence of the looser mesenchymal tissues, Nestin positive areas and cytokeratin 8 positive structures. There are some isolated cytokeratin 8 positive cells, indicating the presence of cells from that lineage. Combined with the evidence of marker expression seen in BMP-2 treated and untreated TERA2.cl.SP12 EBs which were cultured as tissue discs on the surface of the HDFn DE, this highly suggests that the presence of the dermal fibroblasts is resulting in an influence on the function i.e. pluripotency and differentiation of theTERA2.cl.SP12 tissue discs.

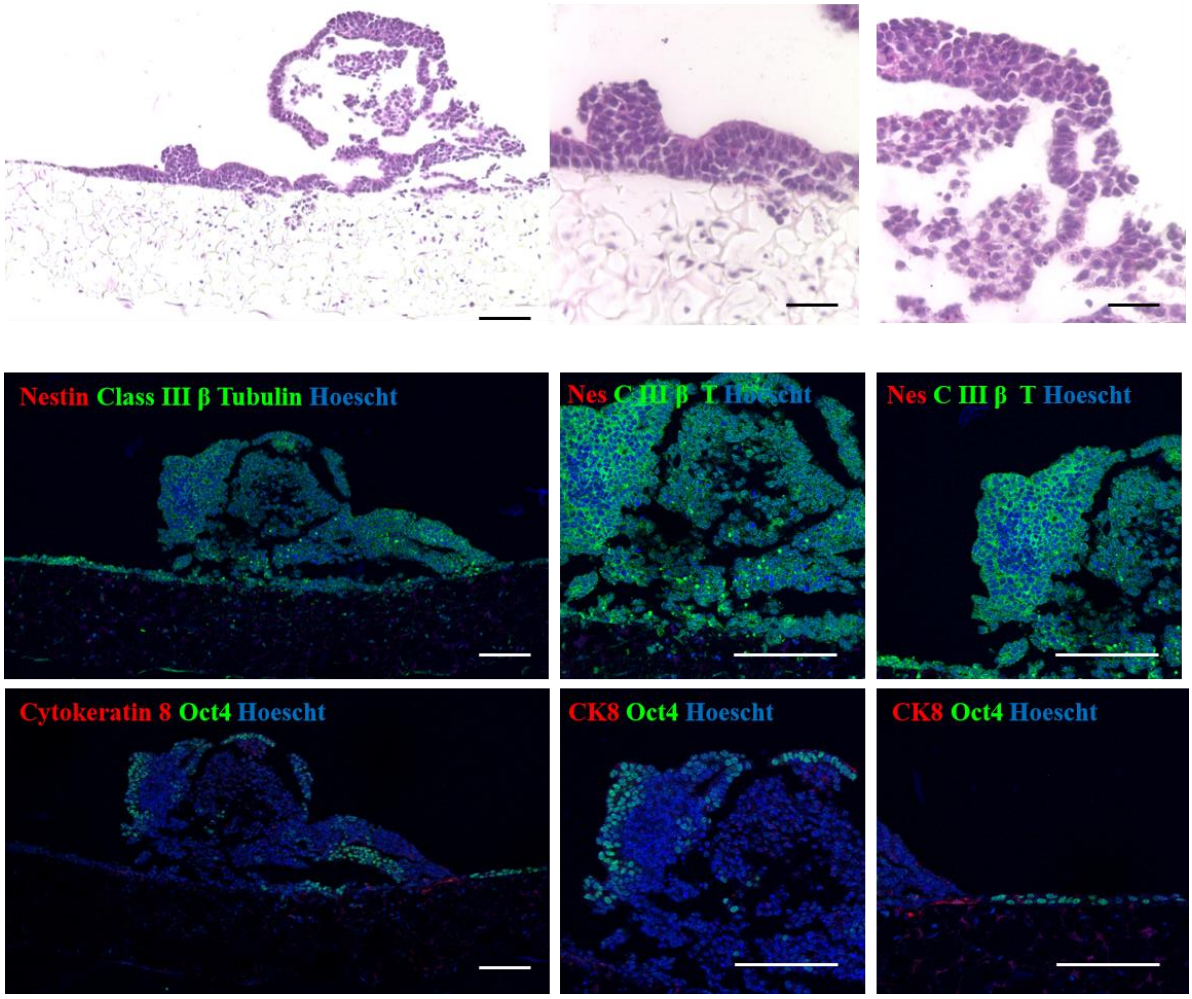


Figure 5.23: Characterisation of TERA2.cl.SP12 EBs treated with BMP-2 and cultured on HDFn dermal equivalents for 7 days: HDFn dermal equivalents were cultured for 21 days as previously described, with TERA2.cl.SP12 EBs seeded onto the DE at this time point and cultured for a further 7 days. As has been previously seen, EBs do not infiltrate the DE scaffold but are successfully maintained on the surface of the DE. Immunostaining shows maintenance of Oct 4 positive pluripotent areas within the EB, as well as positive staining for the neuronal marker Class III β-tubulin. Small areas of staining for the pan-epithelial marker CK8 can also be seen. Representative images shown. Scale bars: 100 µm and 25 µm

5.5.2 Creation and use of more relevant dermal fibroblast model using SCID mouse dermal fibroblasts

The HDFn dermal equivalent model is robust and allows for the successful co-culture of fibroblasts with stem cell EBs. While this is certainly useful for human stem cell models due to the use of a species matched fibroblast population, this is not necessarily representative of the teratoma assay. As the teratoma assay currently represents the most complex differentiation which can be achieved using pluripotent stem cells, it would be pertinent to attempt to recapitulate the microenvironmental conditions of the teratoma assay more closely in the *in vitro* setting, in order to recreate that complexity in a more reproducible and controllable manner.

5.5.2.1 Dermal fibroblast population isolated from a severe combined immunodeficient mouse display a fibroblast phenotype

As previously described in the Materials and Methods in Chapter 2, a dermal explant was taken from the flank of a severe combined immunodeficient (SCID) mouse, cut into small pieces and fibroblasts encouraged to grow out of the tissue pieces, as can be seen in Figure 5.24. Phase contrast and H&E stains show typical fibroblast morphology, with Masson's Trichrome indicating the synthesis of ECM proteins. Cells were immunostained to confirm the fibroblast phenotype; a mixed population of fibroblasts and myofibroblasts was detected, with cells strongly expressing the fibroblast marker vimentin, and a selection of cells also expressing the cytoskeletal protein α smooth muscle actin. Cells also showed secretion of appropriate ECM proteins, including Collagens I, III and IV and fibronectin.

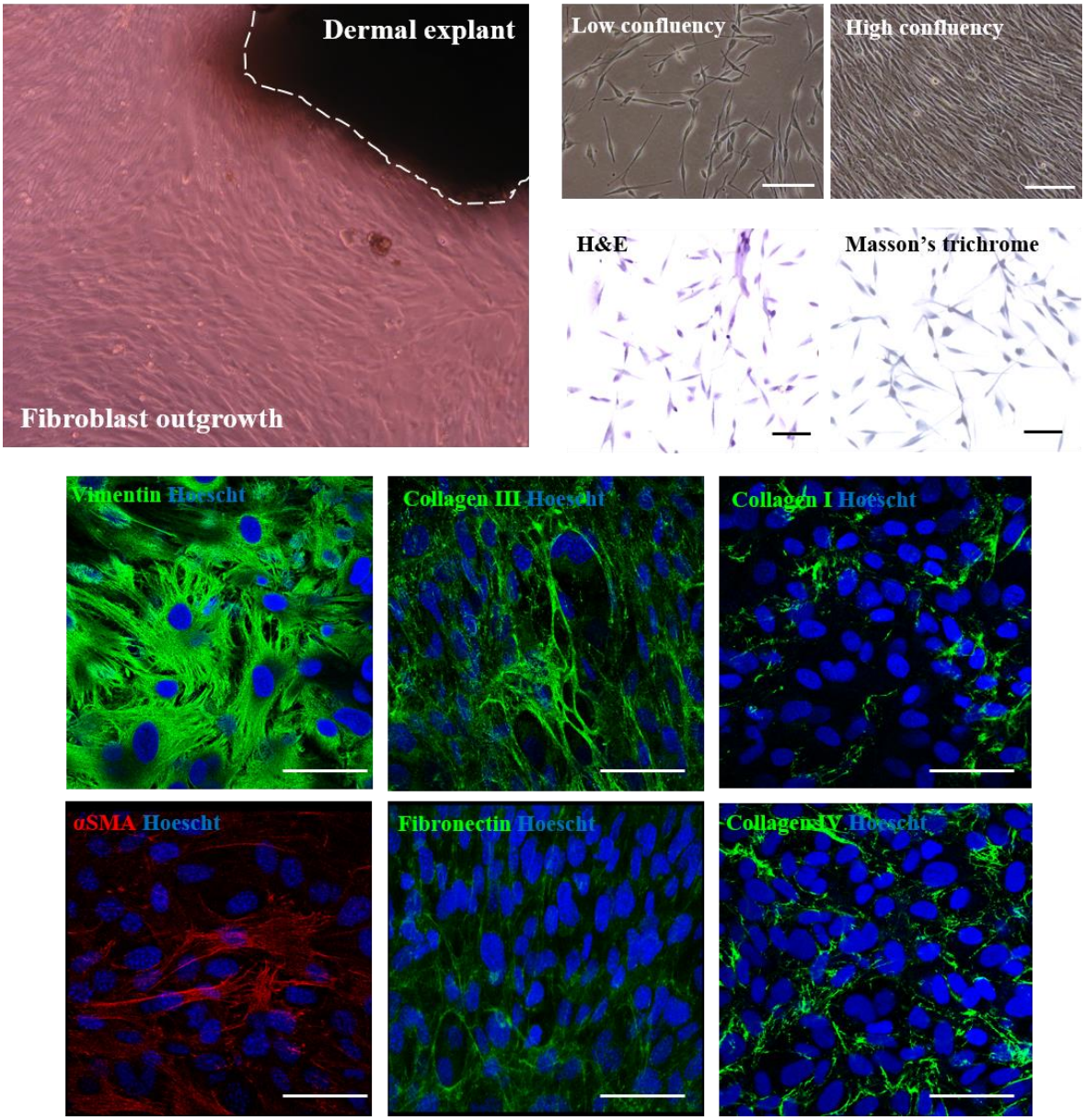


Figure 5.24: Isolation and characterisation of SCID Mouse dermal fibroblast cell line: Dermal explants were removed from the trunk of a SCID mouse, cut into pieces of around 0.5mm^2, and placed onto the surface of a 6 well plate which had been scored with a sterile scalpel to aid attachment. Dermal explants were allowed to attach to the plate for a couple of hours, before topping up with isolation media. After the first 2 passages, media was swapped to a maintenance medium. Phase contrast imaging and staining for appropriate extracellular matrix markers and cellular markers confirms the fibroblast identity of the cellular population, and the ability to synthesise ECM proteins. Scale bar: 100 µm, 50 µm

5.5.2.2 Supplementation of media with TGF-β and ascorbic acid results in the formation of a SCID moue fibroblast dermal equivalent

In the same way that the HDFn dermal equivalent is created, Alvetex® Scaffold was again used as a basis to create the novel SCID dermal equivalent. Initially, cells were seeded at the same ratio as the HDFn dermal equivalent, with 1 million cells seeded per 6 well size format of Alvetex® Scaffold (N.B. this is again a scaling up of the original HDFn dermal equivalent model to facilitate transfer from the previous format use 6 well inserts, particularly the seeding density, and potentially to other formats) and the scaffold cultured in the normal SCID fibroblast maintenance medium. H&E images in Figure 5.25 show poor proliferation of the fibroblasts over a 28 day culture period in the scaffold, and no evidence of layering at the top and bottom of the scaffold. Staining for vimentin and α smooth muscle actin confirms this, with very few cells visible within the scaffold or at the surfaces. ECM protein production is also poor, with very little evidence of endogenous collagen deposition within the scaffold.

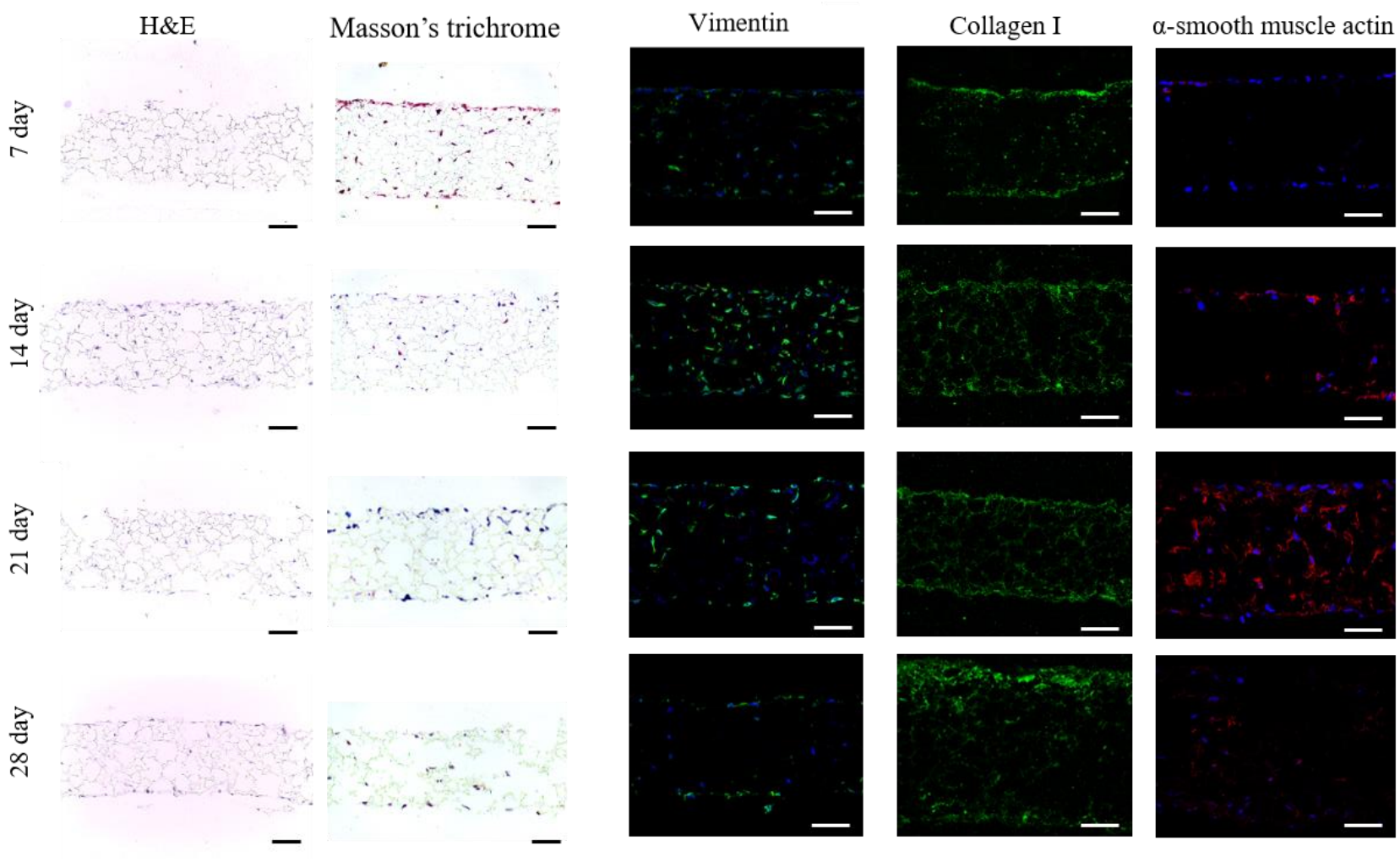


Figure 5.25: Characterisation of SCID Mouse Fibroblast dermal equivalents cultured for up to 28 days in DMEM: Using the previously adopted dermal equivalent seeding protocol, 1M SCID fibroblasts were seeded onto the 6 well format of Alvetex® Scaffold at day 0 and to form a dermal equivalent tissue over 28 days. H&E shows that infiltration of the scaffold by the cells is slow, with few cells visible within the voids, and no evidence of the formation of a barrier. Staining for various ECM proteins and markers shows some evidence of matrix deposition, as well as expression of fibroblast appropriate markers. Representative images shown. Scale bar: 100 µm

Due to the successful growth of the HDFn dermal equivalent through the supplementation of the culture medium with TGF-β and ascorbic acid, the same concentrations of these were added to the SCID maintenance medium during the formation of the dermal equivalent, in an attempt to improve the proliferation of the fibroblasts and their secretion of endogenous ECM. There is a clear difference in the cellular structures which form, which an increased population of the scaffold over increasing time, and some evidence of fibroblast layering at the top and bottom of the scaffold, as seen in the H&E and Masson's trichrome images in Figure 5.26. Vimentin and α smooth muscle actin staining further support this observation, with the cell populations spread throughout the scaffold, and localised in an organised manner at the top and bottom of the scaffold. While the cells do not produce as thick and robust a layer as is seen using the HDFn cells in both the 12 well and 6 well formats of the scaffold, the layering should still be sufficient to support tissue disc formation and limit major infiltration, which is a potential issue when using the Alvetex® Scaffold format. Endogenous ECM production is also increased, as shown by the immunostaining for various proteins including collagens and fibronectin.

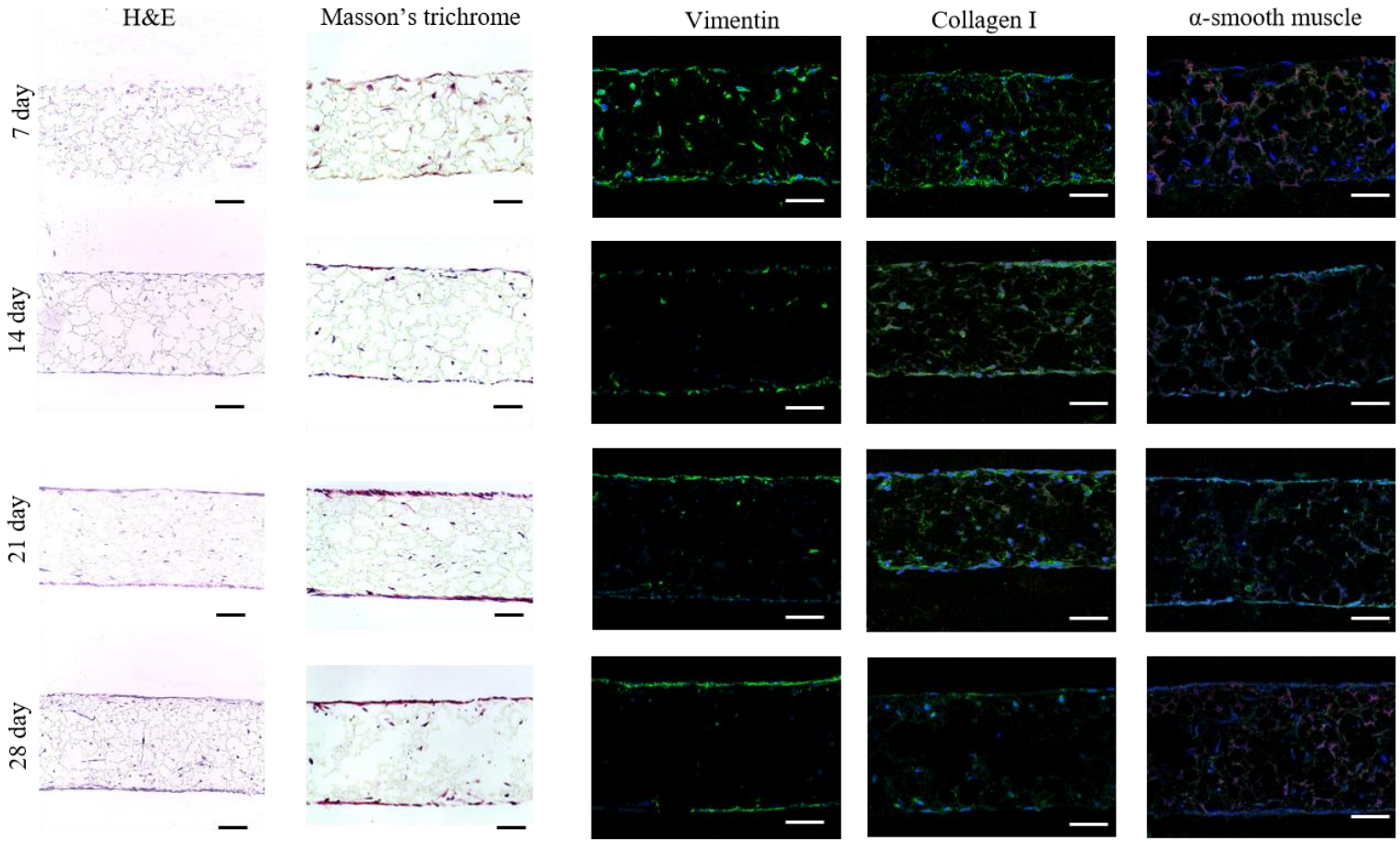


Figure 5.26: Characterisation of SCID Mouse Fibroblast dermal equivalents cultured for up to 28 days in DMEM with ascorbic acid and TGF-β supplementation: Using the previously adopted dermal equivalent seeding protocol and media supplementation of 100 µg/mL ascorbic acid and 5 ng/ml TGF-β, 1M SCID fibroblasts were seeded onto the 6 well format of Alvetex® Scaffold at day 0 and to form a dermal equivalent tissue over 28 days. H&E shows that infiltration of the scaffold by the cells is faster and more complete, with cells visible within the voids, and evidence of the formation of a barrier by 14 days. Staining for various ECM proteins and markers shows evidence of matrix deposition over the culture period, as well as expression of fibroblast appropriate markers. Representative images shown. Scale bar = 100 µm

5.5.2.3 TERA2.cl.SP12 EBs, both untreated and treated, can be successfully co-cultured on the SCID dermal equivalent, displaying an altered phenotype.

Following the successful demonstration of the co-culture of TERA2.cl.SP12 tissue discs with the HDFn dermal equivalent, and the creation of a relevant SCID mouse dermal equivalent, treated and untreated TERA2.cl.SP12 tissues discs were cultured on the surface of the novel SCID dermal equivalent in order to better mimic the *in vivo* environment.

Initially tested with EBs allowed to spontaneously differentiate, the co-culture of the tissue disc is again possible, with no infiltration into the Alvetex® Scaffold, as can be seen in Figure 5.27. The tissue disc is small in size, and shows little histological heterogeneity, although the assessment of the cell phenotype highlights some differences. Small amounts of mature neural differentiation can be observed in the positive Class III β-tubulin staining, and little in the way of neural progenitor marker Nestin. Cytokeratin 8 positive epithelial structures are also not present, although weak positive staining for the pluripotency marker Oct 4 can be detected in the tissue disc. This is weaker and less widespread throughout the tissue disc compared to those cultured on the HDFn model.

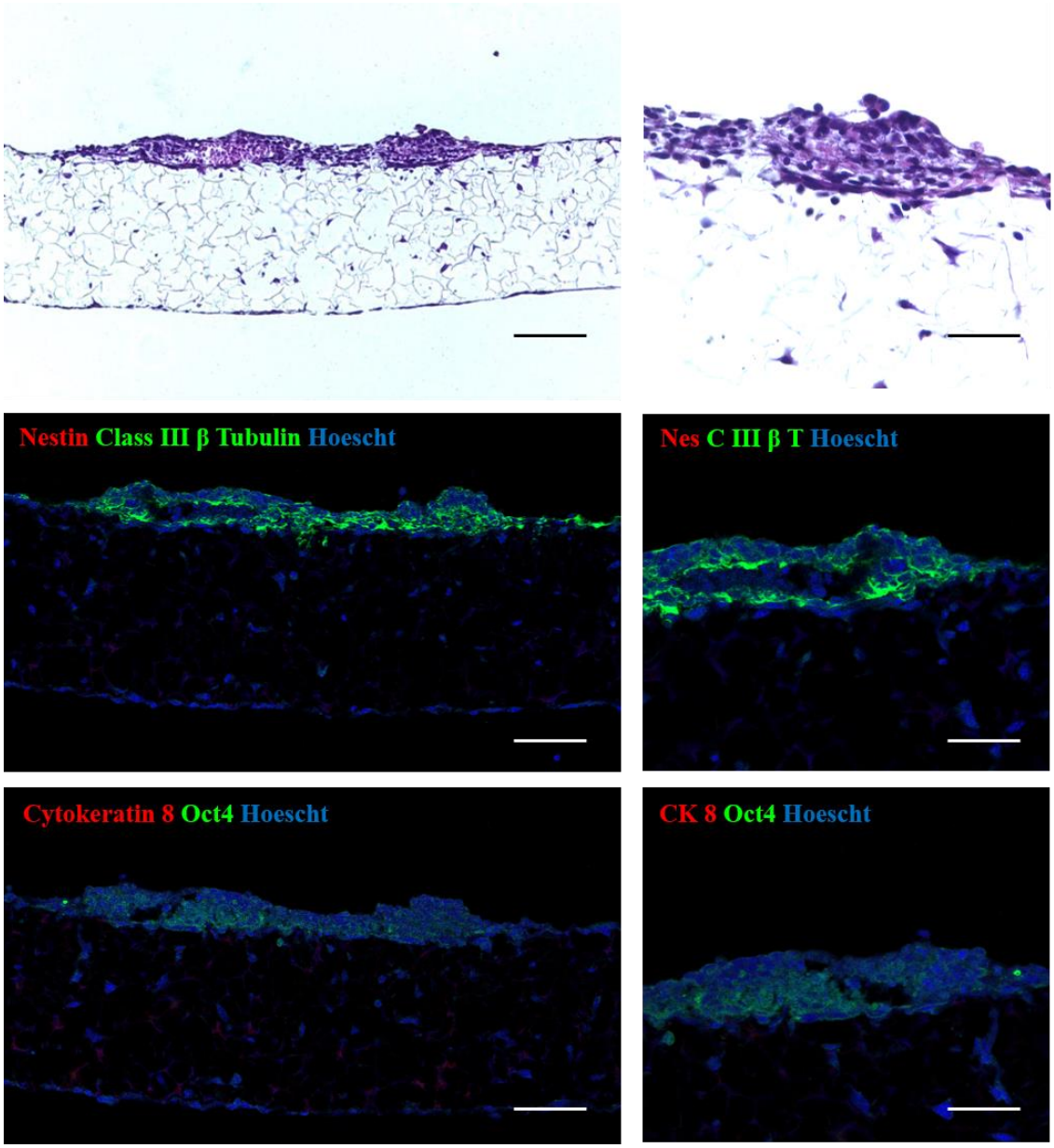


Figure 5.27: Characterisation of T2SP12 EBs cultured on SCID dermal equivalents for 7 days: SCID dermal equivalents were cultured for using the optimised protocol to allow for the formation of the dermal equivalent, including a sufficient barrier and extracellular matrix component. Once sufficiently formed, untreated T2SP12 EBs were seeded onto the surface of the dermal equivalent, and cultured for a further 7 days. As can be seen in the H&E, TERA2.cl.SP12EBs successfully form tissue discs on the surface of the SCID dermal equivalent. The tissue disc shows positive Class III β-tubulin staining, as shown by immunostaining. This area show very weak positive staining for pluripotency marker Oct 4. Representative images shown. Scale bar: 100 µm and 25 µm

The histology in Figure 5.28 of the EC23 treated tissue disc which was cultured on the SCID dermal equivalent is more heterogeneous in nature, with a noticeable area that is unlike the rest of the tissue disc structure. Previously, EC23 tissue discs have been shown to be highly homogenous due to the potent action of the compound. Immunostaining to ascertain the identity of the cells within the tissue disc highlights that most of the tissue disc is relatively strongly positive for the mature neural marker Class III β-tubulin as would be expected using this morphogen. However, the heterogeneous area within the tissue disc shows a negative phenotype for Class III β-tubulin staining, instead showing weakly positive staining for the pluripotency marker Oct 4. There are no epithelial structures within this tissue disc, as there is no positive cytokeratin 8 staining as would be expected and has been previously seen in EC23 treated EBs and tissue discs.

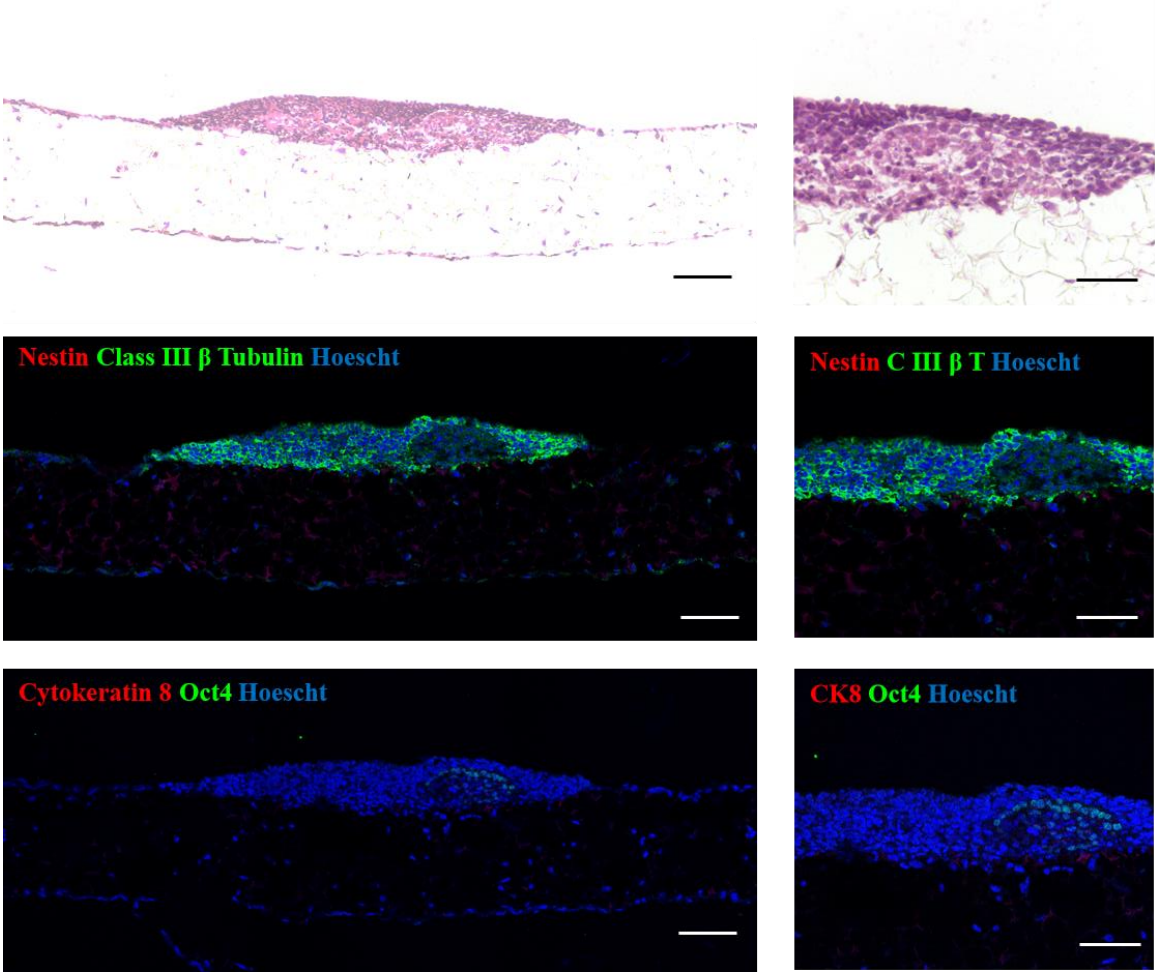


Figure 5.28: Characterisation of T2SP12 EBs treated with EC23 and cultured on SCID dermal equivalents for 7 days: SCID dermal equivalents were cultured for using the optimised protocol to allow for the formation of the dermal equivalent, including a sufficient barrier and extracellular matrix component. Once sufficiently formed, EC23 treated T2SP12 EBs were seeded onto the surface of the dermal equivalent, and cultured for a further 7 days. As can be seen in the H&E, EC23 treated EBs successfully form tissue discs on the surface of the SCID dermal equivalent. Higher magnification images show heterogeneous areas within the tissue disc, which prove to be Class III β-tubulin negative, as shown by immunostaining. This area show weak positive staining for pluripotency marker Oct 4. Representative images shown. Scale bars: 100 µm and 25 µm

EBs which were treated with BMP-2 were also tested in the SCID fibroblast co-culture system. Figure 5.29 shows that the histology of these tissue discs also differs when compared to BMP-2 treated EBs cultured on the surface of Alvetex® Polaris. Tissue discs show a reduced heterogeneity in their morphology, although the loose mesenchymal like structure of the EBs can still be detected in the overall tissue disc. Immunostaining of the tissue disc highlights weak Class III β-tubulin staining within the tissue disc, and a lack of neural progenitors, with no positive staining for Nestin. Cytokeratin 8 staining is present and prevalent within the BMP-2 treated tissue disc, highlighting cells of epithelial lineage rather than structures of this nature. Areas of Oct 4 positive cells can also be detected within the tissue disc throughout the overall structure, although there are much less than identified in the tissue discs culture on the HDFn fibroblasts.

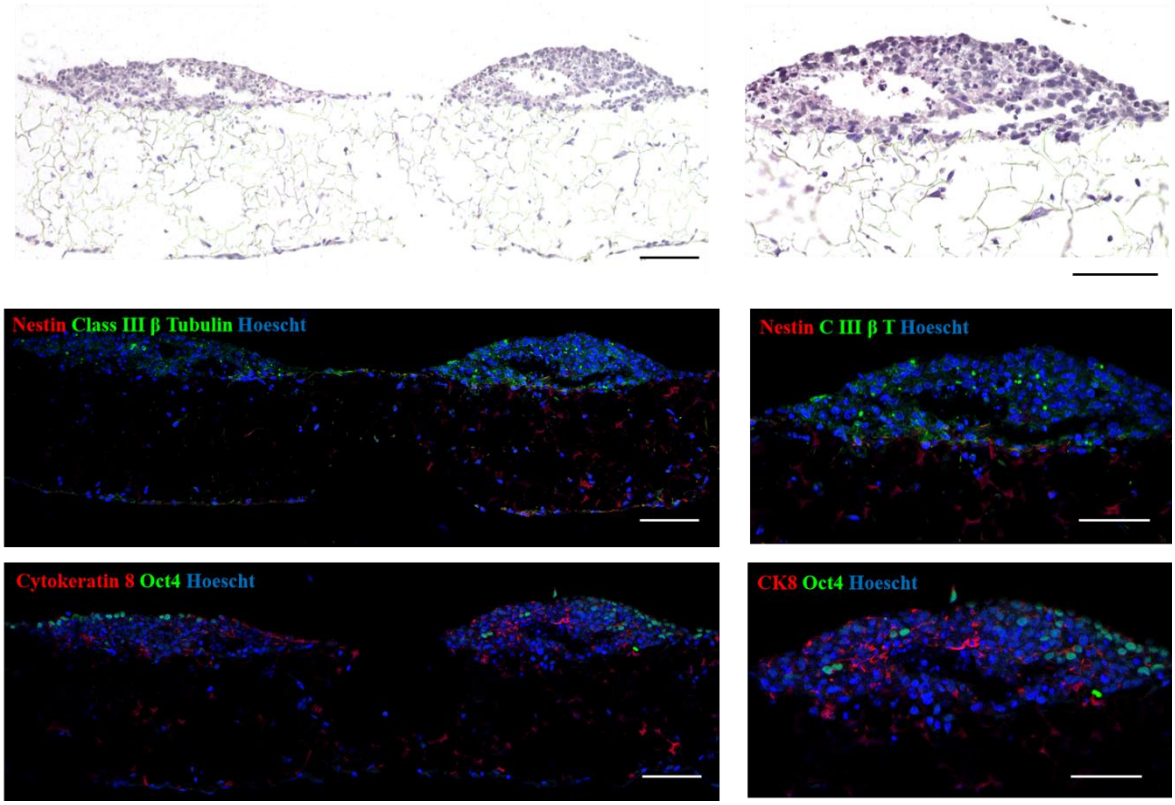


Figure 5.29: Characterisation of T2SP12 EBs treated with BMP-2 and cultured on SCID dermal equivalents for 7 days: SCID dermal equivalents were cultured for using the optimised protocol to allow for the formation of the dermal equivalent, including a sufficient barrier and extracellular matrix component. Once sufficiently formed, BMP-2 treated T2SP12 EBs were seeded onto the surface of the dermal equivalent, and cultured for a further 7 days. H&E staining shows the successful formation of tissue discs and that the diverse morphology of the tissue discs is reduced, showing a loose yet more homogenous structure. Immunostaining confirms the heterogeneity, with some small intermittent areas of Class III β-tubulin as well as cytokeratin 8 staining, indicative of epithelial differentiation. Oct 4 positive areas can also be detected, indicating the presence of undifferentiated embryonal carcinoma cells. Representative images shown. Scale bars: 100 µm and 50 µm

5.5.2.4 Culture of tissue discs on dermal equivalents

The experiments conducted in the first part of this Chapter have revealed a number of interesting results regarding the culture of TERA2.cl.SP12 tissue discs, both treated and untreated, on dermal equivalent compartments.

Table 5.1: Summary of results from co-culture studies

Culture conditions	Results
Untreated TERA2.cl.SP12 tissue discs on HDFn dermal equivalents	Tissue discs could be successfully cultured on the dermal equivalent, demonstrating proof of concept. Some smaller changes to tissue disc structure and phenotype recorded.
EC23 and BMP-2 treated TERA2.cl.SP12 tissue discs on HDFn dermal equivalents	Treated tissue discs can also be successfully cultured on the surface of the dermal equivalent. Significant differences in tissue disc morphology and phenotype are observed, with increased Oct 4 positive populations.
Untreated TERA2.cl.SP12 tissue discs on SCID dermal equivalents	TERA2.cl.SP12 tissue discs can also be cultured on the surface of SCID fibroblast dermal equivalents. Tissue discs show small differences in morphology.
EC23 and BMP-2 treated TERA2.cl.SP12 tissue discs on SCID dermal equivalents	Treated TERA2.cl.SP12 tissue discs can also be maintained on the surface of SCID fibroblast dermal equivalents. Again, significant differences in tissue disc morphology and phenotype are noted, with increased expression of Oct 4 detected within the tissue discs.

In both cases, significant differences in the phenotype of the treated tissue discs was observed, with an increased expression of Oct 4, indicating the presence of an undifferentiated embryonal carcinoma population as a result of the co-culture experiments. The incorporation of physiological conditions in this instance has resulted in some perceptible differences in tissue disc morphology.

5.5.3 The introduction of perfusion to tissue disc culture and technical optimisation

The incorporation of co-culture in the previous part of this Chapter highlighted the impact of increasing the physiological relevance of *in vitro* culture systems; significant differences were observed in the morphology and phenotype of tissue discs in the co-culture setting. However, there are a variety of other microenvironmental cues which impact on cellular structure and function, with perfusion by vasculature noted as particularly important due to providing improved cellular support. Using the novel perfusion system detailed in the Materials and Methods in this Chapter, media perfusion will also be introduced to the model originally developed in Chapter 3.

The novel perfusion system consists of a number of simple pieces of equipment which can be adapted for any number of uses. As shown in Figure 5.8 in the Materials and Method of this Chapter, the entire system is based on a perfusion device composed of two identical pieces of polystyrene. The disc of Alvetex® is placed in between the two pieces, which are clipped together. In this project, the device is to be placed in a glass vessel on a holder, which will direct the flow of the media. To facilitate fluid flow, the vessel will be placed on a magnetic stirrer, with a magnetic stir bar beneath the holder. There were a number of potential options for the device holder, including funnel and table based designs, which required analysis in order to achieve optimum fluid flow.

5.5.3.1 Assessment of fluid flow, turbulence and velocity of anticlockwise flow funnel design reveals impaired fluid recirculation

Two funnel style designs were initially trialled to hold the device, the first of which had slots which directed the fluid flow in an anticlockwise direction. The addition of crystal violet dye to the system with the anticlockwise funnel allowed for the visualisation of the fluid distribution within the system over time. 200 µL of crystal violet dye was added to the glass vessel while on a magnetic stir point, and the perfusion system imaged every 2 seconds for the 30 seconds after the addition of the dye, and again at 60 seconds. The images in Figure 3.30 show that the dye is drawn downwards in a central vortex of fluid through the centre of the funnel, and is recirculated through the slots in the funnel after around 12 seconds. After around 20 seconds, there is full redistribution of the dye throughout the vessel. By 60 seconds, the initial fluid vortex is almost not visible.

The fluid movement in the vessel was assessed more quantitatively by analysing the images taken of the crystal violet dye circulation. Images were of the vessel were split into three sections and the intensity of the dye colour in these was measured, then mean calculated and then plotted as White Intensity against time to attempt to more quantitatively assess fluid flow. All values begin at the highest value of 150 as the dye has not yet been added to the vessel. The graphs in Figure 3.30 show an initial drop in the White Intensity in the top section as would be expected, followed by a steady drop in the white intensity if the middle section as the fluid is pulled down into the funnel. A final, much slower drop in White intensity is seen at the base of the vessel. The White Intensity of the base

of the vessel does not drop as low as that of the other sections due to the fact that only half of the dye recirculation can be visualised in the image due to the opacity of the funnel.

Particle image velocimetry (PIV) analysis of the fluid recirculation was conducted to assess both fluid velocity and turbulence within the system. PIV is used commonly to visualise the direction of fluid flow in a system, as well as other properties such as velocity and turbulence. The plane of measurement was selected as approximately the plane at which the Alvetex® would be positioned within the perfusion device, in order to assess any potential detrimental effects on the cellular material as a result of the system design. Analysis shows a low turbulence overall across the selected plane, with a higher turbulence in the centre where the fluid is drawn down into the funnel, as would be expected. Fluid velocity measurements are of a similar pattern, with the highest fluid velocity recorded in the centre of the plane of measurement, correlating with the centre of the funnel where the fluid is drawn through. In this system, the fluid velocity shows a ring like pattern, where there is a circular area of high velocity, with an area of much mower velocity within.

Repeating the fluid distribution analysis with the crystal violet dye, but with the Alvetex® holder in place, provides a more realistic representation of the fluid flow within the final working system. In a similar manner to the analysis conducted previously, 200 µL of crystal violet dye was added to the vessel and photographs taken every 2 seconds for a total of 60 seconds in order to analyse the fluid distribution within the system. Imaging reveals that although the dye is again drawn through the centre of the funnel, as can be seen in Figure 5.31, full distribution is impaired by the actual perfusion device. Between 10 and 20 seconds, it becomes clear that the majority of the dye remains within the top third of the vessel, unable to be distributed throughout the system. This phenomenon persists from between 10 and 20 seconds until the end of the imaging time course at 60 seconds.

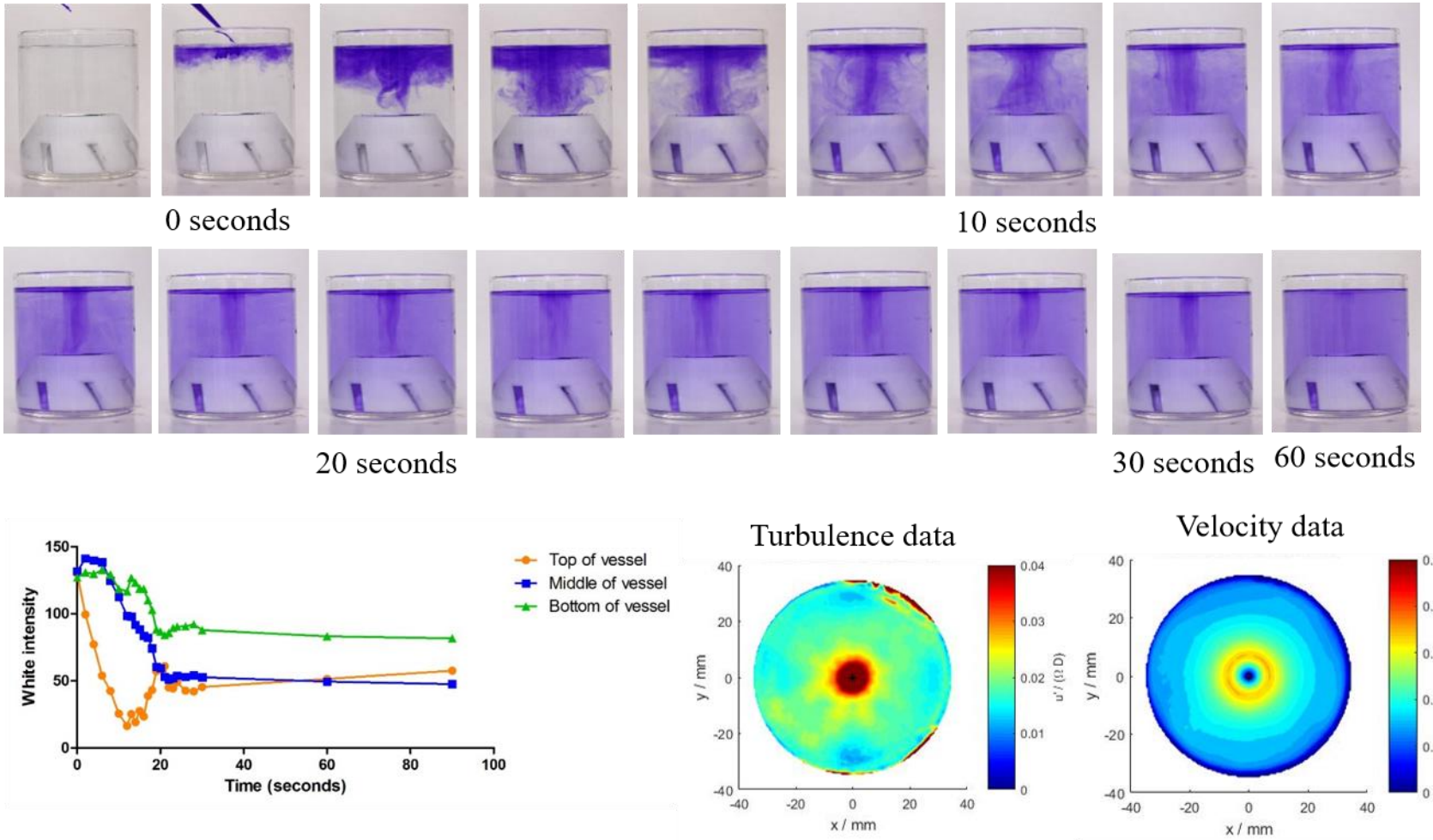


Figure 5.30: Fluid flow analysis data for anticlockwise fluid flow cone design: 200 µl of 0.1 % crystal violet was added to the vessel at the 0 seconds time point, and its distribution monitored over 90 seconds. Images were taken every 2 seconds for the first 30 seconds, and at 60 and 90 seconds time points. A large central vortex of fluid is initially visible, and dye is already recirculating through the system after 20 seconds. By 60 seconds, the dye is well distributed within the vessel. Turbulence data shows a small concentrated area of turbulence at the centre of the cone, where the fluid is drawn in. The velocity of the fluid within the vessel is relatively constant. All analyses conducted at 125 rpm.

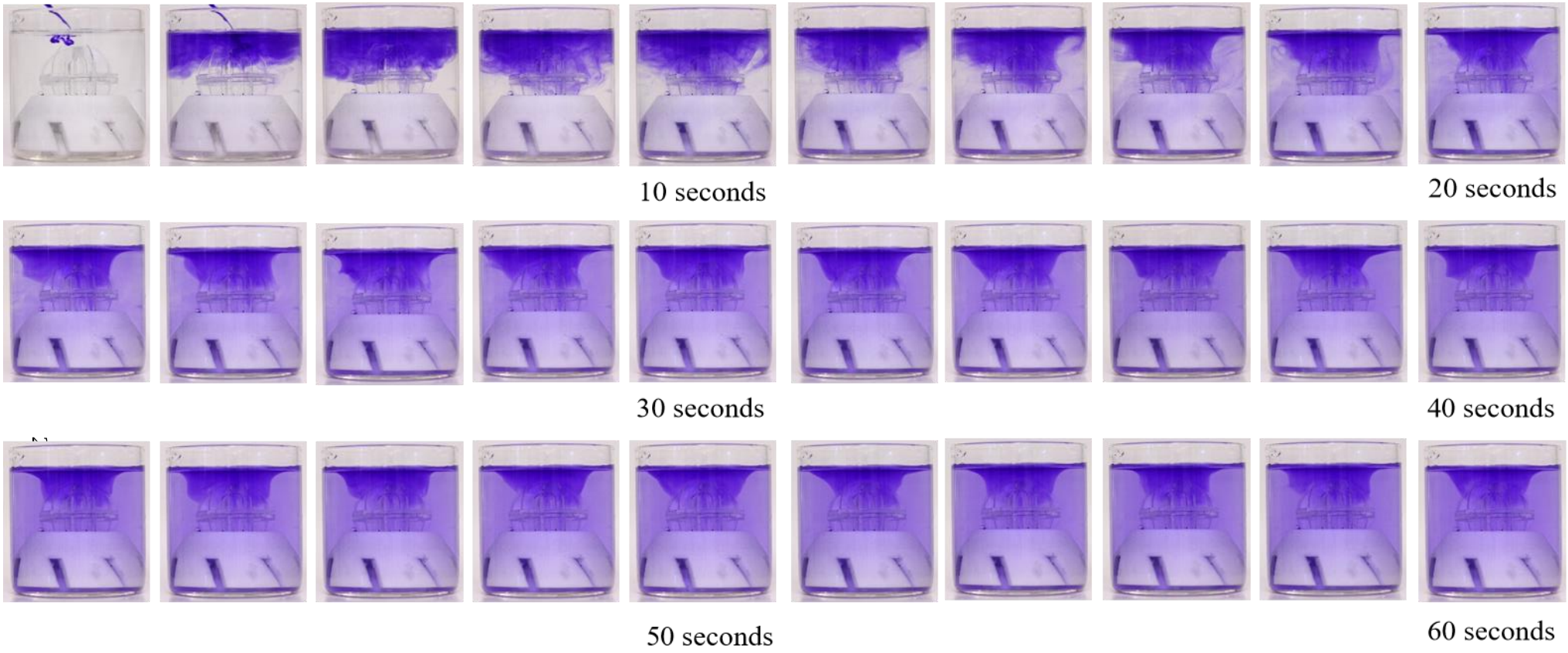


Figure 5.31: Fluid flow analysis data for anticlockwise fluid flow cone design with Alvetex® holder in place: 200 µl of 0.1 % crystal violet was added to the vessel at the 0 seconds time point, and its distribution monitored over 60 seconds, with images taken every 2 seconds. As seen in the previous images, a large central vortex of the dye is seen in the vessel, but the presence of the device shows that it is not well drawn through the centre of the funnel where the device is. This leads to poor redistribution throughout the vessel, and the lack of a defined flow direction. All analyses conducted at 125 rpm.

5.5.3.2 Assessment of fluid flow, turbulence and velocity of clockwise flow funnel design reveals more successful redistribution of fluid

An alternative funnel design which had slots that resulted in the clockwise redistribution of fluid from the funnel was also trialled. Fluid flow analyses using the crystal violet dye and PIV were carried out once again, as on the previous funnel design. In a similar way, fluid is drawn down into the funnel in a central vortex, as can be seen in the photographs in Figure 3.32. Redistribution of the fluid through the funnel and back into the upper area of the vessel can be seen after as little as 10 seconds. Full redistribution of the fluid can be identified after around 30 seconds.

Using this prototype, the fluid flow distribution graph in Figure 3.32 show similar results to the previous funnel design. The White Intensity in the top section drops sharply at the beginning of the time course on addition of the dye, with a steady drop in the middle section following this due to the drawing down of the dye into the funnel. The White Intensity in the base of the vessel also drops after this but in a more steady and prolonged manner compared to the anticlockwise funnel design.

PIV indicates an increase in both turbulence and velocity within this version of the system, with the turbulence in particular showing an increase in both strength and area across the plane of measurement, covering much of the plane. Velocity in the system is also shown to increase in both speed and area, with a more even coverage of the centre of the plane in terms of speed compared to the anticlockwise funnel design.

In Figure 5.33, assessment of the fluid flow with the Alvetex® holder in place shows that fluid is again successfully drawn through the centre of the funnel, and begins to be redistributed between 10 and 20 seconds. While some dye remains in the top section of the vessel at this point, this is successfully recirculated and redistributed over the rest of the time course of photographs shown.

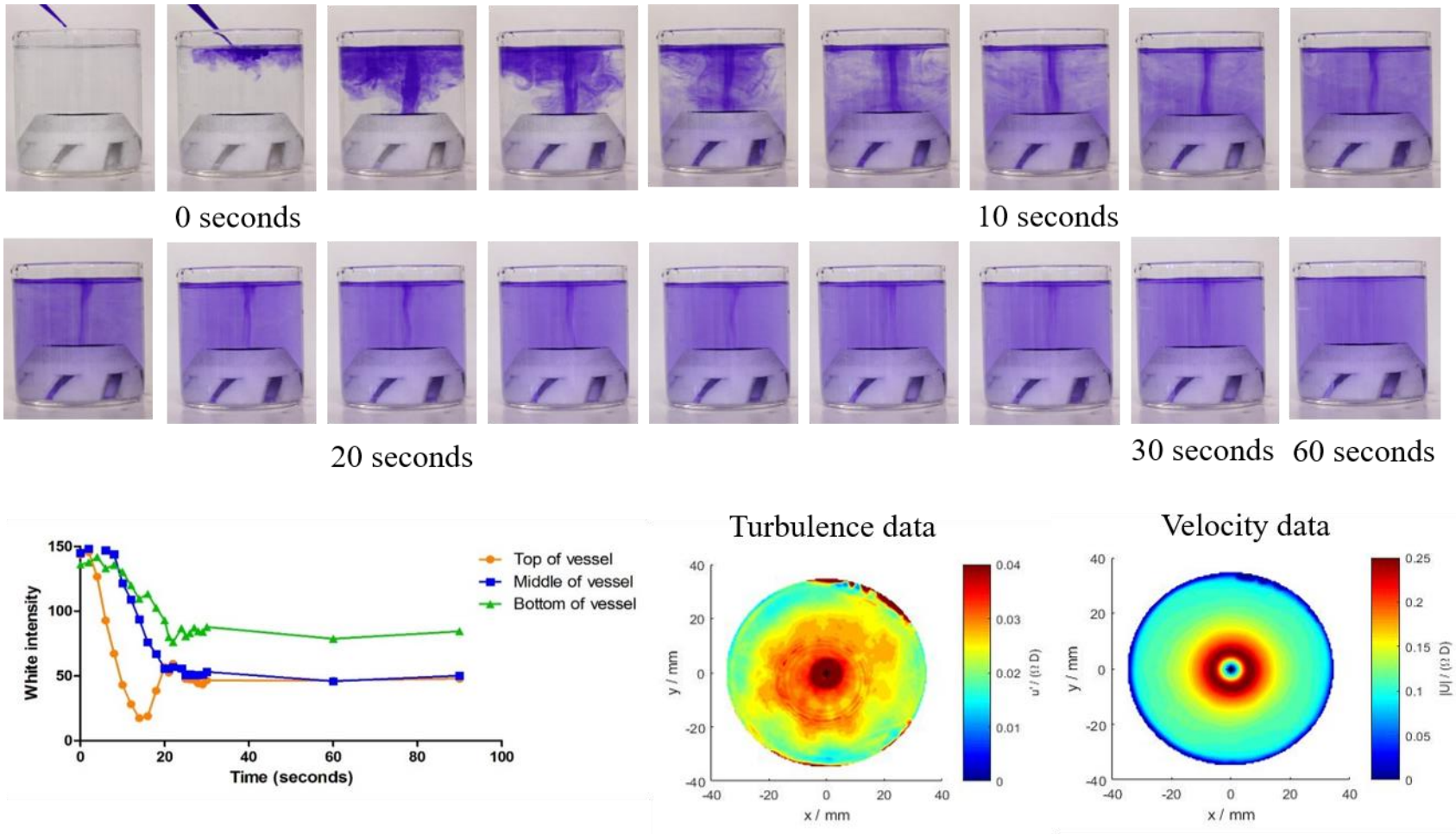


Figure 5.32: Fluid flow analysis data for clockwise fluid flow cone design: 200 µl of 0.1 % crystal violet was added to the vessel at the 0 seconds time point, and its distribution monitored over 90 seconds. Images were taken every 2 seconds for the first 30 seconds, and at 60 and 90 seconds time points. By 20 seconds, dye is just beginning to be recirculated within the vessel. By 60 seconds, the dye has been distributed throughout the vessel. There is significant turbulence across the vessel at the plane where the Alvetex® will sit. There is also a larger area with high fluid velocity in this design of cone. All analyses conducted at 125 rpm.

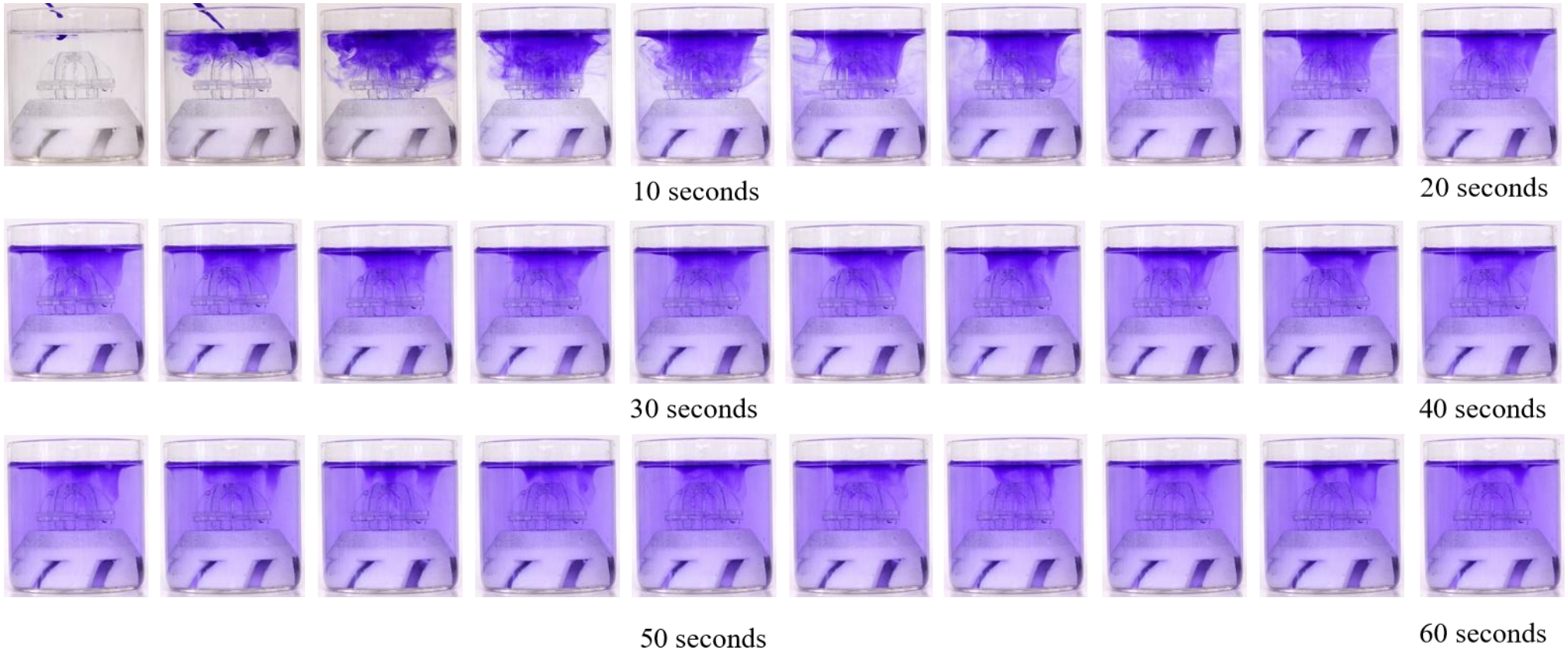


Figure 5.33: Fluid flow analysis data for clockwise fluid flow cone design with Alvetex® holder in place: 200 µl of 0.1 % crystal violet was added to the vessel at the 0 seconds time point, and its distribution monitored over 60 seconds, with images taken every 2 seconds. Images show that the dye is successfully drawn through the centre of the funnel, through the device and is recirculated back into the main part of the vessel. All analyses conducted at 125 rpm.

5.5.3.3 Assessment of fluid flow, turbulence and velocity of platform with angled slots design reveals a highly inefficient design with no fluid recirculation

An alternative design to the funnel style holder was also tested within the system, in order to explore other potential options. The platform style design also had angled slots incorporated into the design in order to allow for the direction of the fluid redistribution. In Figure 5.34, analysis of the fluid flow within the system using the crystal violet dye shows that this style of holder does not produce similar results to the previously tested funnel designs. Fluid is not clearly drawn down through the platform, but is seen to mix in the top half of the vessel. This continues, with the dye becoming completely mixed throughout the system, yet having no clear directionality or recirculation. PIV indicates a very low turbulence across the entire plane of measurement, and a velocity pattern similar to that of the anticlockwise funnel design – a ring around the centre of the plane.

The fluid flow distribution throughout the vessel here is noticeably different to the two previous examples. The White Intensity of the top and middle sections shows a very similar drop and subsequent increase in White Intensity, which is only delayed by a few seconds. This reveals a phenomenon of mixing within the system rather than the drawing through of fluid as is desired. The base of the vessel also shows a drop in White Intensity once the fluid is mixed more thoroughly across the entire vessel.

Assessment of the fluid flow with the Alvetex® holder in place shows similar results, as can be seen in Figure 5.35, with the mixing effect occurring even quicker, after around 10 seconds. The dye is fully mixed within the top half of the vessel, with the same effect occurring within the bottom half of the vessel over the next 10 seconds. This mixing persists throughout the imaging time course.

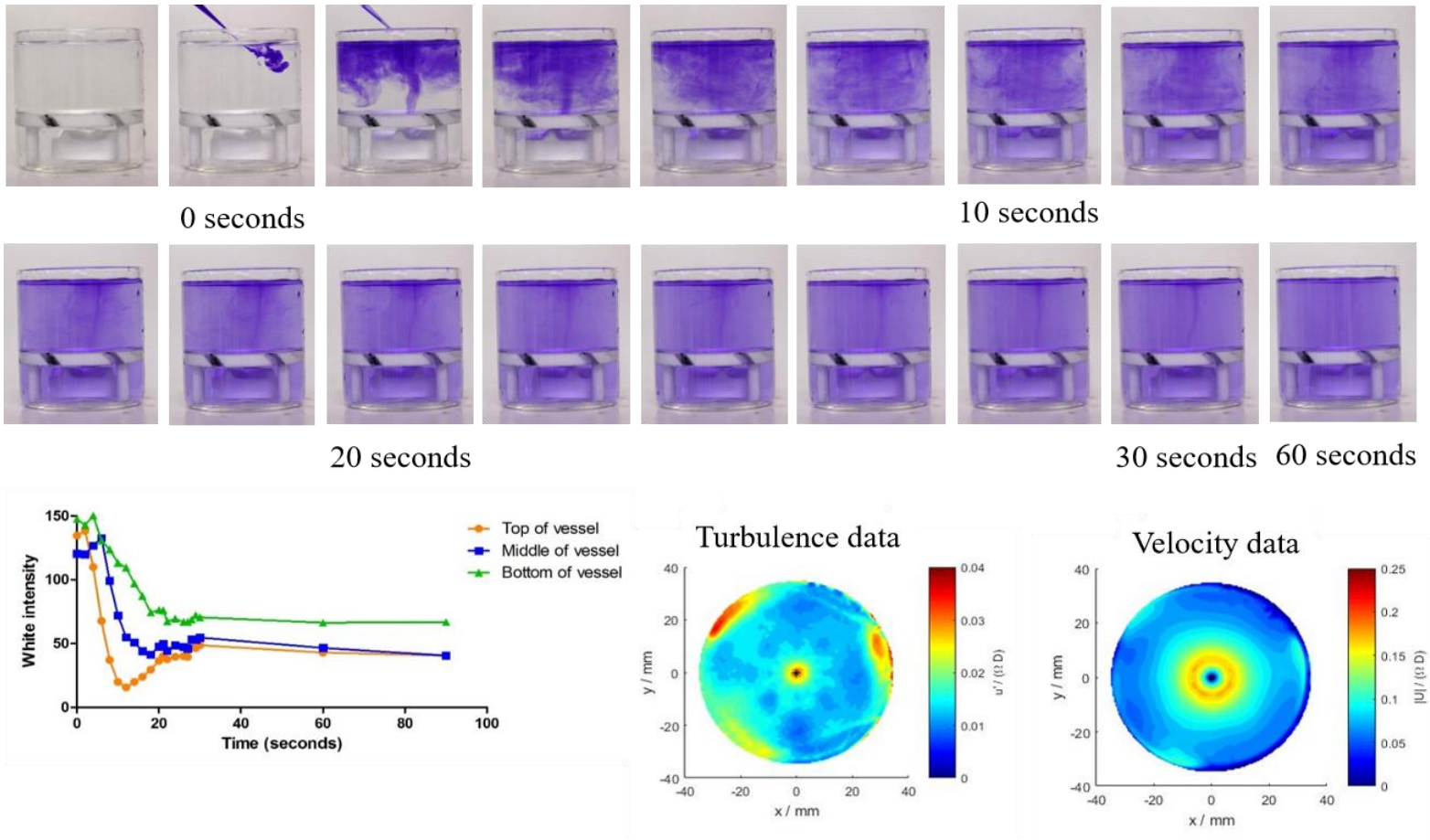


Figure 5.34: Fluid flow analysis data for platform with angled slots design: 200 µl of 0.1 % crystal violet was added to the vessel at the 0 seconds time point, and its distribution monitored over 90 seconds. Images were taken every 2 seconds for the first 30 seconds, and at 60 and 90 seconds time points. By 20 seconds, dye is well distributed within the upper compartment of the vessel, although little is present in the lower compartment. At 30 seconds, more dye is present within the lower compartment, but the recirculation of the dye is not clearly visible. By 60 seconds, the dye appeared to have reached an equilibrium within the vessel. This design shows very little turbulence across the plane at which the Alvetex will sit, the velocity of the fluid is also fairly uniform, with a small ring in the centre where the fluid is drawn into the lower compartment. All analyses conducted at 125 rpm.

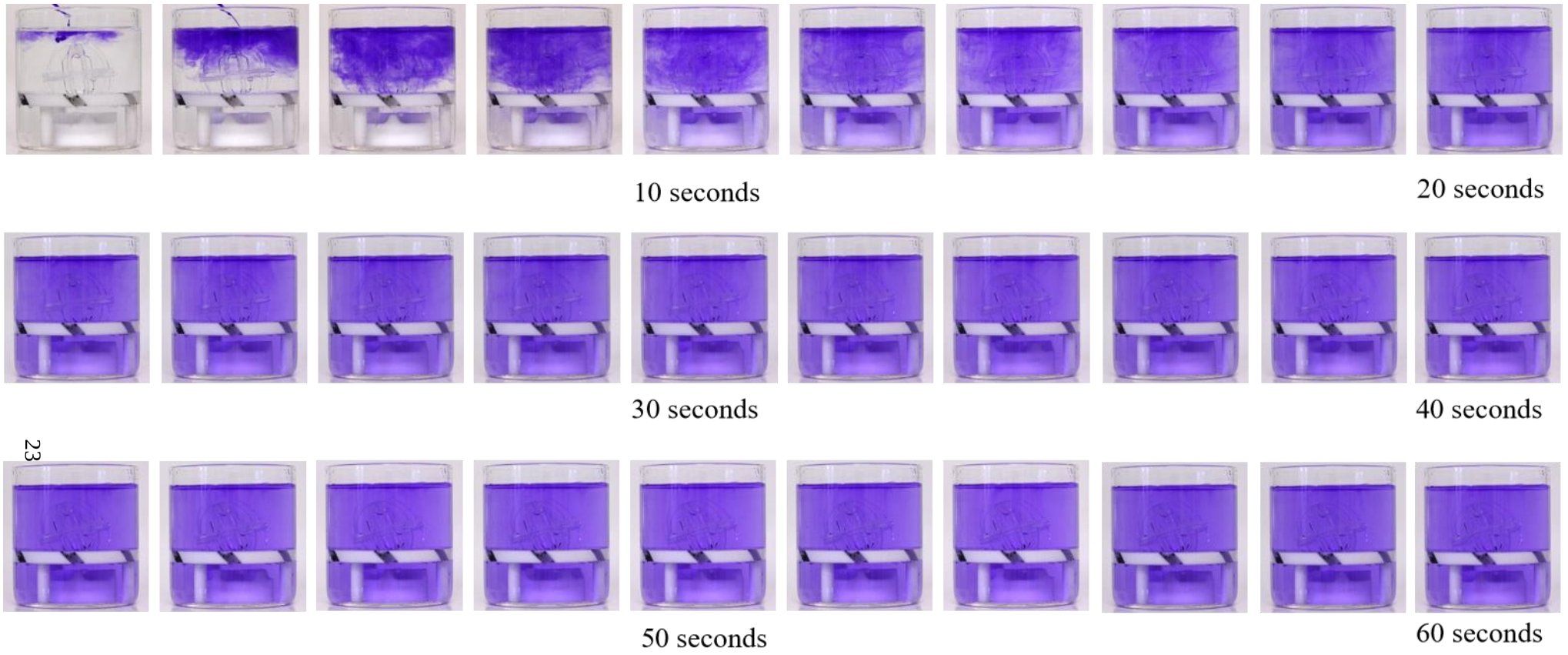


Figure 5.35: Fluid flow analysis data for platform with angled slots design with Alvetex® holder in place: 200 µl of 0.1 % crystal violet was added to the vessel at the 0 seconds time point, and its distribution monitored over 60 seconds, with images taken every 2 seconds. Initially, the dye is well distributed through the upper compartment as previously shown, with some directional flow though the centre, where the device is placed. The dye does not appear to show signs of a flow direction, and reaches an equilibrium in the vessel by around 20 seconds. All analyses were conducted at 125 rpm.

5.5.3.4 Refinement of clockwise funnel design and reassessment of system properties results in improved recirculation and reduced turbulence

Through the previous analyses, the clockwise funnel design was shown to produce effective redistribution of fluid with a better coverage of the central fluid vortex across the plane of measurement. However, the system has a high level of turbulence across much of the plane of measurement. The clockwise funnel design was refined by increasing the height of the funnel by 5 mm. Figure 5.36 shows the data following the refinements, and repeating the crystal violet dye distribution shows that the refined funnel design retains the same physical properties as the original clockwise design system. The dye is drawn through the centre of the funnel and redistributed after around 20 seconds. PIV analysis shows that velocity of the fluid flow is maintained in the centre of the plane of measurement but the turbulence is greatly reduced, with only a small amount of turbulence in the very centre of the funnel. The fluid flow distribution graph shows a much more rapid drawing and recirculation of the fluid through the centre of the funnel and back out into the main body of the vessel, as well as a more consistent maintenance of this state from early on in the time course. Repeating the fluid flow analysis with the Alvetex® holder in place replicates the results seen in the original clockwise funnel, as can be seen in Figure 5.37, with the dye drawn through the centre of the funnel and showing redistribution between 10 and 20 seconds. All of the dye was drawn from the top of the vessel and recirculated within the system.

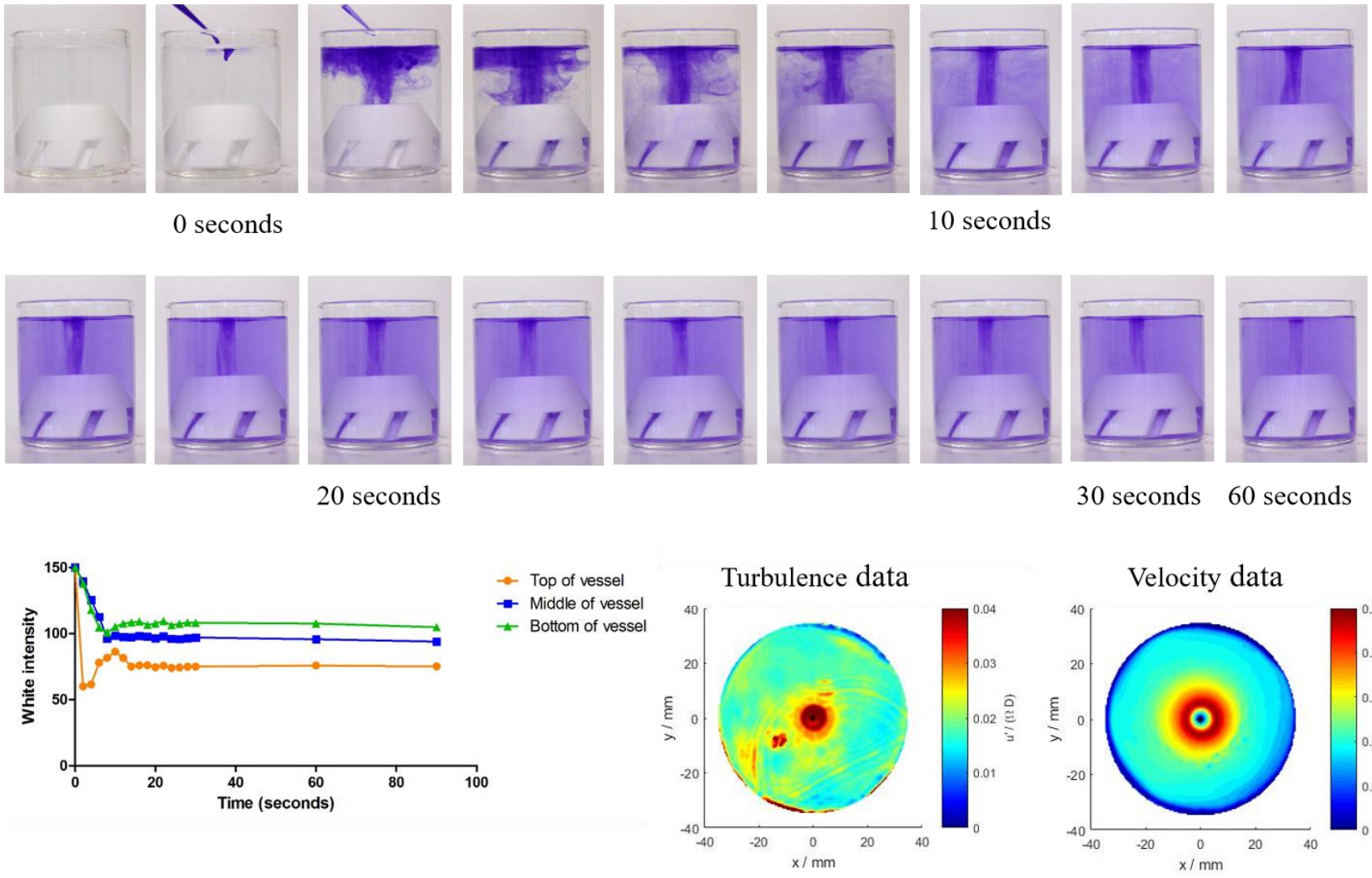


Figure 5.36: Fluid flow analysis data for clockwise fluid flow cone final design: 200 µl of 0.1 % crystal violet was added to the vessel at the 0 seconds time point, and its distribution monitored over 90 seconds. Images were taken every 2 seconds for the first 30 seconds, and at 60 and 90 seconds time points. The turbulence data shows that a more uniform, lower turbulence is achieved across the plane of measurement, with a smaller high turbulence area in the centre of the cone. The velocity measurements for this design are similar to the previous design of the cone. All analyses were conducted at 125 rpm.

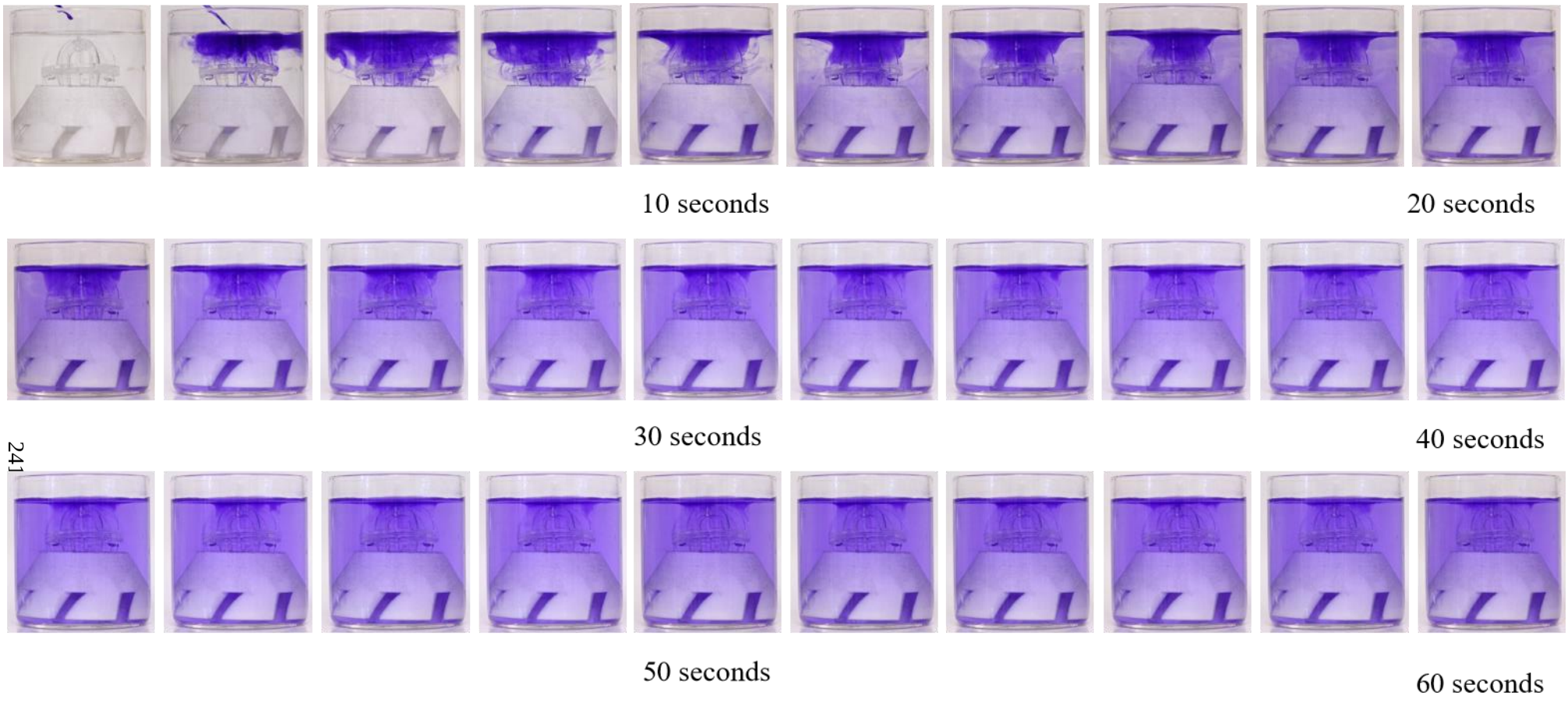


Figure 5.37: Fluid flow analysis data for clockwise fluid flow cone final design with Alvetex® holder in place: 200 µl of 0.1 % crystal violet was added to the vessel at the 0 seconds time point, and its distribution monitored over 60 seconds, with images taken every 2 seconds. As with initial clockwise fluid flow design, images show that the dye is successfully drawn through the centre of the funnel and through the perfusion device. The dye is then recirculated back into the main part of the vessel. All analyses were conducted at 125 rpm.

5.5.3.5 Polytetrafluoroethylene used to create the funnels is not toxic, having no impact on cell viability or growth rate

Once the style of holder for the perfusion device had been selected, brief toxicity testing was undertaken. As the holder for the perfusion device was made of polytetrafluoroethylene (PTFE), it was necessary to ensure that the material did not negatively affect the growth of cells, given that it is not routinely used for cell culture purposes. The PTFE stands were incubated in the cell culture medium at 37°C, 5 % CO_2 for 2-3 days in the event that contaminants leaked from the PTFE, the conditioned media collected and used to culture cells in 2D. Cell morphology, viability and growth rate were assessed and compared to cells cultured in normal maintenance medium incubated in the same way without the PTFE holder. The images in Figure 5.38 show that there is no noticeable difference in morphology of TERA2.cl.SP12 cells cultured in normal maintenance media compared to those cultured in maintenance media conditioned in the PTFE holders. Cell counts show that there is no significant effect on the number of cells when the two media types are compared. Cell viability is also unaffected by the use of the PTFE conditioned media, with MTT values averaging similar values for both the normal maintenance media and the PTFE conditioned media.

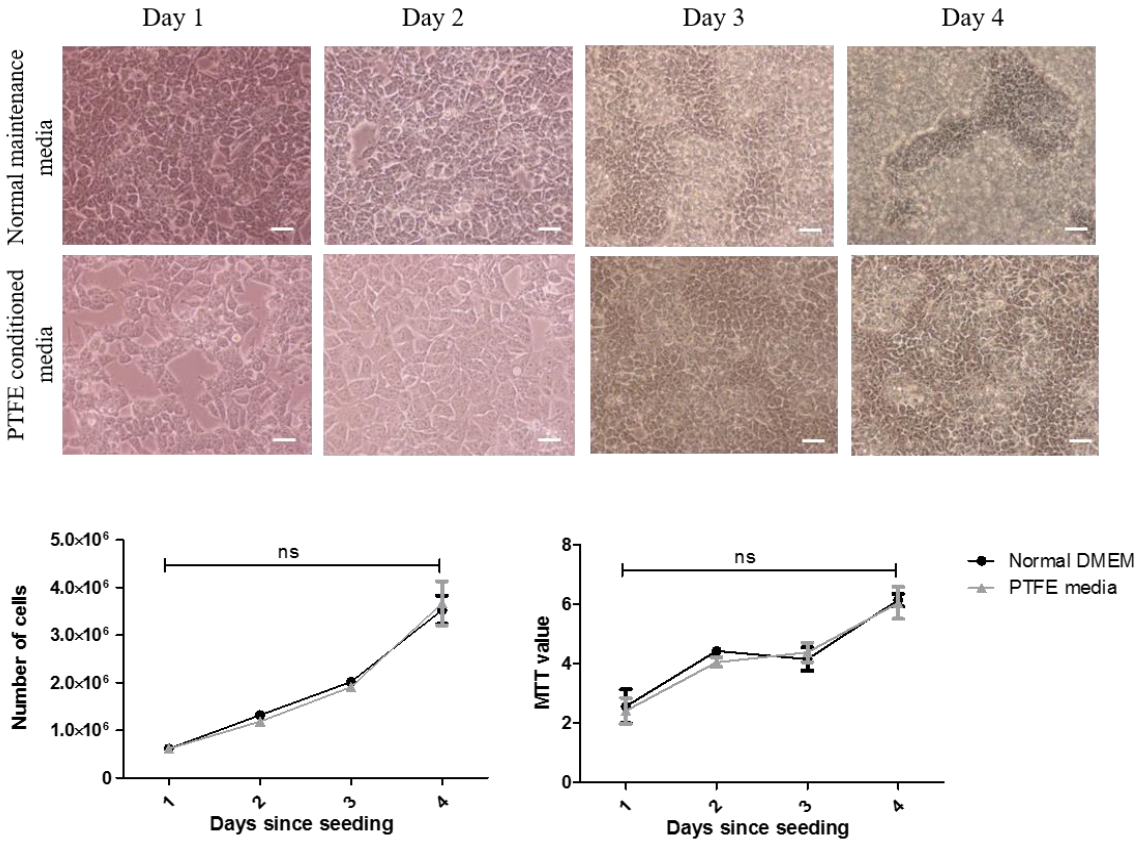


Figure 5.38: Morphology and viability of cells cultured in PTFE conditioned media: To analyse any potential toxic effects from the PTFE stands, TERA2.cl.SP12 cells were seeded at the appropriate passaging ratio with morphology, cell number and viability being monitored over 4 days after initial seeding. Cells were maintained in either normal maintenance media, or maintenance media conditioned in a glass vessel containing the PTFE cone for 48 hours at 37°C, 5 % CO_2. Cell counts and MTT assays were conducted every 24 hours to assess cellular viability and proliferation, and there were no observable differences in cell morphology, growth rate or viability between the two media. Results were found not to be statistically significant by two way ANOVA. Data represents mean ± SEM from 3 independent experiments (n=3). Representative images shown. Scale bars: 50 µm

5.5.4 Optimisation of novel perfusion system using TERA2.cl.SP12

Following the optimisation of the technical aspects of the perfusion system, the biological aspects also required investigation and optimisation, specifically the way in which cells would be seeded. The methods used to introduce perfusion to cells and tissues *in vitro* are highly varied, although many systems employ a solid scaffold to hold cells, with culture media flowing through the construct. Alvetex® lends itself to use in perfusion systems due to its porous nature, but the seeding methods and number of inserts used in this system still requires further optimisation.

5.5.4.1 Use of two Polaris membranes in static sandwich culture is the only culture method which allows for the maintenance of an entire tissue disc.

The decision was made to use an alternative culture setup for the perfusion system, due to the fact that introducing fluid flow, and therefore some shear stress, into the system could result in the disturbance of any cellular material or rudimentary tissue structures. A sandwich culture method was selected in order to protect cells in culture, due to the simplicity of adding another Alvetex® membrane on the top of the membrane seeded with cellular material, and the fact that this culture set up is commonly employed in the perfused culture of hepatocytes to reduce shear stress. The second insert was added to form the sandwich culture 2 days after EBs were initially seeded onto the Alvetex® insert, to allow for attachment. Initially, multiple combinations of Alvetex® were trialled in the static setting, to assess the behaviour of the tissue discs in a sandwich culture setting and ensure that this culture method is both logistically possible and the tissue disc formation process is preserved. Figure 5.40 shows representative histology from testing all three forms of Alvetex® – Scaffold, Strata and Polaris – as both the top and base inserts in the sandwich culture. TERA2.cl.SP12 EBs were cultured in this way for one week; for comparison, typical images of EBs which have formed tissue discs on the three different forms of Alvetex® are also shown. Considering the combinations of Alvetex® sandwich culture in the Figure, while much of the behaviour of the EBs/tissue discs correlates with that which is seen when tissue discs are cultured on the surface of the three forms of Alvetex®, there are also some unexpected results.

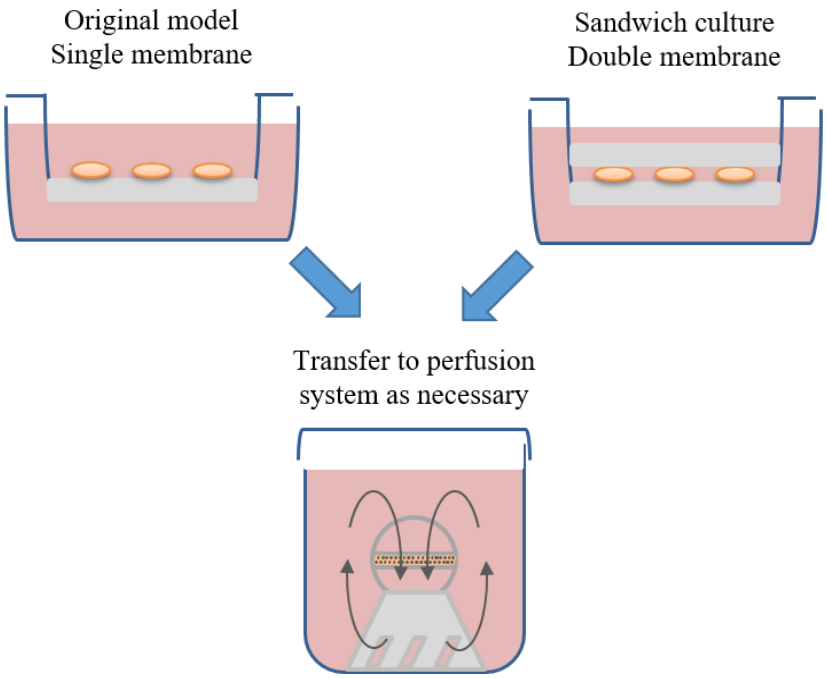


Figure 5.39: The sandwich culture technique used for perfusion experiments: The addition of a second Alvetex® membrane to the original model results in the creation of a sandwich structure, which is commonly used in other perfused culture systems to hold the cellular material.

All of those combinations involving Scaffold and Strata show some level of infiltration, as would be expected and is seen in the original tissue disc model using these forms of Alvetex®, but closer analysis of the combinations in turn is required to select an appropriate culture method. Examining the combinations more closely, those with a Polaris base naturally show no infiltration into the base insert due to the small pore and void size, which is not permissive for cells to enter. The Polaris base/Polaris top combination shows the formation of a homogenous layer of tissue disc from the EB across the insert. The combinations with Strata and Scaffold do not replicate this formation of an even cell layer, with most of the cells of the EB having migrated upwards into the top insert. While with Strata, a residual thin layer of cells remains on the base Polaris insert, with Scaffold as a top there are no cells left on the Polaris base insert; surprisingly the entire EB has disintegrated and infiltrated the Scaffold, rendering it difficult to see the Polaris insert. Those combinations that use Strata as a base also show some expected characteristics, such as moderate infiltration of the EBs into the Strata base in all cases. As with the Polaris base/Strata top, in the Strata base/Polaris top combination the majority of the EB has infiltrated the Strata base insert, with a small layer of residual cells attached to the Polaris top insert. The histology for the Strata base/Strata top combination shows an even amount of infiltration into each insert, which is expected, given that the two inserts are equally permissive to cellular infiltration. Conversely, the Scaffold top/Strata base combination appears to show increased EB infiltration into the top insert when compared to that seen in the base insert, due to increased permissiveness of the Scaffold insert. Scaffold base combinations were investigated for completeness, but as expected, all of these combinations show large amounts of EB

infiltration and full disintegration into the base Scaffold insert. Again, with the Polaris top/Scaffold base, a small number of cells remain attached to the Polaris top, with the majority having infiltrated the Scaffold base. A Strata top/Scaffold base results in complete infiltration into the base insert, whereas Scaffold top/Scaffold base results in significant EB infiltration into both of these inserts.

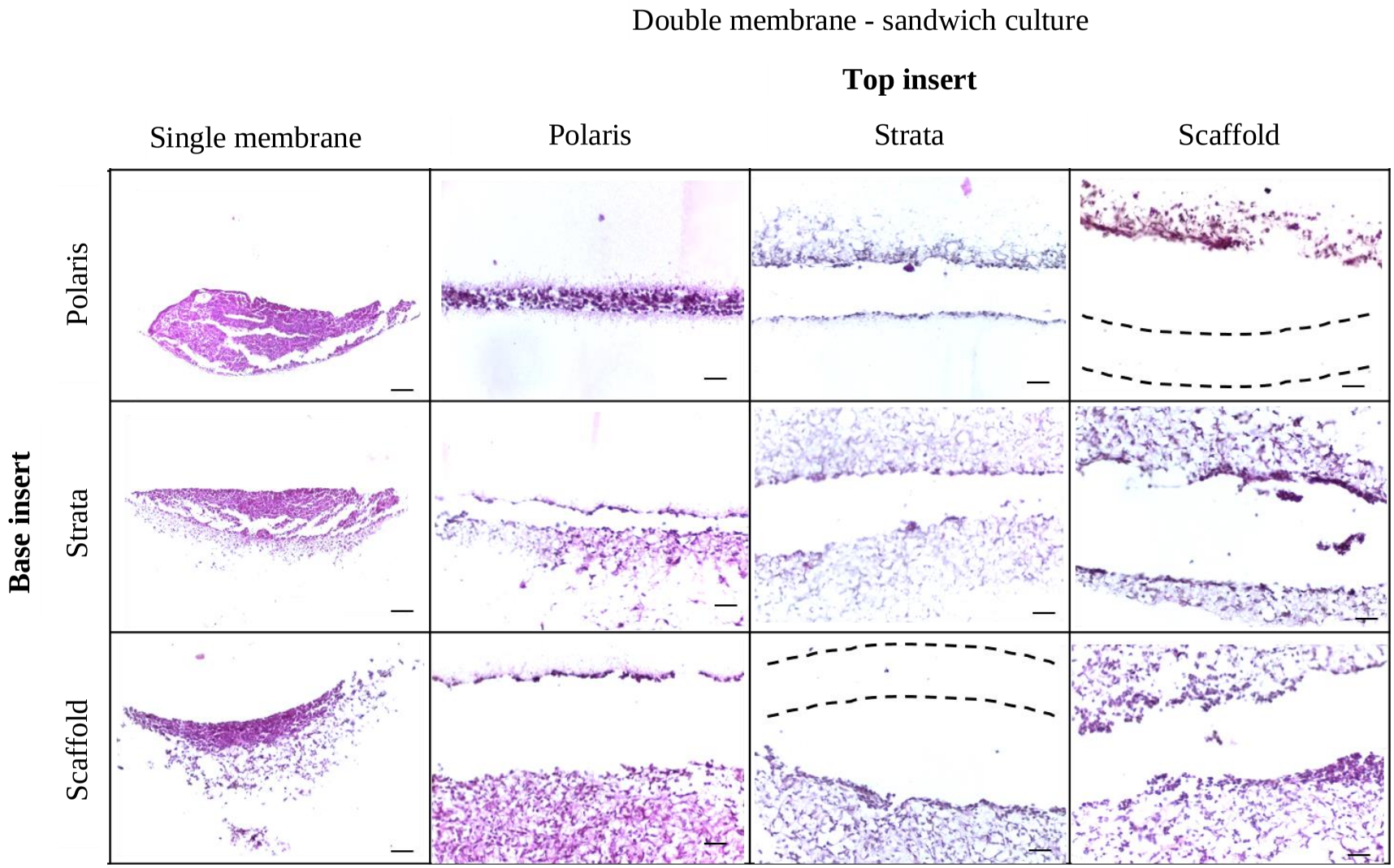


Figure 5.40: Morphology and behaviour of TERA2.cl.SP12 EBs seeded into various combinations of Alvetex® sandwich culture in the static setting: To test an adapted culture methodology before its use in the perfusion system, the current model was cultured in multiple combinations of Alvetex® to assess the behaviour and viability of the EBs. TERA2.cl.SP12 EBs were seeded onto the base insert and cultured for 2 days, before the top insert was attached and cultured for a further 7 days. As can be seen from the H&E images, EB behaviour differs significantly depending on the combination of the Alvetex® inserts. Generally, EBs invade any insert which is permissive i.e. Strata or Scaffold, whether it is the base or top insert. Scale bar: 50 µm.

Quantification of the infiltration of the EBs into the inserts, both top and base, is shown in Figure 5.41. These data correlate with that which was observed in the histology. There is little cellular infiltration into Polaris base combinations. Generally, combinations with a Strata base show a reduction in EB infiltration into the base insert compared to the original surface culture model using Strata, particularly when there is a more permissive top insert available, i.e. Scaffold. Sandwich culture combinations with a Scaffold base also show less infiltration into the base insert compared to the original model using Scaffold, a phenomenon which is likely due to the fact that the EBs are able to attach to or infiltrate the top insert also, reducing the amount of cellular material available to infiltrate each insert. Assessment of infiltration into the top insert in these combinations also confirms the histological findings. Significant EB invasion into the top insert occurs with any permissive insert, i.e. Strata or Scaffold, and is particularly pronounced when the top insert is equally permissive or more permissive to infiltration than the base insert. It is clear from these data that the only Alvetex® sandwich culture combination which allows for the preservation of a tissue disc structure is Polaris base/Polaris top.

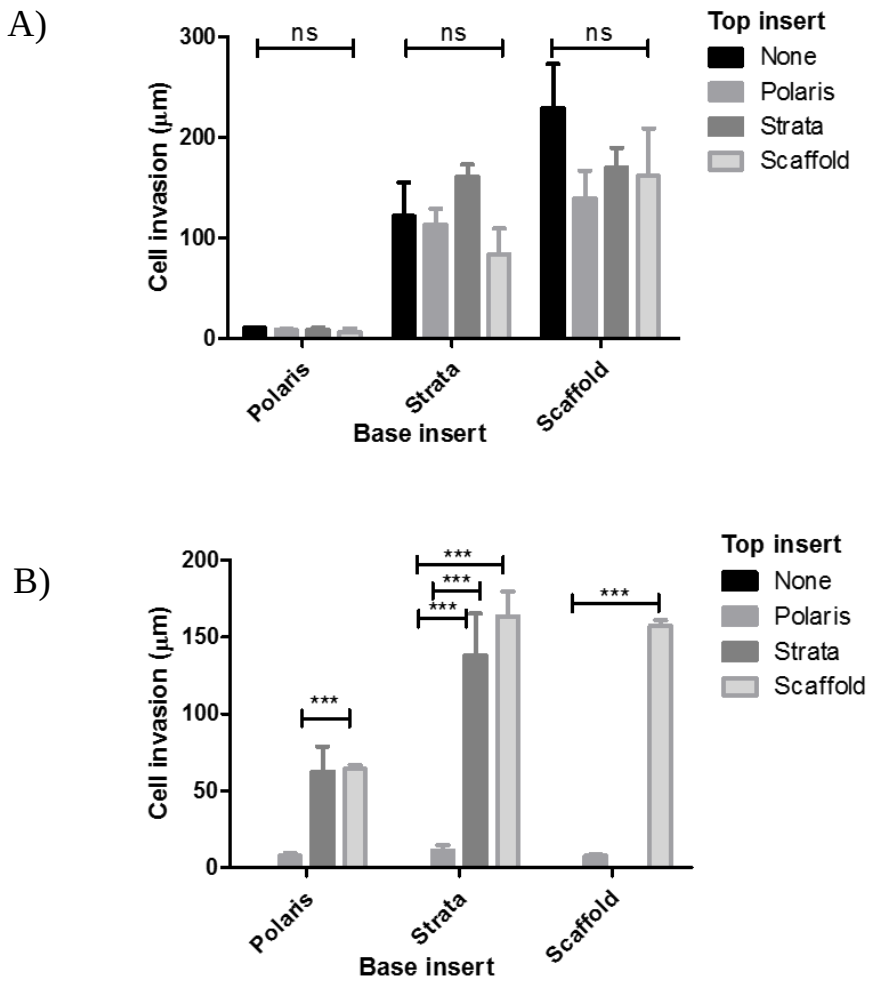


Figure 5.41: Quantification of invasion of TERA2cl.SP12 EBs into base and top membrane of sandwich culture: Histological analysis highlighted the invasion of TERA2.cl.SP12 EBs into inserts used in the sandwich culture model. Invasion of EBs was measured by overlaying a grid, and using a random number generator to select squares to measure. A) Invasion into base membrane of sandwich culture. B) Invasion into top membrane of sandwich culture. Analysis shows that as hypothesised from the histological images, there is increased invasion into permissive inserts. This is true of both the top and bottom inserts, with cellular infiltration occurs whenever there is a permissive insert present. Data represents mean ± SEM from 3 independent experiments (n=3). Statistical significance was calculated using the two way ANOVA. $P \leq 0.001$.

5.5.4.2 Characterisation of Polaris base/Polaris top culture combination shows promise in static culture, but is not suitable for use in the perfused system

As the Polaris base/Polaris top is the only culture combination which allows for the formation of a tissue disc type structure within the Alvetex® sandwich, this culture combination was further investigated to confirm its suitability. High magnification histological images in Figure 5.42 show no obvious signs of cell death within the tissue disc, highlighting the interaction of the cells with the two inserts through the production of cellular processes, which appear to be growing out into the insert. Assessment of apoptotic cell death via TUNEL staining confirms that the tissue discs maintain their viability when cultured in this way, with no areas of cell death identified by the assay. Immunostaining for early neural differentiation marker Nestin and mature pan-neuronal differentiation marker Class III β-tubulin show that the cellular processes stain positively for Class III β-tubulin, resembling possible developing neural processes and indicating a shift to the neural phenotype in this culture system. There are no pluripotent areas which are Oct 4 positive in this tissue disc, or any epithelial structures, correlating with the culture of TERA2.cl.SP12 EBs on Polaris as seen in Chapter 3.

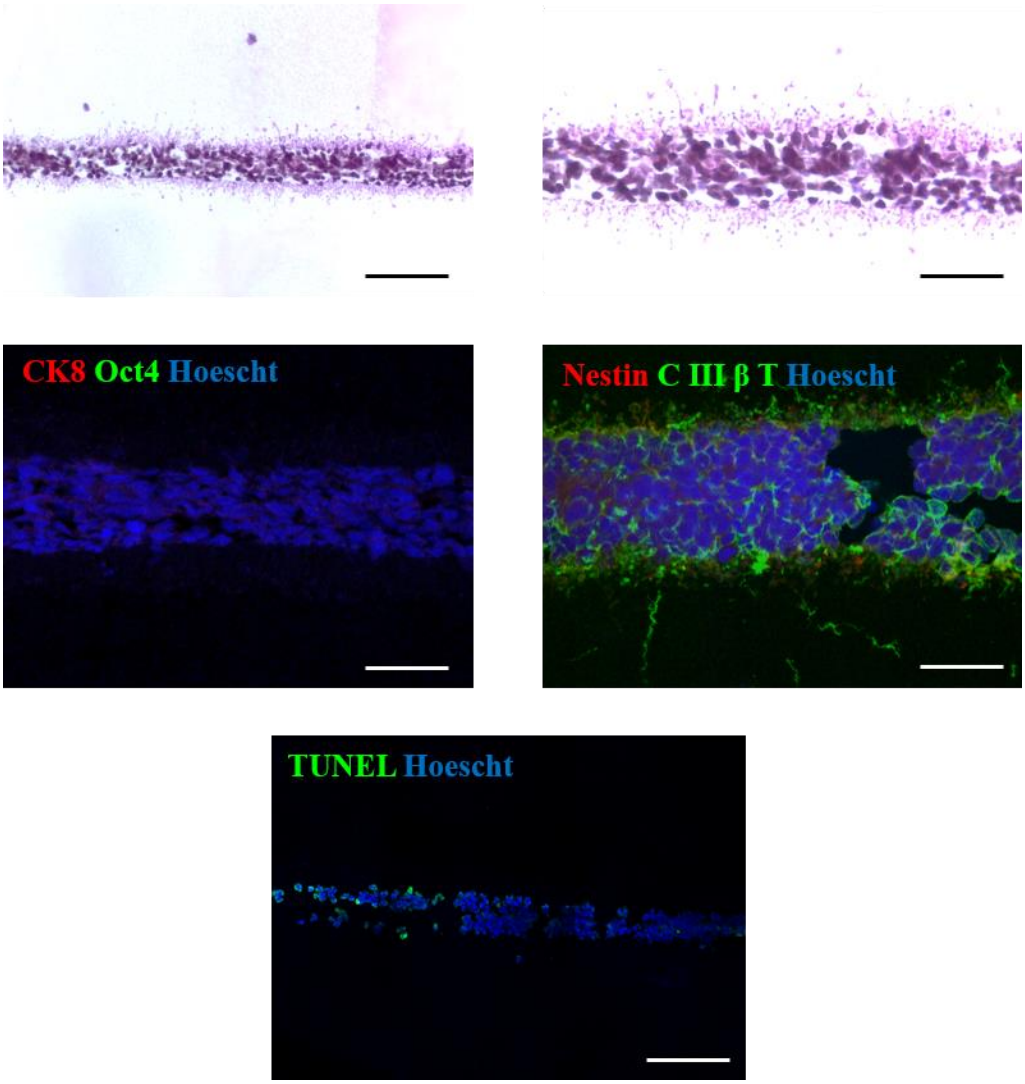


Figure 5.42: Characterisation of TERA2.cl.SP12 EBs cultured in Polaris Polaris sandwich culture combinations: The only sandwich culture combination which yielded the complete maintenance of the EB structure on the insert was the Polaris base/Polaris top combination. The combination was analysed further via immunostaining for TUNEL and appropriate neural protein markers, Nestin and Class III β-tubulin. Culturing untreated EBs in a Polaris base/Polaris top sandwich results in the growth of neural processes into the insert, indicating strong neural differentiation using this culture method after only 7 days, yet a lack of pluripotency or cells positive for epithelial markers. TUNEL staining confirms a lack of cell death. Representative images shown. Scale bars: 50 µm and 25 µm

This optimised culture methodology was transferred to the perfusion system. EBs were seeded onto the first Alvetex® insert and allowed to attach for 2 days, before inserts were unclipped and placed into the perfusion device, with the second insert added at this stage. The cultures were then placed in the perfusion vessels, and the rotation of the magnetic stirrer set to the lowest possible setting, around 100 rpm. Representative images in Figure 5.43 show the typical way in which EBs respond to the introduction of fluid flow. Many EBs showed severe fragmentation and a compromised structure, as can be seen in the examples provided. EBs were unable to form a homogenous, solid tissue disc between the two Alvetex® inserts after 7 days of perfusion within the system, even on the lowest speed setting.

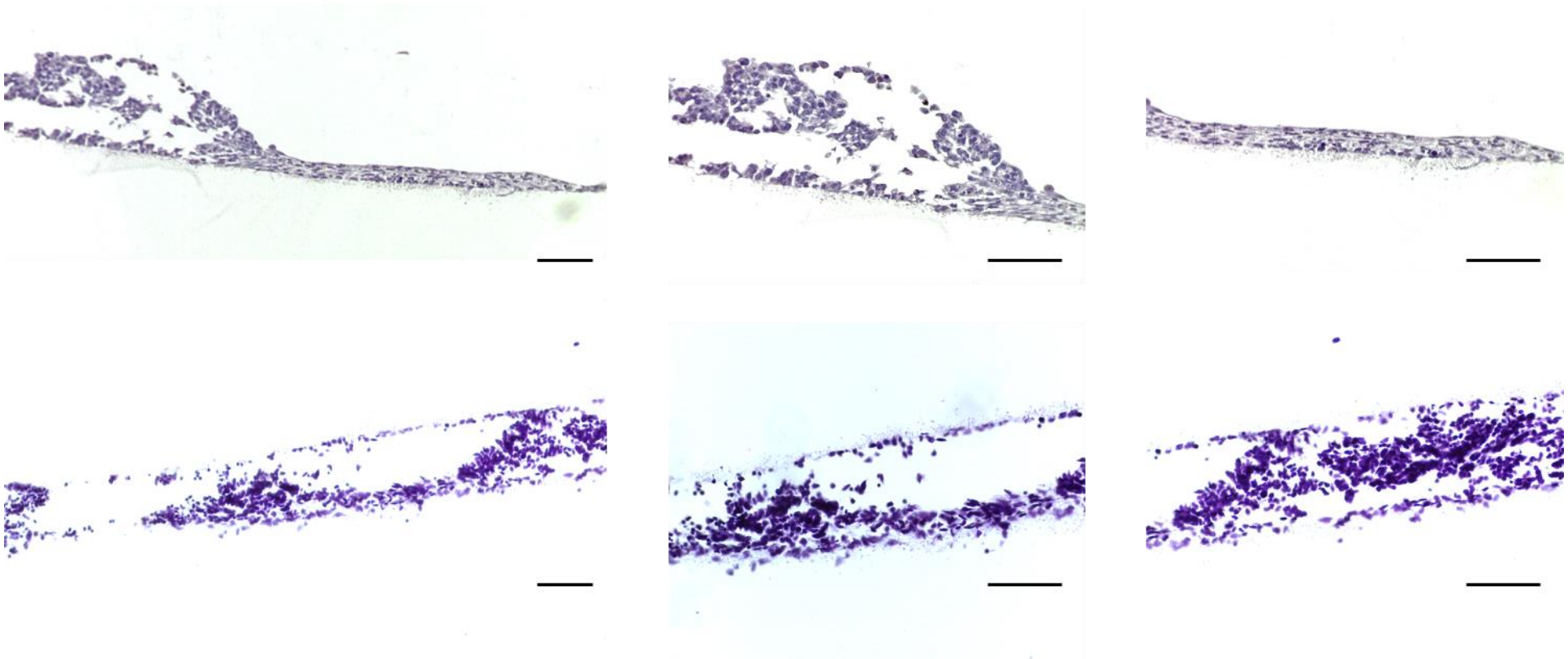


Figure 5.43: TERA2.cl.SP12 EBs cultured in Polaris based sandwich culture combinations in the novel perfusion system: TERA2.cl.SP12 EBs were seeded onto Polaris base inserts and allowed to attach for one day before the second Polaris is insert was added to the top. Cultures were then placed into the perfusion device and cultured for one week. In H&E images, EBs show a very different morphology in the perfused setting, with a either a highly flattened structure or loss of EB structure completely, with no complex structures visible. Scale bars: 100 µm

5.5.4.3 Reoptimisation of perfusion system culture methodology using a cell suspension and Matrigel is successful in static and perfused conditions

The introduction of fluid flow may have imposed significant stress on the structure of the TERA2.cl.SP12 EBs, as by this point the EBs will have formed a number of organised intracellular connections and adhesions within the structure, which will have been put under strain by the flow of the fluid through the scaffold. As many dynamic culture systems and the teratoma assay utilise a single cell suspension, this cell format was selected for reoptimisation of the perfusion system. As with some teratoma assay protocols, cells were combined with Matrigel to provide some support during proliferation and initial placement in the perfusion system.

Reoptimistion of the use of a cell suspension was conducted in static again, to attempt to determine an appropriate seeding density to form a homogeneous tissue layer in the perfusion system. Cells were seeded at 0.5M, 1M, 2M and 5M cells in 3 mg/mL of Matrigel, the lowest recommended dilution of the extracellular matrix, in order to provide as little exogenous modulation as possible while maintaining some cellular support. The cell/Matrigel mixture was allowed to set for up to an hour at 37°C before media was added. Cells were allowed to adhere for up to 2 days before the second insert was added and the sandwich culture clipped together. As shown in Figure 5.44, increasing TERA2.cl.SP12 seeding density results in a decrease in the cellular layer which forms when seeded in the static setting. Masson's trichrome staining highlights the Matrigel component within the cell suspension, with the level of Matrigel still present within the sandwich culture decreasing with the increasing seeding density. Immunostaining for the preferential differentiation route using pan-neuronal maker Class III β-tubulin indicates that there are some areas of neural differentiation within the system. In Figure 5.45, measurement of cell layer height shows a trend which correlated with the observations established in the H&E staining concerning the formation of a cell layer, however, the differences between these were found to be not significant using the one way ANOVA test. Assessment of cell viability using an MTT assay indicates an increased viability with the lower cell density of 0.5M cells, although viability of the other cell densities were much closer in value.

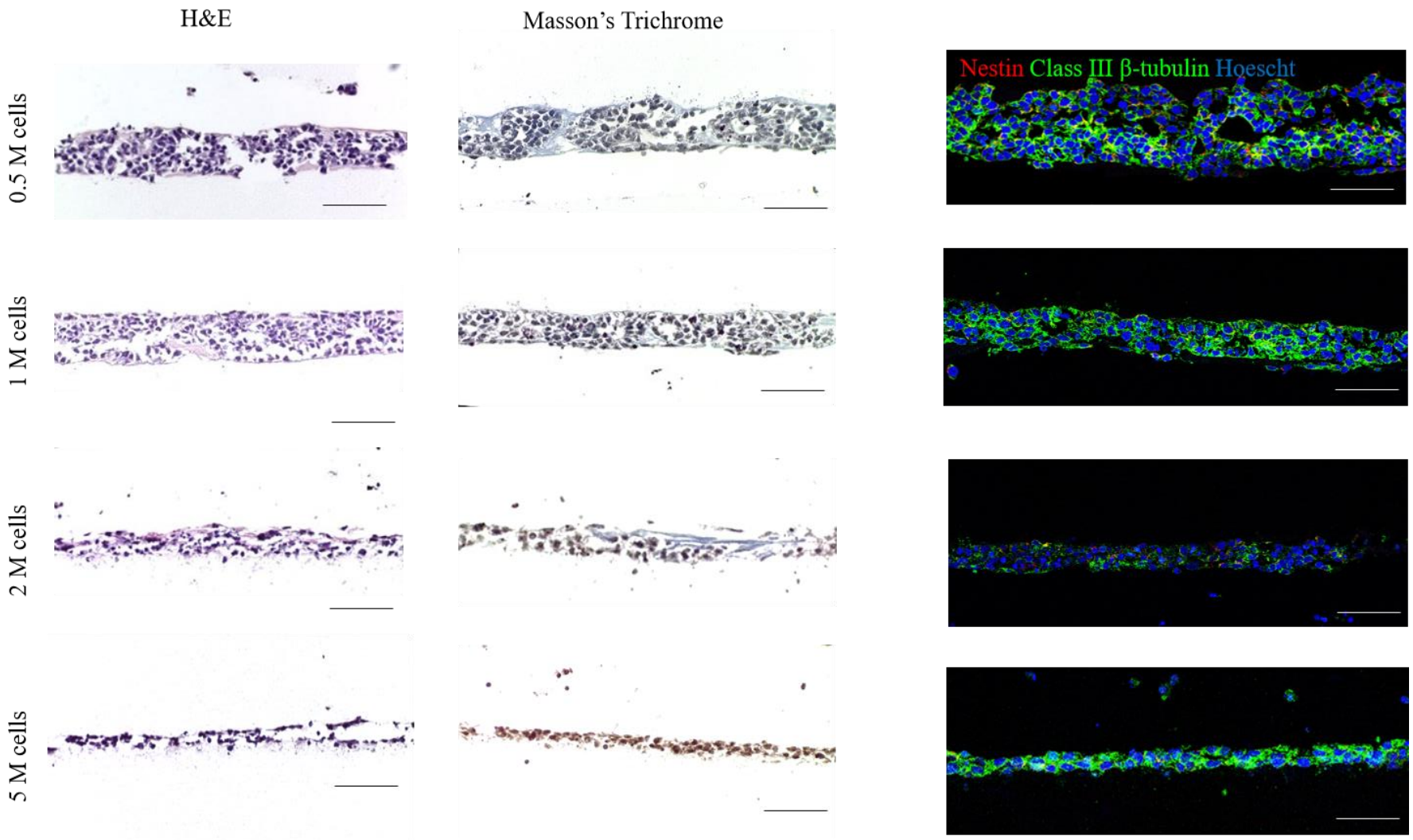


Figure 5.44: TERA2.cl.SP12 cells cultured static culture in the novel sandwich culture setting at varying cell densities: TERA2.cl.SP12 cells were resuspended in 3 mg/ml Matrigel and cultured in Polaris Polaris sandwich culture for 7 days in static culture in a 6 well plate. Inserts were fixed and viability analysed using an MTT assay. H&E images show that as initial cell seeding density increases, the amount of cellular material at the end of the culture period decreases. Masson's Trichrome staining shows the support provided by the Matrigel, indicated by the blue stained extracellular areas. Immunostaining for Nestin and neurone specific marker Class III β-tubulin can be seen to be more variable as the cell seeding number increases. Scale bars: 50 um

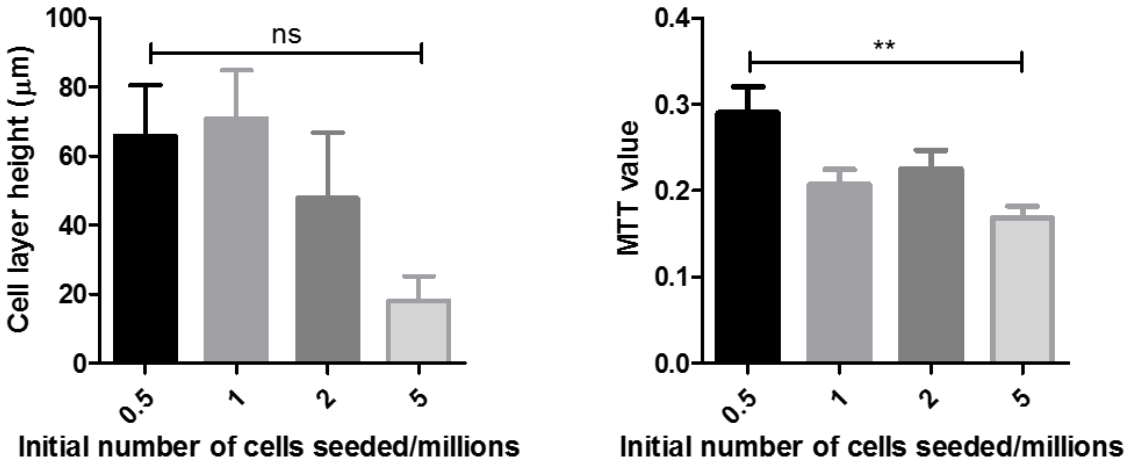


Figure 5.45: TERA2.cl.SP12 cells cultured static culture in the novel sandwich culture setting at varying cell densities: The height of the cellular material within the inserts was measured as previously described for EBs in static using a grid and a random number generator. Although there are clear visual differences with the H&E images, the overall effect was found not to be significant via analysis using the one way ANOVA. MTT values for viable cells at the end of the culture period showed a significant difference between the highest and lowest seeding values after analysis via one way ANOVA at $P \leq 0.01$. Data represents mean ± SEM from 3 independent experiments (n=3)

While all 4 seeding densities were tested in the perfusion system, results were highly variable in terms of viability and culture success as shown by the images and MTT values in Figure 5.46. The most successful results, as shown in Figure 5.47 and sectioned in an orientation parallel to the Alvetex® inserts, resulted in a very different and distinct morphology. TERA2.cl.SP12 cells were cultured in static for 2 days, before the second insert was added and the culture placed into the perfusion system. The most successful results were obtained from seeding 2M cells onto the insert, although there was still variability in viability and structure across the insert, with a large central area of disrupted cells in the centre of the sandwich culture. The morphology of the surrounding cells strongly resembles a colony formation, reminiscent of stem cell colonies. In some areas, cells stain positively for Oct 4, indicating the pluripotent phenotype. Cells also stain weakly positive for differentiation markers such as Nestin and Cytokeratin 8.

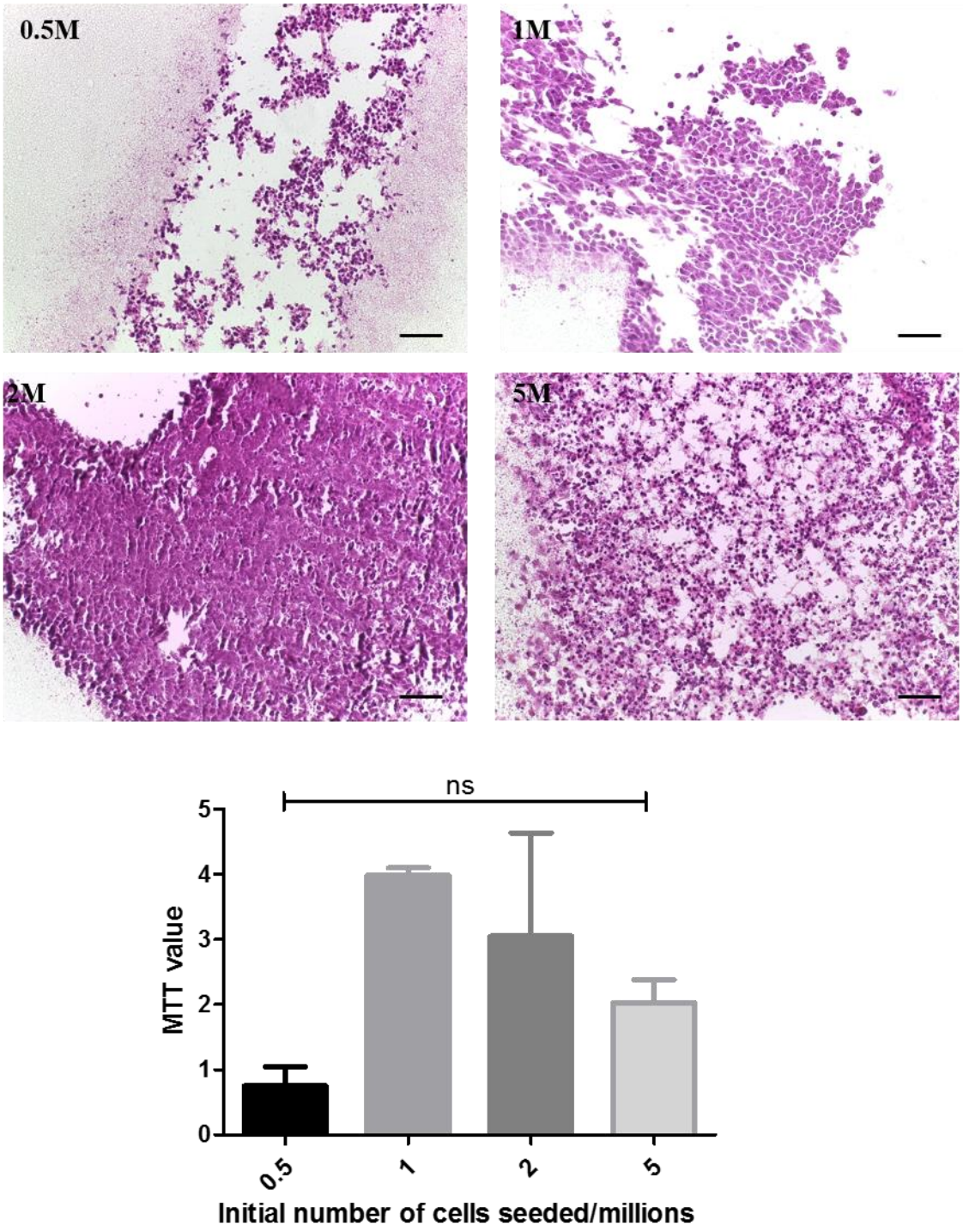


Figure 5.46: Variability of TERA2.cl.SP12 in perfused sandwich culture is dependent on cell seeding density: TERA2.cl.SP12 cells were prepared in Matrigel as described and cultured in the Polaris Polaris sandwich culture combination in the perfusion system for 7 days, at a range of densities. Cells showed a high variability in the ability to form a homogenous cell layer between the two scaffolds. Cell viability was determined via MTT assay, results were not significant according to analysis by one way ANOVA. Data represents mean ± SEM from 3 independent experiments (n=3). Scale bar: 100 µm

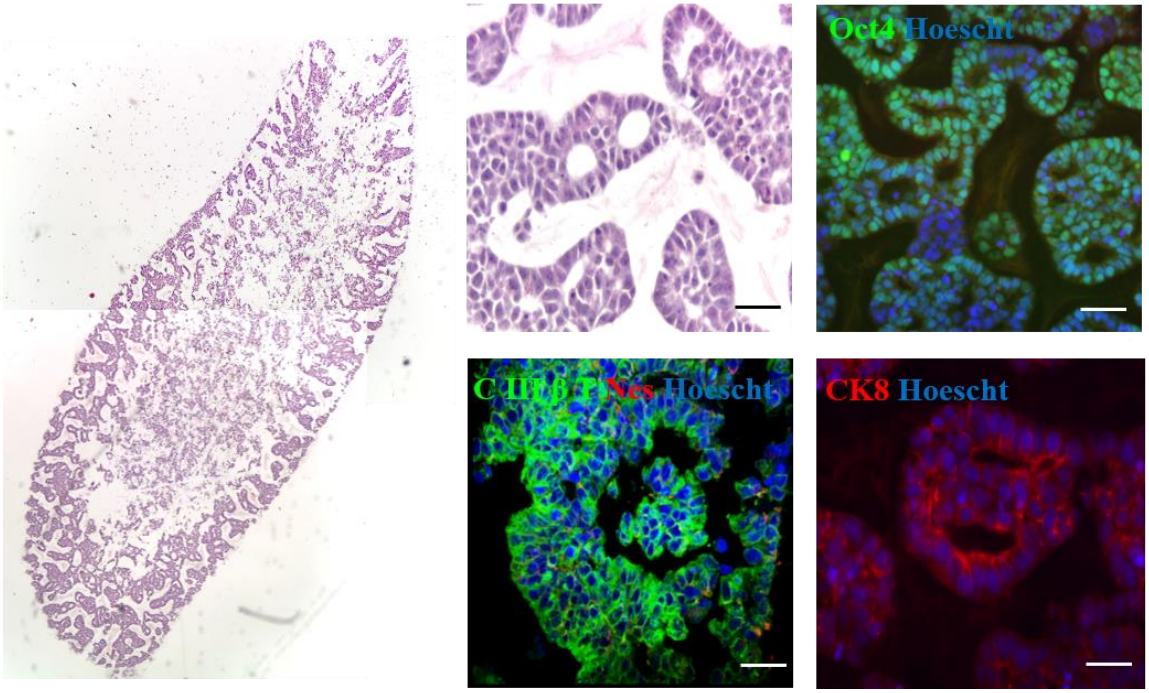


Figure 5.47: Characterisation of TERA2.cl.SP12 cells in perfusion system: TERA2.cl.SP12 cells were prepared in Matrigel as described and cultured in the Polaris Polaris sandwich culture combination in the perfusion system for 7 days. Sections were stained for Oct 4, Nestin, CK8 and Class III β-tubulin. H&E shows that cells grow in a colony-like morphology within the sandwich culture. Cells stain positively for pluripotency marker Oct 4 after 7 days culture in the perfusion system, indicating the persistence of pluripotent cells in the system, as well as the presence of differentiated cell populations. Cells also stain positive for differentiation marker CK8, indicating some movement towards an epithelial phenotype. Scale bar: 50 µm

5.5.4.4 Removal of second insert for perfusion culture is successful, but does not improve on static culture conditions

Due to the fact that the centre of the insert contained a substantial area of cells which were disrupted, the decision was made to remove the second insert from the culture system, due to the fact that this may have been impeding the flow of fluid across the cells to an extent that there was a reduced nutrition and oxygenation. Cells were prepared and seeded as previously described, but without the addition of the second insert on transfer to the perfused system, and maintained for 7 days, with the images in Figure 5.48 showing that culture of TERA2.cl.SP12 in this way is still successful in the perfused system. However, variability was still very present across the insert, with some areas showing the formation of a substantial cell layer, and others showing very few viable cells. MTT assay values reflect the variability more extensively, showing that the use of the same culture conditions in the static setting results in better viability than the perfused culture system. While both culture systems showed some positive neural staining, none showed the ability to maintain pluripotent populations or induce epithelial differentiation.

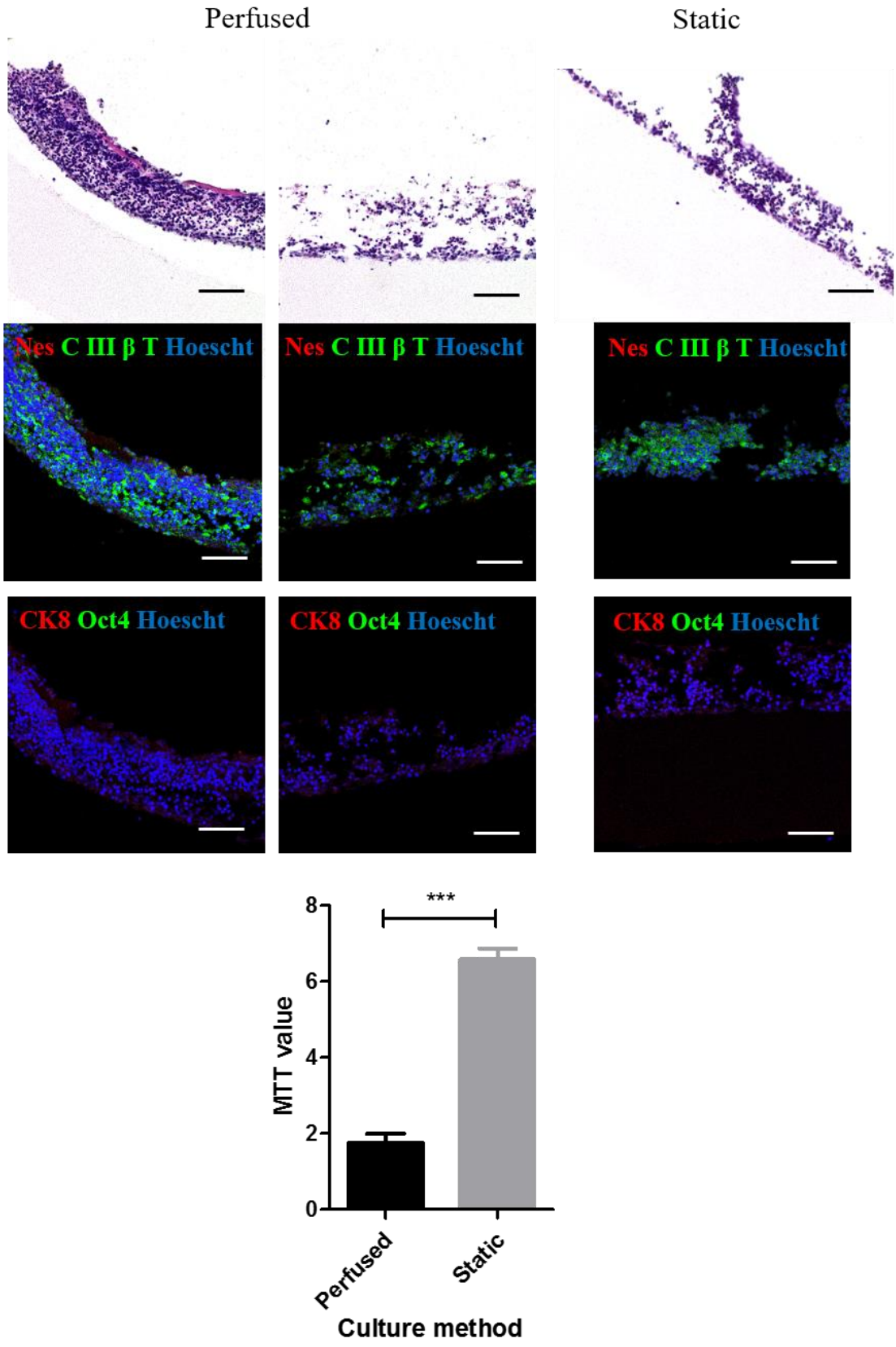


Figure 5.48: Characterisation of TERA2.cl.SP12 cells cultured using a reoptimised culture methodology: Perfusion culture was set up in a similar manner as previously, but without the addition of the top insert when the seeded insert was transferred to the perfusion system. In this case, static culture appeared to result in improved viability, yet perfused culture results in improved structure. Results of MTT assay were found to be significant at $P \leq 0.001$, according to the students t-test. Data represents mean ± SEM from 3 independent experiments (n=3) Scale bars: 100 µm

5.5.4.5 Use of a single insert in the perfusion system without Matrigel results in successful formation of a thick cell layer

Although perfusion culture has shown some success when using Matrigel, the high variability of success is still an issue when attempting to create a reproducible and consistent *in vitro* model. In an attempt to improve the viability and remove a potential source of variation, which could also be interfering with the ability of nutrients and oxygen to access cells, the same culture system as trialled in the previous Figure was used without the inclusion of Matrigel. A pure cell suspension was again seeded onto a Polaris insert, and directly transferred to perfusion after cells had adhered. Figure 5.49 shows that a thick consistent cell layer forms across the insert when this culture method is used, which shows areas of homogeneity. No differentiated structures can be detected initially in the tissue structure, such as neural rosettes and epithelial surfaces, although the cell layer does not appear to have any areas of cell death or disturbance when compared to previous perfused samples. Oct 4 pluripotent areas can also be detected within the perfused sample, indicating an ability to maintain an embryonal carcinoma population also, albeit that the staining is weak. In comparison, the static control shows very little cell proliferation. Neural differentiation is detected through the expression of Class III β-tubulin in the perfused sample, yet there is very little expression in the static sample, as would be expected. Cell viability as assessed by MTT assay shows an increase in viability in the perfused sample, although this is not significant.

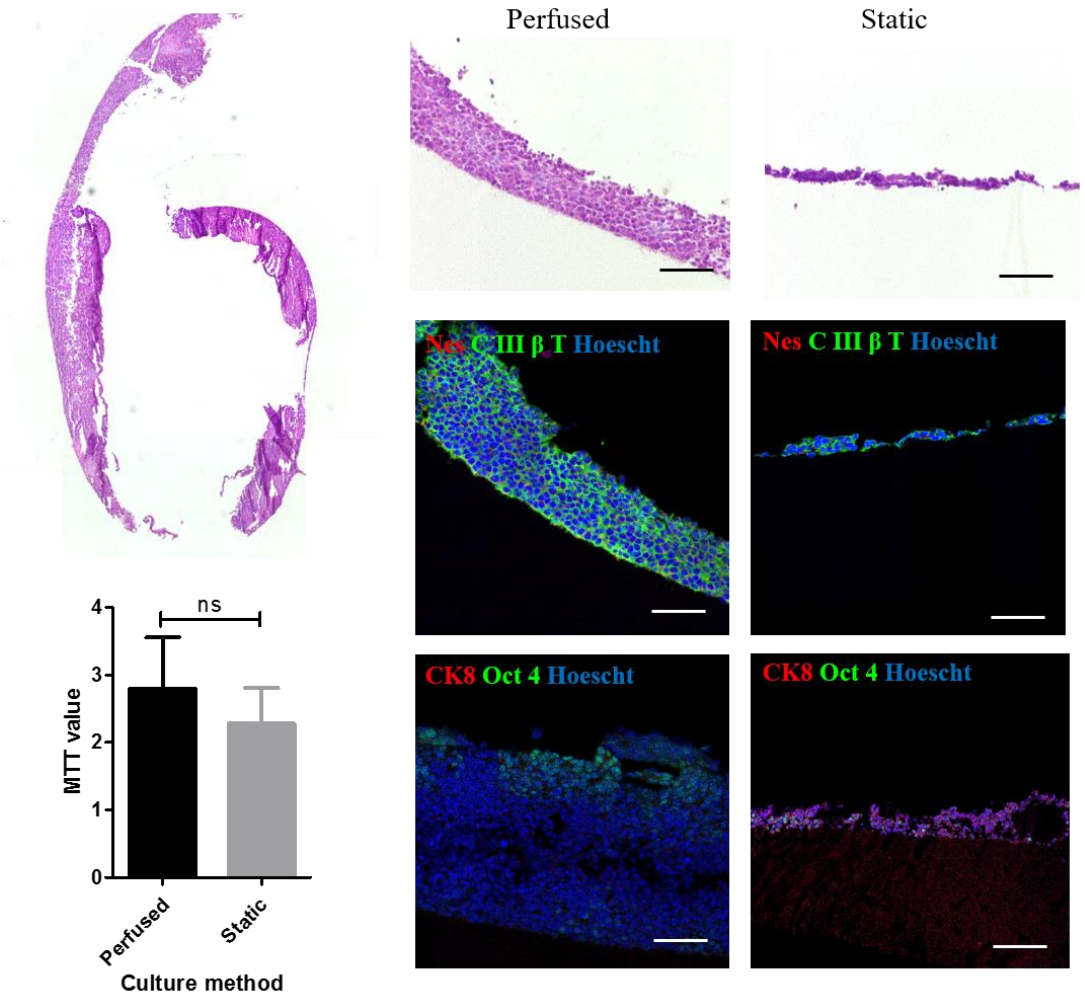


Figure 5.49: Characterisation of TERA2.cl.SP12 cells cultured using a reoptimised culture methodology: Perfusion culture was set up in a similar manner as previously, but without the addition of the top insert when the seeded insert was transferred to the perfusion system. An improvement in the structure and viability of the cultures was observed, and cultured were enhanced in comparison to the static control cultured in a 6 well plate. Results of MTT assay were found not to be significant according to the students t-test. Data represents mean ± SEM from 3 independent experiments (n=3) Scale bar: 100 µm

5.6 Discussion

In this Chapter, the EB based model which was initially developed in Results Chapter 2 was further developed in order to incorporate more physiological cues, with the aim of enhancing the differentiation which occurs in the model. A thorough literature search revealed that two techniques, co-culture and the use of perfusion, have been used in a number of *in vitro* models to increase their physiological relevance, and have previously been shown to affect the pluripotency and differentiation of PSCs. Thus these two factors were introduced separately into the current EB based model and investigated.

5.6.1 The use of an established dermal fibroblast model to undertake proof of concept co-culture studies

Due to the ubiquity of fibroblasts *in vivo*, their multiple roles in the maintenance of tissue homeostasis, including ECM deposition and providing paracrine signalling cues, and their extensive use in many other co-culture studies in the literature, this cell population was deemed as appropriate for a co-culture model of human development and differentiation. These key fibroblast properties are replicated in fibroblasts regardless of origin (Kusindarta and Wihadmadyatami, 2018), a factor which allows for the use of any somatic fibroblast population in the model to create an ECM and provide signalling cues. There are few co-culture studies in the literature specifically regarding the use of EBs in a co-culture situation, although some tumour biology studies involving the culture of tumour spheroids in a fibroblast filled hydrogel share similarities in the aim of creating a more physiologically relevant environment to recapitulate cell responses (Jeong et al., 2016). Due to the infrequent nature of these studies, initially basic proof of concept studies were needed in order to ensure co-culture could be successfully undertaken. Within the laboratory, a human dermal fibroblast based co-culture model of human skin has recently been developed, which has been shown to successfully support the culture and differentiation of human keratinocytes (Roger et al., 2019), examples of which can be seen in Figure 5.16 and 5.17. Dermal fibroblasts are used extensively in organotypic *in vitro* skin models, as well as other *in vitro* modelling situations including vasculogenesis by endothelial cell populations (Sorrell et al., 2007) and tumour biology studies (Flach et al., 2011), making this cell population a suitable choice due to its broad usage. The use of this Alvetex® based model reduces the need to incorporate other culture techniques and methods in addition to the fibroblasts, such as hydrogels, therefore limiting the novel cues in this version to the introduction of the fibroblast population and its subsequent secretions.

Initial optimisation ensured that the human dermal fibroblast properties and ability to create a supportive ECM were retained during culture in an alternative, more cost effective media which was also used as the basis for TERA2.cl.SP12 maintenance media. The HDFns used in this study are commercially available primary cells, and M106 is a synthetic media with a very low serum content

of 2 % ("Low Serum Growth Supplement (LSGS) and LSGS Kit," 2019), whereas the DMEM based media is supplemented with 10 % FBS, highlighting the fact that the nutritional support provided by each would be significantly different, which would naturally impact on cellular growth and function. Immunostaining and assessment of viability and population doubling time in the two different media types confirmed the suitability of the DMEM based media, as would be expected given the wide range of media that is used to support fibroblasts *in vitro*, and even highlighted the benefits of the DMEM based media with a reduced population doubling time. This suitability was also confirmed through the culture of HDFns in Alvetex® Scaffold inserts in the DMEM media. This was completed using 6 well inserts (the skin model mentioned previously uses the smaller 12 well inserts) in order to allow for comparison with the other versions of this model and facilitate any potential transfer to other culture systems later in the project. HDFns showed the ability to successfully form a dermal equivalent compartment in the Scaffold, still forming a consistent barrier across the top of the insert and significant homogenous ECM deposition. The increased population doubling time is likely to have compensated for the difference in media support during the culture period compared to the culture of the skin model.

Seeding of TERA2.cl.SP12 EBs on the surface of the dermal equivalent tissue was successful, as the EBs were maintained during the 7 day culture period and were visible following histological analysis, showing little infiltration into the insert as is observed with keratinocytes in the skin model. This was the case with both treated and spontaneously differentiating EBs. Although the dermal fibroblasts are able to create a continuous barrier, that fact that stem cells are naturally migratory, particularly during the events of embryonic development (Lopez-Lazaro, 2015), and that EC cells such as TERA2.cl.SP12 are tumorigenic in nature could have posed a potential problem in the formation of this co-culture system. However, this was not the case, and the full tissue disc structure was preserved on the top of the dermal equivalent. The phenotype of the tissue discs in this co-culture was of particular interest. All three EBs showed differences in the histology of the tissue disc when compared to the original model with varying cell and tissue morphologies, generally displaying a looser structure in all cases. This was further confirmed through the immunostaining for the four selected markers. While all three stained positive for the mature neural marker Class III β-tubulin, and there was some evidence of epithelial differentiation in the presence of cytokeratin 8 positive staining, all three tissue discs also stained positively for the pluripotency marker Oct 4. This is particularly interesting when previous results from Results Chapter 4 are considered, as tissue discs which were both directed in their differentiation and allowed to spontaneously differentiate showed little staining for Oct 4, with only weak positive staining in the histology of the tissue disc in Figure 4.15 and very low flow cytometry results for Oct 4 positive cells. The presence of significant pluripotent areas, particularly in the tissue disc treated with the potent neural inducer EC23, suggests a phenotype more closely resembling that of the teratocarcinoma as seen in Chapter 4, which contains both pluripotent and differentiated areas.

5.6.2 Development of a relevant, novel co-culture model to enhance the differentiation of PSC derived EBs

The established HDFn dermal equivalent model provided an opportunity to assess whether the co-culture of EBs on a fibroblast compartment would be possible, and whether this elucidated any effects in the tissue disc that subsequently formed. This proved to be the case, and a more relevant co-culture system was developed. Although the analyses in Chapter 3 indicated that the modal response for mouse strain used in the teratoma assay, around a quarter of cell lines, did not provide information regarding the mouse strain used, the use of SCID type strains combined totalled almost 45% of all of the assays (SCID, NOD/SCID, SCID/Beige). Therefore, in line with the popularity of SCID mouse populations, dermal fibroblasts isolated from a SCID mouse were used to create a dermal compartment as previously completed using the HDFns. As shown in Figure 5.24, SCID mouse fibroblasts were a heterogeneous mixed population of fibroblasts and myofibroblasts, as would be found in the dermis *in vivo* (Sorrell and Caplan, 2004; Stunova and Vistejnova, 2018), and did not create a sufficient dermal compartment unless supplemented with ascorbic acid and TGF-β in the same way as HDFns. Ascorbic acid and TGF-β are known to induce proliferation and ECM deposition in human fibroblasts (Clark et al., 1997; Phillips et al., 1994; Russell et al., 1981), and the histology shows a similar effect occurs here when comparing Figures 5.25 and 5.26, with improved scaffold infiltration and barrier formation. The derivation of a mixed fibroblast population is advantageous due to this being more representative of the diversity and heterogeneity found in the *in vivo* environment (Driskell et al., 2013; Sorrell and Caplan, 2004). TERA2.cl.SP12 EBs were subsequently cultured on the surface of the SCID fibroblast dermal equivalent, again, with interesting results. All three tissue discs, treated and untreated, showed evidence of changes in morphology and structure, as can be detected in the histology, as well as phenotype through immunostaining. Again, EBs which were treated with a potent morphogen, EC23, showed heterogeneous structures and evidence of pluripotency within the resultant tissue disc which formed on the SCID fibroblast dermal equivalent. This was also true of the BMP-2 treated EB, with the resulting tissue disc showing a very different structure to that previously identified on Alvetex® Polaris, and a presence of Oct 4 positive cells. These examples are again reminiscent of the TERA2.cl.SP12 teratocacinoma, perhaps more so than the model developed in the previous Chapter.

5.6.3 The impact of fibroblasts on PSC derived tissue discs

The effects of co-culture on the morphology and identity of the TERA2.cl.SP12 tissue discs is clear, as is the fact that both the human and mouse fibroblasts were able to elicit these changes. The data suggests that the enhancement of the cellular microenvironment through the introduction of more signalling cues with the fibroblasts has resulted in this phenotype, yet the ability of both fibroblast populations to induce such strong Oct 4 expression, and particularly in the morphogen differentiated tissue discs, is of high interest.

In feeder based systems, human ES and iPS cell populations are maintained on mitotically inactivated murine embryonic fibroblasts (MEFs), a practice which indicates that fibroblasts have an important role to play in the maintenance of cellular pluripotency. Human pluripotent stem cell populations respond to specific morphogens for the maintenance of pluripotency *in vitro*, one of which is basic Fibroblast Growth Factor (bFGF, also known as FGF-2, see Chapter 6 for more details on the pathways involved in the maintenance of pluripotency in human PSCs). This is synthesised by fibroblasts (Nickel, 2011), and is added to the media in feeder free systems to maintain pluripotency. Morphogens such as bFGF could be responsible for the effects observed in the model here, as other studies have also shown that this molecule is involved in the dedifferentiation of keratinocytes (Sun et al., 2011) and oligodendroglia (Grinspan et al., 1996). Studies investigating the impact of fibroblast identity on the maintenance of cellular pluripotency and the development or differentiation of embryos revealed that the co-culture of bovine embryos with MEFs or murine mesenchymal stem cells (MSCs) resulted in a lower hatching, i.e. less embryos progressed to the next developmental stage, compared to those that were not maintained in a co-culture system (Ascari et al., 2018), indicating the role of fibroblasts in maintaining pluripotency or an undifferentiated state, and contributing further support to the effects noted in the co-culture model in this Chapter. Additionally, in stratified epithelial tissues such as skin, the resident stem cell population is found at the base of the stratified structure, in closer contact with the fibroblast layer and responsive to these signals (Alberts et al., 2002; Blanpain and Fuchs, 2008), indicating another mechanism by which the fibroblasts in the co-culture system could be influencing the tissue discs.

While fibroblasts used to maintain human PSC populations are usually embryonic, the use of MSCs by Ascari et al and the seemingly similar results obtained here (in terms of promotion of an undifferentiated state) suggests a similarity between these cell types, with more recent work suggesting that fibroblasts may simply be aged MSCs which are not quite as efficient at various MSC activities (Soundararajan and Kannan, 2018). This theory suggests that there could be some homogeneity in the responses of fibroblasts if these are derived from a single (MSC) population, and that fibroblasts are also able to elicit a similarly homogenous response in target cells regardless of origin or age – this appears to be the case from the examples found in the literature and the populations used in this study; embryonic populations in the literature, and both neonatal and adult fibroblast populations used in this study all resulted in the promotion of a pluripotent state. It would be expected that there would be differences in the products synthesised and secreted by different fibroblast populations, for example, aged fibroblasts are known secrete more inflammatory cytokines (Coppe et al., 2014) and senescent factors, but further investigation into the cytokines secreted by these populations and their subsequent effects need to be conducted in order to confirm this.

The homogeneity of fibroblast effects has also been shown to be the case using irradiated HDFn and irradiated MEF to maintain and expand human keratinocytes, with favourable results obtained for each (Bisson et al., 2013). Studies such as this also illustrate that the importance of species specific feeder layers is also less crucial than perhaps thought (an idea already highlighted through the use of

murine embryonic fibroblasts to maintain the pluripotent state in human PSCs), and rendering the idea that the two different fibroblast populations used in this study could elicit similar responses quite plausible. It should be noted, however, that although the general morphology and expression between the two fibroblast systems was similar, the HDFn fibroblasts elicited increased Oct 4 expression in the TERA2.cl.SP12 tissue discs compared to the SCID fibroblasts, possibly due to improved cytokine-receptor interaction between the two human populations compared to the mouse cells. Although there is homology between many genes and proteins between the species, human cells would naturally produce an improved reaction. Expression of the transcription factor was stronger and more widespread within the structures, suggesting that there is some significance in the use of species specific fibroblast populations in *in vitro* models, and suggesting that effects such as these could have impact in the formation of a teratocarcinoma during a teratoma assay.

While the effects different fibroblast populations have on PSCs in noted here, the fact that EC cells do not usually require feeder cells for the maintenance of pluripotency cannot be forgotten nor can the fact that cells within a terminally differentiated population were encouraged to revert to an undifferentiated state (in particular the EC23 treated EBs). That said, EC cells, specifically a TERA-2 subclone, have been shown to respond to collagen gels and FGF gradients, growing in tight colonies resembling the pluripotent state and migrating towards the source of FGF (Alanko et al., 1994), explaining in part the pluripotent phenotype established in these models. Further experiments by Tienari have shown that the addition of exogenous bFGF to TERA-2 cultures previously treated with retinoic acid results in an increase in the number of cells proliferating and expressing the proliferation marker Ki67, more so than when compared to RA treated control TERA2 cells and undifferentiated cells (Tienari et al., 1995). While the study by Tienari was conducted on 2D cells, this result is highly similar to that observed here, with treated tissue discs in particular showing an increase in Oct 4 positive areas, and further confirms the validity of the observed effects and the notion that these differentiated tissue discs have been reverted in part to a more pluripotent or undifferentiated state. This phenomenon has also been observed previously through the subculture of differentiated cells from an iPSC derived teratoma in human PSC media containing bFGF, with undifferentiated cells appearing in culture over time (Kumazaki et al., 2014).

EC cells are also tumorigenic in origin and nature, and it has been extensively shown that co-culture systems involving tumour cells and fibroblast populations show improvements in tumour cell survival, even in the presence of therapeutic drugs. Of particular interest are those where tumour spheroid survival and expansion was improved in co-culture with fibroblasts (Jeong et al., 2016). The increase in the expression of the pluripotency marker Oct 4 represents a maintenance of the EC cell phenotype, which are the tumorigenic counterpart of ES cells and the malignant aspects of the teratocarcinoma tumour (Andrews et al., 2005).

5.6.4 The optimisation of the novel perfusion system

The literature review at the beginning of this Chapter outlined the impact of perfusion on the pluripotency and differentiation of PSCs and the opportunity to develop a novel benchtop bioreactor system for the creation of PSC derived tissue constructs. The bioreactor developed in this chapter had elements from both stirred suspension bioreactors and flow through bench top bioreactors, using a magnetic stirrer to induce media recirculation in the system. Optimisation was undertaken, with a number of prototype stands tested to assess media recirculation and fluid flow; this type of optimisation is not required for other flow through type bioreactors due to the fact these have more sophisticated, often technology based, fluid flow control systems, but the inherent simplicity and customisability of this novel system required more optimisation of the technical aspects. The fluid flow and distribution in the system was analysed via photography, calculation of White Intensity as a proxy for dye recirculation and using Particle Image Velocimetry. These analyses revealed that funnel design holders provided better recirculation and dye redistribution than the table style holder due to the ability to direct the recirculated fluid back up into the main vessel. The clockwise distribution design in particular showed excellent recirculation and redistribution with the device in place, most likely due to the fact that the magnetic stirrer in the base of the vessel also rotates in a clockwise direction. However, this system also showed the most turbulence. A minor refinement to the system through increasing funnel height to reduce turbulence from the magnetic stirrer resulted in an improvement in turbulence in the system while maintain the previously established desirable fluid flow properties. Brief toxicity testing confirmed the suitability of the PTFE material that the funnels were made of. Although the substance is generally accepted as non-toxic and non-reactive, its uses in cell culture have previously been very limited (Anamelechi et al., 2005; Garland et al., 1999).

Optimisation of the biological components of the system involved the culture of TERA2.cl.SP12 EBs in sandwich culture between two Alvetex® inserts. This culture set up is used extensively in hepatocyte perfused cultures to protect cells from hydrodynamic damage and severe shear stress (Xia et al., 2012, 2009) as well as provide support and a defined growth area. While PSCs are known to differentiate in response to shear stress as a mechanical cue (Wolfe et al., 2012; Wolfe and Ahsan, 2013), the decision was made to use sandwich culture in order to reduce the impact of this additional cue and focus mainly on the effects of media perfusion, with the option to investigate shear stress further when/if possible. The testing of all combinations of Alvetex® in static resulted in only one combination, using two Polaris inserts, which was able to preserve the entire tissue disc structure, which is not entirely unexpected when the previous interactions of the stem cells EBs and the Alvetex® inserts are considered. The infiltration of the EBs into the upper insert as well as the lower inserts was highly unexpected, and another potential issue to deal with when undertaking perfusion culture, further confirming the use of two Polaris inserts. Static sandwich culture using two Polaris inserts actually enhanced the neural differentiation significantly within the EB, but did not show and pluripotency or epithelial differentiation: this phenotype is similar to that previously observed in

Chapter 4: TERA2.cl.SP12 EBs on Polaris showed mainly neural differentiation with a weakly positive area of Oct positive pluripotent cells. However, the use of EBs in the perfused system did not prove to be successful at all, with evidence of a highly heterogeneous tissue disc morphology, with some areas highly flattened and others highly disturbed and fragmented. This morphology is not consistent with the formation of complex structures, and could not be used as a basis for the model. In the literature, EB based fluid flow systems use EBs in stirred suspension culture rather than fixed cell culture techniques (Lancaster and Knoblich, 2014b; Lei et al., 2014; Shafa et al., 2011; Wu et al., 2014) and as other flow through perfusion systems using solid scaffolds have used cell suspensions, the decision was made to reoptimise the model using a cell suspension. Although EBs are more useful due to their ability to allow cells to undergo lineage commitment and provide a basis for the formation of structure (Desbaillets et al., 2000b; Dvash et al., 2006; Eiraku et al., 2011; Takasato and Little, 2016), the teratoma assay uses a single cell suspension for the formation of a large, complex tumour, so this format of cell preparation is logical.

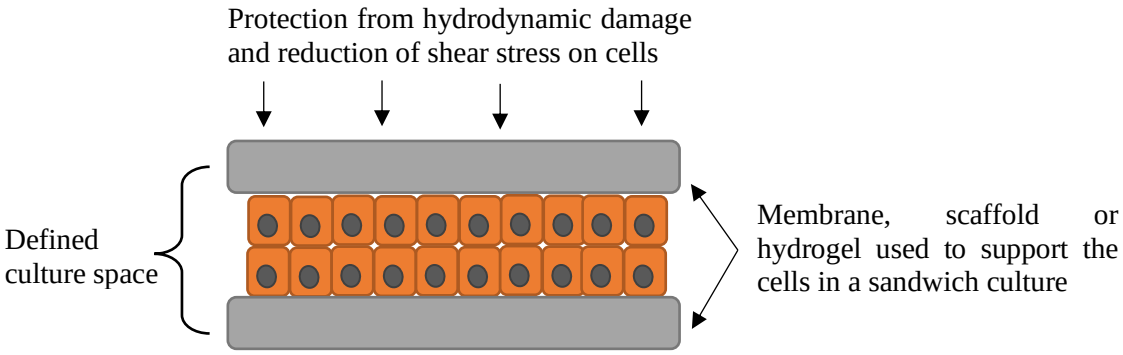


Figure 5.50: The benefits of sandwich culture techniques: Sandwich cultures can be created using solid scaffolds, hydrogels and porous membranes, offering a number of advantages in the perfused culture set up, including a defined culture space and a reduction in shear stress on the cells in culture.

As Matrigel is also used in the teratoma assay, this was used to provide support for the PSCs and encourage successful attachment, proliferation and differentiation as have been seen in the teratoma assay and in other *in vitro* techniques (Hentze et al., 2009; Kaiser et al., 2019; Lam and Longaker, 2012; Prokhorova et al., 2009). Use of a range of densities in static showed that the lowest seeded cell densities formed the thickest cell layers, with these showing the highest viability also. This was not replicated in the perfused system, where the middle values of 1 and 2 million cells showed the highest viability and best overall structure. Further investigation into the value of 2 million cells showed the ability, on occasion, to form highly organised colony like formations. However, heterogeneity was still evident across the insert as well as between inserts. There was a large space in the centre of the cell mass which was disturbed, and showed a fragmented morphology; this was problematic due to its effects on the structure of the cells within the sandwich culture and potential paracrine effects on the rest of the membrane. The upper insert was removed, in order to improve the fluid flow through the system and therefore nutritional and oxygen support, as well as resembling the cell seeding systems used in other flow through bioreactor systems – a single porous scaffold. This improved the structure of the cell layer in part, but still resulted in heterogeneity across the

insert, with areas of density and areas with little cellular material. As Matrigel is a cell derived product which shows lot to lot variation in proteins and growth factors (Caliari and Burdick, 2016), and may show variation across the insert on application and gelling, this also was removed from the culture set up. Matrigel also introduces exogenous signalling cues to the PSCs in the system, which has been shown to influence the differentiation of the PSCs in a manner which cannot be fully controlled (Massumi et al., 2012; Ojala et al., 2012; Patel and Alahmad, 2016) and is commonly used in feeder free maintenance systems in place of inactivated MEFs (Stover and Schwartz, 2011). The removal of the Matrigel resulted in much more homogenous proliferation and differentiation across the insert, with a thick cell layer showing good neural differentiation, some maintenance of pluripotency and an improved viability compared to the static control. This could be due to the fact that the removal of the Matrigel also allowed the cells to be exposed to the constant changes in the surrounding media as a result of the continuous fluid flow, which the hydrogel may have been masking prior to this.

5.6.5 The impact of fluid flow and perfusion on the pluripotency and differentiation of PSCs

The introduction of fluid flow and perfusion to PSCs in the three dimensional model resulted in a number of different outcomes. When PSC derived tissue discs were exposed to these novel cues this resulted in the adoption of an abnormal morphology or destruction of the tissue disc structure itself, most likely due to the fact that structures not usually exposed to large scale fluid flow in this manner are not suited to applications involving this microenvironmental feature; EBs usually exposed to media perfusion in this way are permitted to move in the culture vessel, whereas the adherence of the EBs to the scaffold may have caused increased stress within the structure. While the use of Matrigel with a cell suspension resulted in the successful formation of colony like structures which showed evidence of pluripotency and differentiation into multiple phenotypes, this could have been in part due to the effects of Matrigel on PSCs, both in terms of pluripotency and differentiation rather than the actual perfusion and recirculation of the media. The fact that a more homogenous cell layer was achieved which showed weaker staining for Oct 4 on removal of Matrigel suggests that the Matrigel was both influencing the phenotype of the cells and possibly masking mechanical and chemical cues provided by the perfusion system. These optimisation experiments have shown that the novel system can be used to successfully maintain PSCs and achieve a thick tissue structure showing signs of differentiation, but have only been undertaken for short periods of time with a single PSC population. Successful examples in the literature such as the experiments performed by Stachelsheid were conducted over several weeks in order to allow complex structures to form, indicating the direction and duration that the next studies involving this system and other cell populations should take. Longer term studies can be undertaken due to the large media reservoir, with the aim of achieving more complex and mature differentiation.

5.7 Conclusions

The aims of this chapter were to investigate and incorporate two separate physiological cues into the model developed in the previous Chapter.

The impact of other cell populations on any cell in the *in vivo* environment are myriad, and include the secretion and maintenance of the surrounding ECM and the secretion of paracrine signals. Co-culture with human dermal fibroblasts was successfully introduced into the model with TERA2.cl.SP12 tissue discs, and differences in tissue disc morphology and cell identity were observed. Similar increases in pluripotent cells and changes in tissue disc structure, including a looser structure and more heterogeneity, were observed on the introduction of a more relevant SCID fibroblast dermal population to the TERA2.cl.SP12 tissue discs. These changes to the tissue disc structure are induced by the presence of the fibroblasts, linking to their impact on cellular pluripotency and tumour cell survival, with the resulting tissue disc showing similarities to teratocarcinomas formed from the same cell line.

The introduction of perfusion to the model has also resulted in an impact on the morphology and identity of the cells cultured in the system. In the *in vivo* environment, vasculature maintains a constant nutrient supply and oxygenation of cells and tissues, which is achieved *in vitro* through the introduction of fluid flow and media recirculation. In the model, this also results in the maintenance of pluripotency and the enhancement of stem cell structure when a single cell suspension is used in combination with Matrigel, as well as differentiation towards ectodermal lineages by the TERA2.cl.SP12 cells. Removal of the Matrigel and the sandwich culture set up resulted in an improvement in viability compared to the static controls and more homogenous proliferation and differentiation across the insert. The EB based tissue disc model was not compatible with the perfusion system; although spontaneous EB differentiation was enhanced through the use of sandwich culture alone without perfusion, these structures could not be maintained in the novel bench top bioreactor.

The enhancement of the microenvironment in this Chapter using these methodologies allows for multiple versions of the model depending on the requirements of the developmental process to be studied. Currently, the model has only been tested using human EC cells, but the success with the original version in improving EB viability and differentiation and the two versions presented in this Chapter in enhancing the phenotype of the PSC derived structure indicate that the model can now be trialled using a more relevant cell line

6. The application of novel technologies to enable the formation of rudimentary tissue structures from mammalian PSCs

6.1 Introduction

Populations of embryonal carcinoma cells are a robust tool for the study of human development and the optimisation of novel culture practices using PSCs, however these cells are ultimately not truly representative of the pluripotent phenotype due to their often restricted differentiation capacity. To understand and appreciate the responses of PSCs in *in vitro* models of differentiation, true PSC populations must be used.

6.1.1 EC cells: a truly pluripotent population?

As the first pluripotent stem cell lined successfully derived and cultured *in vitro*, embryonal carcinoma cells have naturally been used extensively in the study of developmental processes and pluripotency (Martin, 1975; Przyborski et al., 2004; Stevens, 1970), with lines such as P19 and N-TERA2 having been used to elucidate the events involved in cardiomyocyte differentiation (van der Heyden and Defize, 2003) and neurogenesis (Pleasure and Lee, 1993; Przyborski et al., 2000) respectively. While considered by many to be the 'malignant counterpart' to embryonic stem cells (Andrews et al., 2005), these cells display the typical hallmarks of pluripotency, including the ability to self-renew and produce differentiated progeny from the three primary germ layers and as such are, according to this definition, a pluripotent stem cell population (Asprer and Lakshmipathy, 2015).

EC cells, however, are not indistinguishable from their ES cell counterparts, with a number of subtle differences in behaviours and expression profile separating the two cell types. Their source of origin, for example, reveals the true embryonic nature of ES cells as cells derived from the blastocyst, and the malignant tumorigenic nature of EC cells, which are derived from germ cell tumours (teratocacinomas). Andrews described EC cells both as 'similar to' and a 'caricature of' ES cells, noting that many EC cells *in vitro* are limited in their differentiation capacity, or are even nullipotent – unable to produce differentiated progeny (Andrews et al., 2005), an example being 2102Ep (Duran et al., 2001), a human testicular carcinoma cell line. These differences in differentiation capacity can be a result of karyotypic abnormalities acquired during their rapid expansion and natural selection for survival as tumour stem cells (Mueller et al., 2006), or the simple fact that genes which promote survival may reduce differentiation capacity. It is not unusual for EC cell lines to have an abnormal number of chromosomes. A characterisation study of 4 different human embryonal carcinoma cell lines revealed modal chromosome numbers ranging from 45 to 72, some of which were consistent to a specific cell line, two of which showed wide variation (Sekiya et al., 1985). EC cells have also been shown to display differences in metabolic signatures (Dawud et al., 2012), with differences in cell membrane components and intermediate proteins in the tricarboxylic acid cycle, suggesting

differences in cell metabolism. It has been posited that the prolonged culture of ES cells *in vitro* can result in some of the genetic and functional changes associated with EC cells, as the ES cells become adapted to culture conditions and an inadvertent selection process takes place, including the accumulation of mutations found in tumour stem cells, such as mutations in the p53 gene (Merkle et al., 2017).

Although EC cells display an expression profile that is typically associated with pluripotent stem cell populations, ultimately their tumorigenic origins predispose these cells to the acquisition of mutations and survival promoting traits which may interfere with their pluripotent stem cell properties and therefore experimental outcomes. While these cells offer an option for use in selected model systems and for the optimisation of novel culture techniques, true pluripotent stem cell populations must be used if a more thorough understanding of pluripotency and differentiation is to be gained.

6.1.2 Alternative pluripotent populations: mouse pluripotent stem cells

The potential flaws and limitations of EC cells in PSC based models have been acknowledged, but the simple culture requirements of these cells make them an attractive tool in the study of human tissue development. The complex requirements of other human PSC populations, including the need for specific coating matrices and a cocktail of cytokines to maintain the pluripotent state, can be a deterrent when undertaking certain experiments, especially during the development of optimisation of new technologies as proposed herein. Murine pluripotent stem cells offer an alternative study population from which to elucidate the events of human development and further test the capabilities of novel culture systems.

The first pluripotent stem cell population derived was a murine EC population (Evans, 1981), with human EC cells derived following the optimisation of derivation techniques and culture practices. The same is true of the derivation of embryonic stem cells and induced pluripotent stem cells: murine populations were successfully derived and cultured (Evans and Kaufman, 1981; Takahashi and Yamanaka, 2006) before attempts were made to derive human populations from the same source (Takahashi et al., 2007; Thomson et al., 1998). Thus, murine PSC populations have long been used by the stem cell field in conjunction with human PSCs for comparison and the development of culture practices. Many of the hallmarks of cellular pluripotency in human PSCs are replicated in murine pluripotent stem cell populations. Murine PSCs are of a small cell size, with prominent nuclei, a high nuclear to cytoplasmic ratio, stain positively for alkaline phosphatase activity and show the ability to differentiate into the three germ layers both *in vitro* (EB and directed differentiation) and *in vivo* (teratomas, germ line transmission and tetraploid complementation) (Pauklin et al., 2011). While expression of the key pluripotency associated transcription factors Oct 4, Sox 2 and Nanog is high, consistent with that seen in human PSCs, there are some differences in extracellular marker

expression. Murine PSCs are positive for the extracellular marker TRA-1-60 and the murine specific PSC marker SSEA-1 (Tielens et al., 2006), but do not express SSEA-3 or SSEA-4 (Fenderson et al., 2006), mimicking the phenotype and expression profile of cells from the murine blastocyst. There are also subtle differences in the pluripotency and developmental potency of murine PSC populations when compared to human PSCs of the same nature. The signalling pathways which maintain the pluripotent state within these cell types differ significantly; mouse PSCs rely on the inhibition of the FGF/ERK pathway and the activation of the LIF/JAK/STAT signalling pathway to maintain pluripotency. Conversely, human PSCs require the activation of the FGF/Activin pathway (Rossant, 2015). There is a suggestion that human PSCs potentially represent a 'primed' pluripotent state, further along the lineage commitment pathway and thus prepared for differentiation, whereas mouse PSCs are thought to be more 'naïve', representing an earlier more pluripotent stem cell population from the developmental process (Davidson et al., 2015). Naïve PSCs are those which have both an unlimited capacity for self renewal and are fully pluripotent, able to contribute to all somatic cell types including the germline (Kumari, 2016). Primed PSCs are also able to self renew, but their differentiation capacity is restricted to the three germ layers only: this population is unable to give rise to germline chimeras in *in vivo* experiments (Kumari, 2016). This is considered by some to be dependent on culture conditions as much as being an actual species difference, and the naïve state has been induced in some human PSC populations, but further studies need to be conducted in this area to confirm this as well as exploring the differences between these two states (Davidson et al., 2015). While differences in pluripotency may not always directly affect experimental outcome, it is

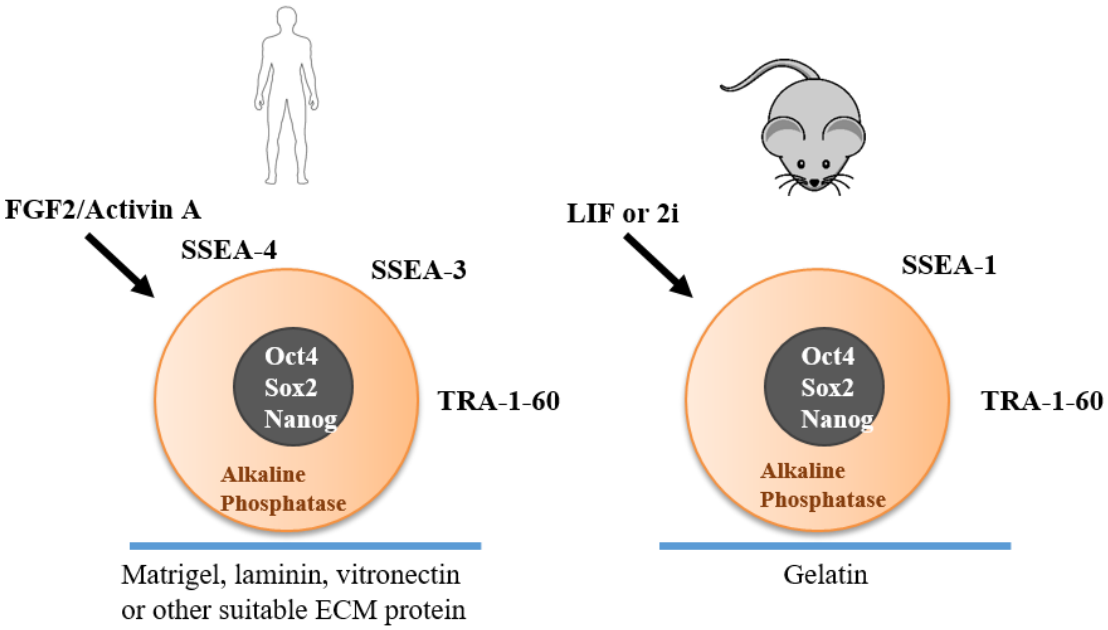


Figure 6.1: Phenotype and culture conditions of human and mouse PSCs: Human and mouse PSC populations are phenotypically similar, with both expressing key transcriptional and extracellular markers of pluripotency, but showing some species specific differences, notably in SSEA antigen expression. The culture requirements for maintaining pluripotency in the two cell lines depend on the signalling pathways involved in this state.

important to note these differences when undertaking work with both cell populations.

The logistics of murine PSC culture are also of note, with their requirements being simpler to manage than human PSCs, a feature which adds to their attractiveness as a model for the study of developmental processes. Murine PSCs can be maintained in the pluripotent state through culture on inactivated feeder layers as human PSCs have previously been, as well as being able to be cultured using feeder free systems based on the use of fetal calf serum, Leukaemia Inhibitory Factor (LIF) and a gelatin coating or two small molecule inhibitors, such as CHIR99021, PD0325901 (commonly known as the 2i method) (Tamm et al., 2013). Both of these methods activate the LIF/JAK/STAT pathway to maintain the pluripotent state. The simplicity of these culture systems and relatively inexpensive nature compared to the costs incurred when using feeder free systems which rely on costly chemically defined media to culture human PSCs allows for larger scale studies and the testing of novel practices in murine populations before transfer to human PSCs.

6.1.3 Comparing mouse and human developmental processes: the use of murine PSCs in developmental studies

The conservation of key signalling pathways between species is well recognised, a fact which is even more pronounced between species within the same phylogenetic Class, including mice and humans. Although the differences in organism size are striking, the inherent processes which govern the development of these organisms during gestation are highly similar and as such much can be learned from the study of murine development using PSCs.

The early phases of embryogenesis in particular, gastrulation, the formation of the anterior posterior body axis, somite formation and limb bud development are very similar in terms of mechanism (Rossant, 2015); many of these were studied and elucidated in depth using model organisms and surrogate methods including mouse PSCs before confirmation of the human developmental process. These embryonic stages are known as the phylotypic phase, during which the activity of evolutionarily conserved genes control the patterning process, leading to the fundamental organisation of the body plan, which is also conserved between organisms (Irie and Kuratani, 2014). Events up to this point and the subsequent differentiation of these progenitor populations into functional, mature adult tissues are points at which more variation is understood to exist in the developmental process. This is due to the fact that genes involved in the phylotypic phase, such as the Hox gene family, are highly conserved between species and those involved in later and earlier developmental events are not (Irie and Kuratani, 2014; Rossant, 2015). This ‘hourglass model of development’, see Figure 6.2, is thought to explain in part why there are subtle differences detected between human and mouse ESCs, as the cells are normally derived from the pre-implantation blastocyst, which is before the phylotypic stage, and so more variable.

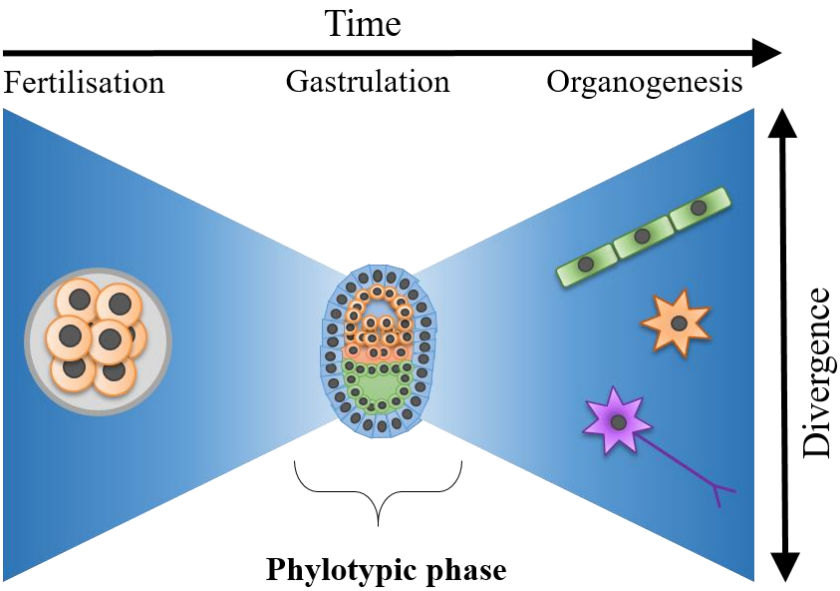


Figure 6.2: The hourglass model of development: The hourglass model predicts that the stages considered to be mid-embryogenesis, the phylotypic phase, represent the period of the processes which is the most conserved. It is considered to be the basic body plan for species within the same taxonomic phylum. Adapted from Irie and Kuratani, 2014.

However, it should not be concluded that a lack of complete conservation in latter developmental processes, mainly those involved in organogenesis, prevents the use of murine PSCs to study the differentiation of mammalian, and by extension human, tissues. There are differences in signalling pathways and cascades involved in the differentiation of the two species, but there are also significant areas of crossover in the maintenance of pluripotency and differentiation, as can be observed in the selection of signalling pathways detailed below (see Figure 6.3). Many of the signalling cascades involved in the maintenance of pluripotency and self-renewal, Oct3/4, Smad2/3, PI3K and Nanog are highly conserved, with their activities almost identical in the two species (Schnerch et al., 2010). The trophoectodermal and neuroectodermal differentiation pathways shown here also demonstrate congruency, possibly due to their involvement in early lineage commitment events, through the modulation of Oct3/4 and Wnt pathways respectively. The differentiation based signalling pathways detailed show some differences in the lineage to which cells commit, such as the BMP-4/Smad1/5/8 directing cells towards trophoectoderm in humans and mesoderm in mice, but only a selection of the canonical pluripotency pathways and key differentiation mediating cascade involved in these processes are shown here.

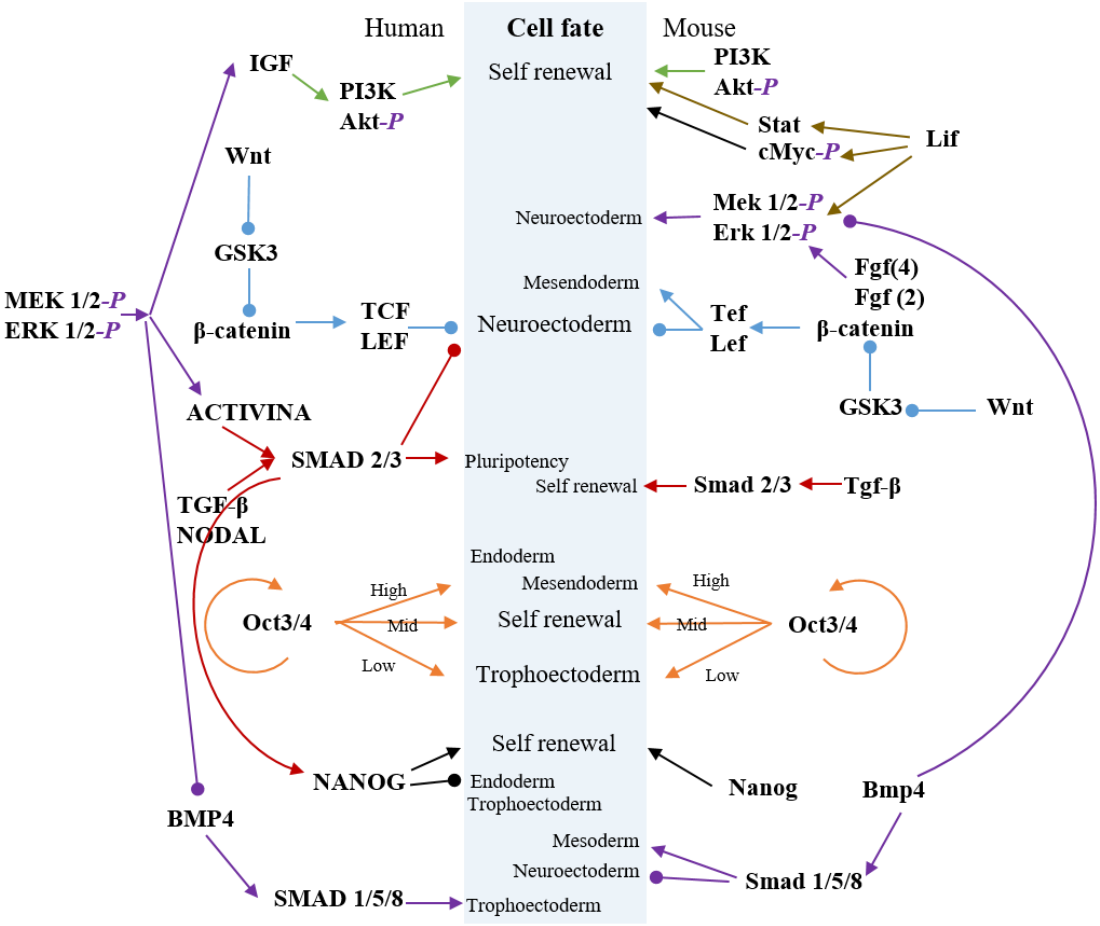


Figure 6.3: Comparison of key signalling pathways involved in pluripotency and differentiation in humans and mice: Several of the key signalling pathways involved in pluripotency and lineage commitment in human and mice ESC are highly similar, showing a high level of conservation in the transcription factors and proteins involved. Many of the signalling cascades involved in pluripotency and self-renewal are fully conserved, with more subtle differences occurring in the lineages cells commit to on the activation of other pathways. Arrows indicate pathway activation, circles indicate pathway repression. Adapted from Schnerch *et al* 2010.

The interactions between genes and transcription factors directing these processes are highly complex and interdependent, but *in vitro* studies comparing the differentiation of murine and human PSCs have shown that the application of similar differentiation protocols results in the differentiation of the same cell populations. Direct comparison studies have shown that successes include, but are not limited to, the use of co-culture with END-2 cells to derive cardiomyocytes from PSCs (Mummery et al., 2002), the combined application of growth factors and M15 cells to differentiate PSCs into hepatocytes (Shiraki et al., 2008) and Wnt/Activin A based protocols to differentiate PSCs towards the endodermal lineage (Borowiak et al., 2009). Many more examples of these can be found in the literature, with mouse PSCs often used to trial novel differentiation protocols in these studies, before their application to human PSC populations.

Due to the conservation of these signalling pathways and the proven ability to apply similar differentiation protocols to achieve the same differentiated tissues, murine PSCs offer a reliable model system for the study of human tissue development.

6.1.4 Organogenesis and the identification of mature complex tissues

Covered briefly in Section 1.2.1.5, organogenesis is the process during which specific tissues and organs are formed, developing from progenitor cell populations into coherent collections of organised tissues, performing a specific function which is essential for survival. The processes involved in these events vary widely, dependent on the physical and structural characteristics of the organ, but are generally guided by the activation of lineage specific genes and responses to local microenvironmental cues including morphogen gradients, extracellular matrix composition and shear stress. Organogenesis culminates in the formation of organs which are distinct not only in their function, but also in their phenotype, allowing for identification using a combination of morphological analysis and the detection of tissue specific markers. The ability to clearly identify specific tissues is crucial in the confirmation of successful differentiation, which is important both in the synthesis of cellular material for regenerative therapies and the assessment of developmental potency in novel PSCs. Differentiated tissue intended for clinical use needs to be fully functional to provide treatment and terminally differentiated to prevent neoplasias following treatment. In the assessment of developmental potency, the teratoma assay in particular relies on the identification of mature, complex tissues from all three germ layers to confirm the property. The main tissues of each germ layer are detailed below, including distinctive histological and protein expression profiles.

The ectoderm is the outermost germ layer, and as such, is responsible for the formation of the epidermis of the skin, the neural appendages associated with skin including mechanosensors, the epithelia of sense organs and the entire nervous system (Webster and de Wreede, 2016). These tissues are highly distinct in their morphology, as shown in the Figures in Table 6.1. The epidermis is characterised by a stratified epithelial structure, which is keratinised, resulting in the formation of an outer cornified layer that is continually shed (Young et al., 2006). Key markers for this tissue include cytokeratins associated with specific layers of the epidermis, as well as proteins associated with the progressive keratinisation which are listed in Table 6.1. Epithelial layers of many organs can be identified similarly through their organisation and morphology with adherens junction markers such as E-cadherin proving useful in their identification due it its almost ubiquitous expression in epithelia. Mature neurones show a distinct cellular shape, with elongated processes termed axons and dendrites radiating out from a small cell body. These cells are tissues can easily be identified through staining for the pan neuronal marker Class III β-tubulin, a cytoskeletal protein strongly associated with the neural axons. Additional identifiable cell populations from this lineage with distinct cell shapes and expression profiles include neuroprogenitors and supportive glial populations.

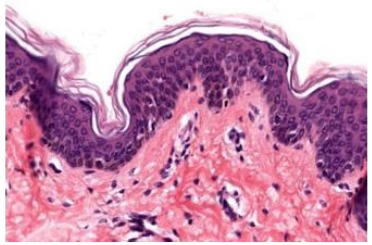
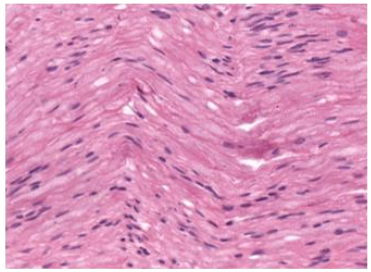
Tissue or organ	Descriptive characteristics	Key identifiers	Histology
Epidermis	Stratified epithelia, with distinct layers including a top keratinised layer.	Cytokeratin 10, Cytokeratin 14, E cadherin, involucrin, filaggrin, loricrin	Thick skin 
Neural tissues	Highly specialised cell shapes: neurones have elongated processes from a small cell body, neuroprogenitors are epithelial and glial cells are often a stellate shape.	Neurones - Class III β tubulin, nestin, Neurofilament Light and Heavy Neuroprogenitors - nestin Glial populations - Glial Fibrillary Acidic Protein (GFAP), Myelin	Peripheral nerve 

Table 6.1. Examples of histology and expression profile of tissues derived from the ectoderm

The tissues derived from the mesoderm layer perform a number of supportive roles, both physically and nutritionally within the body system; the main categories of tissue from this germ layer are described here. All three muscle types, striated, cardiac and smooth are formed from mesodermal progenitors, with each having subtle ultrastructural differences allowing for identification (Young et al., 2006), as described in Table 6.2. Key markers of the striated and cardiac muscle include various isomers of myosin, whereas smooth muscle actin can be used to detect smooth muscle tissues. Structurally important, bone and cartilage tissue share a similarity in their ECM rich tissues and general structure, but are distinct in terms of morphology and matrix composition (see Figures in Table 6.2). Cartilaginous tissue is characterised by the presence of very few isolated cells in a granular ECM, which can be identified through the use of any stains to detect proteinaceous ECM deposits. The secreted ECM associated with bone tissue is also protein rich, although it is denser and can show a more regular arrangement depending on orientation. Naturally, this matrix contains calcium compounds, allowing for a more specific identification process.

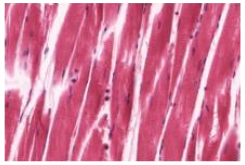
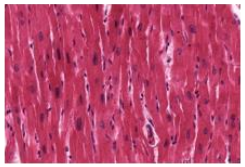
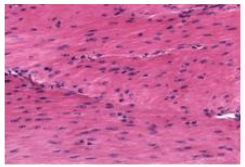
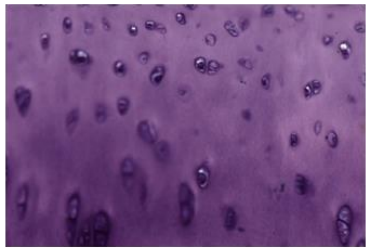
Tissue or organ	Descriptive characteristics	Key identifiers	Histology
Muscle	Striated – striped appearance, regular arrangement, large multinucleated cells Cardiac – branched arrangement, striped cells, intercalated discs between Smooth – no striations, regular fibre arrangement, spindle shaped cells	Striated – Myosin Heavy and Light Chains, Troponin. Cardiac – cardiac isomers of Myosin and Troponin Smooth – α smooth muscle actin	Striated muscle  Cardiac muscle  Smooth muscle 
Bone	Single or small groups of cells isolated in an extensive hard ECM which may show a ring structure or be an open porous network	ECM stains highlight the protein rich matrix, some stains including those with detect calcium can specifically identify bone	
Cartilage	Single or small groups of cells isolated in an extensive granular ECM	ECM stains highlight the protein rich matrix, and some can specifically identify cartilage	

Table 6.2. Examples of histology and expression profile of tissues derived from the mesoderm

The mesoderm also contributes to general connective tissues, including tendon, ligaments and the dermis, which supports the ectoderm derived epidermis. Highly varied in their structure and composition, as shown in Figure 6.3, these tissues can be identified in part due to their high structural protein content, mainly collagens, and the present of fibroblasts to maintain this complex ECM, a vimentin positive cell population (Young et al., 2006). The entire haematopoietic system is also mesoderm derived, with the cells of this system having very distinct morphologies dependent on their function, whether it is oxygen transport or protection from invading organisms. In addition to these distinct structures, the expression of specific extracellular markers on each cell population also allows for accurate identification, often cluster of differentiation (CD) markers specific to each distinct cell lineage. Other mesodermal derivatives include the endothelium, which lines blood vessels and can be detected by a flattened cell morphology and the exclusive expression of cell adherens junction protein VE-cadherin and adipose tissue, which has a highly distinctive tissue appearance, with large lipid droplets within the cells. The reproductive system and urinary systems are also derived from the mesoderm. While the reproductive system comprises of a mixture of specialised organs with very specific markers and various epithelial surfaces which can be detected via their morphology and the expression of typical epithelial adherens junction markers, the renal and urinary system has a number of distinctive tissue structures, such as Bowman's capsule and the nephron. Each of these has associated proteins which can be used in detection, including many transporter proteins such as ion channels and aquaporins (Young et al., 2006).

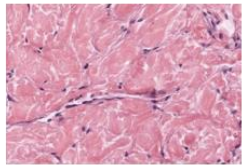
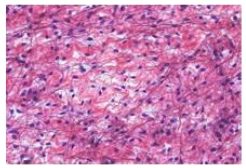
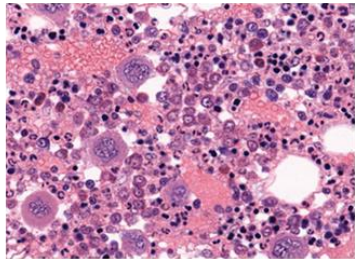
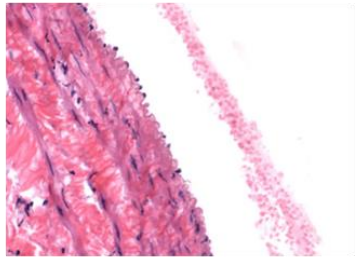
Tissue or organ	Descriptive characteristics	Key identifiers	Histology
Connective tissues	Dependent upon location, function and protein composition, maybe regular or irregular. Presence of stellate fibroblasts and large amounts of extracellular matrix proteins of various types.	Secreted proteins include collagens, fibronectin and elastin. Cellular proteins include vimentin and α smooth muscle actin	Dense irregular  Loose connective 
Haematopoetic tissues	Dependent upon location/ function. Red blood cells and immune cells have a characteristic shape. Bone marrow is heterogeneous due to mixed cell populations.	Cell population specific markers, mainly CD markers. MSCs are positive for vimentin.	Haematopoetic bone marrow 
Endothelia	Distinct flattened morphology of cells lining interior of blood vessels	VE cadherin is only expressed in these cells.	Vein endothelia 

Table 6.3. Examples of histology and expression profile of tissues derived from the mesoderm

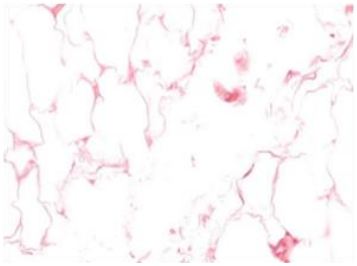
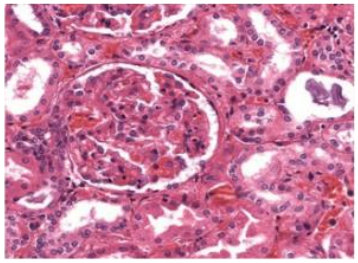
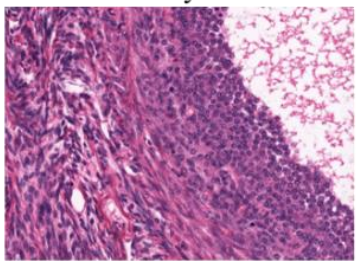
Tissue or organ	Descriptive characteristics	Key identifiers	Histology
Adipose	Cells containing large lipid droplets	Lipid detection methods such as histological stains highlight the lipid contents of the cells.	
Renal system	A number of distinctive structures, including the nephron, as well as varied epithelia.	E cadherin for general epithelia. Kidney specific markers e.g. transport proteins and ion channels, as well as aquaporins.	
Reproductive system	Sex specific germ cell organs, with various epithelia.	Sex specific germ cell organ proteins including . E cadherin for epithelial surfaces, cilia for fallopian tubes.	Ovary 

Table 6.4. Examples of histology and expression profile of tissues derived from the mesoderm

The variety in the tissue structures and organs derived from the mesoderm is replicated in those tissues derived from the endodermal germ layer. The endoderm is the innermost germ layer after gastrulation has taken place, and is mainly responsible for the formation of internal organs (Webster and de Wreede, 2016). While there are some similarities due to the widespread epithelial layers present in many of these tissues which allows for a simple initial identification as an endoderm derivative, these too vary depending on tissue location, and their structures and functions are quite different. All of these can be detected using epithelial adherens junction markers such as E-cadherin, but closer study of the epithelial structure is required for identification as to the organ system. The respiratory system can be broadly split into two areas; the lungs and the respiratory tract, which is characterised by a single layer epithelia surrounded by a complex vasculature or pseudostratified ciliated epithelia with the ability to produce mucus secretions respectively (Young et al., 2006), see Figure. This difference in gross morphology allows for a more careful identification, although detection of mucous secretions using specific stains can also aid in identification. The gastrointestinal tract is another organ system with a location dependent structure, although this too has many variations of epithelial surfaces, several of which are also mucus secreting. The intestine in particular is identifiable from the presence of villi structures, and cells with surface microvilli, in addition to mucous secretions. The liver and pancreas are also associated with the gastrointestinal tract, both of which have a more homogenous structure comprised of repeating functional units, the lobule or acinus, and are detectable through the expression of tissue specific markers such as alphafetoprotein and CYP enzymes or amylases and other digestive enzymes respectively. The endocrine organs are the final broad tissue collection derived from this germ layer, and this group includes the thyroid and thymus. The thyroid comprises of repeating units, follicles, and the thymus is an epithelial organ involved in T cell maturation: both of these organs secrete specific proteins which can be used to identify them in addition to morphological analysis.

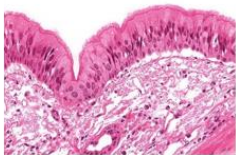
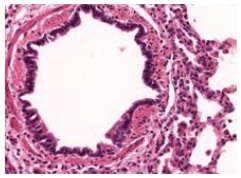
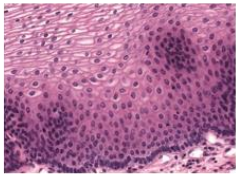
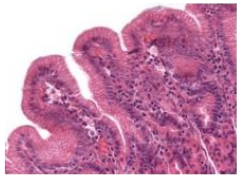
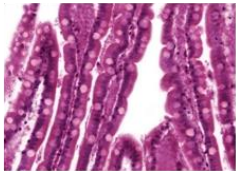
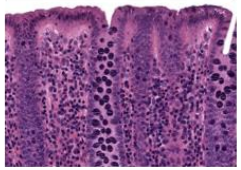
Tissue or organ	Descriptive characteristics	Key identifiers	Histology
Respiratory system	Varied epithelial surfaces, including the trachea and the lung. Trachea including ciliated cells and mucus producing cells. Lung epithelia consists of a single cell layer in alveoli.	E cadherin for epithelia, cytoskeletal and specific cilia markers. Stains to detect mucus production also.	Trachea  Lung 
Gastrointestinal tract	Encompasses a wide range of epithelial organs and surfaces with different functions. The oesophagus is stratified and the stomach and other organs are not. Small intestine possesses folded villi and microvilli on cells, the colon is also a folded tissue to increase surface area. Intestine and colon contain mucus secreting cells also.	E cadherin for epithelia, mucus stains for the small intestine. Specific transporter proteins for the small intestine and colon.	Oesophagus  Stomach  Small intestine  Colon 

Table 6.5. Examples of histology and expression profile of tissues derived from the endoderm

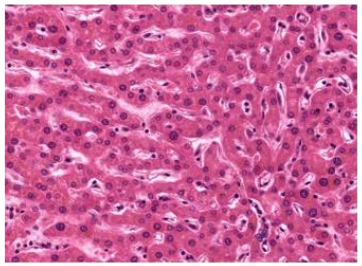
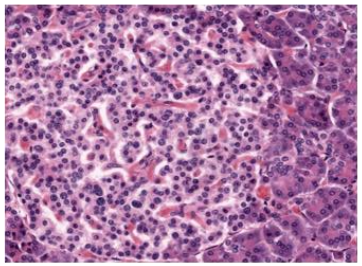
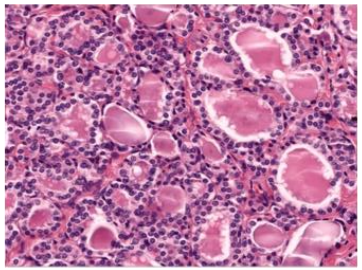
Tissue or organ	Descriptive characteristics	Key identifiers	Histology
Liver	Formed of repeating functional units called lobules including hepatocytes and biliary cells surrounding the vasculature and bile duct.	Liver specific markers include alphafetoprotein in early development, N cadherin and cytoskeletal proteins. Secreted albumin and urea assays can also be used.	
Pancreas	Functional units are acini, consisting of secretory cells.	Secreted hormones such as insulin and glucagon can be used, as well as secreted enzymes such as amylase and trypsin.	
Endocrine organs	The thyroid is made of repeating follicles, with epithelial surrounding a store of the synthesised hormone. The thymus is a dense homogenous epithelial organ, constructed of lobules.	Organ specific hormones such as T3 and T4 can be used, as well as general epithelial markers.	Thyroid 

Table 6.6. Examples of histology and expression profile of tissues derived from the endoderm

The range of tissues and structures present in the human body is far greater than those described here, although this provides an overview of the main organ systems and their general identification. The complex tissues of the human body are very distinct in their nature, when both morphology and protein expression are examined. The correct identification of these tissues is critical following any differentiation process regardless of their intended use and whether they were created *in vitro* or *in vivo*. By exploiting the distinct profiles of these cells and tissues, their identity can be accurately recorded.

6.1.5 The creation of complex tissues *in vitro*

The field of tissue engineering has previously focussed more on the creation of complex tissues for regenerative therapies and clinical applications, but the focus has become more general, with the development of *in vitro* tissue models for a variety of studies including drug efficacy/safety and fundamental physiology, biology and pathophysiology (Griffith and Swartz, 2006). Section 6.1.4 highlighted the diversity of the tissues in the human body, as well as alluding to the complex and varied protocols required to recreate these structures in the *in vitro* setting.

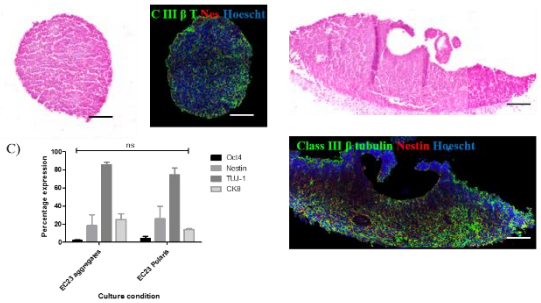
For the creation of any *in vitro* tissue, the minimum requirement is an interaction between growth factors, scaffolds and cells (MIKOS et al., 2006). Understandably, for the creation of complex tissues more than these three factors are required. The complexity of the *in vivo* microenvironment was covered in Chapter 5, with a wide range of chemical, physical and biological cues integrating to create a unique cellular microenvironment which cells sense and respond to. Recreating this *in vitro* is challenging, but is required to ensure tissue complexity and heterogeneity, as was demonstrated in the previous Chapter with the introduction of more physiological culture conditions to the model developed in this project. Up to this point, the importance of time in the developmental process has been acknowledged, but has not been explored in depth in this model. However, as the developmental process and the teratoma assay proves, time is crucial to the formation of complex tissues, and this will be explored more in depth in the following Chapter.

6.1.6 Conclusion

While pluripotent populations such as embryonal carcinoma cells offer a robust culture system for the application of novel technologies, the study of pluripotency and the elucidation of specific differentiation processes, these cells are not representative of true PSCs. Their tumorigenic origin predisposes the cells to the acquisition of survival promoting mutations during rapid proliferation, which in turn impacts on their genomic stability, pluripotency and ability to differentiate. The culture of human ES cells or iPS cells can be technically challenging and incur significant cost, yet murine PSC populations offer an alternative option for the study of human development. Generally, murine PSCs are phenotypically and functionally similar to human PSCs, yet with simpler culture

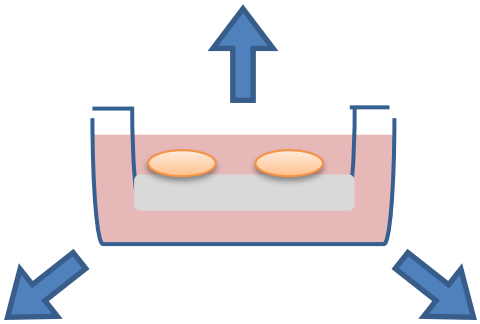
requirements for the maintenance of pluripotency. Many early developmental processes are conserved between the two species, as are the signalling pathways controlling self-renewal, pluripotency and lineage commitment. Murine PSCs are often used to evaluate the success of novel differentiation protocols before their use in human PSC populations, with the same cell populations successfully obtained. Thus murine PSCs can be used as a surrogate in a model to study the development and differentiation of human tissues, including the novel 3D culture model under assessment in this project.

Following the differentiation of PSCs into mature and complex functional tissues, their efficient and accurate identification is essential. Mature functional tissues have distinct morphologies and protein expression profiles depending on their origin and function, which can be exploited in their identification. The ability to do so is crucial in the differentiation of PSCs, to ensure the correct fully differentiated tissue phenotype is achieved for clinical therapies, as well being an essential aspect of the PSC characterisation process. This process will be applied to the identification of mature tissues in the model following the incorporation of murine EBs to form tissue discs, followed by prolonged differentiation *in vitro*.



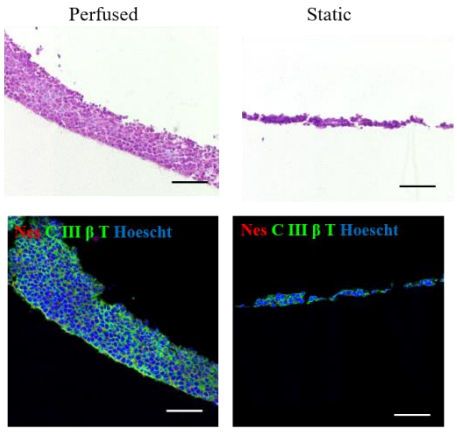
Directed differentiation

\+ addition of known morphogens to direct differentiation towards both ectodermal lineages



Perfusion

\+ introduction of perfusion to the model to improve differentiation and viability



Co-culture

\+ co-culture with HDFn and SCID fibroblast populations to enhance differentiation

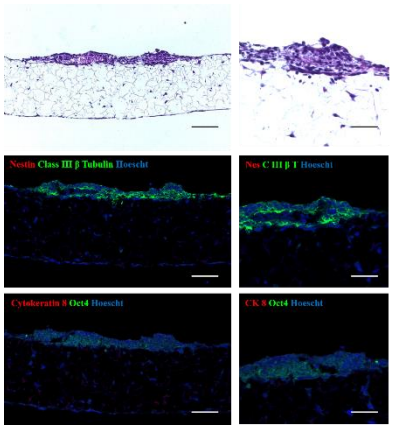


Figure 6.4: Current overview of work completed using TERA2.cl.SP12 EBs as tissue discs in the model: Up to this point, the model has been optimised using embryonal carcinoma cells. EBs can be successfully cultured on the surface of the porous scaffold as tissue discs, and the model adapted in a variety of ways in order to enhance the differentiation of the structures. Tissue discs can be successfully directed towards specific lineages and exposed to additional microenvironemntal cues from other cell populations and physical properties such as perfusion. These varied conditions will now be used in the murine embryonic stem cell version of the model, with CGR8 tissue discs.

6.2 Aims and Hypotheses

The aim of this chapter is to use a more relevant mammalian cell line in the model, both the original static version and the adapted versions which incorporate properties to make the model more physiologically relevant allowing for in depth study of the differentiation occurring within the model. The murine embryonic stem cell line CGR8 will be utilised to make embryoid bodies, which will be maintained in the various versions of the model. Initially, embryoid bodies will be used to form tissue discs in the static model for long term differentiation, with the aim of forming complex structures from the three germ layers. Additionally, embryoid bodies will be differentiated using a variety of morphogen based protocols in order to direct the differentiation and structures which form in the developing tissue disc. Finally, murine PSCs or embryoid bodies will be seeded into the co-culture with dermal fibroblasts and exposed to perfusion, with the aim of simulating the *in vivo* microenvironment, enhancing the differentiation within the tissue discs. It is expected that complex structures from all three germ layers will be formed within the developing tissue discs, with increasingly complex structures forming over time. It is also hypothesised that tissue discs differentiated using a range of morphogens and protocols will be successfully maintained in the model, forming complex tissue like structures as per the differentiation methodologies used. Finally, it is hypothesised that PSCs seeded into the two more physiological versions of the model will show differences in their development, and likely an improvement in the differentiation in the structures present.

6.3 Objectives

- Further explore the capabilities of the model by using a murine embryonic stem cell line to create tissue discs, specifically testing the ability to culture tissue discs for more than 7 days.
- Use a variety of morphogens to differentiate embryoid bodies prior to seeding in the model to study aspects of tissue differentiation.
- Investigate the effects of co-culture of embryonic stem cell derived tissue discs with a relevant SCID fibroblast cell line.
- Introduce the property of perfusion to the murine embryonic stem cells in an attempt to enhance tissue differentiation.

6.4 Materials and Methods

The routine maintenance of CGR8 murine embryonic stem cells is described in the Materials and Methods in Chapter 2 as is the routine maintenance of the dermal fibroblast populations. The creation and seeding of embryoid bodies onto Alvetex® inserts and dermal equivalents is also covered in the Materials and Methods.

6.4.1 Morphogen treatment of CGR8 embryoid bodies

Morphogens were added to the culture medium during culture to direct the differentiation of the embryoid bodies prior to seeding on the Alvetex® membranes.

6.4.1.1 Simple morphogen treatment

Morphogens were added to embryoid bodies during the Petri dish phase prior to seeding on Alvetex® inserts.

Table 6.7: Morphogens used for simple directed differentiation and final concentrations

Morphogen	Final Concentrations
Activin A	50 mg/mL
EC23	0.01 µM

6.4.1.2 Germ layer differentiation

Combinations of morphogens were added to the culture medium during the Aggrewell™ culture stage to direct the differentiation of the embryoid bodies towards specific germ layers, as per the International Stem Cell Initiative study (2018).

Table 6.8: Morphogen combinations used to differentiate the embryoid bodies towards each germ layer and final concentrations.

Germ layer	Morphogens and final concentrations
Ectoderm	Dorsomorphin - 10 µM, SB431542 - 10 µM bFGF - 100 ng/mL
Mesoderm	Activin A - 20 ng/mL BMP-4 - 20 ng/mL
Endoderm	Activin A - 100 ng/mL BMP-4 - 1 ng/mL

6.4.1.3 Ectoderm fate decision experiment

Combinations of morphogens were added to the culture medium during the Aggrewell™ culture stage to direct the differentiation of the embryoid bodies towards specific ectodermal lineages, as per the Li *et al* 2015 paper. Morphogens were used to create three differentiation conditions: BMP-4 only, SB431542 only and BMP-4 and SB43154 in combination.

Table 6.9: Morphogen concentrations used to differentiate the embryoid bodies towards specific ectodermal lineages.

Morphogen combination	Final concentration used
BMP-4	10 ng/mL
SB431542	10 µM

6.4.2 Paracrine and Topography experiments: Preparation of conditioned media and fixed scaffolds

To condition media for the investigation into the paracrine effects of co-culture with fibroblast populations, SCID DEs were set up and cultured until the mature time point, 21 days, in the normal maintenance media. On day 21, inserts were transferred to a fresh plate, and media was swapped to CGR8 differentiation media. Media was harvested and replaced every 3-4 days and stored at 4°C until use.

To prepare fixed scaffolds, SCID DEs were cultured until the mature time point, 21 days. DEs were fixed in sterile filtered 4 % PFA in the cell culture hood, washed twice in sterile PBS and stored in a Parafilm sealed plate in sterile PBS at 4°C until use.

6.4.3 Paracrine and Topography experiments: EB seeding and maintenance

To undertake experiments to investigate the effects of paracrine factors and topography on the behaviour of EBs, the structures were cultured as thus.

For paracrine experiments, EBs were seeded onto 6 well size Alvetex® Polaris as previously described and maintained in 6 well plates in a medium which was composed of a 1:1 mixture of media harvested from 3D dermal equivalents and fresh maintenance media. Media harvested from the SCID DEs was sterile filtered through a 0.2 µm membrane prior to use. Half and full media changes were performed as necessary every 3-4 days.

For topography experiments, EBs were seeded onto a scaffold which had been previously fixed and maintained in normal maintenance medium.

6.4.4 Long term perfusion using CGR8 cells

CGR8 perfused cultures were set up as previously described for TERA2.cl.SP12. Briefly, CGR8 cells were maintained in flasks before detachment using the trypsin/EDTA method to create a single cell suspension. Cells were counted using the Trypan Blue exclusion assay to obtain accurate cell number and seeded at a density of 2 million cells onto the Alvetex® Polaris insert. Cells were allowed adhere over 2 days before transfer to the perfused system, containing 120 mL of media consisting of DMEM, 10 % FBS, 2 mM L-glutamine and 100 U/mL Penicillin and Streptomycin. Cultures were placed on the magnetic stirrer and checked every 7 days, with media topped up as necessary.

6.5 Results

6.5.1 Long term culture of CGR8 embryoid bodies as tissue discs on Alvetex® Polaris

In Chapter 2, it was established that Alvetex® Polaris was the most suitable scaffold form for the culture for tissue discs, in particular the maintenance of the structure of the entire tissue disc on the surface of the scaffold for analysis. Following on from these results, the murine embryonic stem cell line CGR8 was selected for use in the model. This cell line has previously been used to culture tissue discs on Alvetex® Polaris, but only for pilot studies. In this Chapter, CGR8 embryoid bodies were also seeded onto Alvetex® Polaris scaffolds, 6 well format, in order to allow for longer term culture, encouraging complex structure formation and were analysed in a systematic manner. To better define longer term culture, it was decided that tissue discs were to be maintained for up to 35 days in the model to allow for structure maturation; this time frame was chosen as an overall culture time shorter than current teratoma assay protocols, with an aim to improve on turnaround times for the analysis of pluripotent stem cell developmental potential. Additionally, it was deemed that culture times longer than this would be unreasonable and overly lengthy. During analysis, wax sections were cut in an orientation parallel to the scaffold in order to provide a greater overview of the structures present within the tissue disc by allowing a larger area, and in many cases sections through the entire tissue disc, to be viewed simultaneously.

6.5.1.1 CGR8 embryonic stem cells display hallmarks of pluripotency and successfully form embryoid bodies

CGR8 murine embryonic stem cells were subject to a brief characterisation process to confirm pluripotency. Cells show a characteristic stem cell morphology when observed under phase contrast in culture, and express a variety of known stem cell markers including Oct 4, Sox 2, TRA-1-60 and the murine stem cell marker SSEA-1, as shown by immunofluorescent staining and flow cytometry. When seeded into low adherence microwell plates with differentiation medium, CGR8 cells successfully form embryoid bodies which show a loss of pluripotency, through the lack of SSEA-1 expression and signs of spatial organisation and differentiation after a further 5 days culture in suspension conditions. Embryoid bodies, and tissue discs formed from them in the subsequent experiments, were assessed using immunofluorescent staining for a range of proteins and markers which represented many of the common structures and differentiated phenotypes associated with each germ layer. To ascertain ectoderm structures, E-cadherin, the epithelial junctional protein was chosen in addition to those already previously used for the analysis of TERA2.cl.SP12 tissue discs; epithelial marker Cytokeratin 8, Nestin, the early neural marker, and Class III β-tubulin, the pan-neuronal mature differentiation marker. To detect mesodermal differentiation, transcription factor GATA4 was chosen, as was the cytoskeletal protein commonly found in fibroblasts and smooth muscle cells, α smooth muscle actin. E-cadherin was also used to detect epithelial surfaces of

endodermal origin, in conjunction with Collagen 4 staining to highlight the formation of basement membranes. Staining for these proteins, and other germ layer specific proteins, was dependent upon the structures identified within the tissue disc. Within the embryoid bodies seen here, E-cadherin expression is highly organised, and detected at the embryoid body periphery and in the centre, whereas other differentiation markers such as GATA4 and Class III β-tubulin show a more intermittent expression across the embryoid body, again indicating spatially organised distinct groups of cells in a manner reminiscent of early embryonic development.

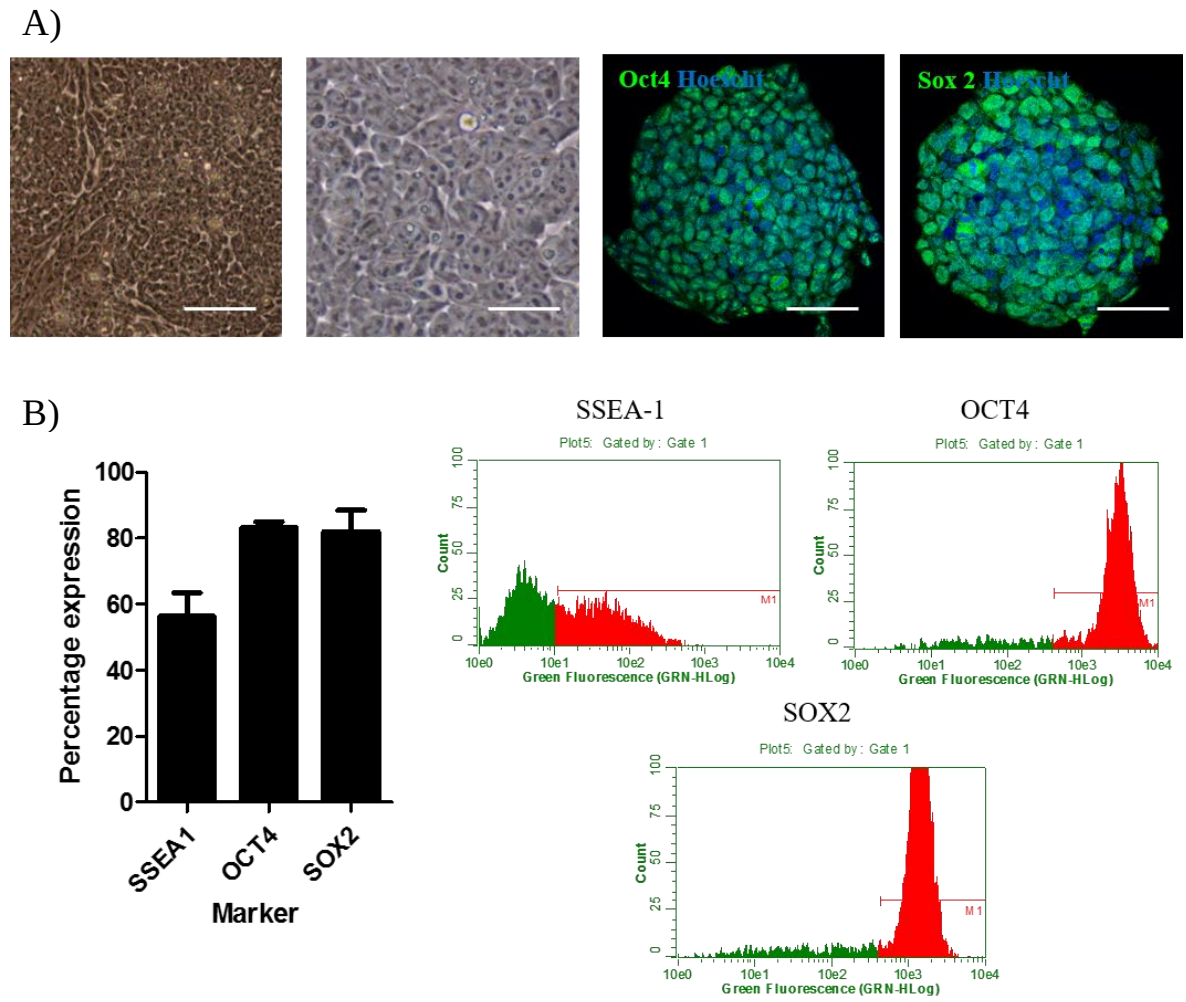


Figure 6.5: Characterisation of 2D CGR8 murine embryonic stem cells in the pluripotent state: CGR8 cells were seeded onto plasma treated glass coverslips or maintained in flasks until 70 % confluent, before fixing in 4 % PFA. Coverslips were stored at 4°C in PBS until immunocytochemistry was performed. A) Phase contrast images of CGR8s show typical stem cell morphology with high nuclear to cytoplasmic ratio and prominent nucleoli. Cells express relevant pluripotency markers also. B) Flow cytometry confirms the expression of various pluripotency markers within the cell population, particularly the mouse specific marker SSEA-1. Representative histograms are shown. Data represents mean ± SEM from 3 independent experiments (n=3). Scale bars: 100 µm and 50 µm

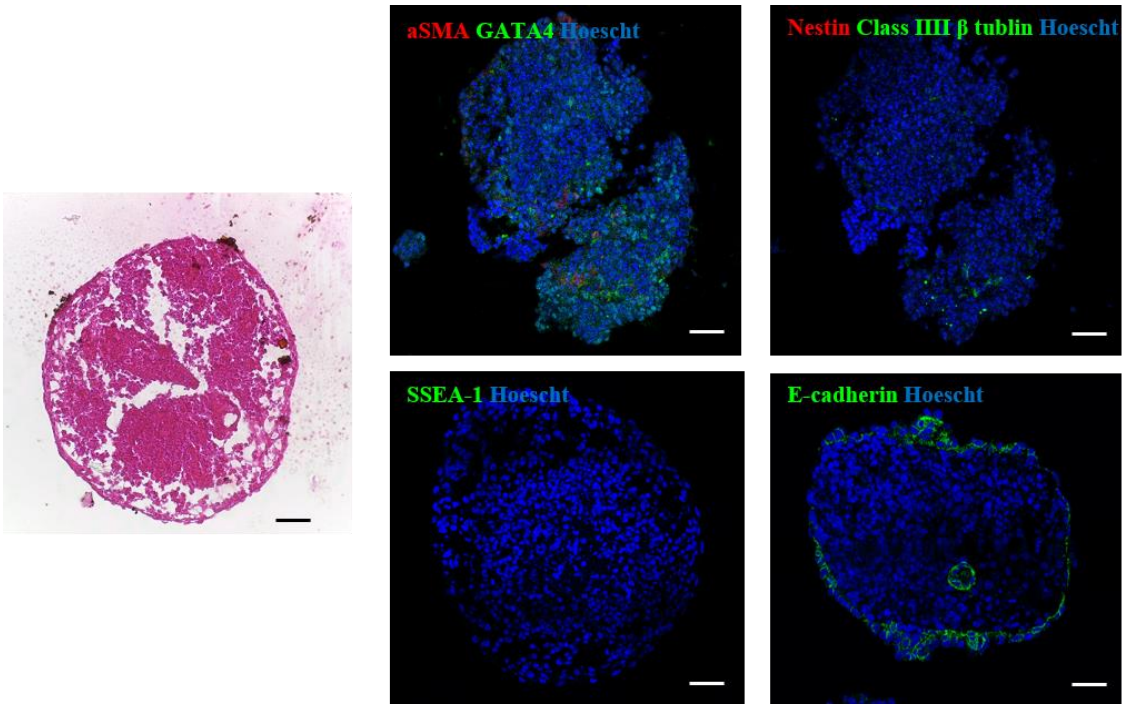
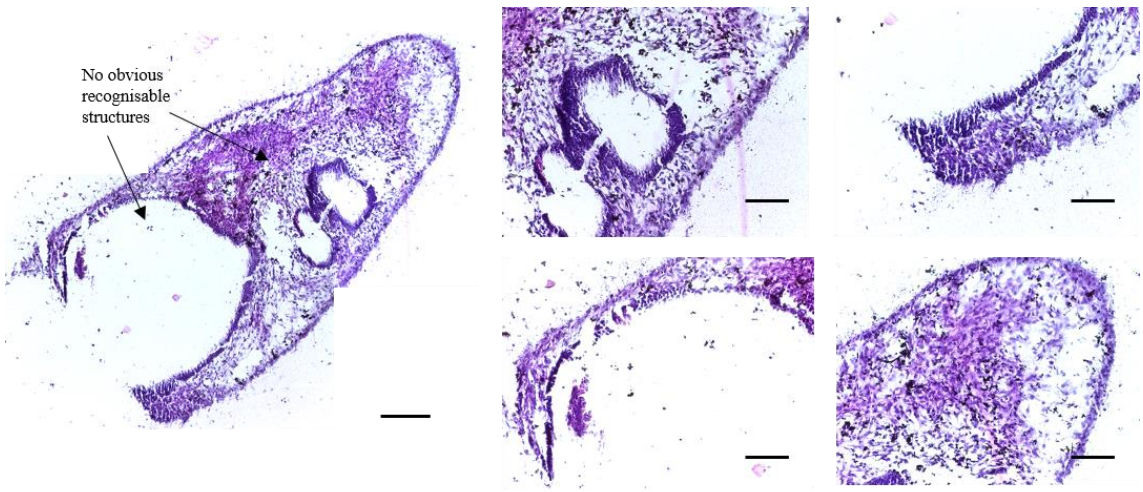


Figure 6.6: CGR8 murine embryonic stem cells successfully form embryoid bodies which show evidence of spontaneous differentiation: CGR8 cells were seeded into the Aggrewell plate at a density of 1000 cells per microwell, and cultured for 3 days before transfer to suspension culture in a Petri dish for a further 5 days. H&E shows a dense spherical structure which appears homogenous. Immunofluorescent analysis of EBs shows the loss of expression of pluripotency of markers such as SSEA-1 and Oct 4, and the expression of various differentiation markers in discrete areas, providing evidence of organisation and polarisation. Scale bars: 100 µm

6.5.1.2 Culture and differentiation of CGR8 tissue discs on Alvetex® Polaris for 7 days results in poor structure formation

CGR8 EBs were seeded onto Alvetex® Polaris as previously done with TERA2.cl.SP2 EBs, and the differentiation of the subsequent tissue discs analysed every seven days As shown in Figure 6.6, histological analysis using H&E staining of tissue discs after 7 days culture on the scaffold indicates tissue disc adherence and formation, but generally poor differentiation, with no recognisable mature structures. Tissue discs do show more complexity than time matched embryoid bodies when histology is compared, with some increased heterogeneity in the tissue discs, a more dense cellular organisation and some highly rudimentary structures present. However, there is very little evidence to suggest that there are differentiated structures derived from each germ layer. Analysis of the tissue discs using immunostaining confirms these findings in Figure 6.7; E-cadherin expression is not organised, with only some small areas of expression which do not resemble the structure of an epithelial surface. Intermittent expression of α smooth muscle actin is detected in contact with the Alvetex® Polaris, with very smaller amounts of Class III β-tubulin expression also present within the tissue disc. Neither of these markers show any level of structural organisation reminiscent of specific tissue structures.

A)



B)

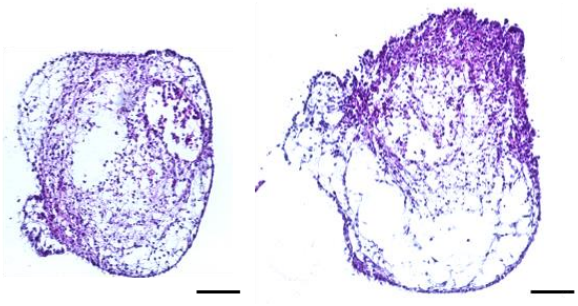


Figure 6.7: Culture and characterisation of murine embryoid bodies on Alvetex® Polaris for 7 days: CGR8 embryoid bodies were seeded onto Alvetex® Polaris inserts and cultured for a specified time in the absence of LIF before fixing in 4 % PFA and processing. Samples embedded in wax were sectioned both in the frontal and transverse planes to analyse the structures within the tissue disc. A) H&E images show that after 7 days cultured on the insert, few complex structures are visible and tissue discs are relatively homogenous, with little evidence of mature tissue formation. B) EBs cultured in suspension for the same length of time also show little heterogeneity or evidence of complex tissue structure formation. Representative images shown. Scale bars: 200 µm and 50 µm

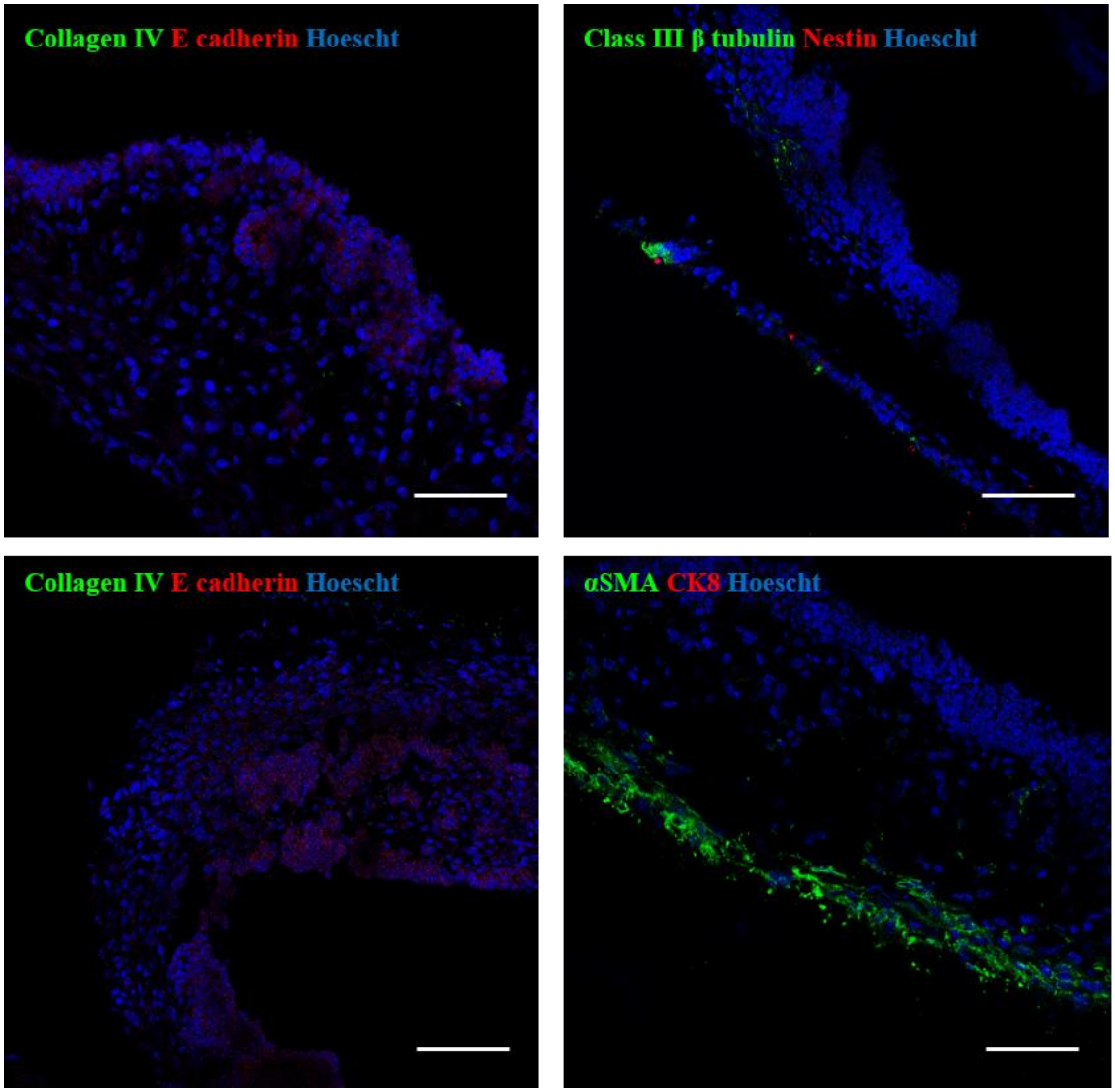


Figure 6.8: Culture and characterisation of murine embryoid bodies on Alvetex® Polaris for 7 days: CGR8 embryoid bodies were seeded onto Alvetex® Polaris inserts and cultured for a specified time in the absence of LIF before fixing in 4 % PFA and processing. Samples embedded in wax were sectioned both in the frontal and transverse planes to analyse the structures within the tissue disc. Immunostaining further confirms that the tissue disc has no complex structures of interest, with a disorganised expression pattern for E-cadherin, indicating poorly organised epithelia, and very little Nestin and Class III β-tubulin expression, suggesting very little neural differentiation. Small amounts of α smooth muscle actin staining indicate mesodermal differentiation. Representative images shown. Scale bars: 100 µm

6.5.1.3 Culture of CGR8 tissue discs for 14 days results in a more complex differentiated phenotype with distinct cellular morphologies

Further culture of the CGR8 tissue discs, resulting in a total time of 14 days culture on the Alvetex® Polaris membrane, reveals a significantly different tissue disc morphology. H&E staining in Figure 6.9 shows a number of distinct cell types visible within the structure, which is randomly organised and larger overall than that seen after 7 days, and larger than the time matched embryoid bodies. Gross morphology suggests the presence of a large area of connective type tissue, cystic cavities and an epithelial type surface, which is possibly differentiating along a gradient due to a progressive loss of nuclei which can be seen in the cells on the outer surface of the tissue disc. These structures indicate the potential for the formation of differentiated structures from all three germ layers. Comparison to time matched embryoid bodies highlights the complexity of the tissue disc and relative simplicity of the embryoid bodies; there is no cell death evident in either structure. Immunofluorescent staining provides some information as to the identity of the structures. E-cadherin staining is highly prominent within the epithelial area, with large amounts of Collagen IV deposited on the surface of the Alvetex® Polaris, indicating an organised polarised morphology. E-cadherin and Collagen IV also highlight a gland like structure on the surface of the tissue disc and an epithelial lined lumen within the tissue disc, structures all of which suggest ectodermal and endodermal differentiation. There are also multiple areas which stain positively for α smooth muscle actin within the tissue disc, indicating the present of myofibroblasts or smooth muscle tissues – myofibroblasts are more likely given that the distribution of the staining doesn't suggest the formation of orientated fibres. The presence of Class III β-tubulin staining within the tissue disc indicates neural differentiation within the tissue disc also, confirming the presence of tissue structures from all three germ layers.

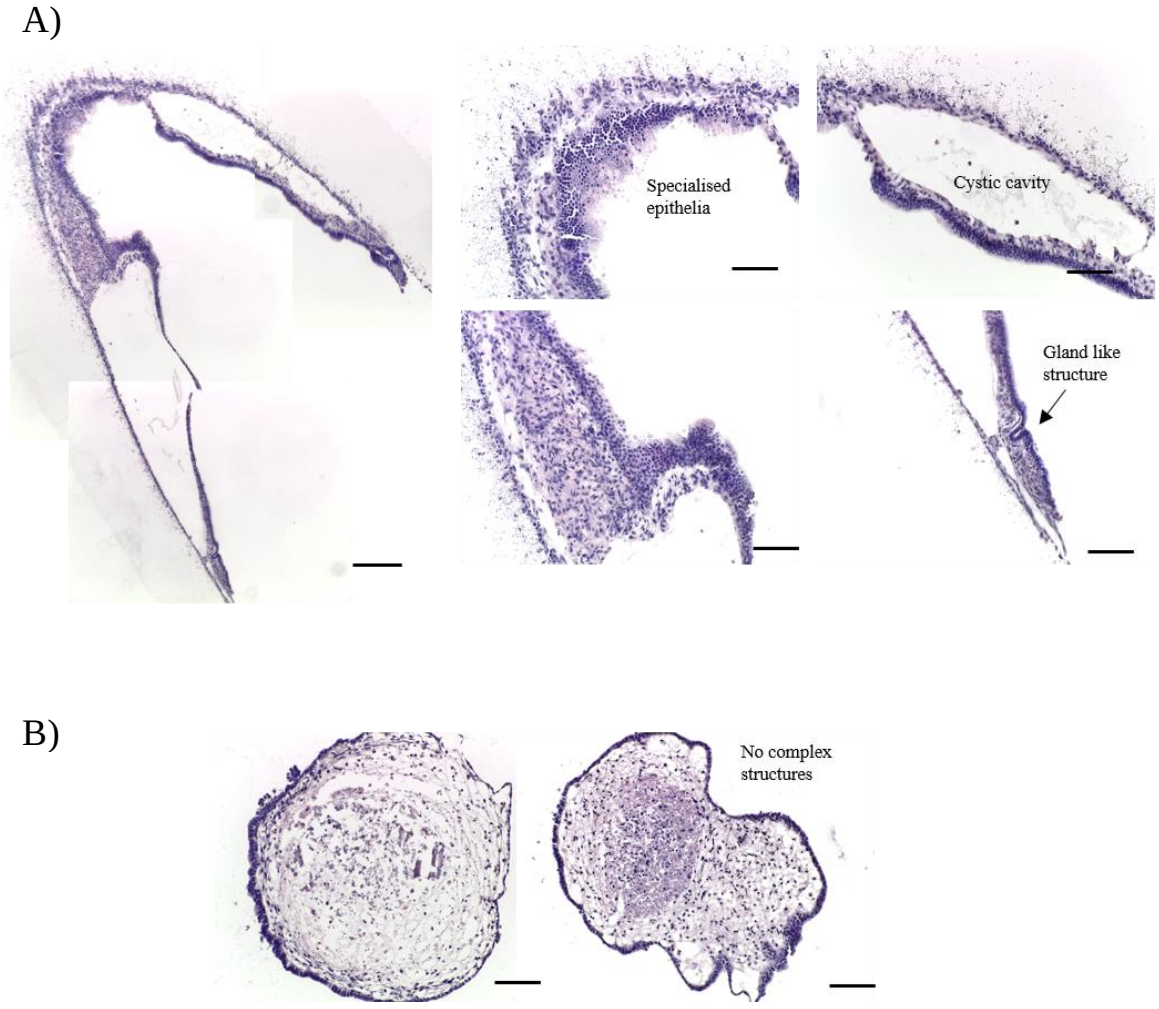


Figure 6.9: Culture and characterisation of murine embryoid bodies on Alvetex® Polaris for 14 days: CGR8 embryoid bodies were seeded onto Alvetex® Polaris inserts and cultured for a specified time in the absence of LIF before fixing in 4 % PFA and processing. Samples embedded in wax were sectioned both in the frontal and transverse planes to analyse the structures within the tissue disc. A) H&E images show that after 14 days, significantly more complex internal structures have formed within the tissue disc, including a specialised epithelial cells, cystic cavities, connective tissues and cellular gradient of differentiation. The tissue disc is also much larger than the EBs culture for the same length of time. B) The EBs cultured in suspension for the same length of time do not contain any recognisable structures, and maintain a relatively homogenous structure. Representative images shown. Scale bars: 200 µm and 100 µm

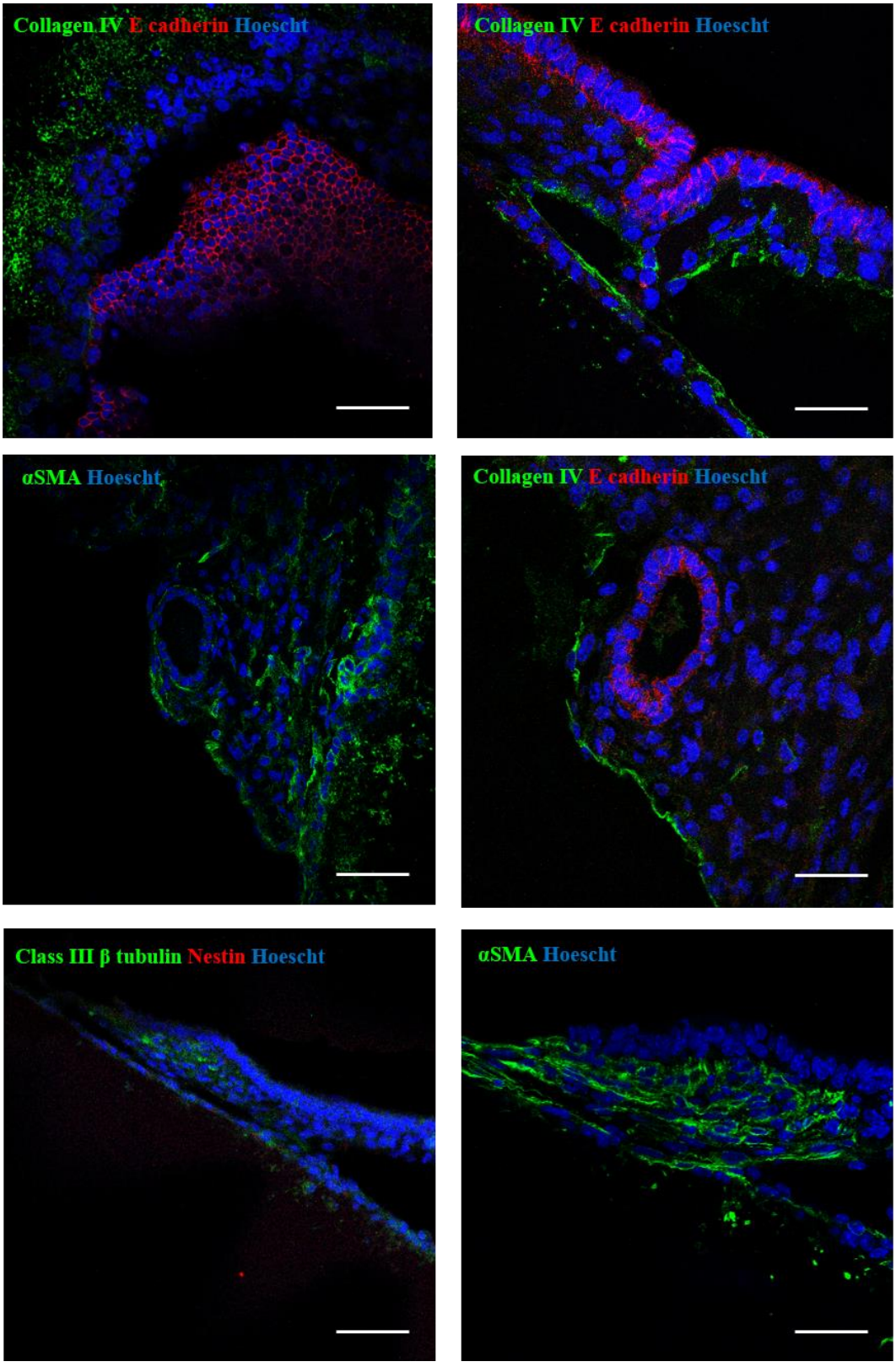
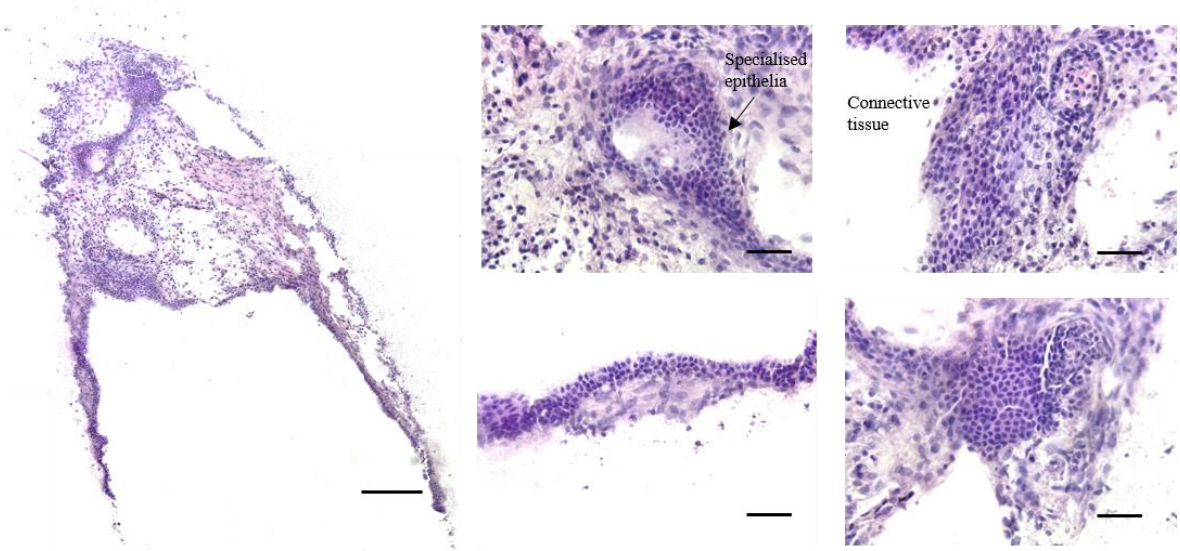


Figure 6.10: Culture and characterisation of murine embryoid bodies on Alvetex® Polaris for 14 days: CGR8 embryoid bodies were seeded onto Alvetex® Polaris inserts and cultured for a specified time in the absence of LIF before fixing in 4 % PFA and processing. Samples embedded in wax were sectioned both in the frontal and transverse planes to analyse the structures within the tissue disc. The immunostaining shown correlates with the H&E images, and identifies the complex structures forming. Structures which can be seen include organised epithelia lining a lumen, gland-like structures and areas of myofibroblast and neural differentiation. Specialised epithelial surfaces are also present. Representative images shown. Scale bar: 100 µm and 50 µm

6.5.1.4 Further culture of tissue discs in the model results in maintaining or increasing complexity of cell differentiation

Figures 6.9 and 6.10 established that after only 14 days culture in the model, CGR8 tissue discs show a highly differentiated phenotype with a number of complex structures. Prolonged culture past this time results in the maintenance of this phenotype, with similar differentiation apparent within the tissue discs. This can be seen in 21 day tissue discs in Figure 6.11, where the epithelial surfaces and connective tissue components are visible. As was seen with the 14 day tissue discs, 21 day tissue discs are also more complex that time matched embryoid bodies. Immunostaining confirms the presence of organised epithelial surface through positive staining for E-cadherin and Collagen IV, myofibroblasts with positive α smooth muscle actin staining and Nestin positive neural progenitor cells. Again, this suggests the continued presence of cells and tissue structures derived from all three germ layers within the tissue disc. Figure 6.13 shows 28 day tissue discs which show similar characteristics to those tissue discs previously encountered: complexity and diversity of tissue structures, with multiple different cellular phenotypes present within the tissue disc – specialised epithelia, connective tissues, smooth muscle, cystic cavities and lumen structures. The repeated presence of these structures indicates a consistency of tissue disc differentiation within the scaffold based model. As with previous tissue discs, immunostaining for the same selected markers highlights the identity of the structures which have formed: E-cadherin positive epithelia, Class III β-tubulin positive neural cells, α smooth muscle actin positive myofibroblasts.

A)



B)

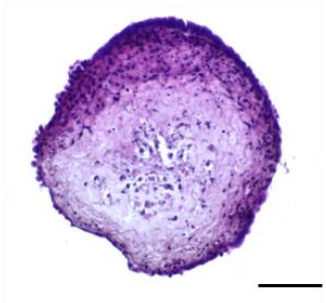


Figure 6.11: Culture and characterisation of murine embryoid bodies on Alvetex® Polaris for 21 days: CGR8 embryoid bodies were seeded onto Alvetex® Polaris inserts and cultured for a specified time in the absence of LIF before fixing in 4 % PFA and processing. Samples embedded in wax were sectioned both in the frontal and transverse planes to analyse the structures within the tissue disc. A) H&E images show that the complexity of the tissue discs is maintained, with multiple cell morphologies present and structures which are similar to those seen at the previous time point. B) As with the previous samples, the EBs cultured for the same length of time show little heterogeneity and no recognisable complex structures. Representative image shown. Scale bars: 200 µm and 100 µm

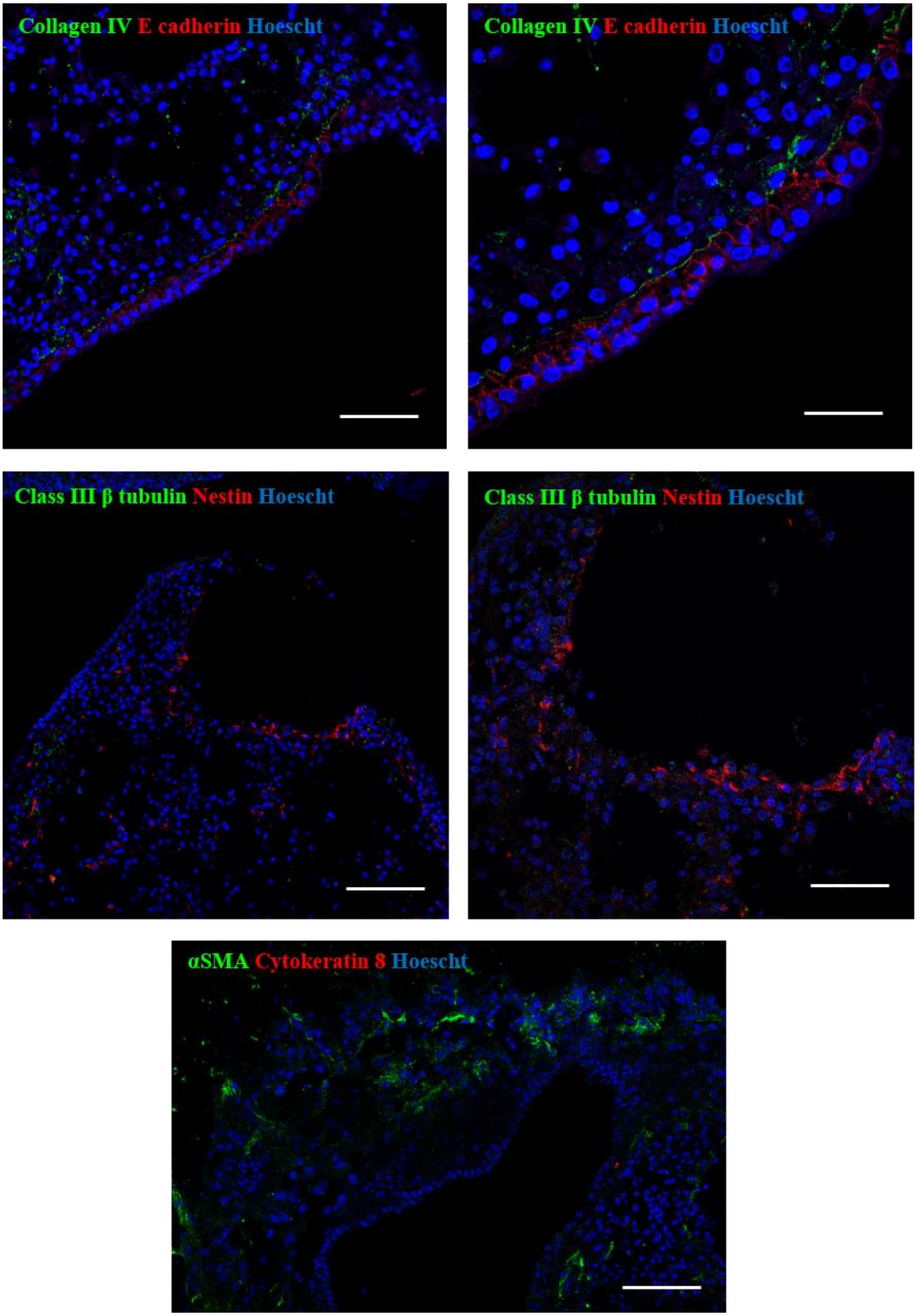


Figure 6.12: Culture and characterisation of murine embryoid bodies on Alvetex® Polaris for 21 days: CGR8 embryoid bodies were seeded onto Alvetex® Polaris inserts and cultured for a specified time in the absence of LIF before fixing in 4 % PFA and processing. Samples embedded in wax were sectioned both in the frontal and transverse planes to analyse the structures within the tissue disc. Again, immunostaining for differentiation markers highlights the complex structures which have formed, pertaining to the three germ layers. These include organised epithelia, Nestin positive neural progenitors and the presence of smooth muscle actin positive muscle cells. Representative images shown. Scale bars: 100 µm and 50 µm

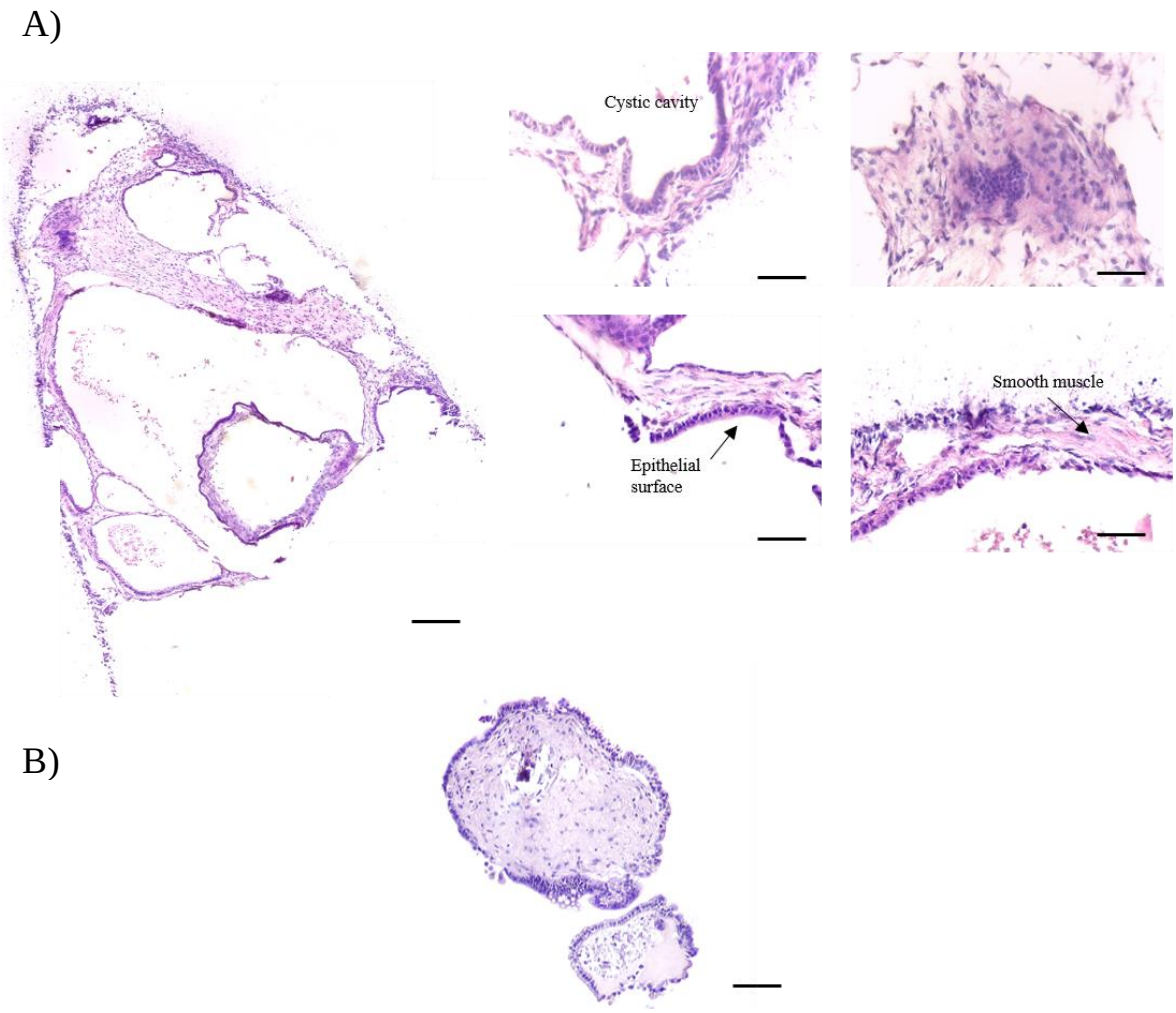


Figure 6.13: Culture and characterisation of murine embryoid bodies on Alvetex® Polaris for 28 days: CGR8 embryoid bodies were seeded onto Alvetex® Polaris inserts and cultured for a specified time in the absence of LIF before fixing in 4 % PFA and processing. Samples embedded in wax were sectioned both in the frontal and transverse planes to analyse the structures within the tissue disc. A) H&E images show that the tissue discs continue to form complex structures which show derivatives from the three germ layers. These include organised epithelia surrounding lumens and cavities, smooth muscle and other connective tissues. B) EBs cultured for the same length of time also appear homogeneous in comparison, with no complex tissues or structures. Representative images shown. Scale bars: 200 µm and 100 µm

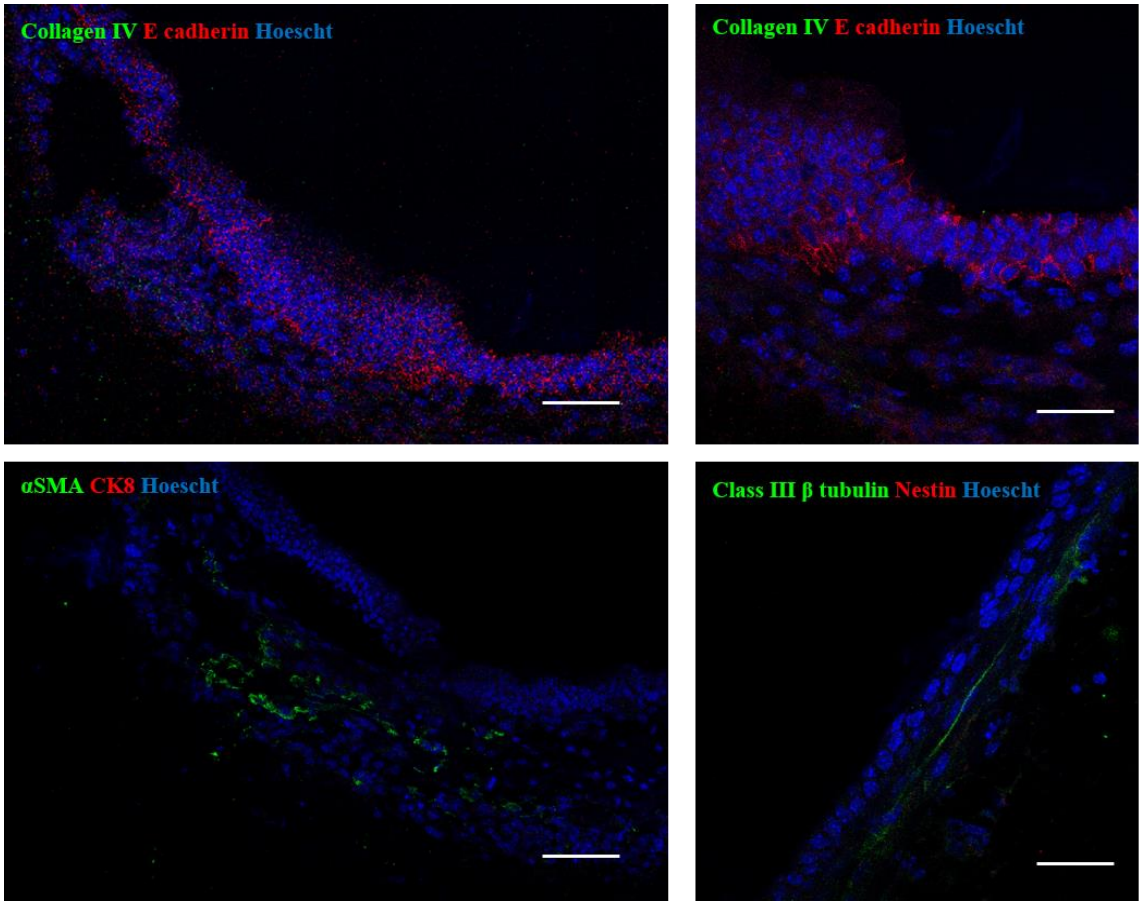


Figure 6.14: Culture and characterisation of murine embryoid bodies on Alvetex® Polaris for 28 days: CGR8 embryoid bodies were seeded onto Alvetex® Polaris inserts and cultured for a specified time in the absence of LIF before fixing in 4 % PFA and processing. Samples embedded in wax were sectioned both in the frontal and transverse planes to analyse the structures within the tissue disc. Immunostaining for differentiation markers supports the identification of the complex structures within the tissue disc, with markers from the three germ layers. Organised epithelia can be identified, as well as areas of smooth muscle and neural differentiation. Representative images shown. Scale bars: 100 µm and 50 µm

Further culture of the tissue discs up to a total time of 35 days on the scaffold results in a continuation of the trends previously seen, with an increase in tissue disc size and the maintenance and increase of the phenotypic diversity and complexity previously established. In particular, the H&E staining in Figure 6.15 shows that the diverse tissues show some increased maturity and definition. Multiple epithelia lined lumen are present, and a large area of epithelial differentiation can be identified easily on the outer surface of the tissue disc. There is also an area reminiscent of cartilaginous differentiation, which has not previously been identified at the earlier time points within the tissue discs, as well as the connective tissue and myofibroblast like populations previously seen. This is in great contrast to the time matched embryoid body samples which show little complexity or diversity by comparison, and are much smaller in size than the tissue discs. Again, immunostaining for a variety of germ layer markers confirms the identity of the tissue structures which have formed. Collagen 4 and E-cadherin expression highlight the epithelia and associated basement membranes,

within the tissue disc, with α smooth muscle actin staining indicating myofibroblasts and smooth muscle tissues in the areas of mesodermal origin.

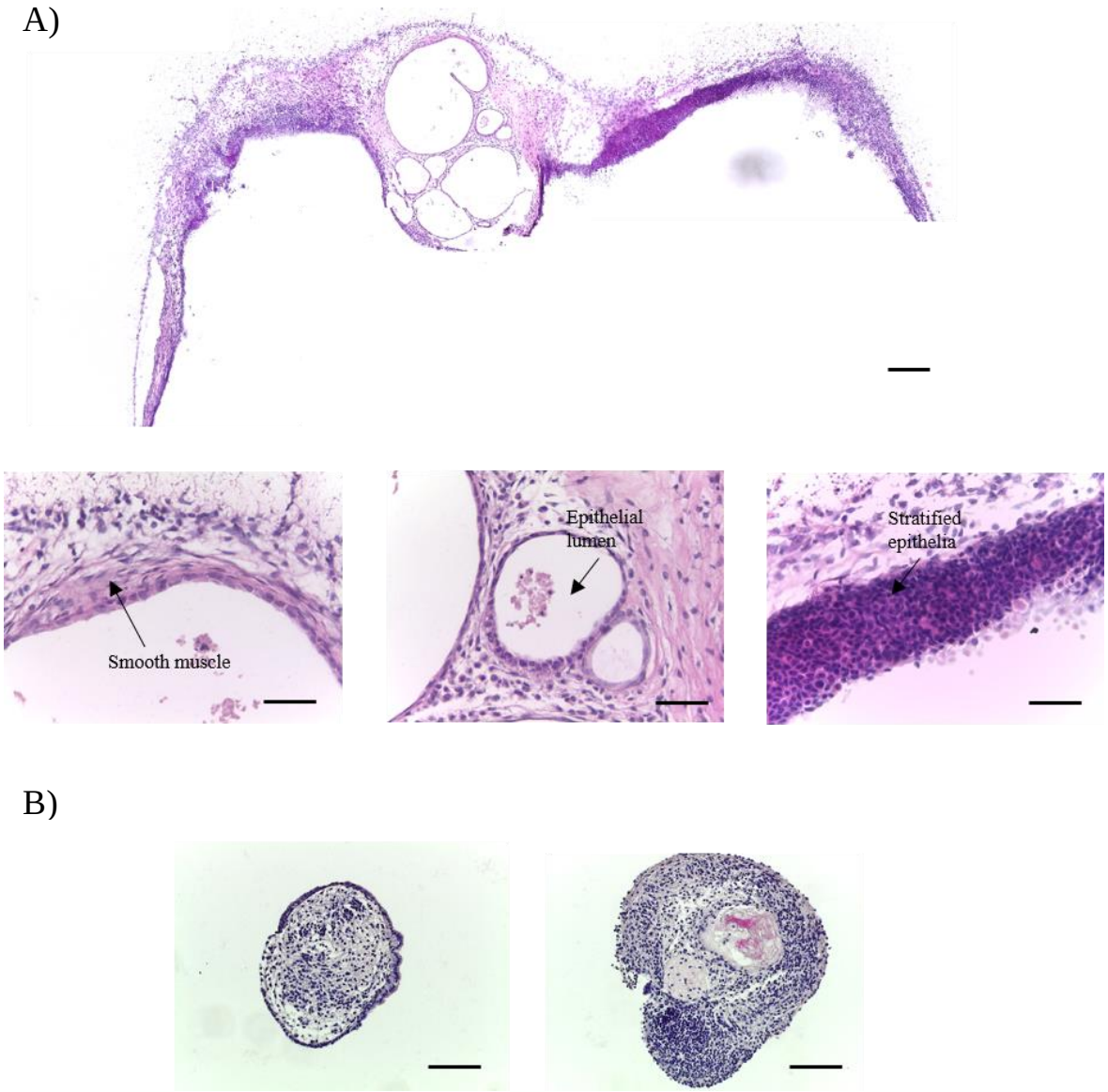


Figure 6.15: Culture and characterisation of murine embryoid bodies on Alvetex® Polaris for 35 days: CGR8 embryoid bodies were seeded onto Alvetex® Polaris inserts and cultured for a specified time in the absence of LIF before fixing in 4 % PFA and processing. Samples embedded in wax were sectioned both in the frontal and transverse planes to analyse the structures within the tissue disc. A) H&E images show the continued presence of complex structures within the tissue disc, even after 35 days culture on the insert. There are a number of epithelia lines cavities, organised epithelia, smooth muscle and connective tissues. B) Even after 35 days in suspension culture, EBs maintain a relatively homogenous morphology and show little evidence of complex organised structures. Representative images shown. Scale bars: 200 µm and 100 µm

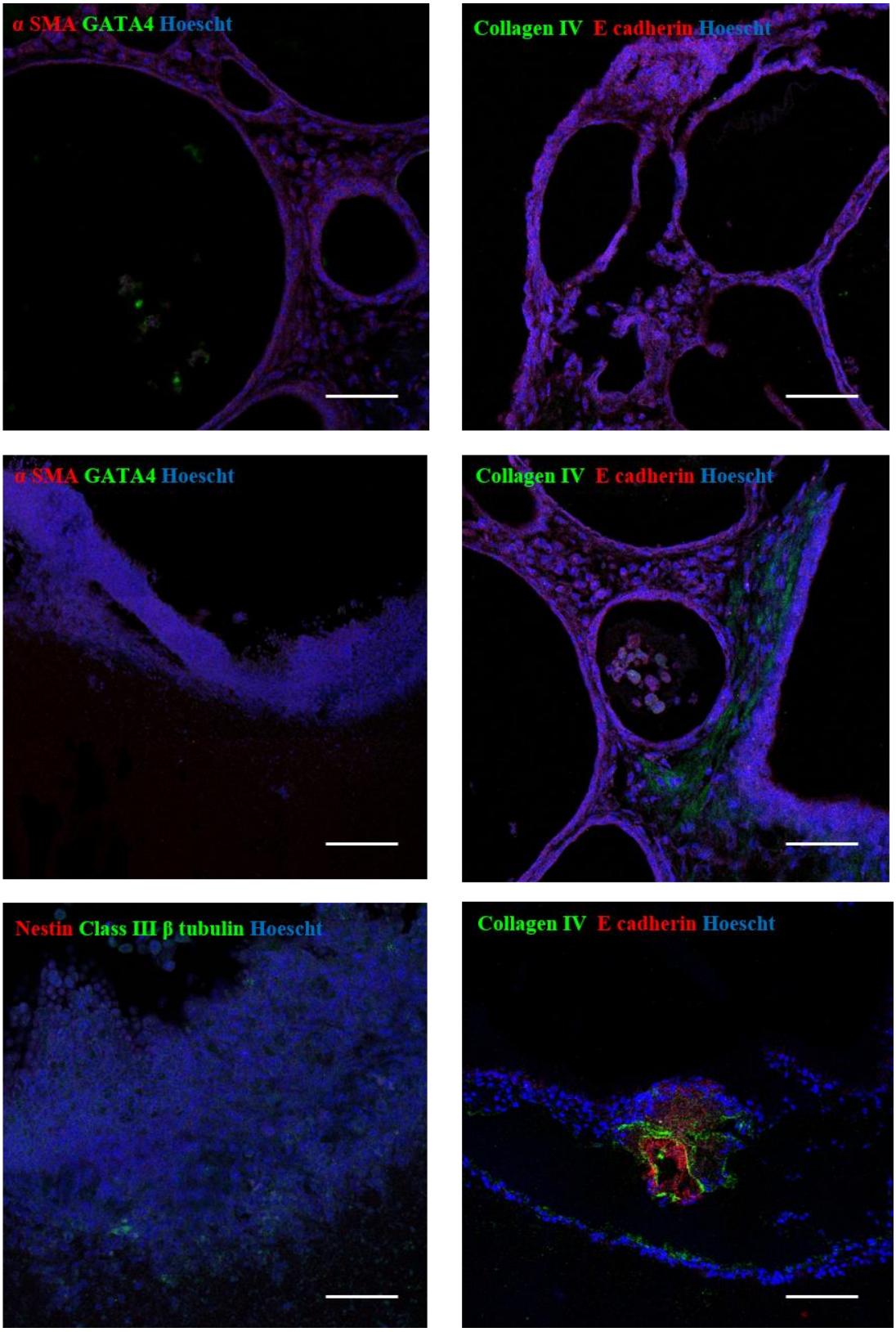


Figure 6.16: Culture and characterisation of murine embryoid bodies on Alvetex® Polaris for 35 days: CGR8 embryoid bodies were seeded onto Alvetex® Polaris inserts and cultured for a specified time in the absence of LIF before fixing in 4 % PFA and processing. Samples embedded in wax were sectioned both in the frontal and transverse planes to analyse the structures within the tissue disc. Immunostaining confirms the identity of the complex differentiation visible in the H&E images, with markers pertaining to the three germ layers, including organised epithelia and neural differentiation. Representative images shown. Scale bars: 200 µm and 100 µm

6.5.2 Modulation of tissue disc differentiation using exogenous morphogen stimulation

Up to this point, CGR8 murine embryoid bodies have been used within the model to successfully form spontaneously differentiated tissue discs, demonstrating their ability to be both maintained and show continued differentiation within the model. Spontaneous differentiation of tissue discs in this way is certainly useful for applications such as the assessment of pluripotency, although given the random differentiation and lack of organisation, this is less useful for studies into the process of human development. While differentiation has shown signs of consistency, it is still a randomly occurring process, and the distributions and relative frequencies of the tissue will also vary from model to model. With this in mind, the decision was made to test the capabilities of the murine stem cell version of the model further through exogenous modulation of embryoid body differentiation prior to seeding onto the scaffold. Simple differentiation with single morphogens would be conducted to ensure CGR8 differentiated tissue discs could form and be maintained in the model, before more complex differentiation was undertaken. Taking inspiration from a recent ISCI paper investigating the methodologies used to assess the developmental potency of human pluripotent stem cell lines, combinations of morphogens were used to direct the differentiation of embryoid bodies more specifically towards the three germ layers prior to seeding on Alvetex® Polaris. Finally, ectodermal differentiation specifically was selected for a more thorough focus, with a view to investigating ectodermal fate decisions as controlled by two morphogen systems; BMPs and Nodal signalling. In this differentiation protocol, experiments previously conducted in 2D were translated to the three dimensional environment, with the intention of investigating whether the interactions seen in 2D are replicated in 3D.

6.5.2.1 Directed differentiation of tissue discs is achievable by the application of single morphogens to embryoid bodies prior to seeding

Initially, embryoid bodies were differentiated very generally towards specific germ layer lineages before seeding as tissue discs, using single exogenous morphogens, to ensure CGR8 differentiated tissue discs could be maintained in the model. The ability to maintain differentiated tissue discs in the model is key to the study of human developmental processes, and the elucidation of the mechanisms involved.

Two morphogens which roughly corresponded to differentiation towards the three germ layers were chosen to differentiate the embryoid bodies during the 5 day suspension stage of culture, while embryoid bodies are undergoing self-organisation. EC23 has been previously used to differentiate TERA2.cl.SP12 EBs in this project, and is a potent inducer of the neural phenotype, allowing for directed differentiation towards an ectodermal phenotype. Activin A is a morphogen which is used extensively in mesodermal (and some endodermal) differentiation protocols.

Applying EC23 to the CGR8 embryoid bodies results in strong differentiation towards the neural phenotype, as evidenced by the strongly differentiated phenotype characterised by the homogeneous structure and dense nuclei within the EBs as seen in Figure 6.17 and the positive staining for the mature neural differentiation marker Class III β-tubulin. EC23 treated embryoid bodies were seeded onto Alvetex® Polaris and maintained for a further 7 days prior to fixing and analysis. The resultant tissue discs show the same homogenous neural phenotype with a dense structure and confirmatory strong positive staining for the neural marker Class III β-tubulin, indicating the ectodermal lineage.

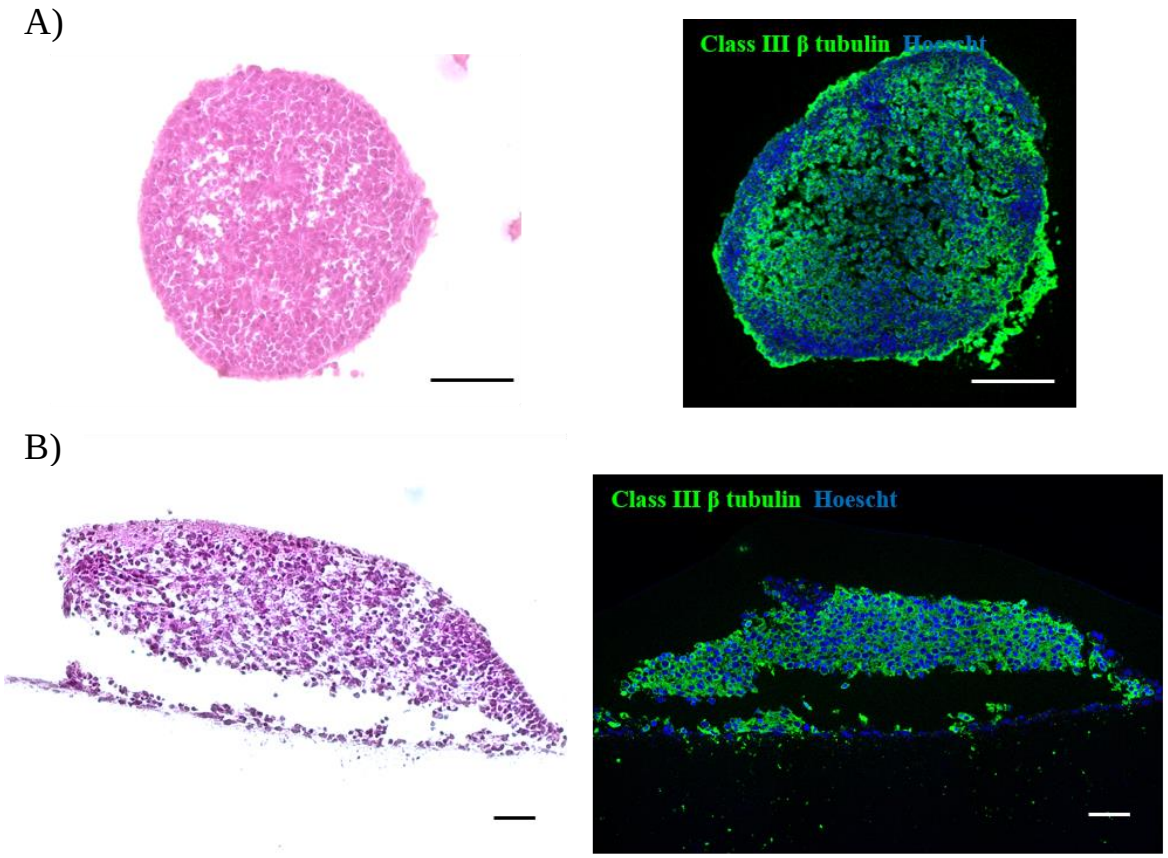


Figure 6.17: Directed differentiation of CGR8 embryoid bodies with synthetic retinoid EC23 and their maintenance on Alvetex® inserts: CGR8 embryoid bodies were treated with 0.01 μM EC23 during the suspension phase in the Petri dish, before subsequent transfer and maintenance on Alvetex® Polaris inserts. A) Embryoid bodies respond well to the EC23 showing a neural phenotype which is morphologically distinct from EBs allowed to spontaneously differentiate, and stains positively for the neural marker Class III β-tubulin. B) These EBs and their phenotype can be maintained on the Alvetex® inserts as tissue discs, also showing strong expression of Class III β-tubulin. Representative images shown. Scale bar: 100 μm

The addition of Activin A to embryoid bodies during suspension culture also results in a strongly differentiated phenotype as seen in Figure 6.18, which stains positive for the early mesodermal differentiation marker GATA4. The strong phenotype is maintained when the embryoid body is cultured as a tissue disc on Alvetex® Polaris for 7 days, showing a similarly dense homogenous

structure within the centre of the tissue disc. This dense centre is surrounded by a distinct outer layer of cells, some of which stain positively for the early mesodermal transcription factor GATA4 and α smooth muscle actin, indicating the presence of myofibroblasts of mesodermal origin.

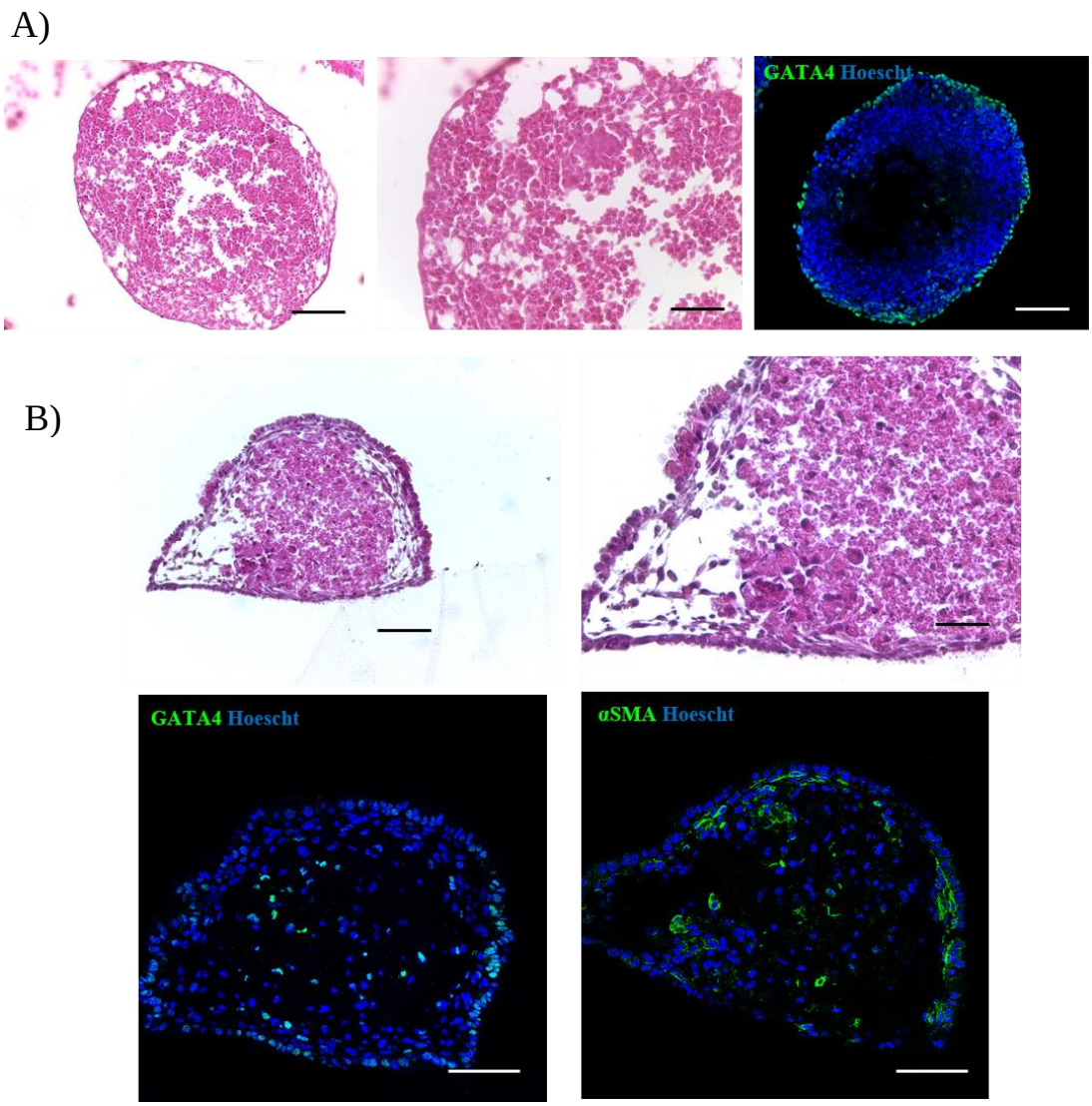


Figure 6.18: Directed differentiation of CGR8 embryoid bodies with Activin A and their maintenance on Alvetex® inserts: CGR8 embryoid bodies were treated with 50 ng/ml Activin A during the suspension phase in the Petri dish, before subsequent transfer and maintenance on Alvetex® Polaris inserts. A) Embryoid bodies respond well to the Activin A, showing a phenotype which is highly morphologically different from EBs allowed to spontaneously differentiate. B) These EBs and their phenotype can be maintained on the Alvetex® inserts as tissue discs, showing evidence of mesodermal differentiation through the expression of GATA4 and α smooth muscle actin. Representative images shown. Scale bars: 100 µm and 50 µm

6.5.2.2 Tissue discs differentiated towards specific germ layers using a combination of morphogens show a shift in the structures which form after 14 days

Simple differentiation of embryoid bodies and the maintenance of their subsequent tissue discs on Alvetex® proved possible, although the tissue structures which formed were not complex or mature when compared to teratoma samples or developed human tissues. In the case of EC23, this represented highly mature neural tissue due to the potent action of the morphogen. The application of Activin A to the EBs resulted in the differentiation of the EBs towards the mesodermal lineage, but the structures mainly show the formation of progenitor populations. The interactions of multiple morphogens are pivotal for complex structure formation during the developmental process. Combinations of morphogens as used in the ISCI 2018 paper to differentiate embryoid bodies towards the three germ layers were again used to direct the differentiation of murine embryoid bodies prior to seeding onto Alvetex® Polaris to encourage the differentiation of multiple complex structures from each germ layer. Two time points were again selected to assess histology, protein and gene expression: 14 days and 28 days. 14 days was the minimum amount of time required for complex, recognisable structured to form during the previous study using spontaneously differentiating tissue discs, so this was used for the following directed differentiation studies. 28 days represents a significant culture period on the scaffold, and is sufficiently lengthy to allow for the assessment of more complex differentiation within the tissue discs. The histology of these tissue discs is only representative of the differentiated samples, as a very wide range of differentiated structures were observed in each germ layer. The quantitative analyses, PCR and Western blotting, are more representative of the differentiation of the tissue disc populations, and so can provide a better indicator as to the phenotype observed.

Ectodermal differentiation was induced by the addition of 10 μM dorsomorphin, 10 μM SB431542 and 100 ng/ml basic-FGF to CGR8 differentiation media during the Aggrewell stage. As shown in Figure 6.19, after 14 days culture on Alvetex® Polaris, these tissue discs show strong differentiation towards ectodermal tissues. Neural differentiation is clearly visible within the tissue disc, which has a dense structure. Fibroblast derived connective tissues are notably absent, as are epithelia lined lumens with other epithelia types, such as columnar, pseudostratified and cuboidal. Immunostaining for a variety of germ layer markers as used previously in this Chapter aids in the identification of the structures present, and confirms the neural nature of the tissue disc. The structure stains strongly for the mature neural marker Class III β-tubulin, and no other germ layer related proteins.

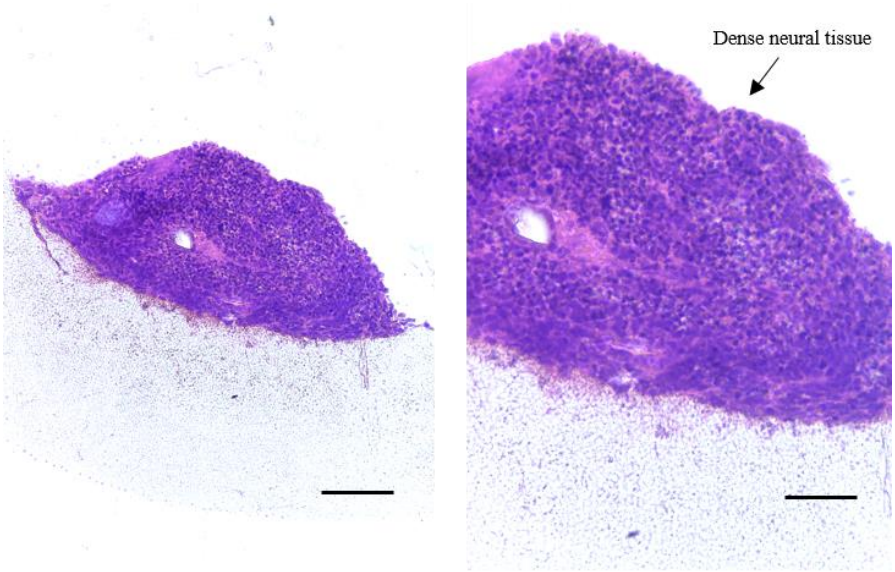


Figure 6.19: Maintenance of embryoid bodies differentiated towards ectodermal lineages as tissue discs on Alvetex® Polaris for 14 days: CGR8 cells were treated with 10 µM dorsomorphin, 10 µM SB431542 and 100 ng/ml basic-FGF during the EB formation stage when cells were in the Aggrewell plate. EBs were then transferred to suspension culture for 5 days, before seeding onto Alvetex® Polaris to form tissue discs. Ectodermal differentiation is apparent within the tissue disc, with clear dense neural tissues and some evidence of neural rosettes. Representative images shown. Scale bars: 100 µm and 50 µm

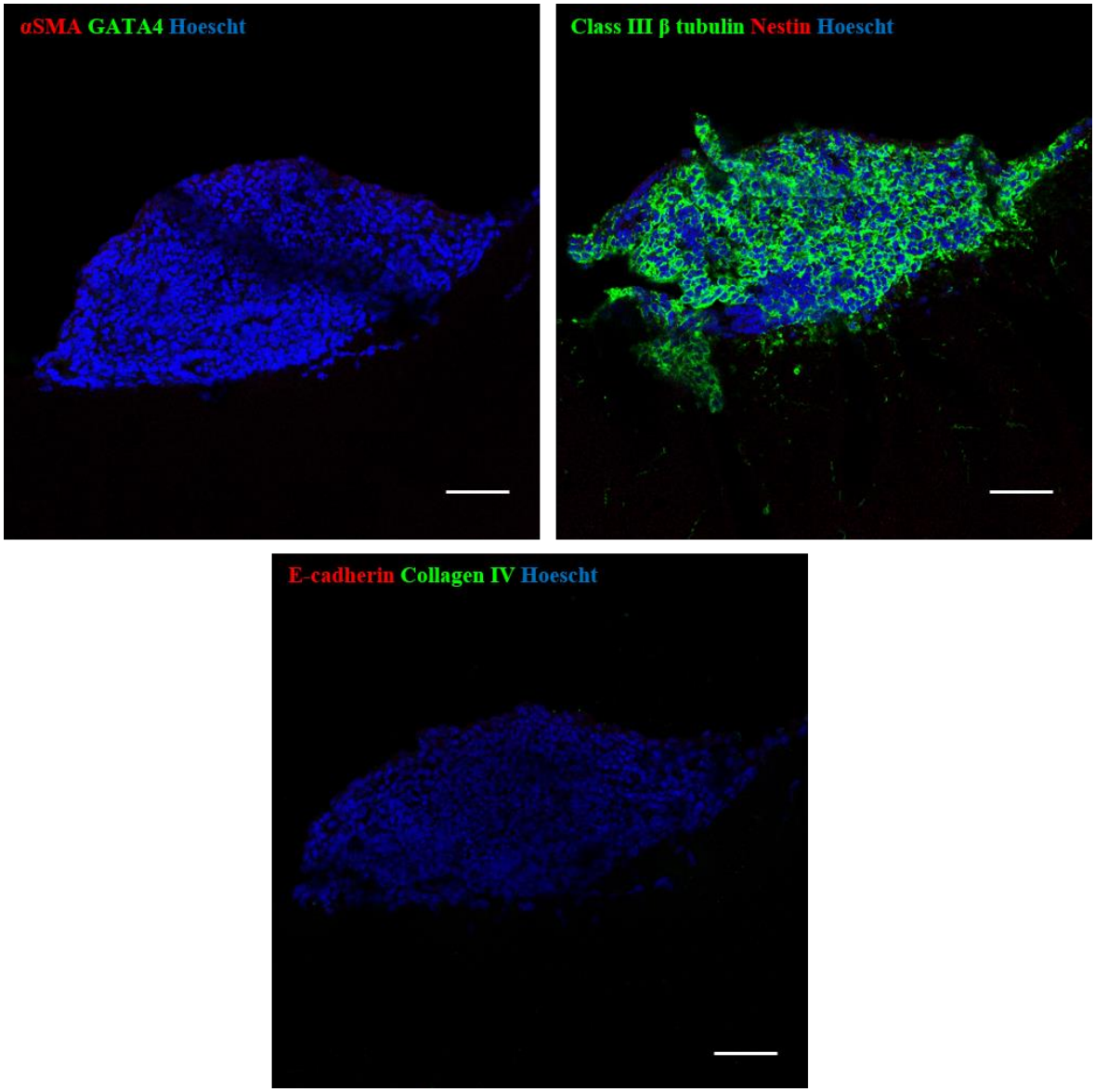


Figure 6.20: Assessment of 14 day ectodermal tissue disc differentiation and structure identity via immunostaining for germ layer markers: Ectodermal differentiation was identified within the tissue disc using histological staining. Immunostaining shows the lack of E-cadherin positive epithelial surfaces. Neural tissue stains strongly positive for mature neural marker Class III β-tubulin, although is not positive staining for early neural marker Nestin. No evidence of α smooth muscle actin staining and GATA4 are present within the tissue disc. Representative images shown. Scale bar: 100 μm

In order to induce mesodermal differentiation, 20 ng/ml Activin A, 20 ng/ml BMP-4 were added to CGR8 differentiation media. Culture on the Alvetex® Polaris scaffold for 14 days results in a tissue disc which shows a very different tissue composition, with a general shift towards the mesoderm in the structures which are present. The tissue disc is comprised mainly of connective tissue and various epithelia, including simple and pseudostratified, as can be seen in Figure 6.21. This is in contrast to that differentiated towards ectoderm; there are few tissues derived from this germ layer immediately visible within the tissue disc, such as neural or skin tissue. Immunostaining shows very little staining for ectodermal markers Nestin and Class III β-tubulin, indicating a lack of neural differentiation within the tissue disc. E-cadherin and collagen 4 staining is minimal or absent within the tissue disc, suggesting that the epithelial surfaces are not fully mature or well organised. Staining for the mesodermal transcription factor GATA4 indicates early mesodermal differentiation. There is limited staining for α smooth muscle actin, another mesodermal marker.

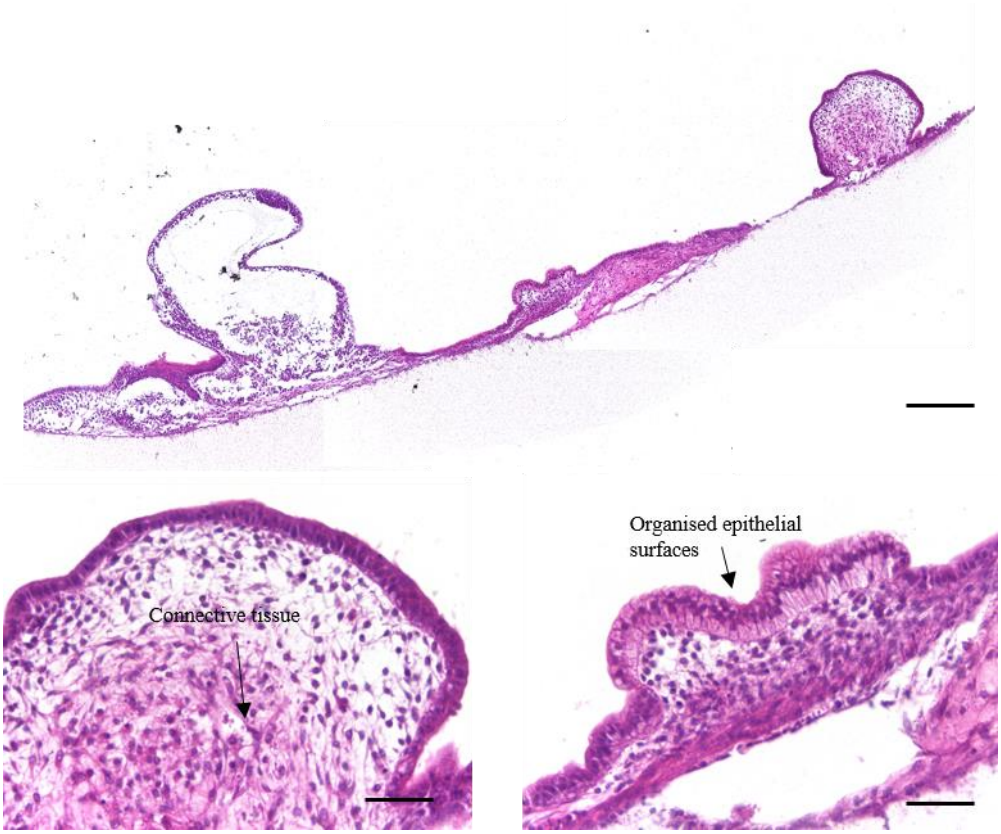


Figure 6.21: Maintenance of embryoid bodies differentiated towards mesodermal lineages as tissue discs on Alvetex® Polaris for 14 days: CGR8 cells were treated with 20 ng/ml Activin A, 20 ng/ml BMP-4 during the EB formation stage when cells were in the Aggrewell plate. EBs were then transferred to suspension culture for 5 days, before seeding onto Alvetex® Polaris to form tissue discs. Mesodermal differentiation is apparent within the tissue disc, with large areas of connective tissue, some organised epithelia and little evidence of ectodermal differentiation, such as epidermal or neural differentiation. Representative images shown. Scale bar: 200 µm and 50 µm

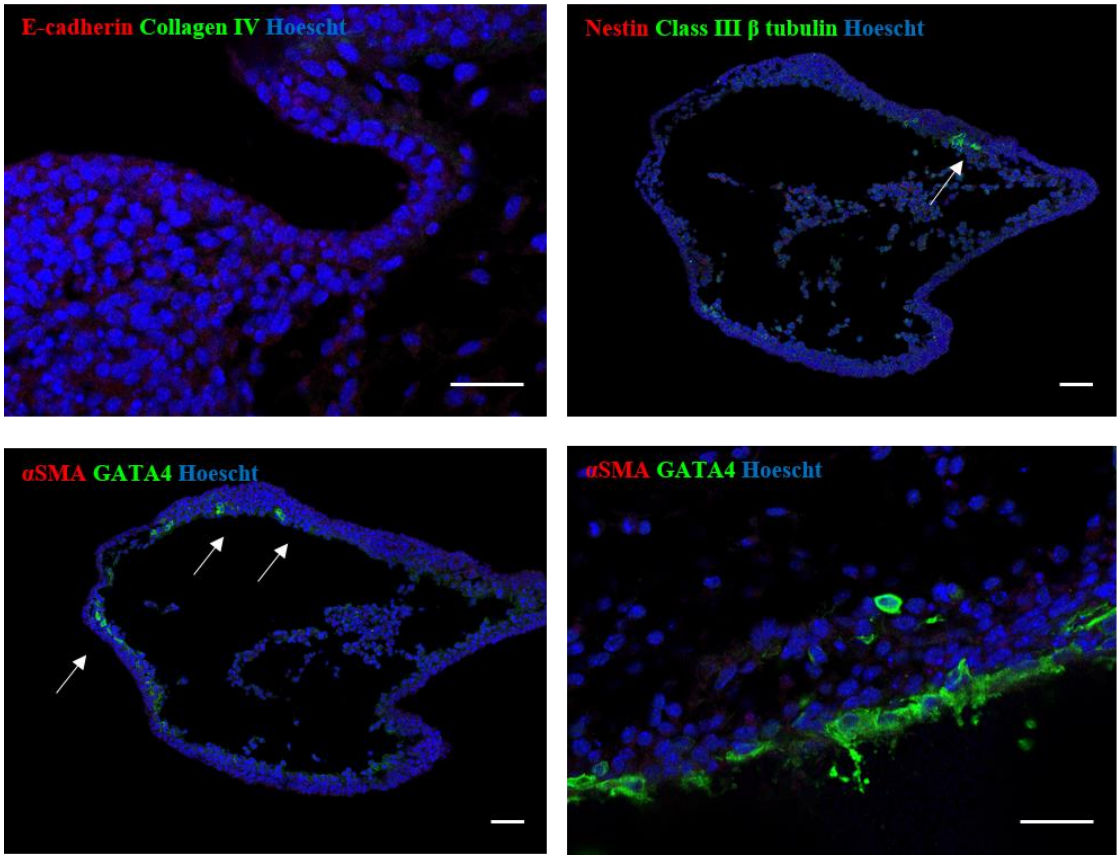


Figure 6.22: Assessment of 14 day mesodermal tissue disc differentiation and structure identity via immunostaining for germ layer markers: Mesodermal differentiation was identified within the tissue disc using histological staining. Immunostaining shows a lack of E-cadherin positive epithelia, suggesting a lack of organisation, and very little neural differentiation as indicated by positive Class III β-tubulin staining. GATA4 positive staining indicates the presence of mesodermal progenitor cells. Representative images shown. Scale bar: 100 µm

The addition of 100 ng/ml Activin A, 1 ng/ml BMP-4 to the CGR8 differentiation media was used to induce endodermal differentiation, and as previously, there are subtle differences in the structures present. Examples of a variety of highly organised polarised epithelial surfaces can be detected, typically associated with endodermal differentiation. A connective tissue component is also present within the tissue disc, which shows a loosely organised structure. Immunostaining shows strongly positive staining of E-cadherin within epithelial surfaces which surround the lumen in the tissue disc, indicating endodermal differentiation and structures which are highly organised. No neural differentiation is detectable through any Nestin or Class III β-tubulin staining, indicating an absence of the ectoderm germ layer. Some areas of weakly positive GATA4 staining are present, indicating small areas of early mesodermal differentiation.

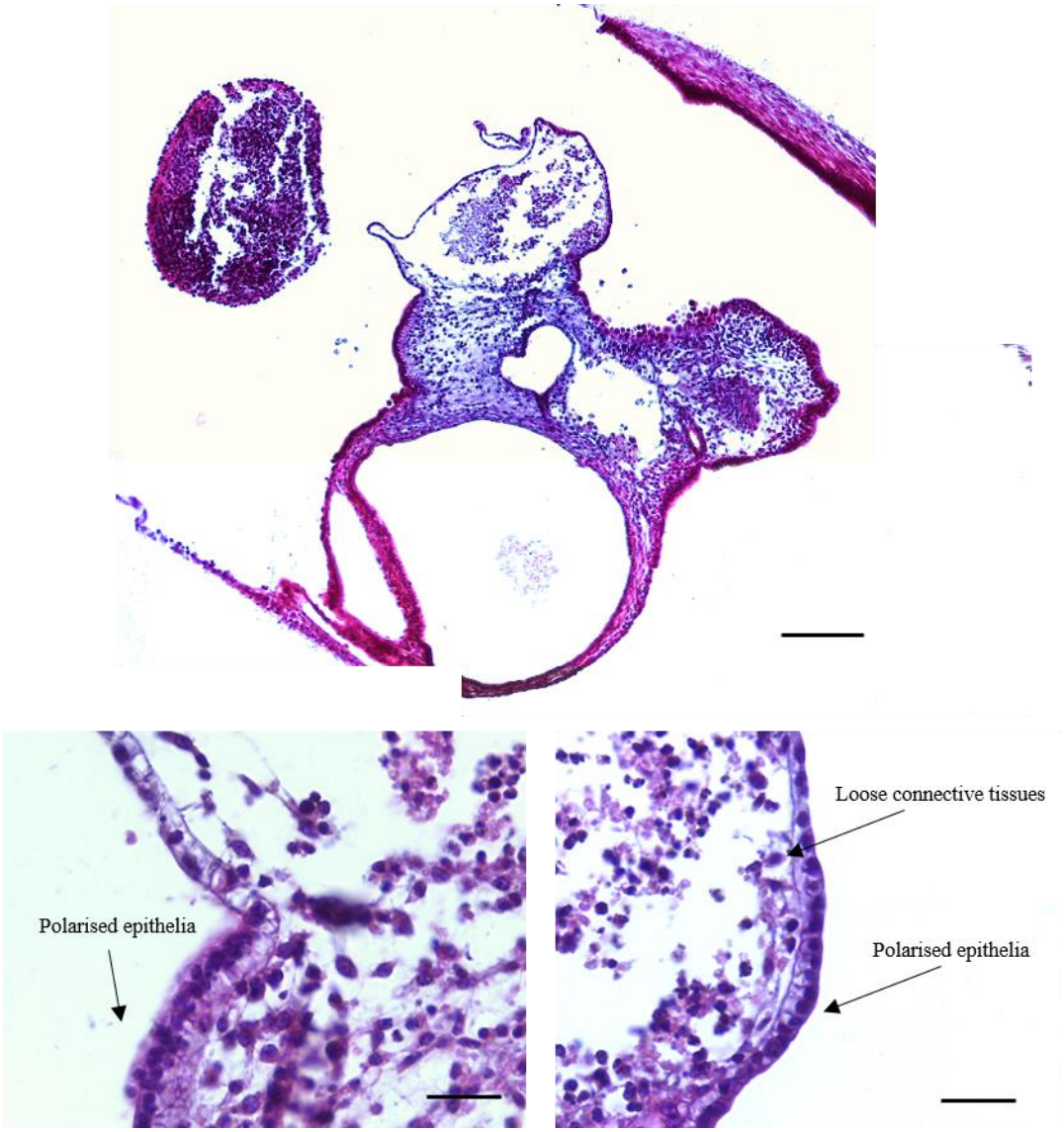


Figure 6.23: Maintenance of embryoid bodies differentiated towards endodermal lineages as tissue discs on Alvetex® Polaris for 14 days: CGR8 cells were treated with 100 ng/ml Activin A, 1 ng/ml BMP-4 during the EB formation stage when cells were in the Aggrewell plate. EBs were then transferred to suspension culture for 5 days, before seeding onto Alvetex® Polaris to form tissue discs. Some endodermal differentiation is detectable within the tissue disc in the form of organised polarised epithelia, along with structures from other germ layers, such as connective tissues. Again, there are few ectodermal derivatives observed. Representative images shown. Scale bar: 200 µm and 50 µm

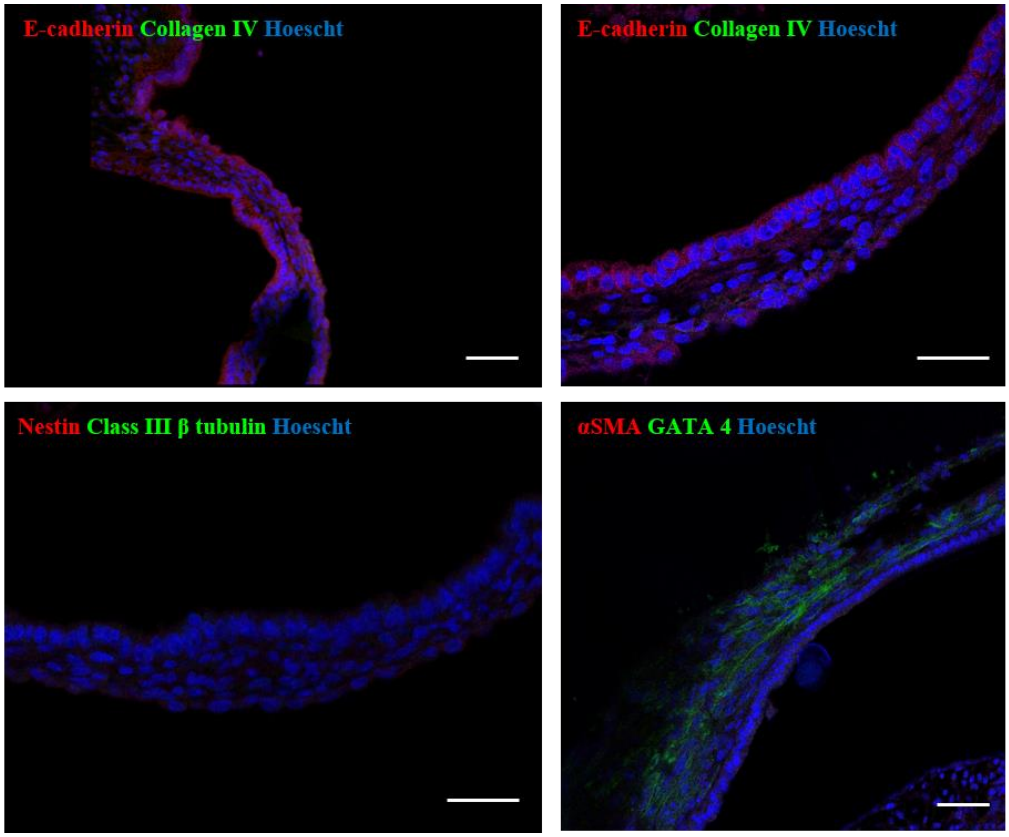


Figure 6.24: Assessment of 14 day endodermal tissue disc differentiation and structure identity via immunostaining for germ layer markers: Endodermal differentiation was identified within the tissue disc using histological staining. Immunostaining shows the presence of E-cadherin positive epithelial surfaces, indicating organisation. Neural tissue is not present in this sample due to the lack of Class III β-tubulin staining. Weak staining for GATA4 indicated some mesodermal progenitors within the sample. Representative images shown. Scale bar: 100 µm

Gene expression was also analysed in order to obtain a better overview of the differentiation of the tissue discs as a population, and to better identify the presence of trends in the differentiation of these structures. A range of genes were selected to correlate with the immunostaining already performed, as well as additional genes to cover the three germ layers. Cytokeratin 10, E-cadherin and Class III β-tubulin were chosen for ectoderm; cytokeratin 14 was also chosen to identify epidermal basal stem cells. Brachyury is a mesodermal lineage commitment marker, and GATA6 is a transcription factor associated with both differentiation towards mesoderm and endoderm. Due to the difficulty in identifying specific markers for endodermal differentiation due to the diversity of the tissues in this germ layer, E-cadherin was used as previously to detect epithelial surfaces derived from the endoderm layer. In addition, a number of commitment markers for endoderm were chosen in order to better understand the differentiation towards this germ layer, as the tissue discs differentiated towards thus germ layer do not show highly complex and specialised structures reminiscent of the tissues associated with this germ layer. After 14 days, the expression of Class III β-tubulin is highly increased in the tissue discs directed towards the ectodermal lineage, as would be expected given the histology and immunostaining data in Figure 6.19. The expression of this gene in the other two germ

layers also correlates with the histology seen in Figures 6.21 and 6.23, as expression is much lower in these tissue discs. The expression of the other two ectoderm specific genes, cytokeratin 10 and cytokeratin 14 does not necessarily fit with what would be expected. Cytokeratin 10 shows an increased expression in mesodermal samples, but this is not significantly different from the expression observed in other germ layer tissues. Cytokeratin 14 is very highly expressed in the endodermal sample at 14 days, with very low level expression detected in the other germ layer samples. Mesoderm specific gene brachyury was elevated in the ectoderm and endoderm samples, yet expression was lower in actual mesoderm differentiated samples. GATA6 expression is noted to be slightly elevated in the endoderm sample, and completely absent in the other two germ layers. All of the genes which were selected to identify the presence of endodermal tissues were highly elevated in the endoderm samples, their expression being several fold times higher than the control samples, as would be expected. All of these genes also showed a slight increase in expression in the mesoderm samples, and were low or absent in the samples which were differentiated towards the ectoderm.

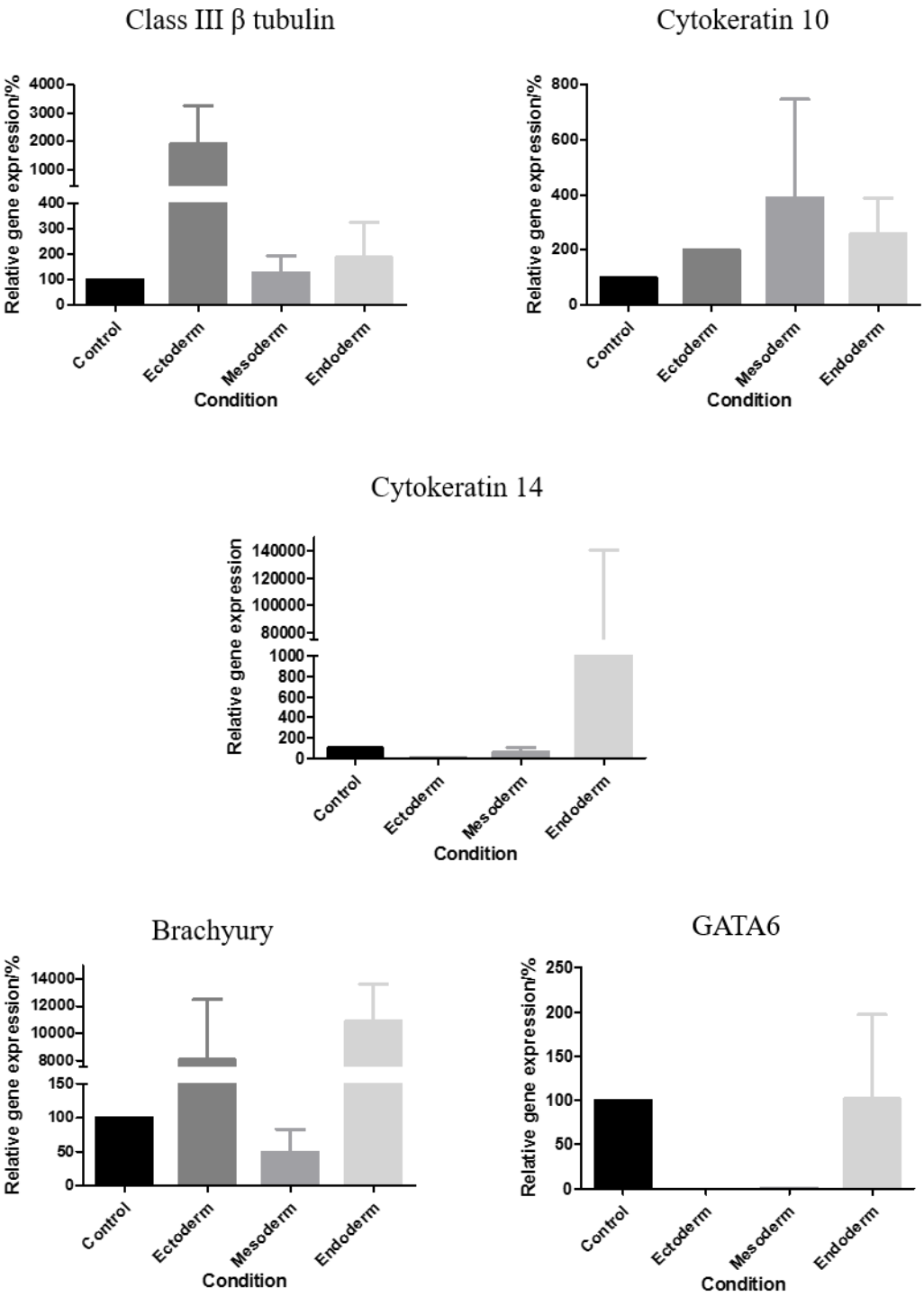


Figure 6.25: Assessment of gene expression in 14 day germ layer differentiated tissues discs: Tissue discs were subject to analysis via qPCR. RNA was extracted from a tissue disc population, converted to cDNA and the expression of a variety of germ layers specific genes quantified. For simplicity, controls are shown as a single bar, as specific germ layer controls were conducted. Differences in gene expression generally correlated with the germ layer to which the tissues discs were differentiated; Class III β-tubulin and GATA6 showed this for ectoderm and endoderm respectively. Cytokeratin 10 and 14 were expressed in an unexpected pattern, in germ layers other than ectoderm at a high level. Brachyury was also expressed highly in other germ layers than was expected. Data represents mean ± SEM from 2-3 independent experiments

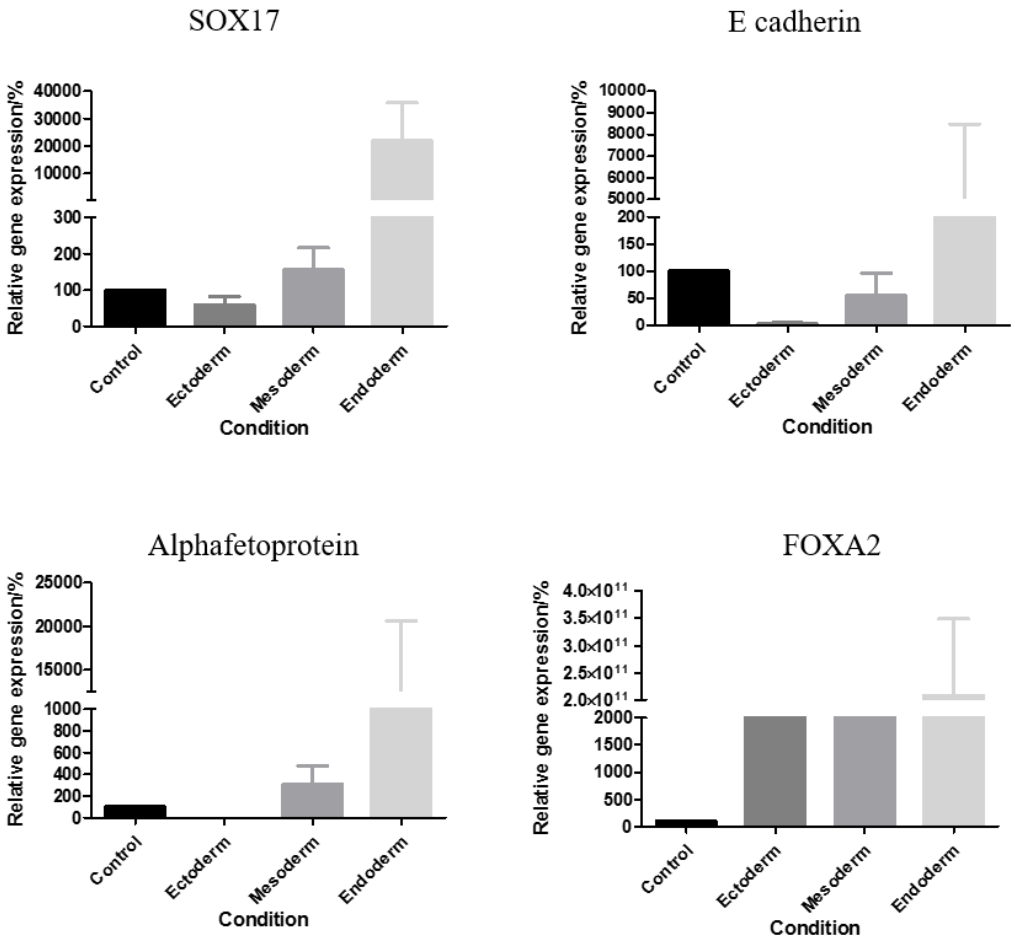


Figure 6.26: Assessment of gene expression in 14 day germ layer differentiated tissues discs: Tissue discs were subject to analysis via qPCR. RNA was extracted from a tissue disc population, converted to cDNA and the expression level of a variety of germ layers specific genes quantified. For simplicity, controls are shown as a single bar, as specific germ layer controls were conducted. Differences in gene expression generally correlated with the germ layer to which the tissues discs were differentiated. The genes in this Figure show very strong association with endoderm samples, as would be expected. Data represents mean ± SEM from 2-3 independent experiments**.**

Brief analysis of protein expression was also undertaken, through conducting SDS PAGE and densitometry on the subsequent bands identified on the membranes. Some of the proteins that were stained for during immunostaining were also selected for Western blotting analysis: Class III β-tubulin for ectoderm, α smooth muscle actin and GATA4 for mesoderm, and E-cadherin for epithelial surfaces of ectodermal and endodermal origin. In the 14 day samples, the expression of E-cadherin is highly elevated in the mesoderm, although shows considerable variation. Class III β-tubulin expression is consistent in the ectoderm and mesoderm samples, but elevated in the endoderm sample and also showing variation. The expression of the mesodermal transcription factor GATA4 appears slightly decreased in the mesoderm samples and increased in ectoderm and endoderm samples. Finally, the expression of α smooth muscle actin is consistent within the mesoderm and endoderm sample, with a small increase in the ectoderm differentiated sample.

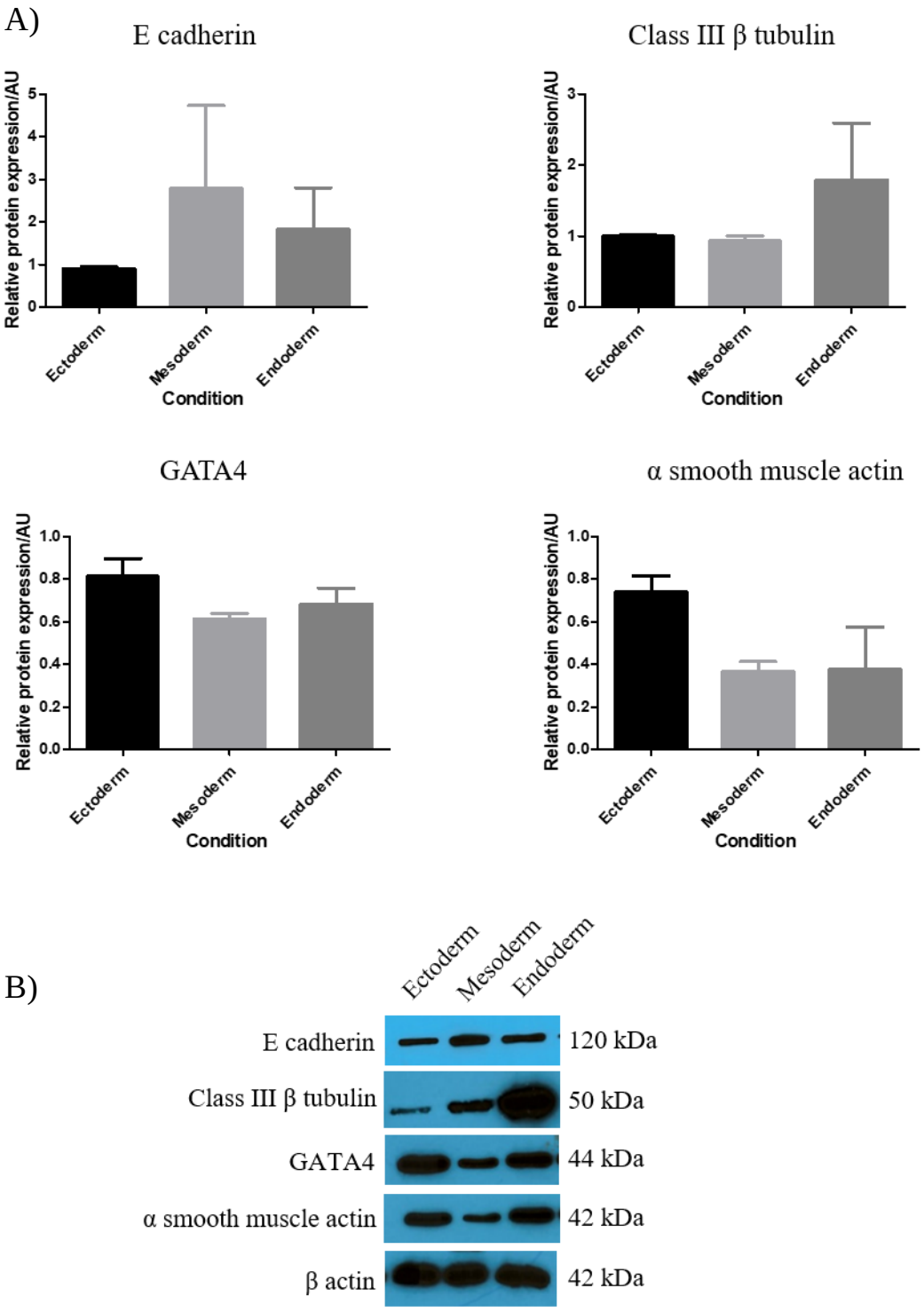


Figure 6.27: Assessment of protein expression in 14 day germ layer differentiated tissues discs: Tissue discs were subject to analysis via Western Blotting. The entire protein contents of the tissue discs on an insert were subject to analysis via Bradford assay and analysed using SDS PAGE, before probing for individual proteins. A) Graphs from densitometry analysis of Western Blotting. This technique in particular highlights the variability in the samples, due to error bar size and the expression patterns of the proteins in relation to the three germ layers. B) Representative images of bands from blots. Data represents mean ± SEM from 2-3 independent experiments

6.5.2.3 Both heterogeneity and increased cellular complexity is observed in tissue discs differentiated for up to 28 days

The short term culture of EBs differentiated towards the three germ layers resulted in a shift towards the intended germ layer after 14 days. However, as complexity was maintained on the prolonged culture of spontaneously differentiating tissue discs, and time is a key aspect of the developmental process, these tissue discs were also allowed to develop over 28 days on the Alvetex® insert.

Further culture of up to 28 days shows increased complexity and recognisable tissue structure formation within the tissue disc differentiated towards ectoderm. Stratified skin tissue is present, with the stratified layers easily distinguished, including the uppermost cornified layer. Neural differentiation is also present within the tissue disc. E-cadherin and Collagen 4 staining identify the presence of epithelial surfaces in the tissue disc, both of endodermal origin, surrounding a lumen, and ectodermal origin, in a stratified organisation on the outer surface of the tissue disc. Significant areas of positive Class III β-tubulin staining exist within the tissue disc, indicating mature neural differentiation, which is also confirmed by the lack of positive staining for Nestin, the early neural differentiation marker. Skin tissue identity is confirmed through E-cadherin staining and positive expression of epidermal differentiation markers cytokeratin 10 and small areas of cytokeratin 14 positive staining in a localised, stratified manner as would be expected in human skin. In keeping with the ectodermal phenotype, there is little staining for mesodermal markers GATA4 and α smooth muscle actin within the tissue disc, correlating with the lack of connective and muscle tissues observed in the histology.

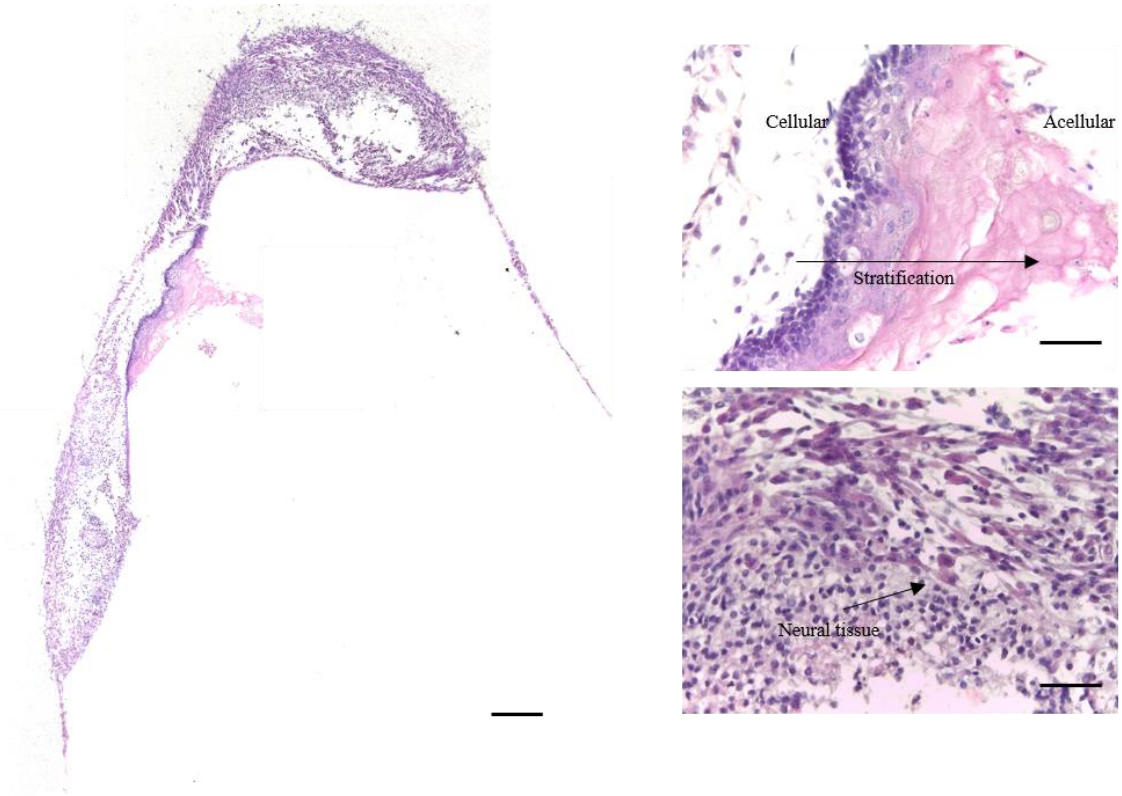


Figure 6.28: Maintenance of embryoid bodies differentiated towards ectodermal lineages as tissue discs on Alvetex® Polaris for 28 days: CGR8 cells were treated with 10 µM dorsomorphin, 10 µM SB431542 and 100 ng/ml basic-FGF during the EB formation stage when cells were in the Aggrewell plate. EBs were then transferred to suspension culture for 5 days as previously described, before seeding onto Alvetex® Polaris to form tissue discs. Ectodermal differentiation is apparent within the tissue disc, with clear areas of neural differentiation and the presence of a significant area of stratified skin which shows clear differentiation. Representative images shown. Scale bar: 200 µm and 50 µm

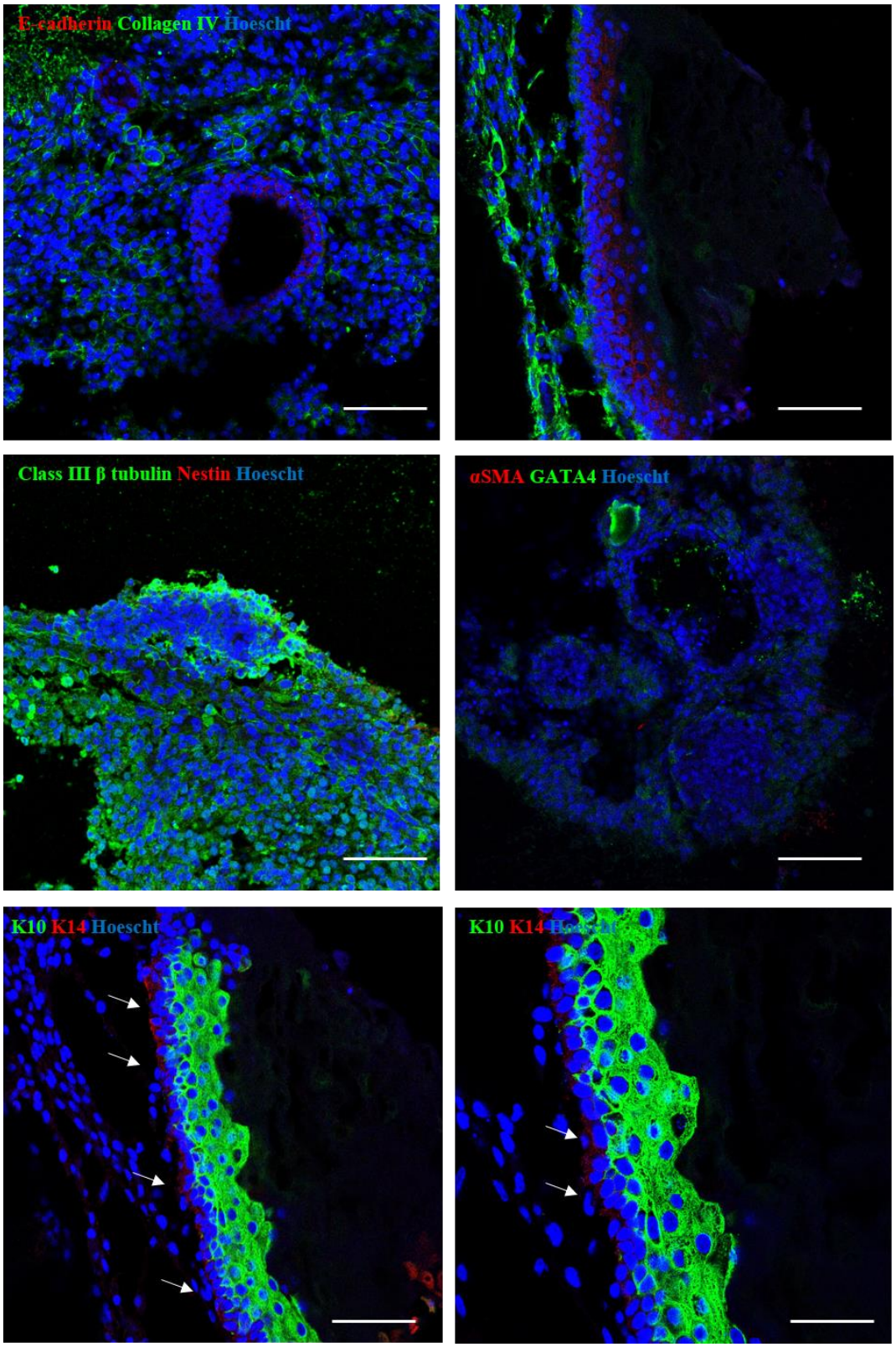


Figure 6.29: Assessment of 28 day ectodermal tissue disc differentiation and structure identity via immunostaining for germ layer markers: Ectodermal differentiation was identified within the tissue disc using histological staining. Immunostaining shows the presence of E-cadherin positive epithelial surfaces. Neural tissue stains positive for mature neural marker Class III β-tubulin and early neural marker Nestin. There are no α smooth muscle actin and GATA4 positive areas, indicating a lack of mesodermal differentiation. Stratified epithelia stains positive for epidermal differentiation markers cytokeratin 10 and basal cell marker cytokeratin 14. Representative images shown. Scale bar: 100 µm and 50 µm

Maintaining the mesoderm differentiated tissue discs on Alvetex® Polaris for 28 days results in the maintenance of this phenotype, with the tissue disc mainly comprising of connective tissue, indicators of smooth muscle and simple epithelia lined lumens, as shown in Figure 6.29. There is a notable absence of tissues derived for ectoderm, such as stratified skin and dense neural areas. Immunostaining for E-cadherin and collagen 4 reveals the presence of some epithelia lined lumens within the tissue disc structure. Intermittent areas of neural differentiation are also present as confirmed by the positive staining for Class III β-tubulin. Mesodermal marker α smooth muscle actin is negative, whereas early differentiation marker GATA4 is positive within the tissue disc.

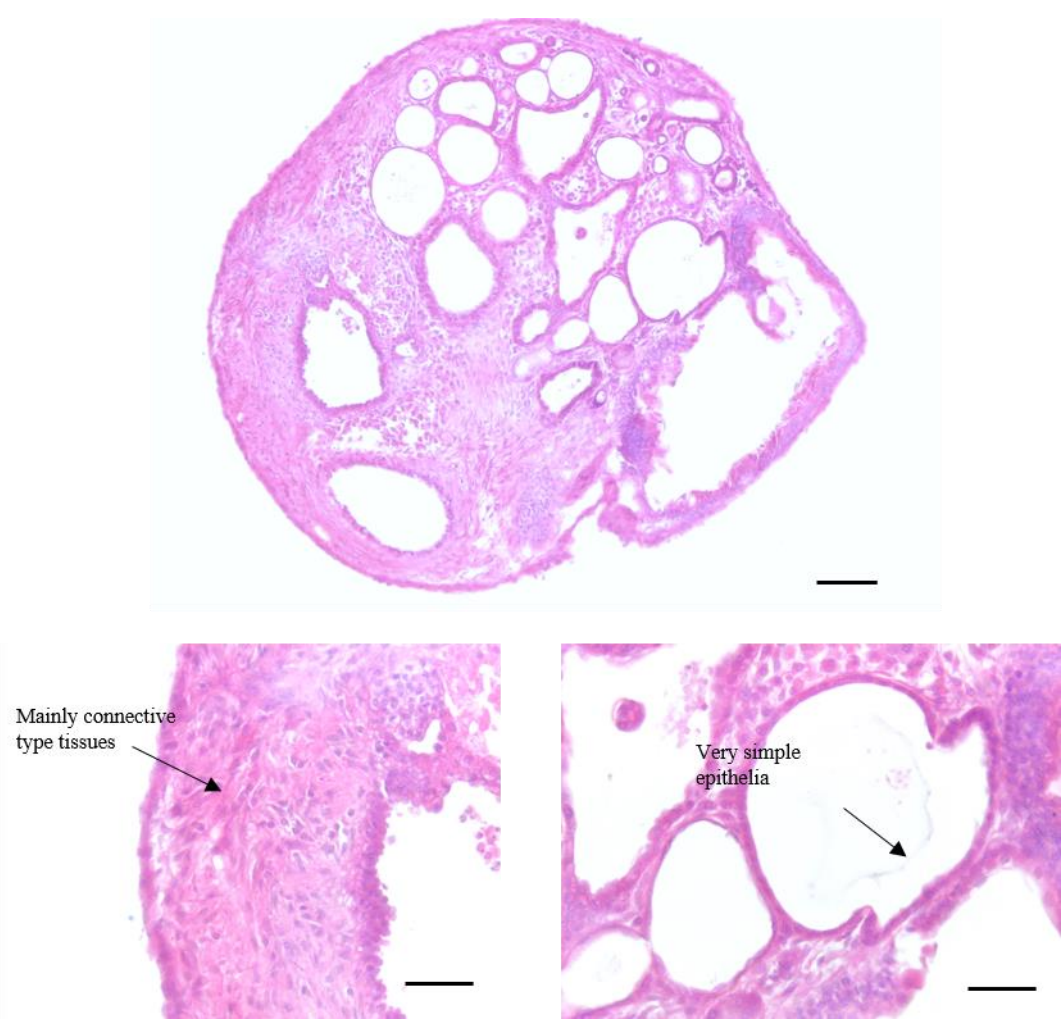


Figure 6.30: Maintenance of embryoid bodies differentiated towards mesodermal lineages as tissue discs on Alvetex® Polaris for 28 days: CGR8 cells were treated with 20 ng/ml Activin A, 20 ng/ml BMP-4 during the EB formation stage when cells were in the Aggrewell plate. EBs were then transferred to suspension culture for 5 days as previously described, before seeding onto Alvetex® Polaris to form tissue discs. Strong mesodermal differentiation is apparent within the tissue disc, with large areas of connective tissue and areas resembling smooth muscle. There are some epithelia and lined cavities, but little evidence of ectodermal differentiation in the form of neural and epidermal structures. Representative images shown. Scale bars: 100 µm and 50 µm

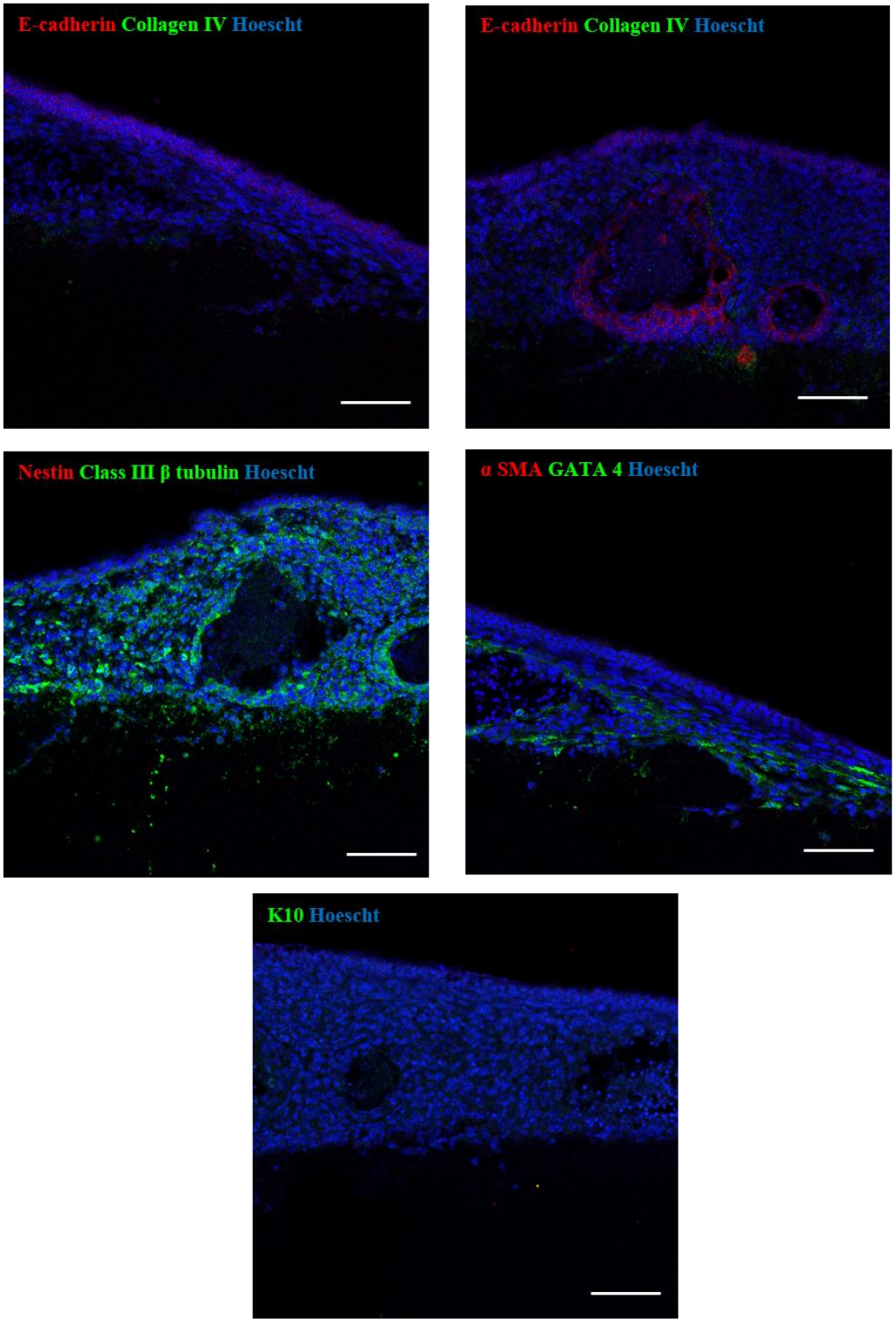


Figure 6.31: Assessment of 28 day mesodermal tissue disc differentiation and structure identity via immunostaining for germ layer markers: Mesodermal differentiation was identified within the tissue disc using histological staining. Immunostaining shows the presence of E-cadherin positive epithelial surfaces. Intermittent neural tissue can be detected within the structure, staining positive for Class III β-tubulin. α smooth muscle actin staining is not detected in the tissue disc, but GATA4 staining indicates mesodermal progenitors within the tissue disc. There are no areas of epidermal differentiation, due to lack of cytokeratin 10 staining. Representative images shown. Scale bar: 100 µm and 50 µm

The 28 day tissue discs differentiated towards endodermal lineages show the development of a number highly organised, polarised epithelial lumens again. In addition, a significant fibroblast based connective tissue component can be seen in the tissue disc, with some areas resembling smooth muscle differentiation also. Immunostaining for a variety of markers confirms these phenotypes. Epithelia stain strongly positive for E-cadherin, showing a strongly organised and polarised phenotype, and some intermittent Class III β-tubulin staining suggests the presence of some neural cells within the tissue. Large areas of GATA4 positive staining indicate a mesodermal phenotype. Interestingly, there is also positive staining for the skin markers cytokeratin 10 and very weak staining for cytokeratin 14, highlighting the presence of a small amount of organised skin differentiation.

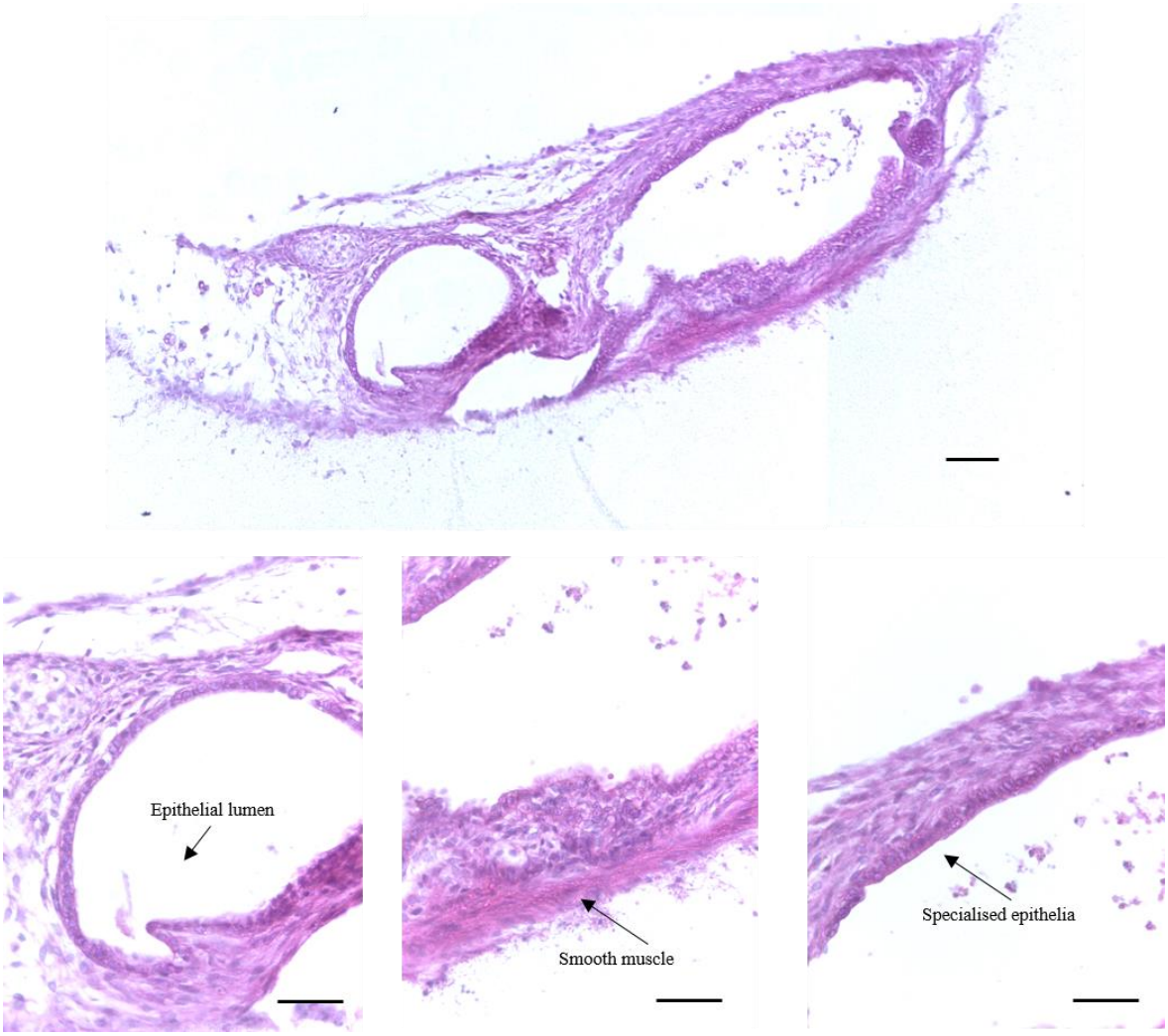


Figure 6.32: Maintenance of embryoid bodies differentiated towards endodermal lineages as tissue discs on Alvetex® Polaris for 28 days: CGR8 cells were treated with 100 ng/ml Activin A, 1 ng/ml BMP-4 during the EB formation stage when cells were in the Aggrewell plate. EBs were then transferred to suspension culture for 5 days as previously described, before seeding onto Alvetex® Polaris to form tissue discs. Some endodermal differentiation is detectable within the tissue disc, with the presence of polarised and specialised epithelial surfaces. Mesoderm derived connective tissue is abundant within the structure, as is stratified epithelia, indicating complex endodermal differentiation. Representative images shown. Scale bar: 100 µm and 50 µm

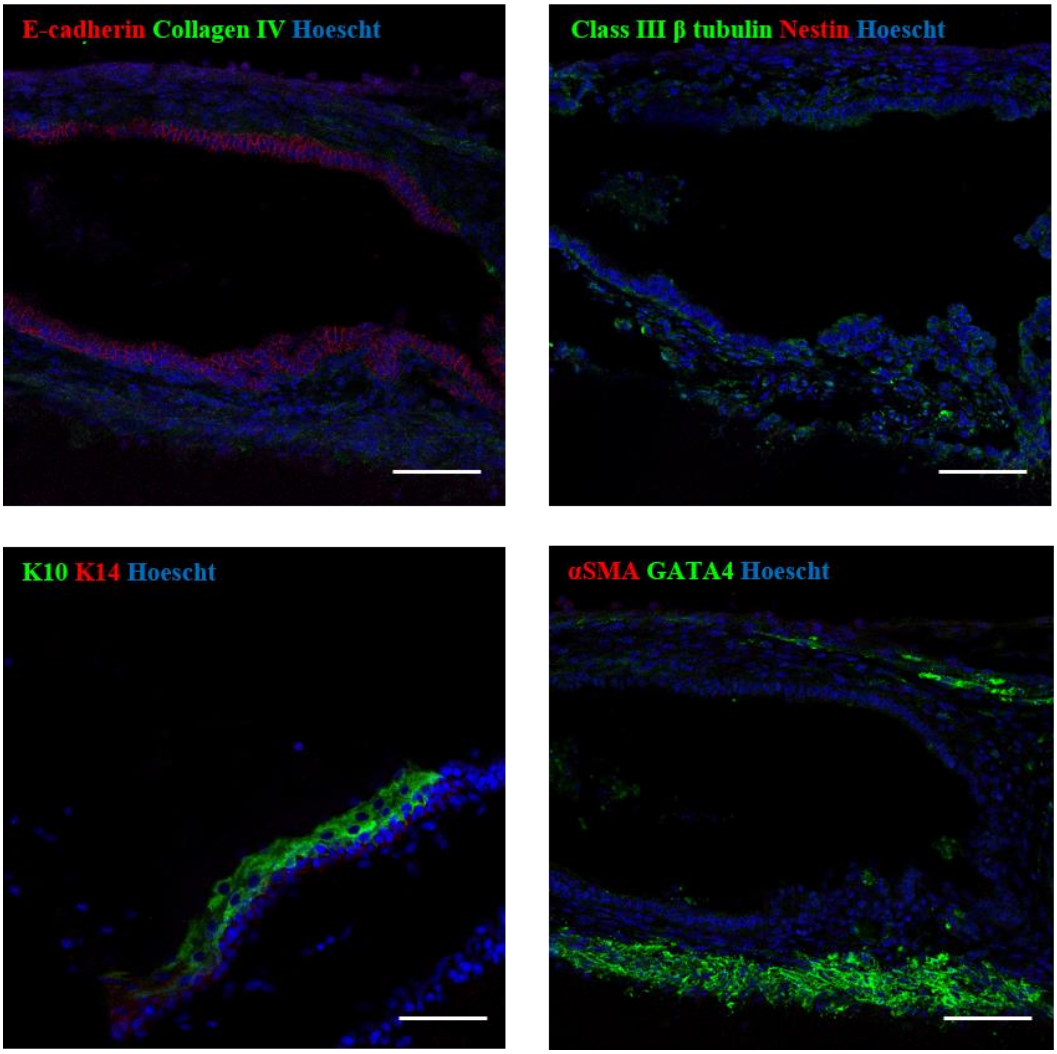


Figure 6.33: Assessment of 28 day endodermal tissue disc differentiation and structure identity via immunostaining for germ layer markers: Endodermal differentiation was identified within the tissue disc using histological staining. Immunostaining shows the presence of well organised E-cadherin positive epithelial surfaces. Small amounts of Class III β-tubulin staining indicate the presence of neural tissues. Positive GATA4 staining indicates the presence of mesodermal progenitors. Epidermal differentiation is also present, with cytokeratin 10 positive epithelial within the structure. Representative images shown. Scale bar: 100 μm

Gene expression analysis was carried out again after 28 days, on a smaller group of genes. Ectoderm gene cytokeratin 10 was found to be elevated in ectoderm and endoderm differentiated samples at this later time point, but almost absent in mesoderm samples, correlating very strongly with the representative histology from Figures 6.28, 6.30 and 6.32. E-cadherin, an indicator for any epithelial surface, was found to be modestly increased in mesoderm and endoderm samples, again showing congruency with the histology as shown in the previous Figures. Interestingly, the expression of E-cadherin was much lower in ectoderm differentiated samples at this time point. The expression of Brachyury was found to be elevated in mesoderm as would be expected, but the expression of this gene was even more elevated in the ectoderm samples, possibly representing a shift in the differentiation occurring. Brachyury expression was absent in endoderm samples. The expression of GATA6 remained elevated in endoderm samples, showing an increase in expression, and remained absent in the other two germ layers. The expression of SOX17 also remained very high in the endoderm samples, with a very small increase in mesoderm tissue discs and a continued absence in ectoderm samples. Differences the expression of the alphafetoprotein gene from 14 days include a decreased expression in endoderm tissue discs and a several fold increase in mesoderm tissue discs.

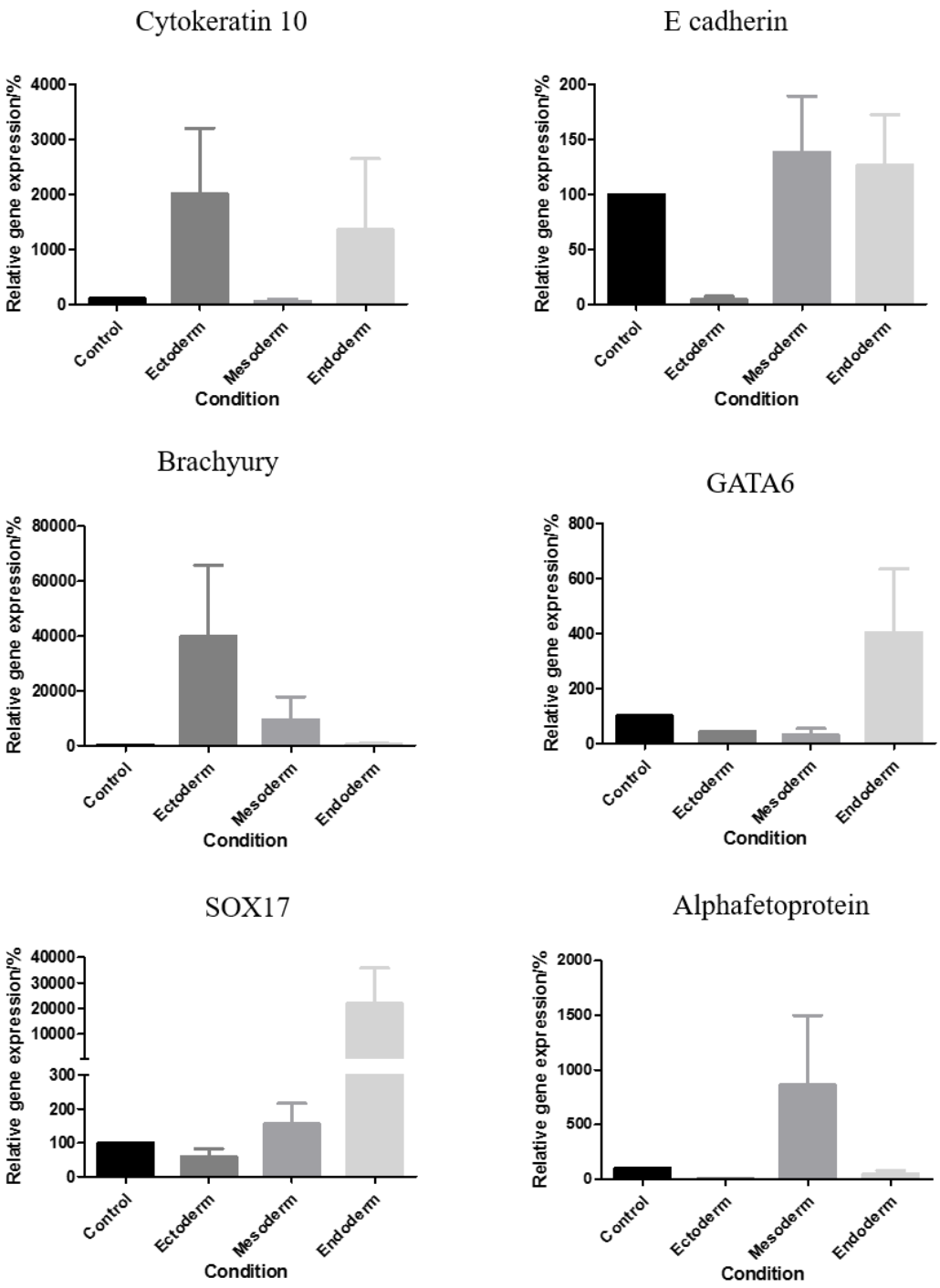


Figure 6.34: Assessment of gene expression in 28 day germ layer differentiated tissues discs: Tissue discs were subject to analysis via qPCR. RNA was extracted from a tissue disc population, converted to cDNA and the expression level of a variety of germ layers specific genes quantified. For simplicity, controls are shown as a single bar, as specific germ layer controls were conducted. Differences in gene expression generally correlated with the germ layer to which the tissues discs were differentiated. Cytokeratin 10 showed increased expression in ectoderm samples, as expected. Endoderm marker SOX17 was elevated in endodermal sample, as was mesoendodermal marker GATA6. The mesoderm and endoderm specific markers Brachyury and alphafetoprotein did not show the expected expression pattern. E-cadherin was elevated in endoderm and mesoderm samples. Data represents mean ± SEM from 2-3 independent experiments.

The expression of proteins as also assessed using Western Blotting, with the same proteins assessed at 28 days as at 14 days. At this time point, the expression of both GATA4 and Class III β-tubulin is relatively consistent between the three samples. E-cadherin expression is consistent between mesoderm and endoderm samples, but shows a small decrease in ectoderm samples. The expression of α smooth muscle actin extremely low in the ectoderm samples, and while the expression appears higher in endoderm than mesoderm, this is not significant due to the variation present.

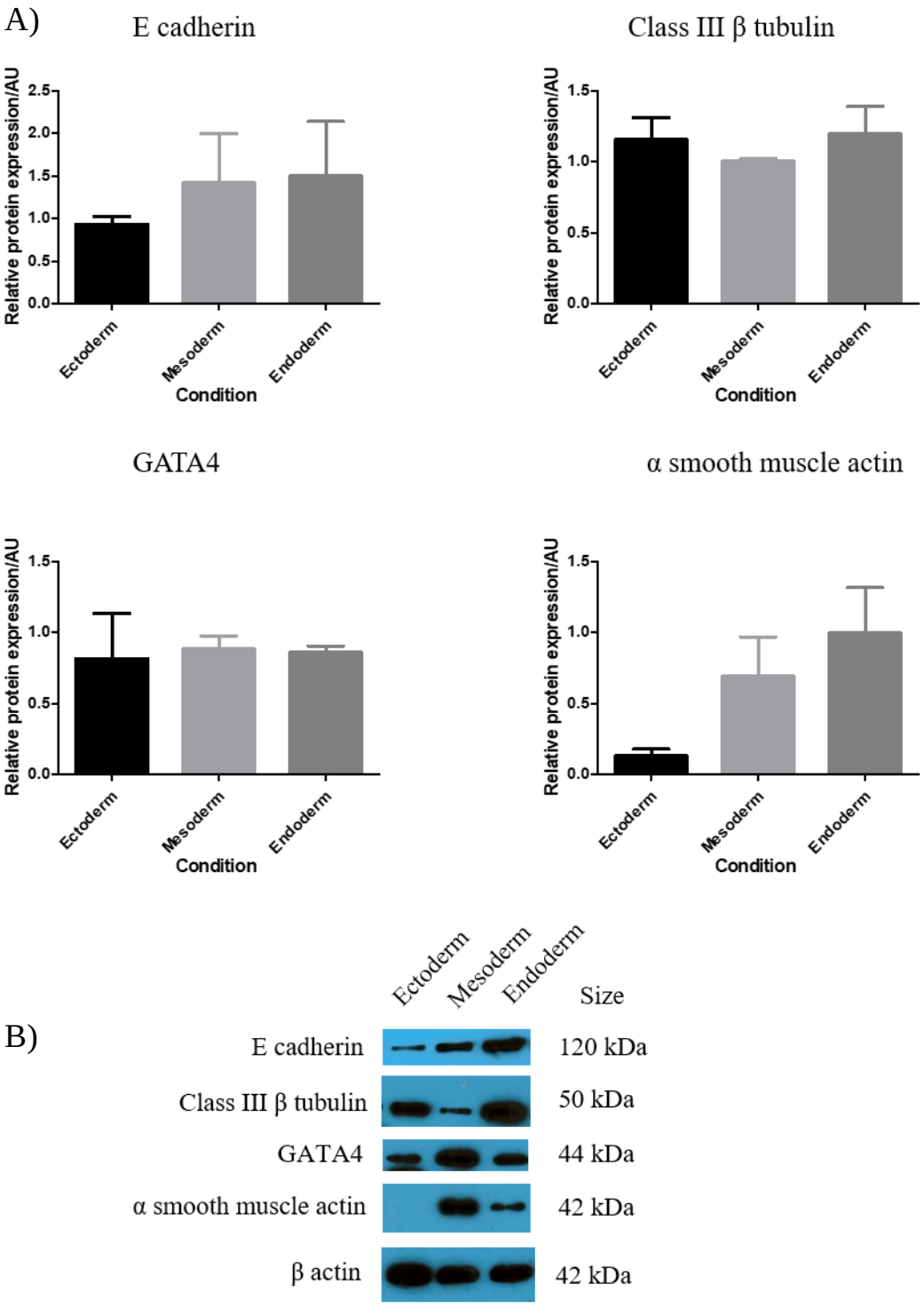


Figure 6.35: Assessment of protein expression in 28 day germ layer differentiated tissues discs: Tissue discs were subject to analysis via Western Blotting. The entire protein contents of the tissue discs on an insert were subject to analysis via Bradford assay and analysed using SDS PAGE, before probing for individual proteins. A) Graphs from densitometry analysis of Western Blotting data. By 28 days, the protein expression in the tissue discs is less variable, with expression of GATA4 and Class III β-tubulin fairly homogeneous between the samples. B) Representative images of bands from blots. Data represents mean ± SEM from 2-3 independent experiments

6.5.3 Investigation into lineage specification events: Ectodermal fate decisions

General differentiation towards each germ layer was achieved in the previous section, which is useful, although more subtle differentiation protocols are required to study the interactions governing cell fate decisions during the developmental process. As detailed in the Introduction, a number of studies have shown the involvement of the BMP and Nodal signalling pathways in controlling ectodermal lineage segregation early on in the developing embryo. Differentiation of the embryoid bodies was modulated using BMP-4 and SB431542 modelled on Li *et al* 2015, during the Aggrewell stage, before embryoid bodies were allowed to mature in suspension culture prior to seeding onto the Alvetex® Polaris scaffold.

6.5.3.1 Modulation of embryoid body differentiation using Nodal inhibitor SB431542 and BMP-4 results in more subtle differentiated phenotypes

As an Activin/Nodal pathway inhibitor, SB431542 is expected to prevent mesoendodermal differentiation within tissue discs, allowing for ectodermal differentiation to occur. Application of this morphogen alone to the tissue discs is expected to induce neural differentiation specifically. After 14 days, this appears to be the case from the histology seen in Figure 6.36. The tissue disc displays a dense, fairly homogenous tissue disc which resembles neural tissues. Immunostaining for epithelial marker E-cadherin is negative, as expected given the lack of epithelial surfaces. No epidermal differentiation is detected, with the absence of cytokeratin 10 staining. Strong positive staining for the mature neuronal marker Class III β-tubulin highlights the mature neural differentiation within the tissue disc, whereas early neural progenitor marker Nestin is negative.

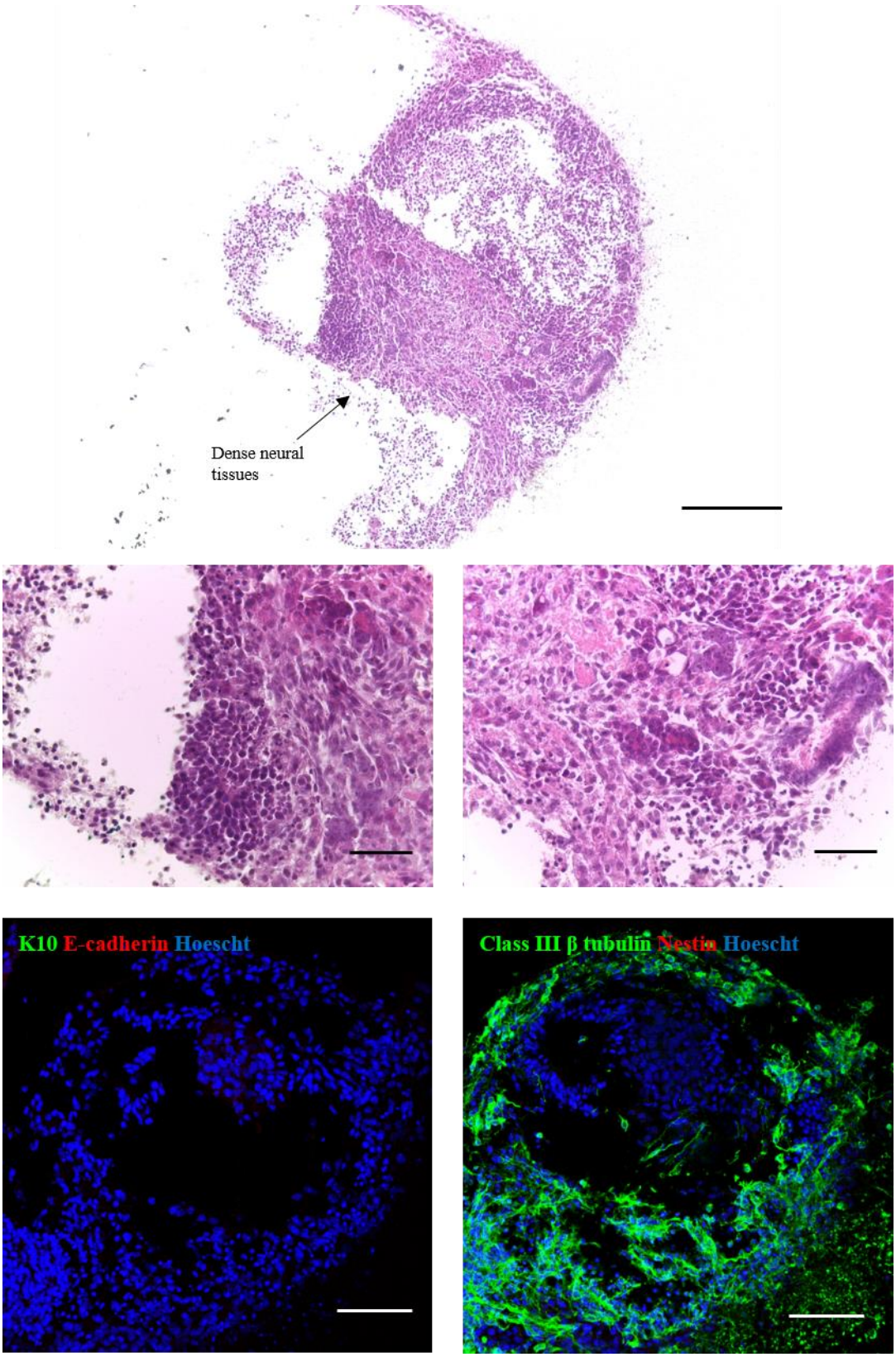


Figure 6.36: SB431542 treated embryoid bodies cultured as tissue discs on Alvetex® Polaris for 14 days: Embryoid bodies were treated during the Aggrewell stage before maturation in suspension and seeding onto the scaffold. Histology shows predominantly neural differentiation with a dense homogenous tissue structure. Neural tissue is confirmed by Class III β-tubulin positive staining. E-cadherin and cytokeratin 10 staining are absent, indicating the lack of endodermal and epidermal differentiation within the tissue disc. Representative images shown. Scale bar: 200 µm, 100 µm and 50 µm

BMP-4 signalling is involved in various developmental processes, including gastrulation and mesodermal/endodermal differentiation. Application of this morphogen to embryoid bodies is expected to lead to differentiation derived from these two germ layers, and prevent the formation of ectoderm derived structures. A variety of structures are visible within the 14 day BMP treated tissue disc as seen in Figure 6.37, which has a heterogeneous composition. These include epithelial lined lumens, large amounts of fibroblast like connective tissue and dense neural type tissues. Immunostaining for a range of markers confirms the identity of these structures. Epithelial lined lumens stain positive for E-cadherin, although there are no areas of stratified epidermis, as cytokeratin 10 staining is absent, highlighting that these lumens are endoderm derived. Class III β-tubulin staining is also present, indicating some areas of neural differentiation. Weak GATA4 staining is visible within the tissue disc, with significant areas of α smooth muscle actin staining surrounding the lumens, indicating areas of smooth muscle, derived from the mesodermal germ layer.

(Next page) Figure 6.37: BMP-4 treated embryoid bodies cultured as tissue discs on Alvetex® Polaris for 14 days: Embryoid bodies were treated during the Aggrewell stage before maturation in suspension and seeding onto the scaffold. Histology shows predominantly mesoendodermal differentiation, with a variety of organised epithelia with a variety of cell phenotypes. Large amounts of connective tissues are also visible in the tissue disc. Epithelial lumens stain positive for E-cadherin, with large areas of Class III β-tubulin positive staining indicating neural tissue and α smooth muscle actin highlighting smooth muscle. Representative images shown. Scale bar: 200 μm, 100 μm and 50 μm

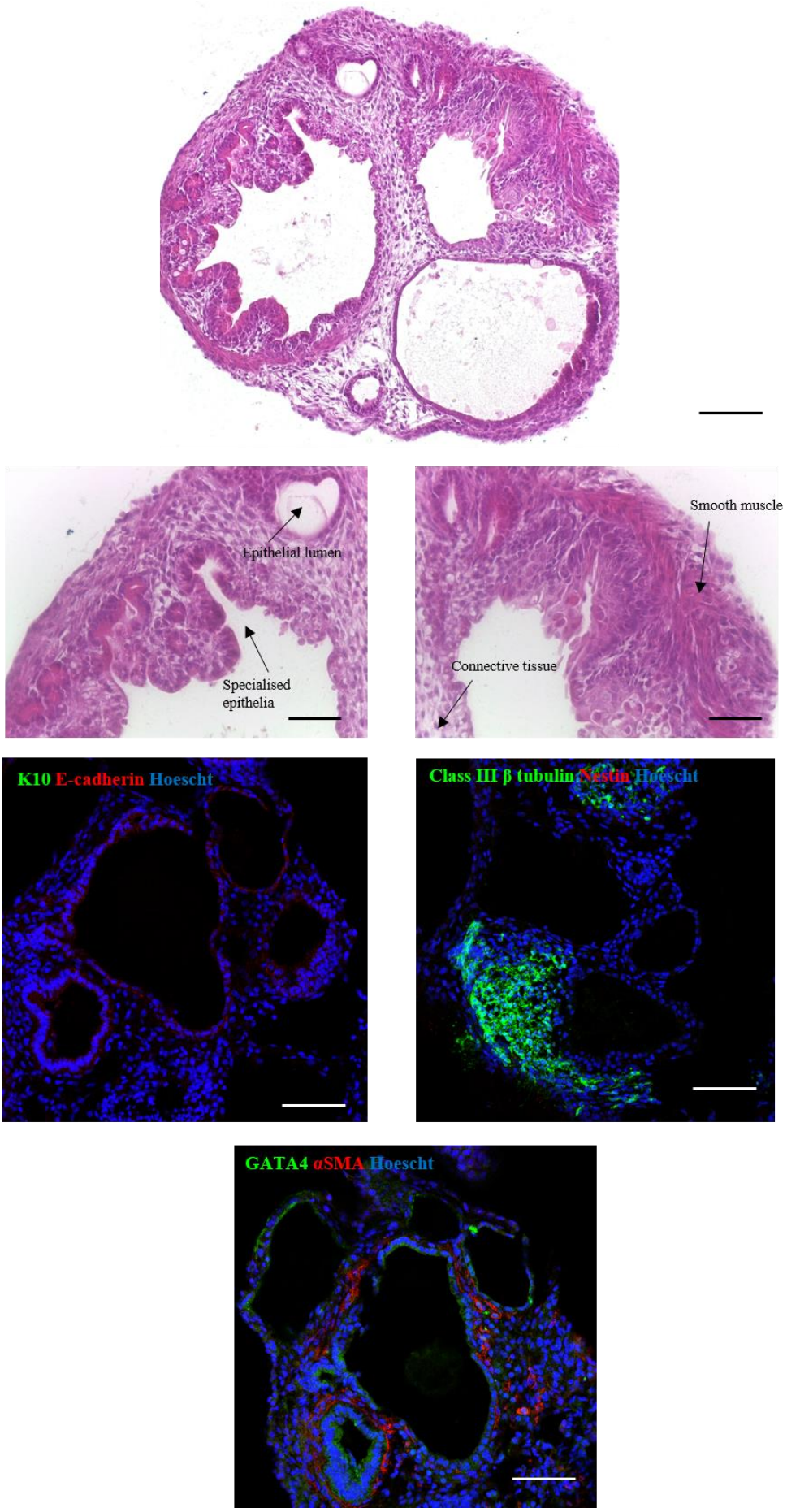


Figure 6.37: BMP-4 treated embryoid bodies cultured as tissue discs on Alvetex® Polaris for 14 days:

Figure legend on previous page

Application of both SB431542 and BMP-4 to the tissue disc is expected to result in the promotion of epidermal differentiation within the tissue disc. Again, the structure and morphology of the tissue discs is heterogeneous, but there is some evidence of potential epidermal differentiation within the centre of the tissue disc, where an acellular area can be identified. Immunostaining demonstrates that this is not epidermal, due to the absence of cytokeratin 10 staining and E-cadherin staining. There are some small areas of neural differentiation within the tissue disc, as shown by the positive Class III β-tubulin staining.

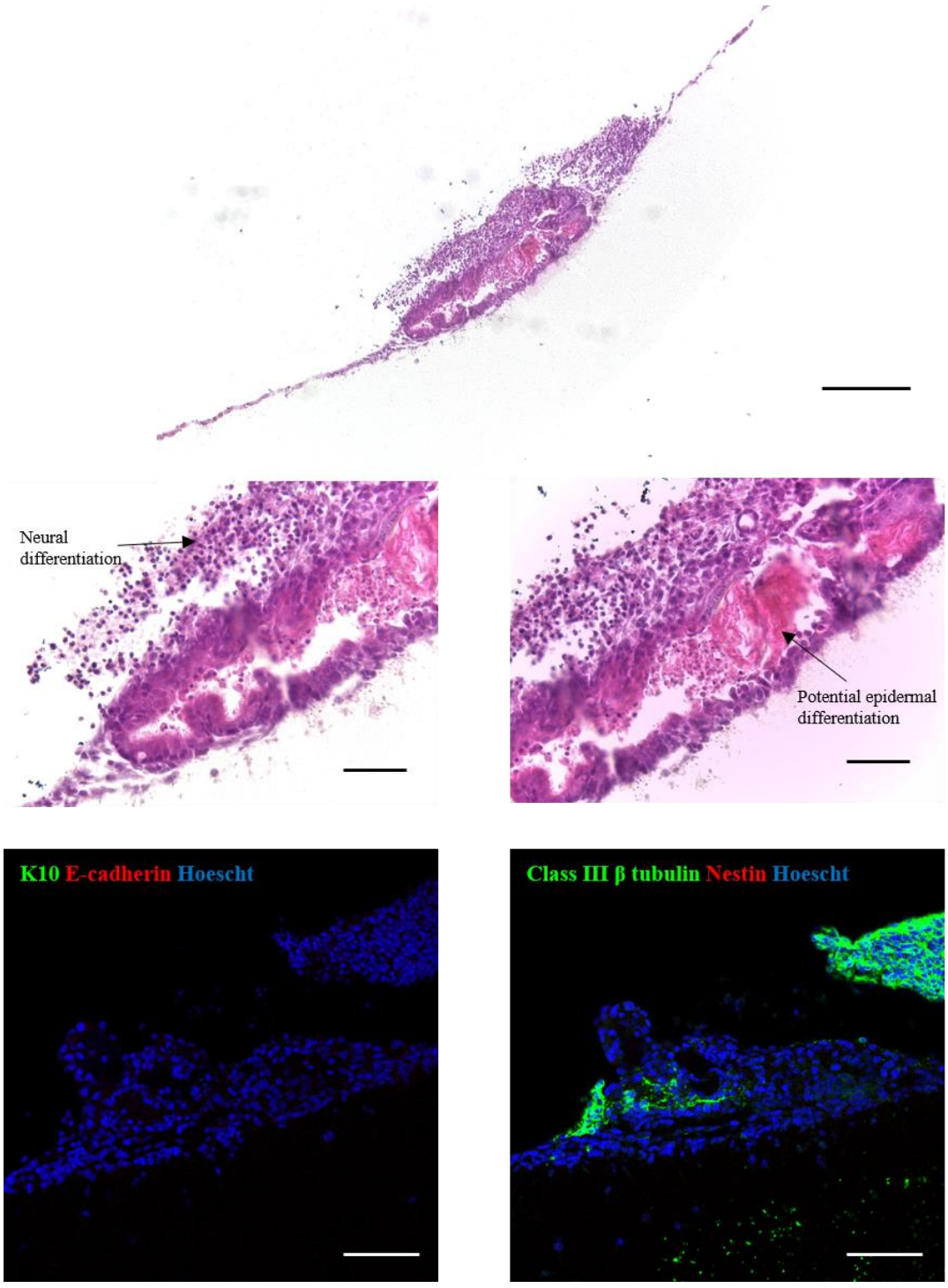


Figure 6.38: SB431542 and BMP-4 treated embryoid bodies cultured as tissue discs on Alvetex® Polaris for 14 days: Embryoid bodies were treated during the Aggrewell stage before maturation in suspension and seeding onto the scaffold. Tissue discs display mainly ectodermal differentiation, with both neural and additional unidentifiable differentiation present within the structure. Immunostaining confirms the neural differentiation with positive Class III β-tubulin staining, but there are no epithelia or epidermal structures. Scale bar: 200 µm, 100 µm and 50 µm

Gene expression was also analysed in this experiment, in order to give a better overview of the differentiation occurring within the tissue disc structures. Although some potential evidence of epidermal differentiation was detected in the histology in the previous Figures, the expression of the gene for the epidermal differentiation marker cytokeratin 10 was increased in the samples treated with SB431542 and BMP-4 compared to other samples, with a modest increase also seen in the samples treated with SB431542 alone. Interestingly, the epidermal basal cell marker cytokeratin 14 is highly increased in the sample treated with SB431542 only, an observation at odds with the intended differentiated tissue from this treatment. As would be expected with this sample, the expression of Class III β-tubulin was significantly higher than the other treated samples, indicating the neural nature of this tissue disc population. While the expression of the mesodermal gene brachyury was increased in all three samples, it was most notably increased in the samples intended for neural and epidermal differentiation. The mesoendodermal marker GATA6 showed decreased expression in both of these samples as would be expected, with expression in the BMP-4 sample being approximately similar to the control sample, indicating no repression of the differentiation of these germ layers. The modest increased expression of E-cadherin and alphafetoprotein in the BMP-4 treated sample correlates with the identification of epithelia lined lumens and the intended differentiation outcome of mesoendodermal tissues, as does the corresponding decrease in the expression of these genes in the other two treated samples. The final two genes selected for analysis, FOXA2 and SOX17, show similar expression across all three treated samples, with a collective increase in the expression of FOXA2 and a decrease in the expression of SOX17.

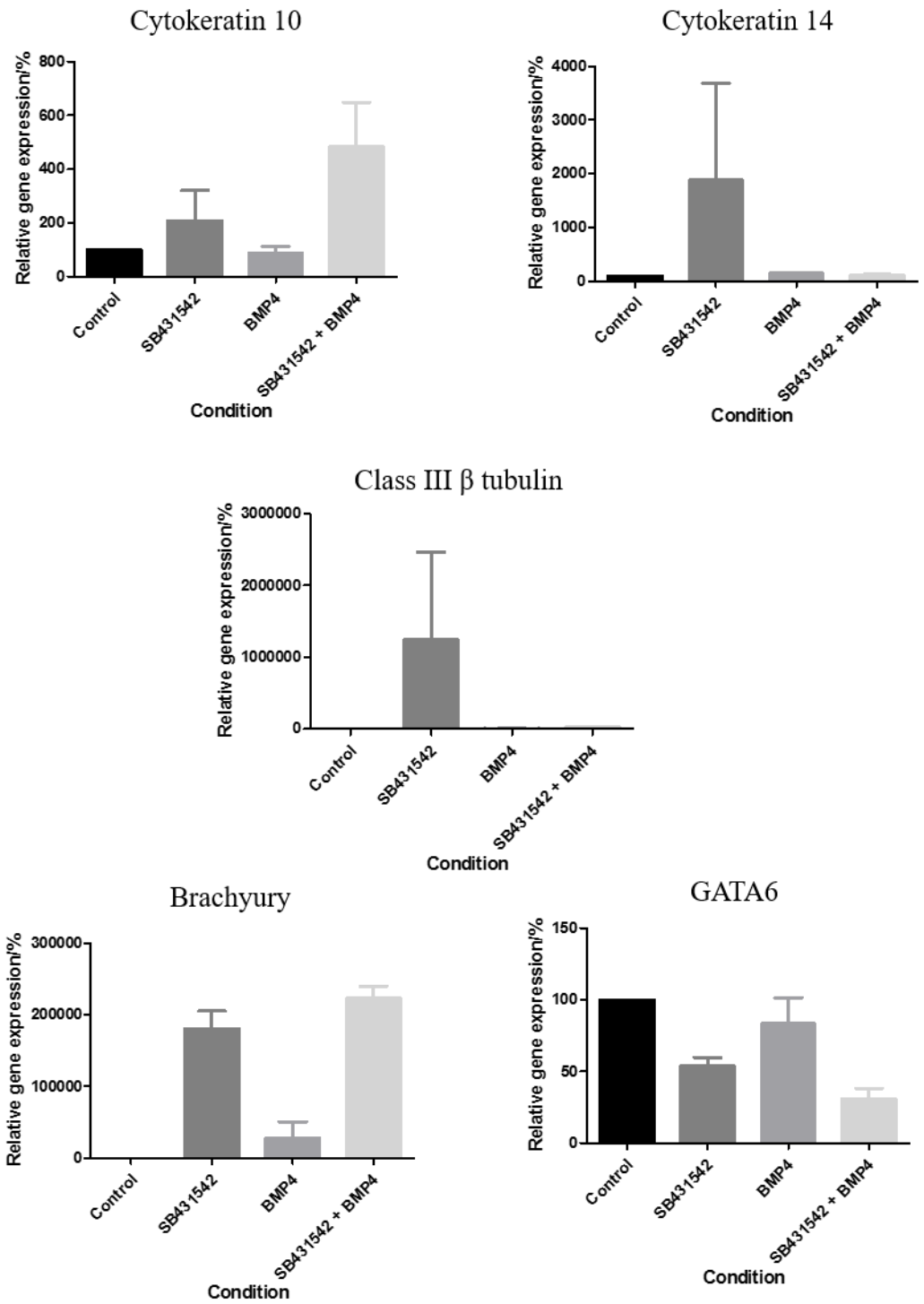


Figure 6.39: Assessment of gene expression in 14 day ectoderm differentiated tissues discs: Tissue discs were subject to analysis via qPCR. RNA was extracted from a tissue disc population, converted to cDNA and the expression level of a variety of germ layers specific genes quantified. For simplicity, the control is shown as a single sample; separate controls were conducted for each germ layer. Some genes were expressed as expected: cytokeratin 14 in the samples differentiated to epidermis and Class III β-tubulin in the neural samples. Data represents mean ± SEM from 2-3 independent experiments

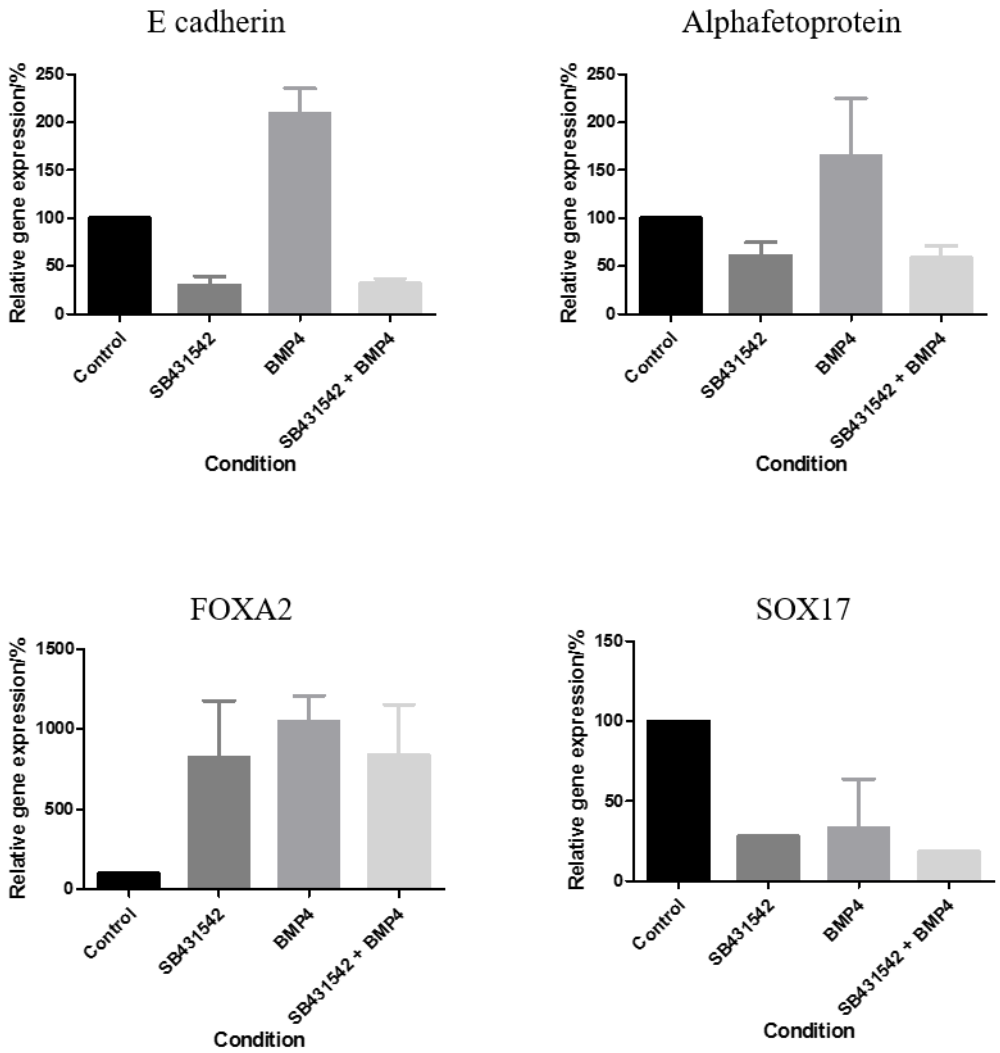


Figure 6.40: Assessment of gene expression in 14 day ectoderm differentiated tissues discs: Tissue discs were subject to analysis via qPCR. RNA was extracted from a tissue disc population, converted to cDNA and the expression level of a variety of germ layers specific genes quantified. For simplicity, the control is shown as a single sample; separate controls were conducted for each germ layer. E-cadherin and alphafetoprotein show increased expression in the mesoendodermal sample, as expected. FOXA2 and SOX17 show a relatively even expression, although at very different levels compared to the control. Data represents mean ± SEM from 2-3 independent experiments

Western blotting and densitometry was also performed on these samples. The analysis of protein expression within these samples showed little difference in the expression of E-cadherin within the samples at this time point, indicating there may be some consistency in the epithelial structures within these tissue discs. The expression of Class III β-tubulin was found to be elevated in those samples which were differentiated towards the ectodermal germ layer, treated with SB431542 or SB431542 and BMP-4, with a relatively small amount of the protein produced in the BMP-4 treated samples. The expression of α smooth muscle actin was found to be relatively consistent between the three treated samples. The epidermal marker cytokeratin 10 was found to be increased in the sample treated for epidermal differentiation, as well as the sample treated for neural differentiation, although to a lesser extent. The BMP-4 treated sample showed very little expression by comparison.

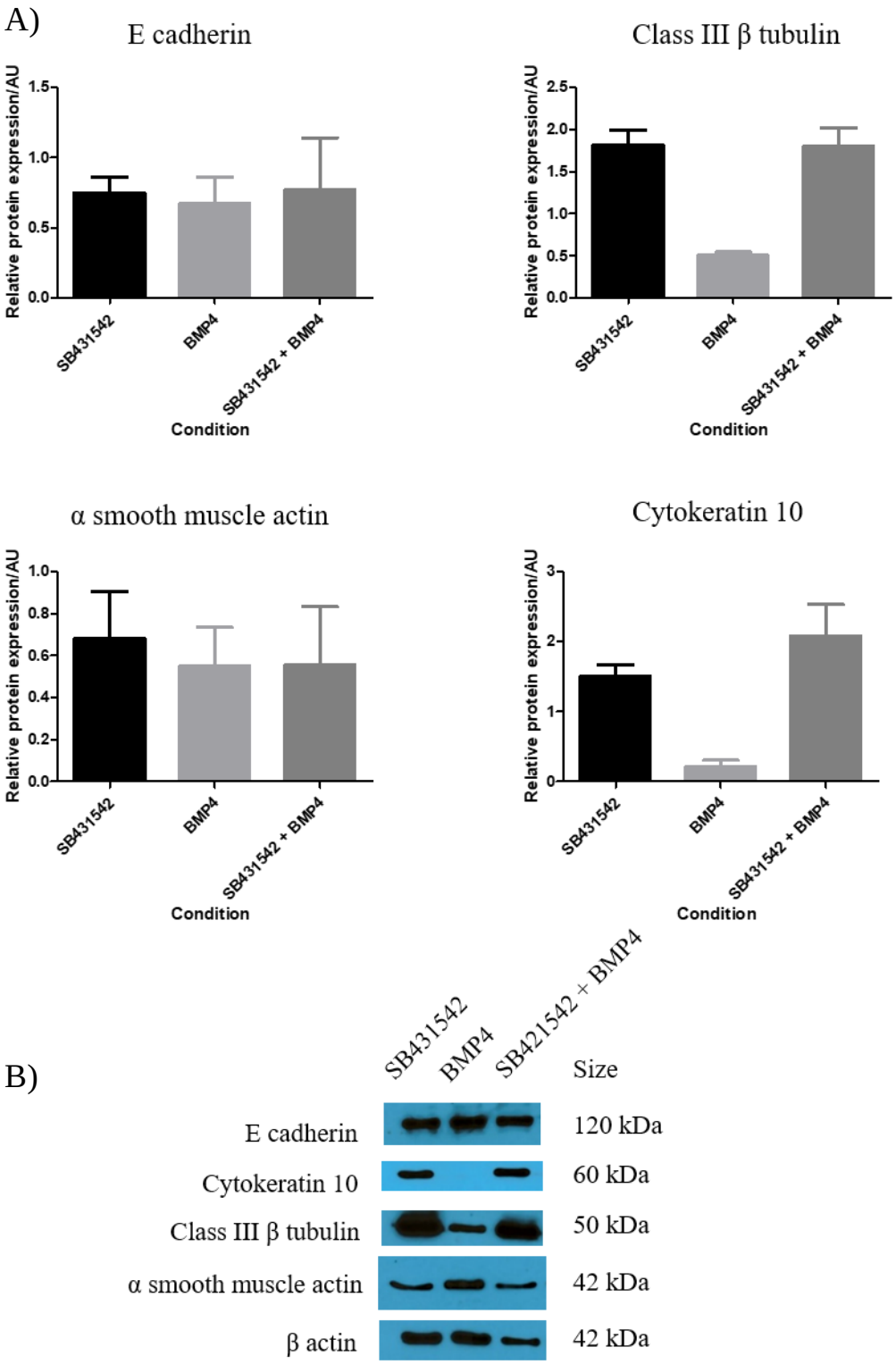


Figure 6.41: Assessment of protein expression in 14 day ectoderm differentiated tissues discs: Tissue discs were subject to analysis via Western Blotting. The entire protein contents of the tissue discs on an insert were subject to analysis via Bradford assay and analysed using SDS PAGE, before probing for individual proteins. A) Graphs from densitometry of Western Blotting data. Expression patterns showed mixed results: E-cadherin and α smooth muscle actin were expressed relatively evenly, whereas the cytokeratins 10 and 14 were expressed more highly in the ectodermal samples. B) Representative images of bands from blots. Data represents mean ± SEM from 2-3 independent experiments

6.5.3.2 Prolonged culture of the differentiated tissue discs results in the maintenance of these phenotypes

The culture of these treated tissue discs for 14 days resulted in their general differentiation towards the structures intended; neural, epidermal and mesoendodermal. As has been discussed on a number of occasions, time is essential to the developmental process, as it is this factor that allows for the formation of these complex tissue structures. In line with this and the previous germ layer differentiation experiment, these treated tissue discs were also allowed to differentiate for 28 days on the Alvetex® Polaris before analysis.

The neural phenotype which was initially established at 14 days in the samples treated with SB431542 appears to be replicated in tissue discs cultured on the scaffold for 28 days, although the tissue discs also appear to be more heterogeneous at this point, but overall still showing a dense neural structure. Immunostaining for Class III β-tubulin is strongly positive again confirming the mature neural identity, with the absence of epithelial marker E-cadherin and the epidermal marker cytokeratin 10 confirming the absence of these tissue structures observed in the histology.

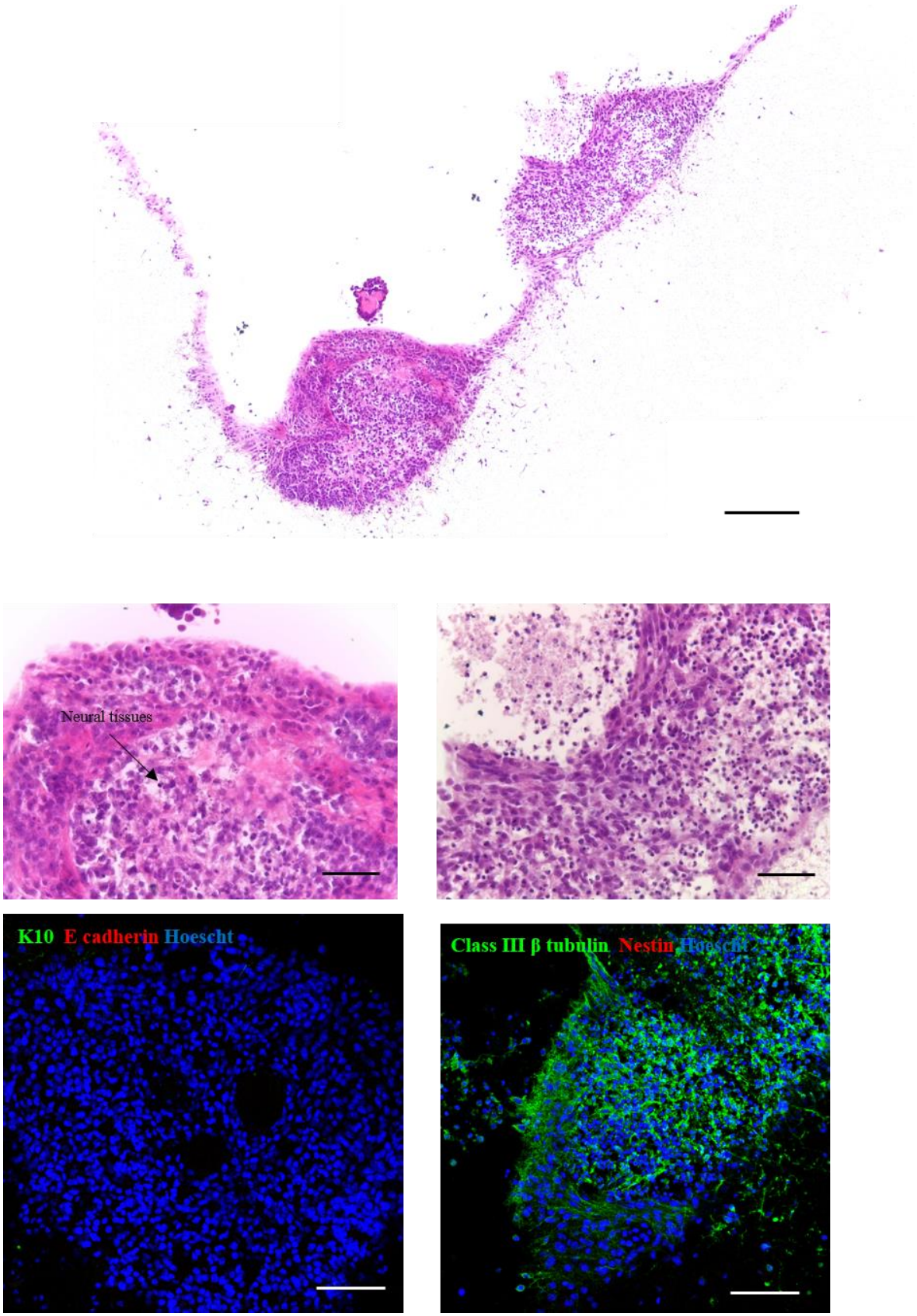


Figure 6.42: SB431542 treated embryoid bodies cultured as tissue discs on Alvetex® Polaris for 28 days: Embryoid bodies were treated during the Aggrewell stage before maturation in suspension and seeding onto the scaffold. As with the earlier time point, histology indicated differentiation is mainly neural, with Class III β-tubulin positive staining. E-cadherin and cytokeratin 10 staining are absent, indicating the lack of endodermal and epidermal differentiation. Representative images shown. Scale bar: 200 µm, 100 µm and 50 µm

A similar differentiation profile is also detected in the tissue disc treated with BMP-4 and allowed to develop on the scaffold for 28 days. The tissue disc contains epithelial lined lumens with fibroblast rich connective tissues, but these do not stain positively for the epithelial marker E-cadherin. The absence of staining for the epidermal marker cytokeratin 10 confirms a lack of epidermal differentiation. The absence of Nestin and Class III β-tubulin staining confirm the lack of neural differentiation within the structure also.

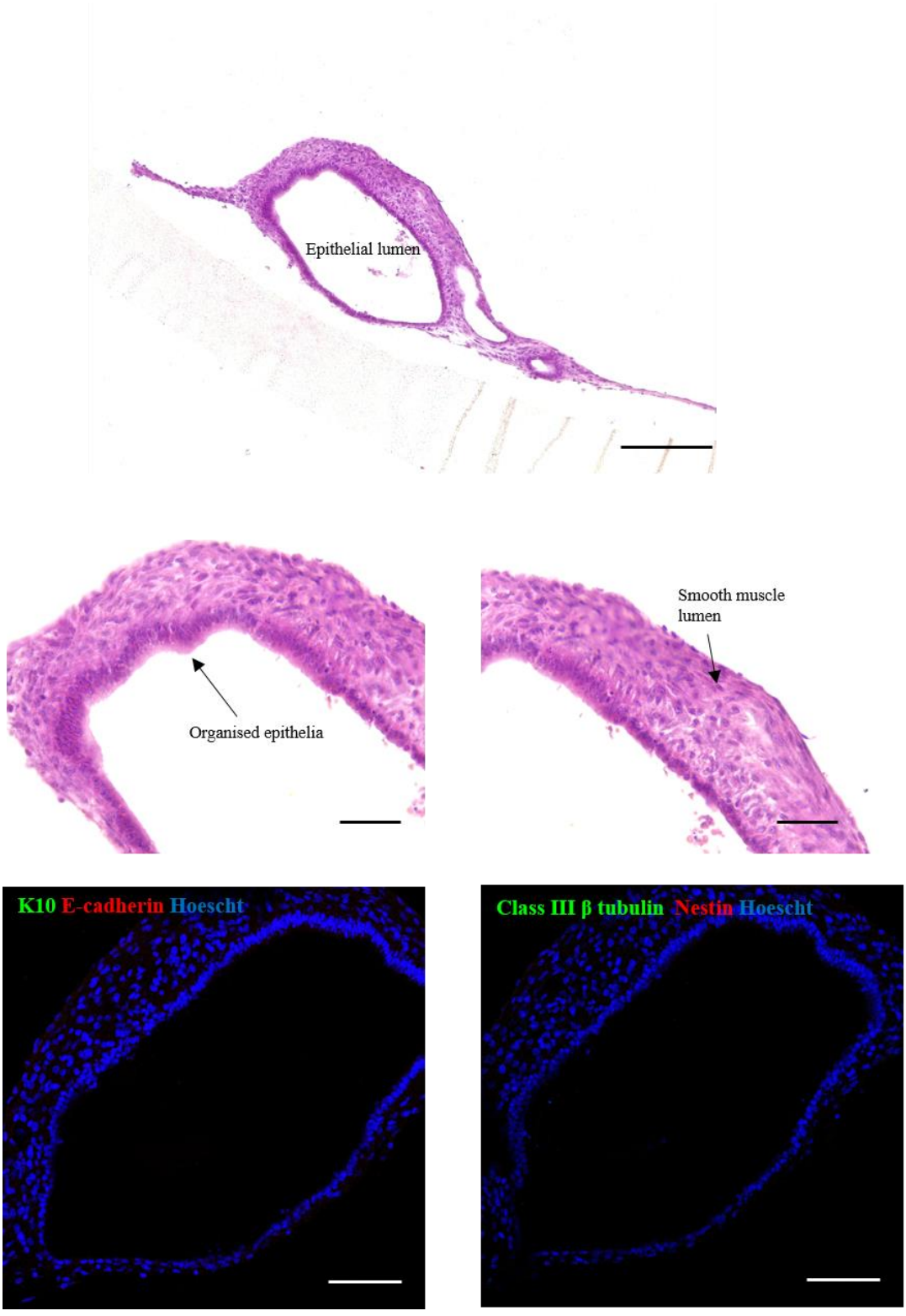


Figure 6.43: BMP-4 treated embryoid bodies cultured as tissue discs on Alvetex® Polaris for 28 days: Embryoid bodies were treated during the Aggrewell stage before maturation in suspension and seeding onto the scaffold. The resultant tissue discs show a variety of structures, particularly mesoderm derived connective tissues and organised epithelia. Immunostaining for a range of markers shows a lack of neural tissues due to the absence of Class III β-tubulin staining. Interestingly, the epithelial surface is E-cadherin negative also. Representative images shown. Scale bar: 200 µm, 100 µm and 50 µm

The tissue disc differentiated using SB431542 and BMP-4 shows a heterogeneous structure, which appears to be mainly dense neural differentiation, which has led to some fragmentation of the tissue disc. There are some structures which suggest epidermal differentiation, but these ae very rudimentary and small in size. Subsequent immunostaining for E-cadherin and cytokeratin 10 confirms that these structures are not mature epidermis. Immunostaining does confirm the presence of mature neural differentiation throughout the tissue disc due to the presence of positive staining for Class III β-tubulin. Mesoderm derived connective tissue elements can also be detected in this structure through the positive staining for the cytoskeletal marker α smooth muscle actin.

(Next page) Figure 6.44: SB431542 and BMP-4 treated embryoid bodies cultured as tissue discs on Alvetex® Polaris for 28 days: Embryoid bodies were treated during the Aggrewell stage before maturation in suspension and seeding onto the scaffold. Tissue discs display mainly ectodermal differentiation, with both neural and potential epidermal differentiation present in the structure. Immunostaining confirms the strong neural differentiation within the tissue disc, as well as mesodermal differentiation with α smooth muscle actin positive areas. There are no epithelial structures, or areas of epidermal differentiation as shown by the lack of staining for both E-cadherin and cytokeratin 10. Scale bar: 200 µm, 100 µm and 50 µm

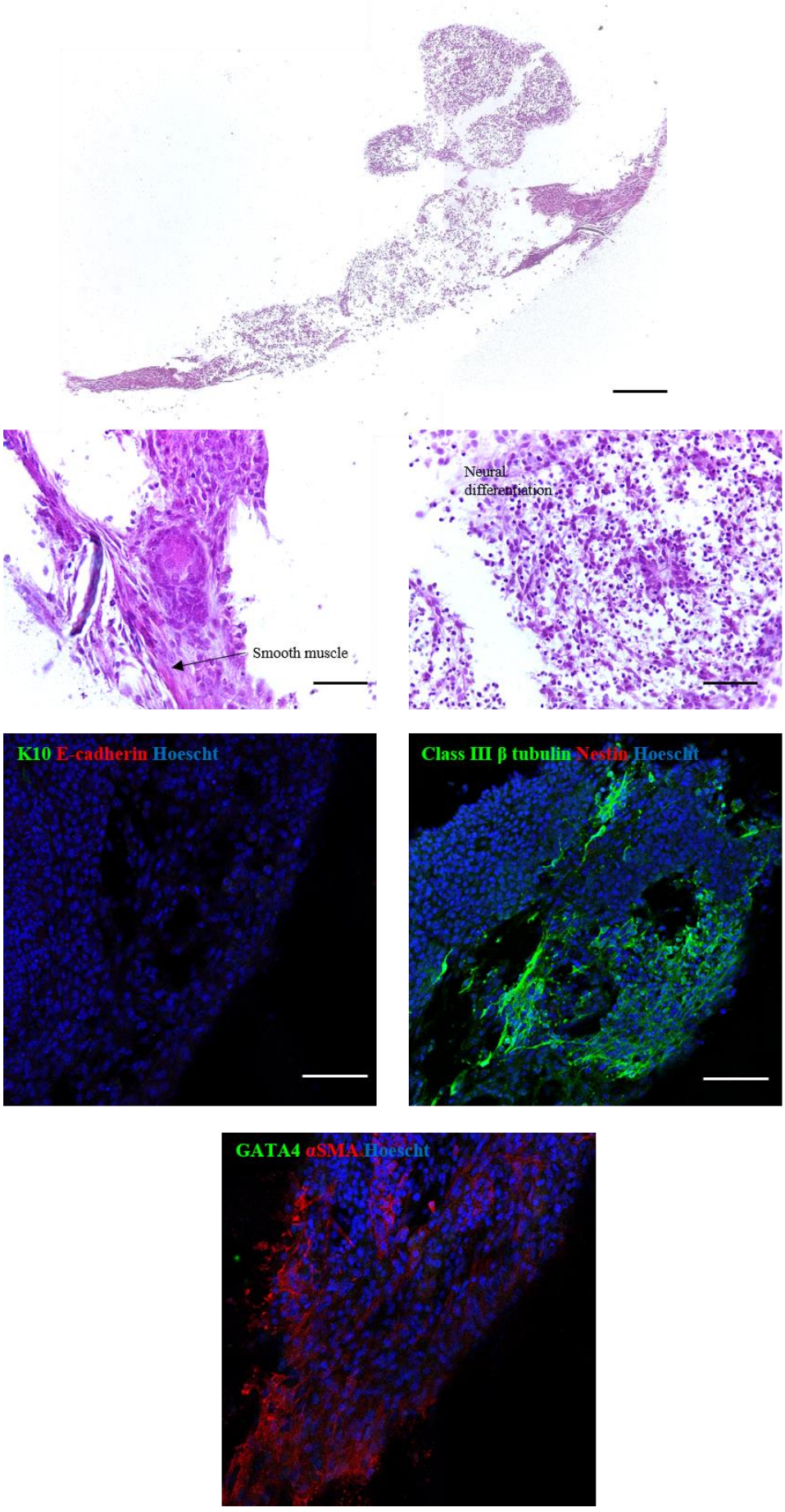


Figure 6.44: SB431542 and BMP-4 treated embryoid bodies cultured as tissue discs on Alvetex® Polaris for 28 days: Figure legend on previous page.

Gene expression analysis was conducted again following qPCR on 28 day samples. Expression of the epidermal marker cytokeratin 10 was found to be increased in samples treated for neural differentiation, with a small increase also in samples treated for mesoendodermal differentiation. Interestingly, the sample which was differentiated towards epidermis showed little difference compared to the control. The expression of cytokeratin 14 was increased in all three samples, with the samples treated with SB431542 only and BMP-4 only showing some similarities. The sample treated with SB431542 and BMP-4 showed less of an increase compared to the other samples. The expression of Class III β-tubulin was strongly increased in the sample differentiated towards the neural phenotype, with some increase in expression also identified in the epidermally differentiated sample. The expression of the gene for the mesoderm transcription factor brachyury was found to be in opposition to that observed at 14 days. All three samples showed very low levels of brachyury, all of which were lower than the control sample. A slightly differential expression of the gene for GATA6 was also observed, with a very slight increase in the neutrally differentiated sample, and slight decreases in the mesoendodermal and epidermal samples. E-cadherin expression was observed to be elevated in the neutrally differentiated SB431542 sample, as was every other endodermal gene chosen for assessment, although these increases were generally modest and variable in term of error. BMP-4 treated samples also displayed an increased expression of E-cadherin; the epidermal sample was similar to the control. Both of these samples showed a small increase in alphafetoprotein expression also. For the expression of FOXA2 and SOX17, both of these samples showed a similar or lower expression than the control sample, indicating a possible shift in the differentiation occurring.

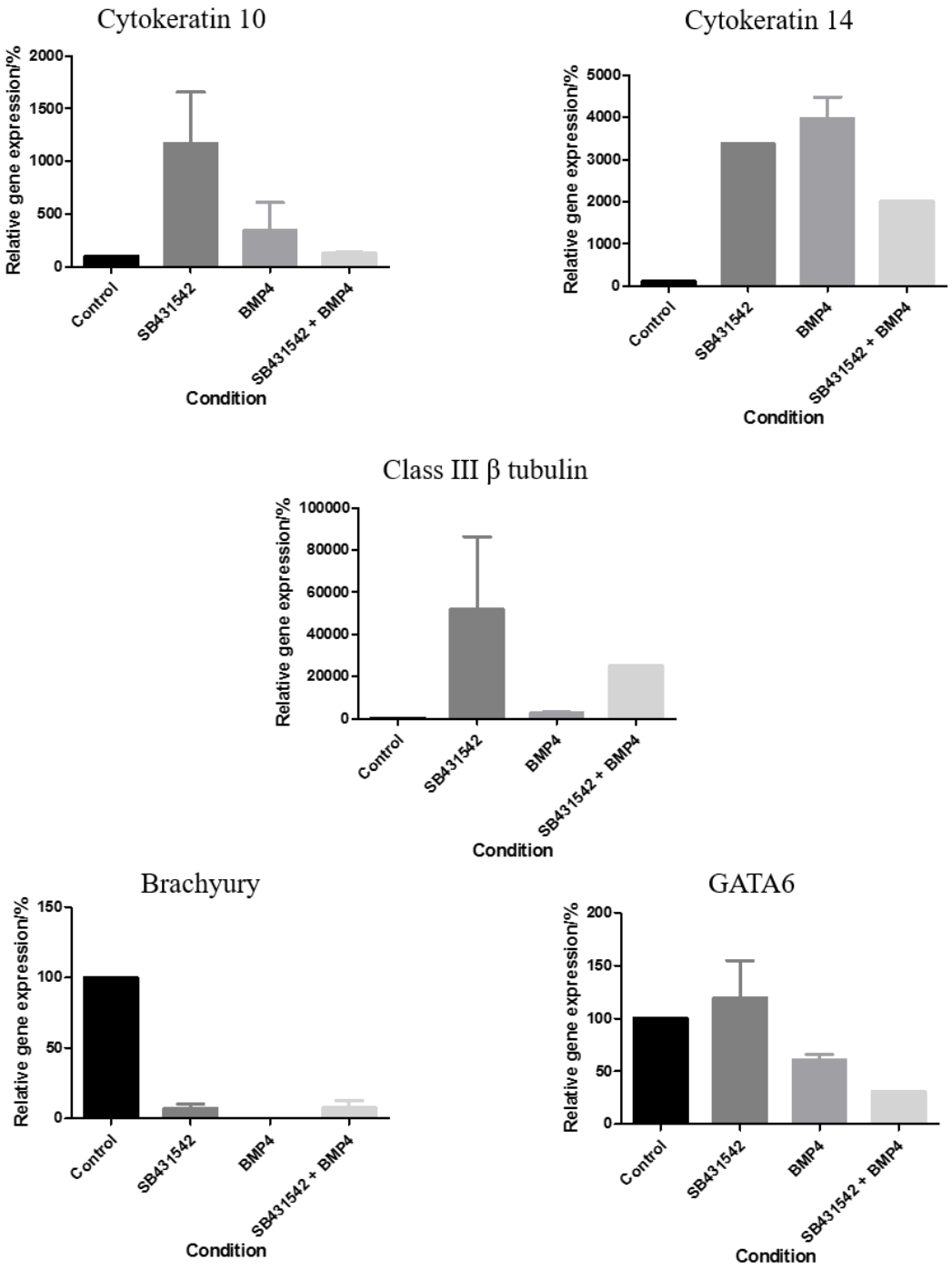


Figure 6.45: Assessment of gene expression in 28 day ectoderm differentiated tissues discs: Tissue discs were subject to analysis via qPCR. RNA was extracted from a tissue disc population, converted to cDNA and the expression level of a variety of germ layers specific genes quantified. For simplicity, the control is shown as a single sample; separate controls were conducted for each germ layer. Expression of some genes was as expected; Class III β-tubulin was strongly expressed in the neural sample, as was cytokeratin 10. Very little expression of brachyury was detected, and GATA6 expression was highest in the neural sample. Data represents mean ± SEM from 3 independent experiments

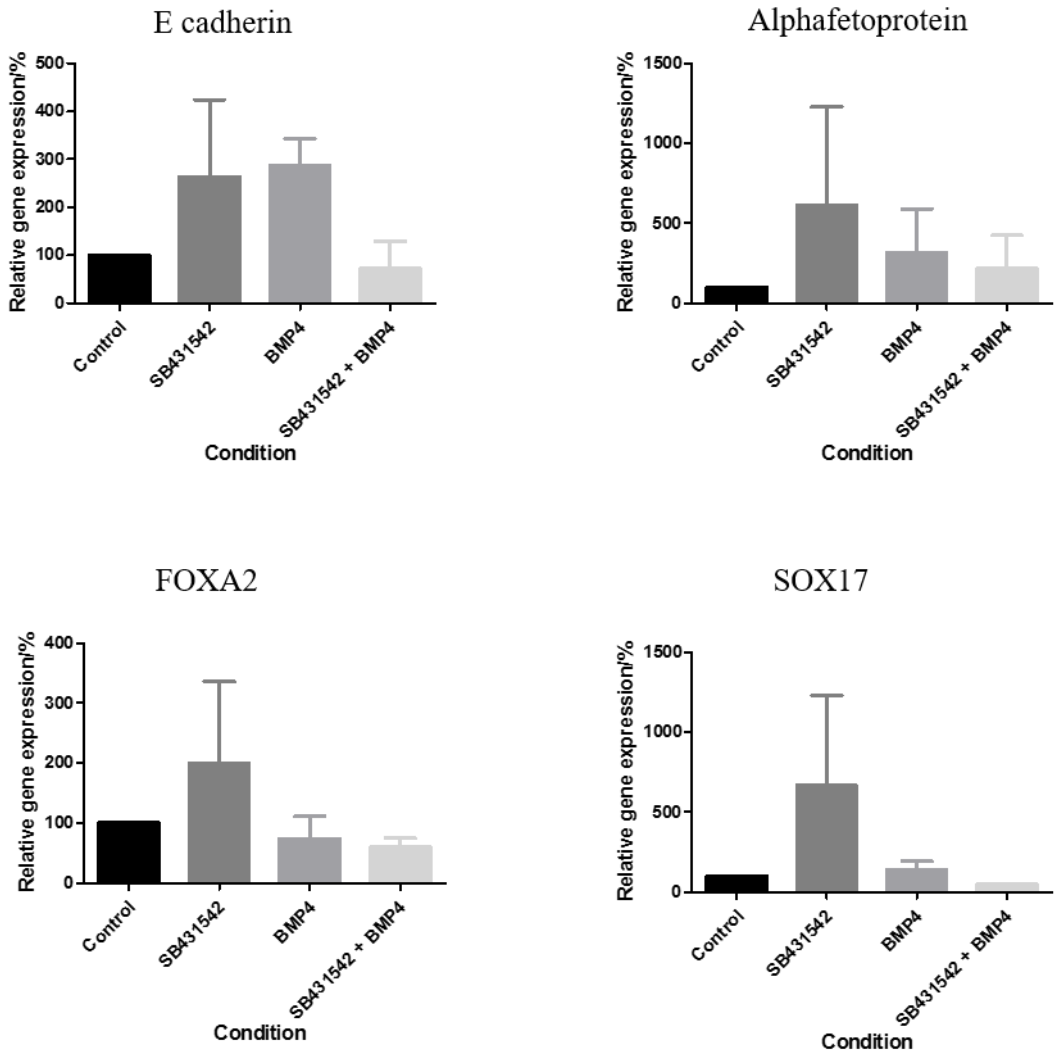


Figure 6.46: Assessment of gene expression in 28 day ectoderm differentiated tissues discs: Tissue discs were subject to analysis via qPCR. RNA was extracted from a tissue disc population, converted to cDNA and the expression level of a variety of germ layers specific genes quantified. For simplicity, the control is shown as a single sample; separate controls were conducted for each germ layer. All of the endoderm associated genes here were found to be highly expressed in the neural samples, with similar expression found for three in the mesoendodermal and epidermal samples. Data represents mean ± SEM from 3 independent experiments

The analysis of protein expression was also carried out on the same proteins analysed at 14 days. Compared to the mesoendodermal and epidermal samples, the expression of E-cadherin was lower in the samples differentiated towards the neural lineage using SB431542, as would be expected. Again, samples differentiated towards the ectoderm showed increased expression of the neural marker Class III β-tubulin compared to the BMP-4 treated samples. While there were some small differences in the expression of α smooth muscle actin between the three samples, overall, there were no real differences in the level of this protein. In a similar way to Class III β-tubulin, cytokeratin 10 was also slightly increased in the samples differentiated towards ectodermal derivatives, the neural and epidermal samples.

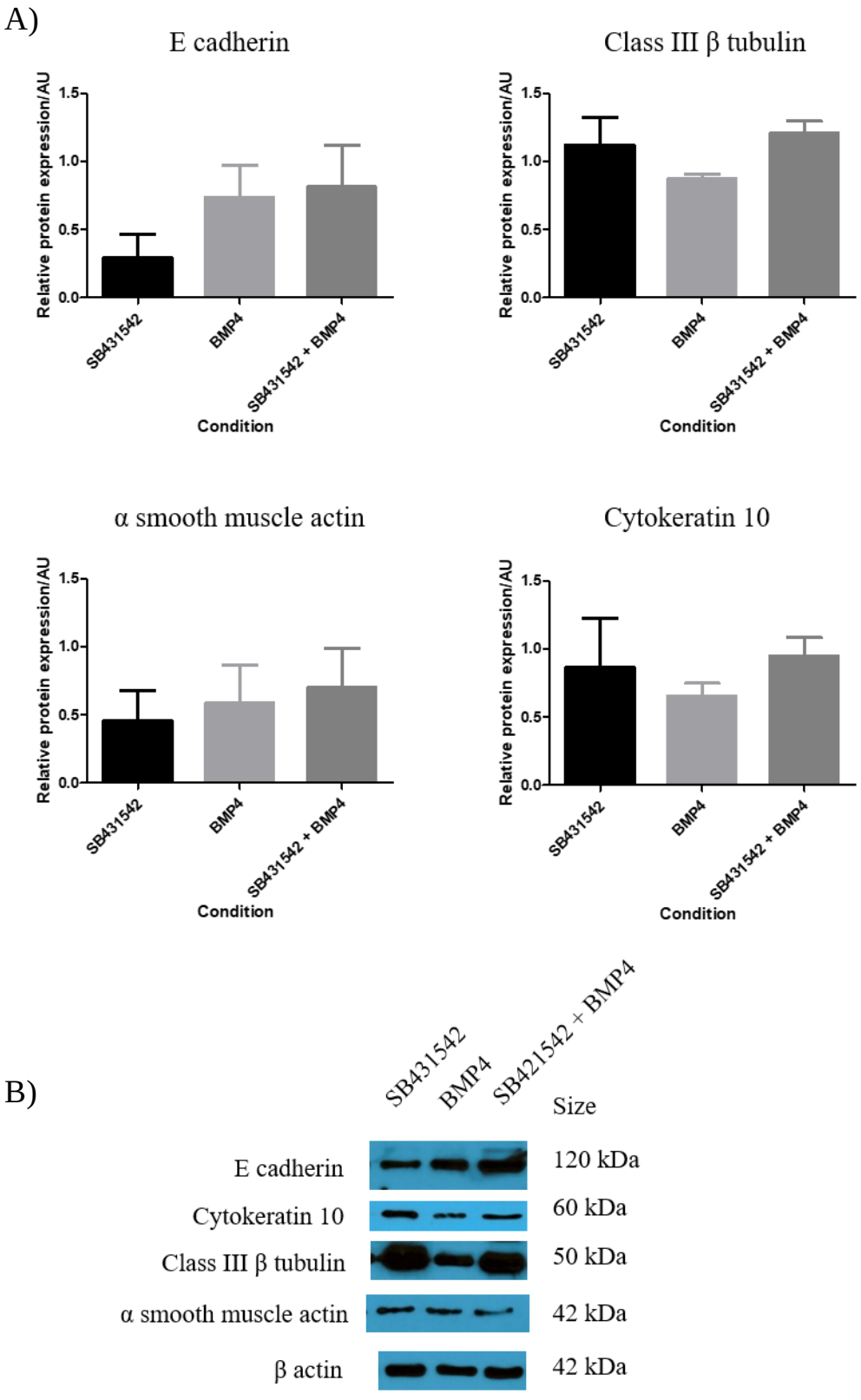


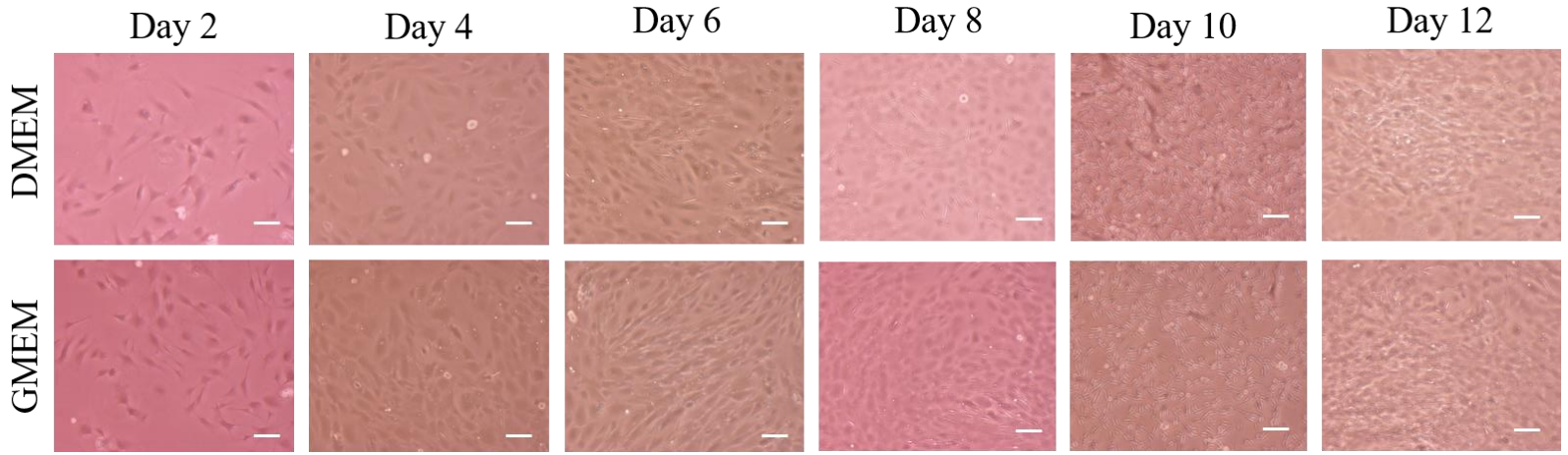
Figure 6.47: Assessment of protein expression in 28 day ectoderm differentiated tissues discs: Tissue discs were subject to analysis via Western Blotting. The entire protein contents of the tissue discs on an insert were subject to analysis via Bradford assay and analysed using SDS PAGE, before probing for individual proteins. A) Graphs from densitometry of Western Blotting data. The ectodermal proteins, Class III β-tubulin and cytokeratin 10 showed varying elevated expression in the ectodermal samples. α smooth muscle actin and E-cadherin expression showed no significant differences across the samples. B) Representative images of bands from blots. Data represents mean ± SEM from 2-3 independent experiments

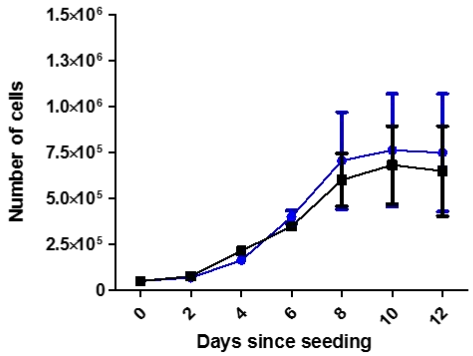
6.5.4 Co-culture of CGR8 tissue discs with SCID fibroblast dermal equivalent

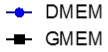
In Chapter 3, a number of optimisation steps were undertaken to develop a dermal equivalent suitable for the culture of tissue disc on the surface. A 21 day formation period was chosen for the SCID dermal equivalent for fibroblasts to populate the scaffold and form a layer across the surface of the insert. Initial investigations using TERA2.cl.SP12 aggregates within the system showed little aggregate infiltration, and that the presence of the fibroblast population influenced the differentiation and pluripotency of the tissue discs in a manner not previously observed in the original version of the model. In a similar way, CGR8 tissue discs were cultured on the surface of the SCID fibroblast dermal equivalents, with the aim of enhancing the differentiation which takes place. Although the overall effect of the fibroblasts on the TERA2.cl.SP12 tissue discs was that of increasing the amount of cells expressing Oct 4, this was hypothesised to be through the bFGF pathway, which maintains pluripotency in human PSCs. As the signalling pathway which maintains pluripotency in murine PSCs is different, as discussed in Section 6.1.3, the effects of the co-culture of murine tissue discs with fibroblast populations is expected to be different to that observed in TERA2.cl.SP12 cells.

6.5.4.1 SCID fibroblasts display a similar phenotype and growth rate in CGR8 differentiation medium in 2D

While the SCID fibroblast dermal equivalent is cultured in a maintenance medium based on DMEM, CGR8 murine tissue discs are differentiated in a medium based on GMEM. To ensure that there are no detrimental effects on the maintenance of the dermal equivalents in the alternative medium, SCID fibroblasts were initially cultured in the two media in 2D conditions, normal fibroblast maintenance media and tissue disc differentiation media, over 12 days. Cell counts were performed every 2 days to assess cell growth rate; cell counts only were performed due to the nature of the cells and the need to maximise their usage (i.e. as the cells were primary cells with a limited replicative ability). Cells do not show any differences in morphology when cultured in the two media types, with both media promoting a typical fibroblast like morphology. As seen in Figure 6.48, phase contrast images also show similarities in cell growth rate and the rate at which confluency is reached over this time. Cell counts confirm there is little difference in the time cells spend in the exponential phase of cell growth and the stationary phase after plateau, with the only noticeable different being that there are slightly more cells grown in DMEM at later time points compared to those in DMEM. Cell counts were analysed by two way ANOVA, with no significant difference detected between the two. The calculation of population doubling time shows a small difference in the value for each.







$$PDT = \frac{T \ln 2}{\ln \frac{Ne}{Nb}}$$

Media	PDT/days
DMEM	1.87
GMEM	2.05

Figure 6.48: SCID Mouse Fibroblast growth curve in DMEM and GMEM: SCID Mouse Fibroblast cells were seeded into 6 well plates at a density of 50,000 cells per well on day 0, with DMEM or GMEM. Cells were counted every two days, and the remaining wells were media changed. Phase contrast images show no morphological differences evident in the cells in the two media types. Average cell number per well was calculated and plotted for each day cells were counted. The Population Doubling Time (PDT) was calculated using the equation shown. T = Incubation time (days), Xb = Cell number at the beginning of the incubation time, Xe = Cell number at the end of the incubation time. The PDT was calculated using the exponential growth phase of the graph. Data represents mean ± SEM from 3 independent experiments. Scale bars: 100 µm

6.5.4.2 SCID fibroblast dermal equivalents maintain their structure and viability when cultured in CGR8 differentiation medium

The culture of SCID fibroblasts in 2D is indicative of success in 3D, although not conclusive given the differences in cellular structure and therefore function when cells are cultured in the three dimensional environment. SCID fibroblast dermal equivalents were also cultured in the CGR8 differentiation medium for 14 and 28 days, the minimum and maximum time tissue discs would be cultured on the scaffold. Histology shows that after 14 days, dermal equivalents cultured in the stem cell differentiation medium are structurally similar to those cultured in DMEM and show a similar distribution of the fibroblasts within the scaffold. Collagen I expression is also similar and found mainly at the top and base of the scaffold. MTT values are highly similar for the two conditions, indicating the preservation of cellular viability. Similarly, when SCID dermal equivalents are cultured for up to 28 days, the structure and morphology of the cells within the scaffold is retained, as is cellular viability as evidenced by the MTT values. Collagen I expression is again similar between the two media types.

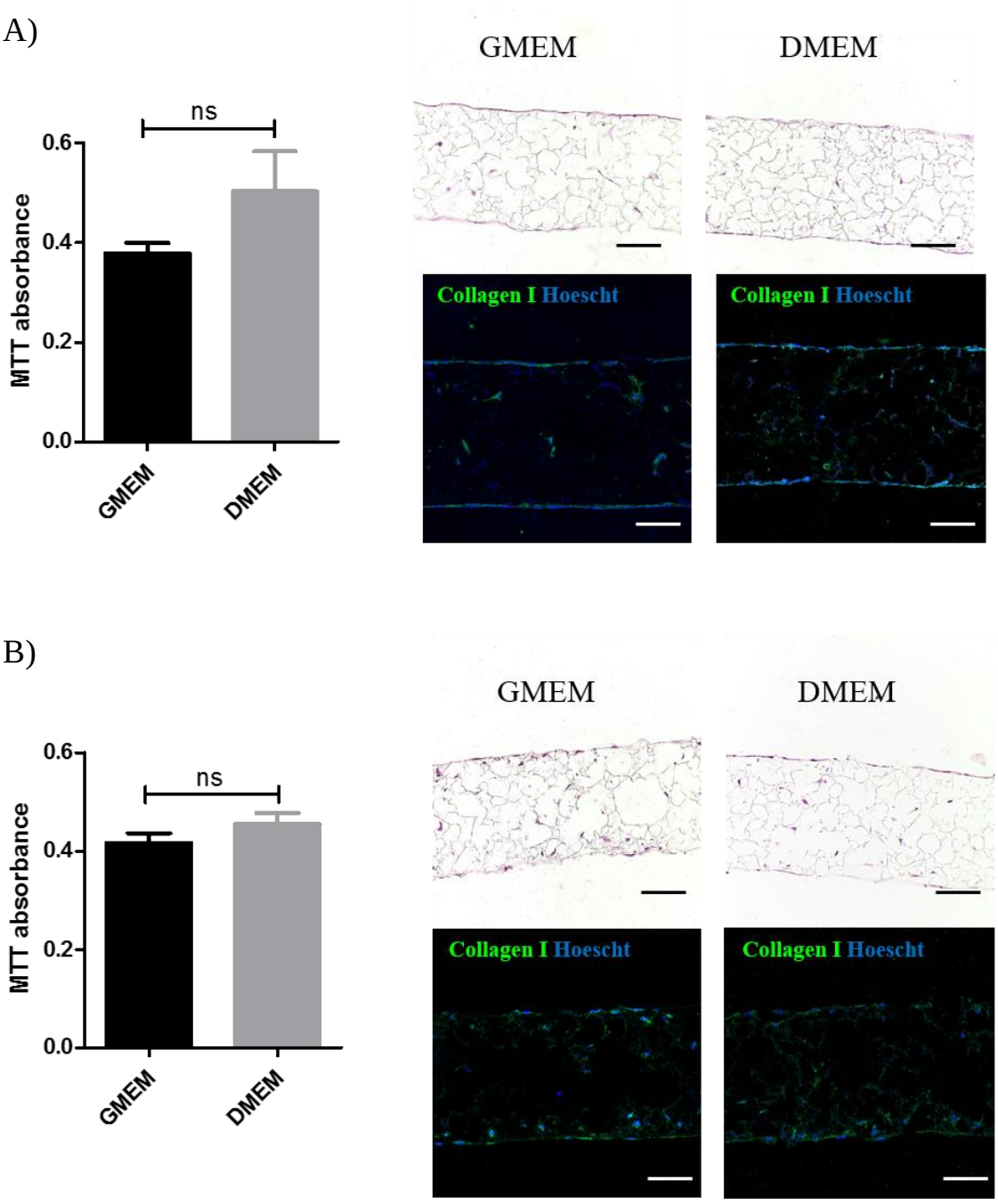


Figure 6.49: Structure and viability of SCID dermal equivalents cultured in stem cell media: SCID fibroblast dermal equivalents were cultured as normal in DMEM until the point of maturity, 21 days. Dermal equivalents were then maintained in DMEM, or the media was swapped to GMEM. A) After 14 days, morphology and distribution of the cells within the dermal equivalent appears to be the same in each media, with viability also the same in each as measured by MTT. Immunostaining also shows a similar expression of ECM protein Collagen 1. B) This morphology and phenotype is replicated following 28 days culture in the two media types also, with little difference in the viability and immunostaining. No significant differences were found in the viability, as assessed by Student's t-test. Data represents mean ± SEM from 3 independent experiments. (n=3) Scale bar: 100 µm

6.5.4.3 Co-culture of murine tissue discs on SCID dermal equivalents does not result in enhanced differentiation

Following the formation of the SCID dermal equivalent over 21 days, CGR8 murine embryoid bodies were seeded onto dermal equivalents which were swapped to GMEM and allowed to spontaneously differentiate. It has previously been established in Section 6.5.1 that 14 days was sufficient time for CGR8 tissue discs to form morphologically complex structures within the tissue disc, so the morphology of tissue discs was assessed after 14 days culture on the SCID dermal equivalent. The size of tissue discs cultured on the SCID dermal equivalent is significantly reduced compared to those allowed to spontaneously differentiation on Alvetex® Polaris. The tissue disc has a homogenous phenotype, with no recognisable structures derived from any germ layers.

A small number of markers representing each germ layer were selected to analyse the tissue discs with a reduced phenotype via immunostaining, to ascertain whether any recognisable differentiation or progenitor cells were able to be detected. A single marker was selected for each germ layer due to the phenotype of the tissue disc: Class III β-tubulin staining identifies neurones, and as neural differentiation is the default differentiation pathway for PSCs, this was selected for ectodermal differentiation. The absence of cells of the myofibroblast or smooth muscle population prevented the use of α smooth muscle actin, but the mesodermal transcription factor GATA4 has been used previously was chosen to identify mesodermal progenitors. Due to the diversity of endoderm derived tissues, E-cadherin was selected again to identify epithelia, a key structural component of many endoderm derived organ systems. Immunostaining reveals some intermittent positive staining for GATA4 and the neuronal marker Class III β-tubulin. E-cadherin staining is negative, confirming the lack of epithelial surfaces and lumens as seen in the histology. Following 21 days culture on the dermal equivalent, a similar tissue disc phenotype is observed, with a reduced size and homogeneous appearance, which does not resemble any specific structure. In the same way, immunostaining shows positive staining for GATA4 and Class III β-tubulin, and negative staining for the epithelial marker E-cadherin. After 28 days culture on the dermal equivalent, the entire tissue disc structure is lost, with the cells having migrated into the dermal equivalent. This is confirmed through the immunostaining, with the positive staining for GATA4 and Class III β-tubulin localised within the scaffold rather than on the top.

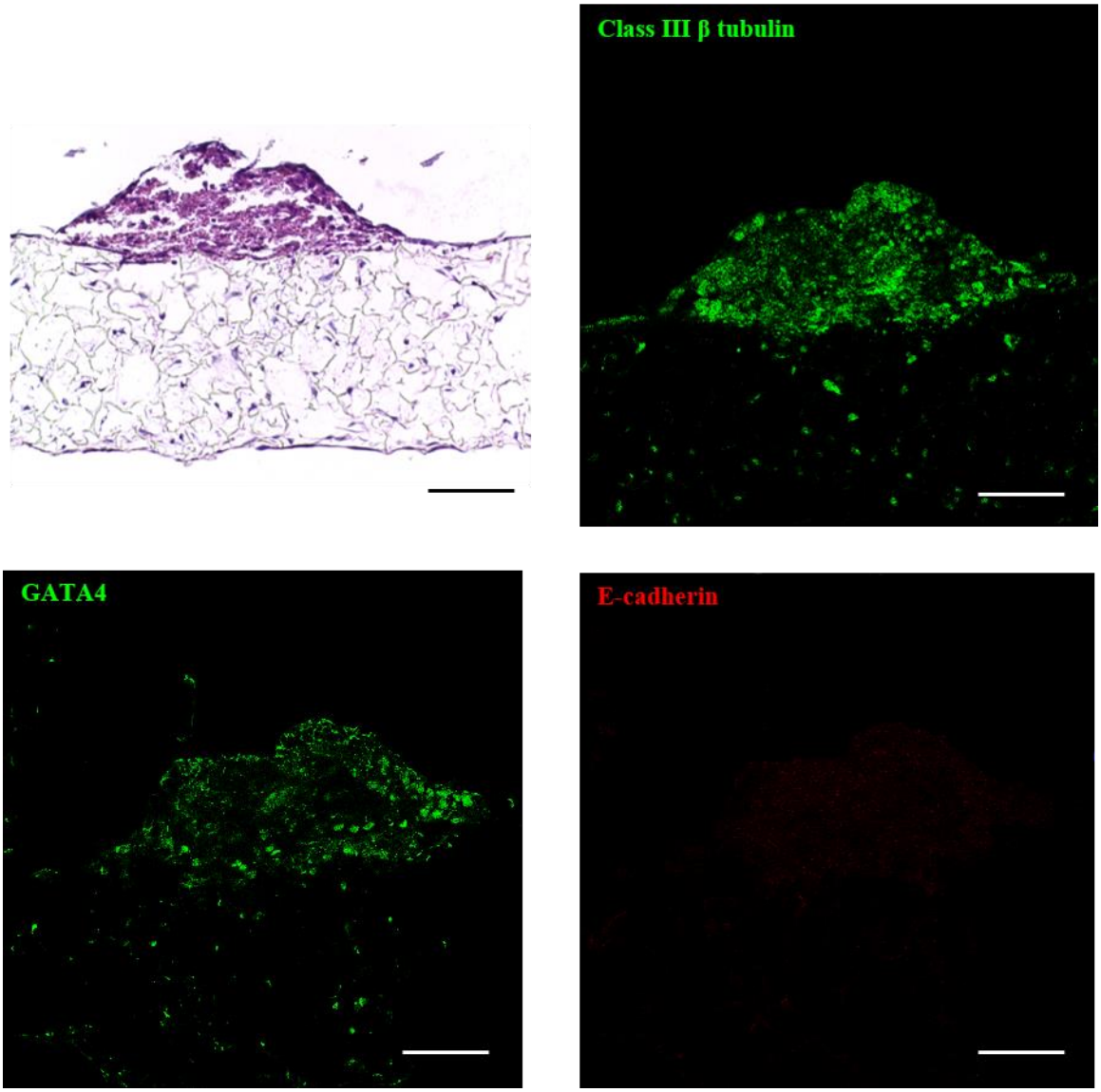


Figure 6.50: CGR8 tissue discs cultured on SCID dermal equivalents for 14 days: CGR8 embryoid bodies were seeded onto 21 day old SCID dermal equivalents and cultured for a further 14 days. Tissue discs show a highly homogenous morphology, with reduced formation of complex structures and very low levels of differentiation, as shown by intermittent expression of germ layer markers across the tissue structure. Differentiation appears to be mainly mesodermal and potentially neural. There are no epithelial structures or complex tissues of any kind. Representative images shown. Scale bars: 100 µm

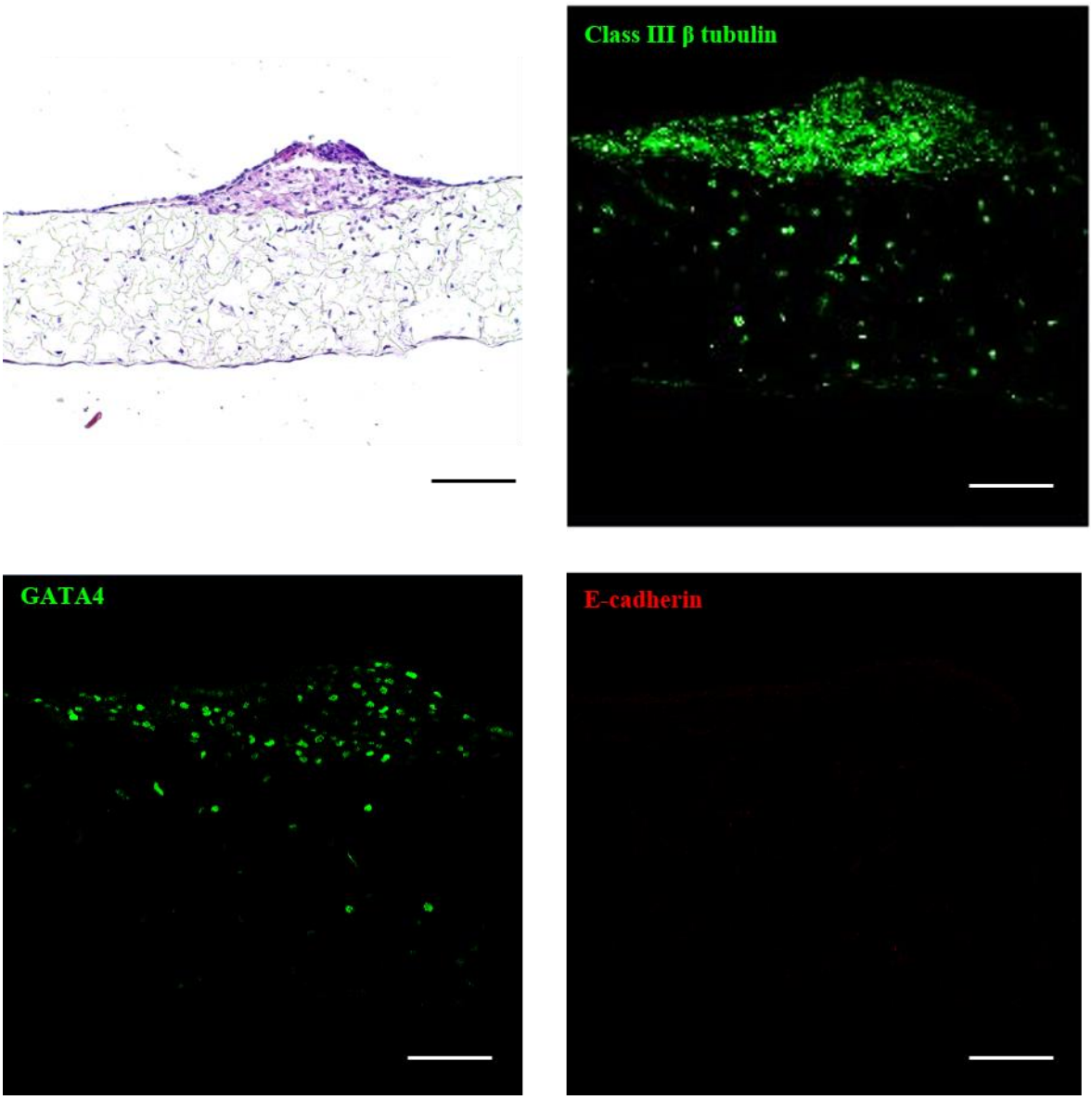


Figure 6.51: CGR8 tissue discs cultured on SCID dermal equivalents for 21 days: CGR8 embryoid bodies were seeded onto 21 day old SCID dermal equivalents and cultured for a further 21 days. Again, tissue discs show a homogenous morphology as previously detected, with reduced structure formation and no complex recognisable differentiation. Intermittent expression of differentiation markers confirms the lack of complexity. Differentiation appears to be mainly mesodermal and potentially neural, with no epithelial surfaces again. Representative images shown. Scale bars: 100 µm

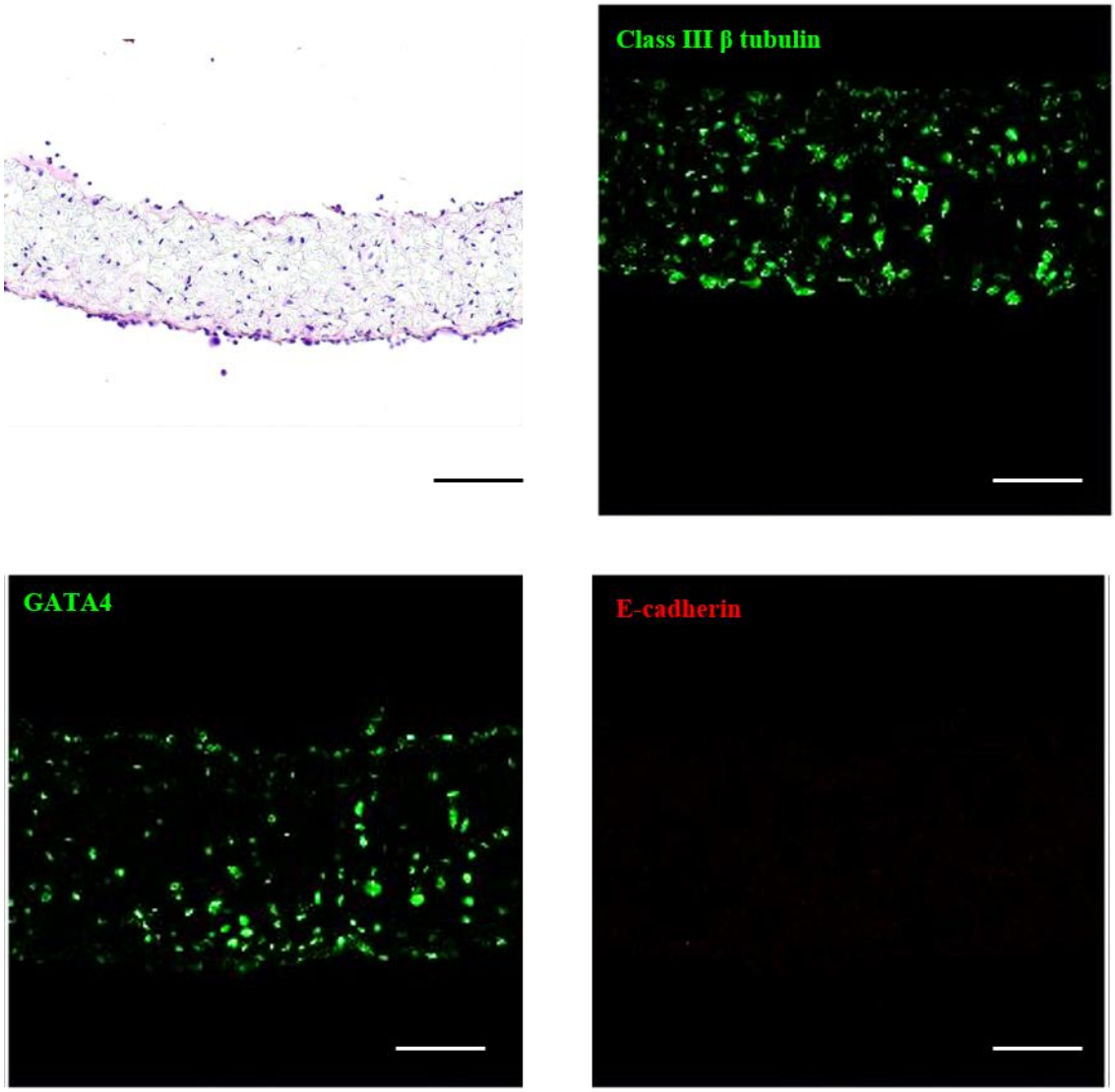


Figure 6.52: CGR8 tissue discs cultured on SCID dermal equivalents for 28 days: CGR8 embryoid bodies were seeded onto 21 day old SCID dermal equivalents and cultured for a further 28 days. Tissue discs completely lose their structure after this prolonged culture on the scaffold, having migrated into the dermal equivalent. Immunostaining for differentiation markers shows that presence of the differentiated stem cells within the scaffold, and again, mesodermal and potential neural differentiation is present. There are no epithelial surfaces. Representative images shown. Scale bars: 100 μm

6.4.4.4 Co-culture of CGR8 tissue discs with an alternative fibroblast population results in the same tissue disc phenotype

As the SCID dermal fibroblasts used in the dermal equivalent were of mouse origin, it was considered that these could have a stronger influence on the differentiation trajectory of mouse embryoid bodies than other fibroblast populations, given that these cells both originated from the same species organism. In order to test this theory, the HDFn dermal equivalent which was originally used to optimise the co-culture methodology was used again for co-culture with CGR8 tissue discs (this study was completed alongside this project). CGR8 tissue discs were cultured on HDFn dermal equivalents for 28 days, with the resultant tissue disc phenotype generally being the same as that seen with the SCID dermal equivalent: a reduced size and homogenous composition, with no clear complex structures. A key difference is that the tissue disc retains its structure after 28 days culture on the HDFn dermal equivalent, which is likely due to the increased cellular layering on the top of the scaffold reducing tissue disc infiltration. Immunostaining for various markers shows a similar expression pattern, with intermittent GATA4 and Class III β-tubulin expression within the tissue disc. Staining for E-cadherin and α smooth muscle actin are absent.

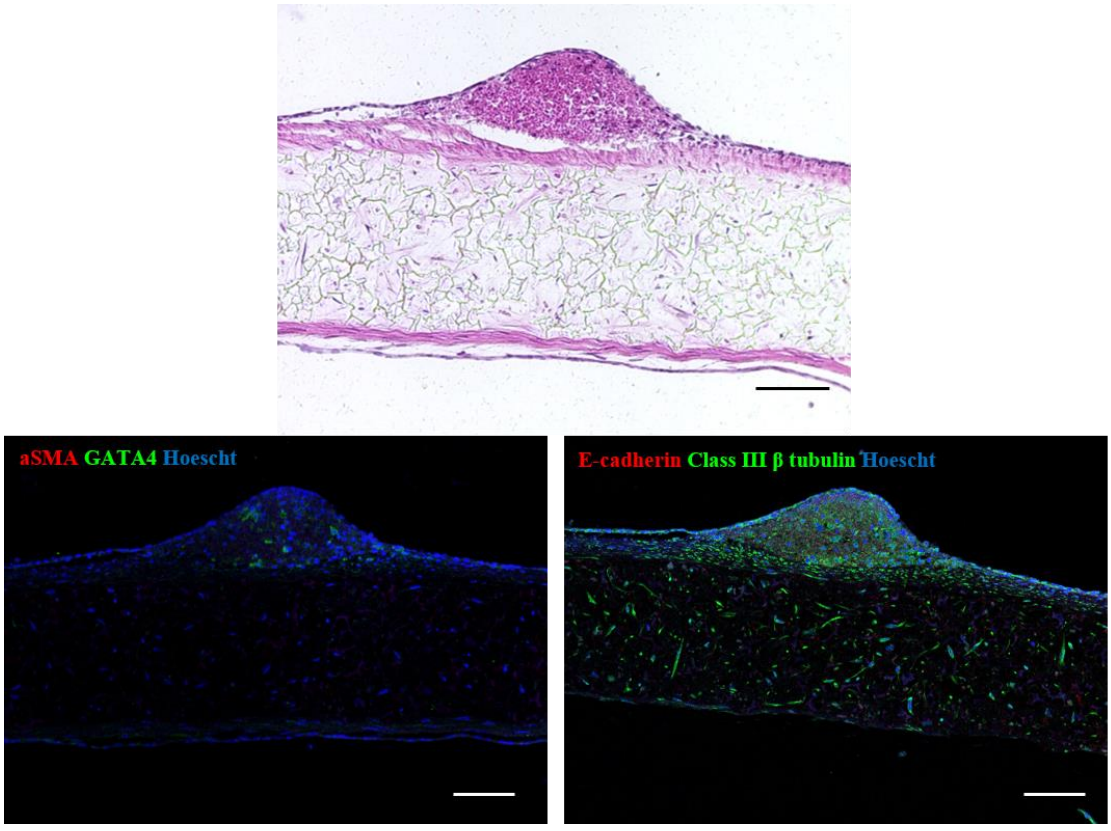


Figure 6.53: CGR8 tissue discs cultured on HDFn dermal equivalents for 28 days: CGR8 embryoid bodies were seeded on 14 day old HDFn dermal equivalents in the 12 well Scaffold format. Tissue discs also show the reduced phenotype in this culture system, with a homogeneous structure and no complex tissue constructs pertaining to any germ layers. Low levels of differentiation are present, with immunostaining highlighting small amounts of mesodermal and neural differentiation. Representative images shown. Slides courtesy of Felicity Liu. Scale bars: 100 µm

6.4.4.5 The effects of SCID dermal fibroblasts on CGR8 tissue discs are due to a combination of paracrine and topographical cues

The effects of culturing the CGR8 tissues discs on the surface of the SCID dermal equivalent are very obviously evident in the histology and immunofluorescence as seen in the previous section. Preliminary studies were conducted to attempt to elucidate how use of the co-culture system led to the tissue disc phenotype observed. This could be due to any number of cellular signals being exchanged by the dermal fibroblasts and CGR8 tissue disc cells, but for simplicity, two main effects were investigated: the effects of paracrine signals secreted into the media by the fibroblasts and the effects of the topography of the fibroblast filled scaffold on the developing CGR8 tissue discs.

Conditioned media was collected from SCID fibroblast dermal equivalents cultured in GMEM after the 21 day time point every 3-4 days, and combined in a 1:1 ratio with fresh GMEM before CGR8 tissue discs were cultured in the media on Alvetex® Polaris. The addition of fresh media was to prevent complete depletion of the media components, which would have been detrimental to tissue disc maintenance overall. After 14 days culture in the conditioned media, CGR8 tissue discs show some similarities to the tissue discs from the co-culture system. Again, a reduced morphology is present, with the tissue disc structure being fairly homogenous overall, showing only small amounts of variation. No complex structures are visible within the tissue discs as was previously seen within the CGR8 tissue discs cultured on Alvetex® Polaris and allowed to spontaneously differentiate.

Fixed fibroblast scaffolds were created by fixing fibroblast populated scaffolds that were at least 21 days old in sterile filtered PFA before washing several times in PBS to ensure complete removal of the PFA from the scaffolds. CGR8 tissue discs were seeded onto the fixed scaffolds and cultured in normal GMEM differentiation media. Tissue discs cultured on the fixed scaffold again show some level of response to the physical cues: after 14 days, a relatively large amount of the tissue disc is still present on the surface of the scaffold. Some cavities are present within the tissue disc, although these are not as complex as has been seen previously. The tissue disc does show more heterogeneity than the tissue discs previously cultured in the co-culture system and with the conditioned media, although this is reduced in comparison to spontaneously differentiated tissue discs, which show a clear range of different cellular morphologies and tissue structures.

As with the original co-culture experiment, these experiments were also conducted for up to a maximum timescale of 28 days, to investigate the effects of prolonged exposure to the chemical and physical cues selected. In a similar manner as was seen with the 14 day exposure to the SCID conditioned media, CGR8 tissue discs cultured for 28 days in the conditioned media also show a reduced differentiation phenotype, as can be seen in Figure 6.53. The histology does show some subtle differences in cellular morphology, most likely the difference between epithelial cells and connective type tissues, but the well-defined lumens and clear epithelial gradients and differentiation from all three germ layers which have previously been observed prior to this time point in the Polaris version of the model characterised in section 6.4.1 are not detected. A mixture of phenotypes was

observed with prolonged culture on the fibroblast filled scaffold, but a similar trend was still observed overall in the behaviour and morphology of the tissue discs. Tissue discs show a highly reduced phenotype and size, with significant infiltration into the scaffold itself. Indeed, there were scaffold which show no evidence of tissue disc structure, either due to complete infiltration or lack of interaction with the fibroblast topography on the scaffold.

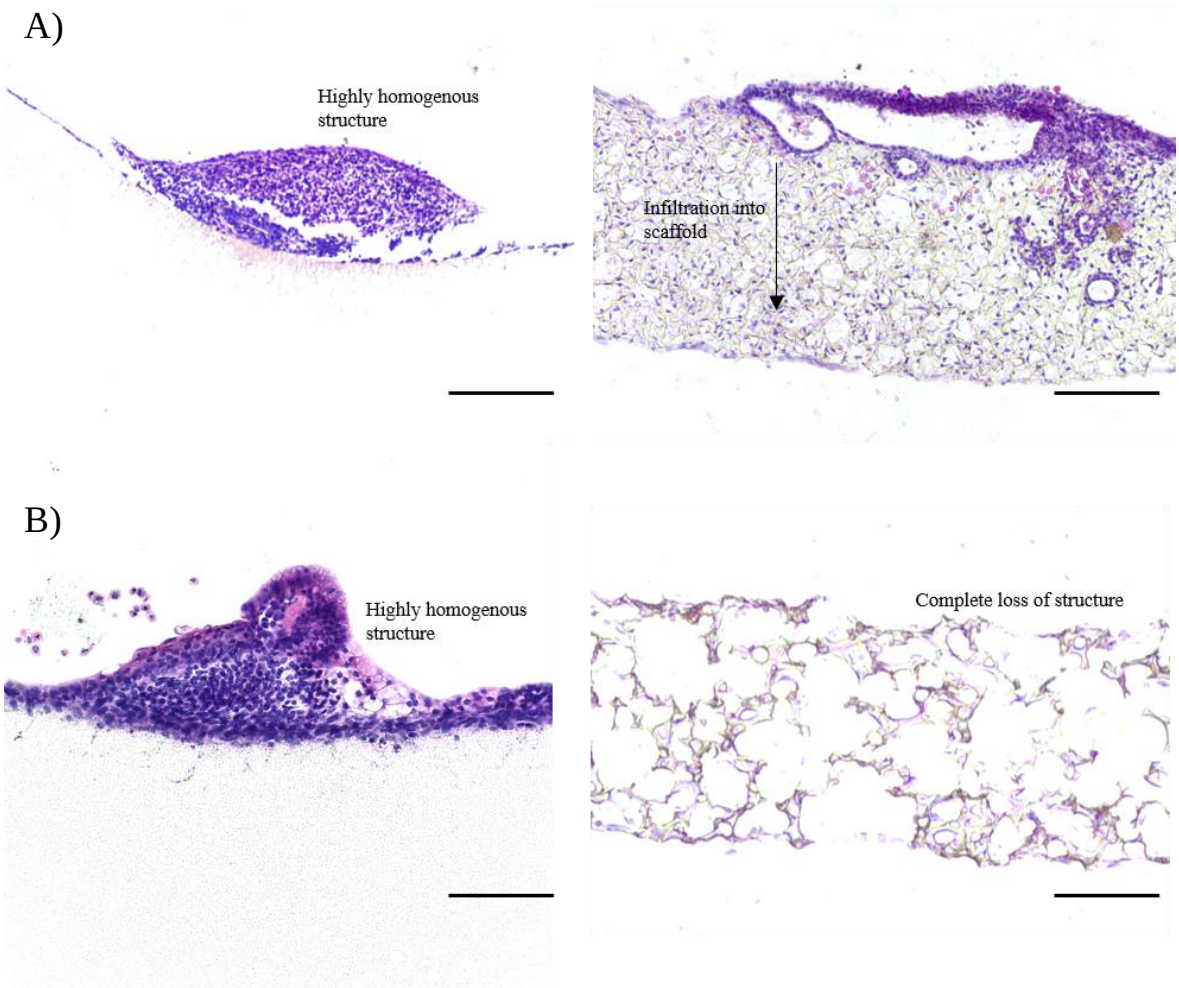


Figure 6.54: CGR8 tissue discs cultured with SCID fibroblast conditioned media or on fixed fibroblast populated scaffolds for up to 28 days: CGR8 embryoid bodies were cultured in one of two conditions: on Alvetex® Polaris with 50 % SCID DE conditioned media, or on fixed Alvetex® Scaffold filled with SCID fibroblasts with normal differentiation maintenance media. A) At 14 days, the paracrine effects from the conditioned media show the reduced phenotype, which is highly homogenous and shows little complexity. There is some level of infiltration into the fixed scaffold, with the tissue disc on the surface also showing a homogenous phenotype. B) The reduced, homogenous phenotype is maintained at the 28 day time point in the paracrine samples, although the tissue disc on the fixed scaffold has fully infiltrated the scaffold. Scale bars: 100 µm

6.5.5 Utilisation of CGR8 murine stem cells in perfusion culture system

Previously, in Chapter 3, the use of a novel perfusion bioreactor was optimised with the culture of TERA2.cl.SP12 embryonal carcinoma cells, with the aim of maintaining cellular viability and enhancing differentiation. This was due to the fact that the *in vivo* microenvironment is highly complex, with perfusion by the vasculature having a critical supporting role. Following on from this, and using the conditions previously optimised and found to be suitable for the culture of stem cells, CGR8 murine embryonic stem cells were used in the perfusion system. Two million CGR8 cells were seeded onto an Alvetex® Polaris insert and allowed to adhere for two days before transfer to the perfusion system and culture under perfused conditions. In line with experiments completed in the literature by Stachelsheid and Gerlach and the generally accepted view that time is a crucial part of the differentiation process, cells were left for 56 days in the perfused system to allow for complex cellular differentiation to occur, and to encourage structure formation. This culture set up strongly resembles the conditions of the teratoma assay, providing a complex perfused cellular microenvironment and allowing significant time for complex structure formation.

The histology of the structures after 56 days is highly complex and different to tissue discs derived from EBs in the static system. As seen in Figure 6.54, these tissue discs are much larger with a variety of different structure visible, making them highly reminiscent of differentiated teratomas. There are large amounts of stratified epidermal differentiation throughout the tissue disc as can be seen in the Figure. This is the predominant differentiated structure within the tissue disc which has formed, as the lumens within the disc also contain highly mature stratified epidermis with stratum corneum like structures within the centre. There are other epithelial structures within the tissue disc, which show organisation and polarisation. Fibroblast like connective tissues are also found within the tissue disc, supporting the overall structure, as well as areas of smooth muscle differentiation. Further analysis of this tissue disc confirms the complexity and diversity of the structures within the tissue disc, including the presence of specialised epithelia, possibly with microvilli, and epithelial lumens potentially representing renal differentiation. Spaces in the epithelial layer indicate the presence of goblet like cells, which indicates the complexity of the epithelial structure, with the use of the Perioidic Acid Schiff stain with Alcian blue confirming the presence of complex proteoglycans, most likely mucins.

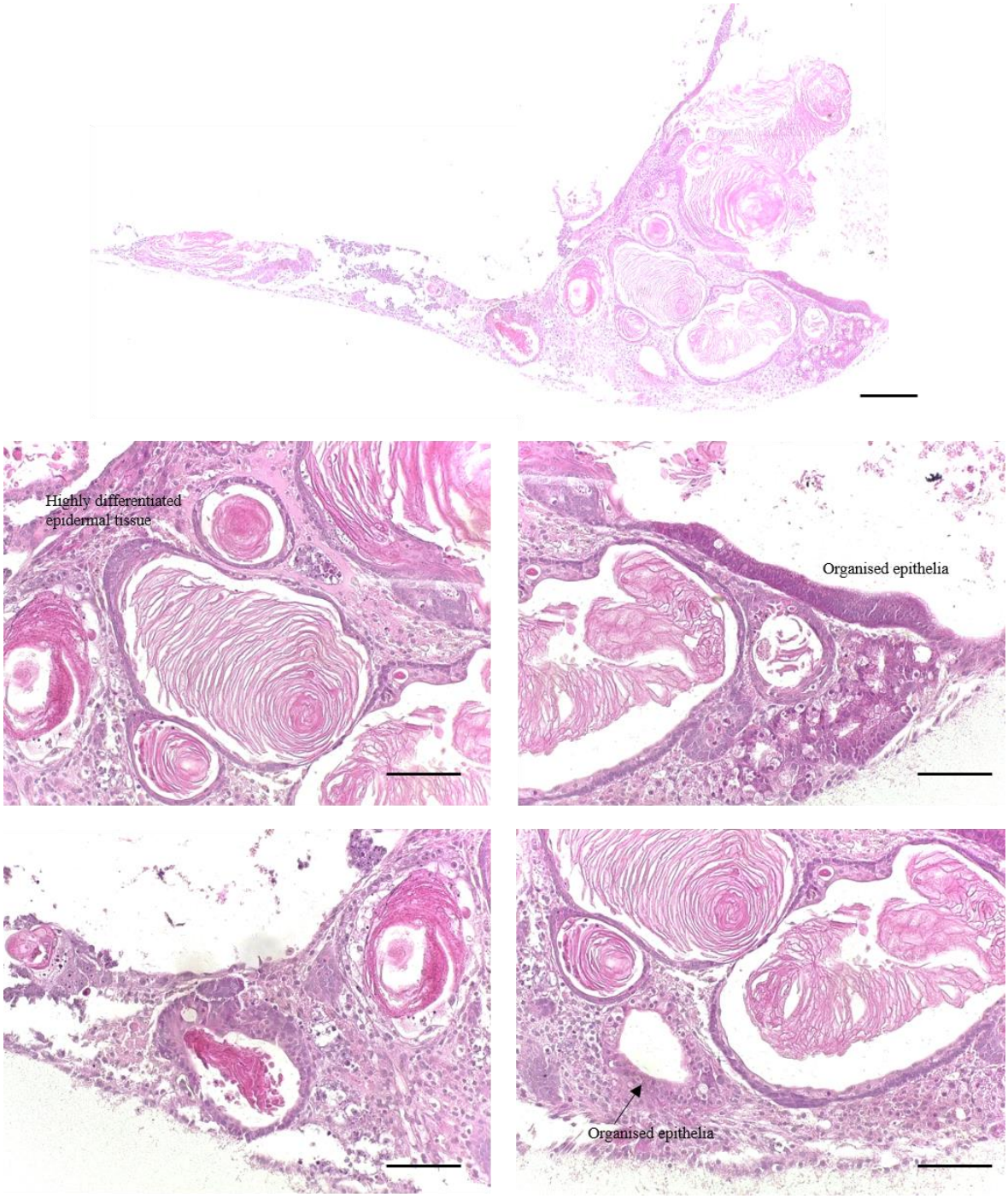


Figure 6.55: Complex structure formation following 56 days of perfusion culture of CGR8 cells: 2 million CGR8 cells were seeded onto the surface of Alvetex® Polaris and allowed to attach over 2 days before transfer to the perfusion system for 56 days culture. Cells show the formation of highly complex tissue structures from all three germ layers within the resultant tissue disc, which closely resembles a mature teratoma. Tissue structures that can be identified include areas of mature epidermal differentiation, well organised epithelial lumens and complex epithelial surfaces, large amounts of connective tissues and various rudimentary structures. Scale bars: 200 µm and 100 µm

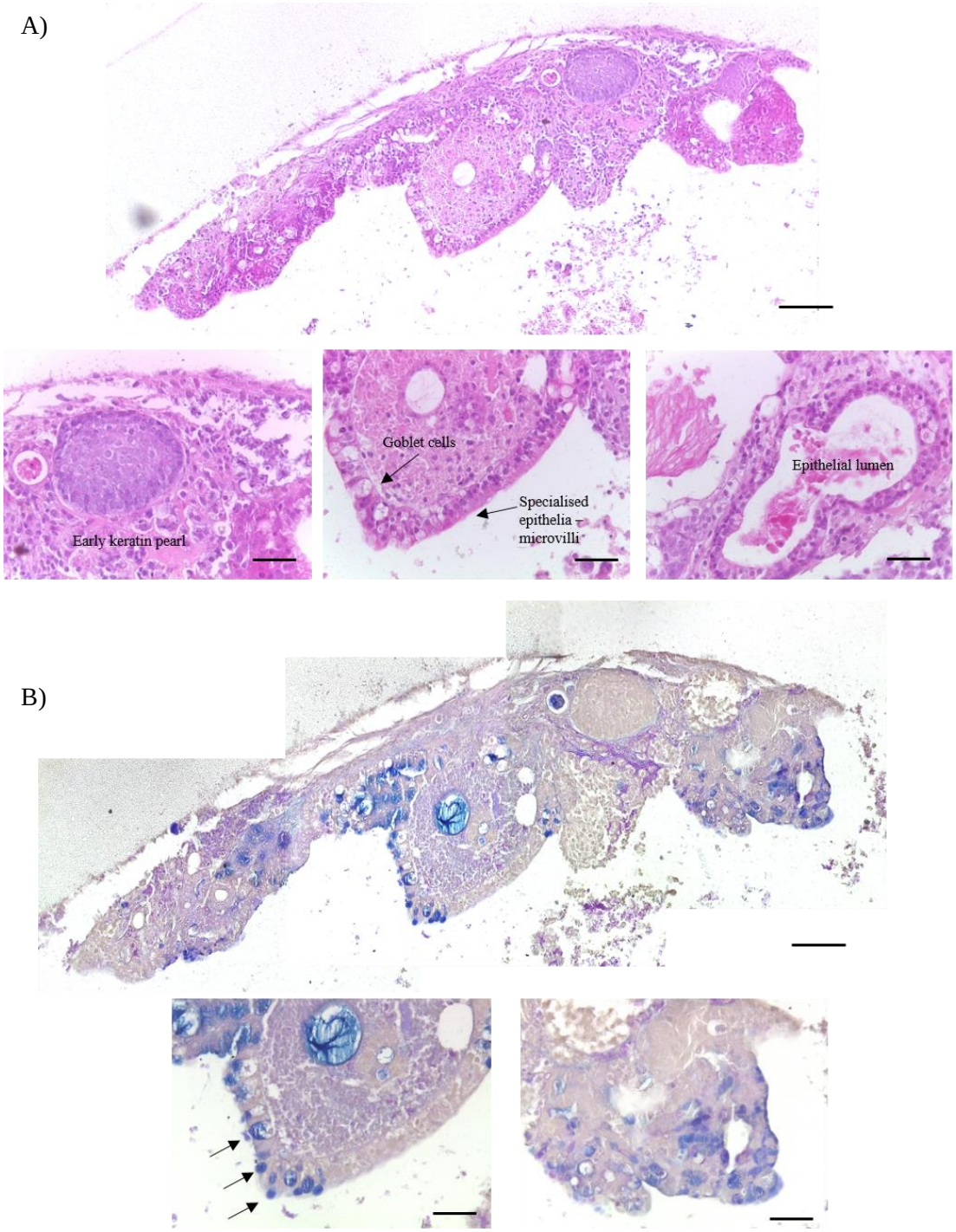


Figure 6.56: Complex structure formation throughout the tissue disc structure of 56 day CGR8 derived tissue disc: Further sectioning through the CGR8 tissue disc confirms the heterogeneity and complexity of the structures which have formed. A) H&E staining highlights complex epithelial surfaces with multiple cell types, lumens and progenitor populations forming complex structures such as keratin pearls. B) Periodic Acid Schiff staining with Alcian Blue identifies the presence of endoderm derived mucous secreting goblet like cells in the epithelial layer and other complex carbohydrates within the tissue disc. Scale bars: 200 µm and 50 µm

Clear evidence of mesodermal differentiation is visible in the tissue disc Figure 6.56, with a structure resembling cartilaginous or bone tissue formation within the centre of the tissue disc, surrounding by

additional stratified epidermis and other epithelial and connective tissues. Masson's trichrome stain confirms the rich extracellular matrix of this structure, but Weighert's stain distinguishes the structure as bone due to the positive red staining, and better highlights the granular nature of the tissue.

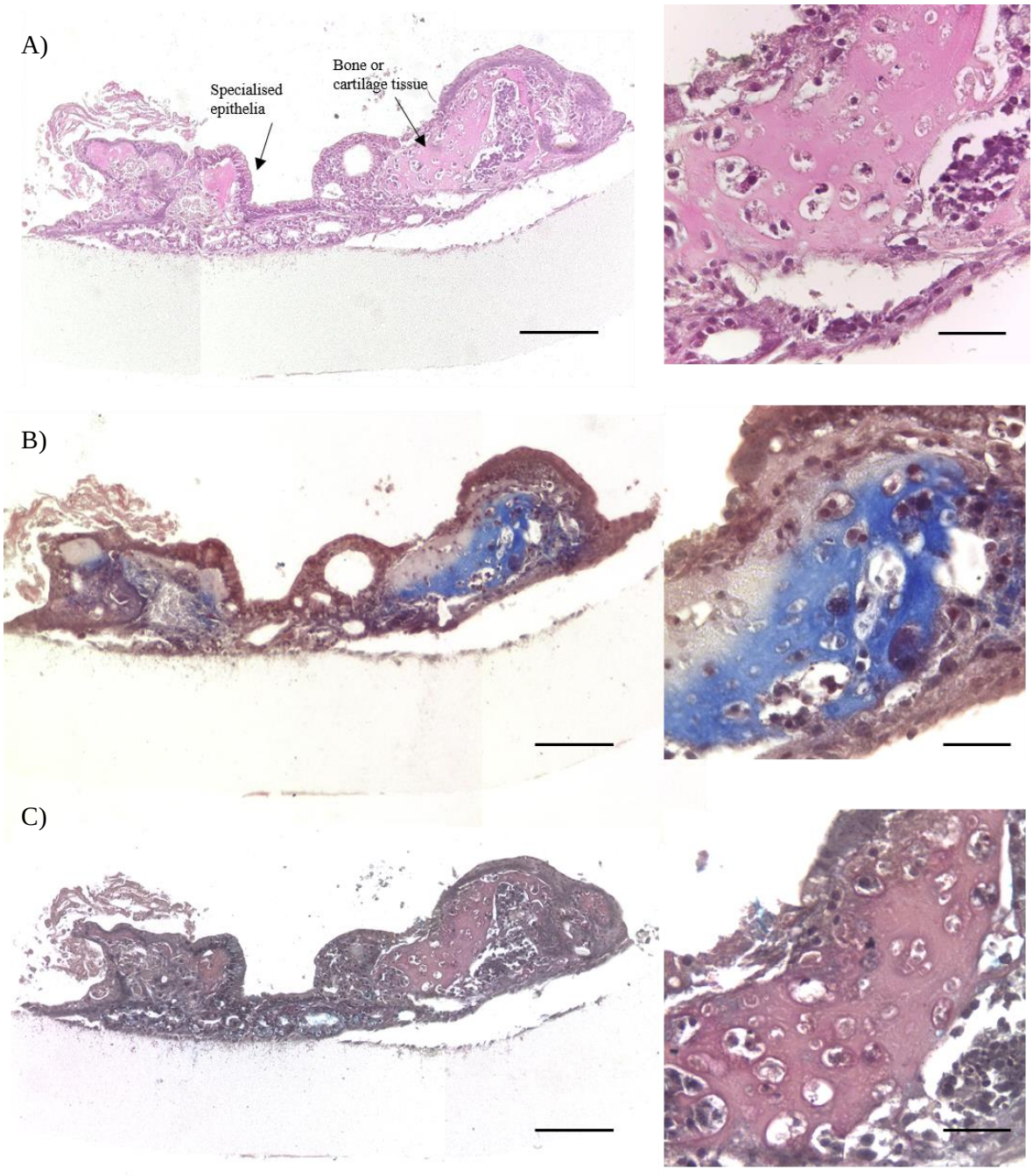


Figure 6.57: Multiple CGR8 derived tissue discs show the formation of complex, mature structures following 56 day perfusion: A) H&E analysis of separate tissue discs shows the formation of other complex structures, including complex varied epithelia, cartilage and bone. B) Masson's Trichrome staining confirms that the structures are rich in extracellular matrix, with positive blue staining. C) Weighert's staining highlights the bone and cartilage structures within the tissue disc, staining red and blue respectively. Scale bars: 200 µm and 50 µm

Immunostaining for a variety of markers aids in the identification of these tissue structures, as is seen in Figure 6.57. Smooth muscle and myofibroblasts stain positively for α smooth muscle actin throughout the tissue disc, with small areas of GATA4 staining also. Epithelial and epidermal structures stain strongly positive for E-cadherin, with stratified epidermal structures also staining positive for the epidermal differentiation marker cytokeratin 10. Loricrin staining is also present within the tissue disc; loricrin is a protein found in cells in the cornified layer, and indicates terminal differentiation within the skin. Filaggrin, another marker of terminal differentiation in skin, is negative, as is staining for the pluripotency marker Oct 4.

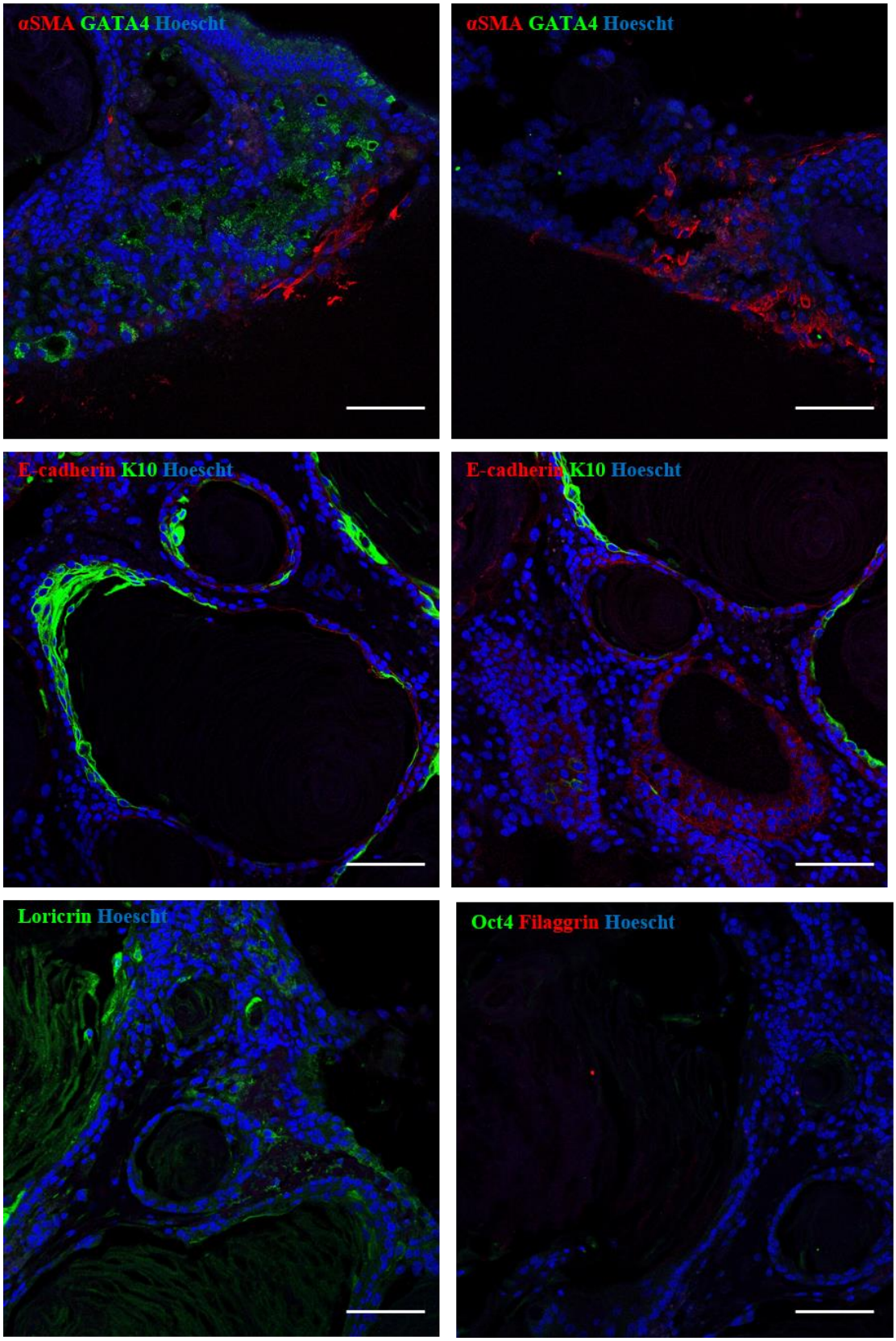


Figure 6.58: Identification of germ layer structures following 56 days of perfusion culture of CGR8 cells: The perfusion of 2 million CGR8 murine stem cells resulted in the formation of a histologically complex structure resembling a teratoma. Immunostaining for a variety of germ layer markers allows for the identification of E-cadherin positive epithelia and epidermal differentiation through presence of positive cytokeratin 10 and loricrin staining. There are also GATA4 mesodermal progenitors and α smooth muscle actin structures within the tissue disc. Scale bars: 100 μm

By contrast, the tissue disc in Figure 6.58 which formed under static conditions strongly resembles the tissue discs previously seen in this Chapter, which were formed using murine EBs. The histology of the tissue disc is heterogeneous, with epithelial structures and connective tissues. The epithelia in this tissue disc are relatively simple, with no additional integrated cell types, and while there is some potential epidermal differentiation, this is not well stratified or organised. There is a heterogeneous connective tissue element, and some evidence of smooth muscle differentiation. The identification of these structures is confirmed using immunostaining. There is weak staining for GATA4, as shown in Figure 6.59, with accompanying staining for α smooth muscle actin confirming the presence of smooth muscle. A small amount of staining is present for cytokeratin 10, but this is also weak in comparison to the tissue disc from the perfused system. Trace amounts of Class III β-tubulin are found within the tissue disc, with no staining for neural progenitor marker Nestin. E-cadherin staining of epithelia is also present but weak.

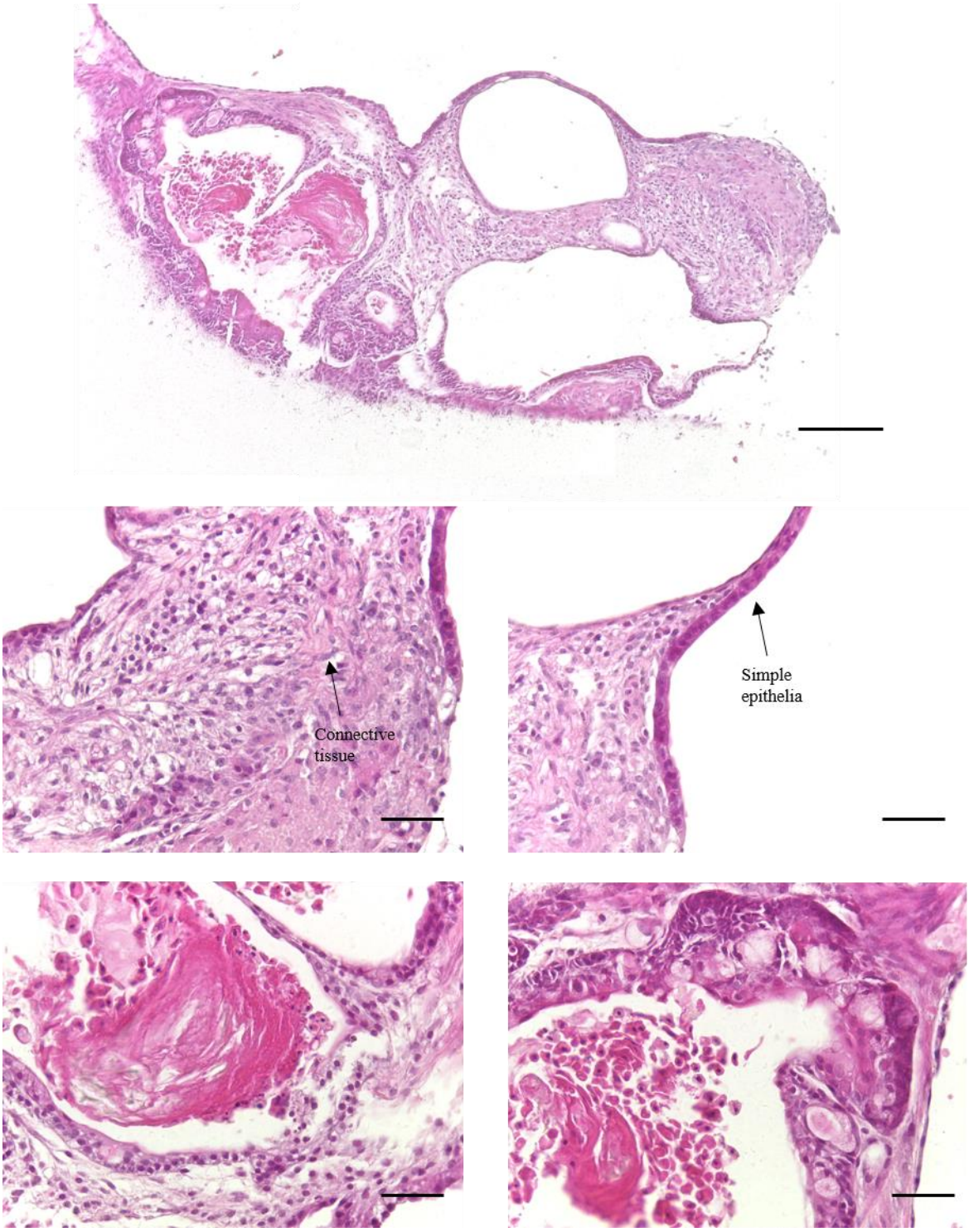


Figure 6.59: Identification of germ layer structures following 56 days of static control culture of CGR8 cells: Alongside the perfused sample, a static control sample was seeded with the same number of cells and cultured in a 6 well plate. After 56 days, this showed the formation of some complex structures similar to those previously seen in the EB derived tissue discs, with the differentiation mainly consisting of epithelial surfaces and large amounts of connective tissues. Some evidence of potential epidermal differentiation is also present, although this is not as complex as that observed in the perfused samples. Scale bars: 200 µm and 50 µm

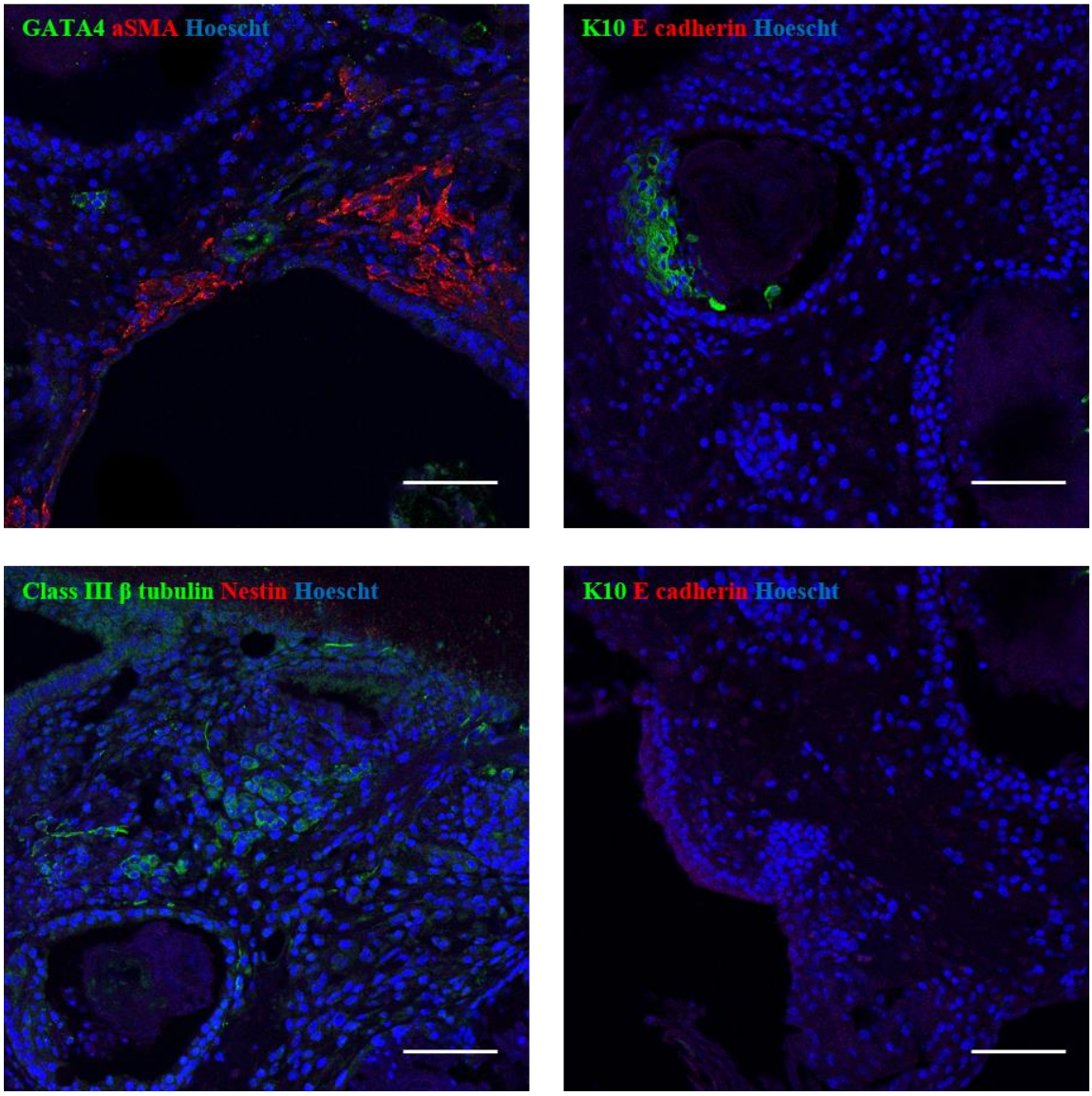


Figure 6.60: Identification of germ layer structures following 56 days of static control culture of CGR8 cells: Immunostaining revealed the presence of areas of α smooth muscle positive tissues, and small amounts of epidermal differentiation as indicated by cytokeratin 10, but these are not as extensive as that observed in the perfused samples. Only small amounts of neural tissue differentiation are present, and the epithelia within the tissue disc do not stain positively for E-cadherin. Scale bars: 100 μm

6.6 Discussion

In this Chapter, the model that was developed in Chapters 4 and 5 using TERA2.cl.SP12 embryonal carcinoma cells was the applied to an alternative stem cell population. While embryonal carcinoma cells are a robust model for the development and assessment of novel technologies or the study of specific developmental pathways, these cells are not representative of true pluripotent stem cell populations, such as embryonic stem cells, due to their tumorigenic origins and properties. Mouse pluripotent stem cell populations represent a suitable intermediate population for the further testing of novel models before the use of human PSCs, which often have expensive and demanding culture requirements. The similarities in mouse and human developmental processes also confirm the suitability of murine PSCs, due to the ability to elucidate mechanisms and processes from work carried out using murine PSCs.

6.6.1 The long term differentiation of murine embryoid bodies as tissue discs on Alvetex® Polaris

The murine embryonic stem cell line CGR8 was chosen for this study as this population has previously been used to create embryoid bodies and subsequently tissue discs on the surface of Alvetex® Polaris (Owens, 2015), which demonstrated the ability to form complex structures. CGR8 cells were briefly subject to pluripotency analysis, with the expression of pluripotency associated factors confirming this phenotype. CGR8 cells also successful formed EBs which displayed evidence of the loss of pluripotency and the beginning of lineage commitment, with evidence of differentiation markers from multiple germ layers as would be expected (Poh et al., 2014). In response to the findings in Chapter 4 which confirmed the presence of a limit to EB size which is independent of seeding density, an EB size of 1000 cells was selected due to the common usage of this seeding density for EB formation and reports of central cell death in EBs larger than this following an initial increase in size (Mansergh et al., 2009). EBs were formed in low adherence microwell plates to achieve a uniform cell number and allowed to mature in suspension for 5 days. This aligns with many protocols in the literature which allow EBs to differentiate for 5 days prior to use or seeding for differentiation (Karp et al., 2006; Kowalski et al., 2012; Son et al., 2011), as well as shortening the time required to create the EBs. CGR8 EBs were seeded onto the Alvetex® Polaris insert as was previously done with TERA2.cl.SP12 EBs, but cultured for up to 35 days, with structural analysis every 7 days, in order to assess the ability to maintain tissue discs on the scaffold for long term differentiation. Examples of the seeding of EBs onto porous scaffold were briefly discussed in the Introduction to Results Chapter 5, namely neural differentiation focussed studies, and further assessment of the literature shows that porous scaffolds are often used for the seeding of single cell suspensions or the creation of EBs rather than the maintenance of EB structures. This is understandable due to the general acceptance of EB formation as representative of early embryonic

development, but provides few examples with which to compare the differentiation observed within this model.

After 7 days culture, although no recognisable structures are visible within the tissue disc, these structures are still more complex and heterogeneous than time matched EBs. This result correlates with that hypothesised by Dang (Dang et al., 2002) and observed in Chapter 4 using the TERA2.cl.SP12, confirming the effects of attachment mediated signals on EB differentiation and providing a homogenous oxygen environment in this second pluripotent stem cell population. Following 14 days culture on Alvetex® Polaris, and the time points after this, tissue discs are highly complex in their nature, with a number of recognisable tissue types and structures observed. As confirmed by the histology and immunostaining at each time point, these are derived from the three germ layers which is of importance in the confirmation of developmental potency and the study of the process of human development from the totipotent zygote to the mature tissues derived from the three germ layers. The structures observed in the tissue discs cultured on the Alvetex® insert are consistently more complex than those observed in the time matched EBs, as well as being consistently more complex than structures that are generally observed in pluripotent stem cell derived EBs (see Figures), due to the fact that EBs are mainly used to study the early events of the differentiation process (Sheridan et al., 2012; Simunovic and Brivanlou, 2017). Overall, these data correlate with that obtained by Owens using the same cell line, confirming the outcome of those initial pilot studies, but also highlighting a level of variability in structure complexity and identity between the tissue discs.

The level of complexity and organisation achieved by the individual structures within tissue discs was particularly interesting, as differences in the structure of the epithelial layer could be detected, although the overall organisation, or rather disorganisation, is similar to that observed in teratomas and therefore does not follow the spatial organisation observed in the developing organism. It can be noted, however, that there are some similarities to the formation of the mammalian body plan; often, there is a specialised epithelial surface reminiscent of the epidermis on the outside of the tissue disc, with the epithelia lined lumens on the inside of the tissue disc. While these structures are not as recognisable as the structures found in a teratoma (see Figures), the fact that these structures can be identified as pertaining to a specific germ layer, and that all three are represented, is sufficient for the assessment of developmental potency for assays such as the teratoma assay. This certainly provides some evidence for the use of this *in vitro* method to test developmental potency.

6.6.2 Directing the differentiation of murine EBs and tissue discs towards specific germ layers

The in depth study of developmental processes requires that the differentiation of PSC populations can be manipulated for the analysis and elucidation of specific mechanisms, thus the culture of

spontaneously differentiating tissue discs is indicative but not representative of the actual studies that would be performed using this novel *in vitro* model.

Simple differentiation studies confirmed the ability to direct the differentiation of CGR8 EBs towards the neural and mesoendodermal lineages using EC23 and Activin A respectively, a feat which has been achieved using CGR8 EBs and alternative differentiation protocols extensively in the literature (Cerdan et al., 2012; Delivopoulos et al., 2015; Sulzbacher et al., 2009; Teo et al., 2012) . In order to definitively prove that structures from the three germ layers could be created using the tissue disc model and attempt to recreate some of the complex morphogen interactions found *in vivo* during the developmental process, multiple morphogens were used to differentiate CGR8 EBs towards each germ layer at the EB formation stage. The morphogen combinations used were taken from the 2018 paper by the International Stem Cell Initiative which compared multiple assays normally used to assess the developmental potency of human PSCs (International Stem Cell Initiative, 2018). In the original paper, treatment of human EBs with these morphogen combinations led to the activation of lineage specific genes appropriate to the morphogens used following up to 16 days culture in a 96 well plate without media change. The paper stated that 'It was anticipated that these protocols would be sufficient to direct differentiation toward the germ layer of interest but would not necessarily support the generation of more mature cell types.' This represented an opportunity to investigate whether these simple treatment protocols could induce the formation of mature tissue structure if given sufficient time and better nutritional support through seeding on a porous scaffold. Additionally, use of this ISCI developed protocol provides an easier route to adoption of these protocols for the assessment of functional pluripotency due to these already being well known from the literature.

The results of this differentiation generally showed that the tissue discs showed a shift in the differentiated structures which formed, which was towards the intended germ layer. This was particularly visible in the histology and immunostaining at 14 days, although these are representative of the sometimes variable differentiation which was found within the tissue discs, with multiple examples of differentiated structures found in each tissue disc (see Figure).

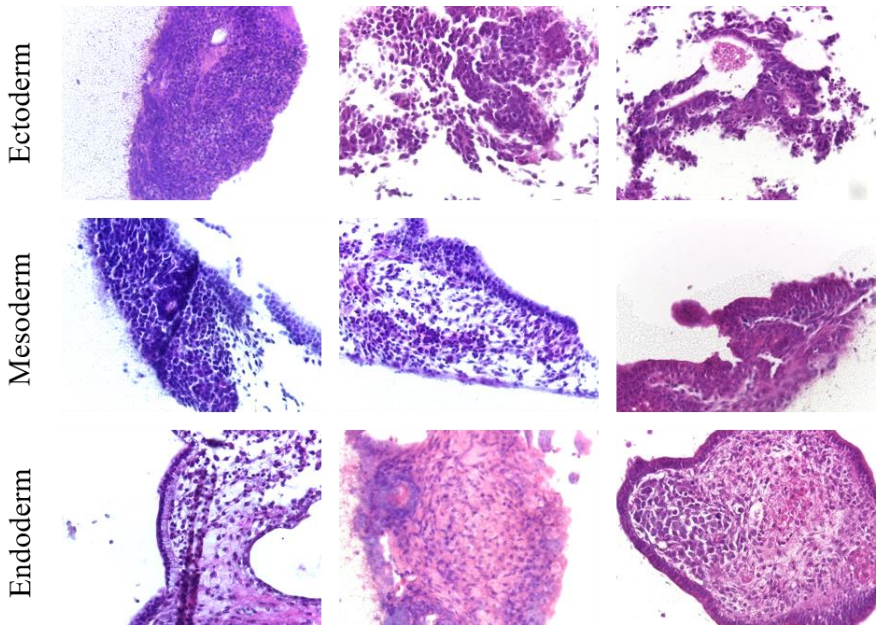


Figure 6.61: Variability in 14 day tissue disc structure formation following differentiation towards specific germ layers: Although much of the data obtained showed that CGR8 tissue discs generally differentiated towards the intended germ layer, variability in germ layer structures was also detected.

Gene and protein expression data provides a better overview of the differentiation within the population, and these too generally correlated with the expected results, shifting towards the intended germ layer. This was particularly prevalent in endoderm tissues, as the genes associated with endodermal differentiation were consistently elevated in these samples. While the ectoderm gene Class III β-tubulin was strongly associated with the ectoderm sample as expected, differences in other ectodermal and mesodermal genes were unexpected. In the case of brachyury, which showed a low expression in mesoderm samples in particular, this could represent the fact that the mesoderm derived tissues in the mesoderm sample have reached an increased level of maturity compared to those in the ectoderm and endoderm samples – this is confirmed by the significant amounts of organised smooth muscle and connective tissues in the histology. Brachyury is a transcription factor which is involved in early lineage commitment to the mesoderm germ layer before the appearance of differentiated cells (Vidricaire et al., 1994); differentiation towards mesodermal tissue structures will have been induced by the application of the mesoderm morphogen combination. Mesoderm tissues are not absent in the other germ layers, but the formation of these is reliant on spontaneous differentiation and supressed in part by the endoderm and ectoderm morphogen combinations, possibly leading to delayed formation and delayed expression of early mesodermal markers. This could also be true of the mesoendodermal marker GATA6 and its elevated expression in endodermal samples. The unexpectedly high expression of the cytokeratins in the mesoderm and endoderm samples could be due to the variability of the tissue disc phenotypes: the error bars for these data are large, reflecting significant variability in the gene expression between samples and while no cytokeratin 14 staining was detected in the immunostaining, these are only representative images. These proteins were used mainly to detect ectodermal epithelial differentiation in this study, but cytokeratins are also key

intracellular proteins in other squamous epithelial surfaces including endodermal epithelial populations during development of the respiratory tract (Hosoya et al., 2010; Pastuszak et al., 2015), thus the unexpected cytokeratin 14 qPCR results could be representative of these populations forming in other tissue discs. Variability in PSC differentiation protocol success, the successful production of terminally differentiated mature cells and the size of the subsequent differentiated cell yield are issues which are currently being addressed by the stem cell field (Rajala et al., 2011; Salimi et al., 2014). The simplicity of this protocol in contrast to more lengthy, tightly managed differentiation procedures naturally introduces more room for variability, as morphogens were applied only once during the initial EB formation to prime the EBs to differentiate towards a specific germ layer rather than to facilitate full differentiation towards ectoderm, mesoderm or endoderm. The application of the morphogens once during the EB formation stage fits well with the current protocol logistically, and further studies are needed to optimise differentiation processes such as these specifically for these structures. This is particularly pertinent when it is noted that many differentiation protocols involving EBs only use the formation of these structures to induce lineage commitment, and that often EBs are subsequently dissociated prior to differentiation (Chadwick et al., 2003; Sottile et al., 2003). While this dissociation solves the problem of differences in cytokine and growth factor concentration in EB structures (Van Winkle et al., 2012) by allowing for single cell or monolayer differentiation, it destroys the primitive spatial organisation and structure formation occurring within the EB. Thus attempts are being made to develop more robust differentiation protocols (Höpfl et al., 2004). In addition to being a complex process, the options and morphogen combinations used for the differentiation of EBs towards specific cell populations are wide ranging; it would be impractical to test many in this project. Simple directed differentiation studies such as these allow for confirmation of the ability to form germ layer specific structures, while allowing for future users to undertake more specific differentiation studies as required.

Prolonged culture of these differentiated samples resulted in increased complexity of the structures which formed, as well as increased variability and divergence away from the intended differentiation outcome. The ectoderm sample in particular showed a complex differentiated epidermal structure which was significantly more mature than the tissue disc from 14 days. Mesoderm tissue discs retained the significant amounts of connective tissues and smooth muscle, as well as simple epithelial surfaces. The tissue discs differentiated towards endoderm continued to show the formation of epithelial lumens, with some specialised epithelia. Tissue disc variability is again acknowledged as a product of the simple differentiation process used and is highlighted in particular by the immunostaining for protein markers. This phenomenon is especially prevalent in the mesoderm and endoderm samples. This could also be due to the length of time since the application of the morphogens, which would naturally lead to a reduction in their effects. This variability is also reflected in part in the gene expression data, with the increase in cytokeratin 10 expression in endodermal samples, increased brachyury in the ectoderm samples and increased alphafetoproein in mesodermal samples. The prolonged expression of early endodermal markers SOX17 and GATA6

may correlate with the absence of mature endodermal derivatives within these samples and within the previously observed spontaneously differentiated samples, such as specialised epithelia with multiple cell types or other endoderm tissues such as pancreas or liver tissues. This prolonged expression may reflect the maintenance of endodermal progenitor populations due to the increased time required for mature endodermal differentiation to occur.

6.6.3 Investigating lineage commitment in the ectoderm germ layer

The ability to broadly differentiate the tissue discs towards each germ layer was assessed in the previous experiment, but creation of specific cell populations from a single germ layer represents the ability to more subtly influence the differentiate of the tissue discs, something which more closely represents differentiation protocols used to study human tissue development.

The study on which the experiment was based used a murine stem cell line, but was completed on cells cultured using traditional cell culture methods (Li et al., 2015). The need to translate differentiation protocols from traditional two dimensional culture methods to more advanced culture methods has been recognised (Centeno et al., 2018; Meier et al., 2017), due to the fact that traditional methods are not representative of *in vivo* complexity and as such, data obtained from these studies may also not be representative of *in vivo* processes. Three dimensional differentiation protocols and study systems in particular represent a more physiologically relevant differentiation and maintenance environment. As the two main tissues derived from the ectoderm are distinct in nature, this provides a relatively simple system in which to test this, as well as offering the opportunity to direct the differentiation of the EBs and tissue discs towards more specific cell populations. Generally, similar results to that obtained in the previous study were found; differentiation generally shifted towards the intended outcome, with particularly accurate results for the neural and mesoendodermal differentiation observed in the histology. These results were observed at both the 14 day and 28 day time points, Epidermal differentiation was less successful in this study according to the histology, with those samples treated with the SB431542 + BMP-4 combination often displaying a heterogeneous tissue disc phenotype with little obvious epidermal differentiation. This could be due to the use of the three dimensional EB culture method during the differentiation stage, as growth factor concentrations have been shown to vary in EB structures (Van Winkle et al., 2012), a phenomenon which would be less likely in the original monolayer culture study, and would result in differential morphogen influences within the developing EB. This is turn would result in a heterogeneous tissue disc structure, as observed.

Gene expression data for the study confirms the neural nature of the SB431542 tissue discs at both 14 and 28 days, which is strongly confirmed by immunostaining and Western blotting data also. The mesoendoderm differentiated tissues discs also display an expression profile as would be hypothesised at the 14 day time point: absence or low expression of ectoderm specific genes and proteins cytokeratins 10, 14 and Class III β-tubulin, and modestly increased expression of some endoderm genes such as E-cadherin, alphafetoprotein and GATA6, by comparison. The analysis of

gene expression in the SB431542 + BMP-4 treated samples, intended for epidermal differentiation, does reflect the heterogeneity observed in the histology of the tissue discs. While a modestly increased expression of cytokeratin 10 is identified, increases in the expression of brachyury and FOXA2 are also observed, as is the expression of the proteins cytokeratin 10 and Class III β-tubulin. Increased variability in gene expression can be observed at the later time point in all three treated samples, possibly replicating the same effect observed in the germ layer differentiation study, that increasing tissue disc variability is observed as the time since morphogen application increases. This is in contrast to the original paper, which saw strong differentiation of each cell population with highly supportive and specific gene expression data. This experiment has shown however, that a level of more subtle differentiation can be achieved within this culture system, with relative success in the transition of the protocol.

6.6.4 The effects of fibroblasts on murine tissue disc formation and differentiation

This Chapter also focussed on the incorporation of the murine PSCs into the two more physiologically representative models developed in Chapter 5. These models were developed due to the importance of the myriad physical and chemical cues that contribute to the *in vivo* microenvironment but which are currently not fully recapitulated in *in vitro* study systems.

The final version of the co-culture model from Chapter 5 including SCID mouse fibroblasts was employed again here for co-culture with CGR8 murine EBs. This SCID model was created to represent the teratoma assay microenvironment, and while the teratoma assay is not the most stringent manner of assessing developmental potency in murine stem cell populations (Aoi, 2016) (and thus this specific co-culture study could be viewed by some to be redundant), the co-culture of murine EBs on the fibroblast compartment can still offer valuable insights into the effects of resident host cell populations on the spontaneous differentiation of pluripotent stem cells in *in vitro* model which recapitulates some aspects of the teratoma assay. Brief optimisation confirmed the viability and phenotype of fibroblasts cultured in the murine PSC media, allowing for the study to take place. The results obtained from this culture system were not as expected. The use of fibroblasts in conjunction with TERA2.cl.SP12 tissue discs in Chapter 5 resulted in the enhancement of pluripotency within the tissue disc structures, which were generally well maintained in the co-culture situation, showing some small reductions in size and differentiation. The culture of CGR8 tissue discs with the SCID fibroblast compartment resulted in a highly homogenous reduced tissue disc morphology, with no recognisable tissue structures within the tissue disc. Immunostaining provided limited information as to the identity of the tissue disc structures, indicating the presence of some mesodermal and ectodermal populations. This phenotype was replicated at the 14 and 21 day time points; after 28 days culture on the fibroblast scaffold, the tissue disc structure was completely lost. This is in stark contrast to the data obtained using the TERA2.cl.SP12, and there may be a number of explanations regarding this cellular behaviour. The tumorigenic properties of TERA2.cl.SP12

cells as an embryonal carcinoma cell populations cannot be overlooked, and the data obtained from those co-culture experiments may be more representative of tumourigenic cell behaviour rather than pluripotent cell behaviour. The widespread reappearance of Oct 4 expression within these structures could be indicative of tumour stem cells rather than pluripotent stem cells, due to the tumorigenic origins and properties of EC cells (Andrews et al., 2005; Mueller et al., 2006; Sekiya et al., 1985). Additionally, co-culture is routinely used to facilitate the differentiation of PSCs towards specific cell populations. Thus, PSC culture on endometrial stromal cells results in their differentiation towards endometrium like cells (YU et al., 2015), co-culture with chondrocytes results in enhanced differentiation towards the chondrocyte lineage (Bigdeli et al., 2009) and the culture of human PSCs with human fetal gondal cells results in improved primordial germ cell differentiation (Park et al., 2009b), to name but only a few examples. The intended differentiation outcomes are directly connected to the co-culture populations used, therefore it is likely that a similar phenomenon could have occurred here, with the fibroblasts directing the differentiation of the murine EBs overwhelmingly towards a fibroblast related mesodermal lineage. The exact cell population cannot be determined using the histology and immunostaining performed here, with no obvious structures visible and the limited markers used, but it is interesting to note that the same phenotype is obtained when murine EBs are culture as tissue discs on HDFn dermal compartments, indicating that this is not a species specific interaction. Brief studies were performed to determine whether this effect was due to the topography of the fibroblasts providing mechanical cues or the influence of secreted factors using the SCID fibroblast model. Fibroblasts are known to secrete a wide range of cytokines to influence epidermal differentiation and proliferation as well as wound healing; these include basic Fibroblast growth factor, which has roles in the pluripotency of human PSCs as mentioned previously, and various other cytokines including Fibroblast growth factor 10, Hepatocyte growth factor and Parathyroid hormone related protein (Sorrell et al., 2007). The effects of the paracrine factors can be seen in Figure 6.53, with the reduced phenotype particularly prominent in these tissue discs at both time points, suggesting that the effects of paracrine factors play a key role in the adoption of the tissue disc morphology observed. Yet, the differences in the signalling pathways maintaining pluripotency in murine and human PSC populations means that it is unlikely that the activity of cytokines such as bFGF are acting on the structures in the manner proposed in the previous Chapter. It is likely that an alternative cytokine is exerting the strong influence on these cells, but without extensive analysis of the cytokines secreted by the fibroblasts and subsequent confirmation through the inhibition of activities of these, few definitive conclusions can be made. The importance of mechanical cues was also demonstrated, with the 14 day time point also showing a slightly reduced morphology when cultured on fixed fibroblast filled scaffolds. Fixed fibroblasts are sufficient to maintain some of the cellular cues delivered by live counterparts as shown in studies investigating the impact of fibroblasts on pluripotency (Huang et al., 2015; Ren et al., 2018; Yue et al., 2012), but in this case, it seems topographical cues alone are insufficient to prevent infiltration of the tissues discs into the scaffold, hinting at a more complex interaction between the fibroblasts and embryoid bodies.

6.6.5 Enhancing the PSC microenvironment using perfusion culture

The novel perfusion system was the final version of this *in vitro* model which was tested using murine PSCs. The introduction of this property to *in vitro* cultures improves the microenvironment in a number of ways, including improving the nutrient and oxygen supply through the prevention of unstirred layers, the prevention of metabolite accumulation and the provision of mechanical cues.

The perfused system required much optimisation in the previous Chapter, and while the inclusion of Matrigel resulted in the ability to maintain pluripotent regions and the two ectoderm tissue phenotypes, neural and epidermal, the decision was made to proceed to use the final optimised culture set up with the CGR8s, with no Matrigel and no second insert. This culture set up provided the best results in terms of viability compared to static culture, and still showed the formation of a thick tissue disc and evidence of differentiation with some weak pluripotency staining. CGR8 cells were seeded onto the Alvetex® insert and cultured for 56 days in total in the system, in part to replicate the study conducted by Stachelsheid using human PSCs over 50 days, and in part to use the system as intended, as a method to maintain PSCs over a longer time period to allow for more complex differentiation. It may be noted that the differentiation media was changed from a GMEM media to a DMEM media. In addition to defined media, Stachelscheid also used a DMEM/FBS media in the hESC perfused study to better represent the nutrient rich environment of the teratoma microenvironment in the host (Stachelscheid et al., 2013), so this was undertaken in this study. Interestingly, this media was unsuccessful in generating differentiated structures in Stachelscheid's study, but the opposite was true here. (This appeared to be due to the differences in the pluripotency maintenance pathways in hESCs, as Stachelsheid attributes this to the secretion of Activin A by feeder like cells which differentiated in the bioreactor early in the culture period. The LIF system which maintains pluripotency in murine PSC populations naturally prevents this phenomenon from occurring in this study.) The resultant structures were far larger and more complex than any of the tissue discs previously analysed in this Chapter, with a highly varied morphology and diverse tissue structures which more closely resembled a teratoma. There were no clear issues with tissue disc viability, and in addition, structures and tissues which had not previously been observed within tissue discs were noted, including epithelia with multiple cell types and bone; similar features were also identified in Stachelscheid's study. The effects of this system were confirmed by the simplicity of the tissue disc which formed in static conditions in the same DMEM based media, confirming the effects of perfusion on the differentiation which occurred. The overall improvements in the differentiated structures which formed aligned with the data obtained by Stachelsheid and Gerlach in particular regarding the use of perfused systems to create tertaoma like tissues *in vitro*. Tissue constructs from each of the germ layers showed increased maturity and complexity, indicating the impact and benefits of introducing properties such as fluid flow to *in vitro* culture systems. The absence of Oct 4 staining in the perfused structure is in contrast to the TERA2.cl.SP12 system, where pluripotent cells were

maintained, and may again be due to their tumorigenic nature and propensity contain embryonal carcinoma regions within developing teratomas (or rather teratocarcinomas). This experiment in particular highlights the impact of introducing this property to three dimensional culture systems, but more studies must be undertaken to better understand the direction of differentiation on the incorporation of this property, and the minimum time for complex structures such as these to form.

6.7 Conclusion

The use of murine PSCs in this novel *in vitro* model has revealed a variety of features, strengths and weaknesses in the protocol and differentiated structures which can be maintained on the polystyrene scaffold.

The long term culture of murine EB derived tissue discs was proven possible, and the ability of these to form more complex tissue structures than time matched EBs was clear after only 14 days culture on the scaffold. The ability to maintain these tissue discs for up to 35 days provides the opportunity to study long term differentiation and potentially use the model to test the developmental potency of cells, although when allowed to spontaneously differentiate, the structures which form within the tissue disc may not be clearly recognisable. Further analysis using immunostaining methods did allow for the identification of structures from the three germ layers. The differentiation of EBs towards specific germ layers and specific cell populations is also possible within the model, as the application of morphogens during the EB formation stage generally resulted in tissue discs which differentiated towards the intended outcome. There was a level of variability in the differentiation which occurred within the tissue disc populations, which is most likely due to the simplicity of the protocols used, the differences in growth factor interactions in EB based differentiation systems and the length of time the differentiated tissue discs were maintained for on the scaffold. This work is preliminary in nature, but does outline the ability to successfully direct the differentiation of EBs towards a number of differentiated phenotypes and maintain these in the model for further study. More complex protocols would be required in order to improve differentiation specificity and yield of the tissue discs cultured on the scaffold.

The introduction of murine EBs to the two more physiologically relevant versions of the model resulted in contrasting outcomes. The co-culture of murine EB derived tissue discs on SCID fibroblasts resulted overall in a reduced phenotype, with no recognisable or complex structures. This was maintained over all time points, with eventual loss of the tissue disc structure. Interestingly, this was also replicated following culture on the HDFn dermal model, indicating that the interactions occurring are not simply species specific, but indicate a more general differentiation phenomenon is occurring through interactions between the fibroblasts and EBs. Further experiments provided some preliminary clarity as to the effects of the fibroblasts, with a combination of paracrine and topographical cues contributing to the tissue disc phenotype, but this ideally needs much more investigation to elucidate both the differentiated nature of the tissue disc and the signalling pathways involved in this. The culture of CGR8 cells in the novel perfusion system resulted in significant enhancement of the differentiated phenotype, with an increased tissue diversity and increased structural complexity in the tissues derived from all three germ layers, in line with studies from the literature. This system also allowed for long term culture surpassing the previous time points used in static, providing a culture option which is highly similar to the microenvironment of the developing teratoma and allows for cells to be maintained for similar time frames.

The use of murine PSCs in this novel scaffold based model has demonstrated the successful culture and differentiation of tissue discs derived from true PSC populations, and demonstrated the ability to differentiate these using exogenous morphogen modulation. The introduction of more microenvironmental cues showed that while co-culture was logistically feasible but led to a diminished tissue disc differentiation the use of a perfused system in the culture of these cells resulted in the formation of tissue structures highly similar to teratoma tissues. Following this validation step using murine PSCs, further model validation needs to be undertaken through direct comparison to teratomas derived from the same cell population, and through the incorporation of other human pluripotent stem cell populations.

7. Further validation and application of the *in vitro* model using the teratoma assay and human pluripotent stem cell populations

7.1 Introduction

The previous Chapters in this thesis have focussed on the development and optimisation of this novel technology to enhance the differentiation of tissue structures from PSCs; further validation steps are now required. The teratoma xenograft assay represents the most complex and mature differentiation that can be achieved using human pluripotent stem cells, providing a suitable sample against which to compare the structures formed in the tissue disc model. If these structures are comparable in complexity, this model provides an opportunity to standardise the characterisation of human PSCs, which does not utilise animals and is more controllable. Finally, the ultimate intended application of the model is the culture of human pluripotent stem cells derived tissue discs, therefore the culture of these stem cell populations also needs to be undertaken to confirm the usability of the model.

7.1.1 Standardising the culture of human pluripotent stem cells and the assessment of cellular pluripotency

Human embryonic stem cell lines have now been available as resource for around 20 years, yet there still remain a number of challenges surrounding the use of human pluripotent cell populations experimentally. Natural variation between pluripotent stem cell populations, differences in derivation methods and culture protocols and the difficulties in these techniques all lead to increasing variability between cell lines, which in turn can affect cellular pluripotency. This property in itself is complex, as discussed in Chapter 3, and so standardisation is needed at a number of points in the use and characterisation of human pluripotent stem cells, a concept which is well understood by the stem cell community. To add further complexity to this issue, the need for regular assessment of the pluripotency and developmental potency of PSCs following culture to assess whether cells have altered in response to passaging and routine culture is also noted, in order to ensure the high quality of PSCs and reproducibility is maintained (Asprer and Lakshmipathy, 2015).

Much progress has been made in the standardisation of PSC culture practices, in addition to the development of feeder free culture systems as discussed in the previous Chapter. The International Stem Cell Banking Initiative (ISCBI) supports those involved in the banking and provision of human PSC populations for study, and has implemented a number of strategies to improve stem cell acquisition and distribution, increasing clarity/access to information and setting minimum operating criteria for stem cell banks as well as providing the ethical and operational framework for the use of clinical grade human PSCs (Crook et al., 2010). There are a number of challenges in the banking of human PSCs, particularly as many countries operate according to slightly different regulatory guidelines, which affect donation, processing, preservation and the use of the cells in clinical

treatments (Isasi and Knoppers, 2011). The largest stem cell registry is the European Human Pluripotent Stem Cell Registry, known as hPSCreg and with an online database at hpscreg.eu, works in collaboration with a number of these stem cell banks, and therefore the ISCBI, and holds data for thousands of hES and hiPS cell populations, providing information on the provenance of these cell lines (Isasi et al., 2019); the submission of human PSC characterisation data to the site is required before cells may be used in European Commission funded studies (Kim et al., 2017). The site itself is funded by the European Commission and provides comprehensive data regarding pluripotency assessment, original source, genetic variation and alternative cell line names. Recommendations have been made by the ISCBI to adopt formal nomenclature systems for hPSC populations to reduce confusion and set standards for the minimum data required for novel hPSC lines. Additional plans include increased testing to monitor hPSC genetic variability, and separate testing for iPSC populations and their derived products prior to clinical use to ensure product safety and that full terminal differentiation has been achieved (Kim et al., 2017).

The International Stem Cell Initiative (ISCI) is a multinational expert panel which has undertaken a large scale multistage plan to characterise and standardise various aspects of the human PSC culture and characterisation processes. Initial work focussed on the identification of key markers of the pluripotent state, including surface antigens and genes, as well as identifying the levels of natural variation within human embryonic stem cell lines (International Stem Cell Initiative et al., 2007). This has allowed for the identification of common markers which are utilised to assess and confirm the pluripotent phenotype, leading to standardisation in the area of pluripotency assessment also. The identification of key criteria for the characterisation of the pluripotent state and the assessment of developmental potency of human pluripotent stem cell lines is critical to their use in both models of development and clinical applications. This is in addition to continually monitoring the variation and safety of PSCs for clinical applications through the organisation of meetings and workshops (Andrews et al., 2017). Guidelines such as these can provide a number of benefits, including quality and safety assurance and potentially allow for the development of more successful differentiation protocols and culture technique, as well as providing a more thorough understanding of the specific properties of specific human pluripotent stem cell lines.

7.1.2 Standardising the assessment of developmental potency

Much effort has been put into the standardisation of culture practices and banking, particularly in the areas of ethics and provenance, and so the standardisation of the assessment of pluripotency is also important, in order to follow through with this high quality work. In addition to the small scale studies discussed in Chapter 3, the ISCI has also conducted studies into the use of various techniques to assess developmental potency and the property of malignancy, including EB formation, the teratoma assay and the bioinformatics application PluriTest (International Stem Cell Initiative, 2018). The main conclusions of the report however, were that the method of assessment should be selected

dependent on the application of the cell population being tested, with more stringent methods such as the teratoma assay required for cells intended for clinical use due to the ability of the assay to assess malignant potential also. It could be considered that clinical therapy is the ultimate intended use of any human PSC population, and this advice, while cautious, provides less clarity, guidance and standardisation for the field. Naturally, the standardisation of culture techniques or processes which quantitatively assess pluripotency is a far simpler task than attempting to standardise a qualitative animal based assay which is performed under highly variable conditions from study to study. While the teratoma assay is considered to have value as a method for the assessment of the malignant as well as developmental potential of PSCs (International Stem Cell Initiative, 2018), culture practices are now highly advanced to allow for the formation of complex tissue structures in the *in vitro* setting, which provides a more controllable and reproducible method of use. The increasing number of iPSCs derived each year further supports the need for a high throughput method to assess this property and the study conducted in Chapter 3 highlighted that the teratoma assay is not performed routinely on these cell population, particularly in large scale derivation studies. Yet it is imperative that the developmental potency of iPSCs is thoroughly examined, and novel models of human development which can allow for the formation of more complex tissue structures could be utilised to assess iPSCs in a controlled and reproducible manner.

7.1.3 Confirming developmental potency using the teratoma assay

While the use of the teratoma assay as a method to assess the developmental potency is still under debate by both individual groups and bodies such as the ISCI, it is still currently the only 'gold standard' method for the assessment of this property. The data analysis conducted in Chapter 3 highlighted the variability of the assay protocol: there are no specific guidelines or consensus as to how the assay should be performed, but there is a general understanding that the tumour which forms from the implanted PSCs should contain derivatives from the three germ layers in order to confirm that a cell line is pluripotent (Aoi, 2016; Brivanlou et al., 2003; Müller et al., 2010b).

In terms of teratoma analysis, histological methods are highly favoured due to their simplicity and the speed with which the identification of tissue structures can be performed, with many researchers focussing on structures which can be definitively confirmed using this method to deem a novel cell line pluripotent, such as neuroepithelia, cartilage and epithelial surfaces (Aleckovic and Simón, 2008), see Figure 7.1 for examples. The identification of structures can be complicated by the fact that many may be embryonic or immature in nature, and as such, recommendations are that a histologist, pathologist or suitably trained individual should identify samples (Andrews et al., 2015). Antibody or chemical based staining methods for the identification of specific proteins can provide more comprehensive information regarding tissue identity and are often used in conjunction with histological analysis to confirm the presence of tissue structures from the three germ layers (Aleckovic and Simón, 2008; Przyborski, 2005). Histological stains in particular are useful due to

their specificity for staining tissue structures based on their physical and chemical properties, allowing for rapid and conclusive confirmation.

There is some anecdotal evidence of the use of PCR and Western blotting to analyse teratomas, but these methods are not widespread, most likely due to the labour intensive tissue processing steps required. TeratoScore is a bioinformatics based method which attempts to make this qualitative assay more quantitative. By comparing the RNA extracted from various teratomas to gene scorecards comprising of 100 tissue specific genes, including the three germ layers and extraembryonic tissues, the method is able to identify teratomas from other tissue specific tumours, the score values obtained were across a range, with there being no obvious explanation as to the differences (Avior et al., 2015). While applications such as TeratoScore can provide some level of standardised quantitative analysis, ultimately histological and antibody based staining methods are used to most commonly to assess teratoma structure and identity.

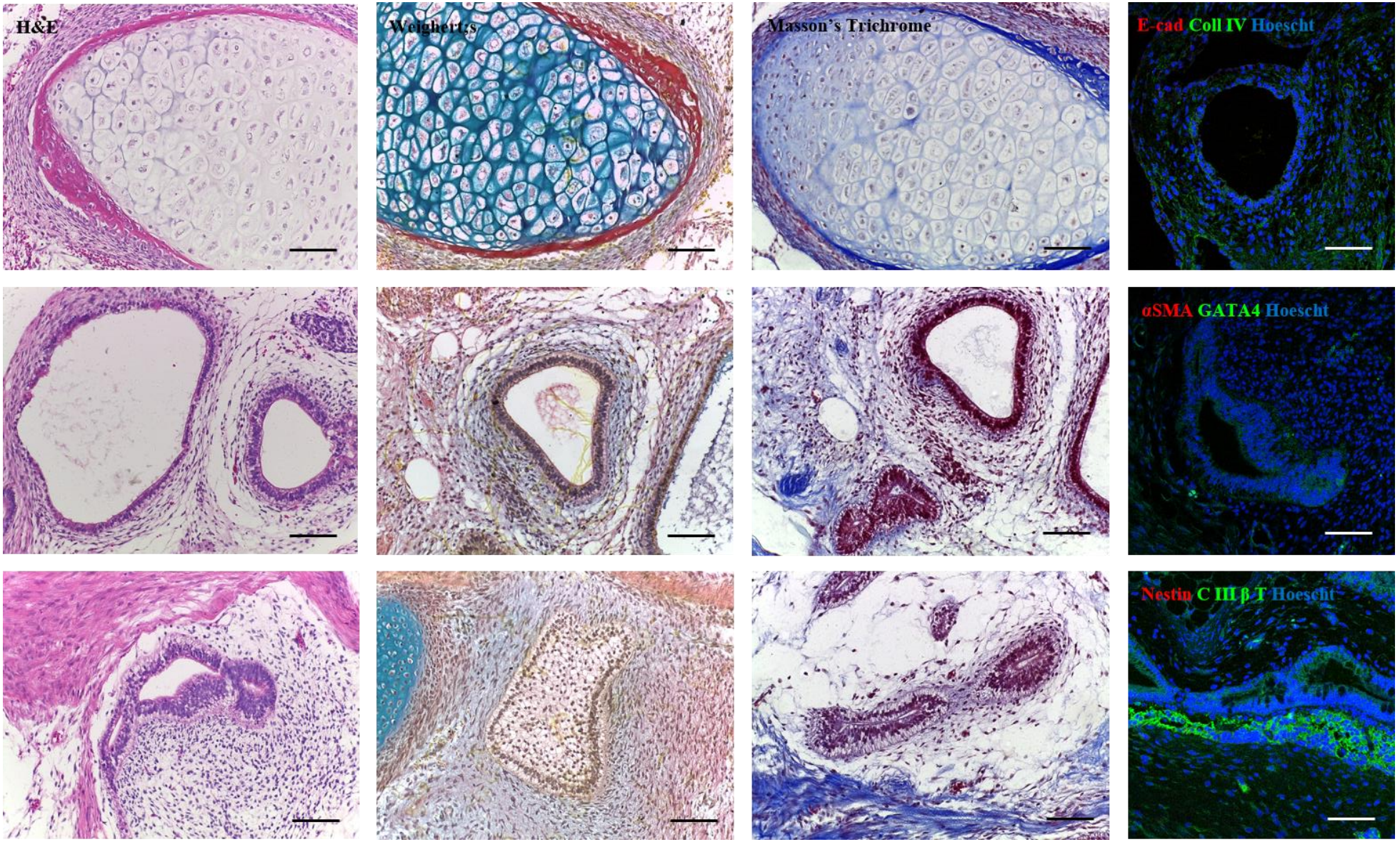


Figure 7.1: Histological and immunofluorescent characterisation of H9 teratomas using various tissue stains: Use of a variety of staining methods reveals the range of tissue structures in a typical human stem cell derived teratoma, with this example formed from H9 human embryonic stem cells. Structures from all three germ layers are visible, including cartilage, bone, neuroepithelia, epithelia, muscle fibres and connective tissues. Scale bars: 100 µm

7.1.4 Human pluripotent stem cells and models of human tissue development

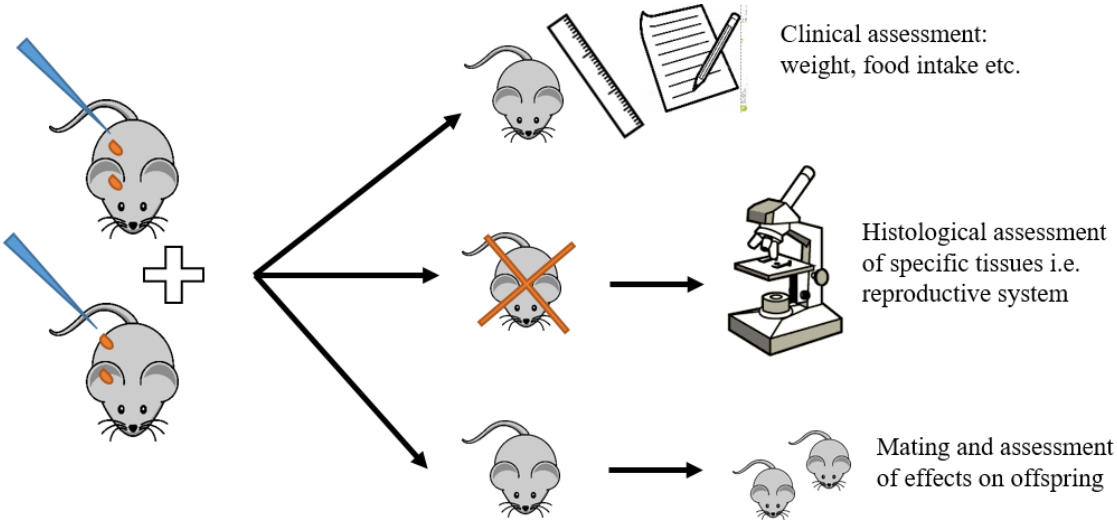
The requirement for a novel model for the study of human development has been addressed a number of times throughout this thesis in regard to a number of issues, with the limitations of current culture techniques and methods having been focussed on in particular. While the spatial limitations of traditional methods and viability issues associated with prolonged EB culture are certainly driving factors in the development of a novel model, the need and applications of the model extend far beyond the study of human development in isolation.

Toxicology is the study of the nature and effects of substances deemed poisonous or at poisonous concentrations on human health and biology, and embryonic toxicity tests deal specifically with the effects of toxic compounds on a developing foetus and the detection of teratogens – substances which are harmful to the developing foetus (Flamier et al., 2017). A variety of regulatory guidelines exist regarding specific testing which should be carried out to confirm product safety, including those provided by the World Health Organisation and the Organisation for Economic Cooperation and Development (OECD). While model organisms such as rodents can provide a wealth of data regarding the detrimental effects of specific compounds on developing tissues and have traditionally been used (Steele, 1991), differences in fundamental physiology, including developmental processes, gestation periods and the concentrations of compound required to induce toxicity mean that studies such as these are indicative rather than conclusive in nature. *In vitro* pluripotent stem cell models are highly valuable due to their human specificity and the ability to undertake high throughput analysis of multiple compounds simultaneously. Traditional culture methods are used due to their simplicity and ability to identify effects on fundamental biological processes. EB based models are popular due to the ability of the structures to recapitulate aspects of the early developmental process, ease of culture and ability to undertake multiple analyses, with many examples of each available in the literature (see Table).

Table 7.1. Current examples of human PSC based embryonic toxicity testing methods

Culture conditions	Measured parameters	Reference
EBs cultured in 24 well plates or suspension with compound of interest	EB growth, EB shape, gene expression of genes from each germ layer	(Flamier et al., 2017)
hESCs cultured in 96 well plates	Viability/cell death, colony attachment, oxygen stress markers	(Erceg et al., 2019)
hECs differentiated towards neural populations in 96 well plates.	Viability and ability to achieve neural differentiation, cell migration	(Stern et al., 2014)

Models which are able to replicate the later stages of the developmental process, particularly organogenesis, would provide further data regarding the effects of toxic compounds and potentially reduce animal testing during the later stages by screening out compounds which are toxic at this stage. Due to the need to undertake cross generation testing to ensure detrimental effects are not transmitted to offspring of those exposed to a particular compound (see Figure 7.2), *in vitro* models cannot replace animal models, but these can reduce the number of animals used for this area of research.



OECD guideline	Evaluation title	Brief overview
OECD 414	Prenatal developmental toxicity study	Provides information on the effects to the mother and the foetus. Continuous dosage of compound to the mother.
OECD 415	One generation reproduction toxicity study	Provides information on the effects on male and female reproductive performance. Dose of compound given to males and females, mating, compound given to females during gestation.
OECD 416	Two generation reproduction toxicity study	Provides information as per OECD 415 and on the growth and development of offspring, and is completed for two generations of offspring. (Parent, F1 and F2)
OECD 421	Reproduction/developmental toxicity screening test	Provides information regarding the effects on male and female reproductive systems. Doses of compound given up to 54 days and clinical and histological analysis performed.
OECD 422	Combined repeated dose toxicity study with the reproduction/developmental toxicity screening test	Provides information as per OECD 421, with animal mating.

Figure 7.2: OECD guidelines for the Testing of Chemicals: There are a number of specific guidelines for the testing of chemicals which are potentially harmful to human health, which cover effects on adult males and females and the developing foetus. Analyses cover a range of parameters, including clinical measurements, histological analysis of tissues and the assessment of the growth of subsequent offspring. Information summarised from the OECD Guidelines for the Testing of Chemicals, Section 4.

Embryonic and developmental toxicity testing represent a key application of novel models of human development, but these can also have crucial applications as an *in vitro* alternative to the teratoma assay.

7.1.5 Conclusions

Human pluripotent stem cells offer a unique opportunity to study the events involved in human tissue development in the *in vitro* setting, but the culture practices and characterisation methods surrounding these cells require standardisation. While progress has been made in the standardisation of routine culture and phenotypic characterisation, the assessment of developmental potency is still in need of improvement. The teratoma assay is the current gold standard method for the assessment of developmental potency in human PSCs, but this method is limited in a number of ways, as previously discussed. Analysis of teratomas is primarily through imaging based methods which allow for the rapid identification of germ layer structures in combination with antibody based staining methods, although some attempts have been made to standardise this process also. Novel models of human tissue development offer an opportunity to undertake complex differentiation *in vitro*, but ideally must be validated against the teratoma assay in order to ensure that the minimum criteria for confirming developmental potency are met. Successful development of models such as this can have applications in other areas involving the use of animal models, including embryonic toxicity testing of compounds, as well as the assessment of developmental potential in novel PSC populations.

7.2 Aims and Hypotheses

There are two aims in this Chapter: to validate the model against the current 'gold standard' method for assessing developmental potency and to use the intended test population, human pluripotent stem cells, to form tissue discs. In order to prove that the model has potential as an *in vitro* alternative to the teratoma assay, the version of the model which has been shown to result in the most complex differentiation – the original static version in which tissue discs form on Alvetex® Polaris – will be directly compared to teratomas formed from the same starting cell population. It is hypothesised that complex structures from all three germ layers will be detected in both the *in vitro* and *in vivo* samples, with the *in vitro* model showing the achievement of this in a reduced timeframe. The final part of this chapter will use human pluripotent stem cells within the model, with a view to the eventual use of the model to study the mechanisms underpinning human developmental processes. Undertaking a series of pilot studies using both embryonic and induced pluripotent stem cells, the aim of these experiments is to successfully form tissue discs on the scaffold, and analyse the differentiation which occurs. Given that this has previously been successful using an alternative format of the scaffold, it is hypothesised that the formation of tissue discs should again be possible, but with the retention of the entire differentiated structure.

7.3 Objectives

- Use the same single cell population to create teratomas and tissue disc samples using TERA2.cl.SP12 and CGR8 stem cell lines.
- Compare the differentiation which occurs in the two sample types, with the aim of detecting the three germ layers in each.
- Use human embryonic stem cell line H9 and human induced pluripotent stem cell line I18002 to create embryoid bodies for maintenance on the Alvetex® Polaris scaffold as tissue discs.

7.4 Materials and Methods

The routine maintenance of H9 and I18002 cells is detailed in the general Materials and Methods found in Chapter 2, as is the creation and seeding of embryoid bodies onto Alvetex® Polaris. The specific techniques used in this Chapter are described below.

7.4.1 Alkaline Phosphatase Staining

To assess cellular pluripotency, human pluripotent stem cells were stained to detect the expression of alkaline phosphatase using the StemAb Alkaline Phosphatase Staining Kit II (Reprocell Europe Ltd). Cells were seeded onto coverslips coated using the appropriate coating matrix at the correct ratio, and cultured in 12 well plates. Staining was completed according to the manufacturer's instructions. Briefly, culture medium was aspirated from the wells, and the coverslips washed in 0.05 % Tween 20 in PBS (PBST). 1 mL of Fix solution was added to each well and incubated for 2-5 minutes at room temperature. Coverslips were washed in PBST and 1 mL of staining solution added to the wells. Staining solution was made by combining 0.5 mL of solution A and 0.5 mL of solution B, incubating for two minutes, and adding 0.5 mL of solution C. Coverslips were incubated in the dark for 5-15 minutes, monitoring the cells for a colour change. Wells were washed in PBST twice to stop the reaction, before storage in PBST for imaging using a brightfield microscope.

7.4.2 Teratoma assay protocols: Cell maintenance and syringe loading

Cells were maintained in the culture conditions described in the Materials and Methods in Chapter 2, detached using the 0.25 % trypsin/ 2 mM EDTA method and the single cell suspension counted using the Trypan Blue Exclusion assay and a Haemocytometer. Cells were resuspended at a density of 5×10^5 cells per 100 µL. 100 µL of the cell suspension was combined with 100 µL of GFR Matrigel matrix maintained on ice and loaded into 1 mL syringes with 21G needles which had been cooled in the freezer prior to use. The loaded syringes were kept covered and on ice for transport to the animal house.

7.4.3 Teratoma assay protocols: Injection and animal maintenance

A single loaded syringe was injected subcutaneously into the flank of young male NOD SCID Gamma mice. 4 mice were injected for each culture condition, with the potential for 4 total tumours per condition. Animals were monitored during the growth period, being weighed on commencing the experiment, prior to injection and twice weekly to assess tumour growth, with tumour measurements also taken when the tumour was visible. Before the tumour reached 5 % of the total body weight of the mouse, the animal was sacrificed according to a Schedule 1 method and the

tumour surgically excised. All procedures were completed with permission and according to the guidelines of Newcastle University and the Home Office, UK.

7.4.4 Teratoma assay protocols: Tumour processing and sectioning

Following excision, tumour samples were fixed in 10 % Neutral Buffered Formalin for at least 12 hours at room temperature. Tumours were then washed in PBS twice for a total of 2 hours, before subsequent dehydration through a series of ethanols at room temperature. Samples were incubated in each ethanol solution for 2 hours as follows: 70 %, 80 %, 90 %, 95 %, 100 % and 100 % again. Samples were incubated in Histoclear II for 2 hours, before incubation in a 1:1 Histoclear II:liquid paraffin wax solution at 60°C overnight. The solution was replaced with 100 % liquid paraffin wax and incubated for 24 hours at 60°C, after which the wax was replaced and incubated for a further 24 hours. Tumours were embedded in Dispomoulds by submersion into a mould filled with liquid paraffin wax, and an embedding cassette placed on top. Wax blocks were left to set overnight, before sectioning using a Leica EG1120 Microtome at 6 µm and mounting onto SuperFrost microscope slides. Slides were stained using methods previously described.

7.5 Results

7.5.1 Histological and immunofluorescent analysis of TERA2.cl.SP12 teratomas and tissue disc samples

In order to test the claim that the *in vitro* model developed in this project can be used as an alternative method to test cellular pluripotency, a teratoma assay was conducted in parallel with the creation of tissue discs, all of which were seeded from the same starting cell population. This was first tested using the embryonal carcinoma cell line TERA2.cl.SP12, which has been used for much of the development and optimisation of the model. TERA2.cl.SP12 cells have been used previously to form teratomas (Knight, 2014), and so further success with this cell line was anticipated in the teratoma assay. While the assay was conducted in conjunction with another stem cell related project and therefore included cells which were cultured in both 2D and 3D conditions, as seen in the Appendix, for the purpose of this project only the tumours derived from cells cultured in 2D were analysed. The endpoint of the teratoma assay was defined as before the tumour reached 5 % of the entire body weight of the mouse. TERA2.cl.SP12 teratomas took between 20 and 30 days to form and of the 4 implantations carried out, all were successful, giving a final success rate of 100 %.

7.5.1.1 TERA2.cl.SP12 teratomas form successfully and show evidence of both differentiated teratoma and pluripotent embryonal carcinoma aspects

Histological analysis of serial sections as seen in Figure 7.3 shows that the tumours display a typical morphology as would be expected of teratoma derived from embryonal carcinoma cells. Examples of neural differentiation and epithelial differentiation are prominent, as are large areas of undifferentiated cells which represent the pluripotent embryonal carcinoma aspect of the tumour. Positive immunostaining for pluripotency marker Oct 4 confirms the identity of the undifferentiated cells while immunostaining the markers used previously with TERA2.cl.SP12, highlights the differentiated teratoma aspects of the tumour. As can be seen in Figure, teratoma display a mixed expression of these differentiation markers, showing areas of early neural differentiation via Nestin expression, mature neuronal differentiation through the expression of Class III β-tubulin and epithelial differentiation as highlighted by cytokeratin 8 expression.

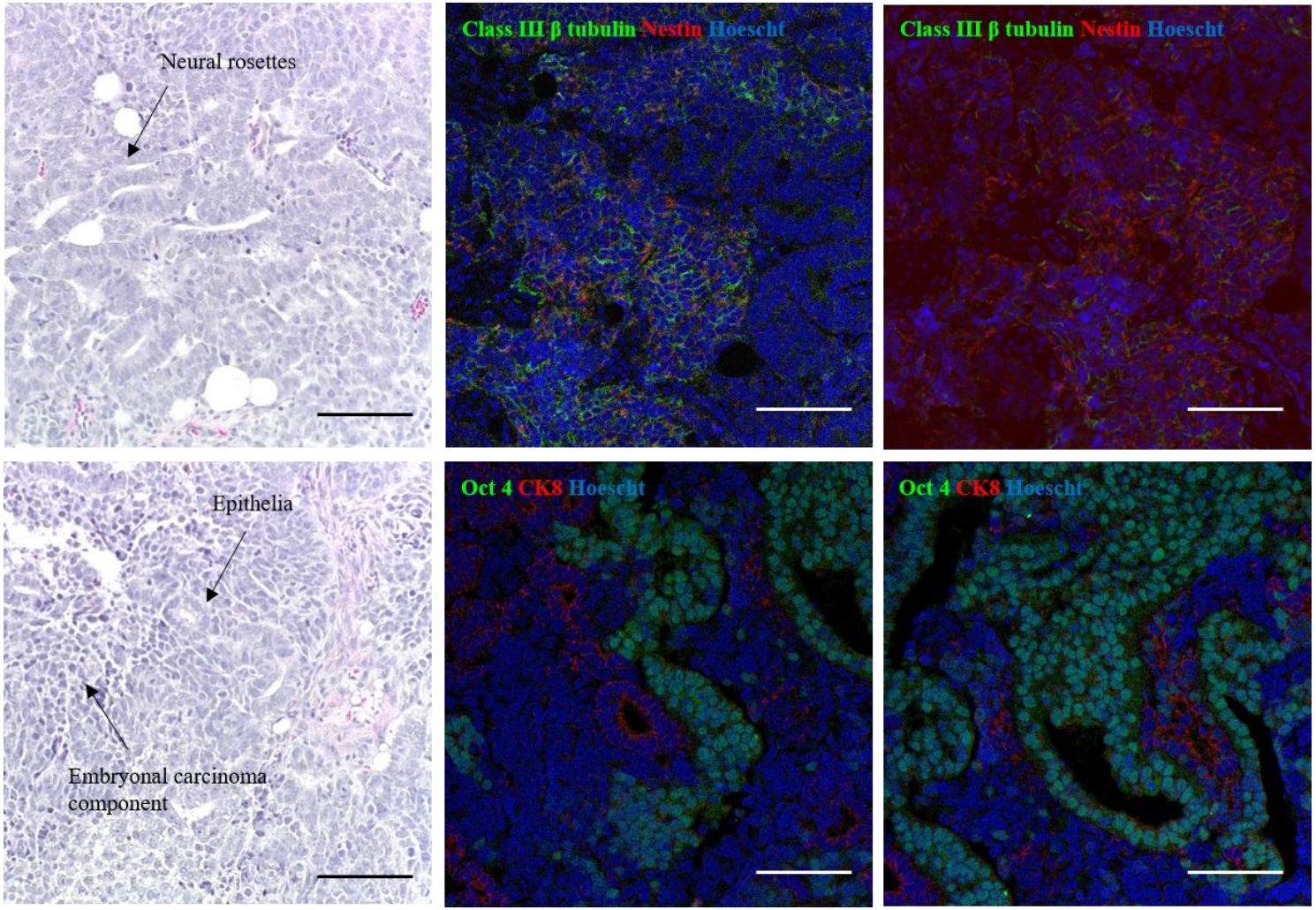


Figure 7.3: Characterisation of TERA2.cl.SP12 teratomas: 1 million TERA2.cl.SP12 cells were removed from traditional culture and combined with an equal volume of Matrigel before subcutaneous injection into a SCID mouse host. The resultant tumours show the formation of a variety of structures, particularly from the ectodermal germ layer including cytokeratin 8 positive epithelia, Nestin positive neural progenitors and Class III β-tubulin positive neurones. There is also evidence of the maintenance of an embryonal carcinoma cell population, which is Oct 4 positive. Representative images shown. Scale bars: 100 µm

7.5.1.2 TERA2.cl.SP12 tissue discs from the same population show a variety of differentiated and pluripotent features following prolonged culture

As stated above, the original version of the model, which was first described in Owens and further investigated in the prior Chapters in this thesis, involves the seeding of tissue discs onto Alvetex® Polaris, and was found to support the most complex differentiation within the tissue discs. Up to this point, TERA2.cl.SP12 tissue discs have only been cultured in the various different versions of the model for 7 days. As the teratoma assay can in extreme cases take up to 3 months for sufficient tumour formation to occur, the decision was made to culture the TERA2.cl.SP12 tissue discs for up to a maximum time of 8 weeks on the scaffold, dependent on the time taken for the tumours to form *in vivo*. This was based on previous work using this cell line by Knight, in which TERA2.cl.SP12 teratomas took around 6-8 weeks to form, and would allow for a direct comparison between the *in vitro* and *in vivo* samples.

Tissue discs were analysed every 14 days using histology and immunostaining on serial sections. As Figure 7.4 shows, after 14 days culture, the TERA2.cl.SP12 tissue disc which has formed resembles those which have previously been seen after only 7 days culture. These are some small areas of histological interest, such as the dense compact and loosely structured areas. It is noted that the tissue disc is fragmented in a similar way to those in Chapter 4; this is likely due to the phenotype and morphology. As the tissue disc only has small areas of differentiation, there are low levels of ECM deposition, resulting in some fragmentation. Immunostaining for pluripotency marker Oct 4 reveals a lack of expression, and therefore no embryonal carcinoma component. Cytokeratin 8 and Nestin expression are also lacking, indicating an absence of early neural and epithelial differentiation. Intermittent positive staining for differentiation marker Class III β-tubulin indicates the presence of some mature neural differentiation. The phenotype of the tissue disc is reduced in complexity and heterogeneity at this point in comparison to the teratoma samples.

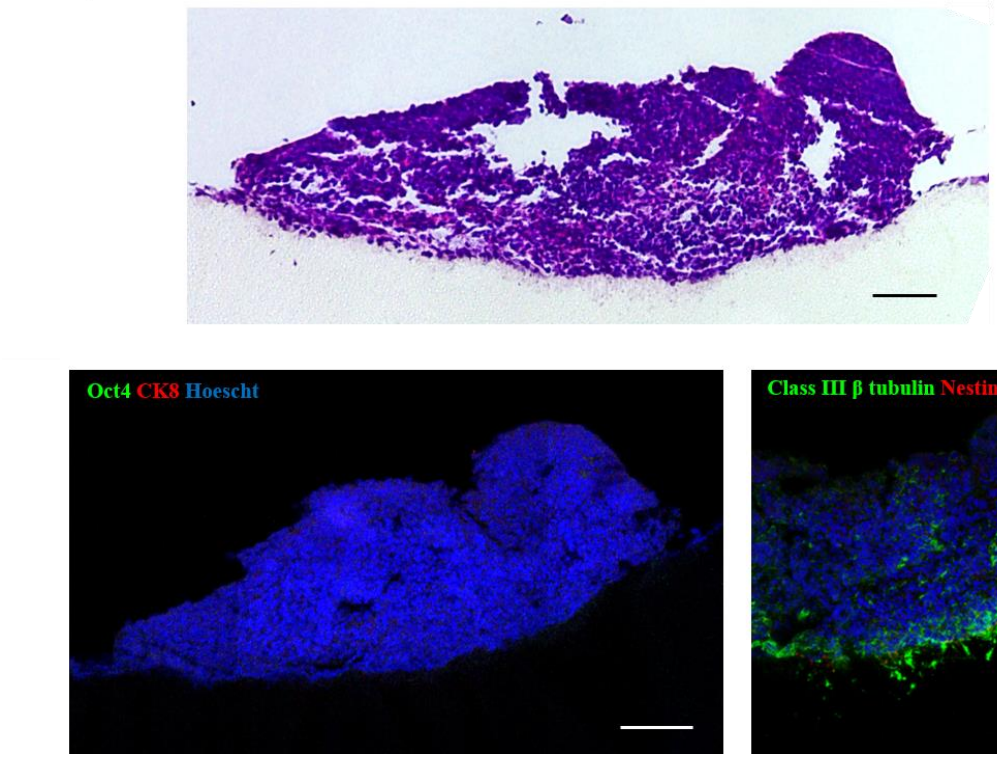


Figure 7.4: TERA2.cl.SP12 tissue discs formed from the same cell suspension show successful tissue disc formation after 14 days on the scaffold: At the same time TERA2.cl.SP12 cells were prepared for the teratoma assay, cells were seeded into Petri dishes to form aggregates, which were subsequently seeded onto Alvetex® Polaris as previously described. Tissue discs maintained for 14 days show no expression of pluripotency marker Oct 4, but show evidence of neural differentiation as shown by Class III β-tubulin staining. No evidence of epithelial differentiation is present, as staining for cytokeratin 8 is negative. Scale bars: 100 µm

Figure 7.5 shows a TERA2.cl.SP12 tissue disc cultured for 28 days, which is a more comparable time point given the range of time that the TERA2.cl.SP12 tumours took to form (for full details see Appendix). The tissue disc shown here is histologically more interesting than those previously allowed to spontaneously differentiate in the model, with the formation of a cavity, potentially cystic as seen in teratomas, and a rosette type differentiated structure. Low level Nestin expression is detected in the centre of the tissue disc via immunostaining, along with a more organised and strong expression of Class III β-tubulin in the structure. Cytokeratin 8 expression is negative again, as is the expression of Oct 4, ruling out any epithelial and pluripotent areas. This tissue disc compares to the teratoma in terms of the neural differentiation detected, both early and mature, although it does not appear to support the maintenance of embryonal carcinoma or epithelial populations as seen in the *in vivo* samples.

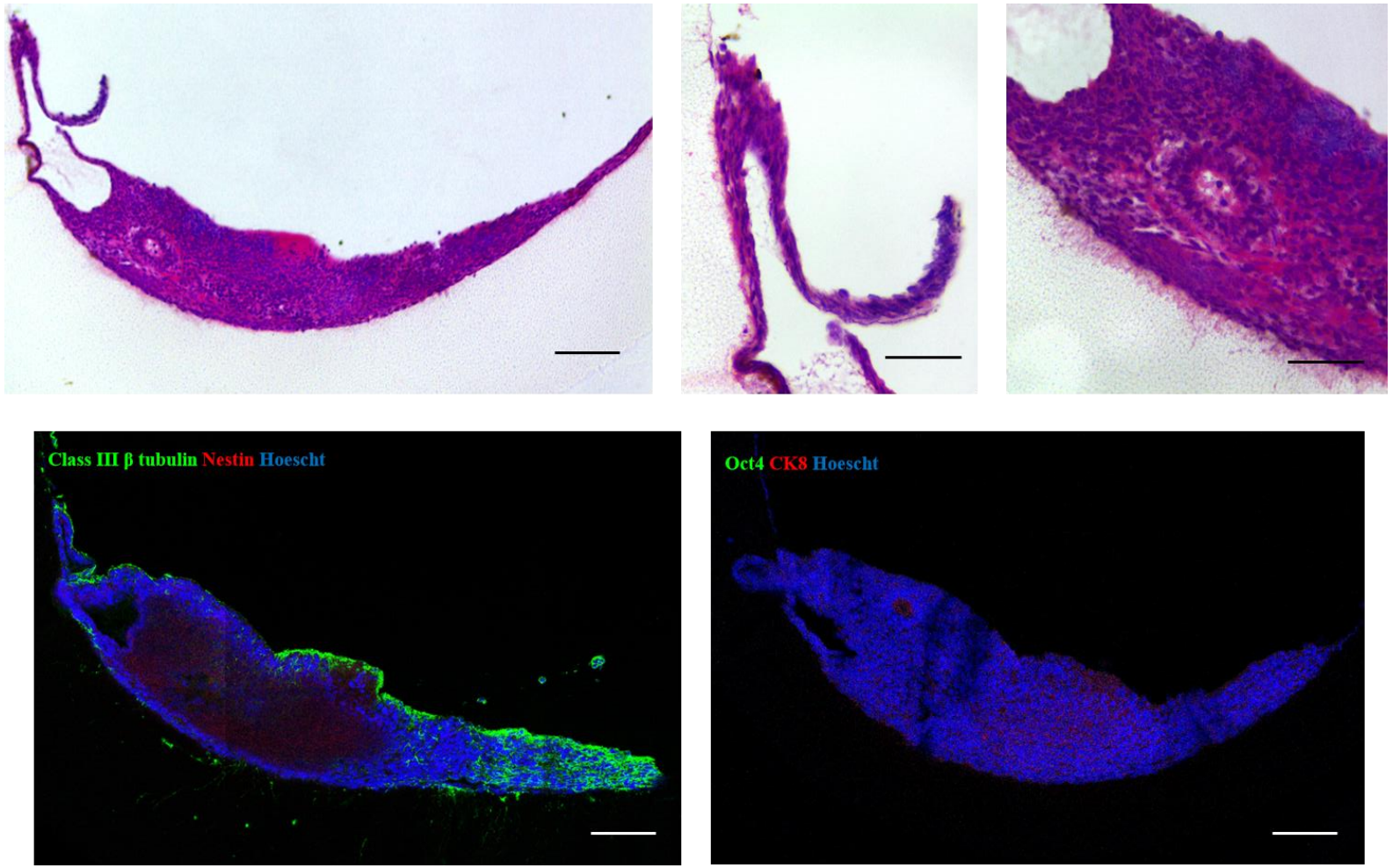


Figure 7.5: TERA2.cl.SP12 tissue discs formed from the same cell suspension show successful tissue disc formation with complex structures after 28 days on the scaffold: TERA2.cl.SP12 aggregates cultured for 28 days show more complex structure formation, including cystic cavities. The tissue disc shows expression of pan neuronal marker Class III β-tubulin, although there is no expression of pluripotency marker Oct 4 to indicate embryonal carcinoma cells or the epithelial marker cytokeratin 8. Scale bars: 100 µm

The final tissue discs were analysed after 42 days culture on the scaffold, due to the fact that all TERA2.cl.SP12 teratomas had been excised from the host mice at this point. H&E staining of the tissue disc as shown in Figure 7.6 shows that the structure that forms after this length of time remains viable, with no signs of cell death (this is noted due to the fact that this represents a growth period six times longer than previously undertaken with this cell line). Histologically, the tissue disc is highly heterogeneous, and again shows the formation of a cavity, as well as areas both dense and loose in terms of their composition. Immunostaining reveals a range of cellular identities. Of the neural differentiation markers, early marker Nestin is absent, with distinct well organised areas of mature marker Class III β-tubulin expression distributed throughout the structure. This highlights the neural differentiation which has been present in all TERA2.cl.SP12 tissue discs. Strong and organised expression of the epithelial marker cytokeratin 8 can also be detected in distinct areas throughout this tissue disc, demonstrating the presence of both ectoderm derived populations as detected in the TERA2.cl.SP12 teratoma samples. Notably, weak expression of the pluripotency marker Oct 4 can also be detected in a discrete area within the tissue disc, highlighting the presence of an embryonal carcinoma aspect to the tissue disc, which is also detected in the teratoma samples around this time point. The immunostaining pattern of the tissue disc suggests that it has now achieved a phenotype highly similar to that of the teratoma cultured in the *in vivo* environment.

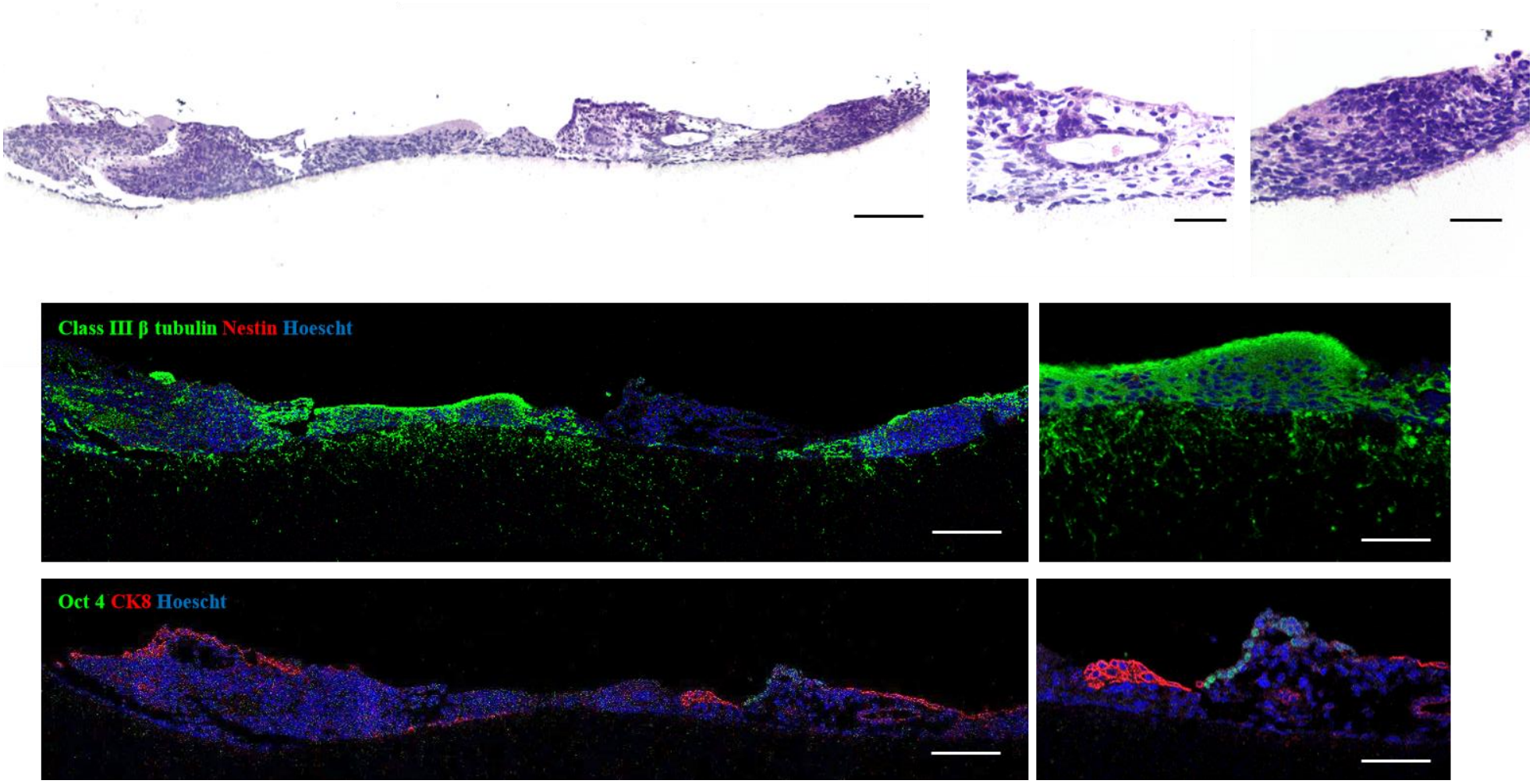


Figure 7.6: Analysis of TERA2.cl.SP12 tissue discs cultured for 42 days on the scaffold: TERA2.cl.SP12 aggregates allowed to form tissue discs over 42 days continue to show a more varied morphology, with various structures. Tissue disc shows expression of pan neuronal marker Class III β-tubulin, as well as positive expression of cytokeratin 8 in epithelial differentiated areas. Weak expression of Oct 4 can also be detected within the tissue disc. Scale bars: 200 µm, 100 µm and 50 µm

7.5.2 Histological and immunofluorescent analysis and comparison of CGR8 teratomas and tissue disc samples

As a murine embryonic stem cell line, the gold standard method of assessing the pluripotency of CGR8 stem cells would normally involve germline transmission or tetraploid complementation. However, as the aim of these experiments are to determine whether the developed model can be used as an alternative to the teratoma assay, CGR8 murine embryonic stem cells were also subject to a teratoma assay in parallel with the formation of CGR8 derived tissue discs, as created from the same cell suspension. The assay was carried out in conjunction with another stem cell related project again, involving the use of cells cultured in 2D and 3D conditions. As previously, only the tumours derived from cells cultured in 2D conditions were appropriate to be compared to the tissue discs which formed. The assay endpoint was determined in the same manner, prior to tumours reaching 5 % of total mouse body weight. CGR8 teratomas took between 9 and 15 days to form, and of the 4 implantations carried out, all were successful. This again gave a success rate of 100 %.

7.5.2.1 Analysis of CGR8 teratomas reveals a variety of structures derived from the three germ layers, and a consistency in their formation

Serial sections of CGR8 teratomas were assessed using a variety of histological methods, in order to identify the structure and tissues present within the teratoma tissues. Histology is used extensively in the assessment of PSC derived teratomas due to their simple nature and the ability to use protocols which preferentially stain for specific structures or tissue types. Haematoxylin and eosin (H&E) staining is a widely used general stain which is distinguishes between acidic and basic structures, and allows for the visualisation of the overall tissue structure. Figure 7.7 shows the initial H&E staining of representative sections of three CGR8 derived teratomas. It is clear that the tumours are highly diverse and heterogeneous in terms of the structures present, with a wide range of organised and complex tissues from each germ layer visible even after such a short timescale. Structures and tissues within the tumours include cartilage, bone, neural tissues, epithelial lined lumens, muscle and connective tissues. In particular, the images in Figure 7.7 highlight a level of consistency in the differentiation present between the tumours, with each displaying a similarly wide range of tissue structures.

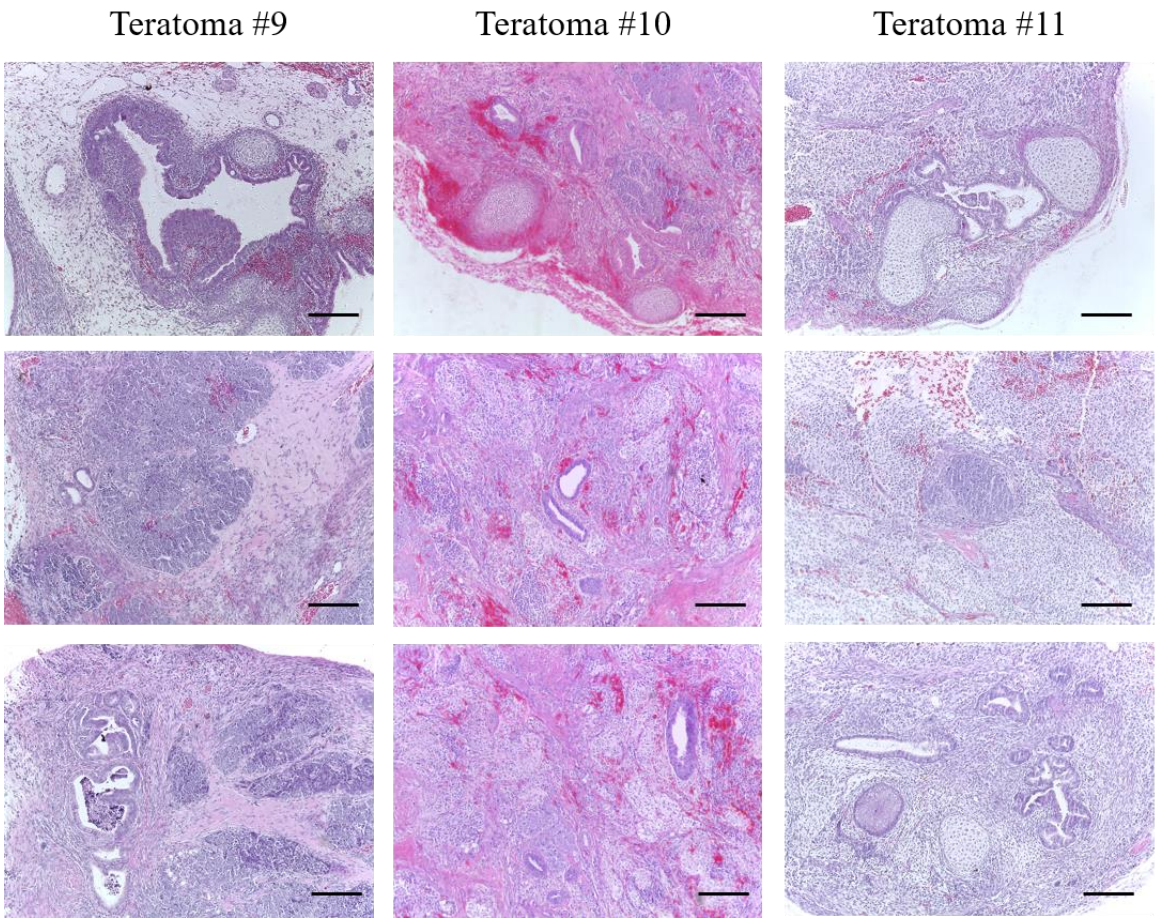


Figure 7.7: Histological characterisation of CGR8 teratomas using H&E: H&E staining of CGR8 teratomas reveals a variety of tissue structures from all three germ layers within these samples, confirming the developmental potency of the cell population. There is also a consistency in the differentiation which occurs within the tumours, indicating an element of reproducibility. Structures which can be observed are wide ranging and easily recognisable, and include epithelial lumens and cavities, specialised epithelia, cartilage, bone and neural tissues. Scale bars: 200 µm

Additional histological stains were used in order to identify structures from specific germ layers. Masson's trichrome was used to identify the tissue structures within the teratoma samples. This stain highlights the extracellular matrix rich tissue structures in blue, allowing for the identification of cartilage, bone and connective tissues, as can be seen in Figure 7.8. Using this stain, keratins and muscle fibres are stained red, although there are fewer of these structures visible within the tumours. Again, there is a consistency overall, with all of these tissues and structures detected in each tumour.

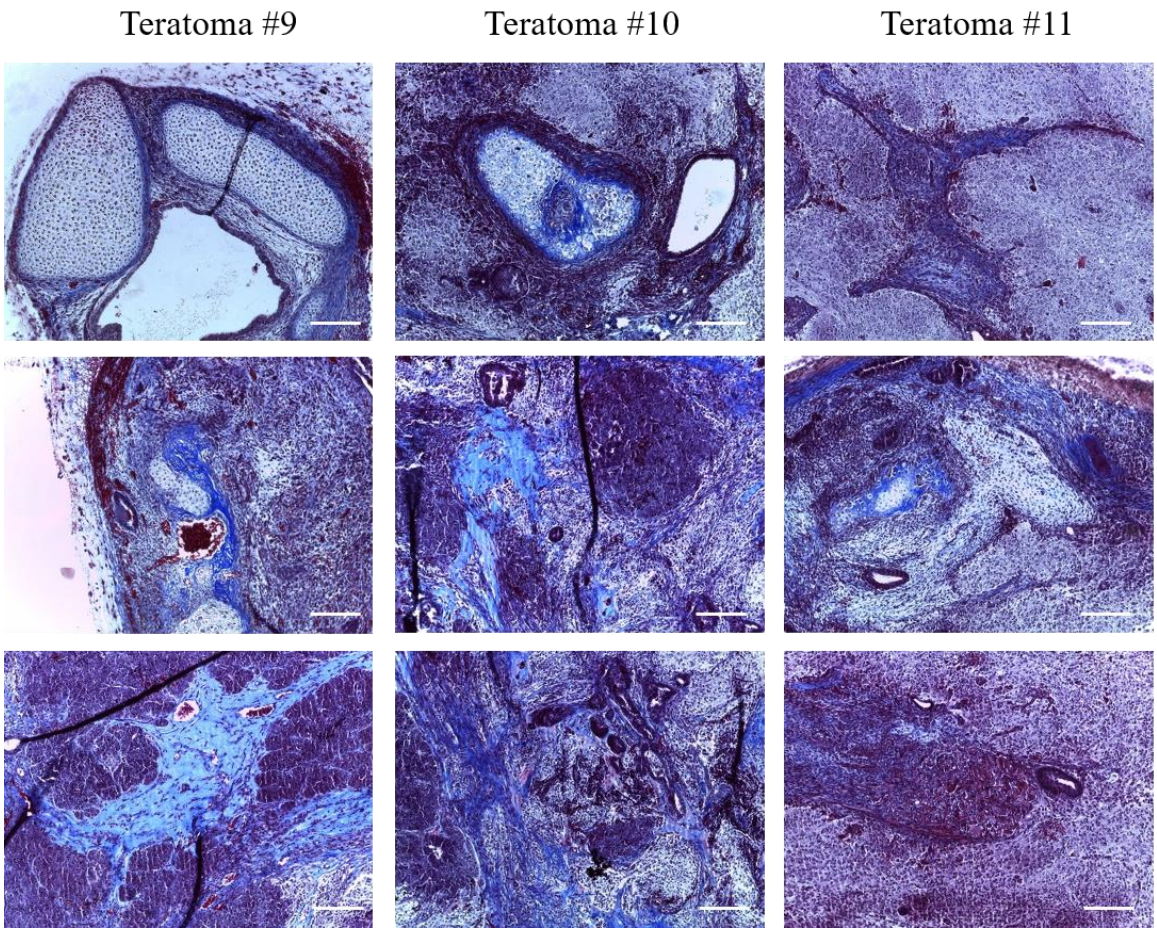


Figure 7.8: Histological characterisation of CGR8 teratoma using Masson's trichrome: Use of Masson's trichrome highlights the extracellular matrix rich areas of the teratoma, stained in blue. These include cartilage, bone and general connective tissue, and are found in all three teratoma samples. Muscle tissue and keratins are stained red, again indicating the presence of a wide variety of tissue structures derived from the three germ layers throughout the three teratoma samples. Scale bars: 200 µm

A third stain, Weighert's stain, was also used to assess the differentiated structures within the teratomas. Weighert's stain allows for more subtle analysis of the mesodermal structures within the teratomas, differentially staining bone and cartilage in red and blue respectively. These particularly complex structures are also present in all three teratoma samples, as can be seen in Figure 7.9, conforming the complexity of these samples and the consistency of the differentiation which occurred. This comprehensive histological analysis indicates their complexity and the presence of structures from all three germ layers.

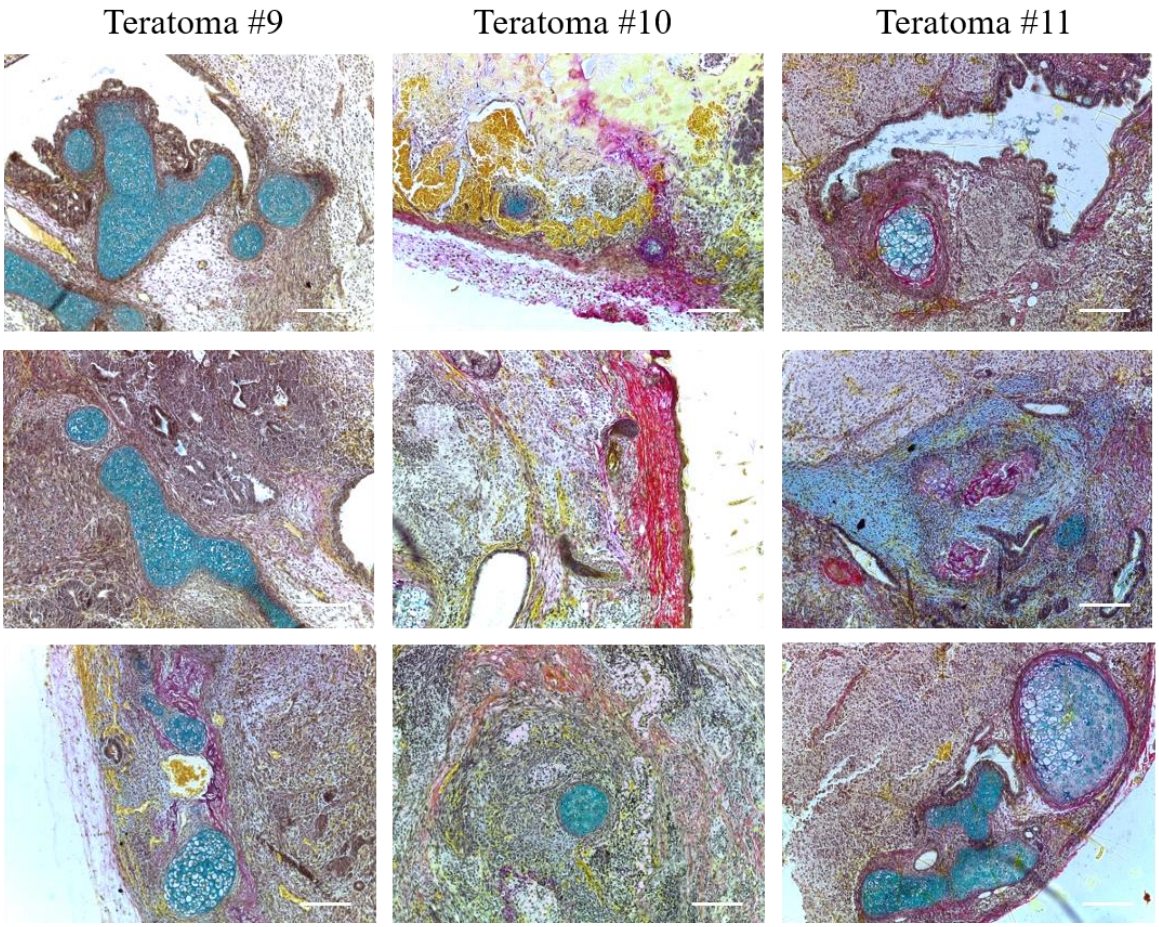


Figure 7.9: Histological characterisation of CGR8 teratoma using Weighert's stain: Weighert's staining highlights the development of bone in red, and cartilage in blue, allowing for confirmation of the presence of these tissue types. Again, all three teratoma samples show evidence of the formation of these tissue structures, indicating their complexity. Scale bars: 200 μm

In keeping with the identification of the structures present, immunostaining for a variety of germ layer markers also reveals the identity of these structures and confirms the expression of relevant proteins as well as appearing histologically identifiable. Structures from all three germ layers can be detected in the tumours. In Figure 7.10, CGR8 teratomas show the expression of ectodermal markers such as Class III β-tubulin indicating the presence of neural tissues, with very low levels of the neural progenitor marker Nestin. Mesodermal markers such as α smooth muscle actin indicate the presence of smooth muscle, whereas staining for the transcription factor GATA4 is absent. Endodermal markers such as E-cadherin and Collagen IV indicate the epithelial surfaces, their organisation and varied structures.

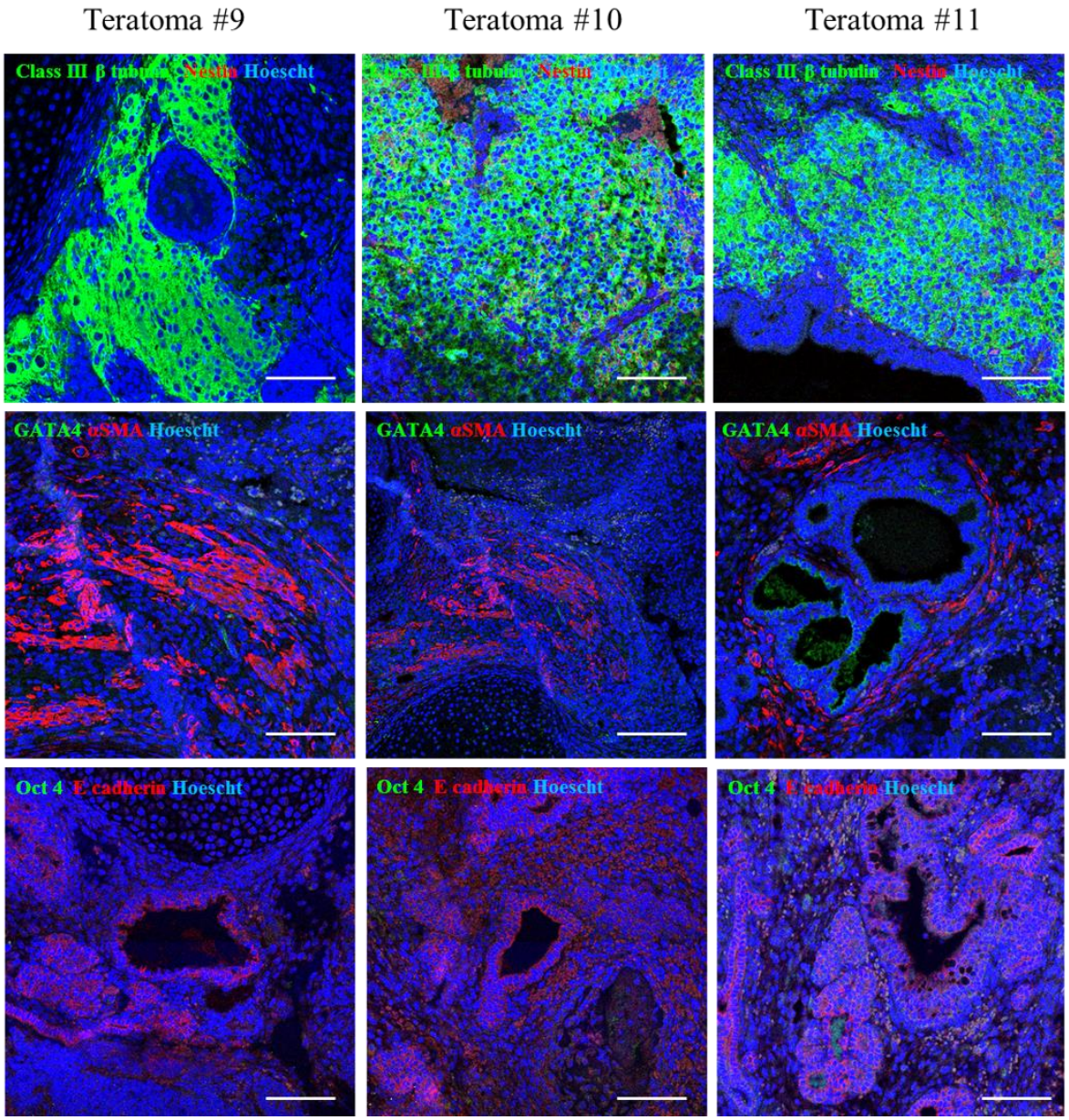


Figure 7.10: Immunofluorescent staining of CGR8 teratoma samples from markers from the three germ layers: Immunostaining for markers from all three germ layers confirms the identity of the tissue structures, and the markers chosen here include ectodermal markers E-cadherin, Nestin and Class III β-tubulin, mesodermal markers αSMA and GATA4 and endodermal markers E-cadherin. All three teratoma samples show positive staining for the markers, confirming their diversity. The pluripotency marker Oct 4 was also stained for, showing no expression in the tumours. Scale bars: 100 μm

7.5.2.2 Analysis of 14 and 28 day CGR8 tissue disc samples also shows a variety of structures and consistency in differentiation.

Archival examples of CGR8 teratomas were available prior to completing the teratoma assay, however no data was available regarding the manner in which the teratoma assay was performed. In particular, the length of time tumour formation would take could not be estimated, providing no guidance as to how long CGR8 tissue discs should be cultured for. In the same way as was completed for the TERA2.cl.SP12 teratomas, CGR8 tissue discs were to be cultured for a maximum of 56 days dependent on tumour formation, with analysis conducted every 14 days to allow for comparison with the tumour samples.

Following 14 days culture on the scaffold, CGR8 tissue discs derived from the same cell population also show highly complex structure formation. The examples of H&E stained tissue discs as shown in Figure 7.11 contain examples of organised epithelia of multiple types, stratified skin, and fibroblast rich connective tissue. Some consistency of differentiation exists between the tissue discs, with similarities in the formation of epithelia and cavities. The immunostaining in Figure 7.12 confirms the identity of the structures. Keratin 10 expression indicates epidermal differentiation and Class III β-tubulin indicated neural differentiation, ectoderm derived tissues, alpha smooth muscle actin and GATA4 expression indicate mesodermal differentiation, and E-cadherin/Collagen IV expression indicate organised epithelia of endodermal origin. Due to the unexpectedly rapid formation of the CGR8 teratomas after only around 11 days, this first time point of tissue discs is the most comparable. While the wide range and complexity of structures as seen in the teratomas is not exactly replicated, the presence of complex tissue structures from all three germ layers is confirmed. As the only criterion of the teratoma assay is the identification of tissue structures derived from all three germ layers, the tissue disc samples fulfil this criterion at roughly the same time point as the teratomas formed from the same initial cell population.

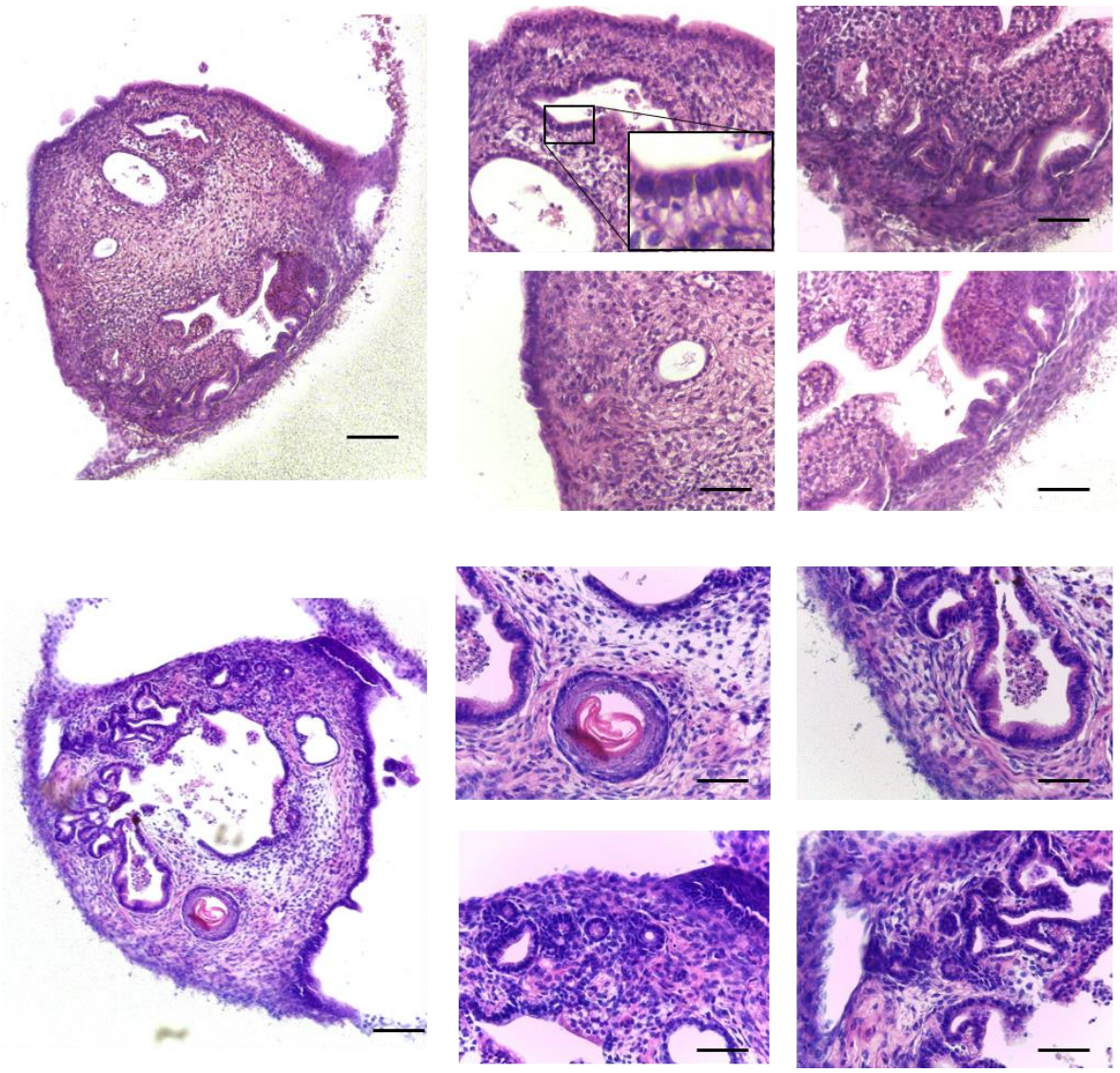


Figure 7.11: Histological analysis of CGR8 tissue disc samples cultured for 14 days using H&E staining: H&E highlights a variety of differentiated structures within the tissue disc sections which again show some consistency in the differentiation present. Structures include highly organised polarised epithelia, epithelia lined lumens and cavities, extensive connective tissues and mature epidermal differentiation, as well as possible rudimentary endodermal differentiation in the form of renal epithelia. Scale bars: 100 µm and 50 µm

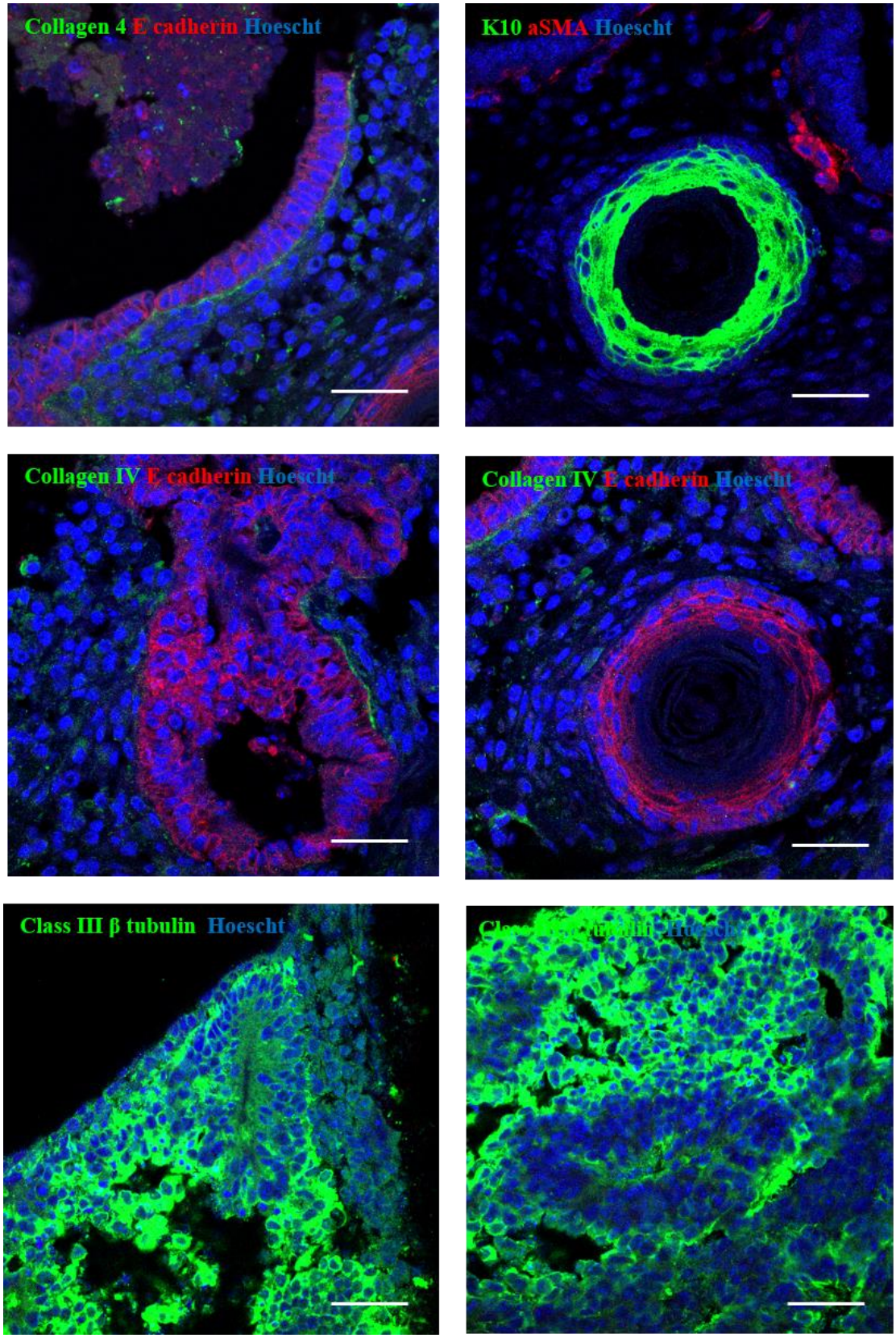


Figure 7.12: Immunofluorescent staining of 14 day CGR8 tissue discs for markers from the three germ layers: Staining of the tissue discs for a variety of germ layer markers confirms the identity the differentiated structures within the tissue disc, confirming the presence of structures from all three germ layers within the tissue discs. These include E-cadherin positive organised epithelia, keratin 10 positive epidermal structures, α smooth muscle actin positive cells and Class III β-tubulin positive neurones. Scale bars: 100 μm

Due to the rapid formation of the teratomas, the decision was made to continue to culture the CGR8 derived tissue discs in order to continue to assess the differentiation which occurred and to ascertain whether the tissue discs could realistically be maintained in culture as long as a typical teratoma assay and whether this impacted significantly on the structures which formed. After 28 days culture, the CGR8 tissue discs continue to show complex structure formation derived from the three germ layers. In the H&E stained images in Figure 7.13, a number of structures can be identified: stratified skin, muscle fibres and multiple different organised epithelial surfaces. There is a small amount of consistency in the differentiation identified between the tissue discs, in the form of muscle fibres, connective tissues and epithelial surfaces, although only one of the tissue discs displays conclusive histological evidence of structures from the three germ layers. As shown in Figure 7.14, immunostaining for various protein markers confirms the presence of structures from the three germ layers. These include α smooth muscle actin positive muscle fibres, small areas of Class III β-tubulin neural differentiation and E-cadherin positive epithelial markers with a defined Collagen IV basement membrane. Keratin 10 positive epidermal differentiation can also be observed. This time point also fulfils the criteria of the teratoma assay through the present of structures from the three germ layers.

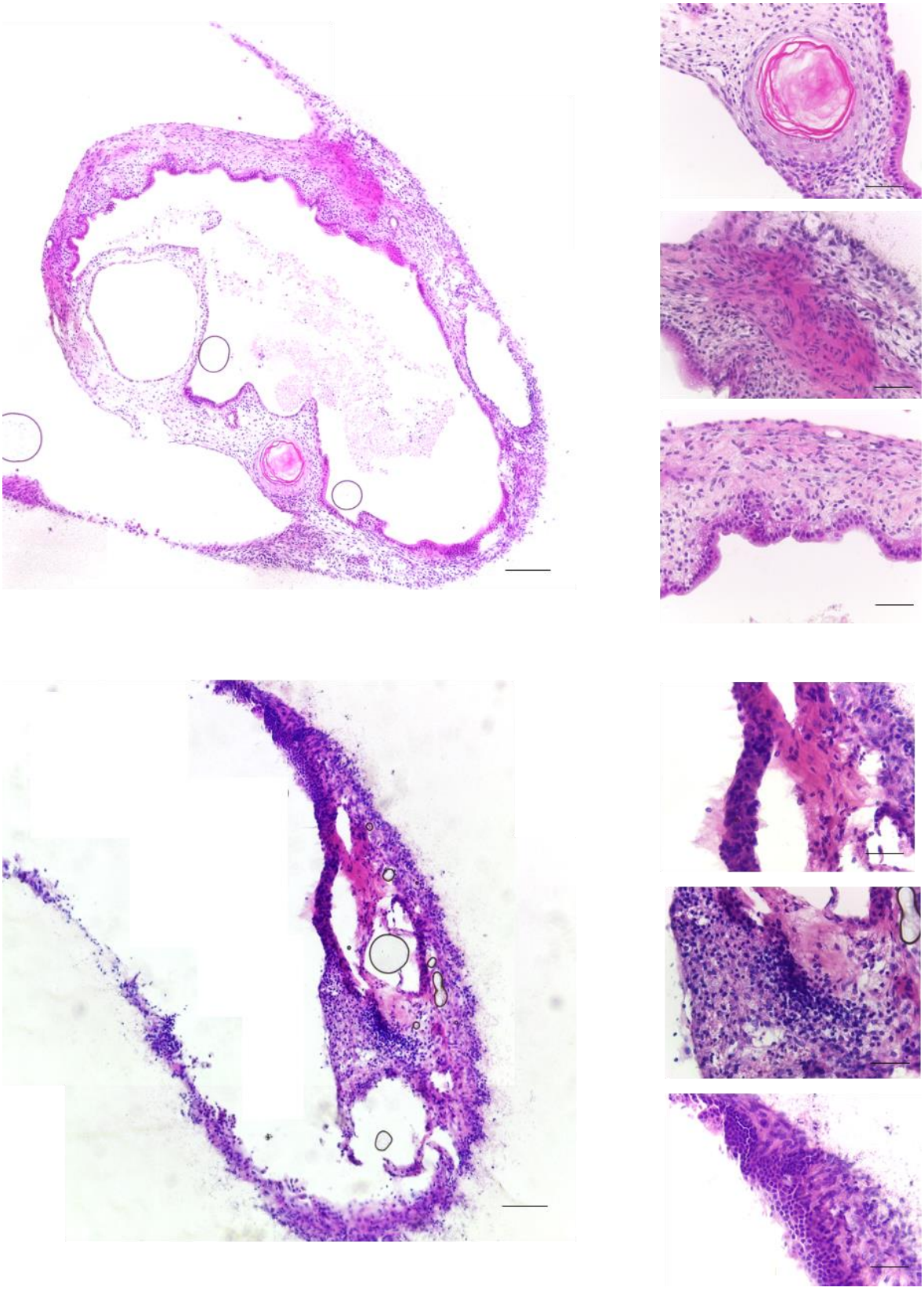


Figure 7.13: Histological analysis of CGR8 tissue disc samples cultured for 28 days using H&E staining: H&E highlights that after 28 days culture, tissues discs continue to show the development of a variety of complex structures derived from the three germ layers, including keratin pearls, aligned muscle fibres, epithelial cavities and lumens and highly organised specialised epithelial surfaces. Scale bars: 200 µm and 50 µm

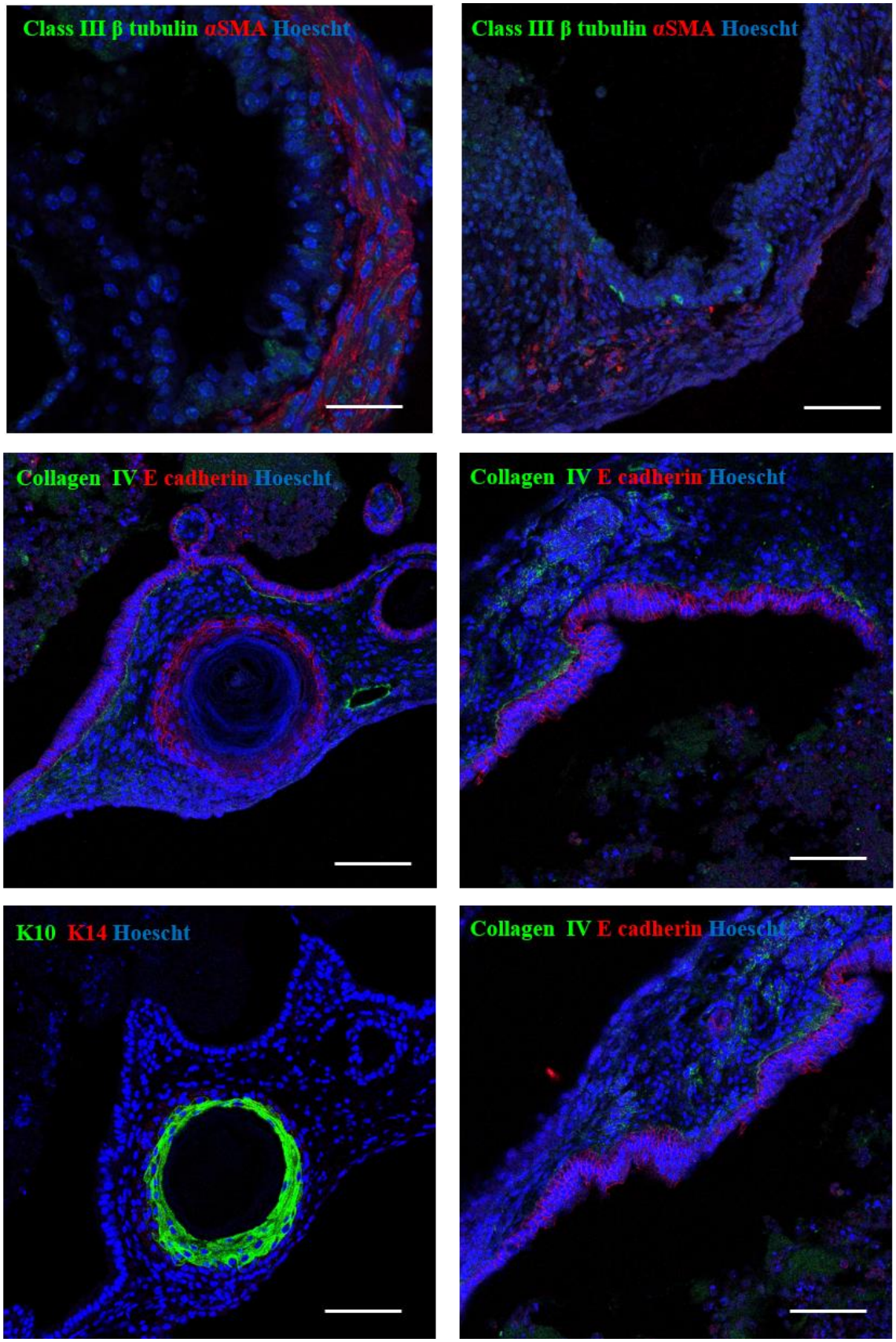


Figure 7.14: Immunofluorescent staining of 28 day CGR8 tissue discs for markers from the three germ layers: Staining of the tissue discs for a variety of germ layer markers confirms the identity the differentiated structures within the tissue disc, confirming the presence of structures from all three germ layers within the samples. These include E-cadherin positive epithelial surfaces, areas of smooth muscle, neurones and keratin 10 positive epidermal structures. Scale bars: 100 μm

7.5.2.3 Consistency and complexity of structure formation is maintained in tissue discs up to 56 days

The tissue discs analysed at the previous time points have already proven the ability of the model to produce recognisable structures derived from the three germ layers, although the decision was made previously to continue to culture the tissue discs up to a time point more representative of a typical teratoma assay length. Analysis of the tissue discs cultured for 42 days as shown in Figure 7.15 shows continued maintenance of the complex differentiation previously seen, with no major differences in the differentiated structures present, other than the possibility of cartilaginous differentiation and the fact that the tissue discs shown here contain no clear keratin pearls. Again, a range of tissue types are present, including connective tissue, muscle fibres, epithelial lines lumens and stratified epithelia resembling skin. Immunostaining as shown in Figure 7.16 confirms the identity of the structures used the markers previously stained for and indicates the germ layer each is derived from. A similar phenotype is observed after 56 days culture on the scaffold, with a similarity in the differentiated structures present within the CGR8 tissue disc, although differences in the gross overall structure. As seen in Figure 7.17, these include connective tissues, muscle fibres, epithelial structures, potential cartilage and neural tissues, displaying a consistency with those tissue discs analysed at previous time points. Immunofluorescent staining as shown in Figure 7.18 further confirms the identity of the structures within the tissue discs, as well as highlighting which germ layer each structure is derived from.

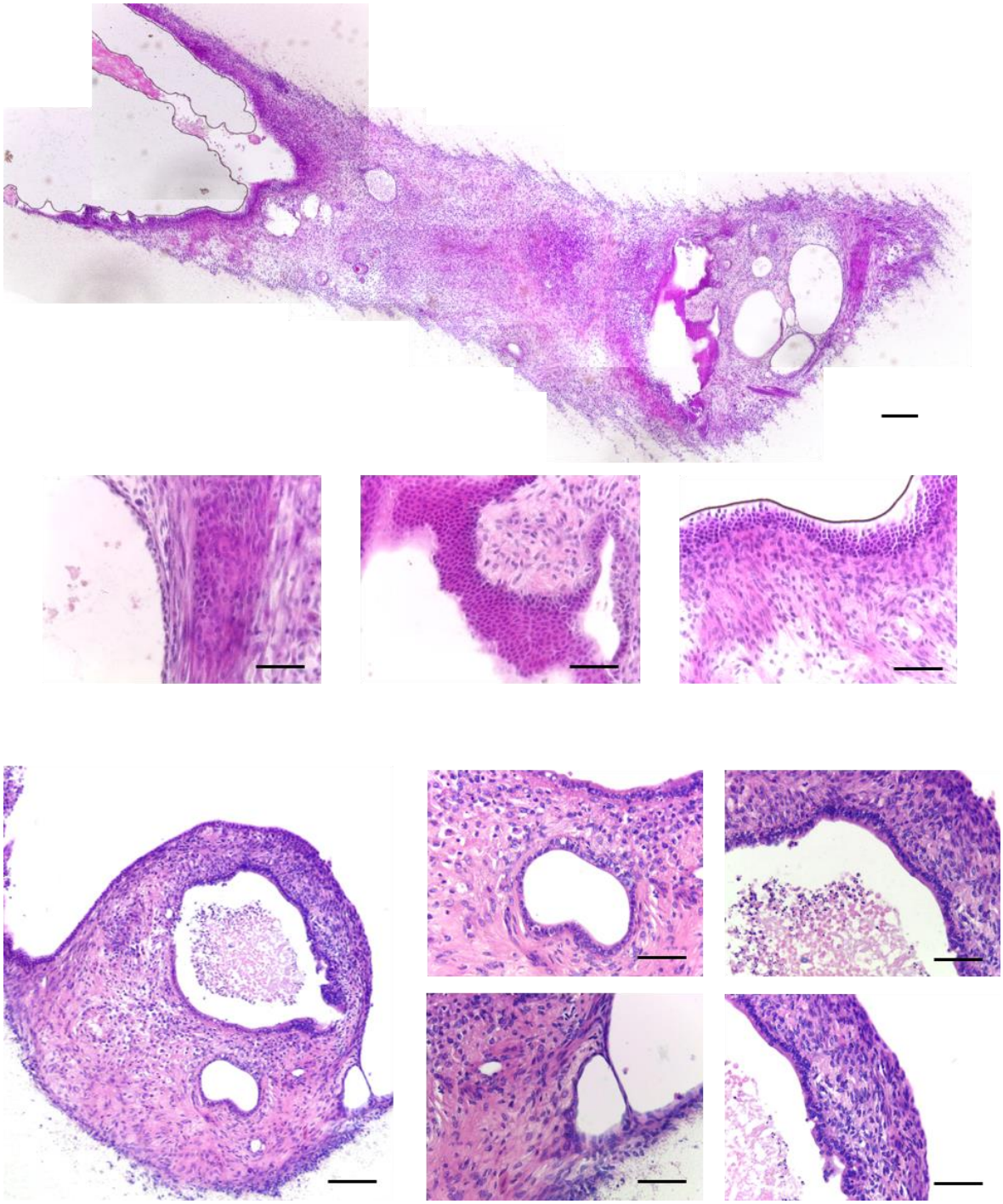


Figure 7.15: Histological analysis of CGR8 tissue disc samples cultured for 42 days using H&E staining: H&E highlights that 42 days culture results in the formation of tissues discs that continue to show the development of a variety of complex structures. These are derived from the three germ layers, and include aligned muscle fibres, connective tissues, epithelial lines cavities and lumens and organised epithelial surfaces. Scale bars: 200 µm, 100 µm and 50 µm

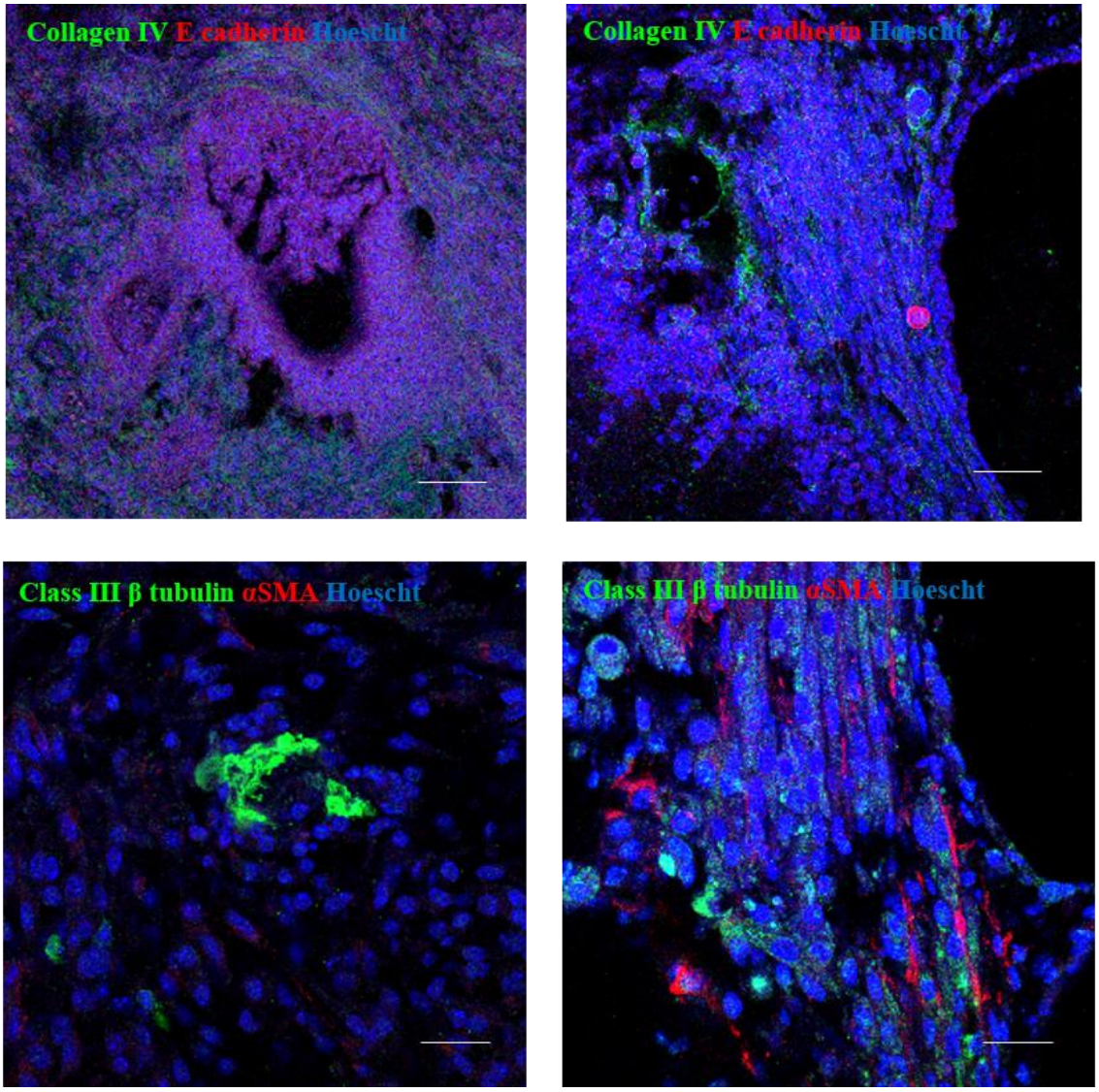


Figure 7.16: Immunofluorescent staining of 42 day CGR8 tissue discs for markers from the three germ layers: Staining of the tissue discs for a variety of germ layer markers confirms the identity the differentiated structures within the tissue disc, showing the presence of structures from all three germ layers within the tissue discs, including E-cadherin positive epithelia, areas of smooth muscle and Class III β-tubulin positive neurones. Scale bars: 100 µm

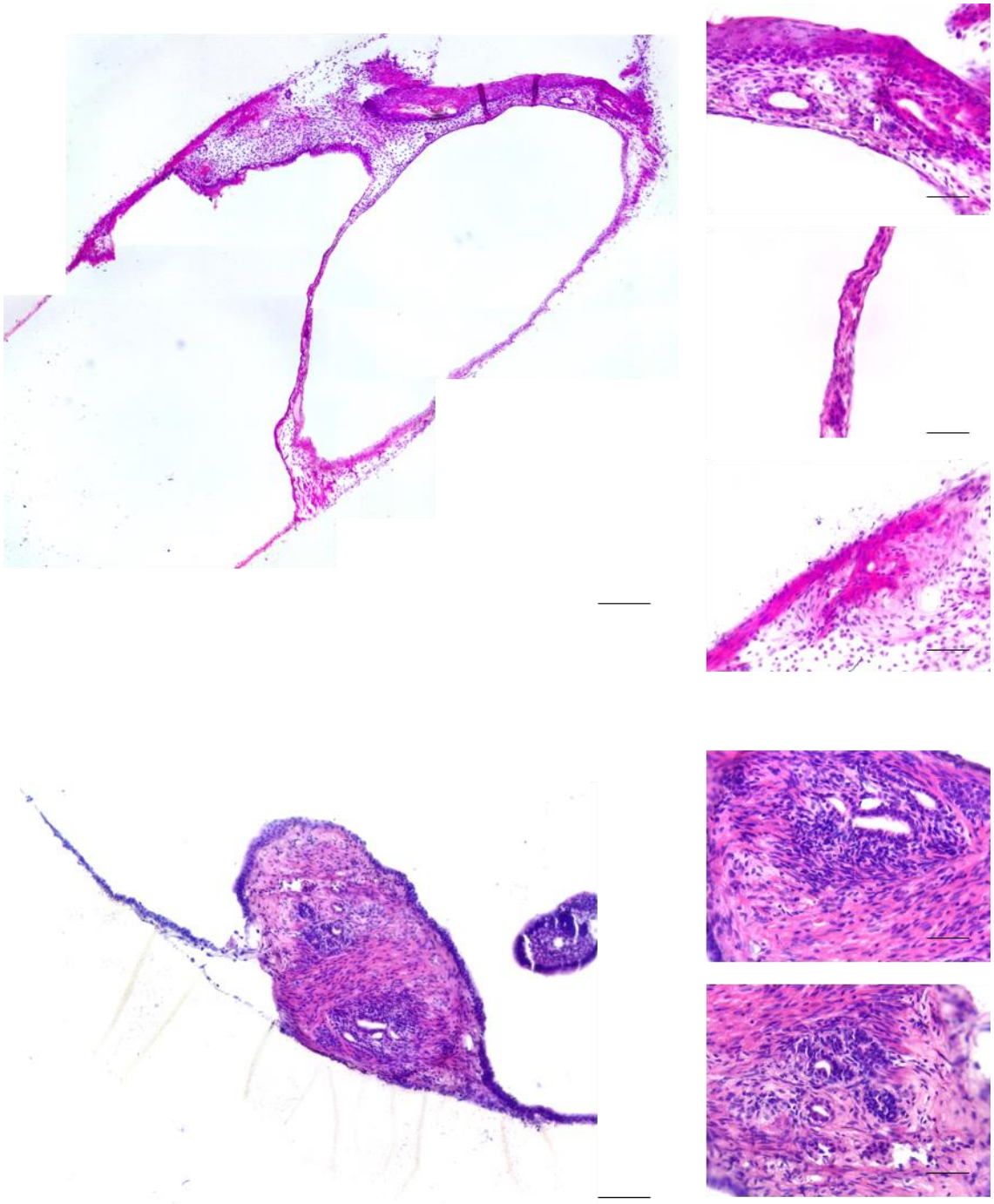


Figure 7.17: Histological analysis of CGR8 tissue disc samples cultured for 56 days using H&E staining: H&E highlights that 56 days culture leads to the formation of tissues discs that still consist of a variety of complex structures derived from the three germ layers. These include neural differentiation, aligned muscle fibres, organised epithelia and potential rudimentary renal epithelia. Scale bars: 200 µm and 50 µm

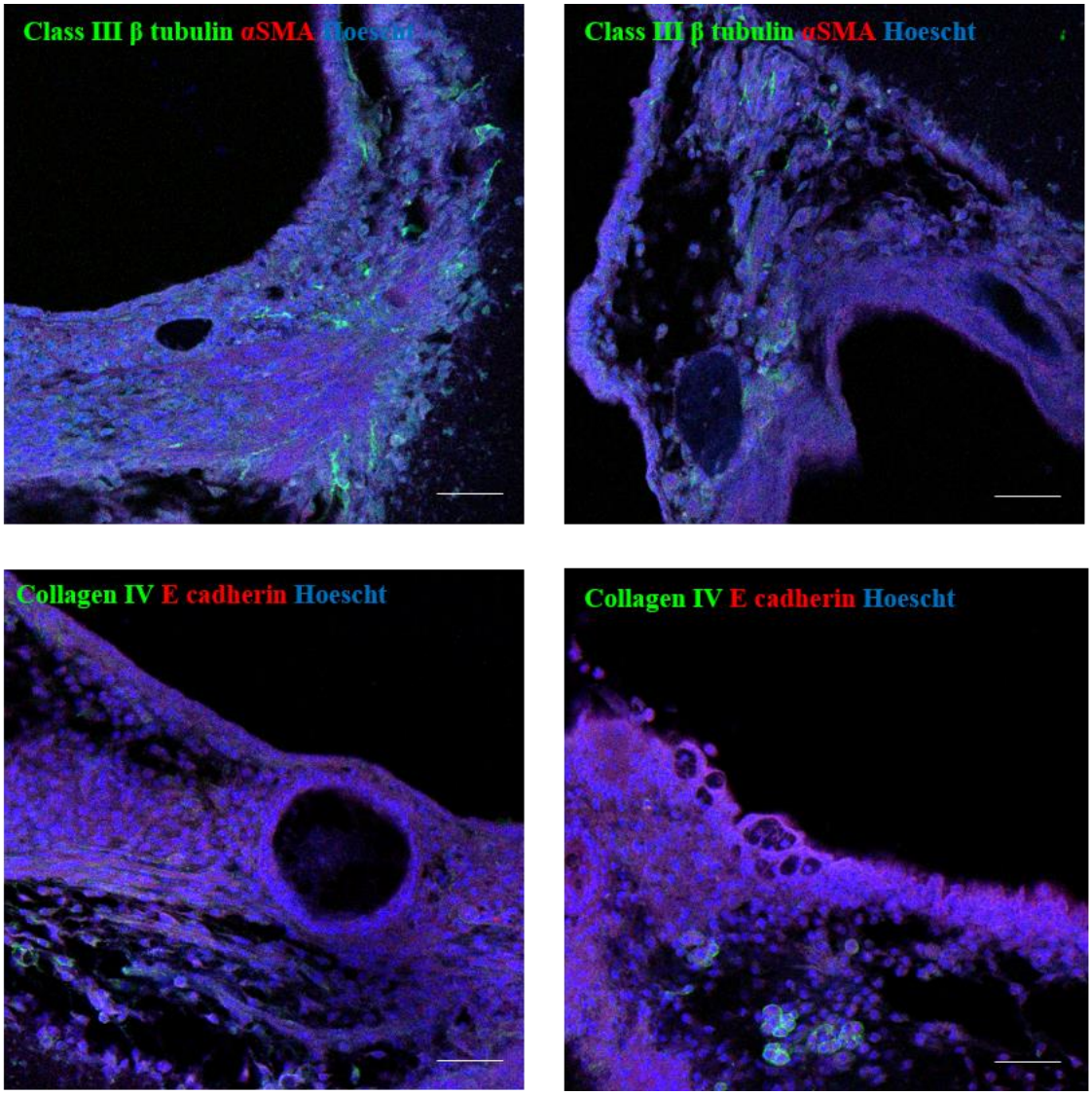


Figure 7.18: Immunofluorescent staining of 56 day CGR8 tissue discs for markers from the three germ layers: Staining of the tissue discs for a variety of germ layer markers confirms the identity the differentiated structures within the tissue disc, showing the presence of structures from all three germ layers within the tissue discs. These include Class III β-tubulin positive neurones and E-cadherin positive epithelia. Scale bars: 100 µm

7.5.3 Use of human pluripotent stem cell lines to form tissue discs

The model developed in this project has been used to study the maintenance and differentiation of a human embryonal carcinoma cell line and a murine embryonic stem cell line. While these stem cell populations have their own applications, and can in part inform the study of the human developmental process, they can never fully replace the use of human pluripotent stem cell populations to better understand the events involved. Additionally, as the teratoma assay is the primary methodology used to assess the pluripotency of putative human pluripotent stem cell lines, it is pertinent that these stem cell populations are tested in the model. In pilot studies, two human pluripotent stem cells were used in the model to test the ability to maintain human stem cell derived tissue discs; one well established embryonic stem cell line, and one novel induced pluripotent stem cell line.

7.5.3.1 H9 human embryonic stem cells display typical hallmarks of pluripotency

The H9 cell line is a well-established embryonic stem cell line originally derived by Thomson *et al* in 1998. A large volume of work has been conducted on this cell line, with the pluripotency and developmental potential of the cell line well documented. H9 cells were kindly donated by Prof M Lako, and were subject to brief characterisation prior to use in the model. As expected, H9 embryonic stem cells display all of the typical hallmarks of pluripotency, including a small cell size and colony morphology and the expression of alkaline phosphatase. The cells also express a range of known markers of pluripotency, as confirmed by immunostaining and flow cytometry, including Oct 4, Sox 2, SSEA-4 and TRA-1-60.

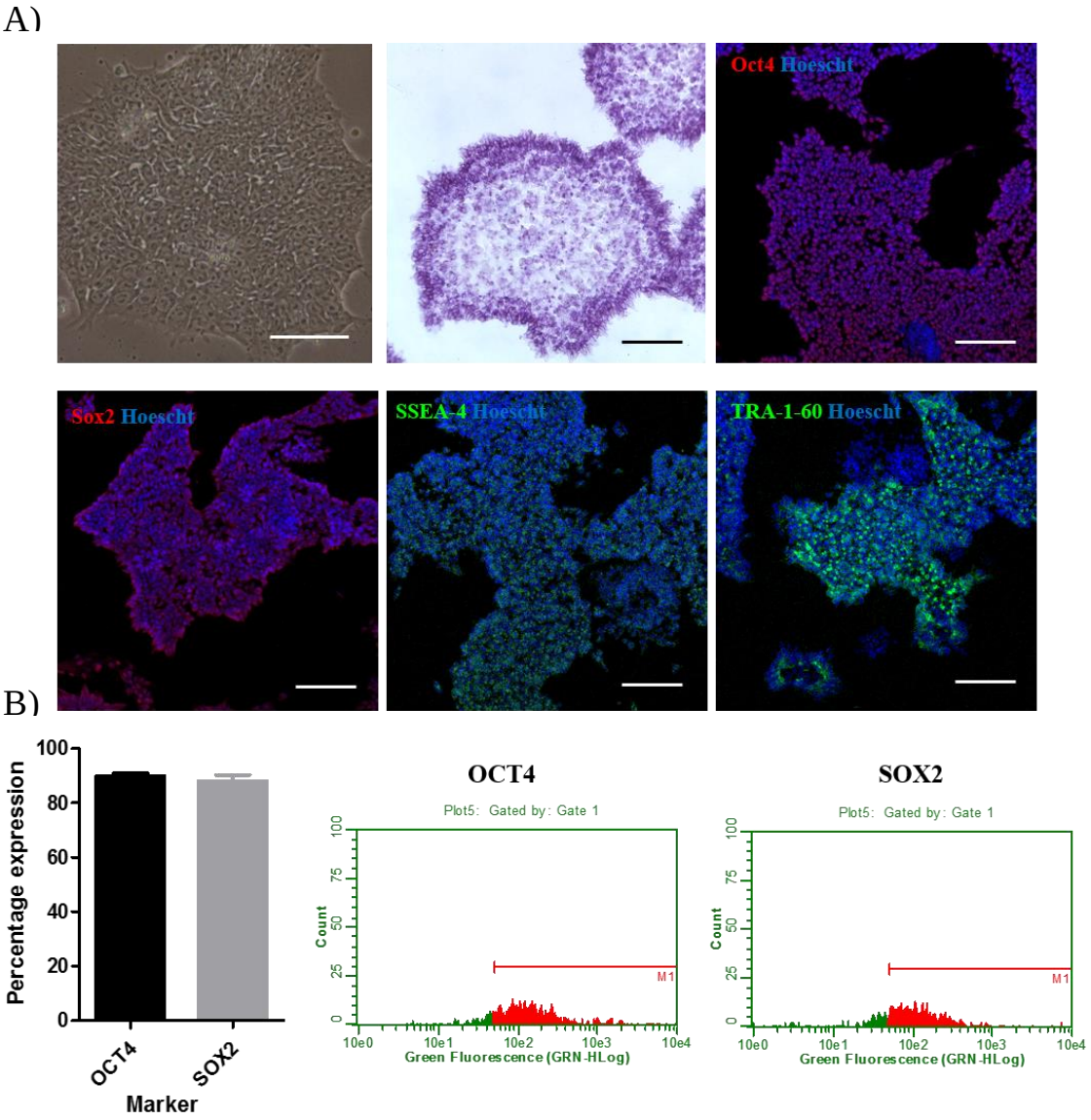


Figure 7.19: Characterisation of human induced pluripotent stem cell line H9: A) H9 embryonic stem cells display the typical stem cell morphology, with a small cell size, prominent nucleoli and high nuclear to cytoplasmic ratio. Cells grow in colonies as expected, expressing the enzyme alkaline phosphatase. H9 cells also express known markers associated with pluripotency, as detected by immunofluorescence. B) Flow cytometry also confirms the expression of known markers. Scale bars: 100 µm

7.5.3.2 H9 hESCs successfully form differentiated tissue discs on the scaffold, and can be maintained for up to 28 days

H9 cells were used to create embryoid bodies which were formed in low adherence microwell plates, cultured in suspension and transferred to the Alvetex® Polaris inserts for maintenance. The images in Figure 7.20 show that the formation of human ESC derived tissue discs is possible for up to 28 days, with the structures showing no evidence of issues with viability. Samples were analysed at 7 days also, but tissue discs were not able to be detected at this early time point. The histology shows a variety of cell morphologies, with connective tissues and neural differentiation dominating the

structure of the tissue discs. The 14 day sample in particular shows evidence of neuroepithelial differentiation, with the 21 and 28 day time points showing a more varied structure and morphology with increasing time in culture. Positive staining for Class III β-tubulin in all of the tissue discs indicates differentiation towards the default neural lineage, but there is no staining for the mesodermal and endodermal markers in the 14 and 21 days samples, highlighting a lack of tissue diversity. The final 28 day sample does show very weak E-cadherin staining, suggesting a maturation of the tissue disc and increase in structure diversity.

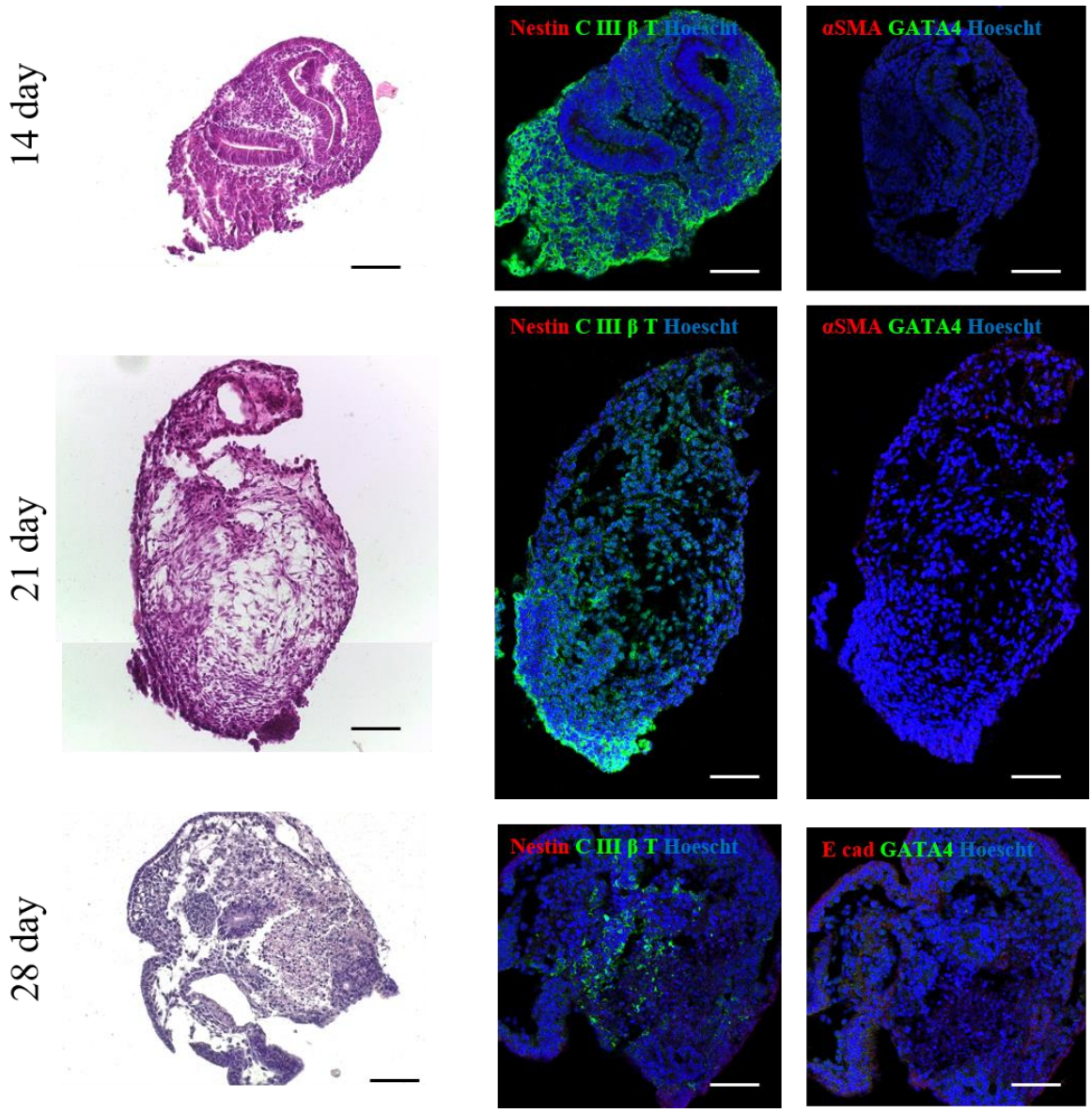


Figure 7.20: Histological analysis of H9 stem cell derived tissue discs cultured for up to 28 days: Histology reveals some complex differentiation has taken place within the tissue discs, with some evidence of neural differentiation in particular at all three time points. Immunostaining confirms the predominantly neural phenotype with positive Class III β-tubulin staining. Staining for other germ layer markers is mainly negative, indicating the tissue discs are still in the early stages of differentiation or have differentiated towards a specific population only. Scale bars: 200 μm

7.5.3.3 I18002 induced pluripotent stem cells display typical hallmarks of pluripotency

The I18002 induced pluripotent stem cell line is a newly derived stem cell line, kindly donated by Reprocell Ltd. As such, it is likely representative of putative stem cell lines that could be tested in the model in the future, given the exponential increase the number of novel iPSC lines derived each year. Characterisation of I18002 shows that this stem cell line also displays the typical colony morphology and expression of the pluripotency associated enzyme alkaline phosphatase. Assessment of pluripotency marker expression confirms the expression of known markers including Oct 4, Sox 2, SSEA-4 and TRA-1-60.

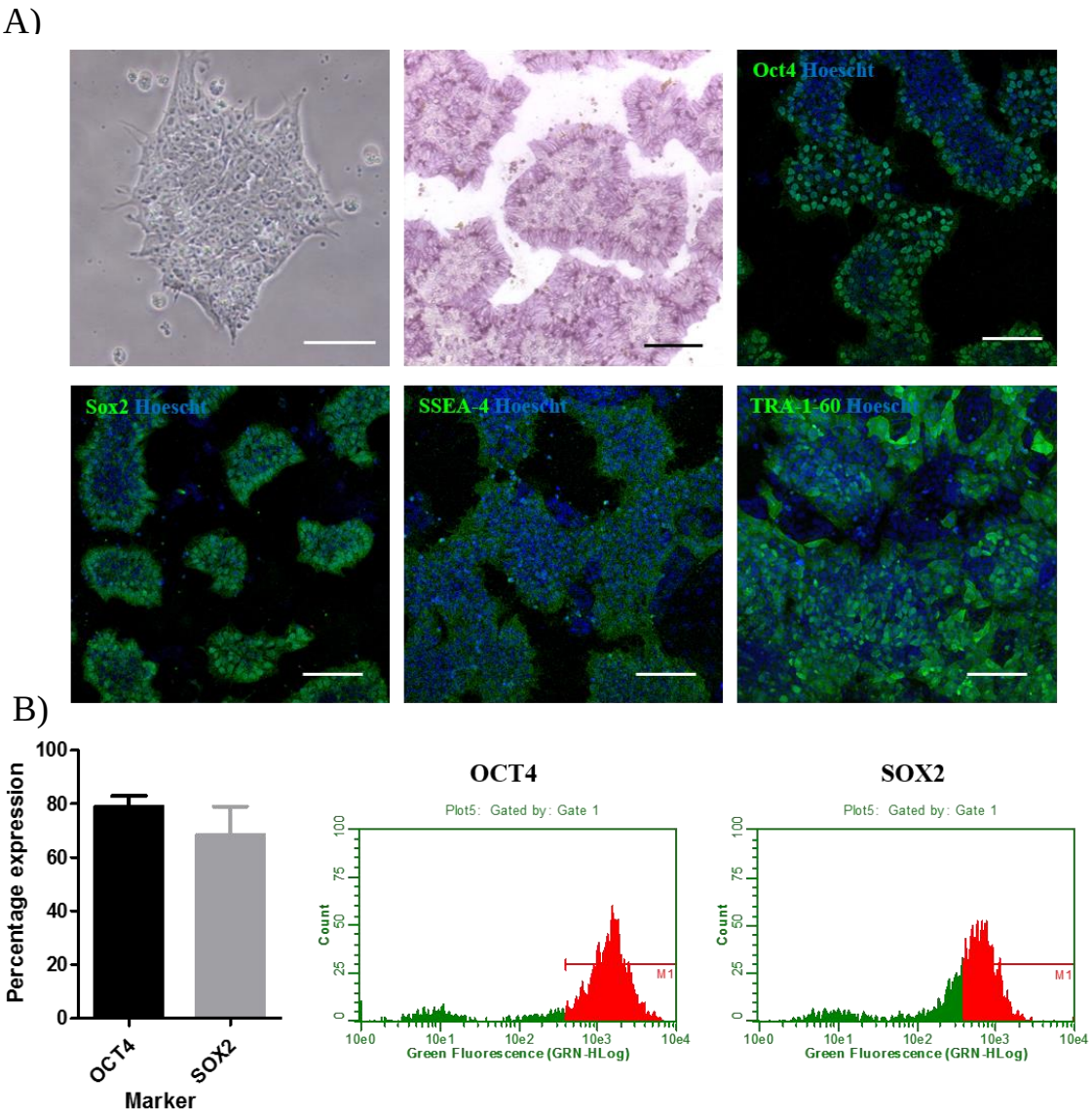


Figure 7.21: Characterisation of human induced pluripotent stem cell line I18002: A) I18002 induced pluripotent stem cells display typical stem cell morphology, growing in colonies. The cells express the pluripotency associated enzyme alkaline phosphatase, as well as known markers associated with pluripotency, as detected by immunofluorescence. B) Assessment by flow cytometry also confirms the expression of known pluripotency markers. Scale bars: 100 µm

7.5.3.4 I18002 iPSCs show the ability to successfully form differentiated tissue discs on the scaffold

I18002 iPSCs were used to form EBs in the same way as the H9 cells, and seeded onto Alvetex® Polaris inserts. While inserts were analysed at four different time points, 7, 14, 21 and 28 days, only the final 28 day sample contained a detectable tissue disc sample which could be analysed. The structure of the tissue disc is heterogeneous in nature, but no recognisable structures can be detected within the tissue disc itself. Immunostaining highlights the strong neural differentiation present within the tissue disc, with Class III β-tubulin staining positive throughout. Additional markers which were stained for show a negative staining pattern, indicating a lack of tissue diversity within the tissue disc.

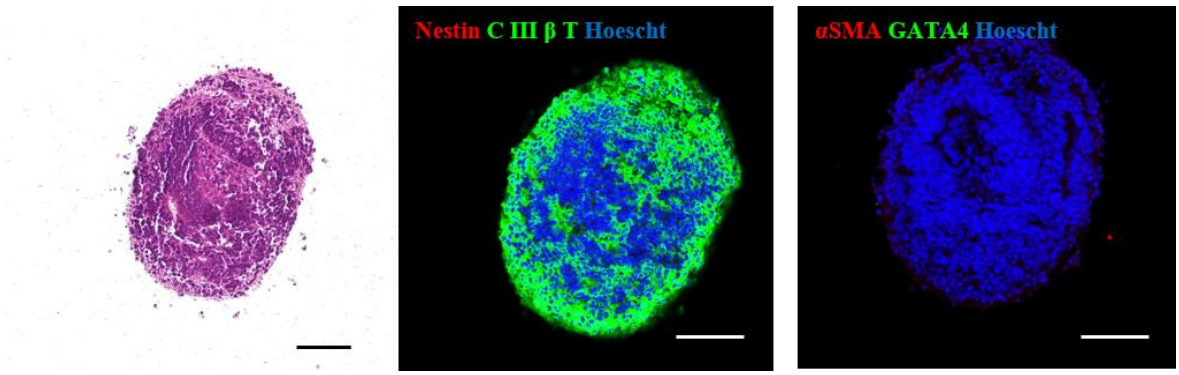


Figure 7.22: Histological analysis of I18002 stem cell derived tissue discs cultured for up to 28 days: Histology reveals complex differentiation has taken place within the tissue discs, with immunostaining partially elucidating the identity of the structures that have formed. Class III β-tubulin staining indicates the neural identity. Scale bars: 100 μm

7.6 Discussion

This final results Chapter sought to validate the model developed in this project in two different ways. Initially, the structures which developed in the model were compared to those formed in teratomas using the same cell populations, in order to ascertain whether comparative complexity could be achieved, and whether this EB based model offers a possible *in vitro* alternative to the teratoma assay. The model was also trialled using two different human pluripotent stem cell populations, in order to better represent the potential cell lines that would be used in the assay in any future applications.

7.6.1 Comparison of the differentiation within tissue disc samples and teratoma samples

It was concluded that the only way in which to directly compare the *in vitro* model and *in vivo* teratoma assay was to undertake these simultaneously using the same starting cell population to form both samples. This was considered an appropriate and ethical rationale for performing the assay, when the costs of animal usage were weighed against the potential to confirm the ability to use the model as an *in vitro* alternative. Full details of the protocol can be found in the Materials and Methods, with additional data found in the Appendix. The success rate of the formation of the teratoma samples used in this project (2D samples) was 100 %. The assay was performed using TERA2.cl.SP12 and CGR8 cells so that the comparability between the *in vivo* and *in vitro* samples for both PSC types, EC and ES, could be understood.

The teratoma samples from the TERA2.cl.SP12 cells contain the structures that would typically be found in an EC cell teratoma formed using this cell line (Knight, 2014). Highlighted here via immunostaining are the ectoderm derived structures, including epithelia and neural differentiation, and, importantly, the embryonal carcinoma aspect of the tumour, with positive Oct 4 staining throughout the teratoma structure. Comparing the tissue disc samples to the teratomas shows that a mixed phenotype, as seen in the teratoma, is not clearly observed in the tissue discs until the final time point at 42 days. Prior to this point, tissue disc structural heterogeneity is observed in the histology but phenotypic heterogeneity is not observed via immunostaining. It is interesting to note the difference in the expression of the pluripotency marker Oct 4 when compared to the tissue discs in Chapter 4, and that there is also a level of heterogeneity in the manner in which the TERA2.cl.SP12 tissue discs develop. This expression however, was again weak. TERA2.cl.SP12 derived tissue discs have the ability to recapitulate the teratocarcinoma phenotype, but this could take up to several weeks, which is a similar time scale to the time taken for a teratoma to form *in vivo*. This provides preliminary results to confirm the success of the *in vitro* model and also underlines the importance of time in the formation of complex and diverse tissue structures, both *in vivo* and *in vitro*.

CGR8 derived teratomas show a very wide variety of complex structures from all three germ layers, as highlighted by the multiple staining methods see in Figures 7.7 – 7.10. These include cartilage, bone, muscle, epithelia and neural tissues, which formed over a much shorter time period of around 11-19 days. In a similar manner to the data shown in Chapter 6, structures from all three germ layers can also be detected in the CGR8 derived tissue discs, which is observed in the first time point assessed at 14 days. Complex epidermal and epithelial differentiation can be observed in particular, as can clear mesoderm derived structures including connective tissues and smooth muscle, all of which can be identified via immunostaining. Variability is again observed between the tissue discs, with differences in the specific structures present. However, this further demonstrates the ability of this novel method to generate samples which fulfil the criteria of the teratoma assay, namely the formation of structures from all three germ layers, and provides promising data for its use as an alternative method to assess the developmental potency of putative stem cell populations. Assay length here also shows correlation between the *in vivo* and *in vitro* samples (11-19 and 14 days respectively). The level of structural complexity and variability is maintained at the next time point of 28 days, which show some comparability in the structures present: epidermal differentiation, organised epithelia and areas of smooth muscle can be identified in one of the tissue discs. This time point is also shorter in length than a typical teratoma assay using human pluripotent stem cells, and provides more options for the culture of tissue discs to form complex differentiated structures. As would be expected and was observed also on Chapter 6, tissue disc viability, complexity and heterogeneity are maintained up to the final time point of 56 days. This length of culture represents a time scale more similar to that of the teratoma as well as the most prolonged culture of tissue discs undertaken in this project, indicating their stability and the ability to culture and compare to teratomas in an even more direct manner. Heterogeneity between the tissue discs and the tissue structures within them persists at these later time points also, as was seen in those featured in both this Chapter and the previous Chapter. While this is more problematic when differentiation protocols are used due to the requirement for homogenous tissues, in the assessment of pluripotency this can be utilised through the assessment of the structures within the tissue discs as a population rather than individually. Multiple mouse hosts are used in typical teratoma assays both to ensure the successful production of samples and to allow for a thorough investigation (Buta et al., 2013). In addition, a teratoma assay assesses the developmental potency of a pluripotent cell population, not individual cells. As discussed in Chapter 3, the phenotype of stem cell populations is known to be heterogeneous, with differences in the relative expression of the various markers which indicate pluripotency (Asprer and Lakshmipathy, 2015; Cahan and Daley, 2013). Evidence also suggests that the transition from pluripotency to lineage commitment is not the difference between two distinct phenotypes, but a ‘continuum of cell states’, thus cells within a population could represent any of a number of pluripotent identities (Hough et al., 2009). While this method could easily be adapted to assess the developmental potential of single clonal pluripotent stem cells through the use of a different EB formation method, in the case of a cell population, the assessment of the structures

within the overall tissue disc population provides a more comprehensive and reliable overview of the developmental potential of the putative PSCs.

7.6.2 The tissue disc model as an *in vitro* alternative to the teratoma assay

Comparing the structures within the *in vitro* produced tissue discs and *in vivo* derived teratomas has highlighted the ability to create complex and varied tissue structures from all three germ layers using both methods, and as such, the *in vitro* model is a promising alternative to the *in vivo* assay. The need for standardisation or an alternative to the animal assay has been well documented in the field and the literature (Buta et al., 2013; Gropp et al., 2012; Müller et al., 2010b), and the review in Chapter 3 confirmed that the assay requires standardisation or replacement due to varied practices and incomplete reporting of protocols and results. The *in vitro* tissue disc model can form complex and recognisable tissue structures in a time scale similar to or shorter than the time taken to undertake a teratoma assay, and is also flexible to analysis using a wide variety of techniques, as demonstrated in Chapter 6 – histology, immunostaining, western blotting and qPCR. However, there are structures within the tissue discs which are not recognisable or do not stain strongly with antibodies to confirm their identity, most likely due to their lack of complexity and maturity. This does make the identification of germ layer derived structures difficult at times, but immature structures also form in teratomas, and so the use of this novel method could be considered no less difficult than the identification of tissue structures in a teratoma sample. In a similar way to the teratoma assay, the *in vitro* model is also able to assess the developmental potency of a PSC population, but could also be adapted for the analysis of single cells through the use of an alternative EB formation method. Most importantly, the *in vitro* nature of the tissue disc model means that the method is more controllable, and likely to be more consistent and reproducible than the teratoma assay. At the very least, the selection of protocol parameters for undertaking tissue disc formation could be considered to be simpler due to the reduced number of variables: EB initial cell seeding number, EB formation time and EB culture time on the membrane to form a tissue disc. While the full adoption of novel technologies and methods can take time in the scientific field, the fact that other novel approaches such as PluriTest have been adopted rapidly and in a widespread manner, as highlighted in Chapter 3, indicates the openness of the field to novel methods for the assessment of pluripotency.

In the Introduction and Chapter 3, the various attempts to standardise the teratoma assay and alternative approaches were discussed. These dealt mainly with standardising the manner in which the assay is performed, but standardisation of the analysis has also been considered through the application of tissue recognition algorithms to histological samples of teratomas (Bhagavatula et al., 2010). The combination of a technology such as this with the controllable *in vitro* assay has to potential to offer a completely standardised process, with reduced subjectivity in the confirmation of pluripotency and removing the need for a trained pathologist or other trained individual as is suggested for the analysis of the teratoma assay.

7.6.3 Use of multiple human pluripotent stem cell populations in the EB based *in vitro* model

The ultimate aim of this project is to create a novel model of human tissue development, which could also be used as an animal free alternative to the teratoma assay. While optimisation work did involve the use of a human pluripotent stem cell line, the embryonal carcinoma cell line used was restricted in its capacity to differentiate. Much of the validation work in this project has been conducted using a murine embryonic stem cell line, and while this has proved a useful for the assessment of the ability to differentiate tissue discs within the model due to inherent similarities with human PSCs, this population is also not representative of the potential cell populations which would be used within the model to study human developmental processes and developmental potential. Thus, in the final part of this project, two different human stem cell populations were used in pilot studies to form EBs, to assess whether it is possible to form tissue discs within the model from true human stem cell populations.

H9 cells were chosen due to their widespread use in a number of differentiation based protocols, and their well characterised nature. A brief analysis of the cells confirmed their expression of relevant pluripotency markers such as Oct 4 and alkaline phosphatase with the associated stem cell morphology also noted. This cell population also showed the ability to form tissue discs when cultured on the surface of Alvetex® membranes; these structures could be maintained for up to 28 days on the scaffold. (This timepoint was selected as the final timepoint to correlate with previous studies with CGR8 EBs when complexity of tissues structures was noted.) Generally, only neural tissues can be definitively identified using immunostaining; there is little evidence of mesodermal and endodermal derived structures, although there are some differing cell morphologies within the tissue discs and weak E-cadherin staining. The tissue discs formed from the H9 cells are noticeably different from those tissue discs which were formed from the murine stem cells; these are smaller and do not display the same level of complexity and heterogeneity as observed in the murine tissue discs. The same phenotype was also observed with I18002 iPSCs. Following a characterisation which confirmed the pluripotent phenotype of the cells, I18002 cells were used to form EBs and seeded to form tissue discs in the same way. Samples were only visible for assessment after 28 days, and these tissue discs were small, showing a predominantly neural phenotype as observed in the H9 tissue discs. While logistically, both human PSCs were able to produce tissue discs, these both lacked the complexity as observed previously.

This lack of complexity is likely due to a number of reasons; human PSCs are known to grow at a slower rate than their murine counterparts (Schwartz et al., 2011), which suggests that their ability to proliferate and spontaneously differentiate as an EB will also be slower. This is true for the teratoma assay; typical assays take around 6-8 weeks, the human EC cell teratomas in this project took three times longer to form in some cases when compared to the murine teratomas. In addition, in this study EBs were allowed to spontaneously differentiate as tissue discs for a prolonged period

on the Alvetex® membrane, a process which is not usually followed using human PSCs – specific differentiation media are used to create specific cell or tissue populations, and these generally contain a cocktail of cytokines and morphogens to direct and promote differentiation. A simple serum free media composition was used in this instance, as this is often the basis of more complex differentiation media used in differentiation based studies and was deemed to represent an animal free system that could be used if the model is employed as an alternative to the teratoma assay. Clearly the media was able to promote human EB and tissue disc survival, but was possibly unsuitable for supporting the prolonged spontaneous differentiation of the structures, requiring further optimisation. Thus, further experiments and studies longer than 28 days were not conducted using the hPSCs due to the need to further optimise a variety of aspects of this version of the model, such as media composition, EB growth and size, and assay length. This data however, indicates that the culture of human PSC derived tissue discs is possible, and with further optimisation work this could provide a viable option for the study of the events of human development and the assessment of developmental potential in putative PSCs.

7.7 Conclusion

The comparison of the *in vitro* model developed during this project with teratoma samples derived from the same cell population has allowed for a more thorough appreciation of the potential to use the model as more standardised and controllable alternative to the *in vivo* assay. The completion of a teratoma assay using both TERA2.cl.SP12 and CGR8 PSC populations has shown that the ability to achieve a similar phenotype both *in vitro* and *in vivo* is possible. While this takes several weeks with the TERA2.cl.SP12 cells in the *in vitro* setting, as is more generally observed with the formation of human PSC derived teratomas *in vivo*, the murine stem cell population was able to fulfil the requirements of the teratoma assay, the confirmation of the presence of structures from the three germ layers, after only 14 days in the *in vitro* setting. Structures are highly complex and recognisable, showing a defined tissue morphology. While there is still variability in the structural composition of the tissue discs, assessing these as a population allows for a more comprehensive understanding of the developmental potential of the putative PSC population as a whole.

Human pluripotent stem cells are the intended test population for a model such as that developed during this project, and so it is prudent to also test these cell populations in the *in vitro* model in order to further validate it. The culture of human PSC derived EBs on Alvetex® resulted in the successful formation of tissue disc, although these showed less complexity and heterogeneity than that observed within murine tissue discs. This provides proof of concept for the use of human PSCs in the model, although highlights the need for further optimisation in order to enhance the differentiation which is achieved.

The validation of this model through comparison with teratoma samples and incorporation of various human PSC populations has further confirmed the flexibility of the model and the ability to use it as an alternative to the teratoma assay, as well as highlighting the need for further optimisation to pursue the use of the model for the study of human pluripotent stem cell populations. The model has been optimised already in a number of different ways in order to enhance the differentiation which occurs, and these data considered in combination with this final Chapter provides a relatively comprehensive overview of its potential uses and differentiation abilities.

8. General Discussion, Future Directions and Conclusion

8.1 Summary of key findings

- Despite its 'gold standard' status and the recognised need for standardisation, the teratoma assay continues to be performed according to no standardised protocol.
- Embryonal carcinoma cell derived embryoid bodies can be maintained on a porous polystyrene scaffold as flattened structures named tissue discs, showing improvements in viability and maintained or enhanced differentiation.
- The creation of a more physiological microenvironment using co-culture or perfusion results in some enhancement of cell differentiation, with the maintenance of pluripotent regions similar to a teratocarcinoma.
- Murine embryonic stem cell derived 3D cultures can also be maintained in the model for long term culture, with a variety of germ layer derived tissue structures present.
- The differentiation of these tissues from PSCs can be successfully manipulated both using morphogens and applying more physiological culture conditions; perfusion in particular resulted in the formation of complex, mature differentiated structures.
- Differentiation of PSC derived structures using novel 3D cell culture technology leads to the formation of structures which are comparable to teratomas formed from the same cell population.
- Pilot studies have indicated similar success with human embryonic and induced pluripotent stem cell lines.

8.2 Discussion

This project has focussed on the development of a novel *in vitro* model using pluripotent stem cells and three dimensional cell culture techniques, which can be used to study the events of human development and potentially be used as an alternative to the xenograft teratoma assay, the current 'gold standard' method for the assessment of developmental potency in putative human PSC populations. This is in light of that fact that although various models are available to study human tissue development, each has a number of limitations, whether that be ethical issues and lack of material (Cavaliere, 2017), species specific differences in developmental events (Holloway et al., 2019) or viability over prolonged culture (Gothard et al., 2009; Son et al., 2011). A wide range of advanced culture techniques are now available to help develop new approaches to create functional tissues *in vitro*, including both three dimensional cell culture and more physiological culture methods. This project has used a range of advanced culture techniques with the aim of enhancing the differentiation of PSC derived EBs as tissue discs *in vitro* in order to achieve increased cell viability and tissue structure complexity.

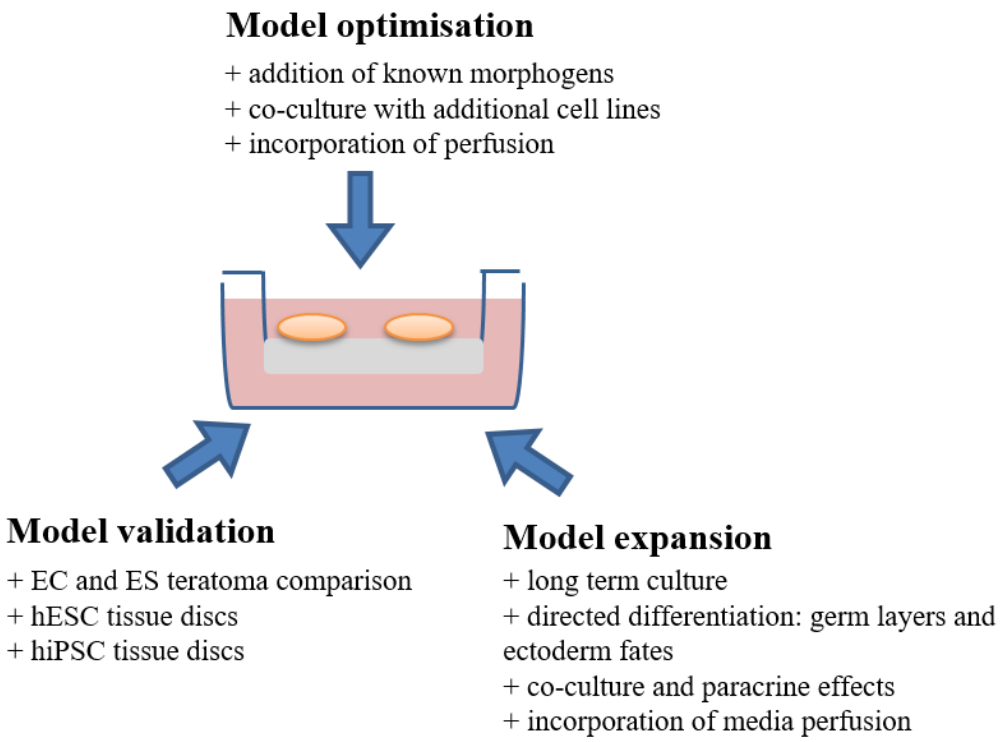


Figure 8.1: Overview of the studies conducted in this project: This project has used a range of pluripotent cell populations and utilised various methods to direct and enhance the differentiation of PSC derived tissue discs cultured on the porous scaffold. Many of these have been used in the literature previously to study the effects of EB differentiation.

8.2.1 The current use of the teratoma assay to assess developmental potency

In order to understand the use of the teratoma assay in the stem cell field at present, a literature review was conducted on human PSCs held at major US and UK registered cell banks and repositories. It was anticipated that this would also be able to inform the *in vitro* work through the identification of common aspects of the protocol, as well as following up on recommendations for standardisation made previously (Buta et al., 2013; Gropp et al., 2012), including the only previous review conducted in this area around 10 years ago (Müller et al., 2010b). Surprisingly, the data obtained aligned closely with that obtained by Müller in the review: there is still currently no evidence of standardisation of the assay within the field. Many of the parameters were highly variable and while there were some indications as to protocol commonalities, the modal value for many of the parameters was that the method/reagent used was not specified. This analysis also indicated that many human pluripotent stem cell lines which are registered for use at public repositories have not previously had a teratoma assay performed, even though the completion of the assay is strongly recommended by multiple reports and regulatory bodies (International Stem Cell Initiative, 2018; International Stem Cell Initiative et al., 2007). This was particularly prevalent with iPSC lines, and although many of these were derived in high throughput studies, this is still concerning given that there is no validated alternative to the teratoma assay. The literature review did not provide clear parameters for the

undertaking of *in vitro* work, but underlined the importance for the demand of a robust, standardised, controllable alternative method that can be used to assess the developmental potency of human PSCs.

8.2.2 Differentiation of EC cell derived structures using advanced cell technology

Embryoid bodies are commonly used in differentiation protocols and to study early events of human development, so the use of these structures in the novel model was deemed logical and appropriate. EB growth/differentiation has been shown to be limited by viability issues and the lack of attachment to surfaces, so building on preliminary work from the literature and within the group (Abbasi et al., 2016; Knight, 2014; Nestor et al., 2013; Owens, 2015), the seeding of EBs onto solid scaffolds was hypothesised and utilised within this study. Prior to seeding EBs onto the scaffolds, studies were conducted to assess the effect of EB seeding density on differentiation and cell death within the structures, as it is critical to achieve high levels of differentiation with minimum cell death in the structures prior to seeding. An upper limit to EB size was found as is hypothesised in the literature (Dang et al., 2002; Gassmann et al., 1996), as was a consistency in the level of cell death in EBs after 14 days. While some trends in the impact of EB seeding density on differentiation were observed, no significant differences in these effects were found. Some seeding densities did show some enrichment for neural markers, which allowed for the selection of specific EB culture conditions prior to seeding. Membranes with the smaller pore sizes, particularly Alvetex® Polaris, were found to be most suitable for the preservation of the entire tissue disc structure, in agreement with previous data (Owens, 2015). The culture of flattened EBs on the scaffold as tissue discs confirmed that the reduction of diffusion distance and attachment to the scaffold resulted in the ability to maintain tissue discs with an improved viability and differentiation. Additional studies confirmed the ability to maintain EBs which had been differentiated using various morphogens on the scaffold, further supporting the ability to use the scaffold for the maintenance and study stem cell differentiation.

8.2.3 Creating a more physiological culture environment

The *in vivo* microenvironment is highly complex, with a wide range of integrated cues which cells respond to, impacting on their structure and function (Yamada and Cukierman, 2007); this is the case with the microenvironments that the developing embryo and teratomas are exposed to. The introduction of a three dimensional space is insufficient to capture this complexity and so two additional aspects of the *in vivo* microenvironment were chosen for incorporation into the *in vitro* model, with the aim of further enhancing the differentiated structured within the tissue discs. Co-culture with fibroblasts has been shown to enhance the structure and function of a number of *in vitro* models, tissue specific (Blom et al., 2016; Roger et al., 2019; Viney et al., 2009) and tumour biology (Majety et al., 2015), and this cell population is ubiquitous throughout the human body performing a number of roles, including ECM maintenance and cytokine secretion. The co-culture of EC cell

derived tissue discs was shown to be possible with the use of human dermal fibroblasts, and was further explored using fibroblasts derived from a SCID mouse, a common choice of mouse host for the xenograft teratoma assay as detailed by the literature review in Chapter 3. Using both fibroblast populations, alterations in tissue disc phenotype and structure were observed when compared to the tissue discs from Chapter 4, with a more heterogeneous internal morphology and evidence of the maintenance of larger Oct 4 positive pluripotent areas than previously noted in the tissue discs, suggesting changes in the tissue disc resembling a teratocarcinoma, with both differentiated and pluripotent areas.

Media perfusion was also introduced into the model in an attempt to mimic some of the functions of the vasculature and microcirculation, another key component of the *in vivo* microenvironment responsible for the support of large tissues through the provision of nutrients and removal of waste metabolites. Dynamic culture systems have been reported in the literature to provide better support to *in vitro* cultures by preventing the formation of unstirred layers adjacent to cells in culture (Ng et al., 1993; Spivak et al., 2006). In the case of pluripotent stem cells, it has been used to differentiate PSCs into teratoma like structures (Gerlach et al., 2010a; Stachelscheid et al., 2013). The introduction of perfusion to EC cell derived tissue discs did not result in any significant improvements to cell differentiation, and so the decision was made to utilise a cell suspension in the perfused system as is generally used in bioreactor cultures. This led to the moderately successful formation of tissue like structures which also showed some evidence of the maintenance of pluripotency, similar to that seen in a teratocarcinoma tumour. It is of interest that both strategies that were used to improve the *in vitro* microenvironment by increasing its physiological relevance resulted in this phenotype, further confirming the need to accurately recapitulate *in vivo* conditions in the *in vitro* setting in order to better understand these interactions and events.

8.2.4 Application of the model to a more relevant murine PSC population

Human embryonal carcinoma cells are a recognised pluripotent cell population, and whilst having a number of applications in the study of tissue development and pluripotency, these cells ultimately do not represent a typical population of human pluripotent stem cells due to their tumorigenic origins and various genetic and functional differences (Andrews et al., 2005; Mueller et al., 2006). In this project, these cells were highly useful for optimisation purposes, but a murine embryonic stem cell line was chosen to undertake further differentiation based work to test the capabilities of the *in vitro* model due to the similarities between mouse and human developmental processes (Schnerch et al., 2010) and relative ease of culture. Differentiating 3D cultures could be maintained in the model for up to 35 days, longer than many embryoid body based studies in the literature, forming multiple complex internal tissue like structures which could be identified and attributed to the three germ layers. A range of differentiation based studies using various morphogens demonstrated the ability to recapitulate in part a number of differentiated phenotypes and maintain these structures as tissue

discs within the model, further confirming the ability to form constructs from all three germ layers and study the developmental events of specific tissues. Variation did exist within the differentiated tissue discs, but this is not entirely unexpected given the manner in which the EBs were differentiated prior to seeding: EBs were primed towards a specific lineage rather than directed specifically towards an endpoint. The introduction of co-culture to the murine tissue discs resulted in a highly reduced homogenous phenotype with little structure formation; some preliminary experiments indicated the effects of factors secreted from the fibroblast populations used, but this phenotype differed from that observed using the EC cells. Long term perfusion culture induced the formation of a large, highly mature tissue disc which contained multiple complex tissue like structures not previously noted, mimicking that seen by other groups conducting similar studies (Gerlach et al., 2010a; Stachelscheid et al., 2013) and indicating a promising option for an *in vitro* alternative to the teratoma assay.

8.2.5 Validation against teratoma samples and with human pluripotent stem cell lines

The final work in this project involved the validation of the *in vitro* model against teratoma samples formed from the same cell population. Analysis of teratoma assay samples is routinely completed through histological and immunostaining for the identification of complex structures (Aleckovic and Simón, 2008), and so these analyses were used to compare the two tissue samples. The application of 3D cell culture technology demonstrated the ability to form complex structures as previously identified, over a time period comparable to that taken for a teratoma to form *in vivo* from the same cell line. Again, variability in the tissue discs was observed, but as the teratoma assay assesses the developmental potency of a cell population rather than a single cell clone and multiple mouse hosts are used, the structures and complexes of multiple tissue discs can be assessed to better ascertain the pluripotency of heterogeneous putative pluripotency cell population (Asprer and Lakshmipathy, 2015; Cahan and Daley, 2013), and in a more controlled and standardised manner than the *in vivo* assay. This is particularly important when it is considered that the teratoma assay is low throughput, with only one sample per host, and that the formation of a successfully differentiated tumour is not guaranteed: tumours may become cystic or not form (see Figure 8.2). The high throughput nature of the tissue disc model allows for increased success of structure formation, and the assessment of the tissue disc population in order to confirm the presence of all three germ layers, as well and providing an opportunity to reduce the number of animals used in the *in vivo* assay. The *in vitro* model was also used in a number of pilot studies with human pluripotent stem cell lines, in order to confirm that these cell populations, which are likely to be used extensively in the model, are able to be cultured as tissue discs successfully. Both human iPS and ES cell lines were cultured as tissue discs in the model and although these were smaller than murine counterparts there was evidence of differentiated tissue structures forming.

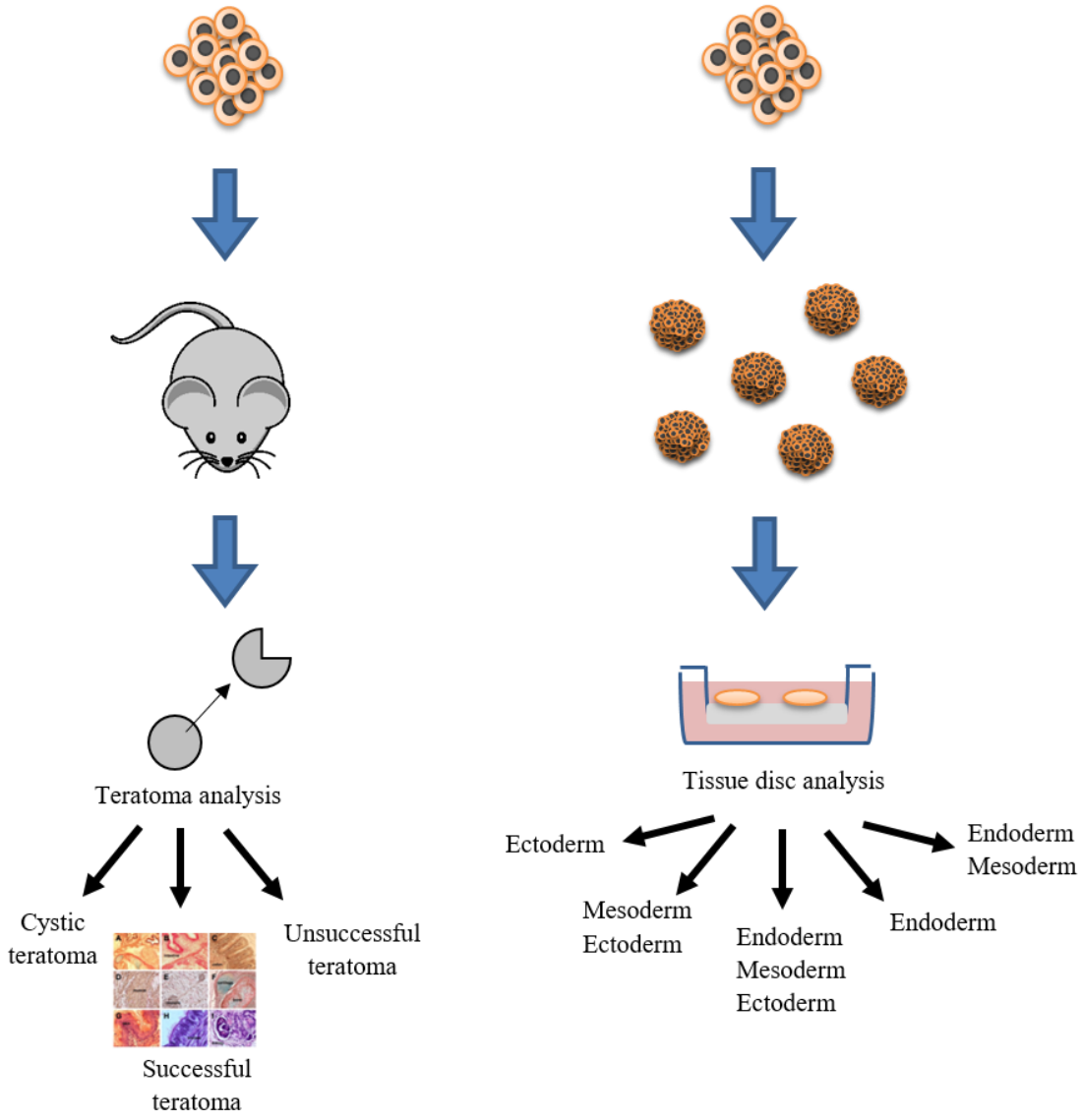


Figure 8.2: Comparing the use of the teratoma assay and the *in vitro* model to assess developmental potency: Both the teratoma assay and the *in vitro* model developed in this project begin with a single cell suspension. When undertaking the teratoma assay, one cell sample has the potential to produce one teratoma, provided the tumour formation is successful. The tumour could form as a fully differentiated, complex structure, a cystic structure with little tissue diversity, or be unsuccessful. In contrast, the high throughout nature of the tissue disc model allows for increased success with multiple tissue discs forming and the opportunity to confirm the presence of all three germ layer through the analysis of many samples within a single experiment.

8.3 Future Directions

The experiments performed in this project, form a foundation for more work to be undertaken in a range of areas, including human development and cellular pluripotency.

8.3.1 Differentiation of specific cell populations using more complex morphogen based protocols

Many of the differentiation based experiments which have been conducted in this project have been relatively simple in nature, primarily to provide preliminary data as to the ability to undertake such studies, directing the differentiation of cells and maintaining their development in the 3D model. Differentiation protocols in the literature are noted to be significantly more complicated, in order to achieve specific cell populations. Following the completion of these simple studies, it would be pertinent to undertake such differentiation protocols in order to study the events of lineage commitment and cellular differentiation more closely, in order to generate more specific cell populations and tissue types.

8.3.2 Integration of multiple cues to create a more complex and physiological microenvironment

The importance of multiple microenvironmental cues on the structure and function of cells was highlighted in various parts of this project, but these were investigated and applied in isolation to the model. *In vivo*, these cues are integrated and act on cells simultaneously, both in a synergistic and antagonistic manner. In order to better mimic the *in vivo* microenvironment, cues such as perfusion and co-culture could be simultaneously applied during the culture of PSC derived tissue discs, as is becoming increasingly popular in other tissue modelling studies with the aim of more faithfully recapitulating the structure and function of *in vivo* organs (Strüver et al., 2017). Additional microenvironmental cues could also be incorporated into the model following initial optimisation (see Section 8.3.4 below).

8.3.3 Further work using human pluripotent stem cell lines

Two human pluripotent stem cell lines, one iPS and one ES cell lineage, were used in this project. Further work is required to optimise the culture of such cell lines, particularly to select a culture medium optimised for the culture of cells and their spontaneous differentiation in order to assess developmental potency. The natural variability in human pluripotent stem cell lines also warrants further culture of more human pluripotent stem cell populations in the model to appreciate the range of structures that can form and note any differences in developmental potency between cell lines. It

would be interesting to identify how this variability presents in the model, whether through the formation of immature tissue structures or differentiation of tissues restricted to a specific germ layer, and allow for a more standardised comparison.

8.3.4 Investigation into the effects of other environmental cues on tissue disc differentiation

A wide range of other microenvironmental cues have been shown to impact on the pluripotency and differentiation of PSCs, including oxygen concentration. The oxygen concentration *in vivo* is known to be variable and lower that atmospheric oxygen, particularly during human development prior to the formation of the vasculature system; hypoxia has previously been shown to affect the formation of specific structures, the expression of lineage specific genes and drive proliferation (Dunwoodie, 2009; Fathollahipour et al., 2018; Simon and Keith, 2008), and is used within the stem cell field to both maintain pluripotent colonies and differentiate PSCs. Thus, the oxygen concentrations cells are normally cultured at are not representative of the oxygen concentration *in vivo* (Csete, 2005). The flexible format of the model would permit exposure to hypoxic conditions at various culture points, allowing for the investigation as to the effects of oxygen concentration on pluripotent stem cell differentiation into three dimensional structures.

8.3.5 Embryonic toxicity testing for therapeutic compounds

The investigation into any potential impact of therapeutic drugs on a developing foetus is a crucial part of the analysis and safety testing of any novel clinical compound, but current methods involve large scale animal testing and have been in use for decades (DeSesso, 2017). Advances in cell culture practices and technologies have allowed for *ex vivo* culture but these do not recapitulate the full *in vivo* activities and influence of the compounds, and *in utero* testing is still required. *In vitro* models such as novel EB methods (Flamier et al., 2017) offer the opportunity to screen out extremely harmful compounds and analyse their effects on developing tissues, potentially reducing the number of animals required for downstream testing. Basic toxicology experiments could also be conducted using human PSCs in the model to investigate the impact of known teratogens on the formation of tissue structures, providing preliminary data on its use as a model to study human tissue development before testing compounds with unknown effects and comparing to animal studies.

8.4 Conclusion

This thesis has focussed on the development, optimisation and validation of a novel *in vitro* model for the study of human tissue development. It has demonstrated that 3D cellular masses derived from various pluripotent stem cell populations can be cultured and maintained on a porous polystyrene scaffold, showing the maintenance or enhancement of the tissue structures which form. The application of various stimuli, morphogens, co-culture and perfusion, have been applied to the model in order to direct and improve the differentiation, with generally successful results. The model can be used to form differentiated cells that show the formation of comparable structures to teratomas from the same cell line, indicating the potential to use this technique for the assessment of the developmental potency of putative stem cell populations. Optimisation of the model continues for human PSC derived 3D cultures, but the work completed with embryonal carcinoma cells and murine embryonic stem cells herein provides good evidence for the further development of this model in the future.

9. Bibliography

Abbasi, N., Hashemi, S.M., Salehi, M., Jahani, H., Mowla, S.J., Soleimani, M., Hosseinkhani, H., 2016. Influence of oriented nanofibrous PCL scaffolds on quantitative gene expression during neural differentiation of mouse embryonic stem cells. J. Biomed. Mater. Res. A 104, 155–164. https://doi.org/10.1002/jbm.a.35551

Adamo, L., García-Cardeña, G., 2011. Directed Stem Cell Differentiation by Fluid Mechanical Forces. Antioxid. Redox Signal. 15, 1463–1473. https://doi.org/10.1089/ars.2011.3907

Aibibu, D., Hild, M., Wöltje, M., Cherif, C., 2016. Textile cell-free scaffolds for in situ tissue engineering applications. J. Mater. Sci. Mater. Med. 27. https://doi.org/10.1007/s10856-015-5656-3

Alanko, T., Tienari, J., Lehtonen, E., Saksela, O., 1994. Development of FGF-Dependency in Human Embryonic Carcinoma Cells after Retinoic Acid-Induced Differentiation. Dev. Biol. 161, 141–153. https://doi.org/10.1006/dbio.1994.1016

Alberts, B., Bray, D., Watson, J., Lewis, J., Roberts, K., Raff, M., 2002. Epidermis and Its Renewal by Stem Cells - Molecular Biology of the Cell - NCBI Bookshelf. Mol. Biol. Cell.

Aleckovic, M., Simón, C., 2008. Is teratoma formation in stem cell research a characterization tool or a window to developmental biology? Reprod. Biomed. Online 17, 270–280. https://doi.org/10.1016/S1472-6483(10)60206-4

Al-Jomard, R., Amarin, Z., 2017. The use of human mature cystic ovarian teratoma as a model to study the development of human lymphatics. Anat. Cell Biol. 50, 104–106. https://doi.org/10.5115/acb.2017.50.2.104

Amann, A., Zwierzina, M., Gamerith, G., Bitsche, M., Huber, J.M., Vogel, G.F., Blumer, M., Koeck, S., Pechriggl, E.J., Kelm, J.M., Hilbe, W., Zwierzina, H., 2014. Development of an Innovative 3D Cell Culture System to Study Tumour - Stroma Interactions in Non-Small Cell Lung Cancer Cells. PLOS ONE 9, e92511. https://doi.org/10.1371/journal.pone.0092511

Anamelechi, C.C., Truskey, G.A., Reichert, W.M., 2005. Mylar and Teflon-AF as cell culture substrates for studying endothelial cell adhesion. Biomaterials 26, 6887–6896. https://doi.org/10.1016/j.biomaterials.2005.04.027

Andrews, P.W., Baker, D., Benvinisty, N., Miranda, B., Bruce, K.A., Bruestle, O., Choi, M., Choi, Y.-M., Crook, J.M., Sousa, P.A.D., Dvorak, P.A., Freund, C., Firpo, M.-C., Furue, M.K., Gokhale, P., Ha, H.-Y., Han, E., Haupt, S., Healy, L., Hei, D.J., Hovatta, O., Hunt, C.E., Hwang, S.-M., Inamdar, M.S., Isasi, R.M., Jaconi, M., Jekerle, V., Kamthorn, P., Kibbey, M., Knezevic, I., Knowles, B.B., Koo, S.-K., Laâbi, Y., Leopoldo, L.P.M., Liu, P., Lomax, G.P., Loring, J.F., Ludwig, T.E., Montgomery, K. evin, Mummery, C.L., Nagy, A., Nakamura, Y., Nakatsuji, N., Oh, S., Oh, S.-K., Otonkoski, T., Pera, M., Peschanski, M., Pranke, P., Rajala, K.M., Rao, M.V.C., Ruttachuk, R., Reubinoff, B., Riccò, L., Rooke, H., Sipp, D., Stacey, G.N., Suemori, H., Takahashi, T.A., Takada, K., Talib, S., Tannenbaum, S.C., Yuan, B.-Z., Zeng, F.A., Zhou, Q., 2015. Points to consider in the development of seed stocks of pluripotent stem cells for clinical applications: International Stem Cell Banking Initiative (ISCBI). Regen. Med. 10, 1–44. https://doi.org/10.2217/rme.14.93

Andrews, P.W., Ben-David, U., Benvenisty, N., Coffey, P., Eggan, K., Knowles, B.B., Nagy, A., Pera, M., Reubinoff, B., Rugg-Gunn, P.J., Stacey, G.N., 2017. Assessing the Safety of Human Pluripotent Stem Cells and Their Derivatives for Clinical Applications. Stem Cell Rep. 9, 1–4. https://doi.org/10.1016/j.stemcr.2017.05.029

Andrews, P.W., Damjanov, I., Simon, D., Banting, G.S., Carlin, C., Dracopoli, N.C., Føgh, J., 1984. Pluripotent embryonal carcinoma clones derived from the human teratocarcinoma cell line Tera-2. Differentiation in vivo and in vitro. Lab. Investig. J. Tech. Methods Pathol. 50, 147–162.

Andrews, P.W., Matin, M.M., Bahrami, A.R., Damjanov, I., Gokhale, P., Draper, J.S., 2005. Embryonic stem (ES) cells and embryonal carcinoma (EC) cells: opposite sides of the same coin. Biochem. Soc. Trans. 33, 1526–1530. https://doi.org/10.1042/BST0331526

Aoi, T., 2016. 10th anniversary of iPS cells: the challenges that lie ahead. J. Biochem. (Tokyo) 160, 121–129. https://doi.org/10.1093/jb/mvw044

Artzt, K., Dubois, P., Bennett, D., Condamine, H., Babinet, C., Jacob, F., 1973. Surface Antigens Common to Mouse Cleavage Embryos and Primitive Teratocarcinoma Cells in Culture. Proc. Natl. Acad. Sci. U. S. A. 70, 2988–2992.

Ascari, I.J., Martins, S.C., Camargo, L.S.A., Mendez-Otero, R., Jasmin, null, 2018. Development of bovine embryos in vitro in coculture with murine mesenchymal stem cells and embryonic fibroblasts. Mol. Biol. Rep. https://doi.org/10.1007/s11033-018-4329-y

Asprer, J.S.T., Lakshmipathy, U., 2015. Current Methods and Challenges in the Comprehensive Characterization of Human Pluripotent Stem Cells. Stem Cell Rev. Rep. 11, 357–372. https://doi.org/10.1007/s12015-014-9580-6

Asthana, A., Kisaalita, W.S., 2012. Microtissue size and hypoxia in HTS with 3D cultures. Drug Discov. Today 17, 810–817. https://doi.org/10.1016/j.drudis.2012.03.004

Atwood, C.S., Meethal, S.V., 2016. The Spatiotemporal Hormonal Orchestration of Human Folliculogenesis,

Early Embryogenesis and Blastocyst Implantation. Mol. Cell. Endocrinol. https://doi.org/10.1016/j.mce.2016.03.039
Aulehla, A., Pourquié, O., 2010. Signaling Gradients during Paraxial Mesoderm Development. Cold Spring Harb. Perspect. Biol. 2, a000869. https://doi.org/10.1101/cshperspect.a000869
Avior, Y., Biancotti, J.C., Benvenisty, N., 2015. TeratoScore: Assessing the Differentiation Potential of Human Pluripotent Stem Cells by Quantitative Expression Analysis of Teratomas. Stem Cell Rep. 4, 967–974. https://doi.org/10.1016/j.stemcr.2015.05.006
Baillie-Johnson, P., van den Brink, S.C., Balayo, T., Turner, D.A., Martinez Arias, A., 2015. Generation of Aggregates of Mouse Embryonic Stem Cells that Show Symmetry Breaking, Polarization and Emergent Collective Behaviour In Vitro. J. Vis. Exp. JoVE. https://doi.org/10.3791/53252
Baker, B.M., Chen, C.S., 2012. Deconstructing the third dimension: how 3D culture microenvironments alter cellular cues. J. Cell Sci. 125, 3015–3024. https://doi.org/10.1242/jcs.079509
Bauwens, C., Yin, T., Dang, S., Peerani, R., Zandstra, P.W., 2005. Development of a perfusion fed bioreactor for embryonic stem cell-derived cardiomyocyte generation: oxygen-mediated enhancement of cardiomyocyte output. Biotechnol. Bioeng. 90, 452–461. https://doi.org/10.1002/bit.20445
Bhagavatula, R., Fickus, M., Kelly, W., Guo, C., Ozolek, J.A., Castro, C.A., Kovačević, J., 2010. AUTOMATIC IDENTIFICATION AND DELINEATION OF GERM LAYER COMPONENTS IN H&E STAINED IMAGES OF TERATOMAS DERIVED FROM HUMAN AND NONHUMAN PRIMATE EMBRYONIC STEM CELLS. Proc. IEEE Int. Symp. Biomed. Imaging Nano Macro IEEE Int. Symp. Biomed. Imaging 2010, 1041–1044. https://doi.org/10.1109/ISBI.2010.5490168
Bhattarai, D.P., Aguilar, L.E., Park, C.H., Kim, C.S., 2018. A Review on Properties of Natural and Synthetic Based Electrospun Fibrous Materials for Bone Tissue Engineering. Membranes 8. https://doi.org/10.3390/membranes8030062
Bigdeli, N., Karlsson, C., Strehl, R., Concaro, S., Hyllner, J., Lindahl, A., 2009. Coculture of human embryonic stem cells and human articular chondrocytes results in significantly altered phenotype and improved chondrogenic differentiation. Stem Cells Dayt. Ohio 27, 1812–1821. https://doi.org/10.1002/stem.114
Bisson, F., Rochefort, É., Lavoie, A., Larouche, D., Zaniolo, K., Simard-Bisson, C., Damour, O., Auger, F.A., Guérin, S.L., Germain, L., 2013. Irradiated Human Dermal Fibroblasts Are as Efficient as Mouse Fibroblasts as a Feeder Layer to Improve Human Epidermal Cell Culture Lifespan. Int. J. Mol. Sci. 14, 4684–4704. https://doi.org/10.3390/ijms14034684
Blanpain, C., Fuchs, E., 2008. Epidermal Stem Cells of the Skin. Annu Rev Cell Dev Biol.
Blom, R.A.M., Erni, S.T., Krempaská, K., Schaerer, O., Dijk, R.M. van, Amacker, M., Moser, C., Hall, S.R.R., Garnier, C. von, Blank, F., 2016. A Triple Co-Culture Model of the Human Respiratory Tract to Study Immune-Modulatory Effects of Liposomes and Virosomes. PLOS ONE 11, e0163539. https://doi.org/10.1371/journal.pone.0163539
Bogdanowicz, D.R., Lu, H.H., 2013. Studying cell-cell communication in co-culture. Biotechnol. J. 8, 395–396. https://doi.org/10.1002/biot.201300054
Borowiak, M., Maehr, R., Chen, S., Chen, A.E., Tang, W., Fox, J.O., Schreiber, S.L., Melton, D.A., 2009. Small molecules efficiently direct endodermal differentiation of mouse and human embryonic stem cells. Cell Stem Cell 4, 348–358. https://doi.org/10.1016/j.stem.2009.01.014
Bouma, M.J., van Iterson, M., Janssen, B., Mummery, C.L., Salvatori, D.C.F., Freund, C., 2017. Differentiation-Defective Human Induced Pluripotent Stem Cells Reveal Strengths and Limitations of the Teratoma Assay and In Vitro Pluripotency Assays. Stem Cell Rep. 8, 1340–1353. https://doi.org/10.1016/j.stemcr.2017.03.009
Brazma, A., Hingamp, P., Quackenbush, J., Sherlock, G., Spellman, P., Stoeckert, C., Aach, J., Ansorge, W., Ball, C.A., Causton, H.C., Gaasterland, T., Glenisson, P., Holstege, F.C., Kim, I.F., Markowitz, V., Matese, J.C., Parkinson, H., Robinson, A., Sarkans, U., Schulze-Kremer, S., Stewart, J., Taylor, R., Vilo, J., Vingron, M., 2001. Minimum information about a microarray experiment (MIAME)-toward standards for microarray data. Nat. Genet. 29, 365–371. https://doi.org/10.1038/ng1201-365
Brimble, S.N., Sherrer, E.S., Uhl, E.W., Wang, E., Kelly, S., Merrill, A.H., Robins, A.J., Schulz, T.C., 2007. The cell surface glycosphingolipids SSEA-3 and SSEA-4 are not essential for human ESC pluripotency. Stem Cells Dayt. Ohio 25, 54–62. https://doi.org/10.1634/stemcells.2006-0232
Brivanlou, A.H., Gage, F.H., Jaenisch, R., Jessell, T., Melton, D., Rossant, J., 2003. Setting Standards for Human Embryonic Stem Cells. Science 300, 913–916. https://doi.org/10.1126/science.1082940
Brons, I.G.M., Smithers, L.E., Trotter, M.W.B., Rugg-Gunn, P., Sun, B., Chuva de Sousa Lopes, S.M., Howlett, S.K., Clarkson, A., Ahrlund-Richter, L., Pedersen, R.A., Vallier, L., 2007. Derivation of pluripotent epiblast stem cells from mammalian embryos. Nature 448, 191–195. https://doi.org/10.1038/nature05950
Buta, C., David, R., Dressel, R., Emgård, M., Fuchs, C., Gross, U., Healy, L., Hescheler, J., Kolar, R., Martin, U., Mikkers, H., Müller, F.-J., Schneider, R.K., Seiler, A.E.M., Spielmann, H., Weitzer, G., 2013. Reconsidering pluripotency tests: Do we still need teratoma assays? Stem Cell Res. 11, 552–562. https://doi.org/10.1016/j.scr.2013.03.001
Cahan, P., Daley, G.Q., 2013. Origins and implications of pluripotent stem cell variability and heterogeneity. Nat. Rev. Mol. Cell Biol. 14, 357–368. https://doi.org/10.1038/nrm3584

Caliari, S.R., Burdick, J.A., 2016. A Practical Guide to Hydrogels for Cell Culture. Nat. Methods 13, 405–414. https://doi.org/10.1038/nmeth.3839
Cannatella, D.C., de Sa, R.O., 1993. Xenopus Laevis as a Model Organism. Syst. Biol. 42, 476–507. https://doi.org/10.1093/sysbio/42.4.476
Carlsson, J., Nederman, T., 1989. Tumour spheroid technology in cancer therapy research. Eur. J. Cancer Clin. Oncol. 25, 1127–1133. https://doi.org/10.1016/0277-5379(89)90404-5
Cavaliere, G., 2017. A 14-day limit for bioethics: the debate over human embryo research. BMC Med. Ethics 18, 38. https://doi.org/10.1186/s12910-017-0198-5
Centeno, E.G.Z., Cimarosti, H., Bithell, A., 2018. 2D versus 3D human induced pluripotent stem cell-derived cultures for neurodegenerative disease modelling. Mol. Neurodegener. 13. https://doi.org/10.1186/s13024-018-0258-4
Cerdan, C., McIntyre, B.A.S., Mechael, R., Levadoux-Martin, M., Yang, J., Lee, J.B., Bhatia, M., 2012. Activin A Promotes Hematopoietic Fated Mesoderm Development Through Upregulation of Brachyury in Human Embryonic Stem Cells. Stem Cells Dev. 21, 2866–2877. https://doi.org/10.1089/scd.2012.0053
Chadwick, K., Wang, L., Li, L., Menendez, P., Murdoch, B., Rouleau, A., Bhatia, M., 2003. Cytokines and BMP-4 promote hematopoietic differentiation of human embryonic stem cells. Blood 102, 906–915. https://doi.org/10.1182/blood-2003-03-0832
Chen, K.G., Mallon, B.S., McKay, R.D.G., Robey, P.G., 2014. Human Pluripotent Stem Cell Culture: Considerations for Maintenance, Expansion, and Therapeutics. Cell Stem Cell 14, 13–26. https://doi.org/10.1016/j.stem.2013.12.005
Chiu, D.T., deMello, A.J., Di Carlo, D., Doyle, P.S., Hansen, C., Maceiczyk, R.M., Wootton, R.C.R., 2017. Small but Perfectly Formed? Successes, Challenges, and Opportunities for Microfluidics in the Chemical and Biological Sciences. Chem 2, 201–223. https://doi.org/10.1016/j.chempr.2017.01.009
Cimetta, E., Sirabella, D., Yeager, K., Davidson, K., Simon, J., Moon, R.T., Vunjak-Novakovic, G., 2013. Microfluidic bioreactor for dynamic regulation of early mesodermal commitment in human pluripotent stem cells. Lab. Chip 13, 355–364. https://doi.org/10.1039/C2LC40836H
Clark, R.A., McCoy, G.A., Folkvord, J.M., McPherson, J.M., 1997. TGF-beta 1 stimulates cultured human fibroblasts to proliferate and produce tissue-like fibroplasia: a fibronectin matrix-dependent event. - PubMed - NCBI [WWW Document]. J. Cell Physiol. URL https://www.ncbi.nlm.nih.gov/pubmed/9012786 (accessed 6.13.19).
Clarke, K.E., Tams, D.M., Henderson, A.P., Roger, M.F., Whiting, A., Przyborski, S.A., 2017. A robust and reproducible human pluripotent stem cell derived model of neurite outgrowth in a three-dimensional culture system and its application to study neurite inhibition. Neurochem. Int. 106, 74–84. https://doi.org/10.1016/j.neuint.2016.12.009
Cooke, M.J., Stojkovic, M., Przyborski, S.A., 2006. Growth of teratomas derived from human pluripotent stem cells is influenced by the graft site. Stem Cells Dev. 15, 254–259. https://doi.org/10.1089/scd.2006.15.254
Coppe, J.P., Desprez, P.-Y., Krtolica, A., Campisi, J., 2014. The Senescence-Associated Secretory Phenotype: The Dark Side of Tumor Suppression. Annu Rev Pathol.
Cosson, S., Lutolf, M.P., 2014. Hydrogel microfluidics for the patterning of pluripotent stem cells. Sci. Rep. 4, 4462. https://doi.org/10.1038/srep04462
Costello, L., Fullard, N., Roger, M., Bradbury, S., Dicolandrea, T., Isfort, R., Bascom, C., Przyborski, S., 2019. Engineering a Multilayered Skin Equivalent: The Importance of Endogenous Extracellular Matrix Maturation to Provide Robustness and Reproducibility, in: Böttcher-Haberzeth, S., Biedermann, T. (Eds.), Skin Tissue Engineering: Methods and Protocols, Methods in Molecular Biology. Springer New York, New York, NY, pp. 107–122. https://doi.org/10.1007/978-1-4939-9473-1_9
Courau, T., Bonnereau, J., Chicoteau, J., Bottois, H., Remark, R., Assante Miranda, L., Toubert, A., Blery, M., Aparicio, T., Allez, M., Le Bourhis, L., 2019. Cocultures of human colorectal tumor spheroids with immune cells reveal the therapeutic potential of MICA/B and NKG2A targeting for cancer treatment. J. Immunother. Cancer 7, 74. https://doi.org/10.1186/s40425-019-0553-9
Crook, J.M., Hei, D., Stacey, G., 2010. The International Stem Cell Banking Initiative (ISCBI): raising standards to bank on. Vitro Cell. Dev. Biol. - Anim. 46, 169–172. https://doi.org/10.1007/s11626-010-9301-7
Csete, M., 2005. Oxygen in the cultivation of stem cells. Ann. N. Y. Acad. Sci. 1049, 1–8. https://doi.org/10.1196/annals.1334.001
Cukierman, E., Pankov, R., Yamada, K.M., 2002. Cell interactions with three-dimensional matrices. Curr. Opin. Cell Biol. 14, 633–640. https://doi.org/10.1016/S0955-0674(02)00364-2
Cunningham, T.J., Duester, G., 2015. Mechanisms of retinoic acid signalling and its roles in organ and limb development. Nat. Rev. Mol. Cell Biol. 16, 110–123. https://doi.org/10.1038/nrm3932
Cyranoski, D., 2018. 'Reprogrammed' stem cells implanted into patient with Parkinson's disease. Nature. https://doi.org/10.1038/d41586-018-07407-9
Cyranoski, D., 2017. Japanese man is first to receive "reprogrammed" stem cells from another person. Nat. News. https://doi.org/10.1038/nature.2017.21730

Dang, S.M., Kyba, M., Perlingeiro, R., Daley, G.Q., Zandstra, P.W., 2002. Efficiency of embryoid body formation and hematopoietic development from embryonic stem cells in different culture systems. Biotechnol. Bioeng. 78, 442–453.

Daud, M.F.B., Pawar, K.C., Claeyssens, F., Ryan, A.J., Haycock, J.W., 2012. An aligned 3D neuronal-glial co-culture model for peripheral nerve studies. Biomaterials 33, 5901–5913. https://doi.org/10.1016/j.biomaterials.2012.05.008

Davidson, K.C., Mason, E.A., Pera, M.F., 2015. The pluripotent state in mouse and human. Development 142, 3090–3099. https://doi.org/10.1242/dev.116061

Davies, E.J., Dong, M., Gutekunst, M., Närhi, K., van Zoggel, H.J.A.A., Blom, S., Nagaraj, A., Metsalu, T., Oswald, E., Erkens-Schulze, S., Delgado San Martin, J.A., Turkki, R., Wedge, S.R., af Hällström, T.M., Schueler, J., van Weerden, W.M., Verschuren, E.W., Barry, S.T., van der Kuip, H., Hickman, J.A., 2015. Capturing complex tumour biology *in vitro*: histological and molecular characterisation of precision cut slices. Sci. Rep. 5, 17187. https://doi.org/10.1038/srep17187

Dawud, R.A., Schreiber, K., Schomburg, D., Adjaye, J., 2012. Human Embryonic Stem Cells and Embryonal Carcinoma Cells Have Overlapping and Distinct Metabolic Signatures. PLOS ONE 7, e39896. https://doi.org/10.1371/journal.pone.0039896

De Los Angeles, A., Ferrari, F., Xi, R., Fujiwara, Y., Benvenisty, N., Deng, H., Hochedlinger, K., Jaenisch, R., Lee, S., Leitch, H.G., Lensch, M.W., Lujan, E., Pei, D., Rossant, J., Wernig, M., Park, P.J., Daley, G.Q., 2015. Hallmarks of pluripotency. Nature 525, 469–478. https://doi.org/10.1038/nature15515

Delivopoulos, E., Shakesheff, K.M., Peto, H., 2015. Neuralization of mouse embryonic stem cells in alginate hydrogels under retinoic acid and SAG treatment. Conf. Proc. Annu. Int. Conf. IEEE Eng. Med. Biol. Soc. IEEE Eng. Med. Biol. Soc. Annu. Conf. 2015, 3525–3528. https://doi.org/10.1109/EMBC.2015.7319153

Desbaillets, I., Ziegler, U., Groscurth, P., Gassmann, M., 2000a. Embryoid bodies: an in vitro model of mouse embryogenesis. Exp. Physiol. 85, 645–651.

Desbaillets, I., Ziegler, U., Groscurth, P., Gassmann, M., 2000b. Embryoid Bodies: An *In Vitro* Model of Mouse Embryogenesis. Exp. Physiol. 85, 645–651. https://doi.org/10.1111/j.1469-445X.2000.02104.x

DeSesso, J.M., 2017. Future of developmental toxicity testing. Curr. Opin. Toxicol., Risk Assessment in Toxicology - relevance of experimental toxicology in human safety evaluation 3, 1–5. https://doi.org/10.1016/j.cotox.2017.04.001

DeWitt, N., 2002. Biologists divided over proposal to create human–mouse embryos. Nature 420, 255–255. https://doi.org/10.1038/420255a

Doetschman, T.C., Eistetter, H., Katz, M., Schmidt, W., Kemler, R., 1985. The in vitro development of blastocyst-derived embryonic stem cell lines: formation of visceral yolk sac, blood islands and myocardium. J. Embryol. Exp. Morphol. 87, 27–45.

Dressel, R., 2011. Effects of histocompatibility and host immune responses on the tumorigenicity of pluripotent stem cells. Semin. Immunopathol. 33, 573–591. https://doi.org/10.1007/s00281-011-0266-8

Driskell, R.R., Lichtenberger, B.M., Hoste, E., Kretzschmar, K., Simons, B.D., Charalambous, M., Ferron, S.R., Herault, Y., Pavlovic, G., Ferguson-Smith, A.C., Watt, F.M., 2013. Distinct fibroblast lineages determine dermal architecture in skin development and repair. Nature 504, 277–281. https://doi.org/10.1038/nature12783

Drury, J.L., Mooney, D.J., 2003. Hydrogels for tissue engineering: scaffold design variables and applications. Biomaterials, Synthesis of Biomimetic Polymers 24, 4337–4351. https://doi.org/10.1016/S0142-9612(03)00340-5

Dunwoodie, S.L., 2009. The Role of Hypoxia in Development of the Mammalian Embryo. Dev. Cell 17, 755–773. https://doi.org/10.1016/j.devcel.2009.11.008

Duran, C., Talley, P.J., Walsh, J., Pigott, C., Morton, I.E., Andrews, P.W., 2001. Hybrids of pluripotent and nullipotent human embryonal carcinoma cells: Partial retention of a pluripotent phenotype. Int. J. Cancer 93, 324–332. https://doi.org/10.1002/ijc.1355

Dvash, T., Ben-Yosef, D., Eiges, R., 2006. Human embryonic stem cells as a powerful tool for studying human embryogenesis. Pediatr. Res. 60, 111–117. https://doi.org/10.1203/01.pdr.0000228349.24676.17

Eiraku, M., Takata, N., Ishibashi, H., Kawada, M., Sakakura, E., Okuda, S., Sekiguchi, K., Adachi, T., Sasai, Y., 2011. Self-organizing optic-cup morphogenesis in three-dimensional culture. Nature 472, 51–56. https://doi.org/10.1038/nature09941

Eiselleova, L., Matulka, K., Kriz, V., Kunova, M., Schmidtova, Z., Neradil, J., Tichy, B., Dvorakova, D., Pospisilova, S., Hampl, A., Dvorak, P., 2009. A complex role for FGF-2 in self-renewal, survival, and adhesion of human embryonic stem cells. Stem Cells Dayt. Ohio 27, 1847–1857. https://doi.org/10.1002/stem.128

El-Sherbiny, I.M., Yacoub, M.H., 2013. Hydrogel scaffolds for tissue engineering: Progress and challenges. Glob. Cardiol. Sci. Pract. 2013, 316–342. https://doi.org/10.5339/gcsp.2013.38

Erceg, S., Mateo, E.M., Zipancic, I., Rodríguez Jiménez, F.J., Pérez Aragó, M.A., Jiménez, M., Soria, J.M., Garcia-Esparza, M.Á., 2019. Assessment of Toxic Effects of Ochratoxin A in Human Embryonic Stem Cells. Toxins 11. https://doi.org/10.3390/toxins11040217

Evans, M., 1981. Origin of mouse embryonal carcinoma cells and the possibility of their direct isolation into tissue culture.
Evans, M.J., Kaufman, M.H., 1981. Establishment in culture of pluripotential cells from mouse embryos. Nature 292, 154–156.
Fathollahipour, S., Patil, P.S., Leipzig, N.D., 2018. Oxygen Regulation in Development: Lessons from Embryogenesis towards Tissue Engineering. Cells Tissues Organs 1–22. https://doi.org/10.1159/000493162
Fenderson, B.A., De Miguel, M.P., Pyle, A.D., Donovan, P.J., 2006. Staining embryonic stem cells using monoclonal antibodies to stage-specific embryonic antigens. Methods Mol. Biol. Clifton NJ 325, 207–224. https://doi.org/10.1385/1-59745-005-7:207
Fernandes, S., Shinde, P., Khan, N., Singh, S., Vardhan, S., Nair, V., Kale, V., Limaye, L., 2017. Derivation of human iPSC line NCCSi002-A from umbilical cord blood (UCB) CD34+cells of donor from Indian ethnicity. Stem Cell Res. 26, 80–83. https://doi.org/10.1016/j.scr.2017.12.006
Fink, S.L., Cookson, B.T., 2005. Apoptosis, Pyroptosis, and Necrosis: Mechanistic Description of Dead and Dying Eukaryotic Cells. Infect. Immun. 73, 1907–1916. https://doi.org/10.1128/IAI.73.4.1907-1916.2005
Flach, E.H., Rebecca, V.W., Herlyn, M., Smalley, K.S.M., Anderson, A.R.A., 2011. Fibroblasts contribute to melanoma tumour growth and drug resistance. Mol. Pharm. 8, 2039–2049. https://doi.org/10.1021/mp200421k
Flamier, A., Singh, S., Rasmussen, T.P., 2017. A standardized human embryoid body platform for the detection and analysis of teratogens. PLOS ONE 12, e0171101. https://doi.org/10.1371/journal.pone.0171101
Freyer, C., Renfree, M.B., 2009. The mammalian yolk sac placenta. J. Exp. Zoolog. B Mol. Dev. Evol. 312, 545–554. https://doi.org/10.1002/jez.b.21239
Fuchs, C., Scheinast, M., Pasteiner, W., Lagger, S., Hofner, M., Hoellrigl, A., Schultheis, M., Weitzer, G., 2012. Self-organization phenomena in embryonic stem cell-derived embryoid bodies: axis formation and breaking of symmetry during cardiomyogenesis. Cells Tissues Organs 195, 377–391. https://doi.org/10.1159/000328712
Gagliano, O., Luni, C., Wei, Q., Bertin, E., Elvassore, N., 2019. Microfluidic reprogramming to pluripotency of human somatic cells | Springer Nature Experiments [WWW Document]. URL https://experiments.springernature.com/articles/10.1038/s41596-018-0108-4 (accessed 6.6.19).
Garland, R., Kaneria, S., Hancock, J., Steward, C., Rowbottom, A., 1999. The use of Teflon cell culture bags to expand functionally active CD8+ cytotoxic T lymphocytes [WWW Document]. J. Immunol. Methods. URL https://www.ncbi.nlm.nih.gov/pubmed/10485254 (accessed 2.3.17).
Gassmann, M., Fandrey, J., Bichet, S., Wartenberg, M., Marti, H.H., Bauer, C., Wenger, R.H., Acker, H., 1996. Oxygen supply and oxygen-dependent gene expression in differentiating embryonic stem cells. Proc. Natl. Acad. Sci. 93, 2867–2872.
Gerlach, J.C., Hout, M., Edsbagge, J., Björquist, P., Lübberstedt, M., Miki, T., Stachelscheid, H., Schmelzer, E., Schatten, G., Zeilinger, K., 2010a. Dynamic 3D Culture Promotes Spontaneous Embryonic Stem Cell Differentiation In Vitro. Tissue Eng. Part C Methods 16, 115–121. https://doi.org/10.1089/ten.tec.2008.0654
Gerlach, J.C., Lübberstedt, M., Edsbagge, J., Ring, A., Hout, M., Baun, M., Rossberg, I., Knöspel, F., Peters, G., Eckert, K., Wulf-Goldenberg, A., Björquist, P., Stachelscheid, H., Urbaniak, T., Schatten, G., Miki, T., Schmelzer, E., Zeilinger, K., 2010b. Interwoven Four-Compartment Capillary Membrane Technology for Three-Dimensional Perfusion with Decentralized Mass Exchange to Scale Up Embryonic Stem Cell Culture. Cells Tissues Organs 192, 39–49. https://doi.org/10.1159/000291014
Ghalia, M.A., Dahman, Y., 2016. Chapter 6 - Advanced nanobiomaterials in tissue engineering: Synthesis, properties, and applications, in: Grumezescu, A.M. (Ed.), Nanobiomaterials in Soft Tissue Engineering. William Andrew Publishing, pp. 141–172. https://doi.org/10.1016/B978-0-323-42865-1.00006-4
Giandomenico, S.L., Mierau, S.B., Gibbons, G.M., Wenger, L.M.D., Masullo, L., Sit, T., Sutcliffe, M., Boulanger, J., Tripodi, M., Derivery, E., Paulsen, O., Lakatos, A., Lancaster, M.A., 2019. Cerebral organoids at the air–liquid interface generate diverse nerve tracts with functional output. Nat. Neurosci. 22, 669. https://doi.org/10.1038/s41593-019-0350-2
Gilbert, S.F., 2000. Early Mammalian Development. Dev. Biol. 6th Ed.
Giobbe, G.G., Michielin, F., Luni, C., Giulitti, S., Martewicz, S., Dupont, S., Floreani, A., Elvassore, N., 2015. Functional differentiation of human pluripotent stem cells on a chip. Nat. Methods 12, 637–640. https://doi.org/10.1038/nmeth.3411
Gleadall, A., Visscher, D., Yang, J., Thomas, D., Segal, J., 2018. Review of additive manufactured tissue engineering scaffolds: relationship between geometry and performance. Burns Trauma 6, 19. https://doi.org/10.1186/s41038-018-0121-4
Goers, L., Freemont, P., Polizzi, K.M., 2014. Co-culture systems and technologies: taking synthetic biology to the next level. J. R. Soc. Interface 11. https://doi.org/10.1098/rsif.2014.0065
Goncalves, K., 2017. Development of Novel Stem Cell Based Neurite Outgrowth Models and their Application to Study Neurite Inhibition in Neurological Disorders. Durham University.

González, S., Ibáñez, E., Santaló, J., 2010. Establishment of mouse embryonic stem cells from isolated blastomeres and whole embryos using three derivation methods. J. Assist. Reprod. Genet. 27, 671–682. https://doi.org/10.1007/s10815-010-9473-9

Gothard, D., Roberts, S.J., Shakesheff, K.M., Buttery, L.D., 2009. Controlled embryoid body formation via surface modification and avidin–biotin cross-linking. Cytotechnology 61, 135–144. https://doi.org/10.1007/s10616-010-9255-3

Grapin-Botton, A., Melton, D.A., 2000. Endoderm development: from patterning to organogenesis. Trends Genet. 16, 124–130. https://doi.org/10.1016/S0168-9525(99)01957-5

Griffith, L.G., Swartz, M.A., 2006. Capturing complex 3D tissue physiology in vitro. Nat. Rev. Mol. Cell Biol. 7, 211–224. https://doi.org/10.1038/nrm1858

Grinspan, J., Reeves, M., Coulaloglou, M., Nathanson, D., Pleasure, D., 1996. Re-entry into the cell cycle is required for bFGF-induced oligodendroglial dedifferentiation and survival. J Neurosci Res.

Groebe, K., Mueller-Klieser, W., 1996. On the relation between size of necrosis and diameter of tumor spheroids. Int. J. Radiat. Oncol. 34, 395–401. https://doi.org/10.1016/0360-3016(95)02065-9

Gropp, M., Shilo, V., Vainer, G., Gov, M., Gil, Y., Khaner, H., Matzrafi, L., Idelson, M., Kopolovic, J., Zak, N.B., Reubinoff, B.E., 2012. Standardization of the Teratoma Assay for Analysis of Pluripotency of Human ES Cells and Biosafety of Their Differentiated Progeny. PLOS ONE 7, e45532. https://doi.org/10.1371/journal.pone.0045532

Gupta, S., Mishra, N., Dhasmana, A., 2017. Decellularization Methods for Scaffold Fabrication | Springer Nature Experiments [WWW Document]. URL https://experiments.springernature.com/articles/10.1007/7651_2017_34 (accessed 5.17.19).

Gutierrez-Aranda, I., Ramos-Mejia, V., Bueno, C., Munoz-Lopez, M., Real, P.J., Mácia, A., Sanchez, L., Ligero, G., Garcia-Parez, J.L., Menendez, P., 2010. Human Induced Pluripotent Stem Cells Develop Teratoma More Efficiently and Faster Than Human Embryonic Stem Cells Regardless the Site of Injection. Stem Cells Dayt. Ohio 28, 1568–1570. https://doi.org/10.1002/stem.471

Henderson, J.K., Draper, J.S., Baillie, H.S., Fishel, S., Thomson, J.A., Moore, H., Andrews, P.W., 2002. Preimplantation human embryos and embryonic stem cells show comparable expression of stage-specific embryonic antigens. Stem Cells Dayt. Ohio 20, 329–337. https://doi.org/10.1634/stemcells.20-4-329

Hentze, H., Soong, P.L., Wang, S.T., Phillips, B.W., Putti, T.C., Dunn, N.R., 2009. Teratoma formation by human embryonic stem cells: Evaluation of essential parameters for future safety studies. Stem Cell Res. 2, 198–210. https://doi.org/10.1016/j.scr.2009.02.002

Hill, D.S., Robinson, N.D.P., Caley, M.P., Chen, M., O'Toole, E.A., Armstrong, J.L., Przyborski, S., Lovat, P.E., 2015. A Novel Fully Humanized 3D Skin Equivalent to Model Early Melanoma Invasion. Mol. Cancer Ther. https://doi.org/10.1158/1535-7163.MCT-15-0394

Ho, H.-Y., Moffat, R.C., Patel, R.V., Awah, F.N., Baloue, K., Crowe, D.L., 2010. Embryoid body attachment to reconstituted basement membrane induces a genetic program of epithelial differentiation via jun N-terminal kinase signaling. Stem Cell Res. 5, 144–156. https://doi.org/10.1016/j.scr.2010.06.001

Holloway, E.M., Capeling, M.M., Spence, J.R., 2019. Biologically inspired approaches to enhance human organoid complexity. Development 146, dev166173. https://doi.org/10.1242/dev.166173

Höpfl, G., Gassmann, M., Desbaillets, I., 2004. Differentiating Embryonic Stem Cells into Embryoid Bodies, in: Schatten, H. (Ed.), Germ Cell Protocols, Methods in Molecular Biology™. Humana Press, pp. 79–98. https://doi.org/10.1385/1-59259-741-6:079

Horrocks, G.M., 2007. Signalling events controlling early cell fate decisions in a human embryonal carcinoma cell line, with relation to neural versus non-neural transitions m human ectoderm development (Doctoral). Durham University.

Hosoya, A., Kwak, S., Kim, E., Lunny, D., Lane, E., Cho, S., Jung, H., 2010. Immunohistochemical localization of cytokeratins in the junctional region of ectoderm and endoderm. - PubMed - NCBI. Anat Rec (Hoboken).

Hough, S.R., Laslett, A.L., Grimmond, S.B., Kolle, G., Pera, M.F., 2009. A Continuum of Cell States Spans Pluripotency and Lineage Commitment in Human Embryonic Stem Cells. PLOS ONE 4, e7708. https://doi.org/10.1371/journal.pone.0007708

Hovatta, O., Rodin, S., Antonsson, L., Tryggvason, K., 2014. Concise Review: Animal Substance-Free Human Embryonic Stem Cells Aiming at Clinical Applications. Stem Cells Transl. Med. 3, 1269–1274. https://doi.org/10.5966/sctm.2014-0129

Huang, B., Ning, S., Zhuang, L., Jiang, C., Cui, Y., Fan, G., Qin, L., Liu, J., 2015. Ethanol Inactivated Mouse Embryonic Fibroblasts Maintain the Self-Renew and Proliferation of Human Embryonic Stem Cells. PLOS ONE 10, e0130332. https://doi.org/10.1371/journal.pone.0130332

Hultman, I., Björk, L., Blomberg, E., Sandstedt, B., Ährlund-Richter, L., 2014. Experimental teratoma: At the crossroad of fetal- and onco-development. Semin. Cancer Biol., Oncofetal signaling as a target for cancer therapy 29, 75–79. https://doi.org/10.1016/j.semcancer.2014.08.005

Hyun, I., Taylor, P., Testa, G., Dickens, B., Jung, K.W., McNab, A., Robertson, J., Skene, L., Zoloth, L., 2007. Ethical Standards for Human-to-Animal Chimera Experiments in Stem Cell Research. Cell Stem Cell 1, 159–163. https://doi.org/10.1016/j.stem.2007.07.015

International Stem Cell Initiative, 2018. Assessment of established techniques to determine developmental and malignant potential of human pluripotent stem cells. Nat. Commun. 9, 1925. https://doi.org/10.1038/s41467-018-04011-3

International Stem Cell Initiative, Adewumi, O., Aflatoonian, B., Ahrlund-Richter, L., Amit, M., Andrews, P.W., Beighton, G., Bello, P.A., Benvenisty, N., Berry, L.S., Bevan, S., Blum, B., Brooking, J., Chen, K.G., Choo, A.B.H., Churchill, G.A., Corbel, M., Damjanov, I., Draper, J.S., Dvorak, P., Emanuelsson, K., Fleck, R.A., Ford, A., Gertow, K., Gertsenstein, M., Gokhale, P.J., Hamilton, R.S., Hampl, A., Healy, L.E., Hovatta, O., Hyllner, J., Imreh, M.P., Itskovitz-Eldor, J., Jackson, J., Johnson, J.L., Jones, M., Kee, K., King, B.L., Knowles, B.B., Lako, M., Lebrin, F., Mallon, B.S., Manning, D., Mayshar, Y., McKay, R.D.G., Michalska, A.E., Mikkola, M., Mileikovsky, M., Minger, S.L., Moore, H.D., Mummery, C.L., Nagy, A., Nakatsuji, N., O'Brien, C.M., Oh, S.K.W., Olsson, C., Otonkoski, T., Park, K.-Y., Passier, R., Patel, H., Patel, M., Pedersen, R., Pera, M.F., Piekarczyk, M.S., Pera, R.A.R., Reubinoff, B.E., Robins, A.J., Rossant, J., Rugg-Gunn, P., Schulz, T.C., Semb, H., Sherrer, E.S., Siemen, H., Stacey, G.N., Stojkovic, M., Suemori, H., Szatkiewicz, J., Turetsky, T., Tuuri, T., van den Brink, S., Vintersten, K., Vuoristo, S., Ward, D., Weaver, T.A., Young, L.A., Zhang, W., 2007. Characterization of human embryonic stem cell lines by the International Stem Cell Initiative. Nat. Biotechnol. 25, 803–816. https://doi.org/10.1038/nbt1318

Irie, N., Kuratani, S., 2014. The developmental hourglass model: a predictor of the basic body plan? Development 141, 4649–4655. https://doi.org/10.1242/dev.107318

Isasi, R., Knoppers, B.M., 2011. From Banking to International Governance: Fostering Innovation in Stem Cell Research. Stem Cells Int. 2011. https://doi.org/10.4061/2011/498132

Isasi, R., Namorado, J., Mah, N., Bultjer, N., Kurtz, A., 2019. A pathway for attesting ethical provenance of cell lines: Lessons from the European human pluripotent stem cell registry (hPSCreg). Stem Cell Res. 40, 101539. https://doi.org/10.1016/j.scr.2019.101539

Ishikawa, S., Ishimori, K., Ito, S., 2017. A 3D epithelial–mesenchymal co-culture model of human bronchial tissue recapitulates multiple features of airway tissue remodeling by TGF-β1 treatment. Respir. Res. 18, 195. https://doi.org/10.1186/s12931-017-0680-0

Itskovitz-Eldor, J., Schuldiner, M., Karsenti, D., Eden, A., Yanuka, O., Amit, M., Soreq, H., Benvenisty, N., 2000. Differentiation of human embryonic stem cells into embryoid bodies compromising the three embryonic germ layers. Mol. Med. Camb. Mass 6, 88–95.

Iwata, K., Yumoto, K., Sugishima, M., Mizoguchi, C., Kai, Y., Iba, Y., Mio, Y., 2014. Analysis of compaction initiation in human embryos by using time-lapse cinematography. J. Assist. Reprod. Genet. 31, 421–426. https://doi.org/10.1007/s10815-014-0195-2

Jamil, S., Cedervall, J., Hultman, I., Ali, R., Margaryan, N.V., Rasmuson, A., Johnsen, J.I., Sveinbjörnsson, B., Dalianis, T., Kanter, L., Orrego, A., Strizzi, L., Hendrix, M.J.C., Sandstedt, B., Kogner, P., Ahrlund-Richter, L., 2013. Neuroblastoma cells injected into experimental mature teratoma reveal a tropism for embryonic loose mesenchyme. Int. J. Oncol. 43, 831–838. https://doi.org/10.3892/ijo.2013.2014

Jammalamadaka, U., Tappa, K., 2018. Recent Advances in Biomaterials for 3D Printing and Tissue Engineering. J. Funct. Biomater. 9. https://doi.org/10.3390/jfb9010022

Jennings, B., 2011. Drosophila – a versatile model in biology & medicine - ScienceDirect [WWW Document]. URL https://www.sciencedirect.com/science/article/pii/S1369702111701134 (accessed 5.18.19).

Jeong, S.-Y., Lee, J.-H., Shin, Y., Chung, S., Kuh, H.-J., 2016. Co-Culture of Tumor Spheroids and Fibroblasts in a Collagen Matrix-Incorporated Microfluidic Chip Mimics Reciprocal Activation in Solid Tumor Microenvironment. PLOS ONE 11, e0159013. https://doi.org/10.1371/journal.pone.0159013

Joshi, P., Lee, M.-Y., 2015. High Content Imaging (HCI) on Miniaturized Three-Dimensional (3D) Cell Cultures. Biosensors 5, 768–790. https://doi.org/10.3390/bios5040768

Jun, I., Han, H.-S., Edwards, J.R., Jeon, H., 2018. Electrospun Fibrous Scaffolds for Tissue Engineering: Viewpoints on Architecture and Fabrication. Int. J. Mol. Sci. 19. https://doi.org/10.3390/ijms19030745

Kaiser, A., Kale, A., Novozhilova, E., Olivius, P., 2019. The effects of Matrigel® on the survival and differentiation of a human neural progenitor dissociated sphere culture. Anat. Rec. Hoboken NJ 2007. https://doi.org/10.1002/ar.24131

Karp, J.M., Ferreira, L.S., Khademhosseini, A., Kwon, A.H., Yeh, J., Langer, R.S., 2006. Cultivation of human embryonic stem cells without the embryoid body step enhances osteogenesis in vitro. Stem Cells Dayt. Ohio 24, 835–843. https://doi.org/10.1634/stemcells.2005-0383

Kiecker, C., Lumsden, A., 2005. Compartments and their boundaries in vertebrate brain development. Nat. Rev. Neurosci. 6, 553. https://doi.org/10.1038/nrn1702

Kim, J.-H., Kurtz, A., Yuan, B.-Z., Zeng, F., Lomax, G., Loring, J.F., Crook, J., Ju, J.H., Clarke, L., Inamdar, M.S., Pera, M., Firpo, M.T., Sheldon, M., Rahman, N., O'Shea, O., Pranke, P., Zhou, Q., Isasi, R., Rungsiwiwut, R., Kawamata, S., Oh, S., Ludwig, T., Masui, T., Novak, T.J., Takahashi, T., Fujibuchi, W., Koo, S.K., Stacey, G.N., 2017. Report of the International Stem Cell Banking Initiative Workshop Activity: Current Hurdles and Progress in Seed-Stock Banking of Human Pluripotent Stem Cells. STEM CELLS Transl. Med. 6, 1956–1962. https://doi.org/10.1002/sctm.17-0144

Kim, Y., Rim, Y.A., Yi, H., Park, N., Park, S.-H., Ju, J.H., 2016. The Generation of Human Induced Pluripotent Stem Cells from Blood Cells: An Efficient Protocol Using Serial Plating of Reprogrammed Cells by Centrifugation. Stem Cells Int. 2016. https://doi.org/10.1155/2016/1329459

Knight, E., 2014. Influence of the Micro-Environment on the Maintenance and Differentiation of Pluripotent Stem Cells. Durham University.

Knöspel, F., Freyer, N., Stecklum, M., Gerlach, J.C., Zeilinger, K., 2016. Periodic harvesting of embryonic stem cells from a hollow-fiber membrane based four-compartment bioreactor. Biotechnol. Prog. 32, 141–151. https://doi.org/10.1002/btpr.2182

Kowalski, M.P., Yoder, A., Liu, L., Pajak, L., 2012. Controlling Embryonic Stem Cell Growth and Differentiation by Automation: Enhanced and More Reliable Differentiation for Drug Discovery. J. Biomol. Screen. 17, 1171–1179. https://doi.org/10.1177/1087057112452783

Kropp, C., Kempf, H., Halloin, C., Robles-Diaz, D., Franke, A., Scheper, T., Kinast, K., Knorpp, T., Joos, T.O., Haverich, A., Martin, U., Zweigerdt, R., Olmer, R., 2016. Impact of Feeding Strategies on the Scalable Expansion of Human Pluripotent Stem Cells in Single-Use Stirred Tank Bioreactors. Stem Cells Transl. Med. 5, 1289–1301. https://doi.org/10.5966/sctm.2015-0253

Kumari, D., 2016. States of Pluripotency: Naïve and Primed Pluripotent Stem Cells | IntechOpen [WWW Document]. URL https://www.intechopen.com/books/pluripotent-stem-cells-from-the-bench-to-the-clinic/states-of-pluripotency-na-ve-and-primed-pluripotent-stem-cells (accessed 1.3.20).

Kumazaki, T., Takahashi, T., Matsuo, T., Kamada, M., Mitsui, Y., 2014. Re-emergence of undifferentiated cells from transplants of human induced pluripotent stem cells as a possible risk factor of tumourigenesis. Cell Biology International Reports.

Kurosawa, H., 2007. Methods for inducing embryoid body formation: in vitro differentiation system of embryonic stem cells. J. Biosci. Bioeng. 103, 389–398. https://doi.org/10.1263/jbb.103.389

Kusindarta, D.L., Wihadmadyatami, H., 2018. The Role of Extracellular Matrix in Tissue Regeneration. Tissue Regen. https://doi.org/10.5772/intechopen.75728

Kyrylkova, K., Kyryachenko, S., Leid, M., Kioussi, C., 2012. Detection of apoptosis by TUNEL assay. Methods Mol. Biol. Clifton NJ 887, 41–47. https://doi.org/10.1007/978-1-61779-860-3_5

Lach, M.S., Kulcenty, K., Jankowska, K., Trzeciak, T., Richter, M., Suchorska, W.M., 2018. Effect of cellular mass on chondrogenic differentiation during embryoid body formation. Mol. Med. Rep. https://doi.org/10.3892/mmr.2018.9272

Lam, M.T., Longaker, M.T., 2012. Comparison of several attachment methods for human iPS, embryonic and adipose-derived stem cells for tissue engineering. J. Tissue Eng. Regen. Med. 6, s80–s86. https://doi.org/10.1002/term.1499

Lancaster, M.A., Knoblich, J.A., 2014a. Organogenesis in a dish: Modeling development and disease using organoid technologies. Science 345, 1247125. https://doi.org/10.1126/science.1247125

Lancaster, M.A., Knoblich, J.A., 2014b. Generation of Cerebral Organoids from Human Pluripotent Stem Cells. Nat. Protoc. 9, 2329–2340. https://doi.org/10.1038/nprot.2014.158

Lancaster, M.A., Renner, M., Martin, C.-A., Wenzel, D., Bicknell, L.S., Hurles, M.E., Homfray, T., Penninger, J.M., Jackson, A.P., Knoblich, J.A., 2013. Cerebral organoids model human brain development and microcephaly. Nature 501, 373–379. https://doi.org/10.1038/nature12517

Lazzari, G., Nicolas, V., Matsusaki, M., Akashi, M., Couvreur, P., Mura, S., 2018. Multicellular spheroid based on a triple co-culture: A novel 3D model to mimic pancreatic tumor complexity. Acta Biomater. 78, 296–307. https://doi.org/10.1016/j.actbio.2018.08.008

Lee, A.S., Tang, C., Cao, F., Xie, X., van der Bogt, K., Hwang, A., Connolly, A.J., Robbins, R.C., Wu, J.C., 2009. Effects of cell number on teratoma formation by human embryonic stem cells. Cell Cycle Georget. Tex 8, 2608–2612. https://doi.org/10.4161/cc.8.16.9353

Lei, X., Deng, Z., Zhang, H., Zhao, H., Zhou, J., Liu, S., Chen, Q., Ning, L., Cao, Y., Wang, X., Zhang, X., Duan, E., 2014. Rotary Suspension Culture Enhances Mesendoderm Differentiation of Embryonic Stem Cells Through Modulation of Wnt/β-catenin Pathway. Stem Cell Rev. Rep. 10, 526–538. https://doi.org/10.1007/s12015-014-9511-6

Lensch, M.W., Schlaeger, T.M., Zon, L.I., Daley, G.Q., 2007. Teratoma formation assays with human embryonic stem cells: a rationale for one type of human-animal chimera. Cell Stem Cell 1, 253–258. https://doi.org/10.1016/j.stem.2007.07.019

Leung, M.C.K., Williams, P.L., Benedetto, A., Au, C., Helmcke, K.J., Aschner, M., Meyer, J.N., 2008. Caenorhabditis elegans: An Emerging Model in Biomedical and Environmental Toxicology. Toxicol. Sci. 106, 5–28. https://doi.org/10.1093/toxsci/kfn121

Li, H., Jiang, H., Zhang, B., Feng, J., 2018. Modeling Parkinson's Disease Using Patient-specific Induced Pluripotent Stem Cells. J. Park. Dis. 8, 479–493. https://doi.org/10.3233/JPD-181353

Li, L., Song, L., Liu, C., Chen, J., Peng, G., Wang, R., Liu, P., Tang, K., Rossant, J., Jing, N., 2015. Ectodermal progenitors derived from epiblast stem cells by inhibition of Nodal signaling. J. Mol. Cell Biol. 7, 455–465. https://doi.org/10.1093/jmcb/mjv030

Lijuan, W., Liu, X., Yu, H., Zhou, F., Chen, H., Liu, Q., 2014. [Integrins mediate the migration of HepG2 cells induced by low shear stress]. Sheng Wu Yi Xue Gong Cheng Xue Za Zhi J. Biomed. Eng. Shengwu Yixue Gongchengxue Zazhi 31, 336–340.

Liu, X., Huang, J., Chen, T., Wang, Y., Xin, S., Li, J., Pei, G., Kang, J., 2008. Yamanaka factors critically regulate the developmental signaling network in mouse embryonic stem cells. Cell Res. 18, 1177–1189. https://doi.org/10.1038/cr.2008.309

Liu, Y., Lu, H., 2016. Microfluidics in Systems Biology – Hype or Truly Useful? Curr. Opin. Biotechnol. 39, 215–220. https://doi.org/10.1016/j.copbio.2016.04.020

Lopez-Lazaro, M., 2015. The migration ability of stem cells can explain the existence of cancer of unknown primary site. Rethinking metastasis [WWW Document]. Oncoscience. URL https://www.ncbi.nlm.nih.gov/pmc/articles/PMC4468332/ (accessed 6.13.19).

Low Serum Growth Supplement (LSGS) and LSGS Kit [WWW Document], 2019. . Fish. Sci. UK. URL https://www.thermofisher.com/document-connect/document-connect.html?url=https%3A%2F%2Fassets.thermofisher.com%2FTFS-Assets%2FLSG%2Fmanuals%2FLSGS__LSGS_Kit_man.pdf&title=TG93IFNlcnVtIEdyb3d0aCBTdXBwbGVtZW50IChMU0dTKSBhbmQgTFNHUyBLaXQ= (accessed 6.16.19).

Luni, C., Giulitti, S., Serena, E., Ferrari, L., Zambon, A., Gagliano, O., Giobbe, G.G., Michielin, F., Knöbel, S., Bosio, A., Elvassore, N., 2016. High-efficiency cellular reprogramming with microfluidics. Nat. Methods 13, 446–452. https://doi.org/10.1038/nmeth.3832

Luo, Y., Zhu, D., Xu, X., Ge, L., Sun, X., Chen, G., Chen, Y., 2018. Generation of an induced pluripotent stem cell line from an adult male with 45,X/46,XY mosaicism. Stem Cell Res. 27, 42–45. https://doi.org/10.1016/j.scr.2018.01.003

MacDonald, C., Finlay, D.B., Jabed, A., Glass, M., Graham, E.S., 2014. Development of positive control tissue for in situ hybridisation using Alvetex scaffolds. J. Neurosci. Methods 238, 70–77. https://doi.org/10.1016/j.jneumeth.2014.09.006

Maehr, R., Chen, S., Snitow, M., Ludwig, T., Yagasaki, L., Goland, R., Leibel, R.L., Melton, D.A., 2009. Generation of pluripotent stem cells from patients with type 1 diabetes. Proc. Natl. Acad. Sci. U. S. A. 106, 15768–15773. https://doi.org/10.1073/pnas.0906894106

Majety, M., Pradel, L.P., Gies, M., Ries, C.H., 2015. Fibroblasts Influence Survival and Therapeutic Response in a 3D Co-Culture Model. PLOS ONE 10, e0127948. https://doi.org/10.1371/journal.pone.0127948

Mansergh, F.C., Daly, C.S., Hurley, A.L., Wride, M.A., Hunter, S.M., Evans, M.J., 2009. Gene expression profiles during early differentiation of mouse embryonic stem cells. BMC Dev. Biol. 9, 5. https://doi.org/10.1186/1471-213X-9-5

Mansour, A.A., Gonçalves, J.T., Bloyd, C.W., Li, H., Fernandes, S., Quang, D., Johnston, S., Parylak, S.L., Jin, X., Gage, F.H., 2018. An in vivo model of functional and vascularized human brain organoids. Nat. Biotechnol. 36, 432–441. https://doi.org/10.1038/nbt.4127

Marrazzo, P., Maccari, S., Taddei, A., Bevan, L., Telford, J., Soriani, M., Pezzicoli, A., 2016. 3D Reconstruction of the Human Airway Mucosa In Vitro as an Experimental Model to Study NTHi Infections. PLOS ONE 11, e0153985. https://doi.org/10.1371/journal.pone.0153985

Martin, G.R., 1981. Isolation of a pluripotent cell line from early mouse embryos cultured in medium conditioned by teratocarcinoma stem cells. Proc. Natl. Acad. Sci. U. S. A. 78, 7634–7638.

Martin, G.R., 1980. Teratocarcinomas and mammalian embryogenesis. Science 209, 768–776.

Martin, G.R., 1975. Teratocarcinomas as a model system for the study of embryogenesis and neoplasia. Cell 5, 229–243. https://doi.org/10.1016/0092-8674(75)90098-7

Martin, G.R., Wiley, L.M., Damjanov, I., 1977. The development of cystic embryoid bodies in vitro from clonal teratocarcinoma stem cells. Dev. Biol. 61, 230–244. https://doi.org/10.1016/0012-1606(77)90294-9

Massumi, M., Abasi, M., Babaloo, H., Terraf, P., Safi, M., Saeed, M., Barzin, J., Zandi, M., Soleimani, M., 2012. The Effect of Topography on Differentiation Fates of Matrigel-Coated Mouse Embryonic Stem Cells Cultured on PLGA Nanofibrous Scaffolds. Tissue Eng. Part A 18, 609–620. https://doi.org/10.1089/ten.tea.2011.0368

Masuda, S., Yokoo, T., Sugimoto, N., Doi, M., Fujishiro, S., Takeuchi, K., Kobayashi, E., Hanazono, Y., 2012. A Simplified In Vitro Teratoma Assay for Pluripotent Stem Cells Injected Into Rodent Fetal Organs. Cell Med. 3, 103–112. https://doi.org/10.3727/215517912X639351

Matic, I., Antunovic, M., Brkic, S., Josipovic, P., Mihalic, K.C., Karlak, I., Ivkovic, A., Marijanovic, I., 2016. Expression of OCT-4 and SOX-2 in Bone Marrow-Derived Human Mesenchymal Stem Cells during Osteogenic Differentiation. Open Access Maced. J. Med. Sci. 4, 9–16. https://doi.org/10.3889/oamjms.2016.008

Mehta, G., Hsiao, A.Y., Ingram, M., Luker, G.D., Takayama, S., 2012. Opportunities and Challenges for use of Tumor Spheroids as Models to Test Drug Delivery and Efficacy. J. Control. Release Off. J. Control. Release Soc. 164, 192–204. https://doi.org/10.1016/j.jconrel.2012.04.045

Meier, F., Freyer, N., Brzeszczynska, J., Knöspel, F., Armstrong, L., Lako, M., Greuel, S., Damm, G., Ludwig-Schwellinger, E., Deschl, U., Ross, J.A., Beilmann, M., Zeilinger, K., 2017. Hepatic differentiation of human iPSCs in different 3D models: A comparative study. Int. J. Mol. Med. 40, 1759–1771. https://doi.org/10.3892/ijmm.2017.3190

Meng, X., Leslie, P., Zhang, Y., Dong, J., 2014. Stem cells in a three-dimensional scaffold environment. SpringerPlus 3. https://doi.org/10.1186/2193-1801-3-80

Merkle, F.T., Ghosh, S., Kamitaki, N., Mitchell, J., Avior, Y., Mello, C., Kashin, S., Mekhoubad, S., Ilic, D., Charlton, M., Saphier, G., Handsaker, R.E., Genovese, G., Bar, S., Benvenisty, N., McCarroll, S.A., Eggan, K., 2017. Human pluripotent stem cells recurrently acquire and expand dominant negative P53 mutations. Nature 545, 229–233. https://doi.org/10.1038/nature22312

Meyers, J.R., 2018. Zebrafish: Development of a Vertebrate Model Organism. Curr. Protoc. Essent. Lab. Tech. 16, e19. https://doi.org/10.1002/cpet.19

MIKOS, A.G., HERRING, S.W., OCHAREON, P., ELISSEEFF, J., LU, H.H., KANDEL, R., SCHOEN, F.J., TONER, M., MOONEY, D., ATALA, A., VAN DYKE, M.E., KAPLAN, D., VUNJAK-NOVAKOVIC, G., 2006. Engineering Complex Tissues. Tissue Eng. 12, 3307. https://doi.org/10.1089/ten.2006.12.3307

Morales, A.R., 2018. Oxygen Availability in Embryonic Development and Stem Cell Maintenance in Three-Dimensional Cell Culture. Durham University.

Mueller, T., Mueller, L.P., Luetzkendorf, J., Voigt, W., Simon, H., Schmoll, H.-J., 2006. Loss of Oct-3/4 Expression in Embryonal Carcinoma Cells Is Associated with Induction of Cisplatin Resistance. Tumor Biol. 27, 71–83. https://doi.org/10.1159/000092324

Müller, F.-J., Brändl, B., Loring, J.F., 2008. Assessment of human pluripotent stem cells with PluriTest, in: StemBook. Harvard Stem Cell Institute, Cambridge (MA).

Müller, F.-J., Goldmann, J., Löser, P., Loring, J.F., 2010a. A Call to Standardize Teratoma Assays Used to Define Human Pluripotent Cell Lines. Cell Stem Cell 6, 412–414. https://doi.org/10.1016/j.stem.2010.04.009

Müller, F.-J., Goldmann, J., Löser, P., Loring, J.F., 2010b. A call to standardize teratoma assays used to define human pluripotent cell lines. Cell Stem Cell 6, 412–414. https://doi.org/10.1016/j.stem.2010.04.009

Müller, F.-J., Schuldt, B.M., Williams, R., Mason, D., Altun, G., Papapetrou, E.P., Danner, S., Goldmann, J.E., Herbst, A., Schmidt, N.O., Aldenhoff, J.B., Laurent, L.C., Loring, J.F., 2011. A bioinformatic assay for pluripotency in human cells. Nat. Methods 8, 315–317. https://doi.org/10.1038/nmeth.1580

Mummery, C., Oostwaard, D.W., Doevendans, P., Spijker, R., Brink, S. van den, Hassink, R., Heyden, M. van der, Opthof, T., Pera, M., Riviere, A.B. de la, Passier, R., Tertoolen, L., 2003. Differentiation of Human Embryonic Stem Cells to Cardiomyocytes. Circulation 107, 2733–2740. https://doi.org/10.1161/01.CIR.0000068356.38592.68

Mummery, C., Ward, D., van den Brink, C., Bird, S., Doevendans, P., Opthof, T., de la Riviere, A.B., Tertoolen, L., van der Heyden, M., Pera, M., 2002. Cardiomyocyte differentiation of mouse and human embryonic stem cells. J. Anat. 200, 233–242. https://doi.org/10.1046/j.1469-7580.2002.00031.x

Murugesan, M., Premkumar, K., 2018. Hypoxia stimulates microenvironment in human embryonic stem cell through inflammatory signalling: An integrative analysis. Biochem. Biophys. Res. Commun. https://doi.org/10.1016/j.bbrc.2018.02.194

Nagy, A., Rossant, J., Nagy, R., Abramow-Newerly, W., Roder, J.C., 1993. Derivation of completely cell culture-derived mice from early-passage embryonic stem cells. Proc. Natl. Acad. Sci. U. S. A. 90, 8424–8428.

Natunen, S., Satomaa, T., Pitkänen, V., Salo, H., Mikkola, M., Natunen, J., Otonkoski, T., Valmu, L., 2011. The binding specificity of the marker antibodies Tra-1-60 and Tra-1-81 reveals a novel pluripotency-associated type 1 lactosamine epitope. Glycobiology 21, 1125–1130. https://doi.org/10.1093/glycob/cwq209

Nayak, S., Dey, S., Kundu, S.C., 2013. Skin Equivalent Tissue-Engineered Construct: Co-Cultured Fibroblasts/ Keratinocytes on 3D Matrices of Sericin Hope Cocoons. PLoS ONE 8. https://doi.org/10.1371/journal.pone.0074779

Nestor, M.W., Paull, D., Jacob, S., Sproul, A.A., Alsaffar, A., Campos, B.A., Noggle, S.A., 2013. Differentiation of serum-free embryoid bodies from human induced pluripotent stem cells into networks. Stem Cell Res. 10, 454–463. https://doi.org/10.1016/j.scr.2013.02.001

Ng, K., Grass, G., Lane, H., Borchardt, R.T., 1993. Characterization of the Unstirred Water Layer in Cultured Brain Microvessel Endothelial Cells. In Vitro Cell. Dev. Biol. Anim. 29A, 627–629. https://doi.org/10.2307/4294096

Niakan, K.K., Han, J., Pedersen, R.A., Simon, C., Pera, R.A.R., 2012. Human pre-implantation embryo development. Development 139, 829–841. https://doi.org/10.1242/dev.060426

Nichols, J., Smith, A., 2012. Pluripotency in the embryo and in culture. Cold Spring Harb. Perspect. Biol. 4, a008128. https://doi.org/10.1101/cshperspect.a008128

Nickel, W., 2011. The Unconventional Secretory Machinery of Fibroblast Growth Factor 2. Traffic 12, 799–805. https://doi.org/10.1111/j.1600-0854.2011.01187.x

O'Connor, M.D., Kardel, M.D., Iosfina, I., Youssef, D., Lu, M., Li, M.M., Vercauteren, S., Nagy, A., Eaves, C.J., 2008. Alkaline Phosphatase-Positive Colony Formation Is a Sensitive, Specific, and Quantitative Indicator of Undifferentiated Human Embryonic Stem Cells. STEM CELLS 26, 1109–1116. https://doi.org/10.1634/stemcells.2007-0801

Ojala, M., Rajala, K., Pekkanen-Mattila, M., Miettinen, M., Huhtala, H., Aalto-Setälä, K., 2012. Culture Conditions Affect Cardiac Differentiation Potential of Human Pluripotent Stem Cells. PLOS ONE 7,

e48659. https://doi.org/10.1371/journal.pone.0048659
Omole, A.E., Fakoya, A.O.J., 2018. Ten years of progress and promise of induced pluripotent stem cells: historical origins, characteristics, mechanisms, limitations, and potential applications. PeerJ 6, e4370. https://doi.org/10.7717/peerj.4370
Ortmann, D., Vallier, L., 2017. Variability of human pluripotent stem cell lines. Curr. Opin. Genet. Dev. 46, 179–185. https://doi.org/10.1016/j.gde.2017.07.004
Owens, D., 2015. Modelling the development of tissues in vitro from pluripotent stem cells.
Palmqvist, L., Glover, C.H., Hsu, L., Lu, M., Bossen, B., Piret, J.M., Humphries, R.K., Helgason, C.D., 2005. Correlation of Murine Embryonic Stem Cell Gene Expression Profiles with Functional Measures of Pluripotency. STEM CELLS 23, 663–680. https://doi.org/10.1634/stemcells.2004-0157
Park, J., Cho, C.H., Parashurama, N., Li, Y., Berthiaume, F., Toner, M., Tilles, A.W., Yarmush, M.L., 2007. Microfabrication-based modulation of embryonic stem cell differentiation. Lab. Chip 7, 1018–1028. https://doi.org/10.1039/b704739h
Park, T.S., Galic, Z., Conway, A.E., Lindgren, A., Van Handel, B.J., Magnusson, M., Richter, L., Teitell, M.A., Mikkola, H.K.A., Lowry, W.E., Plath, K., Clark, A.T., 2009a. Derivation of Primordial germ cells from Human Embryonic and Induced Pluripotent Stem Cells is significantly improved by co-culture with human fetal gonadal cells. Stem Cells Dayt. Ohio 27, 783–795. https://doi.org/10.1002/stem.13
Park, T.S., Galic, Z., Conway, A.E., Lindgren, A., Van Handel, B.J., Magnusson, M., Richter, L., Teitell, M.A., Mikkola, H.K.A., Lowry, W.E., Plath, K., Clark, A.T., 2009b. Derivation of Primordial germ cells from Human Embryonic and Induced Pluripotent Stem Cells is significantly improved by co-culture with human fetal gonadal cells. Stem Cells Dayt. Ohio 27, 783–795. https://doi.org/10.1002/stem.13
Pastuszak, Marek, Groszewski, K., Pastuszak, Malgorzata, Dyrla, P., Wotjun, S., Gil, J., 2015. Cytokeratins in gastroenterology. Systematic review. Prz Gastroenterol 10.
Patel, R., Alahmad, A.J., 2016. Growth-factor reduced Matrigel source influences stem cell derived brain microvascular endothelial cell barrier properties. Fluids Barriers CNS 13. https://doi.org/10.1186/s12987-016-0030-5
Pauklin, S., Pedersen, R.A., Vallier, L., 2011. Mouse pluripotent stem cells at a glance. J. Cell Sci. 124, 3727–3732. https://doi.org/10.1242/jcs.074120
Pazzano, D., Mercier, K.A., Moran, J.M., Fong, S.S., DiBiasio, D.D., Rulfs, J.X., Kohles, S.S., Bonassar, L.J., 2000. Comparison of Chondrogensis in Static and Perfused Bioreactor Culture. Biotechnol. Prog. 16, 893–896. https://doi.org/10.1021/bp000082v
Peng, X., Liu, T., Shi, C., Zhang, L., Wang, Y., Zhao, W., Jiang, L., Wu, M., Zhang, Y., Qian, Q., 2014. Germline Transmission of an Embryonic Stem Cell Line Derived from BALB/c Cataract Mice. PLOS ONE 9, e90707. https://doi.org/10.1371/journal.pone.0090707
Petersen, O.W., Rønnov-Jessen, L., Howlett, A.R., Bissell, M.J., 1992. Interaction with basement membrane serves to rapidly distinguish growth and differentiation pattern of normal and malignant human breast epithelial cells. Proc. Natl. Acad. Sci. U. S. A. 89, 9064–9068. https://doi.org/10.1073/pnas.89.19.9064
Pettinato, G., Wen, X., Zhang, N., 2015. Engineering Strategies for the Formation of Embryoid Bodies from Human Pluripotent Stem Cells. Stem Cells Dev. 24, 1595–1609. https://doi.org/10.1089/scd.2014.0427
Phillips, C.L., Combs, S.B., Pinnell, S.R., 1994. Effects of ascorbic acid on proliferation and collagen synthesis in relation to the donor age of human dermal fibroblasts. J. Invest. Dermatol. 103, 228–232.
Pleasure, S.J., Lee, V.M., 1993. NTera 2 cells: a human cell line which displays characteristics expected of a human committed neuronal progenitor cell. J. Neurosci. Res. 35, 585–602. https://doi.org/10.1002/jnr.490350603
Poh, Y.-C., Chen, Junwei, Hong, Y., Yi, H., Zhang, S., Chen, Junjian, Wu, D.C., Wang, L., Jia, Q., Singh, R., Yao, W., Tan, Y., Tajik, A., Tanaka, T.S., Wang, N., 2014. Generation of organized germ layers from a single mouse embryonic stem cell. Nat. Commun. 5, 4000. https://doi.org/10.1038/ncomms5000
Porter, A.G., Jänicke, R.U., 1999. Emerging roles of caspase-3 in apoptosis. Cell Death Differ. 6, 99–104. https://doi.org/10.1038/sj.cdd.4400476
Prokhorova, T.A., Harkness, L.M., Frandsen, U., Ditzel, N., Schrøder, H.D., Burns, J.S., Kassem, M., 2009. Teratoma formation by human embryonic stem cells is site dependent and enhanced by the presence of Matrigel. Stem Cells Dev. 18, 47–54. https://doi.org/10.1089/scd.2007.0266
Przyborski, S.A., 2005. Differentiation of Human Embryonic Stem Cells After Transplantation in Immune-Deficient Mice. STEM CELLS 23, 1242–1250. https://doi.org/10.1634/stemcells.2005-0014
Przyborski, S.A., 2001. Isolation of human embryonal carcinoma stem cells by immunomagnetic sorting. Stem Cells Dayt. Ohio 19, 500–504. https://doi.org/10.1634/stemcells.19-6-500
Przyborski, S.A., Christie, V.B., Hayman, M.W., Stewart, R., Horrocks, G.M., 2004. Human embryonal carcinoma stem cells: models of embryonic development in humans. Stem Cells Dev. 13, 400–408. https://doi.org/10.1089/scd.2004.13.400
Przyborski, S.A., Morton, I.E., Wood, A., Andrews, P.W., 2000. Developmental regulation of neurogenesis in the pluripotent human embryonal carcinoma cell line NTERA-2. Eur. J. Neurosci. 12, 3521–3528. https://doi.org/10.1046/j.1460-9568.2000.00230.x

Quelch, R., 2018. Dynamic Regulation of the Pluripotent Stem Cell Structure-Function Relationship through Topographical Cues. Durham University.
Raffel, M., Willert, C.E., Scarano, F., Kahler, C.J., Wereley, S.T., Kompenhans, J., 2018. Particle Image Velocimetry: A Practical Guide, 3rd ed. Springer International Publishing.
Rajala, K., Pekkanen-Mattila, M., Aalto-Setälä, K., 2011. Cardiac Differentiation of Pluripotent Stem Cells. Stem Cells Int. 2011. https://doi.org/10.4061/2011/383709
Raza, A., Colley, H.E., Baggaley, E., Sazanovich, I.V., Green, N.H., Weinstein, J.A., Botchway, S.W., MacNeil, S., Haycock, J.W., 2017. Oxygen Mapping of Melanoma Spheroids using Small Molecule Platinum Probe and Phosphorescence Lifetime Imaging Microscopy. Sci. Rep. 7, 10743. https://doi.org/10.1038/s41598-017-11153-9
Ren, Y., Ma, Z., Yu, T., Ling, M., Wang, H., 2018. Methanol fixed fibroblasts serve as feeder cells to maintain stem cells in the pluripotent state in vitro. Sci. Rep. 8, 7780. https://doi.org/10.1038/s41598-018-26238-2
Rhinn, M., Dollé, P., 2012. Retinoic acid signalling during development. Dev. Camb. Engl. 139, 843–858. https://doi.org/10.1242/dev.065938
Rivron, N.C., Frias-Aldeguer, J., Vrij, E.J., Boisset, J.-C., Korving, J., Vivié, J., Truckenmüller, R.K., Oudenaarden, A. van, Blitterswijk, C.A. van, Geijsen, N., 2018. Blastocyst-like structures generated solely from stem cells. Nature 557, 106. https://doi.org/10.1038/s41586-018-0051-0
Roger, M., Fullard, N., Costello, L., Bradbury, S., Markiewicz, E., O'Reilly, S., Darling, N., Ritchie, P., Määttä, A., Karakesisoglou, I., Nelson, G., von Zglinicki, T., Dicolandrea, T., Isfort, R., Bascom, C., Przyborski, S., 2019. Bioengineering the microanatomy of human skin. J. Anat. 234, 438–455. https://doi.org/10.1111/joa.12942
Rohani, L., Karbalaie, K., Vahdati, A., Hatami, M., Nasr-Esfahani, M.H., Baharvand, H., 2008. Embryonic stem cell sphere: a controlled method for production of mouse embryonic stem cell aggregates for differentiation. Int. J. Artif. Organs 31, 258–265.
Rossant, J., 2015. Mouse and human blastocyst-derived stem cells: vive les differences. Development 142, 9–12. https://doi.org/10.1242/dev.115451
Rossant, J., Tam, P.P.L., 2009. Blastocyst lineage formation, early embryonic asymmetries and axis patterning in the mouse. Development 136, 701–713. https://doi.org/10.1242/dev.017178
Rouwkema, J., Koopman, B., Blitterswijk, C., Dhert, W., Malda, J., 2010. Supply of nutrients to cells in engineered tissues. Biotechnol. Genet. Eng. Rev. 26, 163–178.
Russell, S.B., Russell, J.D., Trupin, K.M., 1981. Collagen synthesis in human fibroblasts: effects of ascorbic acid and regulation by hydrocortisone. J. Cell. Physiol. 109, 121–131. https://doi.org/10.1002/jcp.1041090114
Sailon, A.M., Allori, A.C., Davidson, E.H., Reformat, D.D., Allen, R.J., Warren, S.M., 2009. A Novel Flow-Perfusion Bioreactor Supports 3D Dynamic Cell Culture. J. Biomed. Biotechnol. 2009. https://doi.org/10.1155/2009/873816
Salimi, A., Nadri, S., Ghollasi, M., Khajeh, K., Soleimani, M., 2014. Comparison of different protocols for neural differentiation of human induced pluripotent stem cells. Mol. Biol. Rep. 41, 1713–1721. https://doi.org/10.1007/s11033-014-3020-1
Sathananthan, H., Menezes, J., Gunasheela, S., 2003. Mechanics of human blastocyst hatching in vitro. Reprod. Biomed. Online 7, 228–234.
Sato, T., Vries, R.G., Snippert, H.J., van de Wetering, M., Barker, N., Stange, D.E., van Es, J.H., Abo, A., Kujala, P., Peters, P.J., Clevers, H., 2009. Single Lgr5 stem cells build crypt–villus structures *in vitro* without a mesenchymal niche. Nature 459, 262–265. https://doi.org/10.1038/nature07935
Schmelzer, E., Triolo, F., Turner, M.E., Thompson, R.L., Zeilinger, K., Reid, L.M., Gridelli, B., Gerlach, J.C., 2010. Three-dimensional perfusion bioreactor culture supports differentiation of human fetal liver cells. Tissue Eng. Part A 16, 2007–2016. https://doi.org/10.1089/ten.TEA.2009.0569
Schnerch, A., Cerdan, C., Bhatia, M., 2010. Distinguishing Between Mouse and Human Pluripotent Stem Cell Regulation: The Best Laid Plans of Mice and Men. STEM CELLS N/A-N/A. https://doi.org/10.1002/stem.298
Schuldiner, M., Yanuka, O., Itskovitz-Eldor, J., Melton, D.A., Benvenisty, N., 2000. Effects of eight growth factors on the differentiation of cells derived from human embryonic stem cells. Proc. Natl. Acad. Sci. U. S. A. 97, 11307–11312. https://doi.org/10.1073/pnas.97.21.11307
Schutte, M., Fox, B., Baradez, M.-O., Devonshire, A., Minguez, J., Bokhari, M., Przyborski, S., Marshall, D., 2011. Rat primary hepatocytes show enhanced performance and sensitivity to acetaminophen during three-dimensional culture on a polystyrene scaffold designed for routine use. Assay Drug Dev. Technol. 9, 475–486. https://doi.org/10.1089/adt.2011.0371
Schwartz, P.H., Brick, D.J., Nethercott, H.E., Stover, A.E., 2011. Traditional Human Embryonic Stem Cell Culture. Methods Mol. Biol. Clifton NJ 767, 107–123. https://doi.org/10.1007/978-1-61779-201-4_8
Sekiya, S., Kawata, M., Iwasawa, H., Inaba, N., Sugita, M., Suzuki, N., Motoyama, T., Yamamoto, T., Takamizawa, H., 1985. Characterization of human embryonal carcinoma cell lines derived from testicular germ-cell tumors. Differentiation 29, 259–267. https://doi.org/10.1111/j.1432-0436.1985.tb00325.x

Shafa, M., Krawetz, R., Zhang, Y., Rattner, J.B., Godollei, A., Duff, H.J., Rancourt, D.E., 2011. Impact of stirred suspension bioreactor culture on the differentiation of murine embryonic stem cells into cardiomyocytes. BMC Cell Biol. 12, 53. https://doi.org/10.1186/1471-2121-12-53

Shahbazi, M.N., Jedrusik, A., Vuoristo, S., Recher, G., Hupalowska, A., Bolton, V., Fogarty, N.M.E., Campbell, A., Devito, L.G., Ilic, D., Khalaf, Y., Niakan, K.K., Fishel, S., Zernicka-Goetz, M., 2016. Self-organization of the human embryo in the absence of maternal tissues. Nat. Cell Biol. 18, 700–708. https://doi.org/10.1038/ncb3347

Shahbazi, M.N., Scialdone, A., Skorupska, N., Weberling, A., Recher, G., Zhu, M., Jedrusik, A., Devito, L.G., Noli, L., Macaulay, I.C., Buecker, C., Khalaf, Y., Ilic, D., Voet, T., Marioni, J.C., Zernicka-Goetz, M., 2017. Pluripotent state transitions coordinate morphogenesis in mouse and human embryos. Nature. https://doi.org/10.1038/nature24675

Sheridan, S.D., Surampudi, V., Rao, R.R., 2012. Analysis of Embryoid Bodies Derived from Human Induced Pluripotent Stem Cells as a Means to Assess Pluripotency. Stem Cells Int. 2012, e738910. https://doi.org/10.1155/2012/738910

Shiraki, N., Umeda, K., Sakashita, N., Takeya, M., Kume, K., Kume, S., 2008. Differentiation of mouse and human embryonic stem cells into hepatic lineages. Genes Cells 13, 731–746. https://doi.org/10.1111/j.1365-2443.2008.01201.x

Simon, M.C., Keith, B., 2008. The role of oxygen availability in embryonic development and stem cell function. Nat. Rev. Mol. Cell Biol. 9, 285–296. https://doi.org/10.1038/nrm2354

Simunovic, M., Brivanlou, A.H., 2017. Embryoids, organoids and gastruloids: new approaches to understanding embryogenesis. Dev. Camb. Engl. 144, 976–985. https://doi.org/10.1242/dev.143529

Singh, V.K., Saini, A., Kalsan, M., Kumar, N., Chandra, R., 2016. Describing the Stem Cell Potency: The Various Methods of Functional Assessment and In silico Diagnostics. Front. Cell Dev. Biol. 4. https://doi.org/10.3389/fcell.2016.00134

Smith, S.C., Reuhl, K.R., Craig, J., McBurney, M.W., 1987. The role of aggregation in embryonal carcinoma cell differentiation. J. Cell. Physiol. 131, 74–84. https://doi.org/10.1002/jcp.1041310112

Son, M.-Y., Kim, H., Kim, M.-J., Cho, Y.S., 2011. Physical Passaging of Embryoid Bodies Generated from Human Pluripotent Stem Cells. PLOS ONE 6, e19134. https://doi.org/10.1371/journal.pone.0019134

Sorrell, J.M., Baber, M.A., Caplan, A.I., 2007. A Self-Assembled Fibroblast-Endothelial Cell Co-Culture System That Supports in vitro Vasculogenesis by both Human Umbilical Vein Endothelial Cells and Human Dermal Microvascular Endothelial Cells. Cells Tissues Organs 186, 157–168. https://doi.org/10.1159/000106670

Sorrell, J.M., Caplan, A.I., 2004. Fibroblast heterogeneity: more than skin deep. J. Cell Sci. 117, 667–675. https://doi.org/10.1242/jcs.01005

Sottile, V., Thomson, A., McWhir, J., 2003. In Vitro Osteogenic Differentiation of Human ES Cells. Cloning Stem Cells 5, 149–155. https://doi.org/10.1089/153623003322234759

Soundararajan, M., Kannan, S., 2018. Fibroblasts and mesenchymal stem cells: Two sides of the same coin? - PubMed - NCBI [WWW Document]. J. Cell Physiol. URL https://www.ncbi.nlm.nih.gov/pubmed/29943820 (accessed 6.13.19).

Spivak, C.E., Oz, M., Beglan, C.L., Shrager, R.I., 2006. Diffusion delays and unstirred layer effects at monolayer cultures of Chinese hamster ovary cells: radioligand binding, confocal microscopy, and mathematical simulations. Cell Biochem. Biophys. 45, 43–58. https://doi.org/10.1385/CBB:45:1:43

Stachelscheid, H., Wulf-Goldenberg, A., Eckert, K., Jensen, J., Edsbagge, J., Björquist, P., Rivero, M., Strehl, R., Jozefczuk, J., Prigione, A., Adjaye, J., Urbaniak, T., Bussmann, P., Zeilinger, K., Gerlach, J.C., 2013. Teratoma formation of human embryonic stem cells in three-dimensional perfusion culture bioreactors. J. Tissue Eng. Regen. Med. 7, 729–741. https://doi.org/10.1002/term.1467

Steele, C.E., 1991. Whole embryo culture and teratogenesis. Hum. Reprod. 6, 144–147. https://doi.org/10.1093/oxfordjournals.humrep.a137249

Stern, M., Gierse, A., Tan, S., Bicker, G., 2014. Human Ntera2 cells as a predictive in vitro test system for developmental neurotoxicity. Arch. Toxicol. 88, 127–136. https://doi.org/10.1007/s00204-013-1098-1

Stevanato, L., Hicks, C., Sinden, J.D., 2015. Differentiation of a Human Neural Stem Cell Line on Three Dimensional Cultures, Analysis of MicroRNA and Putative Target Genes. JoVE J. Vis. Exp. e52410. https://doi.org/10.3791/52410

Stevens, L.C., 1970. The development of transplantable teratocarcinomas from intratesticular grafts of pre- and postimplantation mouse embryos. Dev. Biol. 21, 364–382. https://doi.org/10.1016/0012-1606(70)90130-2

Stevens, L.C., Little, C.C., 1954. Spontaneous Testicular Teratomas in an Inbred Strain of Mice. Proc. Natl. Acad. Sci. U. S. A. 40, 1080–1087.

Stevens, L.C., Varnum, D.S., 1974. The development of teratomas from parthenogenetically activated ovarian mouse eggs. Dev. Biol. 37, 369–380. https://doi.org/10.1016/0012-1606(74)90155-9

Stover, A.E., Schwartz, P.H., 2011. Adaptation of Human Pluripotent Stem Cells to Feeder-Free Conditions in Chemically Defined Medium with Enzymatic Single-Cell Passaging. Methods Mol. Biol. Clifton NJ 767, 137–146. https://doi.org/10.1007/978-1-61779-201-4_10

Strelchenko, N., Verlinsky, O., Kukharenko, V., Verlinsky, Y., 2004. Morula-derived human embryonic stem cells. Reprod. Biomed. Online 9, 623–629.
Strüver, K., Friess, W., Hedtrich, S., 2017. Development of a Perfusion Platform for Dynamic Cultivation of in vitro Skin Models. Skin Pharmacol. Physiol. 30, 180–189. https://doi.org/10.1159/000476071
Stunova, A., Vistejnova, L., 2018. Dermal fibroblasts—A heterogeneous population with regulatory function in wound healing. Cytokine Growth Factor Rev. 39, 137–150. https://doi.org/10.1016/j.cytogfr.2018.01.003
Suga, H., Kadoshima, T., Minaguchi, M., Ohgushi, M., Soen, M., Nakano, T., Takata, N., Wataya, T., Muguruma, K., Miyoshi, H., Yonemura, S., Oiso, Y., Sasai, Y., 2011. Self-formation of functional adenohypophysis in three-dimensional culture. Nature 480, 57–62. https://doi.org/10.1038/nature10637
Sulzbacher, S., Schroeder, I.S., Truong, T.T., Wobus, A.M., 2009. Activin A-Induced Differentiation of Embryonic Stem Cells into Endoderm and Pancreatic Progenitors—The Influence of Differentiation Factors and Culture Conditions. Stem Cell Rev. Rep. 5, 159–173. https://doi.org/10.1007/s12015-009-9061-5
Sun, X., Fu, X., Han, W., Zhao, Y., Liu, H., Sheng, Z., 2011. Dedifferentiation of human terminally differentiating keratinocytes into their precursor cells induced by basic fibroblast growth factor. Biol Pharm Bull.
Takahashi, K., Tanabe, K., Ohnuki, M., Narita, M., Ichisaka, T., Tomoda, K., Yamanaka, S., 2007. Induction of pluripotent stem cells from adult human fibroblasts by defined factors. Cell 131, 861–872. https://doi.org/10.1016/j.cell.2007.11.019
Takahashi, K., Yamanaka, S., 2006. Induction of pluripotent stem cells from mouse embryonic and adult fibroblast cultures by defined factors. Cell 126, 663–676. https://doi.org/10.1016/j.cell.2006.07.024
Takasato, M., Er, P.X., Becroft, M., Vanslambrouck, J.M., Stanley, E.G., Elefanty, A.G., Little, M.H., 2014. Directing human embryonic stem cell differentiation towards a renal lineage generates a self-organizing kidney. Nat. Cell Biol. 16, 118–126. https://doi.org/10.1038/ncb2894
Takasato, M., Little, M.H., 2016. A strategy for generating kidney organoids: Recapitulating the development in human pluripotent stem cells. Dev. Biol. https://doi.org/10.1016/j.ydbio.2016.08.024
Tam, P.P.L., Behringer, R.R., 1997. Mouse gastrulation: the formation of a mammalian body plan. Mech. Dev. 68, 3–25. https://doi.org/10.1016/S0925-4773(97)00123-8
Tamm, C., Pijuan Galitó, S., Annerén, C., 2013. A Comparative Study of Protocols for Mouse Embryonic Stem Cell Culturing. PLoS ONE 8. https://doi.org/10.1371/journal.pone.0081156
Tao, H., Chen, X., Wei, A., Song, X., Wang, W., Liang, L., Zhao, Q., Han, Zhibo, Han, Zhongchao, Wang, X., Li, Z., 2018. Comparison of Teratoma Formation between Embryonic Stem Cells and Parthenogenetic Embryonic Stem Cells by Molecular Imaging [WWW Document]. Stem Cells Int. https://doi.org/10.1155/2018/7906531
Telpalo-Carpio, S., Aguilar-Yañez, J., Gonzalez-Garza, M., Cruz-Vega, D., Moreno-Cuevas, J., 2013. iPS cells generation: an overview of techniques and methods. J. Stem Cells Regen. Med. 9, 2–8.
Teo, A.K.K., Ali, Y., Wong, K.Y., Chipperfield, H., Sadasivam, A., Poobalan, Y., Tan, E.K., Wang, S.T., Abraham, S., Tsuneyoshi, N., Stanton, L.W., Dunn, N.R., 2012. Activin and BMP4 Synergistically Promote Formation of Definitive Endoderm in Human Embryonic Stem Cells. STEM CELLS 30, 631–642. https://doi.org/10.1002/stem.1022
The 3Rs | NC3Rs [WWW Document], 2019. URL https://www.nc3rs.org.uk/the-3rs (accessed 2.19.18).
Thomson, J.A., Itskovitz-Eldor, J., Shapiro, S.S., Waknitz, M.A., Swiergiel, J.J., Marshall, V.S., Jones, J.M., 1998. Embryonic stem cell lines derived from human blastocysts. Science 282, 1145–1147.
Tibbitt, M.W., Anseth, K.S., 2009. Hydrogels as extracellular matrix mimics for 3D cell culture. Biotechnol. Bioeng. 103, 655–663. https://doi.org/10.1002/bit.22361
Tielens, S., Verhasselt, B., Liu, J., Dhont, M., Elst, J.V.D., Cornelissen, M., 2006. Generation of embryonic stem cell lines from mouse blastocysts developed in vivo and in vitro: relation to Oct-4 expression. Reproduction 132, 59–66. https://doi.org/10.1530/rep.1.00887
Tienari, J., Alanko, T., Saksela, O., Vesterinen, M., Lehtonen, E., 1995. Fibroblast growth factor-mediated stimulation of differentiating teratocarcinoma cells: evidence for paracrine growth regulation. Differ. Res. Biol. Divers. 59, 193–199.
Timmins, N., Dietmair, S., Nielsen, L., 2004. Hanging-drop multicellular spheroids as a model of tumour angiogenesis. Angiogenesis 7, 97–103. https://doi.org/10.1007/s10456-004-8911-7
Titmarsh, D., Hidalgo, A., Turner, J., Wolvetang, E., Cooper-White, J., 2011. Optimization of flowrate for expansion of human embryonic stem cells in perfusion microbioreactors. Biotechnol. Bioeng. 108, 2894–2904. https://doi.org/10.1002/bit.23260
Toxicology, N.R.C. (US) C. on D., 2000. Using Model Animals to Assess and Understand Developmental Toxicity. National Academies Press (US).
Tsankov, A.M., Akopian, V., Pop, R., Chetty, S., Gifford, C.A., Daheron, L., Melton, D.A., Tsankova, N.M., Meissner, A., 2015. An improved ScoreCard to assess the differentiation potential of human pluripotent stem cells. Nat. Biotechnol. 33, 1182–1192. https://doi.org/10.1038/nbt.3387
Tsou, Y.-H., Khoneisser, J., Huang, P.-C., Xu, X., 2016. Hydrogel as a bioactive material to regulate stem cell

fate. Bioact. Mater. 1, 39–55. https://doi.org/10.1016/j.bioactmat.2016.05.001
Ungrin, M.D., Joshi, C., Nica, A., Bauwens, C., Zandstra, P.W., 2008. Reproducible, Ultra High-Throughput Formation of Multicellular Organization from Single Cell Suspension-Derived Human Embryonic Stem Cell Aggregates. PLOS ONE 3, e1565. https://doi.org/10.1371/journal.pone.0001565
van der Heyden, M.A.G., Defize, L.H.K., 2003. Twenty one years of P19 cells: what an embryonal carcinoma cell line taught us about cardiomyocyte differentiation. Cardiovasc. Res. 58, 292–302. https://doi.org/10.1016/S0008-6363(02)00771-X
Van Winkle, A.P., Gates, I.D., Kallos, M.S., 2012. Mass transfer limitations in embryoid bodies during human embryonic stem cell differentiation. Cells Tissues Organs 196, 34–47. https://doi.org/10.1159/000330691
Vidricaire, G., Jardine, K., McBurney, M.W., 1994. Expression of the Brachyury gene during mesoderm development in differentiating embryonal carcinoma cell cultures. Development 120, 115–122.
Viney, M.E., Bullock, A.J., Day, M.J., MacNeil, S., 2009. The co-culture of intestinal epithelial and stromal cells in 3D collagen-based environments. Regen. Med. 4, 397–406. https://doi.org/10.2217/rme.09.4
Walsh, J.G., Cullen, S.P., Sheridan, C., Lüthi, A.U., Gerner, C., Martin, S.J., 2008. Executioner caspase-3 and caspase-7 are functionally distinct proteases. Proc. Natl. Acad. Sci. 105, 12815–12819. https://doi.org/10.1073/pnas.0707715105
Walton, W.H., 1948. Feret‘s Statistical Diameter as a Measure of Particle Size. Nature 162, 329–330. https://doi.org/10.1038/162329b0
Webster, S., de Wreede, R., 2016. Embryology at a glance. Wiley Blackwell, Chichester.
Weimar, C.H.E., Post Uiterweer, E.D., Teklenburg, G., Heijnen, C.J., Macklon, N.S., 2013. Reprint of: In-vitro model systems for the study of human embryo–endometrium interactions. Reprod. Biomed. Online 27, 673–688. https://doi.org/10.1016/j.rbmo.2013.10.004
Wertheim, L., Shapira, A., Amir, R., Dvir, T., 2018. A microfluidic chip containing multiple 3D nanofibrous scaffolds for culturing human pluripotent stem cells. Nanotechnology. https://doi.org/10.1088/1361-6528/aaabf2
Williams, J.A.G., Beeby, A., Davies, E.S., Weinstein, J.A., Wilson, C., 2003. An Alternative Route to Highly Luminescent Platinum(II) Complexes: Cyclometalation with NΛCΛN-Coordinating Dipyridylbenzene Ligands. Inorg. Chem. 42, 8609–8611. https://doi.org/10.1021/ic035083+
Wolfe, R.P., Ahsan, T., 2013. SHEAR STRESS DURING EARLY EMBRYONIC STEM CELL DIFFERENTIATION PROMOTES HEMATOPOIETIC AND ENDOTHELIAL PHENOTYPES. Biotechnol. Bioeng. 110, 1231–1242. https://doi.org/10.1002/bit.24782
Wolfe, R.P., Leleux, J., Nerem, R.M., Ahsan, T., 2012. Effects of shear stress on germ lineage specification of embryonic stem cells. Integr. Biol. 4, 1263–1273. https://doi.org/10.1039/C2IB20040F
Wu, J., Rostami, M.R., Olaya, D.P.C., Tzanakakis, E.S., 2014. Oxygen Transport and Stem Cell Aggregation in Stirred-Suspension Bioreactor Cultures. PLOS ONE 9, e102486. https://doi.org/10.1371/journal.pone.0102486
Xia, L., Arooz, T., Zhang, S., Tuo, X., Xiao, G., Susanto, T.A.K., Sundararajan, J., Cheng, T., Kang, Y., Poh, H.J., Leo, H.L., Yu, H., 2012. Hepatocyte function within a stacked double sandwich culture plate cylindrical bioreactor for bioartificial liver system. Biomaterials 33, 7925–7932. https://doi.org/10.1016/j.biomaterials.2012.06.078
Xia, L., Ng, S., Han, R., Tuo, X., Xiao, G., Leo, H.L., Cheng, T., Yu, H., 2009. Laminar-flow immediate-overlay hepatocyte sandwich perfusion system for drug hepatotoxicity testing. Biomaterials 30, 5927–5936. https://doi.org/10.1016/j.biomaterials.2009.07.022
Xie, Y., Hardouin, P., Zhu, Z., Tang, T., Dai, K., Lu, J., 2006. Three-dimensional flow perfusion culture system for stem cell proliferation inside the critical-size beta-tricalcium phosphate scaffold. Tissue Eng. 12, 3535–3543. https://doi.org/10.1089/ten.2006.12.3535
Yamada, K.M., Cukierman, E., 2007. Modeling tissue morphogenesis and cancer in 3D. Cell 130, 601–610. https://doi.org/10.1016/j.cell.2007.08.006
Yanai, A., Laver, C.R.J., Joe, A.W., Viringipurampeer, I.A., Wang, X., Gregory-Evans, C.Y., Gregory-Evans, K., 2013. Differentiation of Human Embryonic Stem Cells Using Size-Controlled Embryoid Bodies and Negative Cell Selection in the Production of Photoreceptor Precursor Cells. Tissue Eng. Part C Methods 19, 755–764. https://doi.org/10.1089/ten.tec.2012.0524
Yeo, D., Kiparissides, A., Cha, J.M., Aguilar-Gallardo, C., Polak, J.M., Tsiridis, E., Pistikopoulos, E.N., Mantalaris, A., 2013. Improving Embryonic Stem Cell Expansion through the Combination of Perfusion and Bioprocess Model Design. PLOS ONE 8, e81728. https://doi.org/10.1371/journal.pone.0081728
Yoshimitsu, R., Hattori, K., Sugiura, S., Kondo, Y., Yamada, R., Tachikawa, S., Satoh, T., Kurisaki, A., Ohnuma, K., Asashima, M., Kanamori, T., 2014. Microfluidic perfusion culture of human induced pluripotent stem cells under fully defined culture conditions. Biotechnol. Bioeng. 111, 937–947. https://doi.org/10.1002/bit.25150
Young, B., Lowe, J., Stevens, A., Heath, J., Deakin, P., 2006. Wheater’s Functional Histology: A text and colour atlas, 5th ed. Churchill Livingstone.
YU, W., NIU, W., WANG, S., CHEN, X., SUN, B., WANG, F., SUN, Y., 2015. Co-culture with endometrial

stromal cells enhances the differentiation of human embryonic stem cells into endometrium-like cells. Exp. Ther. Med. 10, 43–50. https://doi.org/10.3892/etm.2015.2490

Yue, X.-S., Fujishiro, M., Nishioka, C., Arai, T., Takahashi, E., Gong, J.-S., Akaike, T., Ito, Y., 2012. Feeder Cells Support the Culture of Induced Pluripotent Stem Cells Even after Chemical Fixation. PLoS ONE 7. https://doi.org/10.1371/journal.pone.0032707

Zangrossi, S., Marabese, M., Broggini, M., Giordano, R., D'Erasmo, M., Montelatici, E., Intini, D., Neri, A., Pesce, M., Rebulla, P., Lazzari, L., 2007. Oct-4 Expression in Adult Human Differentiated Cells Challenges Its Role as a Pure Stem Cell Marker. STEM CELLS 25, 1675–1680. https://doi.org/10.1634/stemcells.2006-0611

Zdravkovic, T., Nazor, K.L., Larocque, N., Gormley, M., Donne, M., Hunkapillar, N., Giritharan, G., Bernstein, H.S., Wei, G., Hebrok, M., Zeng, X., Genbacev, O., Mattis, A., McMaster, M.T., Krtolica, A., Valbuena, D., Simón, C., Laurent, L.C., Loring, J.F., Fisher, S.J., 2015. Human stem cells from single blastomeres reveal pathways of embryonic or trophoblast fate specification. Dev. Camb. Engl. 142, 4010–4025. https://doi.org/10.1242/dev.122846

Zhang, W., 2014. Teratoma formation: A tool for monitoring pluripotency in stem cell research. StemBook. https://doi.org/10.3824/stembook.1.53.1

Zhou, J., Zhang, Y., Lin, Q., Liu, Z., Wang, H., Duan, C., Wang, Y., Hao, T., Wu, K., Wang, C., 2010. Embryoid bodies formation and differentiation from mouse embryonic stem cells in collagen/Matrigel scaffolds. J. Genet. Genomics 37, 451–460. https://doi.org/10.1016/S1673-8527(09)60064-3

10. Appendices

Contained within the following appendices are all abstracts, posters and oral presentations given during this project as well as variety of details and data supplementary to that in the previous Chapters, including recipes for the creation of stains and buffers and PCR primer optimisation data.

10.1 Appendix 1 – Abstracts and Posters

10.1.1 Investigating Modelling Human Tissue Development *In Vitro* Using Three Dimensional Cell Culture Technologies (2016) BSCB BSDB Joint Meeting, Coventry, UK

10.1.1.1 Abstract

Authors: L A Smith[1], D Owens[1], S A Przyborski[1,2]

Affiliations: 1. Durham University, Durham, UK; 2. Reprocell Europe, Sedgefield, UK

The culture of pluripotent stem cells as aggregates in suspension has been used as a method for modelling the development of human tissues in vitro for a number of years. However, the development of a necrotic core during long term culturing is a major drawback, limiting their usefulness and ability to form complex tissues. Maintaining aggregates on 3D porous polystyrene scaffolds allows for better nutritional and oxygen support, increasing the length of time over which the cellular aggregates can be maintained. This allows for the formation and study of complex and diverse tissues. This approach can be combined with small molecules to direct differentiation and study specific developmental pathways. As well as allowing for the study of human tissue development, the in vitro model could additionally offer an alternative assay for assessing cell pluripotency.

9.1.1.2 Poster

Investigating Modelling Human Tissue Development *In Vitro* Using Three Dimensional Cell Culture Technologies

L.A.Smith[1], D. Owens[1], M. Roger[1], & S.A. Przyborski[1,2]

1. School of Biological & Biomedical Sciences, Durham University, UK, 2. ReproCELL Reinnervate Ltd, Sedgefield, UK

Introduction

Human tissue development is a highly regulated period of growth which has still not been well characterised, primarily due to **the lack of an *in vitro* model** and the ethical implications of work with embryos and embryonic materials.

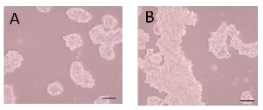
Currently, the sophistication and complexity of **tissue differentiation achieved *in vivo***, including *via* the teratoma assay, **cannot be fully replicated *in vitro***, although many different tissue types have been produced using a variety of cell culture methods. While ***in vivo* methods** can produce **complexity,** there is **little consistency and reproducibility**, which are key aspects of scientific investigation. Three dimensional (3D) cell culture offers a culturing system which is much more similar to the *in vivo* environment, and provides the opportunity to produce tissues which are more like their *in vivo* counterparts. An *in vitro* model of human tissue development created **using three dimensional cell culture techniques** would **provide a model** of the early stages of **human development** that are currently difficult to study, as well as potentially provide an alternative, reproducible and consistent assay to test pluripotency.

Methods and Materials

Creation of embryoid bodies for seeding on Alvetex® inserts

Embryonic pluripotent cells are used to create a model of early human tissue development: **TERA2.cl.SP12 embryonal carcinoma cells** are a useful tool for optimising techniques and protocols, due to their **simple and inexpensive** culture requirements. Method optimisation involved investigating using **versene as an alternative dissociation reagent to trypsin**, an enzymatic method which may result in the loss of external cell surface proteins involved in cellular attachment and signalling.

Figure 1. Untreated TERA2.cl.SP12 aggregates created using different dissociation reagents: (A) 1 day old aggregates created using trypsin (B) 1 day old aggregates created suing versene. Versene created aggregates appear to be larger than trypsin created aggregates at the same time point. Scale bar = 100µm



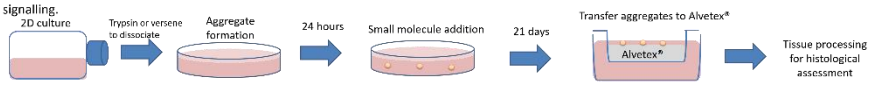
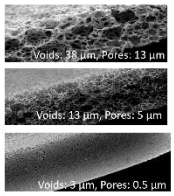


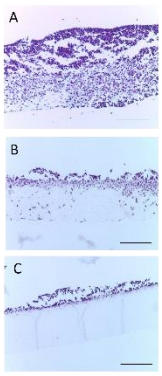
Figure 2. Protocol for differentiation of stem cell derived tissues in 3D on Alvetex® membrane: TERA2.cl.SP12 cells are cultured in 2D flasks. Cells are seeded into Petri dishes to form aggregates. After 24 hours, morphogens are added to the Petri dish to induce differentiation. Aggregates are grown in suspension, before being transferred and pipetted directly onto the Alvetex ®inserts. The tissues are then maintained on the inserts for 7 days. Inserts are then fixed, embedded and analysed histologically.

Fig 3. Three forms of Alvetex® membrane: Images showing the structure of the three forms of Alvetex® (ReproCELL Reinnervate Ltd.), a 3D polystyrene scaffold used for cell culture: (A) Alvetex® Scaffold, (B) Alvetex® Strata, (C) Alvetex® Polaris



Results

Differences in the structure of aggregates grown on three forms of Alvetex® membrane



Aggregates grown on Alvetex® membranes adopt a **flattened disc structure**; resulting in a smaller diffusion distance and better nutritional/oxygen support. From this data, it is clear that **Alvetex® Scaffold is not appropriate** for investigating human tissue development, as cells from the aggregate migrate into the scaffold and **lose their overall tissue structure**. Aggregates seeded onto **Alvetex® Strata** (B) and **Alvetex® Polaris** (C) membranes **retain their tissue structure** on top of the membrane, and so are suitable for this study.

Figure 4. TERA2.cl.SP12 aggregates grown on Alvetex® for 7 days: (A) 21 day old aggregates grown on Alvetex Scaffold for 7 days, (B) 21 day old aggregates grown on Alvetex Strata for 7 days, (C) 21 day old aggregates grown on Alvetex Polaris for 7 days. Aggregates survive significantly past 21 days when grown on Alvetex. Those grown on Polaris retain their structure and do not migrate into the scaffold. Magnification: x10, Scale bar: 200 µm

Formulation of embryonic tissue through modulation of stem cell differentiation

The application of small molecules to aggregates in suspension leads to their differentiation, for example use of BMP2 results in the production of mesenchymal tissues. Growing differentiated tissues on Alvetex® membrane has led to **highly complex differentiation** not previously seen *in vitro*, **similar to** that seen in **teratomas**.

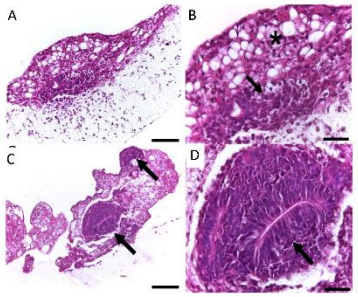


Figure 5. TERA2.cl.SP12 tissue differentiated using a range of small molecules and grown on Alvetex® Polaris for 7 days: Haematoxylin and Eosin stained images (A, B) BMP2 treated 7 day aggregate shows the development of mesenchymal regions in a heterogeneous manner, asterisk indicates low cell density region, arrow indicates high cell density region; (C, D) BMP2 treated 21 day aggregates show mesenchymal tissues as well as complex neuroepithelial tissues as shown by arrows; Magnification: (C)x10 , (A) x20 and (B, D, E) x40, Scale bar: (x10) 200 µm, (x20) 100 µm and (x40) 50 µm

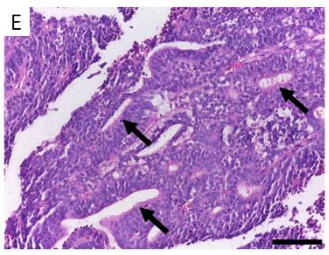


Figure 6. TERA2.cl.SP12 embryonal carcinoma cell teratoma: Haematoxylin and Eosin stained image (E) TERA2.cl.SP12 teratoma, grown under the skin of a nu/nu mouse for 6-8 weeks. Arrows indicate neuroepithelial rosettes. Note the similarity of the neuroepithelial tissue seen in image D, produced by embryonal carcinoma cells *in vitro*, compared to the above image. Magnification: x40, Scale bar: 50 µm

Conclusions

- TERA2.cl.SP12 aggregates maintained on Alvetex® for 7 days show **increased survival** due to a decrease in diffusion distance and **better nutritional and oxygen support**.
- TERA2.cl.SP12 aggregates maintained on **Alvetex® Strata and Polaris** for 7 days fully **maintained their structure** without migrating into the scaffold membrane.
- **Differentiated aggregates** can also be **grown successfully on Alvetex Polaris**, whilst maintaining their tissue structure and **producing complex tissue**.
- **This three dimensional culture system has the potential to create a basic model of human tissue development, with the ability to study developmental pathways.**

References

D Owens (2015) Thesis, S A Przyborski *et al.*, (2004) *Stem Cells and Development*

Future Directions

How do tissues differentiated down different lineages influence each other?

- Combine aggregates differentiated down different lineages and study the effects on tissue development. Are more complex or unusual tissues produced?

What is this effect on embryonic stem cells?

- Use embryonic stem cells, which have a greater differentiation potential, to repeat experiments, focussing on differentiating tissues representing the three germ layers and combining these to create complex tissues.

Can highly developed tissues which reach the complexity of *in vivo* tissues be produced?

- Tissues produced *in vitro* are compared to teratomas in terms of complexity and tissues present, and these are assessed by methods including microscopy, staining and immunofluorescence.

Can a new *in vitro* alternative to the teratoma assay be produced, reducing the need for animals?

- Comparison to teratoma and assessment using other pluripotent cell lines.

10.1.2 Investigating Modelling Human Tissue Development *In Vitro* Using Three Dimensional Cell Culture Technologies (2016) Anatomical Society Summer Meeting, Brighton, UK

10.1.2.1 Abstract

Authors: L A Smith[1], D Owens[1], E Knight[1], M F Roger[1], S A Przyborski[1,2]

Affiliations: 1. Durham University, Durham, UK; 2. ReproCELL Reinnervate Ltd, Sedgefield, UK

Studying the differentiation of human pluripotent stem cells enables the investigation of tissue development in man. Teratomas are tumours derived from pluripotent stem cells in vivo and contain differentiated tissues demonstrating developmental potential. Studying such tissue development in vitro is challenging and it is currently not possible to recreate the complexity of differentiation observed in such tumours in a controlled and reproducible manner. In a proof of concept study, we have used human embryonal carcinoma cells (TERA2.cl.SP12) to recapitulate teratoma formation using a novel two-step three dimensional (3D) cell culture procedure designed to create 3D spatial relationships between cells over time. In brief, stem cells were initially grown as classic organoid suspension cultures prior to transfer onto Alvetex porous polystyrene scaffolds. 3D aggregates subsequently flatten forming a disc of developing cells. This enhanced physical microenvironment allows for the long-term maintenance of cells through increased nutritional and oxygen support. Histological and immunofluorescent characterisation showed that as time progressed the extent of tissue development increased, enabling the formation of more complex structures. Control over such differentiation was demonstrated through the addition of exogenous compounds such as synthetic retinoid ec23 or BMP2, resulting in the formation of neural or epithelial ectodermal derivatives, respectively. These experiments are the first step to developing more sophisticated in vitro models of human tissue development from pluripotent embryonic stem cells. Such technology will advance our understanding of human tissue development, enable production of specific tissue types, and contribute to reducing the use of animals in teratoma models.

9.1.2.2 Poster

Investigating Modelling Human Tissue Development *In Vitro* Using Three Dimensional Cell Culture Technologies

L.A.Smith[1], D. Owens[1], M. Roger[1], & S.A. Przyborski[1,2]

1. School of Biological & Biomedical Sciences, Durham University, UK, 2. ReproCELL Reinnervate Ltd, Sedgefield, UK

Introduction

Human tissue development is a highly regulated period of growth which has not been well characterised, primarily due to **the lack of an *in vitro* model** and the ethical implications of work with embryos and embryonic materials.

Currently, the sophistication and complexity of **tissue differentiation achieved *in vivo***, including *via* the teratoma assay, **cannot be fully replicated *in vitro***, although many different tissue types have been produced using a variety of methods. While ***in vivo* methods** can produce **complexity,** there is **little consistency and reproducibility**; key aspects of scientific investigation. Three dimensional (3D) cell culture offers a system which is much more similar to the *in vivo* environment, providing the opportunity to produce tissues which are more like their *in vivo* counterparts. An *in vitro* model of human tissue development created **using three dimensional cell culture techniques** would **provide a model** of the early stages of **human development** that are currently difficult to study, as well as potentially provide an alternative, reproducible and consistent assay to test pluripotency.

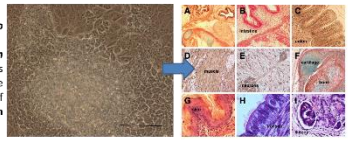


Figure 1. Pluripotent cell colony in 2D and an example of the tissue types which can be achieved in the teratoma assay. Magnification x20. scale bar = 100 µm

Methods and Materials

Creation of embryoid bodies for seeding on Alvetex® inserts

Embryonic pluripotent cells are used to create a model of early human tissue development: **TERA2.cl.SP12 embryonal carcinoma cells** are a useful tool for optimising techniques and protocols, due to their **simple and inexpensive** culture requirements. Method optimisation involved investigating using **versene as an alternative dissociation reagent to trypsin**, an enzymatic method which may result in the loss of external cell surface proteins involved in cellular attachment and signalling.

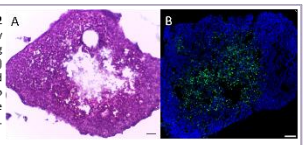


Figure 2. Untreated TERA2.cl.SP12 aggregates: (A) H&E image of 21 day old untreated aggregates, showing loss of viability in the centre. (B) Confocal image of 21 day old aggregates stained using TUNEL to show apoptosis taking place in the centre of the aggregate. Magnification x20. Scale bars = 50 µm

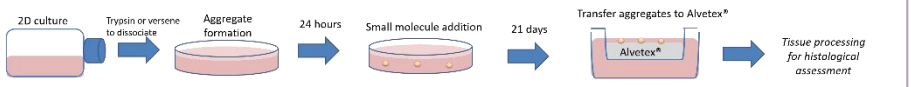


Figure 3. Protocol for differentiation of stem cell derived tissues in 3D on Alvetex® membrane: TERA2.cl.SP12 cells are cultured in 2D flasks. Cells are seeded into Petri dishes to form aggregates. After 24 hours, morphogens are added to the Petri dish to induce differentiation. Aggregates are grown in suspension, before being transferred and pipetted directly onto the Alvetex ®inserts. The tissues are then maintained on the inserts for 7 days. Inserts are then fixed, embedded and analysed histologically.

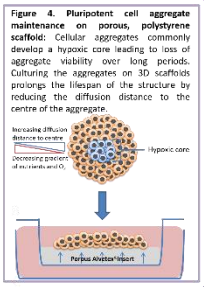
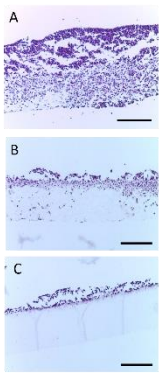


Figure 4. Pluripotent cell aggregate maintenance on porous, polystyrene scaffold: Cellular aggregates commonly develop a hypoxic core leading to loss of aggregate viability over long periods. Culturing the aggregates on 3D scaffolds prolongs the lifespan of the structure by reducing the diffusion distance to the centre of the aggregate.

Results

Differences in the structure of aggregates grown on three forms of Alvetex® membrane



Aggregates grown on Alvetex® membranes adopt a **flattened disc structure**; resulting in a smaller diffusion distance and better nutritional/oxygen support. From this data, it is clear that **Alvetex® Scaffold is not appropriate** for investigating human tissue development, as cells from the aggregate migrate into the scaffold and **lose their overall tissue structure**. Aggregates seeded onto **Alvetex® Strata** (B) and **Alvetex® Polaris** (C) membranes **retain their tissue structure** on top of the membrane, and so are suitable for this study.

Figure 4. TERA2.cl.SP12 aggregates grown on Alvetex® for 7 days: (A) 21 day old aggregates grown on Alvetex Scaffold for 7 days, (B) 21 day old aggregates grown on Alvetex Strata for 7 days, (C) 21 day old aggregates grown on Alvetex Polaris for 7 days. Aggregates survive significantly past 21 days when grown on Alvetex. Those grown on Polaris retain their structure and do not migrate into the scaffold. Magnification: x10, Scale bar: 200 µm

Formulation of embryonic tissue through modulation of stem cell differentiation

The application of small molecules to aggregates in suspension leads to their differentiation, for example use of BMP2 results in the production of non-neural mesenchymal tissues. Growing differentiated tissues on Alvetex® membranes has led to **highly complex differentiation** not previously seen *in vitro,* **similar to** that seen in **teratomas** produced using the same cell line.

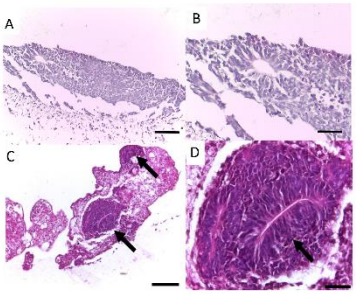


Figure 5. Untreated and differentiated TERA2.cl.SP12 tissue with morphogens applied cultured on Alvetex® Strata and Polaris for up to 14 days: Haematoxylin and Eosin stained images (A, B) Untreated 21 day T2SP12 aggregates cultured on Alvetex Strata for 14 days shows the spontaneous development of neural rosettes; (C, D) BMP2 treated 21 day aggregates show mesenchymal tissues as well as complex neuroepithelial tissues as shown by arrows; Magnification: (C)x10 , (A) x20 and (B, D, E) x40, Scale bar: (x10) 200 µm, (x20) 100 µm and (x40) 50 µm

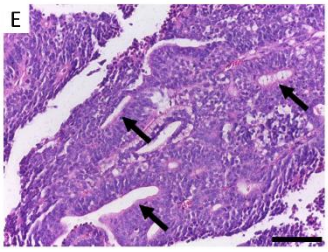


Figure 6. TERA2.cl.SP12 embryonal carcinoma cell teratoma: Haematoxylin and Eosin stained image (E) TERA2.cl.SP12 teratoma, grown under the skin of a nu/nu mouse for 6-8 weeks. Arrows indicate neuroepithelial rosettes. Note the similarity of the neuroepithelial tissue seen in image D, produced by embryonal carcinoma cells *in vitro*, compared to the above image. Magnification: x40, Scale bar: 50 µm

Conclusions

- TERA2.cl.SP12 aggregates maintained on Alvetex® for 7 days show **increased survival** due to a decrease in diffusion distance and **better nutritional and oxygen support**.
- TERA2.cl.SP12 aggregates maintained on **Alvetex® Strata and Polaris** for 7 days fully **maintained their structure** without migrating into the scaffold membrane.
- **Differentiated aggregates** can also be **grown successfully on Alvetex Polaris**, whilst maintaining their tissue structure and **producing complex tissue**.
- **This three dimensional culture system has the potential to create a basic model of human tissue development, with the ability to study developmental pathways.**

References

D Owens (2015) Thesis, S A Przyborski *et al.*, (2004) *Stem Cells and Development*

Future Directions

What is this effect on embryonic stem cells?

- Use embryonic stem cells, which have a greater differentiation potential, to repeat experiments, focussing on differentiating tissues representing the three germ layers.

Can increasingly complex tissue discs representing multiple germ layers be produced?

- Combine embryoid bodies differentiated towards the three germ layers in the 3D *in vitro* model and assess the outcome.

Can highly developed tissues which reach the complexity of *in vivo* tissues be produced?

- Tissues produced *in vitro* are compared to teratomas in terms of complexity and tissues present, and assessed by methods including microscopy, staining and immunofluorescence.

Can a new *in vitro* alternative to the teratoma assay be produced, reducing the need for animals?

- Comparison to tissues produced *via* the teratoma assay and assessment using other pluripotent cell lines in the 3D model.

10.1.3 Modelling the development of human tissues *in vitro* using a combination of three dimensional cell culture technologies (2016) White Rose Consortium Work In Progress Meeting, Durham, UK

10.1.3.1 Abstract

L. A. Smith[1], D Owens[1], M. F. Roger[1], S. A. Przyborski [1,2]

Affiliations: 1.Durham University, Durham, UK; 2.ReproCELL Reinnervate Ltd, Sedgefield, UK

Introduction

The development of mammalian tissues is a critical process that is poorly understood. Current models involve using pluripotent stem cells in various methodologies, including the formation of embryoid bodies. These multicellular structures have been shown successfully to recapitulate events of early mammalian embryogenesis. However, as the size of cell aggregates increases a larger diffusion distance is created, leading to a significant loss of viability and necrosis in the core of the structure. This is a result of the inability of nutrients and oxygen to diffuse into central regions. As a consequence this limits the ability to conduct long-term studies of tissue development. As differentiation processes are time-dependent, this will impact greatly on the maturity and complexity achieved by pluripotent cell derived tissues using in vitro methods. Yet, it is well known that pluripotent cells can form highly differentiated tissues achieving high levels of complexity and maturity, as is seen in a teratoma assay in vivo.

Methods

Through a combination of embryoid body culture and application of an inert three-dimensional porous polystyrene scaffold, we have improved the viability of embryoid bodies by enabling them to form flattened tissue discs, allowing reduced diffusion distances. This improves cell viability, extending their time in culture, resulting in increased cell differentiation. We have increased the complexity of the model by adding exogenous morphogens such as retinoic acid, Activin A and BMP4, each allowing for directed differentiation towards particular primary germ layers and enabling the detailed study of these developmental pathways. Histological staining and immunofluorescence for specific markers have revealed the identity, complexity and maturity of the tissues.

Results

Initial experiments used an embryonal carcinoma cell line to optimise methodology, allowing for proof of concept experiments. Further studies involving mouse embryonic stem cells have revealed the ability to maintain tissue disc structures in the in vitro environment for a significant amount of time without a reduction in viability, whilst forming complex differentiated structures.

Discussion

It is anticipated that this model will provide a novel in vitro alternative to the current pluripotency assessment method, the xenograft based teratoma assay, and provide an approach to investigate the early stages of tissue development.

9.1.3.2 Poster

Modelling the development of human tissues *in vitro* using a combination of advanced cell technologies

L.A.Smith[1], D. Owens[1], M. Roger[1], & S.A. Przyborski[1,2]
1. Department of Biosciences, Durham University, UK, 2. ReproCELL Europe, Sedgefield, UK

Introduction

Human tissue development is a highly regulated period of growth which has not been well characterised, primarily due to **the lack of an *in vitro* model** and the ethical implications of work with embryos and embryonic materials.

Currently, the sophistication and complexity of **tissue differentiation achieved *in vivo***, including *via* the teratoma assay, **cannot be fully replicated *in vitro***. While ***in vivo* methods** can produce **complexity,** there is **little consistency and reproducibility**; key aspects of scientific investigation. Three dimensional (3D) cell culture offers a system which is much more similar to the *in vivo* environment, providing the opportunity to produce tissues which are more similar to *in vivo* counterparts. An *in vitro* model of human tissue development created **using three dimensional cell culture techniques** would **provide a model** of the early stages of **human development** that are currently difficult to study, as well as potentially provide an alternative, reproducible and consistent assay to test pluripotency.

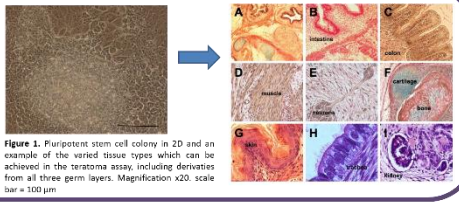


Figure 1. Pluripotent stem cell colony in 2D and an example of the varied tissue types which can be achieved in the teratoma assay, including derivatives from all three germ layers. Magnification x20. scale bar = 100 µm

Methods and Materials

Creation of embryoid bodies for seeding on Alvetex® inserts

Embryonic pluripotent cells are used to create a model of early human tissue development: **TERA2.cl.SP12 embryonal carcinoma cells** are a useful tool for optimising techniques and protocols, due to their **simple and inexpensive** culture requirements. **CGR8 murine embryonic stem cells** allow for the **expansion of the capabilities** of the model and **deeper investigation** into the process of tissue development.

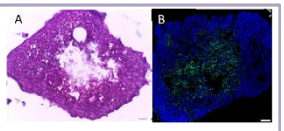


Figure 2. Untreated TERA2.cl.SP12 aggregates: (A) H&E image of 21 day old untreated aggregates, showing loss of viability in the centre. (B) Confocal image of 21 day old aggregates stained using TUNEL to show apoptosis taking place in the centre of the aggregate. Magnification x20. Scale bars = 50 µm

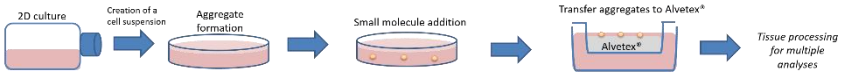


Figure 3. Protocol for differentiation of stem cell derived tissues in 3D on Alvetex® membrane: Pluripotent cells are cultured in 2D flasks, seeded to form aggregates, and cultured in suspension in Petri dishes. Once aggregates have formed, morphogens are added to the media to induce differentiation. After being grown in suspension. Aggregates are transferred to Alvetex ®inserts. The tissue discs are then maintained on the inserts long term. Inserts are then processed and analysed histologically.

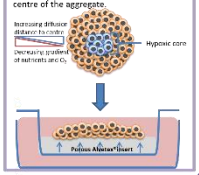


Figure 4. Pluripotent cell aggregate maintenance on porous, polystyrene scaffold: Cellular aggregates commonly develop a hypoxic core leading to loss of aggregate viability over long periods. Culturing the aggregates on 3D scaffolds prolongs the lifespan of the structure by reducing the diffusion distance to the centre of the aggregate.

Results

Formulation of embryonic tissue via modulation of stem cell differentiation

The application of morphogens to aggregates in suspension leads to their differentiation, for example use of BMP2 results in the production of non-neural mesenchymal tissues. Growing differentiated tissues on Alvetex® membranes leads to **highly complex differentiation** not previously seen *in vitro*, **similar to** that seen in **teratomas** produced using the same cell line.

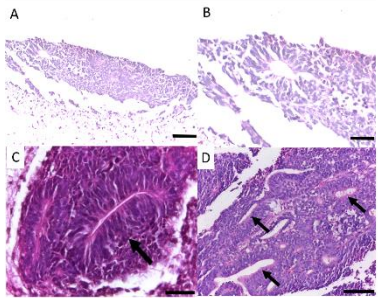


Figure 5. Untreated and morphogen treated TERA2.cl.SP12 tissue cultured on Alvetex® inserts *in vitro* for up to 14 days and TERA2.cl.SP12 teratoma tissue: H&E stained images (A, B) Untreated 21 day T2SP12 aggregates cultured on Alvetex® Strata for 14 days show spontaneous development of neural rosettes; (C) BMP2 treated 21 day aggregates show mesenchymal tissues as well as complex neuroepithelial tissues as shown by arrows; (D) TERA2.cl.SP12 teratoma, grown under skin of a nu/nu mouse for 6-8 weeks. Arrows indicate neuroepithelial rosettes. Note the similarity in images C and D. Magnification: (C) , (A, C) x20 and (B, D) x40, Scale bar: (x20) 100 µm and (x40) 50 µm

Long term maintenance of embryonic tissues in three dimensional culture conditions

The culture of embryonic stem cell derived embryoid bodies on Alvetex membranes results in **the formation of a tissue disc** , with complex internal structures. These tissue discs can be **successfully maintained** on Alvetex membranes long term, with **no impact on viability** or differentiation, and display various tissue markers.

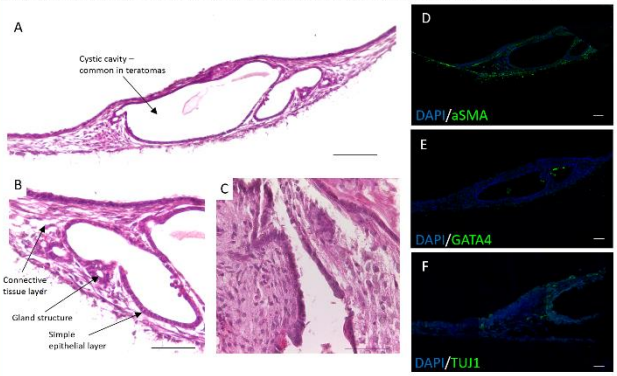


Figure 6. CGR8 murine embryoid bodies cultured on Alvetex® Polaris for 14 days: (A, B) H&E stained images of CGR8 murine embryoid bodies cultures in suspension for 5 days before being transferred to Alvetex® Polaris for up to 14 days. Note the varied cell morphology, and complex cellular organisation within the tissue disc. (C) CGR8 teratoma, gorwn under skin of a nu/nu mouse for 6-8 weeks. (D, E, F) Immunofluorescent images for various tissue markers, including alpha smooth muscle actin, transcription factor GATA4 and class 3 beta tubulin indicate a mesodermal identity. Magnification: (A) x10, (B- F) x40, Scale bar: 100 µm and 25 µm.

Conclusions

- **Pluripotent cell aggregates** maintained on Alvetex® show **increased survival** due to a decrease in diffusion distance and **better nutritional and oxygen support**.
- **Differentiated TERA2.cl.SP12 aggregates** can be **grown successfully on Alvetex® Polaris**, whilst maintaining their tissue structure and **producing complex tissue.**
- **Long term culture** of embryoid bodies on Alvetex® membranes is **highly successful** with no impact on viability or differentiation.
- **This three dimensional culture system has the potential to create a basic model of human tissue development, with the ability to study developmental pathways.**

References

D Owens (2015) Thesis, S A Przyborski *et al.*, (2004) *Stem Cells and Development*

Future Directions

Can increasingly complex tissue discs representing multiple germ layers be produced?

- Use a combination of morphogens to direct the differentiation of the tissue discs towards specific germ layers and lineages
- Investigate the effects of co-culturing other cell lines with the tissue discs to enhance differentiation

Can highly developed tissues which reach the complexity of *in vivo* tissues be produced?

- Tissues produced *in vitro* are compared to teratomas in terms of complexity and tissues present, and assessed by methods including microscopy, staining and immunofluorescence.

Can a new *in vitro* alternative to the teratoma assay be produced, reducing the need for animals?

- Comparison to tissues produced *via* the teratoma assay and assessment using other pluripotent cell lines in the 3D model.

10.1.4 Modelling the development of human tissues *in vitro* using a combination of three dimensional cell culture technologies (2016) Anatomical Society Winter Meeting, London, UK

10.1.4.1 Abstract

Authors: L A Smith[1], D Owens[1], M F Roger[1], S A Przyborski[1,2]

Affiliations: 1. Durham University, Durham, UK; 2. ReproCELL Europe, Sedgefield, UK

The development of mammalian tissues is a critical process that is poorly understood. Current models involve using pluripotent stem cells in various methodologies, including the formation of embryoid bodies. These multicellular structures have been shown successfully to recapitulate events of early mammalian embryogenesis. However, as the size of cell aggregates increases a larger diffusion distance is created, leading to a significant loss of viability and necrosis in the core of the structure. This is a result of the inability of nutrients and oxygen to diffuse into central regions. As a consequence this limits the ability to conduct long-term studies of tissue development. As differentiation processes are time-dependent, this will impact greatly on the maturity and complexity achieved by pluripotent cell derived tissues using in vitro methods. Yet, it is well known that pluripotent cells can form highly differentiated tissues achieving high levels of complexity and maturity, as is seen in a teratoma assay in vivo. Through a combination of embryoid body culture and application of an inert three-dimensional porous polystyrene scaffold, we have improved the viability of embryoid bodies by enabling them to form flattened tissue discs, allowing reduced diffusion distances. This improves cell viability, extending their time in culture, resulting in increased cell differentiation. We have increased the complexity of the model by adding exogenous morphogens such as retinoic acid, Activin A and BMP4, each allowing for directed differentiation towards particular primary germ layers and enabling the detailed study of these developmental pathways. Histological staining and immunofluorescence for specific markers have revealed the identity, complexity and maturity of the tissues. Initial experiments used an embryonal carcinoma cell line to optimise methodology, allowing for proof of concept experiments. Further studies involving mouse embryonic stem cells have revealed the ability to maintain tissue disc structures in the in vitro environment for a significant amount of time without a reduction in viability, whilst forming complex differentiated structures. It is anticipated that this model will provide a novel in vitro alternative to the current pluripotency assessment method, the xenograft based teratoma assay, and provide an approach to investigate the early stages of tissue development.

10.1.4.2 Poster

Same as previous poster

10.1.5 Modelling the Development of Human Tissues *In Vitro* Using a Combination of Advanced Cell Technologies and Mammalian Stem Cells (2017) Anatomical Society Winter Meeting, Dundee, UK

10.1.5.1 Abstract

Authors: L A Smith[1], D Owens[1], M F Roger[1], S A Przyborski[1,2]

Affiliations: 1. Durham University, Durham, UK; 2. Reprocell Europe, Sedgefield, UK

The teratoma assay has long been recognised as a 'gold standard' method to evaluate the pluripotency of human pluripotent stem cells (HPSCs), with further applications in the study of human tissue development. However, the assay is limited due to a high level of variability, with examples including differences in initial cell seeding number, graft site location and assay length. These are known to influence the differentiation trajectory of HPSCs, reducing comparability between assays and influencing assay results. Therefore there is need for a consistent and reproducible method to assess differentiation capacity, which can permit time dependent studies and allow for complex structure formation. We have developed a novel three dimensional in vitro model which permits the extension of embryoid body viability through reducing diffusion distances in these structures, enabling longer in vitro culture and the formation of complex tissue structures. Model optimisation involved using pluripotent stem cell lines to highlight the ability to culture the tissues for up to 35 days. The physiological relevance of the model is being further enhanced through the introduction of a novel perfusion system and co-culture with primary fibroblasts to simulate subcutaneous grafting of cells. These enhancements create a model which more closely mimics the physiology of the teratoma microenvironment, resulting in more complex cell differentiation and tissue structure formation. It is anticipated that this model will provide a novel, standardised animal free in vitro alternative to the current teratoma assay and provide an approach to investigate the early stages of tissue development.

All teratoma samples used were from a previous study conducted at the institution, which was given permission from the University, and was conducted in accordance with UK Home Office Guidelines. No other ethical approval was required for this study.

9.1.5.1 Poster

Modelling the Development of Human Tissues *In Vitro* Using a Combination of Advanced Cell Technologies and Mammalian Stem Cells

L.A.Smith[1], D. Owens[1], M. Roger[1], & S.A. Przyborski[1,2]

1. Department of Biosciences, Durham University, UK, 2. Reprocell Europe, Sedgefield, UK

Introduction

Potency is an **important property** of any cell population; **several methods** are used to assess the pluripotent phenotype and determine differentiation capacity. Amongst these, **the teratoma assay** is considered **the 'gold standard' method.** The formation of a tumour in an immunodeficient mouse host that comprises of **three germ layers is conclusive** of cellular pluripotency, see Fig 1a.

The assay also has **applications in human development**, but **inherent variability** at the technical and biological levels **limits its use/value**, see Fig 1b. This is due to the inability to compare results, and **effects on the differentiation trajectory** of cells, impacting significantly on the resulting tumour. While ***in vitro* methods** such as embryoid body formation are **more consistent**, they do not offer the rigour or complexity of the teratoma assay due to **viability issues** and a limited period of growth which **prevents mature differentiation.**

We hypothesise that an *in vitro* approach can be developed to **replace the use of the animal**, improve **consistency** and enable the **study of stem cell potency** and the formation of rudimentary embryonic tissues representative of all three germ layers. An ***in vitro* model** of human tissue development using **embryoid bodies** and **3D techniques** would provide **a reproducible and controllable alternative** to the teratoma assay. Introducing ***in vivo* like properties** such as **perfusion and co-culture** will mimic the teratoma microenvironment, **enhancing the differentiation** achieved.

*Aim: Produce an **in vitro model of human tissue development** using **pluripotent stem cells** and **3D cell culture techniques**.*

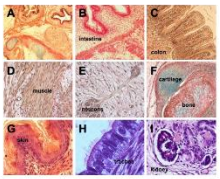


Figure 1a. Examples of structures found within a mature teratoma derived from human pluripotent stem cells: Complex tissues and structures from all three germ layers are present, which is an indicator of cellular pluripotency.

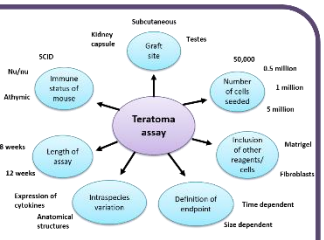


Figure 1b. Variable factors within the teratoma assay protocol

Methods

Embryoid body formation and seeding on Alvetex® Polaris

Aims: enhance cell viability, avoid core of cell death and enable prolonged differentiation

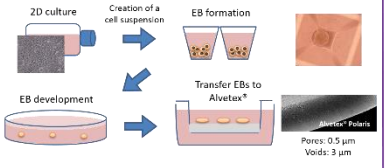


Figure 2a. Protocol for differentiation of stem cell derived tissues in 3D on Alvetex® Polaris: Pluripotent cells are cultured in 2D flasks and seeded into low adherence microwell plates to form embryoid bodies (EB), before culturing in suspension in Petri dishes. Once EBs are formed, these are transferred to Alvetex® inserts to be maintained. Following extended culture, tissue discs can be analysed.

Co-culture with a relevant fibroblast cell line to simulate the subcutaneous teratoma microenvironment

Aims: simulate the microenvironment of a subcutaneous graft, with signalling factors from the fibroblast component

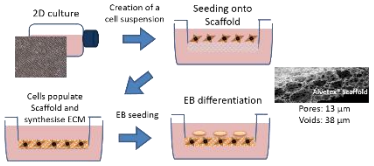


Figure 2b. Protocol for creation of dermal equivalent using fibroblasts in Alvetex® Scaffold: Dermal fibroblasts are seeded onto the membrane, and allowed to infiltrate and synthesise an extracellular matrix. Once dermal tissue has formed, embryoid bodies which have been formed in parallel are seeded onto the surface of the dermal layer and left to develop and differentiate, before fixing and analysis.

Emulation of tissue perfusion using a novel culture system

Aims: improve cell viability and prolong cell culture time, support maturation of tissue formation over time.

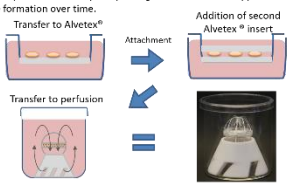


Figure 2c. Protocol for preparing cellular material for culture in the perfusion system: Cells or embryoid bodies are seeded onto the base Alvetex® insert and allowed to attach, before a second insert is placed on the top to form a sandwich culture. This is transferred to the novel perfusion device, and into the perfusion culture system, on a magnetic stirrer to circulate the media within the vessel.

Results

Formation of embryonic tissues in three dimensional culture conditions

Culturing embryonic stem cell derived embryoid bodies on Alvetex® membranes results in the **formation of a tissue disc**, with complex internal structures. These tissue discs can be **successfully maintained** on Alvetex® membranes long term, with **no impact on viability** or differentiation, showing **similarities to teratoma samples** created using the same cell line.

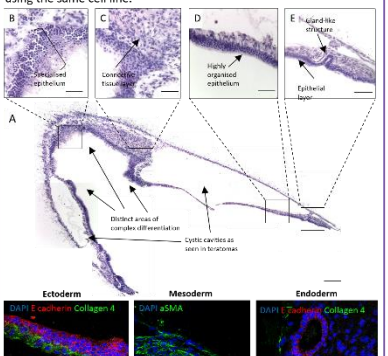


Figure 3a. CGR8 murine embryoid bodies cultured on Alvetex® Polaris: (A-E) H&E stained images of CGR8 embryoid bodies cultured on Alvetex® Polaris for 14 days. Note varied cell morphology, and complex cellular organisation within the tissue disc, including epithelial lined cavities, common in teratoma samples, as well as fibroblast like connective tissue and outer epithelial layers. Evidence of three germ layers shown by immunostaining for E-cadherin, α-smooth muscle actin and collagen 4. Scale bar: 100 µm and 25 µm.

Recapitulation of teratoma microenvironment via co-culture of embryoid bodies with fibroblasts

Introducing **co-culture** to the model using a **relevant fibroblast cell line** allows for **better recapitulation** of the teratoma microenvironment, and **enhanced differentiation** of the embryoid bodies. This is confirmed by **changes in structure** observed in embryoid bodies cultured on the surface of the dermal equivalent.

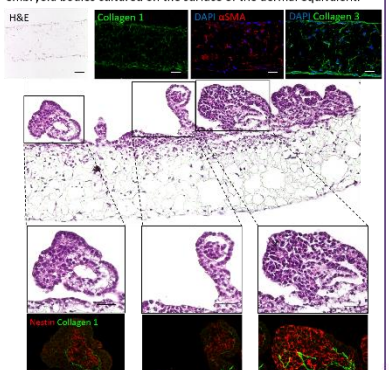


Figure 3b. Characterisation of dermal fibroblasts cultured in Alvetex® Scaffold, with T2SP12 aggregates cultured on the surface: Immunodeficient mouse fibroblasts cultured in the scaffold for 21 days, with H&E, collagen 1 and 3, and α-smooth muscle actin staining to highlight cellular and matrix components. Co-culturing with T2SP12 aggregates results in alterations in the morphology of the tissue discs, with a looser structure and indications of more non-neural differentiation, with nestin negative areas within the aggregate and deposition of collagen 1. Scale bar: 25 µm and 50 µm

Introduction of more physiological properties to enhance the cellular microenvironment

Tissue perfusion via the vasculature is **essential** in the ***in vivo*** environment, and the introduction of this property *in vitro* allows for **enhanced differentiation and viability**, over a **shorter culture period**. Using a cell suspension in a hydrogel, cells form **colony-like structures** reminiscent of embryonal carcinomas, showing both areas of **pluripotency and differentiation**.

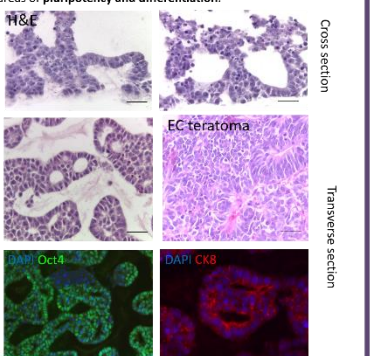


Figure 3c. Morphology of T2SP12 cells cultured in an Alvetex® Polaris sandwich in perfusion culture for 7 days: T2SP12 cells were seeded onto the base insert in a hydrogel before assembly of the sandwich culture in the device and transfer to perfusion culture. H&E staining shows highly organised colony-like structures similar to teratomas of the same cell line, and immunostaining highlights large areas of Oct 4 positive pluripotent cells, as well as areas of non-neural differentiation as indicated by cytokeratin 8 positive staining. Scale bar: 25 µm and 50 µm

Conclusions

- **Long term culture** of murine embryoid bodies on Alvetex® is **highly successful** with evidence of complex tissues which form showing evidence of three germ layers.
- **Co-culture** with a relevant cell line results in the **modulation of the differentiation** achieved by the embryoid bodies, highlighting the **effects of co-culture within the teratoma assay**.
- Cells are able to **survive and proliferate in a novel perfusion system**, showing maintenance of pluripotency and a move towards differentiated phenotypes, **similar to an embryonal carcinoma**.

Future Directions

- **Can the model be used to investigate the effects of co-culture within the teratoma assay?**

Comparison between the differentiation observed in the co-culture model and initial embryoid body model.

Use of known morphogens to direct the differentiation of the embryoid bodies prior to use in the co-culture model.

- **Can this be replicated with human pluripotent stem cell lines?**

Repeat key experiments with human ES and iPS cell lines to highlight the value and capabilities of the model.

- **Can the model be used to investigate the formation of embryonic tissues?**

Use known morphogens to influence the differentiation of cells within the model.

References

S A Przyborski *et al.*, (2004) *Stem Cells and Development*, Aspron and Lakshmipathy, (2013) *Stem Cell Rev and Rep*, Buta *et al.*, (2013) *Stem Cell Reviews*, Stachelscheid *et al.*, (2013) *J Tissue Eng Regen Med*, Xie *et al.*, (2013) *Exp Cell Res*

10.1.6 Modelling the Development of Human Tissues *In Vitro* Using a Combination of Advanced Cell Technologies and Mammalian Stem Cells (2018) EMBO EMBL Symposium: Organoids, Heidelberg, Germany

10.1.6.1 Abstract

Authors: L A Smith[1], D Owens[1], M F Roger[1], S A Przyborski[1,2]

Affiliations: 1. Durham University, Durham, UK; 2. Reprocell Europe, Sedgefield, UK

Human tissue development is a complex process which remains poorly characterised, with current studies utilising pluripotent stem cells (PSCs) to elucidate the events involved. Embryoid bodies are routinely used to model the process; these multicellular structures are partly controllable, self-organising and recapitulate some aspects of early embryogenesis. However, their use is limited due to loss of organisation and viability as size increases. The increasing diffusion distances reduce oxygen/nutrient diffusion into the centre, leading to cell death and impeding long term studies. Yet time is an essential element of the developmental process. The teratoma assay is also a recognised approach to study complex cellular differentiation: putative PSCs are xenografted into an immunodeficient mouse host, demonstrating their ability to form mature tissues derived from three germ layers. But variation in assay protocols brings into question the use and 'gold standard' status of this assay. In this study we extend embryoid body viability through reducing the diffusion distances, enabling longer in vitro culture and therefore allowing for complex 3D tissue formation. Initial studies proved that embryoid body derived tissues can be maintained for at least 35 days in vitro. Current work involves increasing the physiological relevance of the model by mimicking the teratoma microenvironment, introducing perfusion, and co-culture with relevant immunodeficient mouse fibroblast populations to emulate the subcutaneous grafting of cells to enhance cell differentiation. The model has been validated by direct comparison with the teratoma assay, and current studies are focussing on directed differentiation towards specific lineages. This novel model provides an opportunity to study stages of early human tissue development, as well as a reproducible in vitro alternative to the teratoma assay.

9.1.6.2 Poster

Modelling the Development of Human Tissues *In Vitro* Using a Combination of Advanced Cell Technologies and Mammalian Stem Cells

L.A.Smith[1], D. Owens[1], M. Roger[1], & S.A. Przyborski[1,2]

1. Department of Biosciences, Durham University, UK, 2. Reprocell Europe, Sedgefield, UK

Introduction

Potency is an **important property** of any pluripotent stem cell (PSC) population; **several methods** are used to assess the pluripotent phenotype and determine the developmental potency of novel human PSCs. Amongst these, **the teratoma assay** is considered **the 'gold standard' method.** The formation of a tumour in an immunodeficient mouse host that comprises of **three germ layers is conclusive** of the functional pluripotency of PSCs, see Fig 1a.

The assay also has **applications in human development**, but **inherent variability limits its use/value**, see Fig 1b. This is due to **effects on the differentiation trajectory** of cells, impacting significantly on the resulting tumour and preventing comparison. While ***in vitro* methods** such as embryoid body formation are **more consistent**, they do not offer the complexity of the teratoma assay due to **viability issues** and a limited period of growth which **prevents mature differentiation**.

We hypothesise that an *in vitro* approach can be developed to **replace the use of the animal**, improve **consistency** and enable the **study of stem cell potency** and the formation of rudimentary embryonic tissues representative of all three germ layers. An ***in vitro* model** of human tissue development using **embryoid bodies** and **3D techniques** would provide **a reproducible and controllable alternative** to the teratoma assay. Introducing ***in vivo* like properties** such as **perfusion and co-culture** will mimic the teratoma microenvironment, **enhancing the differentiation** achieved.

*Aim: Produce an **in vitro model of human tissue development** using **PSCs** and **3D cell culture techniques**.*

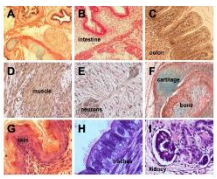


Figure 1a. Examples of structures found within a mature teratoma derived from human pluripotent stem cells: Complex tissues and structures from all three germ layers are present, which is considered a conclusive indicator of cellular pluripotency and developmental potential of putative PSCs.

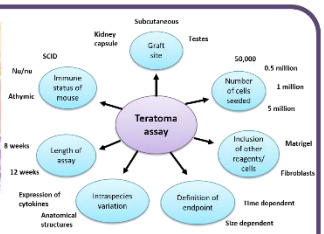


Figure 1b. Variable factors within the teratoma assay protocol: Variation exists both at the technical and biological levels within the assay. Many of these factors are known to have a significant impact on cellular differentiation, and therefore assay results.

Rationale

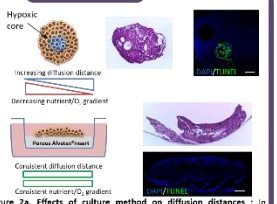


Figure 2a. Effects of culture method on diffusion distances : In suspension, embryoid bodies form a core of cell death, shown by TUNEL, impacting on differentiation and viability. Tissue discs have a reduced diffusion distance, improving viability and differentiation.

Methods

Embryoid body formation and seeding on Alvetex® Polaris

Aims: enhance cell viability, avoid core of cell death, enable prolonged differentiation

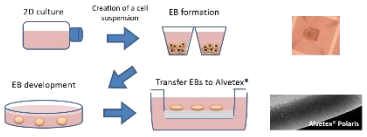


Figure 3a. Protocol for differentiation and maintenance of PSC derived tissues in 3D on Alvetex® Polaris: PSCs are seeded into low adherence microwell plates to form embryoid bodies (EB), before culturing in suspension in Petri dishes. Once EBs have sufficiently matured, these are transferred to Alvetex®, and maintained for an extended culture period.

Emulation of tumour microenvironment using advanced culture methodologies

Aims: improve cell viability over culture time, support maturation of tissue formation over time.

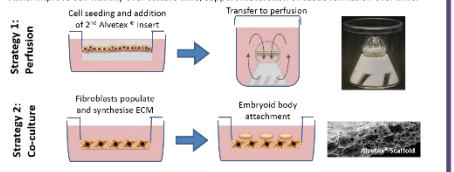


Figure 3b. Protocols for advanced cell culture: Strategy 1: Cells are seeded onto an Alvetex® insert and allowed to attach, before a second insert is placed on top to form a sandwich culture. This is transferred to the perfusion system for culture. **Strategy 2:** Dermal fibroblasts are seeded onto the insert, infiltrate and synthesise an extracellular matrix. Embryoid bodies are seeded onto the surface to differentiate.

Results

Formation of rudimentary embryonic tissues in three dimensional culture conditions

Culturing embryonic stem cell derived embryoid bodies on Alvetex® inserts results in the **formation of a tissue disc,** which can be **successfully maintained** long term, with **no impact on viability.** A variety of complex structures derived from the three germ layers form within the tissue, showing differentiation similar **to teratoma samples** created using the same cell line.

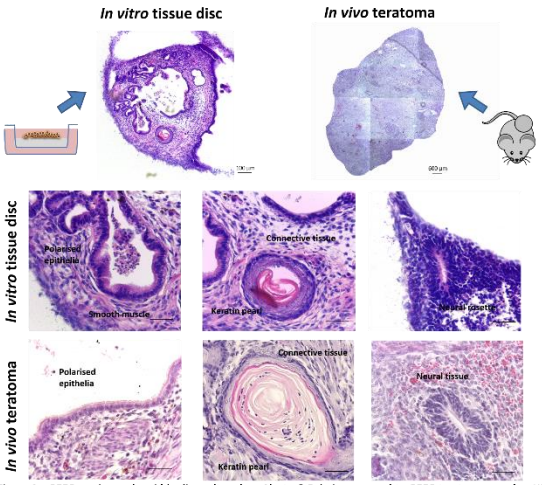


Figure 4a. CGR8 murine embryoid bodies cultured on Alvetex® Polaris compared to CGR8 teratoma samples: H&E stained tissue discs cultured on Alvetex® Polaris for 14 days. Note varied cell morphology, and complex cellular organisation within tissue disc, including structures derived from the three germ layers such as polarised epithelia, connective tissue, smooth muscle, keratin pearls, and neural rosettes Structures show similarities to those seen in the teratoma samples from the animal assay. Scale bar: 50 µm unless stated otherwise.

Introduction of more physiological properties to enhance the cellular microenvironment

The **microenvironment** in which the teratoma tumour forms is **highly complex**; cells are exposed to multiple cues which **affect their differentiation trajectory and survival**. **Perfusion** via vasculature is **essential *in vivo***, and introducing the property *in vitro* allows for **enhanced differentiation and viability,** over a **shorter culture period**. Using a cell suspension in a hydrogel, cells form **colony-like structures** reminiscent of embryonal teratocarcinomas, showing areas of **pluripotency and differentiation**.

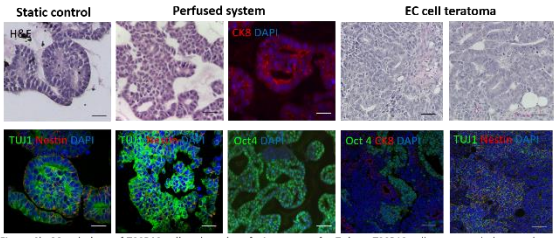


Figure 4b. Morphology of T2SP12 cells cultured perfusion system for 7 days: T2SP12 cells were seeded onto a base insert in a hydrogel, assembled as a sandwich culture in the device and transferred to perfusion. H&E shows highly organised colony-like structures similar to teratomas of the same cell line, and immunostaining highlights areas of Oct 4 positive pluripotent cells, as well as neural and non-neural differentiation. Scale bar: 25 µm and 50 µm

Other cell populations also have a key role in the tumour microenvironment, through the release of **paracrine signals** and the **deposition of the extracellular matrix**. Co-culture with a **relevant fibroblast population** results in **preferential differentiation** of the tissue discs towards **specific germ layers**.

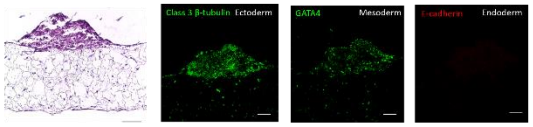


Figure 4c. Characterisation of CGR8 tissue discs cultured on the surface of Alvetex® Scaffold dermal compartment: Immunodeficient mouse fibroblasts cultured in the scaffold for 21 days, before addition of murine embryoid bodies. Co-culture with embryoid bodies for 14 days results in alterations to the morphology of the tissue discs, with, few complex structures and preferential differentiation towards specific germ layers. Scale bar: 50 µm

Conclusions

- **Long term culture** of murine embryoid bodies on Alvetex® is **successful** with evidence of complex tissues derived from three germ layers. The **structures** are **comparable** to those seen in **teratomas**.
- Cells are able to **survive and proliferate in a novel yet simple perfusion system**, showing maintenance of pluripotent and differentiated phenotypes, **similar to teratocarcinoma tumours.**
- **Co-culture** with a relevant **fibroblast population** as a dermal compartment results in a **preferential differentiation** towards specific germ layers.

Future Directions

- Incorporate **human embryonic** and **induced pluripotent stem cells** into the model to further assess the **events of human tissue development.**
- **Direct the differentiation** of the tissues towards **specific germ layers**, focussing more specifically on the pathways involved in **ectodermal fate specification**.
- Evaluate the effects of other **microenvironmental factors** on the **differentiation** of embryonic structures.

References

S A Przyborski et al., (2004) *Stem Cells and Development*, Aspirer and Lakshmipathy, (2015) *Stem Cell Rev and Rep*, Buta et al., (2013) *Stem Cell Reviews*, Stachelscheid et al., (2013) *J Tissue Eng Regen Med*, Kim et al., (2015) *Exp Cell Res*, Müller et al., (2016) *Cell Stem Cell*

10.1.7 Modelling the Development of Human Tissues *In Vitro* Using Advanced Cell Technologies and Mammalian Stem Cells (2018) Anatomical Society Winter Meeting, York, UK

10.1.7.1 Abstract

Authors: L A Smith[1], D Owens[1], S A Przyborski[1,2]

Affiliations: 1. Durham University, Durham, UK; 2. Reprocell Europe, Sedgefield, UK

Human tissue development is a complex, time dependent process, involving morphogen influence on stem cell populations in the developing embryo, and resulting in mature tissue formation. This process remains poorly understood, and current studies utilise pluripotent stem cells (PSCs) to model the events which take place. Specifically, embryoid body (EB) formation is employed, as these multicellular structures are controllable, and recapitulate events of early embryogenesis through their ability to self-organise. However, increasing EB size leads to issues with viability and structure; an increasing diffusion distance limits oxygen and nutrient diffusion, and prevents EB use in long term studies. Yet time is crucial to the tissue development process. The teratoma assay is another approach used to successfully study complex cellular differentiation; putative PSCs are xenografted into an immunodeficient mouse host and allowed to form a tumour. The presence of structures from three germ layers is indicative of pluripotency, yet assay variation brings into question its use and 'gold standard' status. In this study, we extend EB viability by reducing diffusion distances to allow for better nutritional/oxygen support. This enables long term in vitro culture and complex tissue structure formation. Initial investigations showed that EB derived tissues can be maintained for 35 days and further work involved incorporating properties such as perfusion and co-culture, to better mimic the teratoma microenvironment. Model validation through direct comparison to the teratoma assay has shown production of tissues as complex as the in vivo sample. Current focuses on differentiating the model towards specific germ layers to better investigate developmental events, as well as using other PSC populations to fully validate the model and explore its capabilities. The model has potential to be used to study the stages of early tissue development as well as a novel, standardised in vitro alternative to the teratoma assay.

The teratoma assay and associated procedures were completed with permission and according to the guidelines of Newcastle University and the Home Office, UK.

9.1.7.2 Poster

Modelling the Development of Human Tissues *In Vitro* Using a Combination of Advanced Cell Technologies and Mammalian Stem Cells

L.A.Smith[1], D. Owens[1], & S.A. Przyborski[1,2]

1. Department of Biosciences, Durham University, UK, 2. Reprocell Europe, Sedgefield, UK

Introduction

Potency is an **important property** of any pluripotent stem cell (PSC) population; **several methods** are used to assess the pluripotent phenotype and function, determining the developmental potency of novel human PSCs. Amongst these, **the teratoma assay** is considered **the 'gold standard' method.** The formation of a tumour in an immunodeficient mouse host that comprises of **three germ layers is conclusive** of the functional pluripotency of PSCs, see Fig 1a.

The assay also has **applications in the study of human development**, but **inherent variability limits its use/value**, see Fig 1b. This is due to **effects on the differentiation trajectory** of cells, impacting significantly on the resulting tumour and preventing comparison. While ***in vitro* methods** such as embryoid body formation are **more consistent**, they do not offer the complexity of the teratoma assay due to **viability issues** and a limited period of growth which **prevents mature differentiation**.

We hypothesise that an *in vitro* approach can be developed to **replace the use of the animal**, improve **consistency** and enable the **study of stem cell potency** and the formation of rudimentary embryonic tissues representative of all three germ layers. An ***in vitro* model** of human tissue development using **embryoid bodies** and **3D techniques** would provide **a reproducible and controllable alternative** to the teratoma assay. **Directing the differentiation** in the model towards **specific germ layers** using known morphogens would allow for the elucidation of **specific developmental pathways**.

*Aim: Produce an **in vitro model of human tissue development** using **PSCs** and **3D cell culture techniques**.*

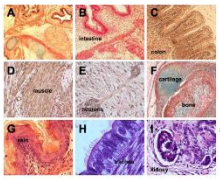


Figure 1a. Examples of structures found within a mature teratoma derived from human pluripotent stem cells: Complex tissues and structures from all three germ layers are present, which is considered a conclusive indicator of cellular pluripotency and developmental potential of putative PSCs.

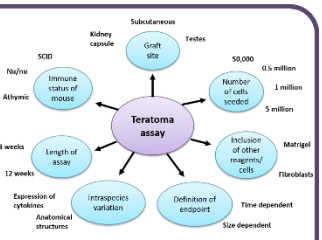


Figure 1b. Variable factors within the teratoma assay protocol: Variation exists both at the technical and biological levels within the assay. Many of these factors are known to have a significant impact on cellular differentiation, and therefore assay results.

Rationale

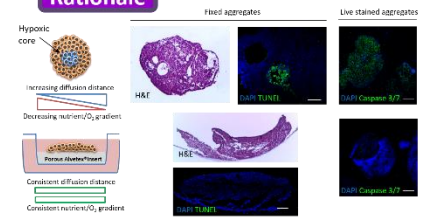


Figure 2a. Effects of *in vitro* culture method on cellular viability: In suspension, embryoid bodies form a core of cell death, shown by TUNEL and live staining with a Caspase 3/7 stain, impacting on differentiation and viability. Tissue discs have a reduced diffusion distance, improving viability and differentiation capacity.

Methods

Embryoid body formation, differentiation and seeding on Alvetex® Polaris

Aims: enhance cell viability, avoid core of cell death, enable prolonged differentiation, differentiate embryoid bodies towards specific germ layers

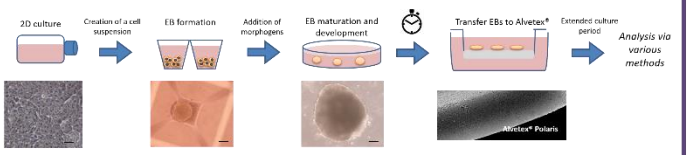


Figure 3a. Protocol for differentiation and maintenance of PSC derived tissues in 3D on Alvetex® Polaris: PSCs are seeded into low adherence microwell plates to form embryoid bodies (EBs), with the addition of morphogens to direct the differentiation towards the three germ layers. EBs are then transferred to suspension culture in Petri dishes. Once EBs have sufficiently matured, these are transferred to Alvetex®, and maintained for an extended culture period, before analysis using a variety of methods.

Results

Formation of rudimentary embryonic tissues in three dimensional culture conditions

Culturing embryonic stem cell derived embryoid bodies on Alvetex® inserts results in the **formation of a tissue disc,** which can be **successfully maintained** long term, with **no impact on viability.** A variety of complex structures derived from the three germ layers form within the tissue, showing differentiation similar **to teratoma samples** created using the same cell line.

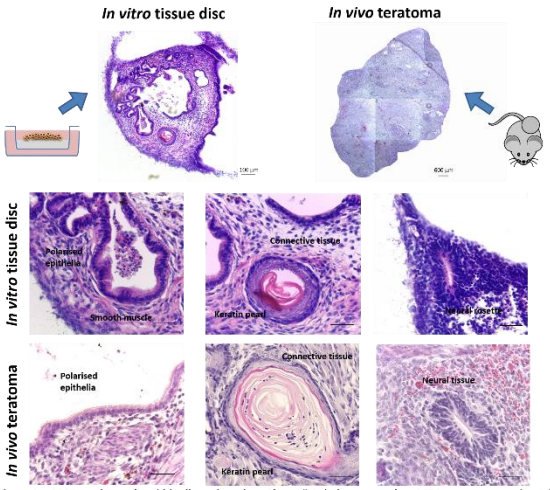


Figure 4a. CGR8 murine embryoid bodies cultured on Alvetex® Polaris compared to CGR8 teratoma samples: H&E stained tissue discs cultured on Alvetex® Polaris for 14 days. Note varied cell morphology, and complex cellular organisation within tissue disc, including structures derived from the three germ layers such as polarised epithelia, connective tissue, smooth muscle, keratin pearls, and neural rosettes Structures show similarities to those seen in the teratoma samples from the animal assay. Scale bar: 50 µm unless stated otherwise.

Induction of germ layer specific structures using a combination of developmental morphogens

During the process of embryonic development, **pluripotent stem cells** from the **inner cell mass** become **progressively more specialised**, and differentiate into one of the **three germ layer lineages**. To recapitulate this *in vitro*, embryoid bodies were exposed to **combinations of morphogens** to direct the differentiation towards specific germ layers: **ectoderm, mesoderm and endoderm.** Tissue discs which formed on the insert showed a shift in the structures present according to the morphogens used.

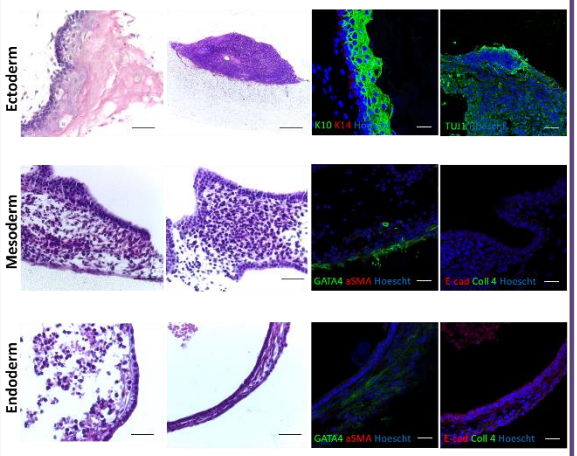


Figure 4c. Culture of germ layer differentiated CGR8 embryoid bodies on Alvetex® Polaris: Embryoid bodies were treated with morphogens during the formation phase before seeding on Alvetex® Polaris. Tissue discs show a preference for the formation of germ layer specific structures, and the absence of structures associated with the other germ layers. Ectoderm tissue disc shows stratified skin and neural tissues, mesoderm tissue disc shows only simple epithelia and connective tissues, endoderm tissue disc shows complex epithelial structures Scale bar: 50 µm

Conclusions

- **Long term culture** of murine embryoid bodies on Alvetex® is **successful** with evidence of complex tissues derived from three germ layers forming within the model. The **structures** are **comparable** to those seen in **teratomas** formed using the same cell line.
- **Directing the differentiation** of embryoid bodies towards **specific germ layers** using combinations of morphogens prior to seeding in the model results in the **preferential differentiation** of the tissue discs towards the **appropriate germ layer**.

Future Directions

- Incorporate **human embryonic** and **induced pluripotent stem cells** into the model to further assess the **events of human tissue development**.
- **Further direct the differentiation** of the tissues towards **specific germ layers**, focussing more specifically on the pathways involved in **ectodermal fate specification**.
- Evaluate the effects of other **microenvironmental factors** on the **differentiation** of embryonic structures.

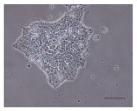


Figure 5: Human iPSC colony in culture

References

S.A Przyborski et al., (2000) *Stem Cells and Development*, Aspirer and Lakshmipathy, (2015) *Stem Cell Rev and Rep*, Balla et al., (2013) *Stem Cell Reviews*, Stachelscheid et al., (2013) *J Tissue Eng Regen Med*, Kim et al., (2014) *Exp Cell Res*, Müller et al., (2012) *Cell Stem Cell*

10.1.8 Modelling the Development of Human Tissues *In Vitro* Using Advanced Cell Technologies and Mammalian Stem Cells (2019) BSCB BSDB Joint Meeting, Coventry, UK

10.1.8.1 Abstract

Authors: L A Smith[1], F Liu[1], D Owens[1], S A Przyborski[1,2]

Affiliations: 1. Durham University, Durham, UK; 2. Reprocell Europe, Sedgefield, UK

Human tissue development is a complex, time dependent process, yet remains poorly understood. Current studies utilise pluripotent stem cells (PSCs) to model these events; embryoid body (EB) formation is employed, as these multicellular structures are controllable, and recapitulate events of early embryogenesis through self-organisation. However, increasing EB size leads to an increasing diffusion distance, limiting oxygen/nutrient access and long term studies. But time is crucial to the development process. In this study, we extend EB viability by reducing diffusion distances, allowing for better nutritional/oxygen support. This enables long term culture and complex tissue structure formation: EB derived tissues can be maintained for up to 35 days. Current work focuses specific germ layer differentiation to better investigate developmental events and using other PSC populations to validate the model. This has potential to be used to study early tissue development as well as a novel in vitro alternative to the teratoma assay.

9.1.8.2 Poster

Modelling the Development of Human Tissues *In Vitro* Using a Combination of Advanced Cell Technologies and Mammalian Stem Cells

L.A.Smith[1], F Liu[1], D. Owens[1] & S.A. Przyborski[1,2]

1. Department of Biosciences, Durham University, UK, 2. Reprocell Europe, Sedgefield, UK

Introduction

Potency is an **important property** of any pluripotent stem cell (PSC) population; **several methods** are used to assess the pluripotent phenotype and function, determining the developmental potency of novel human PSCs. Amongst these, **the teratoma assay** is considered **the 'gold standard' method.** The formation of a tumour in an immunodeficient mouse host that comprises of **three germ layers is conclusive** of the functional pluripotency of PSCs, see Fig 1a.

The assay also has **applications in the study of human development**, but **inherent variability limits its use/value**, see Fig 1b. This is due to **effects on the differentiation trajectory** of cells, impacting significantly on the resulting tumour and preventing comparison. While ***in vitro* methods** such as embryoid body formation are **more consistent**, they do not offer the complexity of the teratoma assay due to **viability issues** and a limited period of growth which **prevents mature differentiation**.

We hypothesise that an *in vitro* approach can be developed to **replace animal usage**, improve **consistency** and enable the **study of stem cell potency** and the formation of rudimentary embryonic tissues representative of all three germ layers. An ***in vitro* model** of human tissue development using **embryoid bodies (EB)** and **3D techniques** would provide **a reproducible and controllable alternative** to the teratoma assay. **Directing the differentiation** in the model towards **specific germ layers** using known morphogens would allow for the elucidation of **specific developmental pathways.**

*Aim: Produce an **in vitro model of human tissue development** using **PSCs** and **3D cell culture techniques**.*

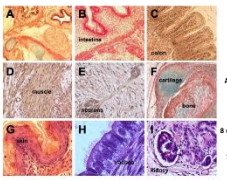


Figure 1a. Examples of structures found within a mature teratoma derived from human pluripotent stem cells: Complex tissues and structures from all three germ layers are present, which is considered a conclusive indicator of cellular pluripotency and developmental potential of putative PSCs.

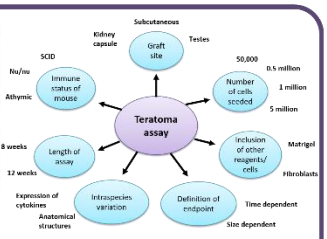


Figure 1b. Variable factors within the teratoma assay protocol: Variation exists both at the technical and biological levels within the assay. Many of these factors are known to have a significant impact on cellular differentiation, and therefore assay results.

Rationale

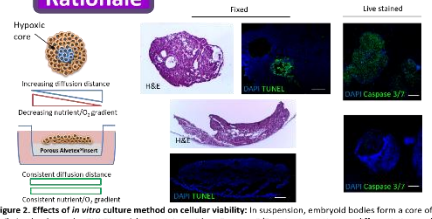


Figure 2. Effects of *in vitro* culture method on cellular viability: In suspension, embryoid bodies form a core of cell death, shown by TUNEL and live staining with a Caspase 3/7 stain, impacting on differentiation and viability. Tissue discs have a reduced diffusion distance, improving viability and differentiation capacity.

Methods

Embryoid body formation, differentiation and seeding on Alvetex® Polaris

Aims: enhance cell viability, avoid core of cell death, enable prolonged differentiation, differentiate embryoid bodies towards specific germ layers

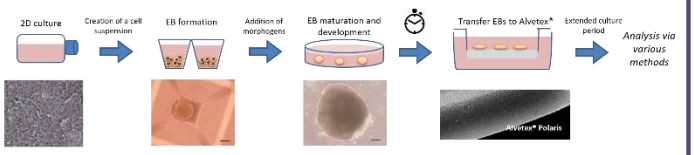


Figure 3. Protocol for differentiation and maintenance of PSC derived tissues in 3D on Alvetex® Polaris: PSCs are seeded into low adherence microwell plates to form embryoid bodies (EBs), with the addition of morphogens to direct the differentiation towards the three germ layers. EBs are then transferred to suspension culture in Petri dishes. Once EBs have sufficiently matured, these are transferred to Alvetex®, and maintained for an extended culture period, before analysis using a variety of methods.

Results

Formation of rudimentary embryonic tissues in three dimensional culture conditions

Culturing embryonic stem cell derived EBs on Alvetex® inserts results in the **formation of a tissue disc,** which can be **successfully maintained** long term, with **no impact on viability.** A variety of complex structures derived from the three germ layers form within the tissue, showing differentiation similar **to teratoma samples** created using the same cell line.

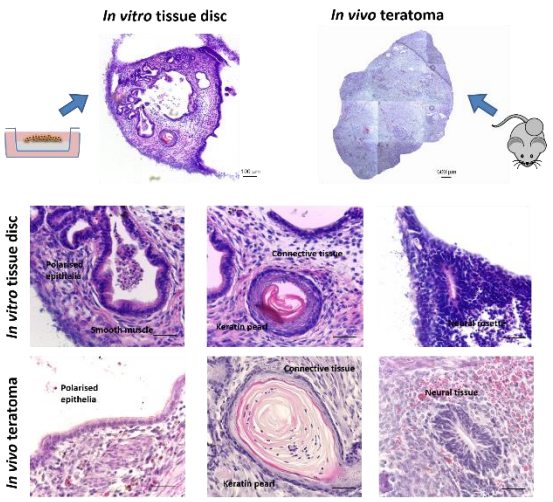


Figure 4a. CGR8 murine embryoid bodies cultured on Alvetex® Polaris compared to CGR8 teratoma samples: H&E stained tissue discs cultured on Alvetex® Polaris for 14 days. Note varied cell morphology, and complex cellular organisation within tissue disc, including structures derived from the three germ layers such as polarised epithelia, connective tissue, smooth muscle, keratin pearls, and neural rosettes Structures show similarities to those seen in the teratoma samples from the animal assay. Scale bar: 50 µm unless stated otherwise.

Induction of germ layer specific structures using a combination of developmental morphogens

To recapitulate the process of **PSC lineage specification** within the developing embryo, EBs were exposed to **multiple morphogens** to direct the differentiation towards specific germ layers: **ectoderm, mesoderm and endoderm**. Tissue discs which formed on the insert showed a shift in the structures present according to the morphogens used.

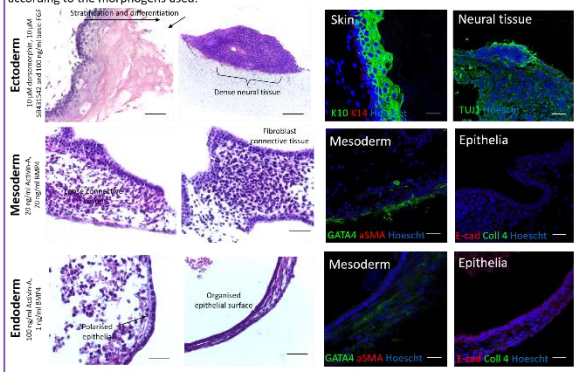


Figure 4b. Culture of differentiated CGR8 embryoid bodies on Alvetex® Polaris: EBs were treated with morphogens during the formation phase before seeding on Alvetex® Polaris. Tissue discs show formation of germ layer specific structures: Ectoderm tissue disc shows stratified skin and neural tissues, mesoderm tissue disc shows only simple epithelia and connective tissues, endoderm tissue disc shows complex epithelial structures Scale bar: 50 µm

Application of technologies to assess the differentiation of human pluripotent stem cell lines

To better allow for the **assessment of human PSC developmental potency** and **study of human tissue development**, human PSCs were used to form EBs to seed in the model. Tissue discs are able to form, showing **heterogeneity** and evidence of **differentiated structures.**

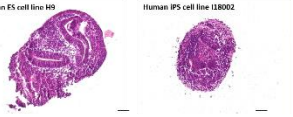


Figure 4c. Histology of human ES and iPS EBs on Alvetex® Polaris: EBs were allowed to form over 7 days before seeding on Alvetex® Polaris for tissue disc formation for up to 28 days. Scale bar: 50 µm

Conclusions

- **Long term culture** of murine EBs on Alvetex® is **successful** with evidence of complex tissues derived from three germ layers, which are **comparable** to those in **teratomas** formed using the same cell line.
- **Directing the differentiation** of EBs towards **specific germ layers** using multiple morphogens results in the **preferential differentiation** of the tissue discs towards the **appropriate germ layer**.
- The technology and methodology used in this model is **applicable to human pluripotent stem cell lines**.

Future Directions

- **Further direct the differentiation** of the tissues towards **specific germ layers**, focussing more specifically on the pathways involved in **ectodermal fate specification**.
- Evaluate the effects of other **microenvironmental factors** on the **differentiation** of embryonic structures, such as **paracrine signals, tissue perfusion and oxygen tension**



Figure 5. Example of a simple bioreactor system to introduce perfusion into a scaffold culture

References

S A Przyborski *et al.*, (2004) *Stem Cells and Development*, Asprer and Lakshmipathy, (2015) *Stem Cell Rev and Rep*, Buta *et al.*, (2013) *Stem Cell Reviews*, Stachelsheid *et al.*, (2013) *J Tissue Eng Regen Med*, Kim *et al.*, (2015) *Exp Cell Res*, Müller *et al.*, (2010) *Cell Stem Cell*

10.1.9 Modelling the Development of Human Tissues In Vitro Using Mammalian Stem Cells and Advanced Cell Technologies (2019) IFAA, London, UK

10.1.9.1 Abstract

Authors: L A Smith[1], D Owens[1], S A Przyborski[1,2]

Affiliations: 1. Durham University, Durham, UK; 2. Reprocell Europe, Sedgefield, UK

Human tissue development is a complex process which occurs within the developing embryo, resulting in the progression from a totipotent zygote to the complex tissues found in the human body. This is a process that remains poorly understood; current studies utilise pluripotent stem cells (PSCs) to model events which take place. Specifically, embryoid body (EB) formation is used, as these multicellular structures are highly controllable and show self-organisation, recapitulating some events of early embryogenesis. Increasing EB size leads to viability and structure issues with an increasing diffusion distance limiting oxygen/nutrient diffusion. This prevents long term EB studies, yet time is crucial to the developmental process. The teratoma assay is also used to study complex cellular differentiation: putative PSCs are xenografted into an immunodeficient mouse host, forming a tumour. The detection of structures from three germ layers is indicative of pluripotency, yet assay variation brings into question its 'gold standard' status. In this study, we have used a polystyrene scaffold in combination with advanced culture methods to improve cellular viability, therefore enabling long term *in vitro* culture. Initial studies extended EB viability through seeding onto the scaffold, showing that the resultant tissue discs produce recognisable mature structures derived from each germ layer. Use of the scaffold in a novel perfusion system shows cells can be maintained *in vitro* for time periods comparable to the teratoma assay. Recent work has focussed on directing the differentiation of EBs towards specific germ layers as well as using human PSC populations to fully validate the model. This model has potential to be used to study early tissue development, as well as providing an *in vitro* animal free alternative to the teratoma assay.

The teratoma assay and associated procedures were completed with permission and according to the guidelines of Newcastle University and the Home Office, UK.

9.1.9.2 Poster

Modelling the Development of Human Tissues *In Vitro* Using Mammalian Stem Cells and Advanced Cell Technologies

L.A.Smith[1], D. Owens[1] & S.A. Przyborski[1,2]

1. Department of Biosciences, Durham University, UK, 2. Reprocell Europe, Sedgefield, UK

Introduction

Potency is an **important property** of any pluripotent stem cell (PSC) population; **several methods** are used to assess the pluripotent phenotype and function, determining the developmental potency of novel human PSCs. Amongst these, **the teratoma assay** is considered **the 'gold standard' method.** The formation of a tumour in an immunodeficient mouse host that comprises of **three germ layers is conclusive** of the functional pluripotency of PSCs, see Fig 1a.

The assay also has **applications in the study of human development**, but **inherent variability limits its use/value**, see Fig 1b. This is due to **effects on the differentiation trajectory** of cells, impacting significantly on the resulting tumour and preventing comparison. While ***in vitro* methods** such as embryoid body formation are **more consistent,** they do not offer the complexity of the teratoma assay due to **viability issues** and a limited period of growth which **prevents mature differentiation**.

We hypothesise that an *in vitro* approach can be developed to **replace animal usage**, improve **consistency** and enable the **study of stem cell potency** and the formation of rudimentary embryonic tissues representative of all three germ layers. An ***in vitro* model** of human tissue development using **embryoid bodies (EB)** and **3D techniques** would provide a **reproducible and controllable alternative** to the teratoma assay. **Directing the differentiation** in the model towards **specific germ layers** using known morphogens would allow for the elucidation of **specific developmental pathways**. The model also has scope for the introduction of more physiological properties, such as perfusion.

*Aim: Produce an **in vitro model of human tissue development** using **PSCs** and **3D cell culture techniques**.*

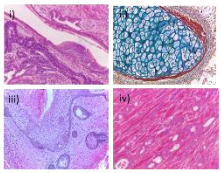


Figure 1a. Example structures found within a mature teratoma derived from human pluripotent stem cells: i) Complex structures from all three germ layers are present: this is considered a conclusive indicator of the developmental potential of putative PSCs. Images show ii) cartilage (blue) and bone (red) detected with Weighert's stain, iii) straitified skin and iv) muscle tissues.

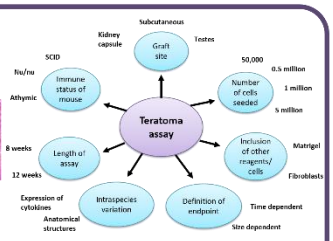


Figure 1b. Variable factors within the teratoma assay protocol: Variation exists both at the technical and biological levels within the assay. Many of these factors are known to have a significant impact on cellular differentiation, and therefore assay results.

Rationale

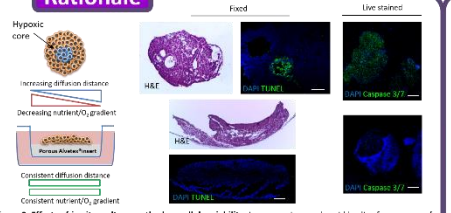


Figure 2. Effects of *in vitro* culture method on cellular viability: In suspension, embryoid bodies form a core of cell death, shown by TUNEL and live staining with a Caspase 3/7 stain, impacting on differentiation and viability. Tissue discs have a reduced diffusion distance, improving viability and differentiation capacity.

Methods

Preparation and seeding of cellular material on Alvetex® Polaris

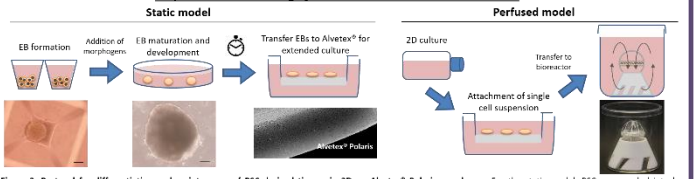


Figure 3. Protocol for differentiation and maintenance of PSC derived tissues in 3D on Alvetex® Polaris membrane: For the static model, PSCs are seeded into low adherence microwell plates to form embryoid bodies (EBs); morphogens are added to direct the differentiation towards the three germ layers. EBs are then transferred to suspension culture in Petri dishes and then to Alvetex® membranes for extended culture once sufficiently matured. To set up the perfused model, a single cell suspension is seeded onto the Alvetex® membrane and allowed to attach before transfer to the insert holder and culture on the perfusion bioreactor.

Results

Induction of germ layer specific structures using a combination of developmental morphogens

To recapitulate the process of **PSC lineage specification** within the developing embryo, EBs were exposed to **multiple morphogens** to direct the differentiation towards specific germ layers: **ectoderm, mesoderm and endoderm**. Tissue discs which formed on the insert showed **a shift in the structures present** according to the morphogens used.

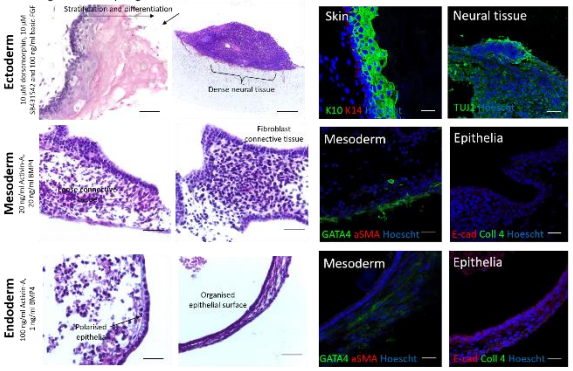


Figure 3a. Culture of differentiated CGR8 embryoid bodies on Alvetex® Polaris: EBs were treated with morphogens during the formation phase before seeding on Alvetex® Polaris. Tissue discs show formation of germ layer specific structures: Ectoderm tissue disc shows stratified skin and neural tissues, mesoderm tissue disc shows only simple epithelia and connective tissues, endoderm tissue disc shows complex epithelial structures Scale bar: 50 µm

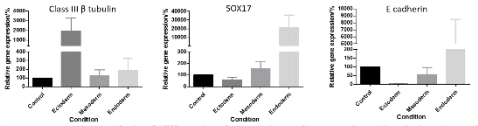


Figure 3b. Gene expression analysis of differentiated CGR8 tissue discs on Alvetex® Polaris: Tissue discs were analysed using germ layer specific genes to assess the differentiation within the tissue disc population. qPCR analysis shows that generally, there is a shift in the differentiation towards the intended germ layer.

Incorporation of more physiological properties to recapitulate the in vivo microenvironment

The *in vivo* microenviroment that cells are exposed to is **highly complex, with multiple integrated physical, chemical and biological cues.** Of particular importance is the maintenance of cellular homeostasis through **the vasculature**; vessels provide a continuous supply of oxygen and nutrients while removing metabolites. Introducing perfusion into the *in vitro* environment **enhances the differentiation** which occurs within PSC derived tissue discs.

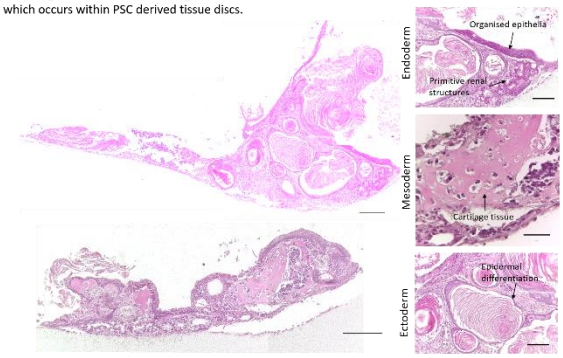


Figure 4a. Creation of CGR8 derived tissue disc on Alvetex® Polaris in a novel perfusion system: CGR8 cells were seeded onto Alvetex® Polaris and allowed to attached before transfer to the perfused system for 56 days. Tissue discs which formed were significantly larger than those previously seen, with evidence of differentiation from the three germ layers; mature stratified skin, specialised epithelial and cartilage formation. Scale bars: 100 µm and 50 µm

Application of technologies to assess the differentiation of human pluripotent stem cell lines

To better allow for the **assessment of human PSC developmental potency** and **study of human tissue development,** human PSCs were used to form EBs to seed in the model. Tissue discs are able to form, showing **heterogeneity** and evidence of **differentiated structures.**

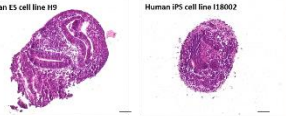


Figure 4b. Histology of human ES and iPS EBs on Alvetex® Polaris: EBs were allowed to form over 7 days before seeding on Alvetex® Polaris for tissue disc formation for up to 28 days. Scale bar: 50 µm

Conclusions

- **Directing the differentiation** of EBs towards **specific germ layers** using multiple morphogens results in the **preferential differentiation** of the tissue discs towards the **appropriate germ layer.**
- Introducing **perfusion allows for long term culture** of murine PSCs on Alvetex®, resulting in the formation of various complex tissue structures derived from **three germ layers**, which are **comparable** to those in **teratomas.**
- The technology and methodology used in this model is **applicable to human pluripotent stem cell lines**.

Future Directions

- **Further direct the differentiation** of the tissues towards **specific germ layers**, focussing more specifically on the pathways involved in **ectodermal fate specification**.
- Evaluate the effects of other **microenvironmental factors** on the **differentiation** of embryonic structures, such as **paracrine signals, tissue perfusion and oxygen tension**

References

S A Przyborski *et al.*, (2004) *Stem Cells and Development*, Asprer and Lakshmipathy, (2015) *Stem Cell Rev and Rep*, Buta *et al.*, (2013) *Stem Cell Reviews*, Stachelsheid *et al.*, (2013) *J Tissue Eng Regen Med*, Kim *et al.*, (2015) *Exp Cell Res*, Müller *et al.*, (2010) *Cell Stem Cell*

10.2 Appendix 2 – Oral presentations

10.2.1 Modelling the Development of Human Tissues *In Vitro* Using a Combination of Advanced Cell Technologies and Mammalian Stem Cells (2017) North East Postgraduate Conference, Newcastle, UK

The development of complex, mammalian tissues remains poorly understood. Pluripotent stem cells (PSCs) are an invaluable tool employed extensively to study tissue development, including the formation of embryoid bodies. These multicellular structures can self organise, recapitulating aspects of early mammalian embryogenesis, but their use is limited by disorganisation and a loss of viability as size increases. This is partly due to the increasing diffusion distance and inability of nutrients and oxygen to fully diffuse into the structure, leading to cell death and impeding the ability to conduct longer term differentiation studies. Yet time is an essential element of the developmental process. The teratoma assay is a recognised approach to study complex cellular differentiation long term using PSCs, demonstrating their ability to form highly mature tissues. In this study we extend embryoid body viability through reducing the diffusion distances, enabling longer *in vitro* culture and enhancing differentiation. By introducing perfusion using a novel yet simple system, the complexity of the model has been further increased to more closely resemble the physiological environment, enabling the formation of complex structures as seen in teratomas. Histological staining and immunofluorescence have enabled the identification and visualisation of the structures. Initial experiments used an embryonal carcinoma cell line to allow for optimisation of methodologies and proof of concept experiments. Further work using a murine embryonic stem cell line has demonstrated the ability to maintain the tissue structures in the *in vitro* environment for a significant time, forming highly complex structures. It is anticipated that this model will provide a novel animal free *in vitro* alternative to the current pluripotency assessment method, the xenograft based teratoma assay, and provide an approach to investigate the early stages of tissue development.

10.2.2 Modelling the Development of Human Tissues *In Vitro* Using a Combination of Advanced Cell Technologies and Mammalian Stem Cells (2018) Durham University Department of Biosciences Postgraduate Conference, Durham, UK

Using functional tests is the most definitive method of assessing stem cell pluripotency, and previously, the teratoma assay has been regarded the ‘gold standard’ for analysing the pluripotency and differentiation capacity of human pluripotent stem cells (HPSCs). However, this assay has limitations, in particular variability in the protocol, including variation in the initial cell seeding number, graft site and assay length, all of which are known to impact on the differentiation trajectory of HPSCs. This results in inconsistency between assays and a lack of comparability. An alternative method is required, which is consistent and reproducible, yet permits long term studies for complex tissue differentiation. We have created a novel model, which extends embryoid body viability by

reducing diffusion distances, therefore allowing for complex tissue structure formation over a longer culture period. Initial model optimisation involved studies proving that embryoid tissues can be maintained for up to 35 days, and current work involves increasing the physiological relevance of the model by mimicking the teratoma microenvironment. This includes introducing perfusion to the culture setting, and co-culture studies using primary immunodeficient mouse fibroblast cells to emulate subcutaneous grafting of cells. These have resulted in more complex structure formation and enhanced differentiation of embryonic tissues. This model has the potential to provide a novel, reproducible, standardised in vitro alternative to the teratoma assay, as well as an opportunity to study stages of early tissue development.

10.2.3 Modelling the Development of Human Tissues *In Vitro* Using a Combination of Advanced Cell Technologies and Mammalian Stem Cells (2018) Anatomical Society Summer Meeting, Oxford, UK

Human tissue development is a complex, time dependent process which remains poorly understood, with current studies utilising pluripotent stem cells (PSCs) to attempt to elucidate the events involved. Embryoid bodies are commonly used to model this process, as these multicellular structures are controllable, and can self-organise, recapitulating early embryogenesis. However, their use is limited due to loss of organisation and viability as size increases. The increasing diffusion distance reduces oxygen and nutrient diffusion into the centre, leading to cell death and impeding long term studies. Yet time is an essential element of the developmental process. The teratoma assay is also a recognised approach to study complex cellular differentiation. Putative PSCs are xenografted into an immunodeficient mouse host, demonstrating their ability to form highly mature tissues derived from the three germ layers, but variation in assay protocols brings into question the use and 'gold standard' status of the assay. In this study we extend embryoid body viability through reducing the diffusion distances, enabling longer *in vitro* culture and therefore allowing for complex tissue structure formation. Initial optimisation studies proved that embryoid body derived tissues can be maintained for up to 35 days, and current work involves increasing the physiological relevance of the model by mimicking the teratoma microenvironment. This includes introducing perfusion to the culture setting, and co-culture studies using primary immunodeficient mouse fibroblast cells to emulate subcutaneous grafting of cells, resulted in more complex structure formation and enhanced differentiation of embryonic tissues. Model validation through direct comparison with the teratoma assay has shown the ability of the model to form equally complex structures derived from the three primary germ layers. This model has the potential to provide a novel, reproducible, standardised *in vitro* alternative to the teratoma assay, as well as an opportunity to study stages of early tissue development.

The teratoma assay and associated procedures were completed with permission and according to the guidelines of Newcastle University and the Home Office, UK.

10.3 Appendix 3 – Histological stain recipes

10.3.1 Haematoxylin and Eosin staining

10.3.1.1 Haematoxylin

Haematoxylin was made as described or purchased from Sigma Aldrich, Dorset, UK.

Haematoxylin – 1 g

Sodium iodate - 0.2 g

Aluminium potassium sulphate – 50 g

Distilled water - 1 L

Above reagents combined and dissolved, left to stir overnight.

Chloral hydrate – 50 g

Citric acid crystals – 1 g

Above reagents added the following day, dissolved and the solution heated to boiling point for 5 minutes, before leaving to ripen for 3 months.

10.3.1.2 Eosin

Eosin Y – 2 g

95 % ethanol – 1 L

10.3.2 Masson's Trichrome staining

10.3.2.1 Weighert's Iron Haematoxylin

Solution A

Haematoxylin – 1 g

95 % ethanol – 100 mL

Solution B

29 % Ferric chloride in dH_2O – 4 mL

Deionised water – 95 mL

Concentrated hydrochloric acid – 1 mL

Working solution – mix Solutions A and B in a 1:1 ratio. Solution is stable for up to 30 days.

10.3.2.2 Biebrich Scarlet- Acid Fuschin solution

1 % aqueous Biebrich Scarlet – 90 mL

1 % aqueous Acid Fuschin – 10 mL

Glacial Acetic Acid – 1 mL

10.3.2.3 Phosphomolybdic-Phosphotungstic Acid Solution

5 % Phosphomolybdic acid – 25 mL

5 % Phosphotungstic acid – 25 mL

10.3.2.4 Aniline blue solution

Aniline blue – 2.5 g

Glacial Acetic Acid – 2 mL

Deionised water – 100 mL

10.3.2.5 1% Acetic acid solution

Acetic acid – 1 mL

Deionised water – 9 mL

10.3.3 Weighert's staining

10.3.3.1 Weighert's iron Haematoxylin

As above.

10.3.3.2 Alcian blue

Alcian blue – 1 g

Glacial Acetic Acid – 3 mL

Deionised water – 100 mL

10.3.3.3 Ponceau S

1 % aqueous Ponceau S – 10 mL

Glacial acetic acid - 1.2 mL

Saturated aqueous picric acid – 90 mL

10.3.3.4 1 % acid wash

Concentrated hydrochloric acid – 1 mL

70 % ethanol – 99 mL

10.4 Appendix 4 – Western Blotting recipes

10.4.1 Gel Casting recipe

Table 10.1. Recipes for making polyacrylymide gels

Components	**5 % Stacking Gel**		**8 % Resolving Gel**		**10 % Resolving Gel**	
	2 Gels	**4 Gels**	**2 Gels**	**4 Gels**	**2 Gels**	**4 Gels**
dH_2O	5.625 mL	11.25 mL	11.4 mL	22.8 mL	10.6 mL	21.2 mL
Prosieve	750 µL	1.5 mL	3.2 mL	6.4 mL	4 mL	8 mL
1.5M Tris pH 6.8	1 mL	2 mL	-	-	-	-
1.5 M Tris pH 8.8	-	-	5 mL	10 mL	5 mL	10 mL
10% SDS	75 µL	150 µL	200 µL	400 µL	200 µL	400 µL
10% APS	75 µL	150 µL	200 µL	400 µL	200 µL	400 µL
Temed	7.5 µL	15 µL	10 µL	20 µL	10 µL	20 µL

10.4.2 Buffer recipes

10.4.2.1 10x Tank buffer recipe

Tris – 30.28 g

Glycine – 144.1 g

SDS – 10 g

Add deionised water up to 1 L

10.4.2.2 1x Tank buffer recipe

10x Tank buffer – 100 mL

Deionised water – 900 mL

10.4.2.3 10x Transfer buffer recipe

Tris – 30.28g

Glycine – 144.1 g

Add deionised water up to 1 L and adjust pH to between 9.0 and 9.4

10.4.2.4 1x Transfer buffer recipe

10x Transfer buffer – 100 mL

Methanol – 200 mL

Deionised water – 700 mL

10.5 Appendix 5 – PCR primer optimisation data

10.5.1 Cytokeratin 10

Optimum running temperature = 60°C

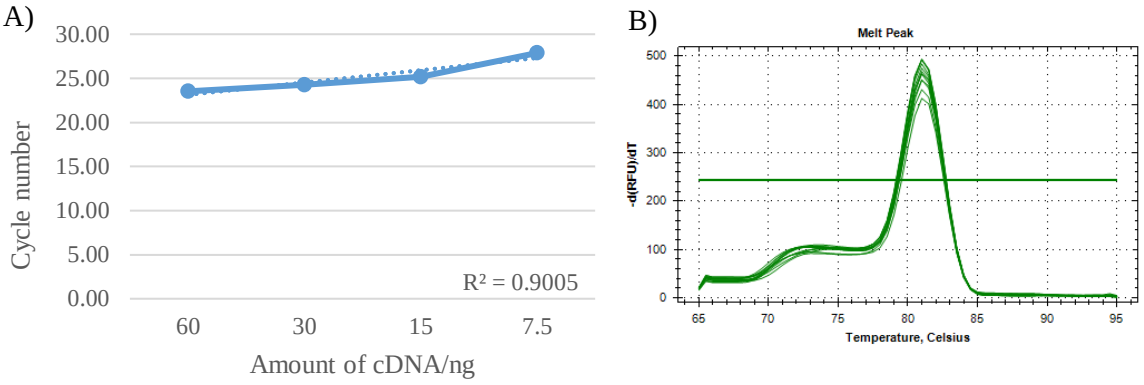


Figure 10.1: Primer optimisation for cytokeratin 10: A) Primers were run at a range of cDNA values. An R^2 value close to 1 indicates primer efficiency. B) The melt curve for the primer provides information on primer specificity, with a single peak indicting the synthesis of a single product.

10.5.2 Cytokeratin 14

Optimum running temperature = 60°C

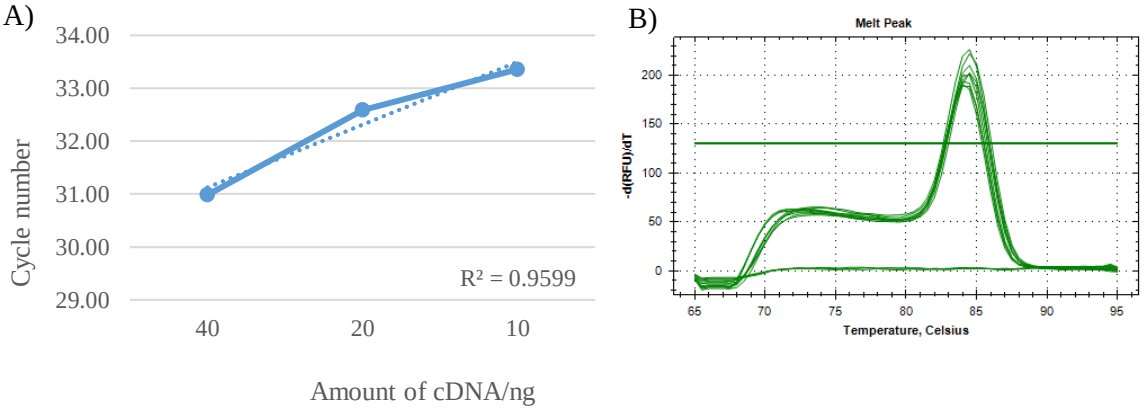


Figure 10.2: Primer optimisation for cytokeratin 14: A) Primers were run at a range of cDNA values. An R^2 value close to 1 indicates primer efficiency. B) The melt curve for the primer provides information on primer specificity, with a single peak indicting the synthesis of a single product.

10.5.3 Class III β tubulin

Optimum running temperature = 60°C

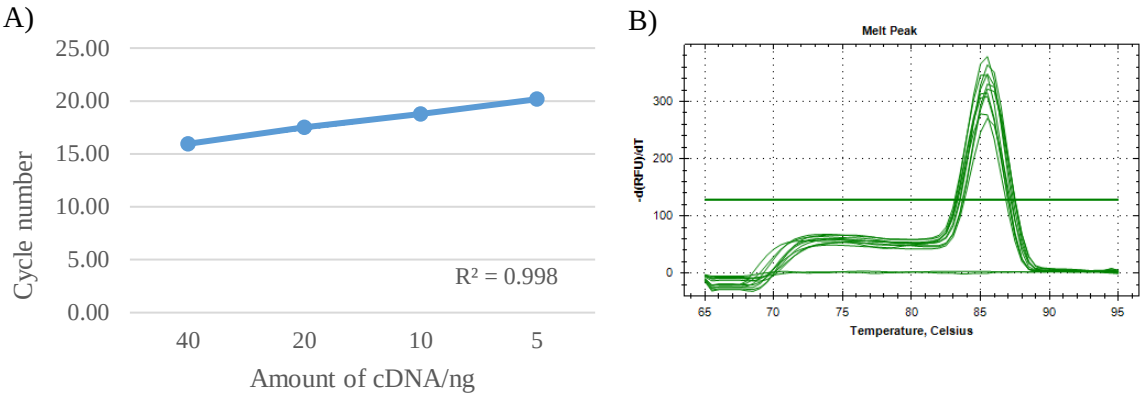


Figure 10.3: Primer optimisation for Class III β tubulin: A) Primers were run at a range of cDNA values. An R^2 value close to 1 indicates primer efficiency. B) The melt curve for the primer provides information on primer specificity, with a single peak indicting the synthesis of a single product.

10.5.4 E cadherin

Optimum running temperature = 60°C

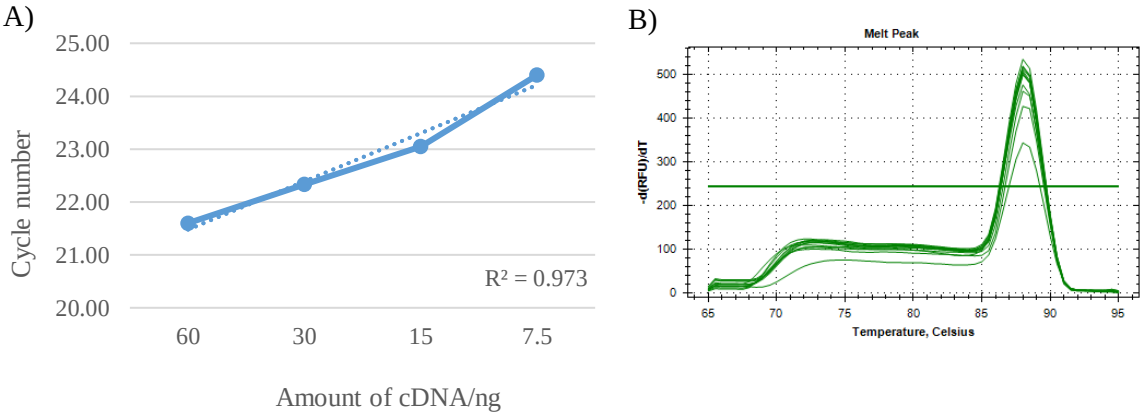


Figure 10.4: Primer optimisation for E cadherin: A) Primers were run at a range of cDNA values. An R^2 value close to 1 indicates primer efficiency. B) The melt curve for the primer provides information on primer specificity, with a single peak indicting the synthesis of a single product.

10.5.5 Brachyury

Optimum running temperature = 60°C

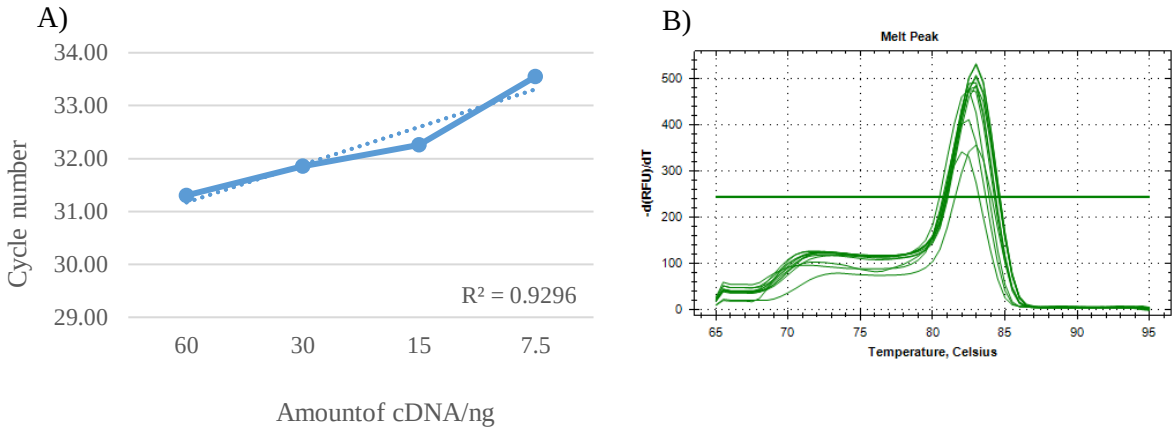


Figure 10.5: Primer optimisation for Brachyury: A) Primers were run at a range of cDNA values. An R^2 value close to 1 indicates primer efficiency. B) The melt curve for the primer provides information on primer specificity, with a single peak indicting the synthesis of a single product.

10.5.6 Alpha fetoprotein

Optimum running temperature = 60°C

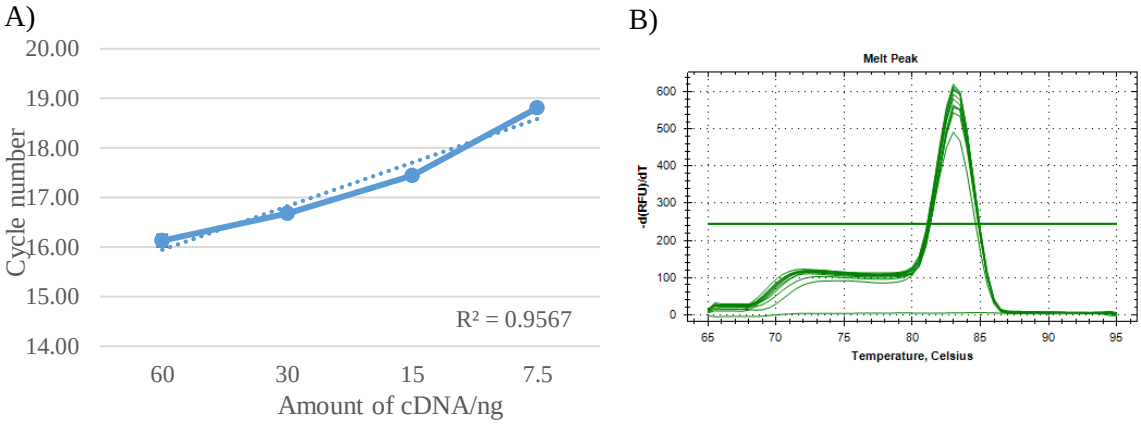


Figure 10.6: Primer optimisation for Alpha fetoprotein: A) Primers were run at a range of cDNA values. An R^2 value close to 1 indicates primer efficiency. B) The melt curve for the primer provides information on primer specificity, with a single peak indicting the synthesis of a single product.

10.5.7 FOXA2

Optimum running temperature = 60°C

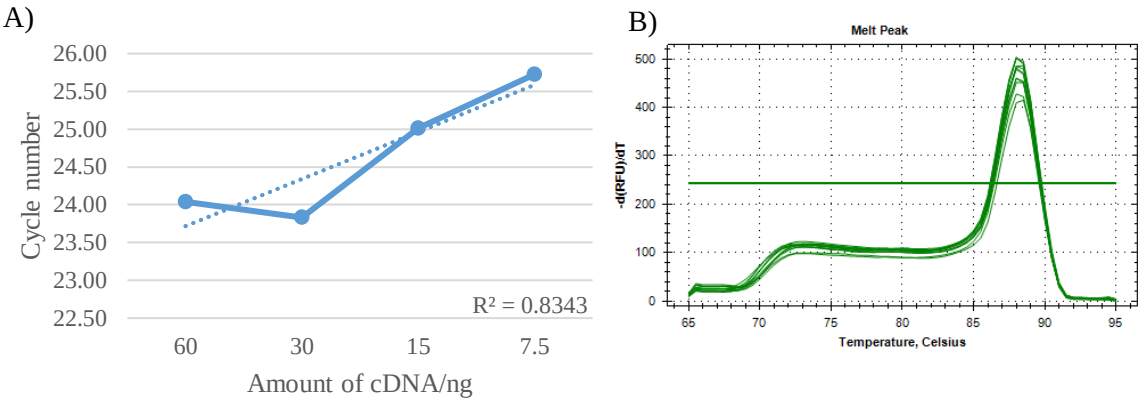


Figure 10.7: Primer optimisation for FOXA2: A) Primers were run at a range of cDNA values. An R^2 value close to 1 indicates primer efficiency. B) The melt curve for the primer provides information on primer specificity, with a single peak indicting the synthesis of a single product.

10.5.8 GATA6

Optimum running temperature = 60°C

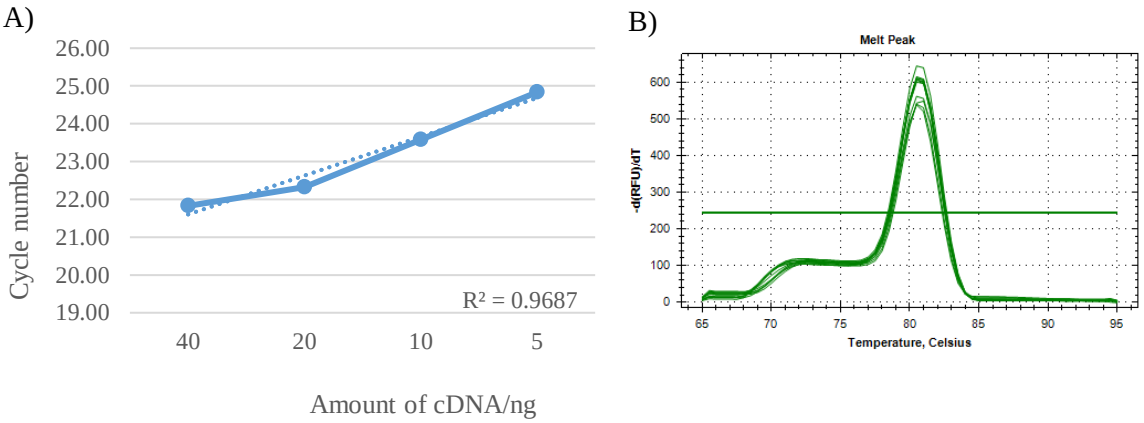


Figure 10.8: Primer optimisation for GATA6: A) Primers were run at a range of cDNA values. An R^2 value close to 1 indicates primer efficiency. B) The melt curve for the primer provides information on primer specificity, with a single peak indicting the synthesis of a single product.

10.5.9 SOX17

Optimum running temperature = 60°C

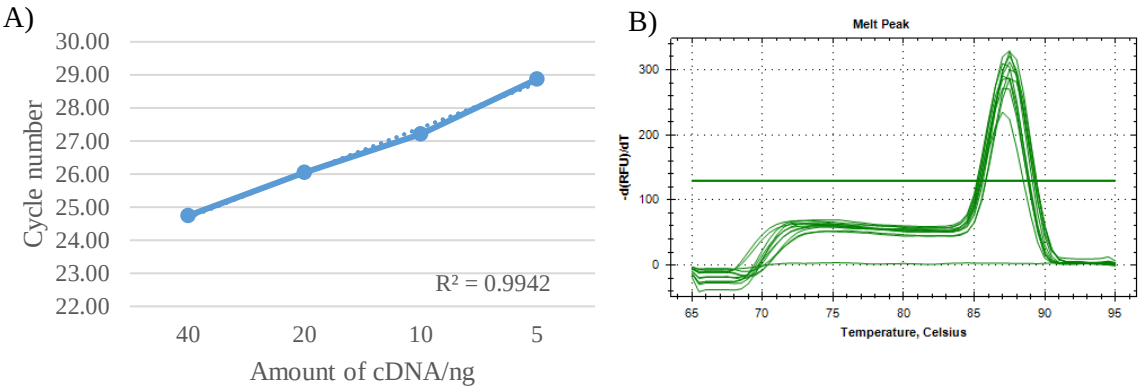


Figure 10.9: Primer optimisation for SOX17: A) Primers were run at a range of cDNA values. An R^2 value close to 1 indicates primer efficiency. B) The melt curve for the primer provides information on primer specificity, with a single peak indicting the synthesis of a single product.

10.5.10 GAPDH

Optimum running temperature = 55°C

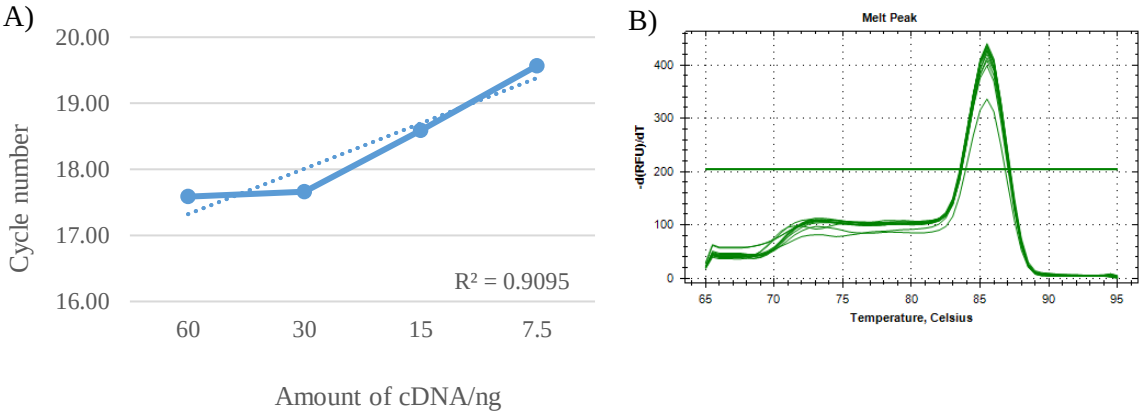


Figure 10.10: Primer optimisation for GAPDH: A) Primers were run at a range of cDNA values. An R^2 value close to 1 indicates primer efficiency. B) The melt curve for the primer provides information on primer specificity, with a single peak indicting the synthesis of a single product.

10.6 Appendix 6 – Teratoma assay supplemental data

The assay was conducted at the Centre for Comparative Biology, University of Newcastle. The assay was commenced on 23/03/18.

Table 10.2. Mouse identification data and assay end dates

Mouse number	Cage number	Ear notches	Cell line	Condition	End date
1	1273	LN	T2SP12	2D	16/04/18
2	2783	LN	T2SP12	2D	14/05/18
3	1149	LN	T2SP12	2D	16/04/18
4	13499	LN	T2SP12	2D	30/04/18
5	1273	RN	T2SP12	3D	14/05/18
6	2783	NN	T2SP12	3D	14/05/18
7	1149	RN	T2SP12	3D	30/04/18
8	13499	RN	T2SP12	3D	30/04/18
9	1273	BN	CGR8	2D	13/04/18
10	787	LN	CGR8	2D	13/04/18
11	1149	BN	CGR8	2D	13/04/18
12	13499	BN	CGR8	2D	13/04/18
13	1273	2LN	CGR8	3D +G	13/04/18
14	787	RN	CGR8	3D +G	16/04/18
15	1149	2LN	CGR8	3D +G	Unsuccessful
16	13499	2LN	CGR8	3D +G	13/04/18
17	1273	NN	CGR8	3D -G	13/04/18
18	787	NN	CGR8	3D –G	13/04/18
19	1149	NN	CGR8	3D –G	13/04/18
20	13499	NN	CGR8	3D -G	16/04/18